Comments on

Dynamic Energy Budget theory

for metabolic organisation

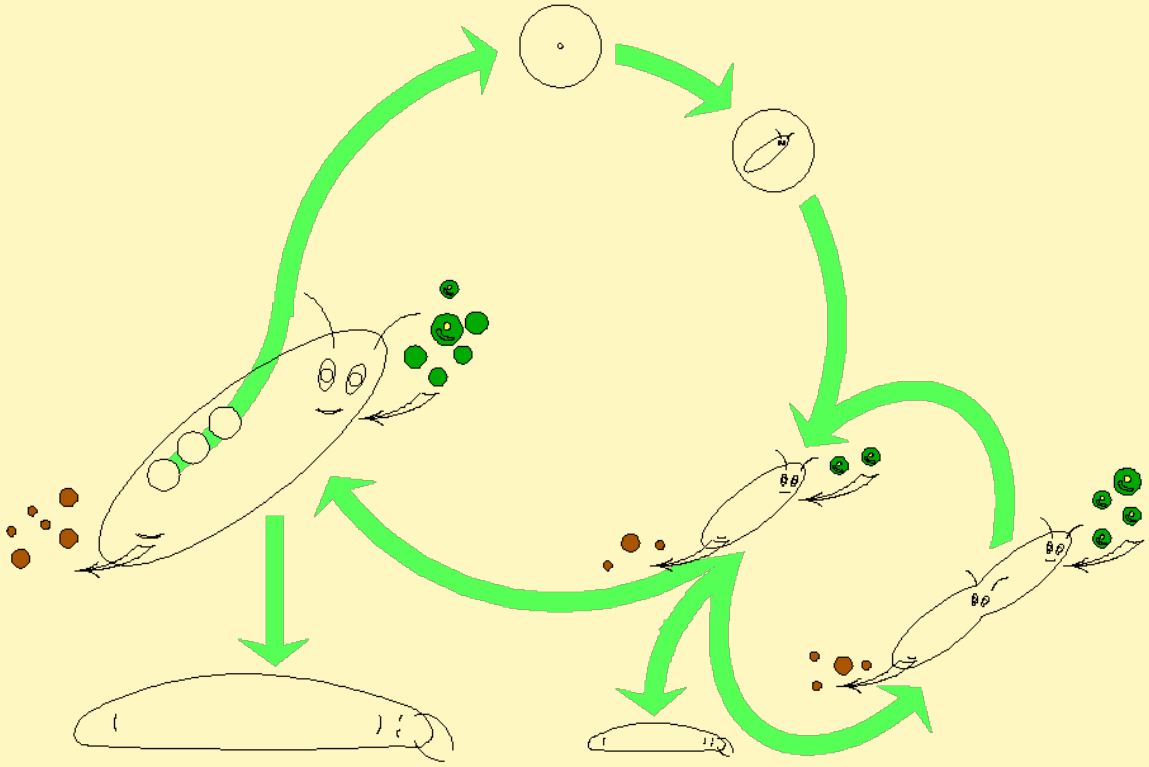

S.A.L.M. Kooijman

Cambridge University Press, third edition 2010

update 2025/07/10

Preface

This document gives comments on my book *Dynamic Energy Budget theory for metabolic organisation*, third edition. The comments follow the section-numbering in that book, which has as consequence that different sections of the comments can have the same section number; clicking on a section number referring within the comments brings you to the correct section. The chapter-titles are identical to that of the book, but the (sub)section-titles refer to the comments.

The types of comments include derivations of particular formulas, further motivation of particular arguments, more biological examples and experimental support, historic backgrounds and discussions of literature, as well as extensions of the theory. If, for instance during the DEB-tele courses, particular sentences in the book turn out to be unclear, I respond by adding explanations in this document. This implies that this document is a dynamic one that is modified many times a year.

Apart from this comments-document, the following DEB-related material is available via the DEBlab

- summary of concepts for each of the sections of the DEB book
- notation document, including notation for new developments of DEB theory
- erratum-list for the 3-rd edition of the DEB book
- software package DEBtool for Matlab (active maintenance) and Octave (maintenance ceased)
- Add_my_Pet (AmP) website with a library of data and parameter values and implied properties for over 1000 animal species, which evolves rapidly
- software package AmPtool for Matlab, which is an DEBtool application for the analysis of the AmP collection
- Basic Methods for Theoretical Biology on methodology, modelling and applied mathematics
- microlectures, a collection of section-wise PowerPoint presentations for the chapters of the DEB-book and the comments
- phylogenetic survey of living organisms, a PowerPoint presentation with an emphasis on life-cycles
- assays, written by participants of DEB tele-courses (no longer maintained)
- Bibliography of DEB papers with pdf's of over 1100 items

In the DEBlab you can find much more, like NicheMapR, DEB and DEBsea Shiny apps, Aquaexcel.

1

Basic concepts

1.1 Individuals as dynamic systems

1.1.3 Why reserves apart from structure?

Argument 3 for delineating reserve needs more context. Chemical composition of the body depends on growth rate in practice if we compare individuals of the same size under different feeding conditions. We don't compare here individuals of different size under the same feeding conditions. Figures 4.16, 4.17 and 4.24 give examples.

Feeding-related changes in chemical composition of the body can be visualized by plotting the inverse of the von Bertalanffy growth rate as function of ultimate length for different food levels. The standard DEB model expect a linear relationship, where the intercept relates to the maintenance rate coefficient, and the slope to the energy conductance. 'No reserve' means an infinitely large energy conductance, implying this line should be horizontal, which is at odds with observations; see Section 2.4 of the comments.

Changes in weight during starvation can only be handled by models without reserve by ignoring length and treating decrease in weight as 'shrinking' and leaving the fact that length does not change, such as during hibernation, as unexplained 'detail'. These models cannot accommodate condition indices, which deal with changes in length-weight relationships.

1.1.4 Stages and switching

Not only aphids, but also some water fleas sport telescoping generations [448]: almost fully developed embryo-like larvae start to produce parthenogenetic subitaneous eggs while they are still being carried in the dorsal brood pouch.

Some insect groups have an imago that does not feed (e.g. mayflies, Ephemeroptera, some antlions, Neuroptera, butterflies of the family Notodontidae, some mosquito's such as chironomids and chaoborids, some wasps), cf subsection 7.8.1, and the allocation to reproduction has already been made in the nymph stage. In DEB terminology, this classifies nymphs as adults, and the adult has a growing nymph and a non-growing imago-stage. Like more family members, the 8 cm long male of the blackdragon *Idiacanthus antrostomus*

does not eat at all, has no teeth, no stomach and only lives long enough to mate; the 61 cm long female has fanglike teeth and a long chin whisker to lure prey. The unability to eat would classify such males as embryo, but allocation to reproduction as adults. This once more illustrates that we should not think in terms of life stages, but in terms of metabolic switching. Some fish species have an isomorphic embryo, a V1-morphic early juvenile stage, which switches back to isomorphy at metamorphisis, see subsection 7.8.2. A lot of stages can be delineated in the development, see Tables 7.3 and 7.4 of the comments, each corresponding with a certain (constant) maturity level.

Not only the paradoxal frog *Pseudis paradoxa* and the midwife toad *Alytes obstetricans* have larvae that are bigger than the adult, but also the deep-sea spiny eels Notacanthidae have leptocephalus larvae that are larger than the adult, see subsection 7. Likewise, pearlfishes *Carapus* have a tenuis larval stage that shrinks to 1/3 of its original length at metamorphosis. Many echinoderms also reduce substantially in body mass at metamorphosis. Embryo's of the parasitic wasp *Venturia* absorb nutrients while still inside the host (some caterpillar), but this is not via a gut. The chlamydomonad *Oophila amblystomatis* lives intra-cellularly in the embryo-tissues of the spotted salamander *Ambystoma maculatum* and returns carbohydrates and dioxygen for ammonia. So, also in this case embryos acquire energy, but not via a gut. Many plants (Tracheophytes), allocate resources to the fertilised ovum and a, sometimes big, seed or fruit develops on the parent plant. In terms of resource allocation this very much resembles foetal development in placentalia. The salp *Thalia democratica* alternates between sexual and asexual stages. After fertilization by an old sexual individual, the young sexual individual first produces a single asexual foetus and then becomes male. The solitary asexual individual produces lots of buds, which become sexual individuals, that aggregate. Bud production is very similar to foetal production, from an energy perspective.

Dung beetles (Scarabaeidae) lay their eggs in dung; the larvae eat dung and the initiation of pupation is modified by food availability [1289]. Parasitic wasps that lay eggs in a host have similar problems to solve once the host is finished by the larvae. Some lizards can switch to a torpor state as embryo to wait with hatching for favourable environmental conditions [1142].

The example of the aphid, sporting telescoping generations, illustrates that the reduction of puberty to a point event is really an idealisation for simplicity's sake that is not always very realistic. This is because puberty is supposed to re-direct allocation to maturity to reproductive output. In reality puberty is a period, and the re-direction is gradual. If puberty would have been an instantaneous event, maturity in aphids would already be arrested in the embryo stage and assimilation would never be switched on.

If maturity is homogeneously distributed in structure and part of the structure is removed, part of maturity is removed as well. You can think of unicellulars that propagate by division, or the daughter cells of a cleaving egg cell of a multicellular organism separate, or a body part is removed (e.g. of plants due to grazing or of a sea anemone that is propagating vegetatively). Each structure should have a maturity. Most organisms can be represented with a single structure, but plants need at least two: root and shoot, each with its own assimilation activity.

Sex-determination is controlled by environmental factors in quite a few species. Changes

in food availability determine sex in daphnids and rotifers (see Section 4.1.8), temperature determines sex in lizards, crocodiles and turtles (see Section 1.3.3). Hymenopterans develop as females from unfertilised eggs and as males from fertilised ones. If larvae of the echiuran annelid *Bonellia* or the siboglinid annelid *Osedax* settle in virgin environment (which is in the latter case the skeleton of a dead whale on the ocean bottom, that is decomposed with help of bacteria in root-like structures), they become female, but if they settle on a female, they become male [1222]. Both groups of annelids produce very small males, that don't feed. This illustrates that the events of metabolic switching matter (initiating feeding, allocation to reproduction), and not the stages (embryo, juvenile, adult). This also holds for the male of the burrowing barnacle *Trypetesa lampas* [403]; males and females are very similar as planktontic larvae, till they settle, when the female grows a mantle sac of 5-11 mm and the tiny male does not develop a gut, only a sexual organ and settles on a female. Males and females moult 3 times as nauplius, slightly increasing in size and transform in a cyprid, with a bivalved shell, that settles. Then follows another metamorphosis and both sexes follow very different trajectories. The eggs remain in the female mantle cavity till the hatch. Females can live and grow upto 3 years; males shrink after at the last metamorphosis, mature in a few days and live upto 3 months.

Western European girls reached puberty at 17 a in 1835, 15 a in 1900 and 13 a in 1945, but the weight at puberty remained the same, 46 kg. These changes in age were due to changes in diet as is further supported by changes in ultimate weight [900, 447].

Diapause, the delay of the onset of development of an egg or foetus, is discussed at several places, e.g. {58} and Subsubsection 8.2.2. This delay can occur before or after fertilisation. Foetal development is initially extremely slow, as if they experience a kind of false diapause, but later sparks off where length increases linearly in time. A delay in fertilisation can involve the storage of sperm. The rattlesnake can store sperm for some 5 years [163]. Such a very long storage time might represent a transition to parthenogenesis, which occurs in 0.6% of the reptile species [701].

The occurrence of many life history events can be understood if they occur at fixed maturity levels, such as hatching in frogs (see Section 2.5.2 of the comments) and morphologically defined life stages in fish (see section 7.8.2 of the comments). The moment of egg-laying is, however, not such a life history event. In many species it occurs as soon as the egg the formed (ovopary), or just before hatching and/or birth (ovovipary). Phytons and boas are related snakes, but boas are ovoviparous, while phytons lay their eggs somewhere during the development of the embryo. The phytoseiid mite *Neoseiulus cucumeris* can delay egg laying in response to the presence of the predatory phytoseiid mite *Iphiseius degenerans* [990]. So the moment of egg laying can depend on environmental factors and part of the buffer handling rules of the mother.

1.1.4 Switching at maturation density?

Nina Marn observed that different populations of loggerheads, *Caretta caretta*, show scatter in size and maturity levels at puberty, but the scatter in maturity density at puberty was much less. If these differences are due to food conditions, rather than to parameter values, this observation suggests that stage switches might be linked to maturity density, $[E_H]$,

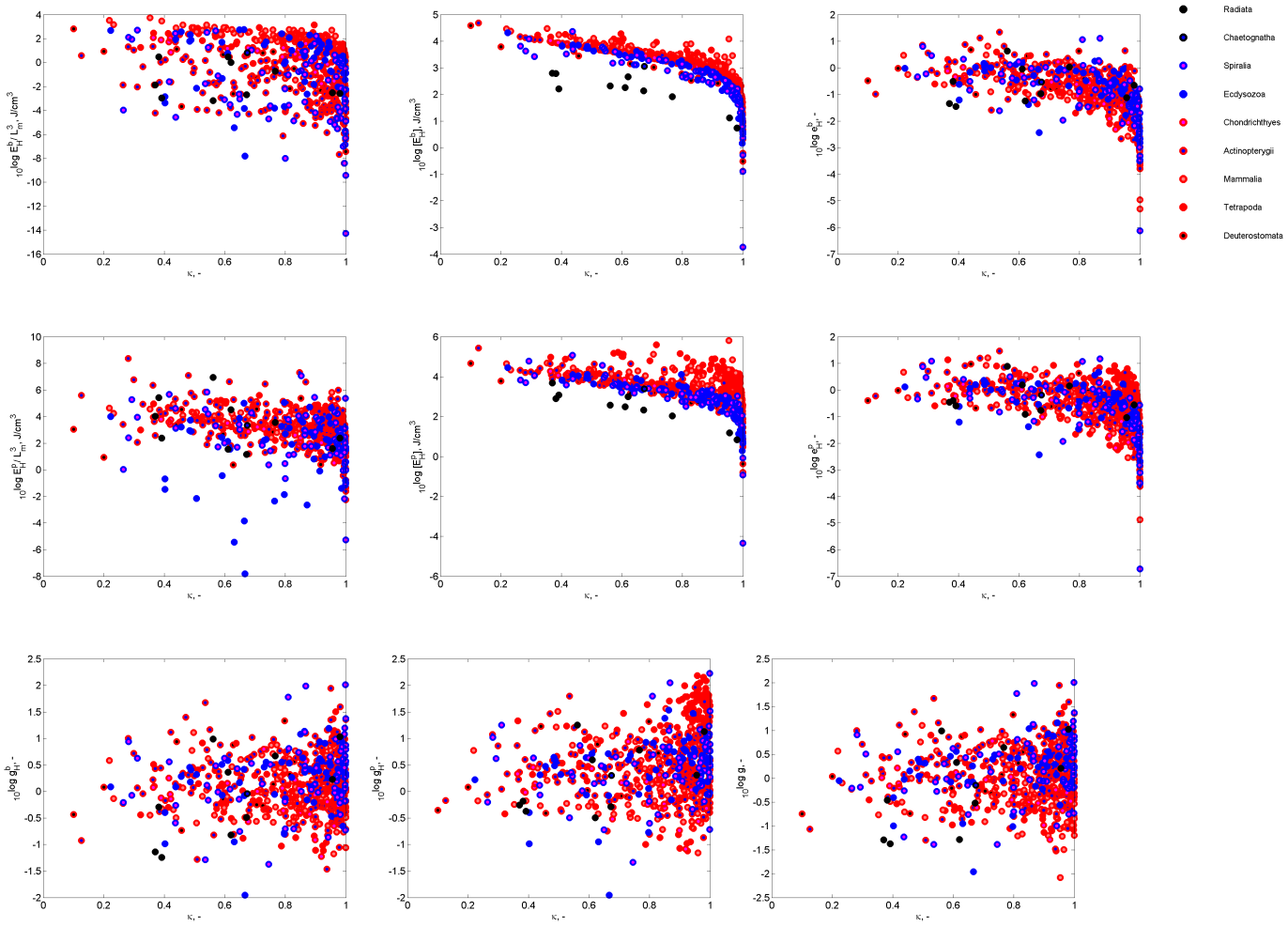

Figure 1.1: Maturity per ultimate structure and actual structure (= maturity density) as functions of κ for the 784 species of the add_my_pet collection. Then maturity density per reserve capacity (= scaled maturity density) and (last row) the maturity investment ratio as functions of κ. Sampling date 2017/05/05.

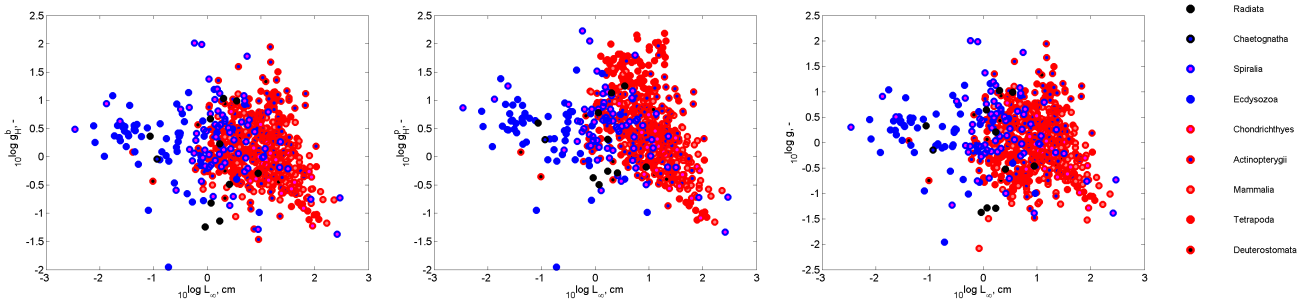

Figure 1.2: Maturity and energy investment ratio as functions of ultimate structural length for the 784 species of the add_my_pet collection. Sampling date 2017/05/05

rather than maturity, E_H. Moreover, Carlos Teixeira noticed that maturity density at birth among bird species turns out to depend on κ. Closer inspection revealed that this holds for all species [50]. The reason is that maturity density at birth does not vary that much. For $k = 1$ is does not vary at all and $[E_H] = [E_G]\frac{1-\kappa}{\kappa}$. This also holds, but to a lesser extend, for the values at puberty, since maturity density can vary in a wider range for $k < 1$. The values for e_H^b for endotherms are larger that for ectotherms. Endotherms have a large reserve capacity, $[E_m]$, which might be linked to compensation for their high body temperature during starvation. An increase of body temperature should come with an increase of reserve capacity to survive a given time of absence of food. The values for energy divestment ratio at birth $g_H^b = \frac{E_H^b/L_b^3}{(1-\kappa)[E_m]} = \frac{[E_H^b]}{(1-\kappa)[E_m]} = \frac{e_H^b}{1-\kappa}$ are the same for all taxa. (The name is inspired by energy investment ratio g, where quantities on the κ-branch in g, are replaced by equivalent quantities on the $(1-\kappa)$-branch in g_H^b. Notice that g remains constant during the life cycle, while g_H^b and g_H^p change if $k \neq 1$.) It is yet unclear why thresholds at stage transition would depend on allocation to maturity via $1-\kappa$, so the larger the allocation to maturation the lower the thresholds at which transitions occur, this is what data indicate. See Figure 1.1, which also shows that $g = \frac{[E_G]}{\kappa[E_m]}$ hardly depends on κ, remarkably enough. This comment aims the access the implications of metabolic switching at threshold values for g_H, rather than E_H.

Differences between switching at maturity or maturity density only become apparent when we compare different food levels. If $\dot{k}_J = \dot{k}_M$, maturity density remains constant during embryo and juvenile stages and it is not possible to link stage transition to maturity density. We now assume that $\dot{k}_J < \dot{k}_M$, in which case maturity density increases till puberty, after which it decreases again, since maturation ceases and growth continues during the adult state. We still keep the maternal effect that reserve density at birth equals mother's reserve density at egg formation. Initial reserve and length at birth (and puberty) have to be re-evaluated.

Maturity density has a strange dynamics at the start of development, since both maturity and structure start at 0. As mentioned below (2.31): $\frac{d}{d\tau}g_H(0) = \pm\infty$ or $\frac{d}{d\tau}g_H(0) = 0$. The latter only occurs if $g_H(0) = g_H^0 = g$, which seems to be the natural initial value for scaled maturity density. This means that for incrementally small initial scaled length l_0, we have $v_H^0 = l_0^3$ and $[E_H](0) = [E_G]\frac{1-\kappa}{\kappa}$.

We cannot work with scaled reserve density e during the embryo stage, since $e(0) = \infty$; eqs (2.26-31) suggest that it is best to work with

$$\frac{d}{d\tau}u_E = -u_E l^2 \frac{g+l}{u_E + l^3}; \quad \frac{d}{d\tau}l = \frac{1}{3}\frac{gu_E - l^4}{u_E + l^3}; \quad \frac{d}{d\tau}g_H = -\frac{g_H^0}{l^3}\frac{d}{d\tau}u_E - g_H\left(k + \frac{3}{l}\frac{d}{d\tau}l\right)$$

The maternal effect amounts to $u_E(\tau_b) = l_b^3 f/g$, where f is the scaled functional response of the mother, with her reserve density in equilibrium. Scaled length at birth l_b can be found from (2.46) and solve l_b from $t(l_b) = \frac{x_b g g_H^b}{v(x_b)g_H^0} - \int_0^{x_b}\frac{r(x)}{v(x)}dx = 0$. DEBtool function get_lb_md computes l_b from parameters.

For scaled structural length at puberty, l_p, it is easiest to work with (2.29-31), but (2.29) replaced by $\frac{d}{d\tau}e = (f-e)g/l$ and (2.30) by $\frac{d}{d\tau}l = r_B(f - l_T - l)$ with $r_B = (3 + 3f/g)^{-1}$. It can be obtained from $\frac{d}{dg_H}l$, where $e = f$, $l(g_H^b) = l_b$ (which is now known) and g_H runs

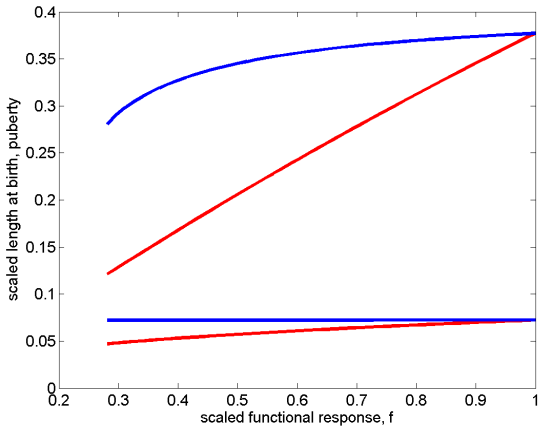

Figure 1.3: Scaled length at birth and puberty as function of scaled functional response, if switches occur at maturity (blue), or maturity density (red). Parameter values: $z = 1$, $\dot{v} = 0.02\,\mathrm{cm/d}$, $\kappa = 0.8$, $[\dot{p}_M] = 18\,\mathrm{J/d.cm^3}$, $\dot{k}_J = 0.002\,\mathrm{d^{-1}}$, $[E_G] = 2800\,\mathrm{J/cm^3}$, $E_H^b = 0.275\,\mathrm{J}$, $E_H^p = 50\,\mathrm{J}$. $g_H^b = 0.3185$, $e_H^p = 4.135$, $g = 3.111$, $k = 0.311$.

from g_H^b to g_H^p. DEBtool function get_lp_md computes l_b and l_p from parameters. Figure 1.2 shows that g_H^b, g_H^p as well as g tend to decrease with ultimate structural length, but the scatter hides the slope.

To compare with switching at maturity, we might choose $e_H^b = E_H^b L_b^{-3}/[E_m] = e_H^0 v_H^b l_b^{-3}$ and $e_H^p = E_H^p L_p^{-3}/[E_m] = e_H^0 v_H^p l_p^{-3}$ (at abundant food). We then select a smaller values for f, keeping E_H^b fixed for switching at maturity and e_H^b for switching at maturity density, and study how l_b depends on f under both switching regimes. Figure 1.3 shows that length at thresholds varies a lot more if switching is at maturity density, rather than at maturity.

Maturity density increases for $\dot{k}_J < \dot{k}_M$, so $e_H(0) < e_H(\tau_b) < e_H(\tau_p)$, which translates to $g < g_H^b < g_H^p < g/k$. The latter condition originates from $l_p < 1$ and $\frac{d}{d\tau} e_H(\tau_p) > 0$. For unscaled scaled parameters we must have $\frac{1-\kappa}{\kappa}[E_G] < E_H^b L_b^{-3} < E_H^p L_p^{-3} < \frac{1-\kappa}{\kappa k}[E_G]$. These constraints clearly show that if $k \uparrow 1$, the possible difference between L_b and L_p shrinks to zero. For given l_b, the scaled maturity density is given by $g_H^b = \frac{v(x_b)}{x_b} \int_0^{x_b} \frac{r(x)}{v(x)} dx$.

Stage transitions at maturity density threshold might be an option for animals that start life with structure and maturity zero and have $k \ll 1$, it is not an option for unicellulars that grow and divide. At division in two (equal) parts, they half their amount of structure and maturity. So maturity density does not change at division. If the division threshold would be at maturity density, maturity density would increase to allocation to maturity maintenance plus maturity being equal to maturity maintenance and further remain constant at constant substrate density.

1.2 Homeostasis is key to life

1.2.1 Strong homeostasis

Empirical evidence for strong homeostasis comes, for instance, from the yolk of developing *Rhea* eggs, where no change in composition could be found and the respiration quotient remained constant during egg development [1133]. This should be seen in the light of yolk dynamics as discussed in Section 2.6.2 in the comment on yolk dynamics, which implies that this finding also supports weak homeostasis.

Notice that strong homeostasis deals with chemical composition of pools, but not with

their dynamics, while weak homeostasis does the opposite: it deals with the dynamics of pools, but assumes strong homeostasis, since pools are defined via their strong homeostatic property: they do not change in chemical composition.

1.2.2 Weak homeostasis

Overwhelming empirical evidence exists for weak homeostasis, which states that reserve density does not change during growth at constant food level, So wet as well as dry weight is proportional to cubed length for isomorphs, with a constant proportionality factor independent of length. The Add_my_Pet (AmP) collection has many examples of length-weight relationships of this type with very good fits, especially for juveniles, where the contribution of gonads to weight has not yet had the chance to disturb the relationship. You can find these entries by searching for `L-Ww` or `L-Wd` in species-list page of the AmP website. Derived from this result, are the many excellent fits in the AmP collection of von Bertalanffy growth curves for length and well as for weigths, where weights are taken proportional to cubed length.

Support for weak homeostasis gains strength by the fact that the AmP collection has many examples where data for males and females have been fitted simultaneously, with excellent fit, assuming that males only differ from females by $\{\dot{p}_{Am}\}$ and E_H^p (so the same shape coefficient). Weights are again found to be proportional to cubed length, but males are heavier for the same length than females, if their ultimate length is larger, but lighter if their ultimate length is less than that of females. This is easy to understand in the context of the std model, since maximum reserve density is $[E_m] = \{\dot{p}_{Am}\}/\dot{v}$, while males and females have the same energy conductance $\dot{v}$. Species for which males are larger than females have, therefore, a larger reserve density and reserve contributes more to weight, compared to females of the same length. Examples in the AmP collection are: *Odorrana swinhoana*, *Podarcis muralis*, *Nerodia sipedon*, *Bothrops insularis*, *Gloydius blomhoffii*.

The AmP collection also shows many time-weight data that fit perfectly to the von Bertalanffy growth curves for weights at constant food, assuming that weight is proportional to cubed length again. This fit involves more assumptions, apart from weak homeostasis, such as assimilation proportional to squared length, maintenance to cubed length and κ being constant. However, many entries show this for both time-length and time-weight data, providing more direct support for weak homeostasis, since the simultaneous fit can only be perfect if weights are proportional to cubed lengths. Notice that, length and weight so not need to have measured at the same time on the same individual; this evidence for weak homeostasis is, therefor, less direct.

Moreover, the AmP collection also has examples of growth at different constant food densities. This data also shows that ultimate length depends on food, and that weight increases with food, for individuals of the same length. This again shows the contribution of reserve to weight and supports the proportionality of weight and cubed length as evidence for weak homeostasis. This links up with the wide use of the ratio of weight and cubed length as condition factor in animal ecology and especially in fisheries research: a good condition means a high reserve density. Its notion goes back to Heincke 1908 [582], according to Nash et al. 2006 [1020], and its success qualifies weak homeostasis as stylised

fact.

Finally, the observation that foetal length is proportional to time, and weight to cubed time [638, 1583], implies that weight is proportional to cubed length, demonstrating weak homeostasis during embryo development, where most relative growth occurs. See further the comment on section 1.2.1 on strong homeostasis, above.

1.2.3 Exoskeletons of isomorphs

Isomorphism itself poses no constraints on shape, but if organisms have a permanent exoskeleton, then stringent constraints on shape exist and as most animals with a permanent exoskeleton actually meet these constraints, it is helpful to work them out. This is done in [764].

A grasshopper remains isomorphic and has an exoskeleton, but it grows by moulting, thus the exoskeleton is not permanent and isomorphism poses no constraints in this case. The same holds for an organism which resembles a sphere, such as a sea urchin; it cannot have a permanent (rigid) exoskeleton, because the curvature of its surface changes during growth. A cylindrical organism that grows in length only, is not isomorphic. A cylindrical organism that grows isometrically has only its caps as a permanent exoskeleton; thus this includes only the caps, i.e. two growing disks separated by a growing distance. The permanent exoskeleton generally represents a (curved) surface in three dimensional space, which can be described in a simple way using logarithmic spirals. The idea of the logarithmic spiral or *spira mirabilis* (in the plane) goes back to Descartes' studies of *Nautilus* in 1638 and to Bernoulli in 1692. The function has been used by Thompson [1418], Rudwick [1226, 1227] and Raup [1156, 1157] to describe the shape of brachiopods, ammonites and other molluscs. I will rephrase their work in modern mathematical terms and extend the idea a bit.

A natural starting point for a description of the isomorphic permanent exoskeleton is the mouthcurve. This is a closed curve in three dimensional space that describes the 'opening' of the permanent exoskeleton (shell). This is where the skeleton synthesizing tissue is found. The development of the exoskeleton can, in most cases, be retraced in time to an infinitesimally small beginning, giving the permanent exoskeleton just the one 'opening'. This method avoids the problem of the specification of the shape of an invisibly small object. To follow the mouth curve back in its development, we introduce a dummy variable l, which has the value 0 for the present mouth curve and $-\infty$ at the start of development. By placing the start of development at the origin, the test on isomorphism of the developing exoskeleton is reduced to mapping one exoskeleton to another by multiplication and rotation only (so no translation). We can always orient the exoskeleton such that the rotation is around the x-axis. Let $\boldsymbol{R}(l)$ denote the rotation matrix

$$\boldsymbol{R}(l) = \begin{pmatrix} 1 & 0 & 0 \\ 0 & \cos l & \sin l \\ 0 & -\sin l & \cos l \end{pmatrix}$$

The closed mouthcurve $\boldsymbol{m}$ at an arbitrary value for the dummy variable l, can be described

by

$$\boldsymbol{m}(l) = c^{l/2\pi}\boldsymbol{R}(-l)\boldsymbol{m}(0)$$

where c is a constant describing how fast the mouth curve reduces in size when the exoskeleton rotates over an angle 2π. If c is very large, it means that the exoskeleton does not rotate during its reduction in size. Size reduction relates in a special way to the rotation rate to ensure (self) isomorphism. It follows from the requirement that for any two points $\boldsymbol{m}_0$ and $\boldsymbol{m}_1$ on the mouthcurve, the distance $\|\boldsymbol{m}_1(l+h) - \boldsymbol{m}_0(l)\|$ depends on l in a way that does not involve the particular choice of points. The rotation matrix is here evaluated at argument $-l$, because most gastropods form left handed coils. For right handed coiling l, rather than $-l$, should be used. The mouth curve, together with the parameter c determine the shape of the exoskeleton.

An arbitrary point on the mouth curve will describe a logarithmic spiral to the origin. To visualize this, it helps to realize that a simple function such as the standard circle is given by $\boldsymbol{f}(l) = (\sin l, \cos l)$, where the dummy variable l takes values between $-\infty$ and ∞. A graphical representation can be obtained by plotting $\sin l$ against $\cos l$. Similarly, the logarithmic spiral with the vertex at the origin through the point $\boldsymbol{m}(0) \equiv (m_1, 0, m_3)$ is given by

$$\boldsymbol{f}(l) = c^{l/2\pi}(m_1, m_3 \sin -l, m_3 \cos -l)$$

It lies on a cone around the x-axis with vertex at the origin, and tangent m_3/m_1 of the diverging angle with respect to the x-axis. For increasing l, the normalized direction vector of the spiral from the vertex, $(m_1, m_3 \sin -l, m_3 \cos -l)/\|\boldsymbol{m}\|$, with $\|\boldsymbol{m}\| = \sqrt{m_1^2 + m_3^2}$, describes a circle in the y, z-plane at x-value $m_1/\|\boldsymbol{m}\|$.

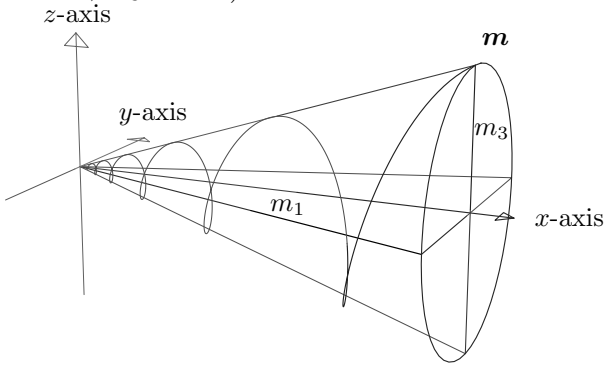

Until now, no explicit reference to time has been made. If the length measure of the animal follows a von Bertalanffy growth pattern, i.e. $1 - \exp\{-\dot{r}_B t\}$ for $t \in (0, \infty)$, the relationship $c^{l/2\pi} = 1 - \exp\{-\dot{r}_B t\}$ results. So, $l = \frac{2\pi}{\ln c} \ln\{1 - \exp\{-\dot{r}_B t\}\}$. This is realistic when food density and temperature remain constant. In winter, when growth ceases in the temperate regions and calcification partially continues in molluscs, a thickening of the shell occurs, which is visible as a ridge ringing the shell. If the gradual transitions between the seasons can be neglected, these ridges will be found at $l = \frac{2\ pi}{\ln c} \ln\{1 - \exp\{-\dot{r}_B i\}\}$, $i = 1, 2, 3, ..,$ when the unit of time is one growth season. In principle, this offers the possibility of determining the von Bertalanffy growth rate $\dot{r}_B$ from a single shell found on the sea shore.

The mouth curve in living animals with a permanent exoskeleton frequently lies more or less in a plane, which reduces the specification of the three dimensional mouth curve to a two dimensional one, plus the specification of the plane of the mouth curve, which involves two extra parameters. The exoskeleton can always be oriented such that the plane of the mouth curve is perpendicular to the x, y-plane and the mouth opening is facing negative y-values.

Let $\boldsymbol{p} \equiv (p_1, p_2, 0)$ denote a point in the plane of the mouth curve, such that this plane is perpendicular to the vector $\boldsymbol{p}$ and $p_2 \leq 0$. (Remember that the axis of the spiral is the x-axis with the vertex at the origin so that the orientation of the exoskeleton is now completely fixed.) The mouth curve $\boldsymbol{n}$ in the plane is now measured using the point $\boldsymbol{p}$ as origin. If the mouth curve is exactly in a plane, a series of two coordinates suffice to describe the exoskeleton together with c, p_1 and p_2.

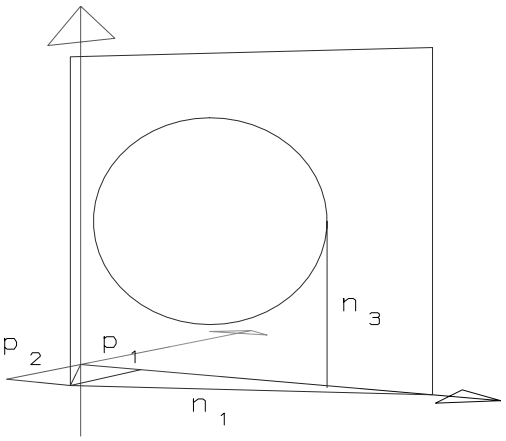

If it is not exactly in a plane, we can interpret the plane as a regression plane and still use three coordinates, where the y-values are taken to be small. The relationship between $\boldsymbol{n}$ measured in the coordinate system with the plane of the mouth curve as x, z-plane and $\boldsymbol{p}$ as origin with the original three dimensional mouth curve $\boldsymbol{m}$ is:

$$\boldsymbol{m} = \boldsymbol{p} + \begin{pmatrix} -p_2/\|\boldsymbol{p}\| & -p_1/\|\boldsymbol{p}\| & 0 \\ p_1/\|\boldsymbol{p}\| & -p_2/\|\boldsymbol{p}\| & 0 \\ 0 & 0 & 1 \end{pmatrix} \boldsymbol{n}$$

More specifically, if the mouth curve is a circle with radius r and the centre point at $(q_1, 0, q_3)$, we get $\boldsymbol{n}(\phi) = (q_1 + r\sin\phi, 0, q_3 + r\cos\phi)$, for an arbitrary value of ϕ between 0 and 2π. This dummy variable just scans the circle. The 6 parameters c, p_1, p_2, q_1, q_2 and r completely fix both shape and size of all isomorphic exoskeletons with circular mouth curves. If only the shape is of interest, we can choose r as the unit of distance, which leaves 5 free parameters for a full specification.

This class of morphs is too wide because it includes physically impossible shapes. The orientation of the mouth curve should be such that a mouth opening results and the shape may not 'bite' itself when walking along the spiral. This constraint can be translated into the constraint that the intersections of the exoskeleton with the x, z-plane should not intersect each other. The intersections of the mouth curve with the x, z-plane are easy to construct, given points on the mouth curve. When the point $\boldsymbol{m}_1 \equiv (m_1, m_2, m_3)$ on the mouth curve $\boldsymbol{m}(0)$ spirals its way back to the vertex, it intersects the x, z-plane at $c^{l_i/2\pi}\boldsymbol{R}(l_i)\boldsymbol{m}_1$, with $l_i = i\pi - \arctan m_2/m_3$ for $i = 0, -1, -2, \cdots$.

The distinction Raup [1156] made between a generating curve and a biological one is purely arbitrary and has neither biological nor geometric meaning; Raup raises the problem that realistic values for the parameters he uses to characterize shape tend to cluster around certain values. Schindel [1255] correctly pointed out that this depends on the particular way of defining parameters, and he used the intersection of mouth curve with the x, z-plane to characterize shape and showed that realistic values for parameters of this curve did not cluster. Any parameterization, however, is arbitrary unless it follows the growth mechanism. This shape of permanent exoskeletons is dealt with here to show that the shape is a result of the isomorphic constraint.

Nautilus has a fixed number of septa per revolution. This is to be expected as it makes a septum as soon as the end chamber in which it lives exceeds a given proportion of its body size. (The fact that the septa in subsequent revolutions frequently make contact implies that *Nautilus* somehow knows the number π.) These septa cause the shell to be no longer isomorphic in the strict sense, but to be what can be called periodically isomorphic, by which I mean that isomorphism no longer holds for any two values of l, but for values that differ by a certain amount. Many gastropods are sculptured at the outer surface of their shell; this sculpture is formed by the mantle curling around the shell edge. The distance from the shell edge and the height of the sculpture relates to the actual body size, the result being a shell that is also periodically isomorphic. Sculpture patterns that do not follow the mouth curve, but follow the logarithmic spirals, do not degrade isomorphism. Some shells of fully grown ammonites and gastropods have a last convolution that deviates in shape from the previous ones, showing a change in physiology related to life stage.

Most shapes are simple and correspond to special cases where the mouth curve lies in a plane. For $p_1 = 0$, the mouth curve lies in a plane parallel to the x, z-plane; shapes such as *Planorbis* and *Nautilus* result if the mouth curve is symmetrical around the x, y-plane. A growing sheet is obtained when $p_1 \to 0$ and $p_2 = 0$ so that the mouth curve lies in the y, z-plane. Age ridges can still show logarithmic spirals (in the plane), depending on the value of c. Figure 1.4 gives a sample of possible shapes. Although the shell of *Spirula* is internal rather than external, this does not spoil the argument.

From an abstract point of view, the closed mouth curve can secrete exoskeletons to either side and no formal restrictions exist for the parameters describing their surfaces. (The biological reality is that two mouth curves are lined up and can be moved apart to let the animal interact with the environment.) Animals such as bivalves have two logarithmic spirals sharing the same mouth-curve, one turns clockwise, one anti-clockwise. Many gastropods also have a second exoskeleton, the plane-like operculum, which is so small that it easily escapes notice. Gastropods of the genera *Berthelinia*, *Julia* and *Midorigai* have two valves, much like the bivalva. As illustrated in figure 1.5, more complex shape are possible when the mouth curve is branched.

1.2.3 Age of shell material

Work with Laure Pecquerie shows the age of shell material in bivalves, which can be used for reconstructing environmental conditions from isotope signals in matter sample from the shell.

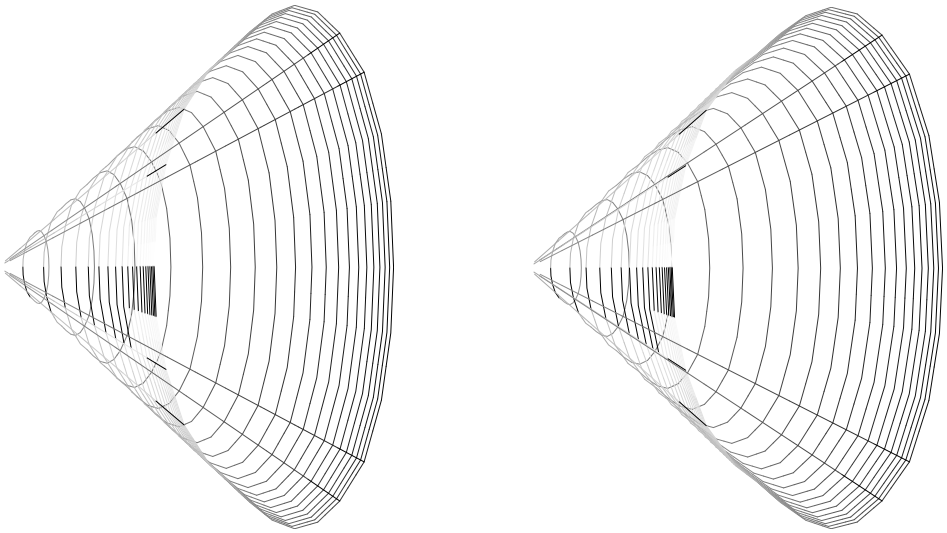

Patella, $c \to \infty$, $p_2 = 0$

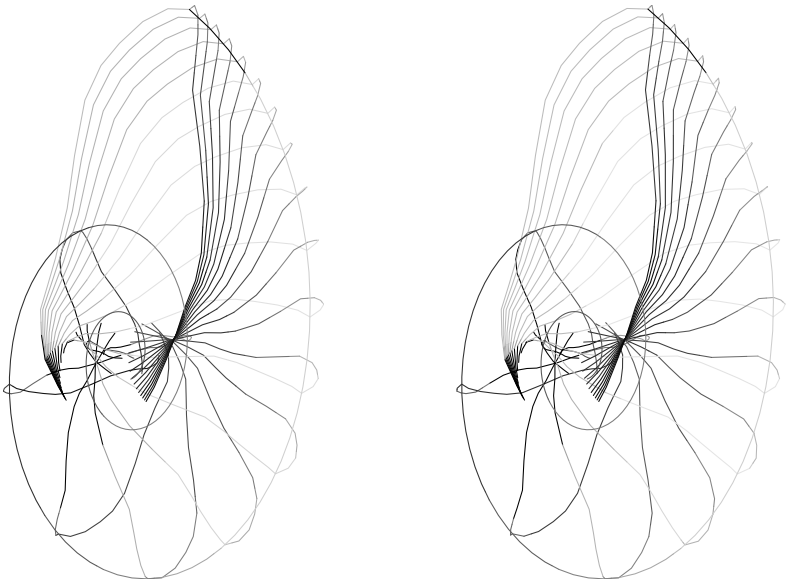

Nautilus, $c = 3$, $p_1 = 0$, $p_2 \to 0$

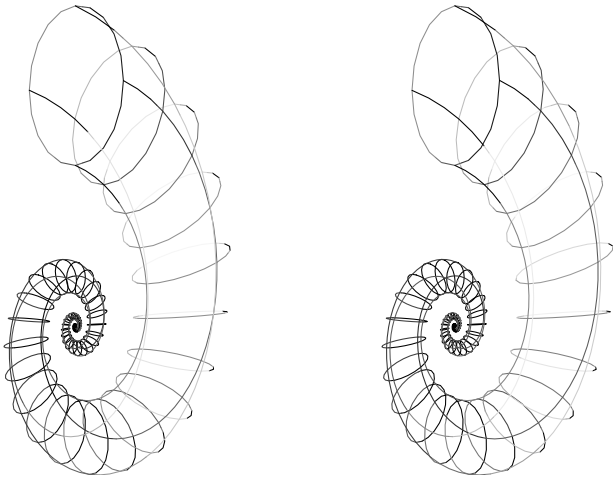

Spirula, $c = 5$, $p_1 = 0$, $p_2 \to 0$

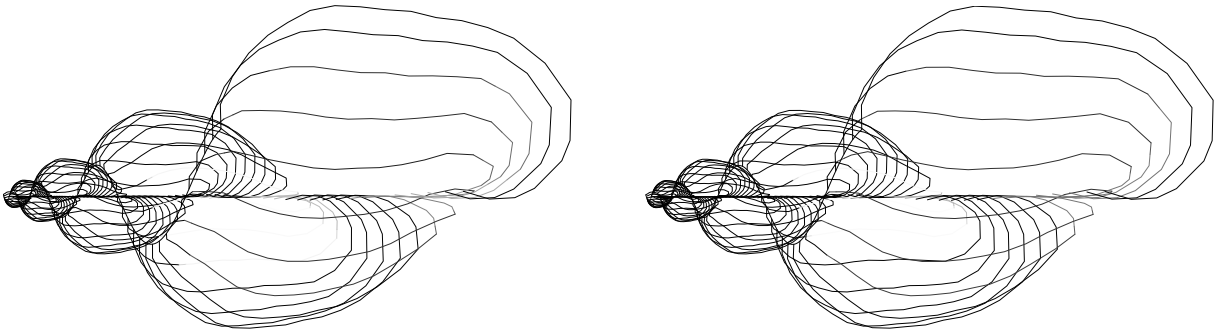

Lymnaea, $c = 2$, $p_1 = 0$, $p_2 \to 0$

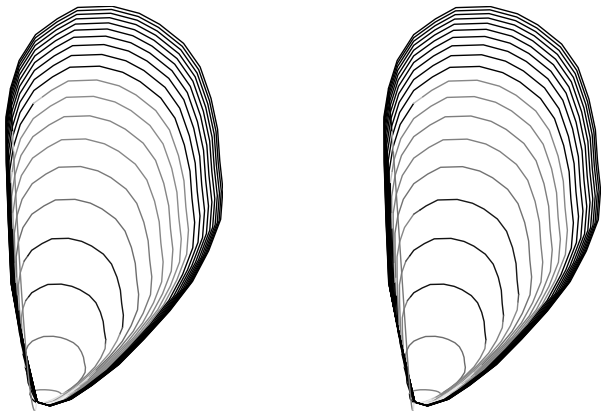

Mytilus, $c = 10^4$, $p_1 \to 0$, $p_2 = 0$

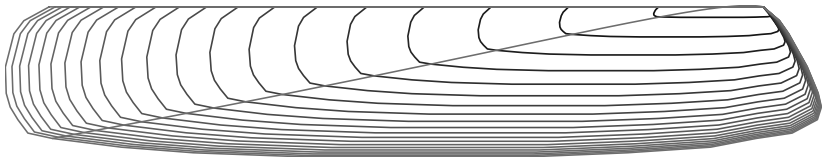

Ensis, $c = 10^5$, $p_1 \to 0$, $p_2 = 0$

Figure 1.4: A sample of possible shapes of isomorphs with permanent exoskeletons. The mouth curves are shown at equal steps for the dummy argument (*Lymnaea*, *Spirula*) or for time. Illuminate well and evenly to obtain the stereo effect. Hold your head about 50 cm from the page with the axis that connects your eyes exactly parelell to that for the figures. Do not focus at first on the page but on an imaginary point far behind the page. Try to merge both middle images of the four you should see this way. Then focus on the merged image. If this fails, try stereo glasses. If the grey is in front, rather than at the background, you are looking with your right eye to the left picture. Prevent this with a sheet of paper placed between your eyes and the page. About 10% of people actually look with one eye only and thus fail to see depth. If necessary, test this by raising one finger in front of your nose and counting the number of raised fingers that you see while focusing at infinity.

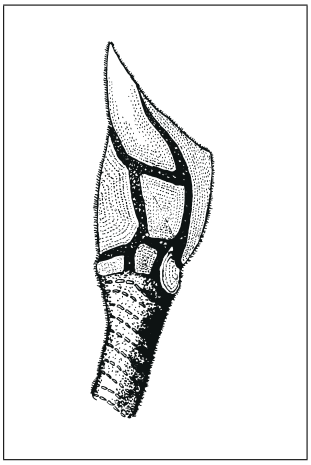

Figure 1.5: The goose barnacle (*Scalpellum scalpellum*) has an exoskeleton with a large number of components; it is an example of a branched mouth curve. Tetrahedrons provide an example of permanent exoskeletons with three branching points in the mouth curve and cubes with eight. If the (branched) mouth curve is a globular network, the exoskeleton can even resemble a sphere.

$L \in (0, L_\infty)$	structural length of bivalve (soft tissue)
$L_s \in (0, L_s^m)$	distance from hinge along shell surface
L_h	thickness of shell
W_s	weight of shell
$l \in (0, L_h)$	depth in shell from outside inwards

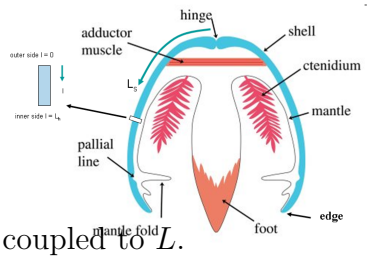

$L_s = 0$ at hinge and $L_s = L_s^m$ at edge, but L_s^m changes in time, coupled to L.
Let us assume that

1 the shell is growing at the edge and at the inner surface
2 $L_h = L\delta_h$
3 $L_s^m = L\delta_s^m$
4 $\frac{d}{dt}L = L\dot{r}/3 = r_B^{\cdot}(L_\infty - L)$ in constant environment

An implication of assumptions 2 and 3 is that the weight of the shell can be written as $W_s = d_s(L\delta_s)^3$. The shell extends at the edge (outward direction) and becomes thicker by deposition from the inside

$$\frac{d}{dt}W_s = d_o L_h L_s^m \frac{d}{dt}L_s^m + d_i L_s^{m2}\frac{d}{dt}L_h$$

leading to

$$\frac{d}{dt}L_h = \delta_h \frac{d}{dt}L \quad \text{with } \delta_h = \frac{3d_s\delta_s^3/\delta_s^{m2}}{d_i + d_o}$$

At t, the bivalve has structural length $L(t)$. the edge is at distance $L_s^m(t) = L(t)\delta_s^m$ from the hinge and the thickness is $L_h(t) = L(t)\delta_h$.

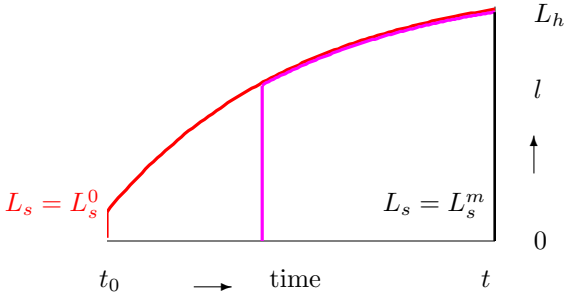

Figure 1.6: The depth in the shell l is plotted against the time of deposition of shell material t for three choices of distances from the hinge of the shell L_s: close to the hinge (red), somewhere in the middle (magenta) and at the edge of the shell. The bivalve settled at time t_0. The outer side of the shell is at depth $l = 0$, the inner side at $l = L_h$.

Suppose we drill a core in the shell with tiny diameter at distance L_s from the hinge and the environment was constant, so

$$\begin{aligned} L(t) &= L_\infty - (L_\infty - L_0)\exp(-\dot{r}_B(t - t_0)) \\ t - t_0 &= \frac{1}{\dot{r}_B}\ln\frac{L_\infty - L_s}{L_\infty - L} \end{aligned}$$

where $t_0 < t$ is the time at settlement and L_0 the length at settlement. We refrain from monitoring the environment before settlement and choose the smallest value of $L_s^0 = L_0\delta_s^m$ at the edge of the shell when it just settled, which was at time t_0 when structural length was L_0. The oldest material of the shell that we are interested in has been deposited at t_0 and can be found at the outer side of the shell at distance L_s^0 from the hinge.

At the time the site of the sample was at the edge of the shell, $L_s = L_s^m$, the structural length of the bivalve was $L = L_s/\delta_s^m$, which was at time $t_L = t - \frac{1}{\dot{r}_B}\ln\frac{L_\infty - L_s/\delta_s^m}{L_\infty - L_s}$. At the inner side of the shell, at $l = L_h(t)$, the material was deposited at t. At the outer side of the shell, at $l = 0$, the material was deposited at t_L.

Let us consider too extreme choices for L_s, close to the hinge $L_s = L_s^0$ and at the edge $L_s = L_s^m$.

Near the hinge, $L_s = L_s^0$, and at the innerside of the shell, $l = L_h(t)$, the material was deposited at t; while at the outer side of the shell, $l = 0$, the material was deposited at t_0. At the edge, $L_s = L_s^m$, the material at outer, $l = 0$, as well as the inner, $l = L_h(t)$, side of the shell is deposited at t.

When the environment is varying in terms of food availability and temperature, von Bertalanffy growth no longer applies, but as long as the specific growth rate is positive, the relation between t and L is monotonous, so the inverse of $L(t)$ exists. The standard DEB model specifies how the specific growth rate $\dot{r}$ varies in time, given trajectories of food density and temperature. Given observations on isotope ratios in the shell, these environmental trajectories can be reconstructed.

1.3 Temperature affects metabolic rates

The issue of temperature dependence of metabolic rates is a complex one. Think of the enzyme(E)-mediated transformation of substrate A to product B: $A + E \to y_{AB}B + E$. Like all transformations it depends on temperature in an instantaneous way. If temperature changes, the rate is changing because of the velocity of molecules. If this transformation

occurs in a living organism, it depends on temperature in a more complex ways, because the cell/individual changes the properties of E qualitatively. This change is not instantaneous (involving enzyme turnover), so the way the rate depends on temperature becomes dependent on temperature history. I don't see yet attempts to capture this dynamically and without such a model, experimental data are hard to interpret (see below).

The point that I make in chapter 1 of DEB3 is: IF y_{AB} does not depend on temperature, then all rate parameters should depend on temperature in the same way in the standard DEB model (does not hold that strict in more-reserve models). If rate parameters depend on temperature in different ways, conversion coefficients (like yield coefficients) become temperature dependent and in fact all parameters can depend on temperature. Even if we use one temperature-parameter per parameter to express how, we have already 13 temperature parameters in the standard DEB model, rather than one (T_A). A challenging question is how y_{AB} can depend on temperature, while the same metabolic machinery is doing the conversion. The above-mentioned transformation is generally not complete and involves other products and probably O_2 as extra substrate. If y_{AB} depends on temperature, product formation depends on temperature in complex ways. To convince me the necessity to go through all this pain (and say farewell to models with few parameters), it is necessary to measure the substrate and product balances and demonstrate mass conservation. It is not likely that this will be done. If done in the proper way, such a development can still be consistent with DEB principles. The many parameters will make the resulting model inapplicable, however. When I see that the standard DEB model has to work with completeness levels of some 2.5 till 3.5 using literature data (while level 10 determines all balances dynamically), it seems safe to choose different priorities to application to many species. Responses of feeding, growth, reproduction not only depends on temperature, but also on feeding history. When people with no attention for metabolic memory analyse temperature responses, signals become connected to temperature, while, in fact, other causes apply. Moreover temperature history cannot be ignored (another form of metabolic memory). We should distinguish between short and long term responses to changes in temperature; short term responses involve temperature history fundamentally. A lot more can be said about this complex topic.

1.3.7 Temperature correction factor

The metabolic rates relate to temperature, by first choosing a reference temperature T_1, and then using the Arrhenius factor on the rate at T_1 of $s_A(T) = \exp\left(\frac{T_A}{T_1} - \frac{T_A}{T}\right)$, given in Eq (1.3). The correction factor satisfies the natural constraint $s_A(T_1) = 1$.

This factor can be multiplied by a term to account for a low-temperature reduction outside the temperature range (T_L, T_H), namely $s_L(T)/s_L(T_1)$ with $s_L(T) = \left(1 + \exp\left(\frac{T_{AL}}{T} - \frac{T_{AL}}{T_L}\right)\right)^{-1}$, or a term to account for a high-temperature reduction, $s_H(T)/s_H(T_1)$ with $s_H(T) = \left(1 + \exp\left(\frac{T_{AH}}{T_H} - \frac{T_{AH}}{T}\right)\right)^{-1}$, or a term to account for both, $s_{LH}(T)/s_{LH}(T_1)$ with $s_{LH}(T) = \left(1 + \exp\left(\frac{T_{AL}}{T} - \frac{T_{AL}}{T_L}\right) + \exp\left(\frac{T_{AH}}{T_H} - \frac{T_{AH}}{T}\right)\right)^{-1}$, see Eq (1.3). Notice that the terms $s_L(T_1)$, $s_H(T_1)$ and $s_{LH}(T_1)$ just serve the function to ensure that the correction factors equal 1 for $T = T_1$.

Intuitive and natural constraints on these reduction factors are $s_L(T) \leq s_L(T_1)$, $s_H(T) \leq s_H(T_1)$ and $s_{LH}(T) \leq s_{LH}(T_1)$. This translates to constraints on T_L, T_H, T_{AL} and T_{AH}. For s_L this works out as $T \leq T_1$ and for s_H as $T \geq T_1$. This suggests that if we want to implement low-temperature reductions, the factor $s_L(T)/s_L(T_1)$ is only applied for temperatures $T < T_1$. Likewise high-temperature reduction is only applied for temperatures $T > T_1$. This imposes constraints on the choice of T_1, which might force us to choose this reference temperature in a species-specific way. The conditions $T_1 > T_L$ and $T_1 < T_H$ seem natural, but not necessary for the condition that the reduction factors are less than 1. For s_{LH}, the 5-parameter temperature-correction variant, the situation is more complex. We must have $\exp\left(\frac{T_{AL}}{T_1} - \frac{T_{AL}}{T_L}\right) + \exp\left(\frac{T_{AH}}{T_H} - \frac{T_{AH}}{T_1}\right) \leq \exp\left(\frac{T_{AL}}{T} - \frac{T_{AL}}{T_L}\right) + \exp\left(\frac{T_{AH}}{T_H} - \frac{T_{AH}}{T}\right)$. A necessary, but not sufficient, condition is $T_L < T_1 < T_H$.

The AmP collection has chosen 293.15 K as reference temperature, but the polar cod, *Boreogadus saida*, for instance, has a T_H that is lower, with the implication that the factors that should reduce metabolic rates actually increase them. This suggests a species-dependent choice of the reference temperature, e.g. 2 ° for (ant)arctic species, and the avoidance of the use of temperature-dependent pseudo-data for parameter estimation for such species. This can be done by using reserve density $[E_m]$, rather than energy conductance $\dot{v}$, and maintenance ratio k, rather than maturity maintenance rate coefficient $\dot{k}_J$.

Figure 1.8 compares the Arrhenius factor with the 5-parameter temperature-correction variant. In the latter, the factor $s_{LH}(T_1)$ is omitted, so the population growth rate at T_1 is multiplied by $s_A(T)/s_{LH}(T)$ to correct for the effect of temperature. This is the reason why the drawn curve is below the stippled line for all temperatures and don't meet the line at T_1, since $s_{LH}(T) > 1$ for all T. This illustrates that the problem of choosing T_1 sometimes in a species-specific way originates from the normalisation (our wish that the temperature correction factor should equal 1 at the reference temperature). Notice that the issue of reference temperature is not discussed in connection to Figure 1.8.

The comparison of temperature-dependent parameter values across species has problems. Depending on the species, endotherms don't tolerate substantial deviations from their target body temperature. When comparisons are made at 20 °C, they typically would simply die at that temperature.

2

Standard DEB model in time, length & energy

2.1 Feeding

2.1.2 Food transport is across surface area of individual

Most animals have guts to process food before absorption, but this does not exclude simultaneous resource uptake through the skin. Hagfish (*Myxini*) have a gut, but can also absorb dissolved organic matter across the skin and gill, possibly an adaptation to a scavenging lifestyle.

2.1.4 Functional response

The text should separate the microscopic and macroscopic levels more clearly. Let us first look at the microscopic level, which is discussed in detail in Section 3.7 and focus on a mussel that filters algae. Suppose that these algal cells arrive at a rate $\dot{h}_X$ per time at the mussel in a given situation. Each cell needs a processing time of $\dot{h}_m^{-1}$, so the mussel is busy during a fraction $\frac{\dot{h}_X}{\dot{h}_X+\dot{h}_m}$ of its time and accepts cells only when it is not busy. So a fraction $\frac{\dot{h}_m}{\dot{h}_X+\dot{h}_m}$ of the arriving cells is accepted and the feeding rate amounts to $\dot{h} = \frac{\dot{h}_m \dot{h}_X}{\dot{h}_X+\dot{h}_m}$ cells per time.

Now we link the microscopic to the macroscopic level, where we can't observe the rate at which algae arrive at the mussel, but we can quantify the filtering rate of the mussel. If the mussel manages, somehow, to organise its feeding process such that all the filtered water is swept clean, the feeding rate $\dot{F}$ (volume of water per time) amounts to $\dot{h} = \dot{F}N$, where the algae have a density of N cells per volume of water. Feeding rate is at maximum in absence of cells: $\dot{F}_m = \dot{h}_X/N$ for very small $\dot{h}_X$ and N. The arrival rate of algae to the mussel is $\dot{h}_X = N\dot{F}_m$. In other words: the arrival rate of cells to the mussel is proportional to the cell density, which is quite natural, and the maximum filtering rate represents the proportionality factor. The feeding rate amounts to $\dot{h} = \frac{\dot{h}_m N}{N+K}$ for half saturation constant $K = \dot{h}_m/\dot{F}_m$.

The dimension of $\dot{h}$ is number of cells per time. This formulation treats cells as identical copies (which is implied by the assumption of a fixed handling time per cell), but for metabolic purposes we need to think about masses and energies and allow for differences between cells. If M_X denotes the mass of a cell in C-mol, we can quantify the ingestion rate as $\dot{J}_{XA} = M_X \dot{h}$. This is too simple for many applications, where we need more compositional information about the cells (reserves, structure), and specify the feeding process in more detail, [1244].

Functional response f is defined as the ingestion rate of food of a given (constant) food quality as fraction of the maximum possible one for an individual of given size. It takes values between 0 (absence of food) and 1 (abundant food). Two types of food can differ in nutritional quality and the maximum specific assimilation rate $\{\dot{p}_{Am}\}$ can depend on food quality. In more detail, the energy content of ingested food can be written as $\dot{p}_X \kappa_X = f(X)\{\dot{p}_{Am}\}L^2$, where κ_X is the digestion efficiency and $\{\dot{p}_{Am}\} = s_X\{\dot{p}^{\mathrm{ref}}_{Am}\}$, where s_X is a dimensionless food quality parameter, relative to some standard; $s_X = 1$ for that standard food quality. So κ_X and s_X play similar, but slightly different roles, where quality coefficient s_X relates to the variation of the maximum specific assimilation rate as function of food quality.

The cumulative amount of food eaten at puberty since birth amounts to $M_X^p - M_X^b = \int_{a_b}^{a_p} \dot{J}_{XA}(a)\, da$, with $\dot{J}_{XA}(a) = f\{\dot{J}_{XAm}\}L(a)^2$. If food density is constant, $L(a) = L_\infty - (L_\infty - L_b)\exp(-\dot{r}_B a)$ with $L_\infty = fL_m - L_T$ and $\dot{r}_B = \frac{\dot{k}_M/3}{1+f/g}$. Substitution gives

$$M_X^p - M_X^b = f\{\dot{J}_{XAm}\}(L_\infty^2(a_p - a_b) + (3L_\infty + L_p)\frac{L_\infty - L_p}{2\dot{r}_B})$$

The amount of food that the mother required to make an egg is $M_X^b = M_E^0/y_{EX}$, which completes the evaluation of the cumulative amount of consumed food at puberty M_X^p. The food-equivalence of a sperm cell is probably small, but most sperm cells are wasted. This evaluation includes overheads in the form of (somatic and maturity) maintenance and maturation.

The remark that organizational simplicity is essential for robustness and evolutionary change is further illustrated by the recent finding that, within the process of deuterostome evolution, tunicates reduced their genome substantially in size (that of *Oikipleura* is the smallest i animal kingdom), and evolved very rapidly, while vertebrates doubled their genome size twice, and evolved much slower [470].

Figure 2 shows that the cumulative amount of food eaten at puberty is a U-shaped function of the functional response, with a minimum close to the minimum functional response that allows for full maturation. At this minimum function response, the cumulative amount of food must go to infinity since it lasts infinitely long to reach the maturity level at puberty, while the maintenance costs grow without boundary. The yield of (dry) biomass on (dry) food, $Y_{WX}^p = W_d^p/(w_X M_X^p)$, has a maximum at a somewhat higher function response than that minimizes cumulative food intake. Applications at population level should consider that most individuals don't make it till puberty, and much more food is required to replace an individual for one of the next generation.

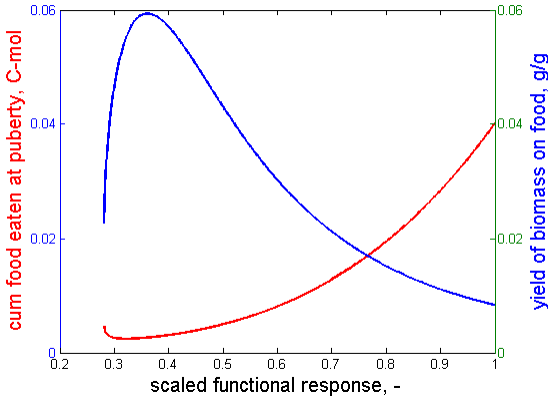

The cumulative amount of food eaten at puberty (red), including overheads, plus the amount of food eaten by the mother to make the egg as function of the scaled functional response. The yield of dry biomass on cumulative food (blue) has maximum at a higher function response than that minimizes cumulative food intake. The parameter values are from the generalized animal, given in Table 8.1.

2.3 Reserve dynamics: simplified derivation

Work with James Maino, Mike Kearney and Roger Nisbet shows that a much simpler (but somewhat less rigorous) derivation of reserve dynamics can be based on three steps:

1 mobilisation only depends on reserve and structure and fuels all metabolism other than assimilation. Only in this way, the resulting growth and reproduction can capture a set of empirical stylised facts [859].

2 gross mobilisation is proportional to E/L. Only in this way gross mobilisation is a function of reserve and structure only and reserve density remains constant at constant food density with a feeding rate that is proportional to squared length.

3 part of mobilised reserve is rejected for growth of structure such that the ratio of the rejected reserve and synthesized structure equals the existing reserve density. Only in this way does mobilisation not affect reserve density, which is required for weak homeostasis.

Reserve dynamics follows from these two rules as follows. Nett mobilisation equals gross mobilisation minus rejection: $\dot{p}_C = \dot{p}_C^g - \dot{p}_C^r$. Gross mobilisation can be written as $\dot{p}_C^g = \dot{v}E/L$. A fraction κ_C , say, of the gross mobilisation is rejected, so $\frac{\kappa_C \dot{p}_C^g}{\dot{r}V} = \frac{E}{V}$ and $\dot{p}_C^r = \kappa_C \dot{p}_C^g = \dot{r}E$ and $\dot{p}_C = E(\dot{v}/L - \dot{r})$.

Somatic maintenance can be introduced as a demand process by subtracting it from gross mobilisation before allocation to growth. Allocation to maturity maintenance and maturation (or reproduction) can be introduced as (constant) fraction of the mobilisation (the κ-rule). None of these modifications affect the expression for mobilisation other than via the specific growth rate $\dot{r}$. It can be shown that the proper rejection flux results naturally from the dynamics of Synthesizing Units for all reserve densities, if these units represent a fixed fraction of structure. Unnecessary mobilisation of reserve can subsequently be avoided with a self-inhibition of monomerisation of polymerous reserve.

2.3 Reserve dynamics: Derivation of (2.4)

The derivation of (2.4) can be as follows. The general formula for reserve dynamics is $\frac{d}{dt}[E] = [\dot{p}_A] - F([E], V)$, for some function F of the state variables $[E]$ and V. We now use the weak homeostasis assumption, which states that $[E]$ is independent of V if $\frac{d}{dt}[E] = 0$, while $[\dot{p}_A] \propto V^{-1/3}$. The essential point of this assumption is that the individual can grow under constant environmental conditions, but does this in such a way the the reserve density does not change. This means that the function F has to be inversely proportional to length as well, and, at equilibrium, F can be written as $F([E]^*, V) = V^{-1/3} H([E]^* | \boldsymbol{\theta})$, where function H does not depend on V, but on $[E]$ only. Weak homeostasis only applies at equilibrium. When we generalize this result to non-equilibrium conditions, we must add a general term that disappears in the equilibrium. We do this by choosing some general function G, like F, and multiply it with the factor $([E]^* - [E])$ to make sure that it disappears at equilibrium. This directly results in (2.4). To demonstrate that the function $G^\circ([E]^*, [E], V) = ([E]^* - [E]) G([E]^*, [E], V)$ must equal zero, we differentiate to $[E]^*$ and require that it is independent of $[E]^*$ by imposing $\frac{d}{d[E]^*} G^\circ = 0$, which leads to $0 = G + ([E]^* - [E]) \frac{d}{d[E]^*} G$. Separation of variables leads to the solution $G([E]^*, [E], V) = G^*([E], V)/([E]^* - [E])$, for some general function G^*. When we substitute this result back into the equation for $\frac{d}{dt}[E]$, the third term amounts to $G^*([E], V)$, about which we know that is does not depend on $[E^*]$ while $G^*([E^*], V) = 0$. This can only be true if $G^*([E], V) = 0$, which leaves us at $\frac{d}{dt}[E] = [\dot{p}_A] - V^{-1/3} H([E] | \boldsymbol{\theta})$ at steady state, as well as non-steady state conditions. The key argument around function G is that an arbitrary function of $[E]$ and V that disappears at steady state $[E]^*$ must depend on the value $[E]^*$, while this value depends on food density. We assumed, however, that the use of reserve does not depend on food density, so we can forget about such a function G and $\frac{d}{dt}[E] = [\dot{p}_A] - V^{-1/3} H([E] | \boldsymbol{\theta})$ fully covers the set of all possibilities, given the assumptions.

2.3 Reserve dynamics: Derivation of (2.6)

The derivation of (2.6) is as follows: We have $\frac{d}{dt} E = \dot{p}_A - \dot{p}_C$, while $[E] = E V^{-1}$, so

$$\begin{aligned}
\frac{d}{dt}[E] &= V^{-1} \frac{d}{dt} E - E V^{-2} \frac{d}{dt} V \\
&= V^{-1} \frac{d}{dt} E - [E] V^{-1} \frac{d}{dt} V \\
&= V^{-1} \frac{d}{dt} E - [E] \frac{d}{dt} \ln V \\
&= \dot{p}_A / V - \dot{p}_C / V - [E] \frac{d}{dt} \ln V \\
&= [\dot{p}_A] - [\dot{p}_C] - [E] \frac{d}{dt} \ln V
\end{aligned}$$

Eqn. (2.6) follows from (2.5) and $\kappa \dot{p}_C = \dot{p}_M + [E_G] \frac{d}{dt} V$, by realizing that $\frac{d}{dt} \ln V = V^{-1} \frac{d}{dt} V$.

2.3.1 Partitionability (2.9)

The definition of partitionability in (2.9) should be read as follows: if we multiply $[E]$, $[\dot{p}_M]$ and $[E_G]$ with some number κ_A between 0 and 1 (as is done in the right-hand side), the effect is that $[\dot{p}_C]$ is multiplied with that number (as is done in the left-hand side). The criterion applies to the dynamics of the reserve density $[E]$, not to the dynamics of the amount of reserve E. The reason is in the smooth merging of reserves in an evolutionary time frame. Single-reserve systems evolved from multi-reserve systems. Moreover, symbiogenesis frequently occurred in evolution, where two syntrophic species merge into a single one. Since DEB theory is supposed to apply to all organisms, consistency arguments show that both partners prior to merging, as well are the merged new species must follow the DEB rules. To do this in a smooth way, we need a mergeability argument, which is the inverse partitionability argument. The reasoning is spelled out in [781].

The step from the partitionability requirement to the requirement for H and κ follows after substitution of (2.7) in the definition of partitionability, together with the observation that it must apply for all values of V. The latter observation boils that to the argument that the substitution of $[\dot{p}_C]$ in the left- and right-hand side of the partitionability definition results in the equality of two ratios of terms in V, and so to equality of each of the terms.

2.3.2 Mergeability (2.15)

Using (2.14), the mergeability constraint $\kappa_A \dot{F}([E], V) = \dot{F}(\kappa_A[E], V)$ can be written as

$$\kappa_A \left(1 + \frac{\kappa[E]}{[E_G]}\right) [\dot{p}_C]([E], V) - \kappa_A \frac{[E]}{[E_G]} [\dot{p}_S] = \left(1 + \frac{\kappa_A \kappa[E]}{[E_G]}\right) [\dot{p}_C](\kappa_A[E], V) - \frac{\kappa_A[E]}{[E_G]} [\dot{p}_S]$$

or

$$\kappa_A \left(1 + \frac{\kappa[E]}{[E_G]}\right) [\dot{p}_C]([E], V) = \left(1 + \frac{\kappa_A \kappa[E]}{[E_G]}\right) [\dot{p}_C](\kappa_A[E], V)$$

From this (2.15) follows.

2.3.3 Mechanism for strong homeostasis

The proposed mechanism in Section 2.3.3 assumes that the (constant) fraction of structure that consists of growth SUs is such that the ratio of the rejected reserve flux and the synthesised structure flux equals the existing reserve density. The beauty of the argument is that such a faction can actually exist, and the property applies even if the flux of reserve allocated to these SUs varies. Fig. 2.2 illustrates that the standard deviation of the specific use of reserve for growth and somatic maintenance during a stochastic feeding process is very sensitive for the value of the rejection strength. This property suggests a possible scenario for the evolution of strong homeostasis, in this case with respect for the growth SUs in structure, via weak homeostasis. Originally the density of SUs would not have been the value that results in weak homeostasis, so the setting of their specific abundance might have been linked to a minimisation of variation, see [799].

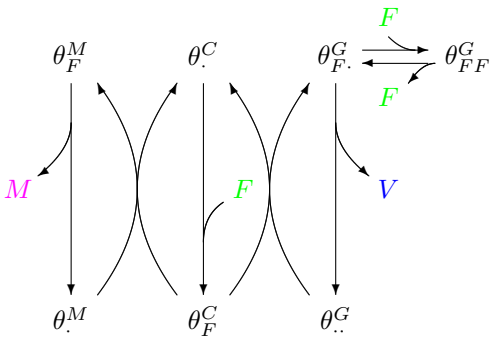

Figure 2.1: The SU-complex for mobilisation, maintenance and growth is inhibition of reserve monomers. The monomer-polymer ratio in reserve is constant and small.

M maintenance substrate
F monomer reserve
V structure

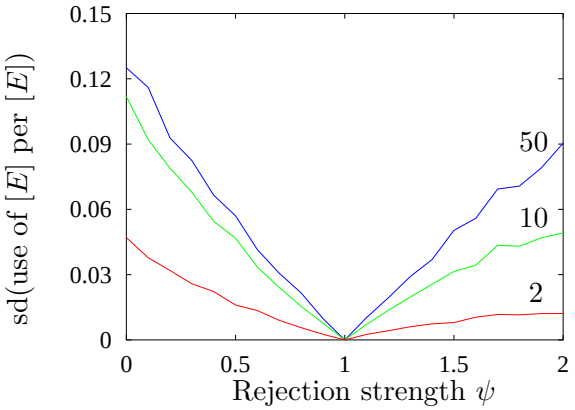

Figure 2.2: The standard deviation of the specific use of reserve density as a function of the rejection strength, if the assimilation rate $\dot{k}_A$ jumps randomly between 0 and 1 h^{-1}. The hazard rate at level 0 is 2, 10 and 50 h^{-1} and at level 1 is 10 h^{-1}. The standard deviations are estimated from Monte Carlo simulations over 200 h, using reserve turnover rate $\dot{k}_E = 1.5\,\mathrm{h}^{-1}$ and maintenance rate coefficient $\dot{k}_M = 0.01\,\mathrm{h}^{-1}$.

The surface area of the interface of reserve and structure is proportional to the amount of reserve M_E for V1-morphs and to M_E/L for isomorphs (for which length $L \propto M_V^{1/3}$, where M_V is the amount of structure) if structural homeostasis applies. To see this, think of a growing sphere of radius L_r; it has volume $V = \frac{4}{3}\pi L_r^3$ and surface area $S = 4\pi L_r^2 = \frac{1}{3}\frac{V}{L_r} \propto V/L$, where $L = V^{1/3}$. The volume of reserve is proportional to its mass (or energy content) due to strong homeostasis and coupled to the volume of structure due to weak homeostasis. The reserve is mobilised at rate $\dot{J}_{EC} = M_E\dot{k}_E$ for V1-morphs and at rate $\dot{J}_{EC} = M_E\dot{v}/L$ for isomorphs. So the reserve turnover rate $\dot{k}_E$ is constant for V1-morphs, but its equivalent for isomorphs, $\dot{v}/L$, changes in time because the energy conductance $\dot{v}$ remains constant, while length L changes in time.

The dynamics of the fraction of unbounded SUs for growth and somatic maintenance, $\theta_\cdot$, for V1-morphs is

$$\frac{d}{dt}\theta_\cdot = (1-\theta_\cdot)\dot{k} + j_{EM}/n - \theta_\cdot \dot{k}_E m_E/n, \tag{2.1}$$

where $n = N/M_V$ denotes the specific number of SUs, $\dot{k}$ the dissociation rate of the SUs, $m_E = M_E/M_V$ the reserve density, $j_{EM} = \dot{J}_{EM}/M_V$ the specific somatic maintenance costs and $\dot{J}_{EM}$ the somatic maintenance costs. Because maintenance is a demand process that has a fixed specific rate, and growth a supply process with a varying rate, maintenance has absolute priority above growth and takes mobilised reserve instantaneously at the moment it arrives at the SUs. It, therefore, appears with the term j_{EM}/n in the change of the unbounded fraction.

The steady state fraction of unbounded SUs then amounts to

$$\theta^*_{\cdot} = \frac{\dot{k} + j_{EM}/n}{\dot{k} + \dot{k}_E m_E/n}, \tag{2.2}$$

while the specific growth rate equals $\dot{r} = (1-\theta^*_{\cdot})n\, y_{VE}\, \dot{k} = \frac{m_E \dot{k}_E - j_{EM}}{m_E \psi + y_{EV}}$ for rejection strength $\psi = \frac{y_{EV}\dot{k}_E}{n\dot{k}}$ and yield of structure on reserve $y_{VE} = y_{EV}^{-1}$. The mobilised reserve flux of size $M_E \dot{k}_E$ is partitioned into the flux $M_E(\dot{k}_E - \dot{r})$ that is accepted and used for somatic maintenance at rate $j_{EM} M_V$ and growth (*i.e.* structure is synthesised at rate $\dot{r} M_V$), and the flux $M_E \psi \dot{r}$ that is rejected and returned to the reserve. The latter flux can be seen (formally) as a synthesis of reserve, which helps to see that for $\psi = 1$ (so $n = y_{EV}\dot{k}_E/\dot{k}$), homeostasis is most effective because reserve is then synthesised at the same specific rate as structure, so the reserve density is not affected.

The dynamics of the reserve density becomes

$$\frac{d}{dt} m_E = j_{EA} - m_E(\dot{k}_E + \dot{r}(1-\psi)), \tag{2.3}$$

where j_{EA} is the specific assimilation rate, which depends on substrate density and so typically fluctuates in time. The mobilising SUs at the reserve-structure interface experience a local chemical environment that changes with $-\frac{d}{dt} \ln m_E|_{j_{EA}=0}$, so with $\dot{k}_E + \dot{r}(1-\psi)$. Let us call this quantity $\dot{k}_C$, the normalised mobilisation rate. Fig. 2.2 gives the standard deviation of $\dot{k}_C$ as function of rejection strength ψ, when the assimilation rate $\dot{k}_A$ jumps randomly between 0 and some fixed value; so the assimilation process follows an alternating Poisson process with the consequence that the reserve density changes in time as does the specific growth rate $\dot{r}$. The standard deviation of $\dot{k}_C$ equals zero for $\psi = 1$ (because $\dot{k}_C = \dot{k}_E$ in that case), but increases almost proportional to the deviation from this value. The tuning of the number of SUs n can then be seen as one of the mechanisms organisms use to improve homeostasis.

The specific flux that is mobilised from the reserve, the specific mobilisation flux $[\dot{p}_C]$, relates to the energy costs per unit of structure $[E_G]$ and the specific maintenance costs $[\dot{p}_M]$ as $[\dot{p}_C] = [E_G]\dot{r} + [\dot{p}_M] = [E](\dot{k}_E - \psi\dot{r})$, where $[E]$ is the reserve density. It is partitionable for all positive values of ψ because $[\dot{p}_C] = [E]\frac{[E_G]\dot{k}_E + \psi[\dot{p}_M]}{\psi[E] + [E_G]} = [E]\frac{[E_G]'\dot{k}_E + [\dot{p}_M]}{[E] + [E_G]'}$. So, rejection strength ψ only affects the apparent growth costs, $[E_G]' = [E_G]/\psi$. The abundance of SUs n, therefore, affects parameter values, not model structure.

Table 2.1 presents the specific mobilisation flux and the reserve density dynamics for the first-order process; this is compared with that for V1 and isomorphs according to DEB rules. Three types of dynamics might represent steps in an evolutionary sequence. The specific growth rate appears in either the specific mobilisation flux or the reserve density dynamics because of the chain rule for differentiation (*i.e.* dilution by growth).

If the reserve capacity is large, which is the case for large bodied species, and for eggs and seeds in an early stage of development, most of the mobilised reserve is rejected and fed back to the reserve. This unnecessary mobilisation is avoided by self-inhibition of monomerisation of reserve-polymers, as illustrated in Figure 2.1.

Module	Specific mobilisation flux $[\dot{p}_C]$	Specific growth rate $\dot{r} = \frac{d}{dt} \ln V$	Reserve density $\frac{d}{dt}[E]$
First-order	$[E]\dot{k}_E$	$\frac{[E]\dot{k}_E - [\dot{p}_M]}{[E_G]}$	$[\dot{p}_A] - [E](\dot{k}_E + \dot{r})$
V1-morphs	$[E](\dot{k}_E - \dot{r})$	$\frac{[E]\dot{k}_E - [\dot{p}_M]}{[E] + [E_G]}$	$[\dot{p}_A] - [E]\dot{k}_E$
Isomorphs	$[E](\dot{v}/L - \dot{r})$	$\frac{[E]\dot{v}/L - [\dot{p}_M]}{[E] + [E_G]}$	$(\{\dot{p}_A\} - [E]\dot{v})/L$

Table 2.1: Three steps in the evolution of reserve dynamics, and the implications for the specific mobilisation flux, the specific growth rate and the dynamics of the reserve density. Symbols: $[E] = E/V$ reserve density, V structural volume, $L = V^{1/3}$ structural length, $[\dot{p}_C] = \dot{p}_C/V$ specific mobilisation flux, $[\dot{p}_M] = \dot{p}_M/V$ specific somatic maintenance flux, $[\dot{p}_A] = \dot{p}_A/V$ (volume-)specific assimilation flux, $\{\dot{p}_A\} = \dot{p}_A/L^2$, surface-area-specific maintenance flux, $[E_G]$ specific costs for structure, $\dot{k}_E$ reserve turnover rate, $\dot{v}$ energy conductance.

2.3 Turnover time of reserve

The turnover time for reserve equals the mean time that a randomly selected (generalised) reserve 'molecule' stays in the reserve compartment; for this reason it is also called residence time. Using (2.20), this time amounts at constant food ($e = f$) for juveniles and adults to

$$t_E = \frac{E}{\dot{p}_C} = \frac{1 + f/g}{\dot{v}/L + \dot{k}_M(1 + L_T/L)}.$$

So t_E increases with structural length L. By comparison, the residence time of food particles in the stomach t_s and gut t_g, see Section 7.3.1 and (7.68), are proportional to structural length. So t_E, t_s and t_g all increase with the length of the individual. This links to the observation that distances across which metabolites have to be transported also increase with a length measure.

Effects of the scaled functional response work out very different for the residence times in reserve, stomach and gut. t_E increases with f, t_s is independent of f and t_g decreases with f. So the residence times of particles in the gut and the reserve respond almost oppositely to changes in food density. The fact that t_E increases with f enhances the buffering capacity of reserve for changes in food availability. The residence time of 'molecules' in the reproduction buffer very much depends on the buffer handling rules.

The maximum value for t_E is reached for $f = 1$ and $L = L_m = \frac{\dot{v}}{g\dot{k}_M}$. For $L_T = 0$ that gives $t_{Em} = (g\dot{k}_M)^{-1}$, so $L_m = \dot{v}t_{Em}$: maximum (structural) length is the product of the energy conductance and the maximum (mean) residence time of 'molecules' in the reserve. The residence time can thus be written as $t_E = \frac{f+g}{1+(L_T+gL_m)/L} t_{Em}$. Scaled maximum turnover time $\tau_{Em} = t_{Em}\dot{k}_M = g^{-1}$ is thus inverse to the energy investment ratio. Since energy investment ratio does not have a direct interpretation, apart from its definition $g = \frac{[E_G]\dot{v}}{\kappa\{\dot{p}_{Am}\}}$, we now uncovered a direct interpretation of the energy investment ratio: the inverse scaled maximum reserve turnover time.

A (constant) fraction of reserve consists of proteins that catalyse particular metabolic transformations (enzymes). Enzymes are thermally rather unstable and functional at for-

mation, but sooner of later loose their activity as catalyst. So when an individual grows bigger, a larger fraction of its enzymes in the reserve is in the non-functional state, which partly explains the loss of metabolic performance that is typically associated with ageing in the literature, but has in fact nothing to do with that. The fully grown individual at abundant food represents a worst case in terms of performance of compounds in its reserve (and in terms of vulnerability for shrinking).

The maximum reserve density equals $m_{Em} = \frac{y_{EV}}{g\kappa}$. When we compare different species, the maximum reserve density increases proportional to the maximum length L_m, because g is inversely proportional to L_m (see Section 8.2). If a large-bodied species makes use of the same enzymes as a small-bodied one, a smaller fraction of its enzymes is in the active state. By increasing the maximum reserve density, the density of active enzymes can become independent of the maximum body size. This is another way to look at the implied result that $\frac{t_{Em}}{m_{Em}} = \frac{\kappa}{k_M y_{EV}}$ is independent of maximum body size across species: The number of active enzymes decays by a first order process, so it decreases exponentially in time, and the density of active enzymes in the reserve is independent of the maximum body size of a species.

Large reserve capacities smooth out fluctuations in food intake rates much more effectively than small ones, as reflected in the turnover rate. This determines a typical temporal scale of living. By 'choosing' for a reserve density proportional to maximum structural length, big-bodied species not only solve the problem of preserving the integrity of their reserve relative to their structure, but also increase the time they can survive starvation in proportion to maximum structural length as an aspect of the smoothing capacity of a large reserve. The (walking, swimming, flying) speed and the diameter of the home range also increase with maximum body length, which combines nicely with the feeding rate scaling with cubed length inter-specifically (with squared length intra-specifically). When there is no food, the combination of speed and starvation time scaling with length nicely combines with the fraction of the home range that is searched for food being independent of maximum body length. I mention this to demonstrate the natural coupling of scales in space and time, and of behavioural, physiological and even molecular traits.

Enzymes not only occur in reserve, but also in structure. A (large) fraction of somatic maintenance relates to the turnover of structure and different chemical compounds can have different turnover rates. So the turnover of structure is paid from somatic maintenance and the turnover rate is independent of food availability and body size. The turnover of reserve is paid from overheads of assimilation and mobilisation and the turnover rate depends on food availability and body size. The overhead of assimilation is in the yield of reserve on food y_{EX} (mass frame of reference), or in the assimilation efficiency κ_X (energy frame of reference). The overhead of mobilisation translates into the overheads of all of the endpoints of mobilised reserve: somatic and maturity maintenance, growth and maturation (or reproduction). The primary difference between reserve and structure is in the way turnover is paid and in how the turnover depends on food availability and body size. One might speculate that enzyme 'species' that loose their activity rapidly are subjected to the structure-regime to avoid that the fraction of inactive enzymes becomes large.

The residence time of atoms of element i in an individual without a reproduction buffer

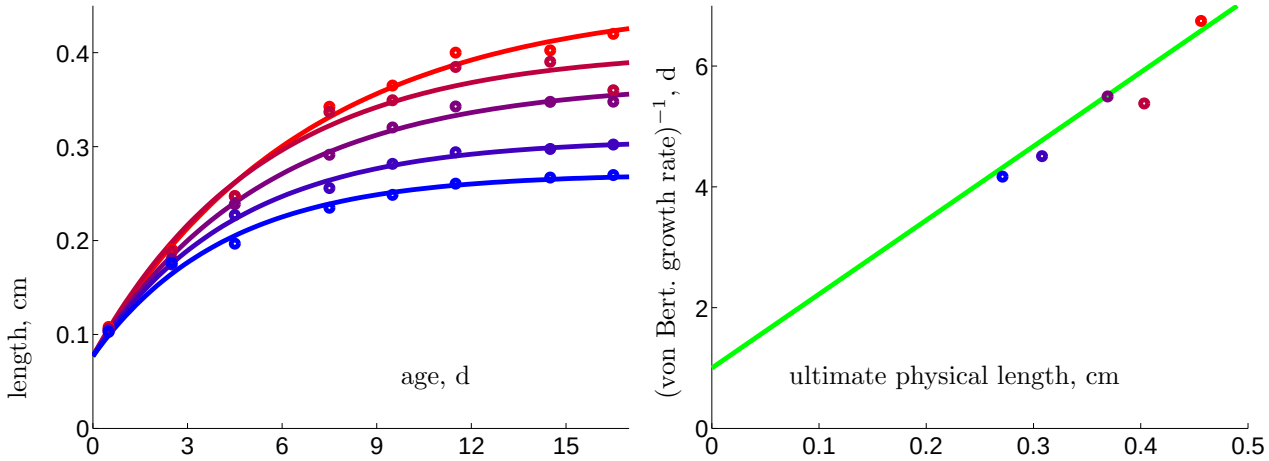

Figure 2.3: Left: Von Bertalanffy growth curves can be fitted separately to the five data sets in the lower right panel of Figure 2.10 for *Daphnia magna* for various food densities. Right: The inverse of the estimated von Bertalanffy growth rates, $\dot{r}_B^{-1}$, is plotted against estimated ultimate lengths and a linear relationship results as expected by the standard DEB model. From [769].

is given by

$$t_W^i = t_s + t_g\left(1 - \frac{n_{iE}}{n_{iX}}\frac{y_{EA}}{2}\right) + t_E\frac{n_{iE}}{n_{iX}}y_{EX} + t_V^i\frac{n_{iV}}{n_{iE}}\frac{\dot{r}}{j_{EC}} \quad \text{with } j_{EC} = m_E(\dot{v}/L - \dot{r})$$

where it is assumed that atoms that enter the reserve stay in the gut half as long as atoms that enter faeces or minerals. The residence time in structure, t_V^i, is independent of food intake and amount of structure and can depend on the compound (in structure) in which the atom is sitting.

Residence times have tight links with chemistry and in fact define metabolic organisation. The main carbohydrate storage of plants is starch, a poly-glucose see Table 3.2, while animals use glycogen, which is another poly-glucose, that can be digested by the same enzymes. The main difference between starch and glycogen is that glycogen is much more branched and enzymes unlock glucose at the tips of the branches. So glycogen can be monomerised more quickly. Animals can also convert carbohydrates into lipids, a very slow and concentrated form of energy storage, which is typically localised in specialised (adipose) tissue, see Subsubsection 3.3.2 of the comments. So animals convert food-derived starch in more rapid (glycogen) and a more slow (lipid) pools. The residence times of metabolic pools have links with differentiation, cell-to-cell communication and activity dynamics of the individual as a whole, see Section 10.5.1; plants don't need to respond instantaneously on signals from sensors, animals do.

2.4 κ is constant

If the allocation fraction to soma, κ, is constant, the inverse von Bertalanffy growth rate increases linearly with ultimate length, $\dot{r}_B^{-1} = 3\dot{k}_M^{-1} + 3L_\infty/\dot{v}$ for $\{\dot{p}_T\} = 0$, cf. (2.24); this is supported by empirical evidence, see Figure 2.3.

Suppose now that κ is not constant and decreases with size as $\kappa = 1 - L/L_\kappa$, where L_κ is a parameter, see [859]. The von Bertalanffy growth $\frac{d}{dt}L = \dot{r}_B(L_\infty - L)$ no longer

applies, meaning that $\dot{r}_B$ is no longer constant at constant food, but (2.21) still holds. Let us define the generalised von Bertalanffy growth rate as

$$\dot{r}_B \equiv L_\infty^{-1} \frac{d}{dt} L \Big|_{L=0} = \lim_{L \to 0} \frac{\dot{r} L}{3 L_\infty} \quad \text{for } \dot{r} \equiv \frac{d}{dt} \ln L^3$$

and evaluate how $\dot{r}_B^{-1}$ would depend on L_∞ for this choice of κ at constant food, so constant reserve density $[E]$. Let us take $\{\dot{p}_T\} = 0$ for simplicity's sake, and we arrive at

$$\begin{aligned}
\dot{r} &= \frac{[E]\dot{v}/L - [\dot{p}_M]/\kappa}{[E] + [E_G]/\kappa} = \frac{[E]\dot{v}/L - [\dot{p}_M]/(1 - L/L_\kappa)}{[E] + [E_G]/(1 - L/L_\kappa)} \\
L_\infty &= \left(\frac{[\dot{p}_M]}{[E]\dot{v}} + \frac{1}{L_\kappa} \right)^{-1} \quad \text{or} \quad [E] = \frac{[\dot{p}_M]/\dot{v}}{L_\infty^{-1} - L_\kappa^{-1}} \\
\dot{r}_B &= L_\infty^{-1} \frac{[E]\dot{v}/3}{[E] + [E_G]} = \frac{\dot{v}/3}{L_\infty + (1 - L_\infty/L_\kappa)\dot{v}[E_G]/[\dot{p}_M]} \\
\dot{r}_B^{-1} &= 3L_\infty/\dot{v} + 3(1 - L_\infty/L_\kappa)[E_G]/[\dot{p}_M] = 3L_\infty/\dot{v} + 3(1 - L_\infty/L_\kappa)/\dot{k}_M
\end{aligned}$$

The conclusion is that $\dot{r}_B^{-1}$ is still linear in L_∞, but the slope is $\frac{3}{\dot{v}} - \frac{3}{L_\kappa \dot{k}_M}$, which is negative for $L_\kappa < \dot{v}/\dot{k}_M$. If we substitute typical values, as given in Table 8.1, the slope is negative if $L_\kappa < 3.1\,\mathrm{cm}$. Notice that L_κ can't be very large, because that would suppress reproduction, and only positive slopes have been found empirically, so far.

Maximum length equals L_∞ for $[E] = [E_m] = \frac{\{\dot{p}_{Am}\}}{\dot{v}}$, so $L_m = \left(\frac{[\dot{p}_M]}{[E_m]\dot{v}} + \frac{1}{L_\kappa} \right)^{-1} = \left(\frac{[\dot{p}_M]}{\{\dot{p}_{Am}\}} + \frac{1}{L_\kappa} \right)^{-1}$ and $L_m^{-1} = L_\kappa^{-1} + \frac{[\dot{p}_M]}{\{\dot{p}_{Am}\}}$. The value of κ for $L = L_m$ is $\kappa_{\min} = 1 - \frac{L_m}{L_\kappa} = 1 - \left(1 + L_\kappa \frac{[\dot{p}_M]}{\{\dot{p}_{Am}\}}\right)^{-1}$ or $L_\kappa = \frac{\{\dot{p}_{Am}\}}{[\dot{p}_M]} \frac{\kappa_{\min}}{1 - \kappa_{\min}}$. Expressed in terms of $\kappa_{\min}$, rather than L_κ, maximum length equals $L_m = \kappa_{\min}\{\dot{p}_{Am}\}/[\dot{p}_M]$. The slope of $\dot{r}_B^{-1}$ against L_∞ is zero if $L_m^{-1} = \frac{\dot{k}_M}{\dot{v}} + \frac{[\dot{p}_M]}{\{\dot{p}_{Am}\}}$.

How would the body size scaling relationships work out for this choice of κ on the assumption that $\kappa_{\min}$ is an intensive parameter, so it does not depend on maximum body size, comparing species? We again have the result that $\{\dot{p}_{Am}\}$ is proportional to the zoom factor, so is L_κ. So for small bodied species we would expect that the slope of $\dot{r}_B^{-1}$ against L_∞ would become negative. Such a pattern has not been observed, however. Figure 2.4 shows that the slope does not depend on maximum body length; notice that the slope (and the intercept) is sensitive for the temperature.

An alternative choice for κ has been worked out by Dina Lika, where κ decreases hyperbolically in L: $\kappa = (1 + L/L_\kappa)^{-1}$, where L_κ is again a parameter. Following the same reasoning, we find:

$$\begin{aligned}
\dot{r} &= \frac{[E]\dot{v}/L - [\dot{p}_M]/\kappa}{[E] + [E_G]/\kappa} = \frac{[E]\dot{v}/L - [\dot{p}_M](1 + L/L_\kappa)}{[E] + [E_G](1 + L/L_\kappa)} \\
L_\infty &= \frac{L_\kappa}{2} \left(\sqrt{1 + \frac{4[E]\dot{v}}{[\dot{p}_M] L_\kappa}} - 1 \right) \quad \text{and} \quad [E] = \frac{[\dot{p}_M]}{\dot{v}} L_\infty \left(1 + \frac{L_\infty}{L_\kappa} \right) \\
\dot{r}_B &= L_\infty^{-1} \frac{[E]\dot{v}/3}{[E] + [E_G]} = \frac{\dot{v}/3}{L_\infty + \frac{[E_G]\dot{v}}{[\dot{p}_M]} \left(1 + \frac{L_\infty}{L_\kappa}\right)^{-1}} \quad \text{and} \quad \dot{r}_B^{-1} = \frac{3}{\dot{v}} L_\infty + \frac{3/\dot{k}_M}{1 + L_\infty/L_\kappa}
\end{aligned}$$

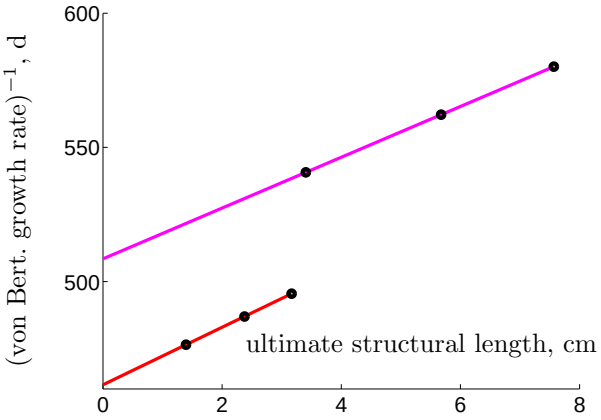

Figure 2.4: The inverse von Bertalanffy growth rate as function of ultimate length for *Rattus norvegicus*, see Figure 4.7 and *Mus musculus*, see Figure 6.2. The slope of the lines does not decrease for decreasing maximum body length across species; in this case the slope slightly increases with decreasing maximum body length.

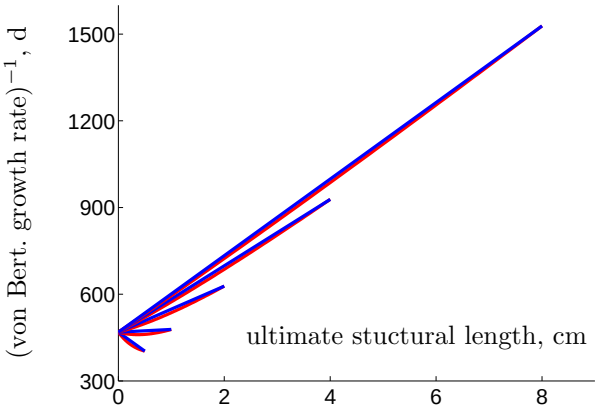

Figure 2.5: The inverse von Bertalanffy growth rate as function of ultimate length (running from zero to maximum length) if κ decreases linearly (blue) or hyperbolically (red) as function of length for several choices of maximum length. Parameters $\dot{v} = 0.02\,\mathrm{cm\,d^{-1}}$, $\dot{k}_M = 0.0064\,\mathrm{d^{-1}}$ and $\kappa_{\min} = 0.7$. Other choices of parameter values don't change the picture qualitatively.

The inverse von Bertalanffy growth rate $\dot{r}_B^{-1}$ is now a non-linear function of ultimate length L_∞; the slope of $\dot{r}_B^{-1}$ for very small values of L_∞ is $\frac{3}{\dot{v}} - \frac{3}{L_\kappa \dot{k}_M}$, which is, again, negative for $L_\kappa < \dot{v}/\dot{k}_M$.

Maximum length L_m equals L_∞ for $[E] = [E_m] = \frac{\{\dot{p}_{Am}\}}{\dot{v}}$, so $L_m = \frac{L_\kappa}{2}\left(\sqrt{1 + \frac{4\{\dot{p}_{Am}\}}{[\dot{p}_M]L_\kappa}} - 1\right)$. The minimum value of κ for is $\kappa_{\min} = (1 + L_m/L_\kappa)^{-1} = 2\left(1 + \sqrt{1 + \frac{4\{\dot{p}_{Am}\}}{[\dot{p}_M]L_\kappa}}\right)^{-1}$ or $L_\kappa = \frac{\{\dot{p}_{Am}\}}{[\dot{p}_M]}\frac{\kappa_{\min}^2}{1-\kappa_{\min}}$. Expressed in terms of $\kappa_{\min}$, rather than L_κ, maximum length again equals $L_m = \kappa_{\min}\frac{\{\dot{p}_{Am}\}}{[\dot{p}_M]}$. On the assumption that $\kappa_{\min}$ is an intensive parameter, we again have that $L_\kappa \propto L_m$, so for small-bodied species we should expect the relationship between $\dot{r}_B^{-1}$ and L_∞ that is very different from a linearly increasing one as have been found empirically. As illustrated in Figure 2.5, a hyperbolic decrease of κ as function of L works out similarly to a linear decrease; this contributes to the robustness of the argument.

This analysis supports the conclusion that a constant κ captures the general pattern best; a constant κ also offers the best basis for generalisations of the κ-rule, cf Sections 5.3.1 and 5.3.2, which link up with the well-known (near-)allometric growth of body parts. Some workers proposed that κ decreases with size to capture the idea that reproduction competes with growth in the context of ideas on evolutionary optimisation; cf Section 8.1.3 of these comments. Apart from the consequences of a decreasing κ on the relationship between $\dot{r}_B^{-1}$ and L_∞, we have the counter intuitive problem that in such a case little is allocated to maturation initially, while the need for it is high. We need maturation as energy sink to understand that no allocation to reproduction occurs during the juvenile stage, while the onset of reproduction hardly seem to affect growth. We can't include maturity maintenance

into somatic maintenance at the expense of allocation to growth because in such a case we should expect to see some reproduction at low food levels, while the general empirical pattern is that no reproduction occurs at very low food densities; emergency reproduction, including suicide reproduction, in response to reducing food availability is a variation sported by a few taxa only. Notice that if κ would decrease with length, reproduction more rapidly decreases with decreasing food.

The concept of von Bertalanffy growth goes back to August Pütter [1139], who proposed in 1920 that the von Bertalanffy growth rate is inversely proportional to ultimate length: $\dot{r}_B^{-1} = 3L_\infty/\dot{v}_B$ (my notation), so $\frac{d}{dt}L = \frac{\dot{v}_B}{3}\left(1 - \frac{L}{L_\infty}\right)$ and $\dot{v}_B = \frac{\dot{r}L}{1-L/L_\infty}$. I tried hard to understand his argument and came to the following reconstruction. Like DEB theory, Pütter (and later von Bertalanffy) did not link growth directly to feeding but to the intensity of metabolism (i.e. the generation of anabolic substrates), that he took proportional to a surface area and decay (of structure) to a volume. Pütter then compared growth with the filling of a leaking cistern of height L_∞ with water. When the water level L increases, the change in length decreases and the conductance $\dot{v}_B$ being a kind of universal constant linking all species, small and large bodied. He motivated this analogy between growth and water filling with the reasoning that some compound accumulates in structure with a concentration proportional to L that inhibits growth using $\dot{v}_B = \dot{r}L$ for $L \ll L_\infty$. I can't quite follow the reasoning, but I assume that the compound appears at a rate proportional to the decay (volume) and disappears a rate proportional to the supply of anabolic substrate (surface area); these rates have to be high relative to the dilution by growth. Growth ceases if the concentration of this compound exceeds a threshold value. Pütter thus thought that the growth rate decreases proportionally to the concentration of this compound. It is striking that the more elaborate reasoning of DEB works out that similarly, quantitatively, and that the link between energetics and concentrations of compounds has been made that long ago. Roff [1205] saw the negative correlation between the von Bertalanffy growth rate and ultimate length as proof that the model was invalid on statical grounds. He probably had no idea about the arguments of Pütter and just took the model as a curve.

Von Bertalanffy modified the idea of Pütter, did not consider length, but mass, and removed the link with surface area. He modelled growth as a difference between two allometric functions of weight, $\frac{d}{dt}W = aW^\alpha - bW^\beta$; allometric functions meanwhile had become very popular in this field. Since this model has 5 parameters, including initial weight, he took $\beta = 1$ for simplicity's sake. The nice logic of Pütter became lost and von Bertalanffy degraded the model to a purely descriptive one. So, while Bertalanffy wanted to step away from surfaces, so from the growth rate $\dot{v}_B$, which is inherent to this idea, cruel history attached his name to Pütter's growth rate, and Pütter became almost forgotten. Clark [260] recently made things even worse, by mixing up the role of Pütter and von Bertalanffy and presents Pütter as the inventor of von Bertalanffy's model, and von Bertalannfy as the inventor of the role of surface area's. The cacophony is complete now; I imagine that both men turn in their graves, if they knew (and could).

The effects that parasites can have on hosts of inducing gigantism in combination with reducing reproduction, and that this can be captured by increasing κ in the standard DEB model is also reported by [540].

The κ-rule has many consequences, such as the waste-to-hurry phenomenon (see section

8.2.1 of the comments), where species increase somatic maintenance to boost growth and reproduction while staying small, and the existence of supply stress as quantifier for the position of species in the supply-demand spectrum (see section 10.5.5 of the comments). Supply stress is defined as the maturity maintenance times the squared somatic one over cubed assimilation. The topology of the allocation scheme is key to this statistic (see section 11.3 of the comments) and plays a dominant role in the range of possible values κ can take (see section 4.10.0 of the comments).

2.5 Dissipation

2.5.1 Somatic maintenance linked to volume

Based on physical models, Stokes [1376] estimates the energy costs for locomotion for a neonate Florida lancelet, *Branchiostoma floridae* to be around 10^{-9} W at 30 °C. The Arrhenius temperature for this species was estimated at $T_A = 9369$ K, so rates differ by a factor 2.87 for a reference temperature of 20 °C. The structural length at birth was estimated at $L_b = 0.011$ cm (see add_my_pet) and the volume-specific somatic maintenance costs at 20 °C at $[\dot{p}_M] = 67.52\,\mathrm{J\,d^{-1}cm^{-3}}$. The total somatic maintenance costs of a neonate is thus $\dot{p}_M = [\dot{p}_M]L_b^3 = 2.97\,10^{-9}$ W If all of this would be correct, the cost of swimming would represent some 30% of the somatic maintenance costs, which seems a bit high.

Around metamorphosis Stokes [1376] arrives at an estimate of 10^{-8} till 10^{-6} W for swimming. Structural length at metamorphosis was estimated at $L_j = 0.092$ cm, so $\dot{p}_M = [\dot{p}_M]L_j^3 = 1.8\,10^{-6}$ W. DEB theory assumes that investment in locomotion is a fixed fraction of the somatic maintenance costs (as a first crude approximation). These numbers are thus more or less consistent.

A comment on the legends of Figure 2.8: The leaves of some sclerophyllic trees last longer than a year; averaging three years in *Quercus ilex* (holm oak) and *Olea europaea* (olive), and five to six years in *Quercus coccifera* (kermes oak) [149]. The champion is probably the Rocky Mountain bristlecone pine *Pinus aristata* with leaves lasting some 30 years; its grows at an altitude of around 3 km, where it is very cold and the growing season lasts some 6 weeks per year. The life span of the trees is about 1500 year.

2.5.1 Somatic maintenance linked to surface area

The importance of osmotic work in growth is still an open question; experimental studies found no effect of ionic strength of water on growth of fish [207].

Like the costs for the heat increment of feeding (or specific dynamic action, SDA), the costs for food handling is included in the overhead costs for assimilation; it determines the value of digestion efficiency $\kappa_X = \frac{\mu_E}{\mu_X} y_{EX}$. What about the costs for food searching, which is maximal in absence of food? Think e.g. of the filtering costs, discussed in Section 2.5.1. As part of the energy costs for movement it is, in the standard DEB model, included as a (rather small) fixed fraction of volume linked maintenance costs. That the fraction is small is further empirically supported by [1034] for fish fry. So food searching is at the expense

of other types of movement. There are other options, however, that should be considered if more detail is required (necessarily leading to more parameters). One is based on the observation made in Section 5.3.2 on the dynamic generalisation of the κ-rule, that food searching (filtering) is proportional to $(1-f)$, while feeding is proportional to f. Suppose now that the costs for food searching for food is proportional to surface area and that the costs for SDA is paid from mobilised reserve, see Section 4.4.2 of the comments. If the maximum costs for food searching is not too different from the maximum costs of SDA, $\kappa_F \dot{p}_{Am}$, the sum of these two costs would become independent of f, and become a fixed part of the surface area linked somatic maintenance costs. These considerations help to understand why the parameter-sparse standard DEB model is robust for contributions of minor fluxes. The remarkable coincidence is that both fluxes relate to feeding, and don't apply to embryos, just like the other surface linked maintenance costs.

2.5.2 Maturation at constant food

If food density is constant, scaled length reduces for scaled time since birth τ and scaled von Bertalanffy growth rate ρ_B to $l(\tau) = l_\infty - l_d \exp(-\rho_B \tau)$ for $l_\infty = 1 - l_T$ and $l_d = l_\infty - l_b$. Scaled maturity changes as $\frac{d}{d\tau} v_H = b_2 l^2 + b_3 l^3 - k v_H$, with $b_3 = f/(f+g)$ and $b_2 = f - b_3 l_\infty$. This is an inhomogeneous first order differential equation that can be integrated analytically, resulting in

$$v_H(\tau) = -a_0 - a_1 \exp(-\rho_B \tau) - a_2 \exp(-2\rho_B \tau) - a_3 \exp(-3\rho_B \tau) + a_k \exp(-k\tau)$$

with $a_0 = -(b_2 + b_3 l_\infty) l_\infty^2 / k$, $a_1 = -l_\infty l_d (2b_2 + 3b_3 l_\infty)/(\rho_B - k)$, $a_2 = l_d^2 (b_2 + 3b_3 l_\infty)/(2\rho_B - k)$, $a_3 = -b_3 l_d^3/(3\rho_B - k)$ and $a_k = v_H^b + a_0 + a_1 + a_2 + a_3$.

Maturation ceases as soon as it hits v_H^p, so the complete solution is $\min(v_H(\tau), v_H^p)$. Since $v_H(\infty) = \frac{f}{k} l_\infty^2$, puberty cannot be reached if $k v_H^p > f l_\infty^2$.

The scaled time since birth at puberty τ_{bp} and the scaled length at puberty l_p have to be found from $l(\tau_{bp}) = l_p$ and $v_H(\tau_{bp}) = v_H^p$.

2.5.2 Maturation and heterochrony

Maturity is defined as a maintenance requiring quantity that is used to trigger metabolic switches. It has no mass or energy. Maturation is the increase in maturity and is assumed to be proportional to the investment of reserve into maturation. Maturity is quantified as energy or mass of reserve. Adults don't invest in maturation. Maturity maintenance is proportional to maturity. If not fully paid, rejuvenation occurs, i.e. maturity decreases.

The first argument that is mentioned for maturation is that volume at first appearance of eggs hardly depends on food density. As Figure 2.4 shows, this should not be taken too literally. If stage transitions occur at fixed levels of maturity, volume at stage transitions can depend on food density in the context of DEB theory if $\dot{k}_J < \dot{k}_M$. The variation at puberty being larger than that at birth.

Heterochrony is an evolutionary change in the timing of expression of a phenotype trait [1520, p 241], such as the onset of reproduction and can represent an acceleration or retardation [509] or a deletion. In the DEB context heterochrony translates into a

change in the maturity threshold for that trait (typically inter-species). Horticulturists can manipulate the maturity threshold at puberty in many plant species, but this also occurs naturally. Understory representatives of the dipterocarps *Hopea*, *Stemonoporus* and *Vatica* flower in an early life stage, compared to their canopy relatives [45]. The life cycles of some *Clusia* (a Rosid belonging to the Malpighiales) resemble those of animal species with sport direct development, such as some sea urchins and salamanders [1520, p 251]. Sea urchins typically have a plankton-feeding pluteus larve, which is so similar to that of hemichordates that is mode was likely ancestral in both groups [1520]. If true, deletion of the pluteus stage has occurred independently in 6 of the 10 echinoid orders at least 27 times [1144]. Heterochrony explains the origin of numerous examples of inducible defenses in plants and invertebrates [1520]; spines in some juvenile pants are lost in later-developing tissues, but sometimes they reappear again at regeneration from damage. See [1520] for many more examples.

Work with Casey Mueller and Starrlight Augustine showed that maturation is accelerated at hatch before birth in the frogs *Crinia nimbus* and *C. georgiana* by lowering κ, which increases respiration and maturation [1002]; at metamorphosis, κ is reset to its value before hatching. The result is that metamorphosis is reached much earlier, compared to the equally sized frogs *Pseudophryne bibronii* and *Geocrinia vitellina*, which do not sport such an acceleration. The acceleration of maturation is very functional; *C. georgiana* lays eggs in temporal pools that typically disappear soon after the froglets left it. These observations strongly support the way DEB theory deals with maturation. See further Section Subsubsection 7.8.2.1 of the comments.

Tadpoles of the common frog *Rana temporaria* and the green frog *Pelophylax ridibundus* can over-winter in Europe, with the result that they grow to much larger sizes and metamorphose in early spring. So temperature and/or light affect the process, but the observation further supports the view that growth and maturation are parallel processes.

2.5.3 Maturity maintenance

The situation of absence of maturity maintenance, $\dot{k}_J = 0$, is a special case that has the implication that birth and puberty always occur (if survival allows), even in extremely poor nutritional situations. This does not seem to be realistic. Moreover the model then becomes ill-posed in the situation of constant $f = l_p$: allocation to reproduction $\dot{p}_J$ eventually becomes either 0 or $(1-\kappa)l_p^3\dot{p}_{Am}$. The point is a bit academic, since we have to wait for this moment infinitely long, i.e. much longer than aging allows.

The condition that $\dot{k}_J = \dot{k}_M$, labeled C1, is equivalent to the condition that the volume-specific maturity maintenance costs $[\dot{p}_J] = [\dot{p}_M]\frac{1-\kappa}{\kappa}$, labeled C2, during the embryo and juvenile stages in absence of surface-specific somatic maintenance, so $\{\dot{p}_T\} = 0$, and have as implication that maturity density remains constant at value $[E_H] = [E_G]\frac{1-\kappa}{\kappa}$, labeled I1. Stage transitions then not only occur when maturity reaches threshold values, but also when structural volume reaches threshold values. Notice that during the adult stage E_H remains constant at level E_H^p, but structural volume can grow (or shrink during prolonged starvation), so $[E_H]$ cannot remain constant during the adult stage. Structural length at

birth, for instance, then equals $L_b = \left(\frac{\kappa}{1-\kappa}\frac{E_H^b}{[E_G]}\right)^{1/3}$ and it is no longer necessary to get it from Eq (2.37) of DEB3. These are implications of the κ-rule, combined with the priority-rule for somatic maintenance for allocation to growth and for maturity maintenance for allocation to maturation.

To see the equivalence of the conditions C1 and C2, we need to realize that maturity maintenance $\dot{p}_J$ amounts, according to Eq (2.19) of DEB3, to $\dot{p}_J = \dot{k}_J E_H$ and that the somatic maintenance rate coefficient $\dot{k}_M$ is defined as $\dot{k}_M = \frac{[\dot{p}_M]}{[E_G]}$, see {45}, 9 lines from below. If we substitute this in C2, we get $\dot{k}_J[E_H] = \dot{k}_M[E_G]\frac{1-\kappa}{\kappa}$. If we now substitute I1, then condition C1 directly follows, or, alternatively, if we substitute C1, then implication I1 directly follows.

So it suffices to show that C2 implies I1. This can be seen from how E_H and V change: $\frac{d}{dt}E_H = (1-\kappa)\dot{p}_C - \dot{p}_J$ and $\frac{d}{dt}V = (\kappa\dot{p}_C - [\dot{p}_M]V)/[E_G]$. The chain rule for differentiation learns that maturity density does not change if $\frac{d}{dt}E_H = [E_H]\frac{d}{dt}V$. Substitutions of the changes leads to the condition $(1-\kappa)[\dot{p}_C] - [\dot{p}_J] = (\kappa[\dot{p}_C] - [\dot{p}_M])\frac{[E_H]}{[E_G]}$. This must hold for all possible trajectories of $\dot{p}_C$, from which follows condition C2.

Although condition C1, or C2, leads to a nice simplicity, there is no biological reason why it should apply and, moreover, it cannot apply as soon as κ or $[E_G]$ or $[\dot{p}_M]$ start to change, due to e.g. effects of a toxic compound, unless maturity maintenance follows such changes exactly. Generally $\dot{k}_J \ll \dot{k}_M$, which has the consequence that structural length at birth and puberty become food-dependent and decrease for decreasing food availability, which can be seen as a stylized empirical fact.

2.5.4 Reproduction overhead

The energy allocation to reproduction, $\dot{p}_R$, is given by (2.55); females translate this in a reproduction rate $\dot{R} = \kappa_R\dot{p}_R/E_0$, see (2.56), where E_0 represents the cost of an egg and $1-\kappa_R$ the overhead costs for reproduction, which is typically low. Some taxa, such as pond snails, are hermaphroditic in a way that they synthesize sperm and oocytes simultaneously. If the ratio of the allocation to sperm and oocytes would be constant, hermaphrodites produce eggs at rate $\dot{R} = \kappa_R^\circ\dot{p}_R/E_0$, where $\kappa_R^\circ < \kappa_R$.

The reproduction efficiency κ_R only quantifies the efficiency of the conversion from the reproduction buffer to embryo reserve. These metabolic pools have, theoretically, the same chemical composition (ignoring that yolk consists of lipo-proteins, but the conversion is efficient) and covers the wrapping. This should not be confused with the overall reproduction efficiency, where the energy investment per offspring, E_0/κ_R, is converted in a neonate with energy $L_b^3[M_V]\mu_V$ locked in structure and $L_b^3 f[E_m]$ in reserve. So the overall reproduction efficiency amounts to $\kappa_R L_b^3([M_V]\mu_V + f[E_m])/E_0$. The extra losses now include maturity and somatic maintenance, maturation and growth overheads of the embryo.

Placentalia produce neonates and placentas. The energy costs of the placenta might be proportional to that of the neonate, with the consequence that the reproduction rate can again be written as $\dot{R} = \kappa_R\dot{p}_R/E_0$, where overhead $1-\kappa_R$ now includes the costs of the placenta and will be large relative to that of egg layers. This more or less compensates the

fact that the cost for a foetus is somewhat less than that of a comparable egg, see Section 2.6.2. Quite a few species eat their placenta and recover some of these losses.

Some toxic compounds affect reproduction, but not feeding, growth, respiration or anything else, see Section 6.5.4. Such perturbations on the energy budget strongly support the existence of parameter κ_R.

2.6 Growth: increase of structure

Rotifers, nematodes and dicyemida are examples of small animals that have a fixed number of cells in adults and sport eutely: their cells divide till puberty, all further growth is only by cell growth; gastrotrichs complete all cell divisions even at birth. Cells of some types of tissue or organs of animals that don't sport eutely loose their ability to divide and further growth only results from cell growth. The relationship between cell growth and body growth is a complex one in multicellulars.

While the specific change in volume and weight $\dot{r}$ at constant food density is decreasing with age after birth in the standard DEB model, the growth rate $\dot{r}W$ or $\dot{r}L^3$ has a maximum for $\frac{d}{dt}\dot{r} + \dot{r}^2 = 0$ (this follows from $\frac{d}{dt}\dot{r}L^3 = 0$ with $\frac{d}{dt}L = L\dot{r}/3$), which occurs at $L = \frac{2}{3}L_\infty$, with $L_\infty = fL_m - L_T$ and $a - a_b = \dot{r}_B^{-1} \ln \frac{L_\infty - L_b}{L_\infty/3}$. Change in length is given by $\frac{d}{dt}L = \dot{r}_B(L_\infty - L) = L\dot{r}/3$. So, the relationship $\dot{r} = 3\dot{r}_B(L_\infty/L - 1)$ follows, and the maximum specific growth for $L = L_\infty 2/3$ is $\dot{r}_m = \dot{r}_B 3/2$. This gives a simple biological interpretation for the von Bertalanffy growth rate [793].

The chicken-meat industry harvests at the age of maximum integrative production, so if $\frac{W(a)-W_b}{a-a_b}$ has a maximum. At constant food density this maximum coincides with the maximum of $\frac{L^3(a)-L_b^3}{a-a_b}$, which occurs when $(a-a_b)\dot{r} = 1-(L_b/L)^3$, i.e. if $\frac{\dot{r}}{\dot{r}_B} \ln \frac{L_\infty - L_b}{L_\infty - L} = 1 - \frac{L_b^3}{L^3}$ with $\dot{r}_B = \frac{\dot{v}}{f+g} 3L_m$ and $\dot{r} = \frac{\dot{v}}{f+g}\left(\frac{f}{L} - \frac{1+L_T/L}{L_m}\right)$. The length at which that maximum is reached, and so the age, must be obtained numerically.

For accelerating species that follow the abj model, the specific growth rate directly after birth remains constant till the end of acceleration at $\dot{r}_j = \dot{k}_M \frac{(fL_m - L_T)/L_b - 1}{1+f/g} = 3\dot{r}_B((fL_m - L_T)/L_b - 1)$, see the comment for section 7.8.2. This rate is larger than the maximum growth rate if $\dot{r}_j > \dot{r}_m$, i.e. if $2L_\infty > 3L_b$. Since metabolic acceleration typically occurs in species with small eggs, this always the case in practice. So accelerating species have a constant high specific growth rate till the end of acceleration, after which the specific growth rate decreases. This decrease is smooth, not abrupt, since asymptotic structural length after the end of acceleration is $L_\infty = s_\mathcal{M} fL_m - L_T$ and acceleration factor $s_\mathcal{M} = L_j/L_b$, where length at end of acceleration L_j is controlled by the maturity level at the end of acceleration E_H^j. The smoothness of the decay in growth also follows from the structure of the DEB model, where growth is fueled from mobilized reserve, and the reserve density as well as the energy conductance, which controls reserve mobilization, make no jumps.

2.6.2 Constraints on maturation thresholds

For $\dot{k}_M = \dot{k}_J$ (so $k = 1$), (2.32) gives $L_b^3 = \frac{E_H^b/[E_m]}{(1-\kappa)g}$. $U_H = \frac{E_H}{\{\dot{p}_{Am}\}}$, with $\dim(U_H) = t\,L^2$, replaces E_H to avoid using energy as dimension. Since $L_b < L_m = \frac{\dot{v}}{g\dot{k}_M}$, we have for $[E_m] = \frac{\{\dot{p}_{Am}\}}{\dot{v}}$ the constraint $\frac{U_H^b \dot{v}}{(1-\kappa)g} < L_m^3$ or $U_H^b < \frac{(1-\kappa)gL_m^3}{\dot{v}} = \frac{(1-\kappa)\dot{v}^2}{\dot{k}_M^3 g^2}$.

$u_H = \frac{U_H \dot{v}}{gL_m^3}$, with $\dim(u_H) = 0$, replaces U_H to avoid using time and length as dimension as well. The constraint translates into $u_H^b < 1-\kappa$, and for $v_H = \frac{u_H}{1-\kappa}$ into $v_H^b < 1$. Since $L_b < L_p < L_m$, we also have $U_H^p < \frac{(1-\kappa)gL_m^3}{\dot{v}}$, $u_H^p < 1-\kappa$ and $v_H^p < 1$, while we have $E_H^b < E_H^p$ or $U_H^b < U_H^p$ or $u_H^b < u_H^p$ or $v_H^b < v_H^p$.

For $\dot{k}_J < \dot{k}_M = \frac{[\dot{p}_M]}{[E_G]}$, which seems most realistic, we know from the comment-section 2.6.2 that $L_b^3 < \frac{E_H^b/[E_m]}{(1-\kappa)g}$. Let us consider the extreme scenario of zero maintenance ratio, $k = 0$. Eq (2.28) can be rewritten as $\frac{d}{d\tau} v_H = -\frac{d}{d\tau} u_E - k v_H$. For $k = 0$, this leads to the solution $u_E(v_H) = u_E^0 - v_H$, so at birth we then have $u_E^b = e_b l_b^3/g = u_E^0 - v_H^b$. Using (2.42), this directly leads to l_b as a root of a 6th degree polynomial in l_b. Only one of the 6 roots is valid, i.e. the smallest real positive root between 0 and 1. For any value of the maintenance ratio k between 0 and 1, scaled length at birth l_b must be between this root and $\left(\frac{E_H^b/[E_m]}{(1-\kappa)g}\right)^{1/3}$. Since $l_b < 1$, $v_H^b < \left(\frac{3g}{3gx_b^{1/3} - B_{x_b}(\frac{4}{3},0)}\right)^3 - \frac{e_b}{g}$ (but see below). For the foetal value for u_E^0, as given in (2.51), $k = 0$ leads to $v_H^b = l_b^3 + \frac{3}{4}\frac{l_b^4}{g}$. Since $l_b < 1$, $v_H^b < 1 + \frac{3}{4g}$.

For foetal development we have $l(\tau) = g\tau/3$ and (2.48) reduces for $k = 0$ to $\frac{d}{dt} v_H = l^2(g + l)$ or $v_H(\tau) = l^3(1 + \tau/4)$. Scaled age at birth obeys $v_H^b = l_b^3(1 + \tau_b/4)$, so it is the root of a 4th degree polynomial in τ_b. Since $l_b < 1$ and $\tau_b = 3l_b/g$ we have $v_H^b < 1 + \frac{3}{4g}$ for $k = 0$, while from (2.50) we have $v_H^b < 1$ for $k = 1$.

2.6.2 Numerical solution for scaled length at birth

The start of the life cycle as egg is in DEB theory implicitly defined by the rule that reserve density at birth equals that of the mother at egg formation and structure and maturity start at zero; birth being defined as the moment assimilation is switched on (when food would be present). The initial amount of reserve of an egg can, in principle, be evaluated with a shooting method, where an arbitrary amount is chosen first (with zero structure and maturity), egg development is followed (in terms of reserve, structure and maturity) till maturity exceeds its threshold value for birth, reserve density is evaluated, and the initial amount of reserve is corrected. This process is then repeated till sufficient accuracy is reached. Although straightforward, this method is computationally intensive, which is a problem if we want to do this for all individuals in a population; we need to do this for each time increment, because food varies, so does the reserve of the mother at egg laying. To reduce computational effort, the number of variables (reserve, structure, maturity) is first reduced to one, and then a weird transformation of variables is found to make the resulting differential equation for this single variable linear. Although all this does reduce the computational effort substantially, it is hardly exciting reading, especially for people with a biological interest. The best reading strategy, therefore, is to skip most of the

technical material in this section and in the knowledge that efficient DEBtool routines exist that do all the required computational work.

The shooting method in one variable turns out to be rather stable, where $y(x_b) = y_b$ is evaluated by integrating $\frac{d}{dx}y$ using $l_b = \left(v_H^b\right)^{1/3}$ as starting value. It is exact for $k = 1$ and has been the motivation for the choice of the symbol v_H^b, which appears to have the interpretation as a scaled volume.

Alternatively the Newton Raphson procedure $l_b^{i+1} = l_b^i - t(l_b^i)/t'(l_b^i)$ can be used to solve (2.46) with

$$\begin{aligned}
l(x) &= \left(\frac{1}{l_b}\left(\frac{x_b}{x}\right)^{1/3} - \frac{B_x(\frac{4}{3},0) - B_{x_b}(\frac{4}{3},0)}{3gx^{1/3}}\right)^{-1}; \quad l'(x) = \frac{l^2(x)}{l_b^2}\left(\frac{x_b}{x}\right)^{1/3} \\
v(x) &= \exp\left(-\int_0^x \frac{k-x_1}{1-x_1}\frac{l(x_1)}{g}\frac{dx_1}{x_1}\right); \quad v'(x) = v(x)\exp\left(-\int_0^x \frac{k-x_1}{1-x_1}\frac{l'(x_1)}{g}\frac{dx_1}{x_1}\right) \\
r(x) &= g + l(x); \quad r'(x) = l'(x) \\
t(l_b) &= \frac{x_b g u_H^b}{(1-\kappa)v(x_b)l_b^3} - \int_0^{x_b}\frac{r(x)}{v(x)}dx \\
t'(l_b) &= -\frac{x_b g u_H^b}{(1-\kappa)v(x_b)l_b^3}\left(\frac{3}{l_b} + \frac{v'(x_b)}{v(x_b)}\right) - \int_0^{x_b}\left(\frac{r'(x)}{r(x)} - \frac{v'(x)}{v(x)}\right)\frac{r(x)}{v(x)}dx
\end{aligned}$$

The problem here is in the accurate evaluation of the integrals. Euler integration requires many steps if $k > 1$, but is nonetheless much faster.

DEBtool has three routines to obtain l_b: get_lb (Euler integration), get_lb1 (advanced integration) and get_lb2 (shooting in one variable).

2.6.2 Yolk dynamics

Chordate embryos develop on the periphery of a blob of yolk, which reduces the problem of dioxygen supply and allow large developmental rates, compared to other animals. They internalize yolk fully at birth, while they still have that reserve density equals that of the mother at egg formation (the maternal effect). The way to include this dynamics, without adding parameters, is to assume that yolk Y has the same composition as reserve E, and reserve is formed in constant ratio with structure, so $[E]$ and M_E/M_V remain constant during embryo development, $E_Y(0) = E_0$, $E_Y(a_b) = 0$. Reserve is transported yolk, not requiring chemical transformation. This is, in fact, not fully true, since yolk consists of lipoproteins, while reserve mostly consists of lipids, proteins and carbohydrates. We assume, however, that this conversion does not require energy and does not produce (mineral or other) products. The dry weight of embryo, excluding the yolk, amounts to $W_{emb}(t) = w_V M_V + w_E M_E = (w_V + w_E e_b m_{Em})M_V = (w_V + w_E e_b m_{Em})\frac{d_V}{w_V}V(t)$. The trajectory of yolk dry weight then becomes $W_Y(t) = E(t)w_E/\mu_E - e_b m_{Em}\frac{w_E}{w_V}d_V V(t)$, where $E(t)$ is the energy in yolk plus reserve. This can be checked by converting to moles: $\frac{W_Y(t)}{w_E} = M_Y(t) = \frac{E(t)}{\mu_E} - \frac{e_b m_{Em}}{w_V}d_V V(t) = M_E(t) + M_Y(t) - e_b m_{Em} M_V(t) = M_E(t) + M_Y(t) - M_E(t) = M_Y(t)$. The dynamics of $E(t)$ and $V(t)$ for embryos is given in Eqns (2.26-28) in scaled form. This has been applied e.g. in [1002].

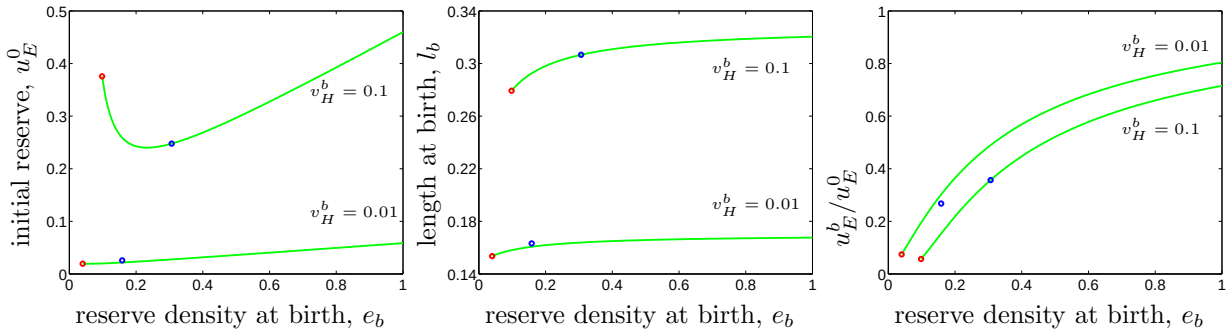

Figure 2.6: Scaled reserve u_E^0 (left), scaled length at birth l_b (middle) and fraction of reserve left at birth u_E^b/u_E^0 (right) as function of scaled reserve density at birth e_b. The red dot indicates where maturation ceases at birth, the blue one where growth ceases at birth. Parameter values: $g = 0.1$, $k = 0.1$, $v_H^b = 0.01$ and 0.1 (curves starting at highest e_b).

2.6.2 Maturation ceasing at birth

The maternal effect in the standard DEB model states that the reserve density at birth equals that of the mother at egg formation. This rule not only captures the dominant empirical pattern, but also avoids a parameter for the initial amount of reserve and it has the property that growth at constant food is of the von Bertalanffy type at all food densities directly since birth. In starving mothers, this might be a low value, but lower boundaries exist for viable eggs.

The initial amount of reserve can be low enough to cause shrinking during the embryo stage; this occurs if $e_b < l_b$, see routine get_eb_min of DEBtool. It then depends on the rule for death by shrinking if the embryo survives that shrinking, see 4.1.5 of the comments. If the initial amount of reserve is lower than the level that causes the ceasing of maturation at birth, shrinking to zero results if death by shrinking does not arrest the process. From (2.29) follows that maturation ceases at birth if

$$(1-\kappa)e_b(g+l_b) = e_H^b(k(e_b/g+1)l_b + e_b - l_b)$$

If $k = 1$, we have $e_H^b = (1-\kappa)g$ and the equation collapses to $e_b = l_b = \left(\frac{u_H^b}{1-\kappa}\right)^{1/3} = (v_H^b)^{1/3}$; this is also the condition for which growth ceases at birth. For other values of k, the equation has to be solved numerically; see routine get_eb_min of DEBtool.

Figure 2.6 shows that for $k < 1$ length at birth increases with reserve density at birth, so does the cost of an egg, expressed as initial amount of reserve. For $k < 1$, the value of e_b for which maturation ceases is smaller than that for which growth ceases, and the embryo shrinks prior to birth between these two values. For $k > 1$ the opposite holds, and shrinking cannot occur prior to birth since below the value of e_b for which maturation ceases at birth, the embryo will not reach the state at birth; for $k = 1$ maturity and growth cease at birth at the same value for e_b. For decreasing reserve density at birth, the costs

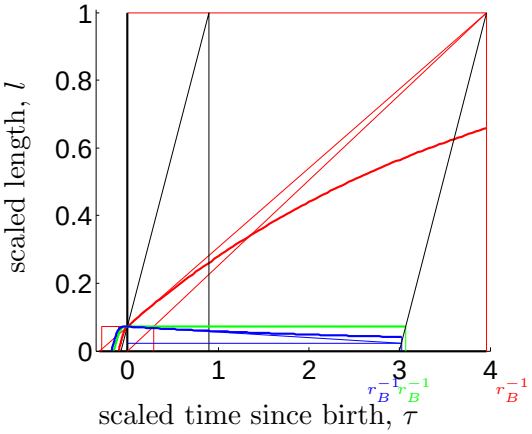

Figure 2.7: Scaled length $l = \frac{L\dot{v}}{g\dot{k}_M}$ as function of scaled time $\tau = (a - a_b)\dot{k}_M$ of the standard DEB model for $f = 1$ (red), f such that growth ceases at birth (green) or maturation ceases at birth (blue). Parameters: $g = 3.1111$, $k = 0.3111$, $v_H^b = 0.0004$ and $l_T = 0$, like in the generalised animal for $z = 1$. For $f = 1$ we have the scaled von Bertalanffy time $r_B^{-1}(1) = 3 + 3/g$. The black line from $(3, 0)$ to $(r_B^{-1}(1), 1)$ connects the asymptotes of the growth curves at their von Bertalanffy times. All embryo growth curves depart parallel to this line (so for all nutritional levels), $\frac{d}{d\tau}l(0) = g/3$.

for an egg can go up again, i.e.

$$\frac{d}{de_b}u_E^0 = 0 \quad \text{if} \quad \frac{d}{de_b}l_b = \frac{l_b}{3}\frac{l_b/e_b - 1}{e_b + g} = \frac{d}{de}l\Big|_{e=e_b}$$

which can only occur in the case of shrinking prior to birth ($e_b < l_b$). The figure also illustrates that the smaller v_H^b, the smaller e_b can be and the higher the fraction of reserve is left at birth.

Figure 2.7 illustrates how the energy investment ratio appears in growth curves at various nutritional levels. The extremes are shown in red ($f = 1$) and blue. For maintenance ratio $k = 1$, the curve where growth ceases at birth (green) coincides with that where maturation ceases at birth (blue). The growth rate at birth equals $\frac{d}{d\tau}l(a_b) = (f - l_b)r_B = \frac{f-l_b}{3+3f/g} \simeq (3+3/g)^{-1}$ for $f = 1$. So the curvature of the growth curve during the embryonic stage decreases with g and large-bodied species will hardly show such a curvature.

For given energy investment ratio g and maintenance ratio k, scaled length at birth l_b increases with scaled maturity at birth v_H^b. The maximum value for l_b equals 1 for $e_b = 1$, so a maximum value for v_H^b exists. To find this value, we rewrite (2.28) as

$$\frac{d}{d\tau}v_H = u_E l^2 \frac{g + l}{u_E + l^3} - kv_H \tag{2.4}$$

and remove scaled time be considering

$$\frac{d}{du_E}l = \frac{-1}{3u_E l^2}\frac{gu_E - l^4}{g + l}; \qquad \frac{d}{du_E}v_H = \frac{kv_H}{u_E l^2}\frac{u_E + l^3}{g + l} - 1 \tag{2.5}$$

For $e_b = 1$ and $l_b = 1$, we have $x_b = \frac{g}{1+g}$ and $\alpha_b = 3gx_b^{1/3}$. Moreover $u_E^0 = \left(\frac{3g}{\alpha_b - B_{x_b}(4/3,0)}\right)^3$ and $u_E^b = \frac{1}{g}$ This set of 2 ODE's should now be integrated for u_E is u_E^0 till u_E^b, where $l(u_E^0) = \epsilon$ and $v_H(u_E^0) = \epsilon^3$ for very small ϵ, e.g. some 10^{-4}. We should test that $l(u_E^b) = l_b = 1$.

2.6.2 Foetal development

From an energy allocation point of view, an important difference between egg and foetal development is that allocation to reproduction is typically continuous in case of egg de-

Figure 2.8: This picture of a dolphin foetus clearly shows the substantial placenta, which is formed by mother and foetus. The shape of the placenta directly suggests that reserve transfer from mother to foetus is proportional to the surface area of the foetus if the diameter of the placenta is proportional to the length of the foetus.

velopment, but cyclic in foetal development. The mother initially allocates little to the developing foetus, but this increases during development and continues as milk production after birth till weaning in mammals. The maternal rule that reserve density at birth equals that of the mother at egg formation becomes somewhat fuzzy for foetal development if food density is not constant, since foetal development concerns a period, not an event. Foetal development evolved several times independently in *Poeciliopsis* [1175] and many (gradual) transitions exist between egg and foetal development. This illustrates that it makes sense to minimize the formal difference, pay allocation to the foetus from the reproduction buffer and treat it as a buffer handling rule, not unlike the preparation of batches of eggs in multiple batch spawners.

Work with Jess Roberts and Mike Kearney, in the light of up-regulation of the intake and assimilation of the mother during pregnancy and lactation, see Section 7.7 of the comments, has led to some re-formulation of allocation to foetal development.

Most mammals have a preparation period t_0 after fertilisation that is used for hormonal regulation, construction of placenta and vascular system in the mother and the foetus, see e.g. [1215]. During this period there is hardly any significant size increase of the foetus, even in absence of a diapauze. During this preparation stage till time t_0, investment into foetal development, $\dot{p}_F$, is taken to be small in absence of other overheads costs. The realism of the latter still needs checking.

The simplest implementation of foetal development at scaled reserve density e of the mother, here called slow development, is an allocation flux to foetal reserve of $\dot{p}_F = e\{\dot{p}_{Am}\}L_F^2/\kappa_R$, where L_F is foetal structural length and e the scaled reserve density of the mother. The foetus mobilises its reserve as (2.11):

$$\frac{d}{dt}e_F = (e - e_F)\dot{v}/L_F$$

where e_F is the scaled reserve density of the foetus and e that of the mother. The specific growth rate of the foetus is given by (2.21) with $L_T = 0$ (no heating or osmotic costs)

$$\dot{r}_F = \dot{v}\frac{e_F/L_F - 1/L_m}{e_F + g} \overset{L_F \ll e_F L_m}{\simeq} \frac{\dot{v}}{L_F}\frac{e_F}{e_F + g}$$

At constant food density, foetal length grows (almost) linearly in time $L_F(t) = \dot{r}_B L_\infty t$, with $\dot{r}_B = \frac{\dot{k}_M/3}{1+f/g}$, as in (2.24), and $L_\infty = fL_m$. Age at birth amounts to $a_b = (1 + g/f)3L_b/\dot{v}$.

Expressed in scaled time and length, we have $\frac{d}{d\tau}l_F = \frac{g}{3}\frac{e_F - l_F}{e_F + g}$, which reduces for $l_F \ll e_F$ to $\frac{d}{d\tau}l_F = \frac{g/3}{1+g/e_F}$ and for $e_F = f$, scaled length as function of scaled time is $l_F(\tau) = \frac{g\tau/3}{1+g/f}$. Scaled age at birth amounts to $\tau_b = 3l_b\frac{f+g}{fg}$.

The subsection on foetal development suggests that foetuses development is speeded up by assuming that $e_F \gg g$, here called fast development. The motivation was that foetal development then resembles egg development closely with the only difference that egg development eventually slows down, due to depletion of reserve (and/or yolk), while foetal development remains fast till birth. In that case the specific growth rate reduces to $\dot{r}_F = \dot{v}/L_F$, see (2.47), and the von Bertalanffy growth rate to $\dot{r}_B = \frac{\dot{r}L_F/3}{L_\infty - L_F} \simeq \frac{\dot{r}L_F}{3L_\infty} = \frac{\dot{v}}{3L_\infty}$. Length grows approximately linearly in time, $L(t) = \dot{r}_B L_\infty t = t\dot{v}/3$, see (2.47). Fast development implies that gestation time hardly depends on the nutritional status of the mother.

To bridge the gap between slow and fast foetal development, we might multiply e_F with stress coefficient s_F, say, and take $s_F = 1$ for slow and $s_F \gg 1$ for fast foetal development. The changes in scaled length and maturity then become

$$\frac{d}{d\tau}l = \frac{g}{3}\frac{s_F e_F - l}{s_F e_F + g}; \quad \frac{d}{d\tau}v_H = \frac{d}{d\tau}l^3 + l^3 - kv_H$$

In both situations foetal length is (about) proportional to time, $L(t) = \dot{v}_F t$, but for slow development $\dot{v}_F = \dot{r}_B L_\infty$ and for fast development $\dot{v}_F = \dot{v}/3$.

Most non-mammalian taxa that sport foetal development do not produce milk, so maturity at weaning E_H^x equals that at of birth E_H^b for them. The amount of milk fed to the baby mammal varies a lot among species. Being highly precocial, baby guinea pig *Cavia porcellus* starts feeding directly on solid food, while still accepting some milk. Most mammalian babies exclusively feed on milk till weaning and the conversion efficiency from milk to foetal reserve will be typically high. Since milk is synthesised from mothers' reserve and converted to baby's reserve, both conversion efficiencies are probably rather high. This in-between step allows to accommodate baby's need for water during the stage that it is not yet able to drink directly. The water content of milk typically reduces during the lactation period since the baby starts to drink an increasing amount of water. The amount of milk is partly adjusted to the offspring needs (demand driven), but still depends on the nutritional status of the mother (maternal effect), with the implication that the allocation to milk production is about $\dot{p}'_F = e\{\dot{p}_{Am}\}L_F^2$, where L_F is the structural length of the baby till weaning, which happens then the maturity of the foetus reaches E_H^x. Milk production production has an overhead fraction $(1 - \kappa_R^L)$, so the allocation to milk production is $\dot{p}_L = e\{\dot{p}_{Am}\}L_F^2/\kappa_R^L$, where L_F is the structural length of the baby. After weaning $\dot{p}_L$ drops till zero till the next cycle starts. Baby's transition to normal diet is typically gradual, but we may neglect this 'detail' at first approximation. Surface area-linked somatic maintenance might become important for the baby, $L_T > 0$, and mother might assist the baby to bring to costs down. The body temperature of the baby might not be constant, which affects rate parameters.

Scaled lengths at birth, weaning and puberty at constant food, are obtained from scaled maturity thresholds, by integrating $\frac{dl}{dv_H} = \frac{dl}{d\tau}\frac{d\tau}{dv_H}$ with $\frac{d}{d\tau}v_H = fl^2\frac{g+l}{g+f} - kv_H$ and

$\frac{d}{d\tau}l = \frac{g}{3}\frac{l_\infty - l}{g+f}$ and $l_\infty = f - l_T$ and $l_T = 0$ if $v_H < v_H^b$. The scaled ages are obtained from $\tau = -3(1+f/g)\ln(l_\infty - l)$.

The cumulative energy investment in the foetus is

$$E_F = \int_0^{a_b} \dot{p}_F(a)\,da = \frac{f\{\dot{p}_{Am}\}}{\kappa_R}\int_0^{a_b} L^2(a)\,da \quad \text{or } U_E^{0F} = \frac{\kappa_R E_F}{\{\dot{p}_{Am}\}} \simeq L_b^3\frac{f+g}{\dot{v}}\left(1+\frac{3}{4}\frac{l_b}{f}\right)$$

and in milk production

$$E_L = \int_{a_b}^{a_x} \dot{p}_L(a)\,a = \frac{f\{\dot{p}_{Am}\}}{\kappa_R^L}\int_{a_b}^{a_x} L^2(a)\,da$$

The total mean investment rate is $\dot{p}_R = \frac{E_F+E_L}{t_0+a_x}$, which has to be multiplied by the number of young per litter if relevant. The dimensionless scaled energy investment in the slowly developing foetus amounts to $u_E^{0F} = \frac{\dot{v}U_E^{0F}}{gL_m^3} = l_b^3\frac{f+g}{g}\left(1+\frac{3}{4}\frac{l_b}{f}\right)$, which can be compared with $u_E^{0F} = u_E^b + l_b^3 + \frac{3}{4}\frac{l_b^4}{g}$ that was found for fast foetal development, (2.51). For $e_b = f$, we have $u_E^b = fl_b^3/g$ and the latter expression can be written as $u_E^{0F} = l_b^3(1+\frac{f}{g}+\frac{3}{4}\frac{l_b}{g})$. This is slightly smaller than for slow development, due to less cumulative maintenance; the difference in u_E^{0F} is $\frac{3}{4}gl_b^4$.

Section 7.7 of the comments discusses up-regulation of mothers' intake during pregnancy and lactation dynamically.

2.6.2 Foetal costs

The foetal costs in (2.51) can be re-written in terms of scaled age at birth, $\tau_b = a_b\dot{k}_M$ as follows. Table 2.1 learns that $u_E^b = fl_b^3/g$ and $l_b = g\tau_b/3$ (see above 2.47). The scaled foetal cost is $u_E^0 = l_b^3\left(1+\frac{f}{g}+\frac{3l_b}{4g}\right) = \frac{g^3\tau_b^3}{27}\left(1+\frac{f}{g}+\frac{\tau_b}{4}\right)$. The unscaled foetal cost amounts according to (2.51) to $E_0 = u_E^0 g[E_m]L_m^3 = [E_m]L_m^3\frac{g^3\tau_b^3}{27}\,(f+g+g\tau_b/4)$

2.6.2 States at birth and initial amount of reserve

The foetus has no assimilation; maturity, structure and reserve develop directly from the supplies by the mother. Eqn (2.47) states that $\frac{d}{dt}L^3 = \dot{v}L^2$, so $\frac{d}{dt}L = \dot{v}/3$. This equals Eqn (2.21) for $e \to \infty$ and $L_T = 0$ Weak homestasis implies that $E(t) = [E_m]L(t)^3$, so $\frac{d}{dt}E = [E_m]3L^2\frac{d}{dt}L = [E_m]L^2\dot{v}$. Change in maturity is given by Eqn (2.48) in scaled form, where $E_H = u_H g[E_m]L_m^3$ and $\tau = t\dot{k}_M$. So

$$\begin{aligned}
\frac{d}{dt}E_H &= \dot{k}_M g[E_m]L_m^3\frac{d}{d\tau}u_H \\
&= \dot{k}_M g[E_m]L_m^3\left((1-\kappa)l^2(g+l) - ku_H\right)) \\
&= \dot{k}_M g[E_m](1-\kappa)L^2(gL_m+L) - \dot{k}_J E_H \\
&= \frac{1-\kappa}{\kappa}[E_G]L^3(\frac{\dot{v}}{L}+\dot{k}_M) - \dot{k}_J E_H
\end{aligned}$$

. This amount to $\frac{d}{dt}E_H = (1-\kappa)\dot{p}_C - \dot{p}_J$ as given in Eq (2.20) for $e \to \infty$ and $L_T = 0$.

2.6.2 Respiration and mobilisation

The respiration curves in Figure 2.12 were fitted with the assumption that respiration is proportional to mobilization. This was in a period where advanced methods for parameter estimation were not yet available. This approximation can only be very crude and does not deserve further advertisement. It was inspired by lack of knowledge of values of some other parameters. The add_my_pet entries don't make use of this crude approximation. There is also no need for it, since all relevant parameters are estimated simultaneously from a set of data.

2.6.3 Maturation ceasing at puberty

Maturation ceases at puberty if $\dot{p}_J = (1-\kappa)\dot{p}_C$ (see (2.18)) and $L = L_\infty = fL_m - L_T$ (see (2.25)) and $[E] = f[E_m]$ (see (2.10)) and $E_H = E_H^p$. This determines f as follows from (2.19), (2.17) and (2.12) for $v_H^p = \frac{E_H^p}{(1-\kappa)g[E_m]L_m^3}$ and $l_\infty = f - l_T$

$$\frac{\dot{k}_J E_H^p}{1-\kappa} = f[E_m]L_\infty^3 \frac{[E_G]\dot{v}/L_\infty + [\dot{p}_M] + \{\dot{p}_T\}/L_\infty}{\kappa f[E_m] + [E_G]} \tag{2.6}$$

$$= f[E_m]L_\infty^3 \frac{\dot{v}/L_\infty + \dot{k}_M(1 + L_T/L_\infty)}{f/g + 1} \tag{2.7}$$

$$kv_H^p = fl_\infty^2 \quad \text{with } l_\infty = f - l_T \tag{2.8}$$

For $l_T = 0$, this gives $f = (kv_H^p)^{1/3}$. See routine DEBtool/animal/get_ep_min. Contrary to the situation at birth, if maturation ceases at puberty, growth ceases as well.

In the case of metamorphosis, see Section 7.8.2, we only need to substitute $l_\infty = fl_j/l_b - l_T$ to find f at which maturation and growth are ceasing at puberty. See routine DEBtool/animal/get_ep_min_metam.

Length at puberty can be found by integrating change in length as function of maturity from birth (or metamorphosis) to puberty. Since integration is computationally intensive and inaccurate, we can also obtain it at constant food from numerically solving the equation $v_H(\tau_p) = v_H^p$ as function of l_p, starting from $l_p = (v_H^p)^{1/3}$. This is discussed in Section 7.8.2. See routines DEBtool/animal/get_lj and DEBtool/animal/get_lp.

2.6.4 Twinning

Section 2.6.2 of the comments discusses the minimum reserve density at birth, such that maturation just ceases. This corresponds with a minimum initial amount of reserve, that can be compared with the maximum amount of initial reserve (at $f = 1$). Many reasons might exist for why twinning via separation of cells at the 2, 4, 8, $\cdots$ cell-stage is not possible, *Mnemiopsis* develops in only half an adult this way [922], but one of them is that the remaining amount of reserve is not sufficient to complete the embryo stage. Since reserve density tends to increase with maximum (structural) length, we might expect that cells in the 2-cell stage cannot be separated in small species, but can be in large species [774]. Using estimated parameter values of some 130 species, Figure 2.9 shows that this

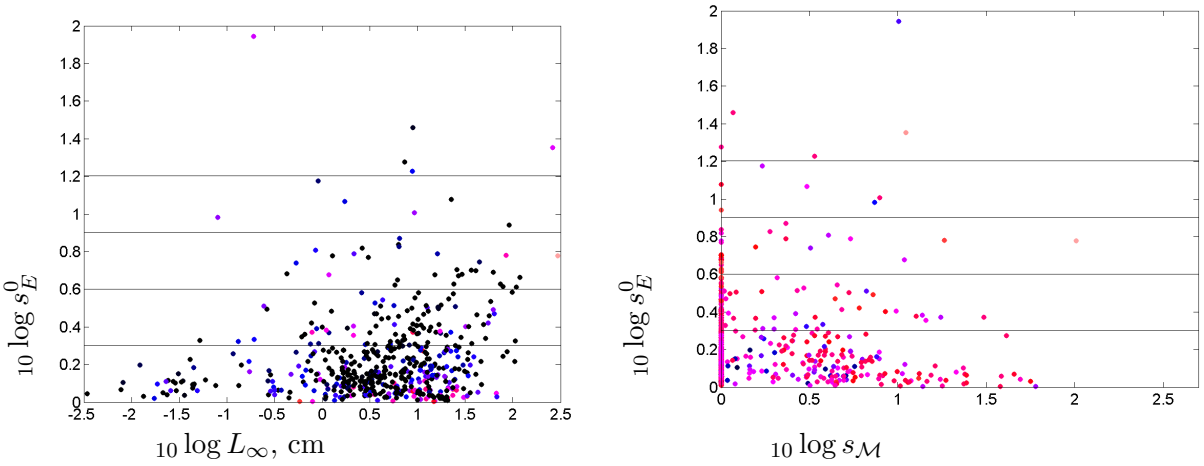

Figure 2.9: The yolkiness , i.e. the maximum initial reserve (at $f = 1$) as fraction of the one at which growth ceases at birth and as function of the maximum structural length of a species that sports egg development, not foetal development. The calculations are based on parameter estimates from the add_my_pet library, sampling date 2017/05/05, 864 species. The colours on the left refer to $_{10}\log(s_{\mathcal{M}})$, ranging for 0 (black) to 2.77 (white), and on the right to $_{10}\log(L_\infty)$. The lines are at values 2, 4, 8, 16

tendency is rather obscured by the huge variability of maturity levels at birth. Notice that large $E_0^{\max}/E_0^{\min}$ ratios hardly occur for $L_\infty < 1\,\mathrm{cm}$; this seems to be the threshold for the 'waste to hurry' phenomenon, see Section 8.2.1 of the comments. Since all the yolky eggs come from accelerating species, yolkiness might relate to accearation. Figure 2.9 suggests that the yolkiness of eggs might relate to metabolic acceleration. Part of the explanation is possibly the fact that specific maturity at birth, E_H^b/L_∞^3, decreases with acceleration. It can only be part of the explanation because the scatter in yolkiness is much less than that of specific maturity at birth.

2.6.5 Back-up production

Crested penguins produce a small egg followed, two days later, by a big one and the incubation of the small one is ceased if the big one proves to be fertile. They can't raise two chicks.

Mothers reduce the number of offspring also in placentalia(e.g. pronghorn, elephant shrews, bats, viscacha), where the mother reduces a considerable number of ova to usually two, early in the development, but also later on, by killing embryos, see 1.1.4. Parent coots, *Fulica* can do it in a later stage, if their litter is too large given the local food availability. Mother Romanian hamsters and gerbils can eat some of their babies, preferring to eat female babies in small litters and male ones in large litters [889].

Siblicide occurs frequently; it is obligatory in the nazca booby *Sula granti* of the Galapagos Isles and the masked booby *Sula dactylatra* of the western and south Pacific. They

typically lay two eggs (of equal size), 4–7 days apart, and if both are healthy, the big chick throws the smaller one out of the nest, with lethal consequences. These two closely related masked boobies are the largest boobies with 1.5 kg body weight, 81–91 cm length and 152 cm wing span; the incubation is 45 d. Like the crested pinguins, these boobies can't raise two chicks.

Siblicide is also known in the cattle egret *Bubulcus ibis*, the common grackle *Quiscalus quiscula*, the spotted hyena *Crocuta crocuta*, parasitic wasps *Ichneumonoidea*, salamanders *Salamandra*, some sharks (sand tiger sharks *Odontaspidae*, mackerel sharks *Lamnidae*, thresher sharks *Alopiidae*), coelacanth *Latimeria* and the sea star *Patiriella*, see 1.1.4 and 5.1.1.

As mentioned in 5.1.1, another variant is sported by some species of poison dart frog *Dendrobatus*, which feed their offspring with unfertilised eggs.

2.6 Maternal effect

The literature on maternal effects is difficult to interpret, because the reports are conflicting, they concern field situations where conditions are complex and varying (allowing for a variety of interpretations) and egg size variation is typically large. A summary, partly composed by Tjalling Jager, is as follows: Neonate size in *Daphnia* sometimes seems to increase with lower food availability [499, 530, 275, 155, 943], sometimes it depends on the clone [497], but starved mothers are also found to produce smaller neonates [1441]. Egg size can also increase with the age of the mother in *Daphnia* [155], salamander (*Ambystoma* [1277]) and chicken (*Gallus* [1274]) or with the size of the mother in fish [684, 469] or decreases with old age in fish [469]. Egg size decreases for lower food availability (as qualitatively assumed in the standard DEB model) in wolf spiders (*Lycosa* [1001]), dung flies (*Scathophaga* [142]), pine beetles (*Dendroctonus* [384]), sea slugs (*Tenellia* [251]), sea urchins (*Pseudechinus* [1117]), fish [469, 208] and owls (*Strix* [689]), but the opposite was found in cichlid fish [1400], fruit flies (*Drosophila* [1467]) and nematods (*Caenorhabditis* [562]), while egg size was found to be independent of food in ground beetles (*Pterostichus* [160]), lizards (*Takydromus* [362]), butterflies (*Bicyclus* [690], *Speyeria* [157]), gastropods (*Nassarius* [252]) and copepods (*Drepanopus* [23]). Egg size sometimes decreases or increases with food availability in rotifers (*Brachionus* [720, 463]), or remained constant (*Synchaeta* [1368]). Postnatal growth also depends on the nutritional condition of the mother [722, 951], as demonstrated in white-tailed deer (*Odocoileus* [989]), for instance.

The empirical evidence is rather weak due to lack of careful control of the conditions of the environment and of the detailed nutritional status of the mother; in most situations information is missing that is critical in a DEB context and adaptation processes might be involved that must be captured by changes in parameter values. In the case of *Daphnia*, the bigger eggs at low food densities do not survive longer during starvation [529]. In view of the observation that the eggs in the brood pouch substantially increase in volume during incubation due to the uptake of water, see Section 4.11.3, and low food densities lead to small clutch sizes, the least problematic interpretation is that *Daphnia* eggs take up less water at high food levels due to lack of room in the brood pouch. Since reserve

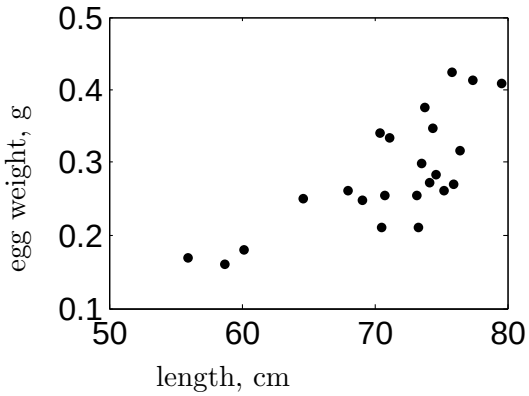

Figure 2.10:
Egg (wet) weight as function of the postorbital-hypural length in the chinook salmon *Oncorhynchus tshawytscha*. Data from [95]

density changes rapidly in small individuals (namely proportional to $\dot{v}/L$), the maternal effect as implemented in the standard DEB model hardly affects the time till death by starvation. The range in egg size is rather limited in the DEB context, so some variation can easily obscure maternal effects. Egg size seems to be related to the size of the mother in fish, see Figure 2.10, not only to weight, but also to length. The maternal effect rule can't explain this. Crowding might be a reason, since reproduction rate scales somewhere between surface and volume, so the mass-specific reproduction rate decreases with the size of the individual. This might also be the case in other taxa.

Despite this conflicting empirical evidence, the maternal effect as implemented in the standard DEB model seems most attractive. A constant egg size, as a possible alternative, introduces a parameter that might be difficult to estimate in practice since allocation to reproduction is a hidden variable. Moreover, the maximum assimilation rate is sensitive to the diet. The normalisation of the scaled functional response f is sensitive to this maximum, so is the scaled reserve at birth. The assimilation rate that corresponds to $f = 1$ for one diet, might correspond to $f < 1$ for another diet. The rule that the reserve density at birth equals that of the mother at egg formation avoids this problem. Moreover, this rule is in beautiful harmony with vegetative propagation that is sported by many species; some species (e.g. some sea cucumbers and anthozoans) sport them simultaneously. This links up with the evolutionary origin of embryos from organism that propagated vegetatively. The maternal effect as implemented in the standard DEB model avoids at least one parameter (the costs of an egg), and possibly more (e.g. to implement that egg size increases with the nutritional status of the mother). It is also the only possibility that ensures von Bertalanffy growth at constant food density, which allows to solve the ODE's for the changes in state explicitly and important mathematical properties can be obtained from that. How the von Bertalanffy growth rate depend on ultimate length under the various food conditions plays an important role in the theory, and also how it changes at abundant food with the maximum body size among species. All that becomes quite a bit more complex for other maternal effects.

If the parameters of the offspring equal to that of the mother, reserve density at birth equals that of the mother at start of development, implies that the scaled reserve densities are also equal. This does not need to hold for the case the parameters differ. If the ultimate size of males and females differ, for instance, this is typically caused by a difference in $\{\dot{p}_{Am}\}$. This implies that, if the reserve density $[E]$ of male and female neonates are

the same, their scaled reserve densities $e = [E]/[E_m]$ differ, since the maximum reserve capacity $[E_m] = \{\dot{p}_{Am}\}/\dot{v}$. The same holds for the scaled length at birth. At constant scaled functional response f, e initially differs from f for males. The time required to reach $e = f$ will be small, since the change in reserve density is linked to $\dot{v}/L$ and l is small.

2.7 Puberty

Puberty is the event at which further maturation ceases and allocation to reproduction starts, such that no other flux is affected. Since allocation to maturation increases over time at constant food in embryo's and juveniles, the natural constraints $(1-\kappa)f\{\dot{p}_{Am}\}L_p^2 a_p > E_H^p$ and $(1-\kappa)f\{\dot{p}_{Am}\}L_\infty^2 a_p > E_H^p$ must apply as long as f is large enough to reach puberty. In scaled quantities, these constraints translate to $f l_p^2 \tau_p > v_H^p$ and $f l_\infty^2 \tau_p > v_H^p$. For the standard model, for which $l_\infty = f - l_T$, the latter becomes $f(f-l_T)^2\tau_p > v_H^p$.

To reach puberty, allocation to maturation just before puberty must be positive, so $(1-\kappa)f\{\dot{p}_{Am}\}L_p^2 > \dot{k}_J E_H^p$ at constant food. In scaled quantities, this constraint translates to $f l_p^2/k > v_H^p$. The combination of these different constraints learns that $k\tau_p > 1$ and $f(f-l_T)^2 > k v_H^p$ and also $1 > k v_H^p$. While l_p and τ_p must be obtained numerically from core parameters and f, the latter constraint can be checked without numerical work.

2.7 Reproduction in *C. elegans*

The nematode *Caenorhabditis elegans* has a remarkable reproduction strategy [1494, 656]. There are males ♂and hermaphrodites ☿, differing in genetics, males being smaller. A hermaphrodite fertilises itself if males are absent. One sperm cell is used to fertilise one egg cell; sperm cells are produced first in a number that more or less matches the number of egg cells to be produced, so $L_p^\sigma < L_p^\varsigma$ in absence of males. Any extra eggs remain unfertilised. The post-reproductive period is typically long in absence of males. In the presence of males, hermaphrodites hardly produce sperm and $L_p^\varsigma \to L_p^\sigma$; reproduction does not cease (no post-reproductive period), but reproduction reduces with old age.

The effects of exposure to cadmium are similar to those of a reduction of assimilation [13]: L_p^ς of individuals in isolation tends to that for individuals in the presence of males, while the latter does not seem to be affected by cadmium.

2.7 Reproduction and moulting in ecdysozoans

Many taxa of ecdysozoans have a fixed number of moults, such as nematodes, copepods, most insects, spiders. For them, moulting seems to be linked to growth to accommodate a growth body and the costs for moulting is a fixed fraction of the specific cost of structure, $[E_G]$. Moulting in juveniles can perhaps better be linked to thresholds in maturity, but some species also moult as adults, which can be linked to $[E_R]$ Some taxa, however, have a undetermined number of moults and continue to moult while growth already ceased.

Examples are daphnids, krill [294], collemboles, silverfish. These taxa linked reproduction to moulting and the costs for moulting is a fixed fraction of the specific cost of somatic maintenance [$\dot{p}_M$]. Decapods show a wide variety of allocation strategies [1163].

In the hep model, imago's do not allocate to reproduction. In the minute pirate bug *Orius*, egg laying is well modelled using assumptions:

- life history events b(=birth), p(=puberty), j(=emergence of imago), i(=death)
- isomorphy during $0b$ and pj, no growth or allocation to reprod during ji
- moults occur when maturity exceeds thresholds
- reproduction buffer at j is $E_R^j = [E_R^j]L_j^3$, where $[E_R^j]$ is a parameter, but L_j depends on food
- egg production rate $\dot{R}(t) = -\frac{d}{dt}E_R\kappa_R/E_0$ for cost E_0 per egg; κ_R is reproduction efficiency
- reproduction buffer dynamics $\frac{d}{dt}E_R = -E_R\dot{k}_R$, but mobilisation rate $\dot{k}_R$ varies in time
- buffer mobilisation rate dynamics $\frac{d}{dt}\dot{k}_R = (\dot{k}_R > \dot{k}_R^0)(\dot{k}_R^m - \dot{k}_R)\dot{k}_R^E$
- constant temperature; all rates depend on temperature, but κ_R might decrease with temperature

Buffer mobilisation rate $\dot{k}_R(t) = 0$ if $t < t_0$ or else $\dot{k}_R^m\left(1 - \exp(-\dot{k}_R^E t)\right)$ for t is time since emergence. Threshold time $t_0 = \log(\dot{k}_R^m/\dot{k}_R^0)/\dot{k}_R^E$.
Egg production rate $\dot{R}(t) = E_R(t)\dot{k}_R(t)\kappa_R/E_0$ with $\frac{d}{dt}E_R = -E_R\dot{k}_R$ and $E_R(0) = E_R^j$.
Cumulative number of eggs $N(t) = \int_0^t \dot{R}(s)\,ds$.

The hep model states that the instar 6/imago transition occurs when $[E_R]$ exceeds threshold $[E_R^j]$, after which growth and further allocation to reproduction cease; after puberty, i.e. at the instar 5/6 transition, further maturation ceases and allocation to reproduction starts and growth switches from V1- to iso-morphic. The imago is not adult in the DEB definition, since it does not allocate to reproduction. An argument for the fact that allocation to reproduction in *Orius albidipennis* only occurs during instar 6, is that temperature-dependence of imago survival just follows the 1-parameter Arrhenius relationship, while egg laying hardly depends on temperature; the increase in allocation to reproduction in instar 6 with temperature is (partly) compensated but a reduction in instar duration.

Temperature dependence is complex in *Orius laevigatus*; survival follows the 1-parameter Arrhenius model, growth needs a 3-parameter one, and reproduction, via κ_R, is again different.

2.7 Age at first brood in birds

Birds typically grow fast to an ultimate weight, and approach that well before they breed for the first time. Many species are fed by their parents during growth, and typically reach a larger weight than their parents, before the parents cease feeding. The young increase their motivation to search for food during starvation and finally their weight settles at the adult level. Birds also have a long life span, and they have the ultimate weight during most of their life span. Time since birth at first brood is frequently reported, but this is well after puberty has been reached. We here evaluate t_R: the time since birth at the first brood on the assumption that brooding starts if the reproduction buffer density reaches some threshold level, food density is constant and the reproduction buffer is fully emptied when littering.

Suppose that an individual at ultimate weight produces clutches at rate $\dot{h}_N$. The reproduction buffer density at littering thus equals $[E_R] = \int_0^{\dot{h}_N^{-1}} [\dot{p}_R]\, dt$, where allocation to reproduction $\dot{p}_R = (1-\kappa)\dot{p}_C - \dot{k}_J E_H^p$ and mobilisation $\dot{p}_C = f[E_m]L^3(\dot{v}/L - \dot{r})$ and specific growth rate $\dot{r} = \frac{f[E_m]\dot{v}/L - [\dot{p}_S]/\kappa}{f[E_m]+[E_G]/\kappa}$. For fully grown individuals $\dot{p}_C$ reduces to $\dot{p}_C = f[E_m]L_\infty^2\dot{v} = f^3[E_m]L_m^3\dot{k}_M g$ and $\dot{p}_R$ to $\dot{p}_R = (1-\kappa)L_m^3[E_m]\dot{k}_M g(f^3 - kv_H^p)$, so $[E_R] = (1-\kappa)[E_m]\dot{k}_M g(1 - kv_H^p/f^3)/\dot{h}_R$. We now apply this to the first brood, where weight might not be ultimate. Allocation to reproduction is zero for $a < a_p$. The time at first breeding t_R now equals

$$\begin{aligned}(1-\kappa)[E_m]\dot{k}_M g(1 - kv_H^p/f^3)/\dot{h}_N &= \int_{t_p}^{t_R} ((1-\kappa)f[E_m](\dot{v}/L - \dot{r}) - \dot{k}_J E_H^p L^{-3})\, dt \\ 1 - kv_H^p/f^3 &= \dot{h}_N \int_{t_p}^{t_R} \left(f\frac{1 + (g + l_T)/l}{f+g} - \frac{kv_H^p}{l^3}\right) dt\end{aligned}$$

The problem that time of first appearance of eggs does not coincide with puberty applies generally, and becomes worse for increasing clutch size. For birds the problem is large, since typically $t_R >> t_p$.

2.9 Standard DEB model in scaled variables

The summary of the complete standard DEB model (including the ageing module as discussed in section 6.1) in scaled variables is as follows (some of the more subtle components are discussed in section 4.1 and in sections 4.1.5 and 4.1.5 of the comments). In addition to the primary parameters in Table 8.1 we need the Weibull ageing acceleration $\ddot{h}_a$, Gompertz stress coefficient s_G, rejuvenation stress coefficient s_H, specific maturity decay $\dot{k}'_J$, maximum shrinking fraction δ_X and food particles have mass M_X. We first introduce the compound parameters and scaled variables as given in Table 2.2. We assume that temperature, and so $\dot{k}_M$, is constant.

The scaled function response is now supposed to jump up and down between 0 and 1. The time intervals for $f = 0$ are exponentially distributed with an intensity that changes in time due to growth and the time intervals for $f = 1$ are deterministic and also change in time; a big individual can handle of a food particle faster than a small one.

Table 2.2: Compound parameters and scaled variables as used in the standard DEB model

half-saturation coefficient $K = \frac{\{\dot{J}_{EAm}\}}{\{\dot{F}_m\}y_{EX}}$	scaled food density $x = X/K$
specific scaled handling rate $\rho_h = \frac{\{\dot{J}_{EAm}\}\dot{v}^2}{M_X y_{EX}\dot{k}_M^3 g^2}$	scaled functional response $f = \frac{X}{X+K} = \frac{x}{x+1}$
scaled feeding rate $h_X = \dot{h}_X/\dot{k}_M$	scaled reserve density $e = [E]/[E_m]$
somatic maintenance rate coefficient $\dot{k}_M = \frac{[\dot{p}_M]}{[E_G]}$	scaled length $l = L/L_m$
maintenance ratio $k = \dot{k}_J/\dot{k}_M$	scaled heating length $l_T = \frac{[\dot{p}_M]}{\{\dot{p}_T\}L_m}$
maximum reserve capacity $[E_m] = \{\dot{p}_{Am}\}/\dot{v}$	scaled maturity $v_H = \frac{E_H}{g[E_m]L_m^3(1-\kappa)}$
energy investment ratio $g = \frac{[E_G]}{\kappa[E_m]}$	scaled time $\tau = t\dot{k}_M$
growth efficiency $\kappa_G = \frac{\mu_V[M_V]}{[E_G]} = \frac{\mu_V}{\mu_E}y_{VE}$	scaled maturity decay $k' = \dot{k}'_J/\dot{k}_M$
reproduction efficiency $\kappa'_R = (1-\kappa)\kappa_R$	scaled reproduction $R = \dot{R}/\dot{k}_M$
maximum length $L_m = \frac{\dot{v}}{\dot{k}_M g}$	scaled hazard $h = \dot{h}/\dot{k}_M$
	scaled ageing acceleration $q = \ddot{q}/\dot{k}_M^2$
	scaled Weibull ageing acceleration $h_a = \ddot{h}_a/\dot{k}_M^2$

No feeding ($f = 0$, $h_X = 0$) occurs before birth, i.e. if $v_H < v_H^b$. After birth, a food handling interval has length $\tau_h = (\rho_h l^2)^{-1}$, the searching intervals have mean $\tau_s = \tau_h/x$ and the mean ingestion rate (in number of particles per scaled time) is $h_X = (\tau_s + \tau_h)^{-1} = f/\tau_h$.

The change in scaled reserve density is

$$\frac{d}{d\tau}e = g(f-e)/l$$

where $f = 0$ for $v_H < v_H^b$, otherwise f, and so x, is a given function of (scaled) time. The maternal effect specifies the condition e of the neonate equals e of the mother at egg formation. With $l(0) = 0$, the change in scaled length is

$$\frac{d}{d\tau}l = lr/3 \quad \text{with} \quad r = \frac{\dot{r}}{\dot{k}_M} = g\frac{e/l - 1 - l_T/l}{e + \kappa_G g}$$

where $\kappa_G = 1$ for $r \geq 0$, otherwise κ_G is some value < 1 (see comments for 4.1.5).

With $v_H(0) = 0$, the change in scaled maturity is

$$\frac{d}{d\tau}v_H = -k'(v_H - l^2 e(1 - lr/g)/k) \quad \text{if } v_H < v_H^p \text{ or } v_H^p > l^2 e(1-lr/g)/k \text{ else } \frac{d}{d\tau}v_H = 0$$

where $k' = k$ for $v_H \leq el^2(1 - rl/g)/k$, otherwise k' is some value (see comments for 4.1.5). Reserve allocated to reproduction is first accumulated in a reproduction buffer with handling rules that vary between species. The mean reproduction in scaled time amounts to

$$R = \frac{\kappa'_R}{u_E^0}\left(\frac{el^2}{e+g}(g + l_T + l) - kv_H^p\right) \quad \text{for } v_H = v_H^p \text{ else } R = 0$$

where scaled initial reserve u_E^0 is given in (2.42) as a function of k, g, v_H^b and e (routine available in DEBtool). Viable eggs satisfy $\frac{d}{dt}v_H\big|_{v_H^b} > 0$, which translates to the constraint $e_b l_b^2 \frac{g+l_b}{g+e_b} > kv_H^b$ (routine available in DEBtool). Maturation ceases at puberty for $kv_H^p =$

fl_∞^2, which reduces to $f = (kv_H^p)^{1/3}$ for $l_T = 0$; for lower mean values of f the adult stage is not entered.

Death is by ageing, rejuvenation or shrinking. The change in scaled ageing acceleration and scaled hazard due to ageing is (cf Section 6.1)

$$\frac{d}{d\tau}q = (ql^3 s_G + h_a)e(g/l - r) - rq \quad \text{and} \quad \frac{d}{d\tau}h = q - rh$$

Death by starvation occurs instantaneously if length shrinks too much, i.e. when $l = \delta_X \max l$, and the hazard rate increases with increasing rejuvenation, $h_H = s_H(\max v_H - v_H)$. This hazard due to rejuvenation adds to the hazard due to ageing; the change in survival probability is $\frac{d}{d\tau}S = -S(h + h_H)$.

Summing up, we have 1 forcing variable (apart from the temperature) and 7 state variables (apart from the reproduction buffer)

$$x \quad \text{and} \quad e, l, v_H, \max l, \max v_H, q, h$$

and 13 parameters

$$v_H^b, v_H^p, \rho_h, g, \kappa_R', \kappa_G, l_T, k, k', s_H, \delta_X, h_a, s_G$$

Together they determine 2 life history events (birth, puberty) separating 3 life stages (embryo, juvenile, adult) and 9 processes (feeding, digestion, somatic & maturity maintenance, growth, reproduction, maturation, reproduction, ageing); 4 of 7 variables and 6 of 13 parameters deal with starvation and death (printed in red). At constant food densities 2 variables ($\max l, \max v_H$) and 4 parameters ($\kappa_G, k', s_H, \delta_X$) don't matter; 2 other variables (q, h) and 2 other parameters (h_a, s_G) concern ageing only. Since most species have $l_T = 0$, 6 parameters ($v_H^b, v_H^p, \rho_h, g, \kappa_R', k$) and 3 variables ($e, l, v_H$) determine 8 processes at constant food densities. The rescaling of scaled time and scaled length to real time and structural volumetric length (which is proportional to physical length) involves 2 additional parameters ($\dot{k}_M, \dot{v}$); this also gives access to the feeding rate (particles per time) and the reproduction rate (eggs per time).

The covariation of parameter values, as discussed in Chapter 8, and typical values, as presented in Table 8.1, lead to the ballpark estimates for zoom factor z

$v_H^b = 4\,10^{-4}$	$v_H^p = 0.25$	$\rho_h = 8z/M_X$	$g = 3/z$	$\kappa_R' = 0.2$	$\kappa_G = 0.8$	
$l_T = 0$	$k = 0.3$	$k' = 0.2$	$s_H = 2$	$\delta_X = 0.8$	$h_a = 3\,10^{-4}z$	$s_G = 0$

where $L_m = 1\,\text{cm}$ for $z = 1$ and the mass of a food particle, M_X, in mmol.

If searching follows a time-inhomogeneous Poisson process, which is a natural choice [536] and section 4.1.1 and sections 2.3.3 and 7.2.4 of the comments, the rules for shrinking, rejuvenation and associated survival become important even at constant food densities, due to stochastic perturbations. Notice that in practice the mass of food particles will not be constant, but follows a varying frequency distribution, with the effect that the handling times will also be stochastic; these model elements are beyond the standard DEB model. Moreover, the hazard rate will have more contributions, such as from predation, which is generally size and probably also maturity dependent.

The consequences of this stochasticity for the mineral fluxes are discussed in Section 4.3.1 of the comments. Scaling is ideal for the analysis of model properties, but if temperature varies, the scaling of time is no longer a good idea.

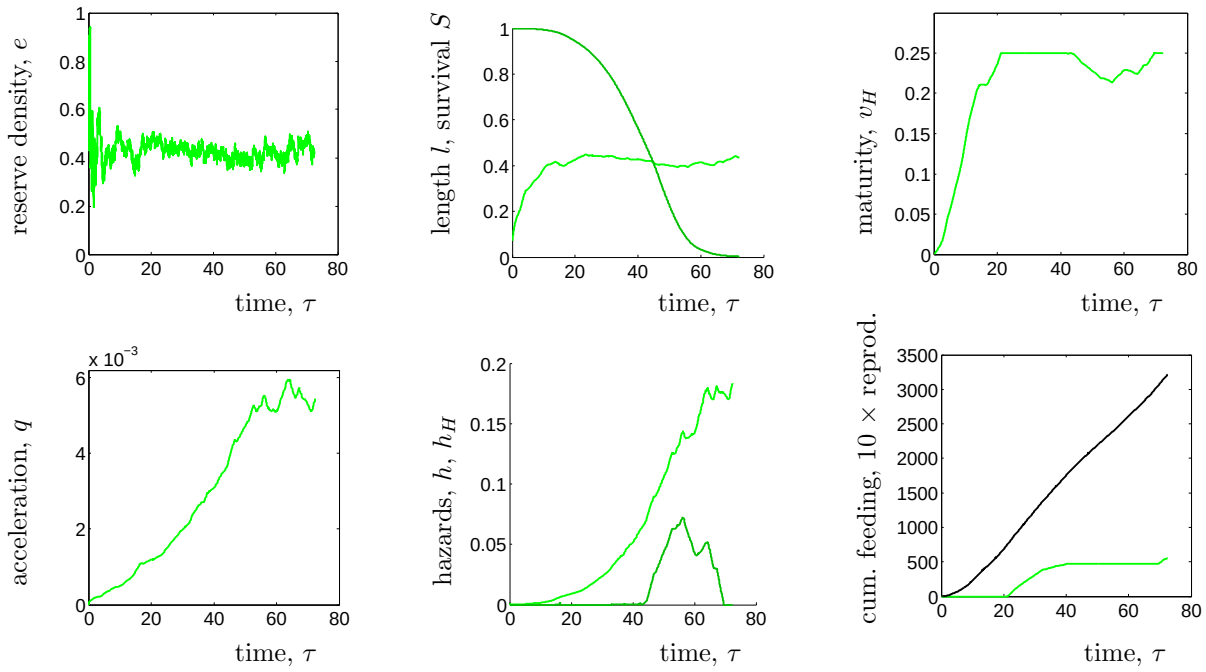

Figure 2.11: If searching follows a time-inhomogeneous Poisson process, the scatter increases for decreasing zoom factor z, decreasing food density x, increasing food particle mass M_X. The scatter in the reserve density decreases with increasing length (upper left panel). The hazard rates due to ageing (upper curve) and rejuvenation (lower curve) are given in the middle lower panel; both contribute to the survival probability S (upper curve in middle upper panel). Death due to shrinking did not occur in this case. The cumulative number of eaten food particles (black) and of produced eggs (green) are shown. Reproduction is here initiated well after growth ceased, but this is not determinate growth. Parameter values: $x = 0.75$, $z = 5$, $M_X = 5\,10^{-4} z^3$, $v_H^b = 0.0004$, $v_H^p = 0.25$, $\rho_h = 8z/M_X$, $g = 3/z$, $\kappa_R' = 0.2$, $\kappa_G = 0.8$, $l_T = 0$, $k = 0.3$, $k' = 0.2$, $\delta_X = 0.8$, $s_H = 2$, $h_a = z3\,10^{-5}$, $s_G = 0.001$

3

Energy, compounds and metabolism

3.2 Body mass and composition

A data base on composition, mass and energy content can be found in [186]

3.2.1 Mass quantified as gram

The relationships between volumes, wet and dry weights, as given in (3.1 - 3.3), are very sensitive for ideas about the water content of structure and reserve; see Section 3.3.1 of the comments. The dry- over wet-weight ratio of structure and reserve is $\frac{w_{Vd}}{w_{Vw}} = \frac{d_{Vd}}{d_{Vw}}$ and $\frac{w_{Ed}}{w_{Ew}} = \frac{d_{Ed}}{d_{Ew}}$, respectively. If $\frac{d_{Vd}}{d_{Vw}} = \frac{d_{Ed}}{d_{Ew}}$, the water content of reserve equals that of structure. The molecular weight of reserve, w_E, as presented in (3.1) and (3.2) includes water in reserve and can be substantially larger than w_{Ed} in (3.3), which excludes water. If we take $w_E = w_{Ed}$ or $d_{Ew} = d_{Ed}$, we essentially say that reserve has no water. If we take $d_{Vw} = 1\,\mathrm{g\,cm^{-3}}$, we assume that the specific density of wet structure equals that of water, which will typically hold by approximation. Excluding the contribution of the reproduction buffer, wet weight can be written as

$$\begin{aligned} W_w &= d_{Vw}L^3 + E\frac{w_{Ew}}{\mu_E} = d_{Vw}L^3 + E\frac{w_{Ed}}{\mu_E}\frac{d_{Ew}}{d_{Ed}} = L^3\left(d_{Vw} + fm_{Em}\frac{w_{Ed}}{w_{Vd}}\frac{d_{Vd}}{d_{Ed}}d_{Ew}\right) \\ &= L^3\left(d_{Vw} + f\omega d_{Ew}\right) \overset{d_{Vw}=d_{Ew}}{=} d_{Vw}L^3\left(1 + f\omega\right) \end{aligned}$$

with $m_{Em} = y_{EV}\frac{[E_m]}{[E_G]} = \frac{[E_m]}{\mu_E[M_V]}$ is the reserve capacity, $[M_V] = \frac{d_{Vd}}{w_{Vd}}$, see Table 3.3, and $\omega = m_{Em}\frac{w_{Ed}}{w_{Vd}}\frac{d_{Vd}}{d_{Ed}} = \frac{[E_m]}{\mu_E}\frac{w_{Ed}}{d_{Ed}}$. Likewise, dry weight can be written as

$$W_d = d_{Vd}L^3 + E\frac{w_{Ed}}{\mu_E} = d_{Vd}L^3\left(1 + fm_{Em}\frac{w_{Ed}}{w_{Vd}}\right) = L^3\left(d_{Vd} + f\omega d_{Ed}\right)$$

If the water contents of reserve and structure are the same on a gram-per-gram basis, $d_{Vd} = d_{Ed}$, we have $\omega = m_{Em}\frac{w_{Ed}}{w_{Vd}}$ and dry weight can be written as $W_d = d_{Vd}L^3(1 + f\omega)$. Only in this case is the dry-wet weight ratio independent of feeding conditions and amounts to $\frac{W_d}{W_w} = \frac{d_{Vd}}{d_{Vw}}$. If the water contents of reserve and structure differ, the dry-wet ratio depends

on feeding conditions, and is, generally, variable. If reserve has no water, $d_{Ew} = d_{Ed}$, wet weight reduces to $W_w = L^3 \left(d_{Vw} + f m_{Em} \frac{w_{Ed}}{w_{Vd}} d_{Vd}\right) = d_{Vw} L^3 + E \frac{w_{Ed}}{\mu_E}$.

Since reserve initially declines faster than structure during starvation, the relative decrease in wet and dry weight has information about the water content of reserve, relative to that of structure. If the relative declines are the same, the water content of reserve and structure are the same.

Maximum reserve density, $[E_m] = \{\dot{p}_{Am}\}/\dot{v}$, is not a primary parameter. Energy conductance has dimension length over time, and this length is in fact the ratio of volume and surface area. This links this concept of energy conductance directly to isomorphs. Since surface area of dry mass has little physical significance, we need surface area of wet mass, so also volume of wet mass. This is why we need w_E in (3.1), which includes water in reserve.

How the chemical indices of wet mass $n^w_{*_1*_2}$ relate to that of dry mass $n^d_{*_1*_2}$ for $*_1 \in \{H, O\}$ and $*_2 \in \{X, V, E, P\}$ can be derived as follows on the basis of the assumption of strong homeostasis. Let us call the number of H_2O molecules per C atom x, so $n^w_{H*_2} = 2x + n^d_{H*_2}$ and $n^w_{O*_2} = x + n^d_{O*_2}$, while $n^w_{C*_2} = n^d_{C*_2}$ and $n^w_{N*_2} = n^d_{N*_2}$. The molecular weights of wet mass relates to that of dry mass as $w_{*_2w} = w_{*_2d} + 18x$, so $x = \frac{w_{*_2w} - w_{*_2d}}{18} = \frac{1 - d_{*_2d}/d_{*_2w}}{18}$, while $d_{*_2w} \simeq 1\,\mathrm{g/cm^3}$.

3.2.2 ATP

The role of energy in cellular metabolism, in particular the generation and use of ATP, is the main focus of bioenergetics [1004]. This compound is called the energy currency of the cell. Together with NADPH and NADH, which provide reducing power, it drives the anabolic processes. Compounds involved in the decomposition processes are important for the cell in two ways: through the production of ATP from ADP and P, which is produced in anabolic processes, and through the production of elementary compounds that are substrates for anabolic processes [614]. The final stages of the catabolic processing of lipids, carbohydrates and proteins all make use of the same cellular machinery: the Krebs cycle. To some extent, these substrates can substitute each other for fueling purposes. The cell chooses between the different substrates on the basis of their availability and its need for particular substrates in anabolic processes.

After this introduction, it perhaps comes as a surprise that ATP is not the main focus in DEB theory. This is because ATP itself does not play a leading role in energy fluxes. It has a role similar to that of money in your purse, while your bank account determines your financial status. A typical bacterial cell has about 5×10^6 ATP molecules, which is just enough for 2 seconds of biosynthetic work [839]. The mean lifetime of an ATP molecule is about 0.3 seconds [553]. The cell has to make sure that the adenylate energy charge $(\frac{1}{2}\ \mathrm{ADP} + \mathrm{ATP})\ (\mathrm{AMP} + \mathrm{ADP} + \mathrm{ATP})^{-1}$ remains fairly constant (usually around 0.9, but this matter is not settled yet). It does so by coupling endergonic (energy requiring) and exergonic (energy releasing) reactions. If the energy charge is reduced, the energy yield of the reaction $\mathrm{ATP} \rightarrow \mathrm{ADP} + \mathrm{P}$ declines rapidly. The situation where the energy charge as well as the concentration of $\mathrm{AMP} + \mathrm{ADP} + \mathrm{ATP}$ remain constant relates to the concept of homeostasis. Cells keep their purses well filled, which makes the dynamics of the purse

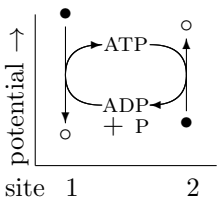

Figure 3.1: The ATP/ADP shuttle transports energy from a site where an energy producing transformation occurs, to a site where an energy requiring transformation occurs. If both transformations occur at the same place and time, and thermodynamics allows, the shuttle is not required. Variations in the free energy of an ATP molecule affect the speed of the shuttle, but not necessarily the transformation rates. Form [770].

contents less interesting. ATP is part of the machinery used to harvest or mobilize energy.

A varying energy yield per mole of ATP does not necessarily complicate metabolic dynamics. It primarily affects the rate at which ATP is produced in energy-yielding transformations or consumed in energy-requiring transformations, and therefore also the rate at which ATP and ADP commute between the sites where these transformations occur, see Figure 3.1. The analogy with money can be extended one step further: the big bank-money is in a stable currency, while the exchange rate of the small purse-money may vary. The focus on ATP/ ADP versus polymers is primarily a question of relevant time scales. Cell division cycles and stages in the development of individuals last too long for a focus on ATP.

The chemiosmotic theory was developed to explain the molecular mechanism of ATP generation. It has boosted biochemical research in cellular energetics, and it is now a central issue in all texts on molecular biology [1031], although competing theories do exist [864]. The focus of bioenergetics on the processes of ATP synthesis and use, matches the classic division of metabolism into catabolic and anabolic processes very well [1522]. This division, however, is less straightforward in the context of the DEB theory, where reserves play an essential role, and processes of synthesis and decomposition occur repeatedly in metabolism. Other differences exist as well. Cell size influences cellular processes through the ratio between membrane surface area to cell volume. This gives the DEB theory a natural focus on cell and life cycles. The link between activity coupled to a surface area (membrane) and mass of metabolic substrate and product coupled to volume is a cornerstone in the DEB theory for the uptake and use of energy.

3.3 Classes of compounds

3.3.1 Terrestrial adaptations in mineral production

Lungfish are supposed to be closest related to ancestors that made the transition from fish to amphibians, so from water to land. This not only concerns the way they respire, as their name suggests, but also to the use of ammonia versus urea as nitrogen waste [865, p 187]. The Australian lungfish *Neoceratodus* is most 'primitive' among lungfish, lives in water that does not become deoxygenated and cannot aestivate. It can only live for 20 min out of the water (at night) and their larvae have no external gills and has a inefficient unpaired lung. The South American lungfish *Lepidosiren* and the four African ones *Protopterus* have paired lungs, live in water that frequently becomes deoxygenated, the larvae have external gills and can aestivate, especially the African species where the swamps in which they live

Table 3.1: Typical values for the ash-free-dry-weight over wet-weight ratio. Any shell is excluded. Measured values can differ considerably due to differences in protocol. This ratio affects $[E_G]$, $[M_V]$, d_E and d_V. The values $[E_G] = 2800\,\mathrm{J\,cm^{-3}}$ and $[M_V] = 4\,\mathrm{mmol\,cm^{-3}}$ of DEB3, Table 8.1 correspond with a ratio of 0.1. Values derived from [1176, 186, 985]. Values for bivalves of 0.2 correspond to the situation where all body fluids have been removed after rupturing the animal. These body fluids should, however, be included for comparative reasons.

Scyphomedusa	0.04	Ctenophora	0.04	Ascidia	0.06	Ectoprocta	0.07
Priapulida	0.07	Cheatognata	0.07	Actinaria	0.08	Bivalvia	0.09
Echinodermata	0.09	Porifera	0.11	Sipuncula	0.11	Gastropoda	0.15
Polychaeta	0.16	Crustacea	0.17	Cephalopoda	0.21	Pisces	0.22
Turbellaria	0.25	Aves	0.28	Reptilia	0.30	Mammalia	0.30

can completely dry up for 9 months in a year. *P. aethiopicus* can even aestivate up to four years. In the water lungfish use ammonia and some urea, while on land, they only use urea, suppressing the formation of (toxic) ammonia via the ornithine cycle. Their kidneys cannot excrete urea, they use their gills for this, like the spiny dogfish *Squalus acanthias* [424]. Gills are, however, inoperative on land, so urea accumulates in the tissues. Adaptation to the terrestrial environment involved many adaptations, including the transfer of excretory function from gills to kidneys. Although the four species of African lungfish *Protopterus* retain gills as adults, 70 % of dioxygen is taken in via the gills in the young post-larval stage, but only 15 % in the adult stage; the rest is taken in via the lungs. The lungs remove carbon dioxide inefficiently in lungfish. In the water lungs remove only 28 % of carbon dioxide, the gills doing the rest, and on land the carbon dioxide level in the blood increases. The receptors that detect carbon dioxide are external in the gills of lungfish and internal in tetrapods. See Section 4.4 of the comments for gill-like structure in breeding *Lepidosiren* males that work inverse to typical gills.

Frogs typically use ammonia in the tadpole stage, but convert to using urea as nitrogen waste during and after metamorphosis [365]. Urea production typically starts at low intensity in the embryo already and gradually becomes more important. Embryos of iguanas produce urea, while after hatching iguanas produce uric acid [1247]; their eggs double their weight during incubation due to water absorption. Eggs of terrestrial reproducers hardly produce ammonia. Excretion of urea through the skin in known in *Bufo* and *Rana* species.

The Chinese soft-shelled turtle, *Pelodiscus sinensis*, excretes urea mainly through the mouth instead of the kidney [650].

3.3.2 Water in tissues

Water in biomass can, like any other compound, belong to reserve or structure or both. On of the ways to find out where it belongs is to study the relative decrease in wet and dry weights during starvation. If both decrease equally fast initially, while only reserve is used, the fractions of reserve and structure that are water are the same. The importance of the water content for energetics is, o.a. in the volume-specific costs for structure $[E_G]$. If most of the structure is water, these costs are expected to be low. The water content

of structure also affects the mass-volume couple $[M_V]$. Given a fixed growth efficiency $\kappa_G = \mu_V[M_V]/[E_G]$ and chemical potential of structure $[M_V]$ and $[E_G]$ are affected by the water content is the same way. Table 3.1 gives typical values. At this moment, it is an open question to what extent $[\dot{p}_M]$ is affected by the water content of structure. If most somatic maintenance is linked to protein turnover, this parameter will decrease for increasing water content. Intra-organismal water transport might become more costly for increasing water content. It is not yet fully clear to what extent water content follows the rules for strong homeostasis.

3.3.2 Segregation of reserve

Embryos of many species have a storage deposit, called yolk, composed of lipo-proteins. These are proteins with large amounts of carbohydrates, lipids and cholesterol bound to it, which are transformed to proteins, lipids and carbohydrates around birth. This transformation is generally considered to be efficient from an energetic perspective, and DEB theory does not account for it explicitly. Animal species vary a lot in the extent of segregation of yolk from the rest [204]. Some species, e.g. mammals, hardly have yolk; such eggs are called alecithal. Some have a small amount that is hardly segregated, such as many echinoderms, annelids, mollusks (except cephalopods), nematodes and tunicates; these eggs are called isolecithal. Others have a large amount that is central in the egg, called centrolecithal with arthopods as example, or the non-yolk is floating on a big blob of yolk, called telolecithal, with cephalopods and vertebrates as examples, see Figure 3.2. (These are also the groups with capillaries, so a closed blood circulation system.) The mitotic apparatus can be in the center of the egg and cleavage is complete, a situation called holoblastic cleavage. If yolk is segregated, the eggs are centrolecithal. The mitotic apparatus can also be displaced from the center and cleavage can be incomplete, a situation called meroblastic cleavage with telolecithal eggs as result. The egg segregates into a number of separate blastomeres and a residue, i.e. a continuous mass of cytoplasm that is specialised in storing. The blastomeres become separated from the yolk by a periblast, a syncytial layer that is supposed to play a role in the mobilisation of yolk. Even in the case of holoblastic development there is some segregation of the storage function.

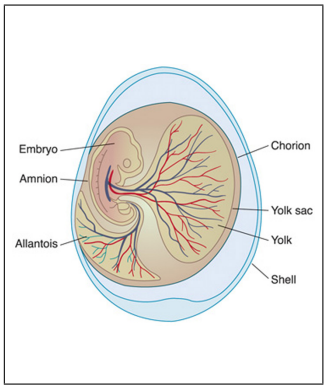

The eggs of amniotes (reptiles, birds and mammals) have a number of membranes: amnion, allantois, yolk sac, and chorion. The amnion surrounds the embryo directly and the amniotic fluid provides it with a stable fluid environment. The allantois takes care for gas diffusion and removal of wastes. Yolk in the yolk sac is mobilised through an umbilical cord. Surrounding all the other membranes is the chorion, which prevents bacteria to invade. Around the chorion is the albumin, or 'white' of the egg, and an outer shell protects the whole egg mechanically, preventing drying while still permitting air to reach the embryo and providing calcium carbonate for the bones of the bird embryo. An air space provides an extra internal buffer for environmental conditions.

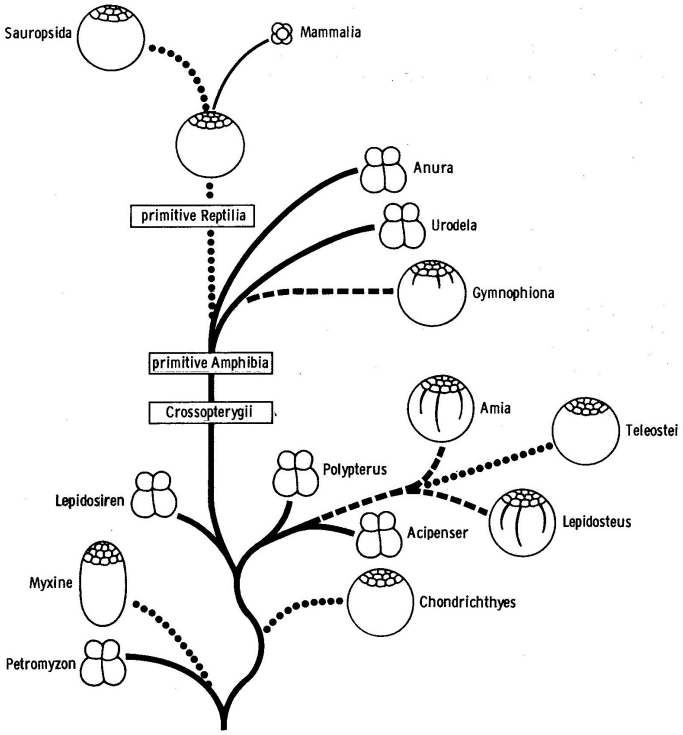

Figure 3.2: Meroblastic development (dotted lines) as it evolved from holoblastic development (drawn) among vertebrates. From Schwartz [1275].

The allantois and yolk sac are modified to an elongated umbilical cord in the foetal embryo, providing a connection through which maternal reserve and dioxygen reaches the foetus, and wastes are removed. Together with part of the chorion, these membranes make up the placenta, which physically attaches the embryo to the uterine wall of its mother. Around the whole is the fluid-filled chorion.

The umbilical cord allows to separate yolk from the rest of the embryo, which calls for an interpretation of the measurements. Mobilised yolk converts to reserve and structure, as mentioned at {80}, where the conversion efficiency from yolk to reserve is very close to one and reserve density remains constant. This conversion of yolk Y to reserve can formally be considered as a transport process, i.e. a spatial reorganisation, with hardly any consequence for the dynamics of development; the total mass of reserve of the embryo is thus the sum of the mass of yolk and the reserve that has already been transported to the embryo tissues and organs. On the assumption that yolk is zero at birth, in combination with the maternal effect that reserve density equals that of the mother at egg formation e_b, quantifies yolk dynamics: $M_Y(t) = M_E(t) - e_b m_{Em} M_V(t)$, where body yolk and the rest of reserve are mobilised to fuel embryo development. This relationship not only interprets measurements on yolk mass, but also gives the relationship between egg and foetal development, where foetal mass corresponds with $(1 + e_b m_{Em}) M_V(t)$.

DEB theory treats the yolk sac as an temporary organ for storage, not unlike adipose tissue in juveniles and adults. The fact that some organs have a temporary role, or that the role can change during development, is certainly not unique. The thymus is an example of an mammalian organ that is mainly active in the early juvenile stage where it regulates

growth, but its role in the immune-system lasts much longer; the size of the thymus shrinks considerably around puberty.

Segregation of reserve comes with a transport issue. The general pattern is that some reserve compounds can be mobilised rapidly and are stored near the site of intensive use, and other compounds are mobilised slowly and are stored in specialised tissues. The distant slow pools need to be mobilised and transported, which takes time. It is no coincidence that the change in reserve density is proportional to $\dot{v}/L$, so the mobilisation rate decreases for increasing transport distance within an organism. All cells in a multicellular body have reserve and structure; the reserve density might differ between organs or tissues in isomorphs, without giving theoretical complications.

3.4 Conversions of energy, mass and volume

Additional to Table 3.3 other useful conversions are:

relationship	unit	description
$\kappa_X = y_{EX}\frac{\mu_E}{\mu_X}$	–	digestion efficiency
$u_E = \frac{\kappa E}{[E_G]L_m^3}$	–	scaled reserve
$v_H = \frac{E_H}{[E_G]L_m^3}\frac{\kappa}{1-\kappa}$	–	scaled maturity
$\kappa_G = \mu_V\frac{[M_V]}{[E_G]} = \frac{\overline{\mu}_V}{\overline{\mu}_E y_{VE}}$	–	growth efficiency

3.6 Isotope dynamics

Isotopes can be used to infer about body temperature from the fossil record. By comparing δ^{1*}O in the phosphate of teeth of Mesozoic reptiles with that of fish, Bernard *et al* [115] conclude that ichthyosaurs, plesiosaurs, and, to a lesser extent mosasaurs, were homeothermic in the range 35–39 °C, swimming in seawater of 12 °C. Eagle *et al* [371] conclude that big non-avian dinosaurs had a body temperature of 37 °C, cf Subsection 8.2.2 of the comments. Montani [987] warns, however, that the interpretation needs to account of the linear increase in δ^{18}O in biogenic carbonates and phosphates during the last 500 Ma at a rate of some 0.02 Ma^{-1}.

3.6.1 Reshuffling

The literature on isotope dynamics typically talks about mixing rather than reshuffling and actually treats this dynamics as if atoms (and so isotopes) travel independently. DEB theory, however, accounts for the fact that atoms are locked in molecules and that molecules are transformed. The atoms of product molecules correspond to particular atoms in substrate molecules in simple transformations. In complex transformations, involving metabolic networks, we still should deal with frequency distributions of originating atoms in substrate molecules. A similar problem is in stochiometric constraints on production, where most literature discusses chemical elements, as if they travel independently, see e.g. [1371]. We only have to remember that N is frequently limiting primary production, but N_2 is very

abundant (but only few species can use N in this form). We can't avoid to consider chemical transformations, which complicates the problem quite a bit.

3.6.2 Derivation of (3.26)

The definition of the odds ratio is the ratio of probabilities of two isotopes being selected for a particular target. Its meaning requires the identification of the isotopes (and the one that is in the numerator) and of the target. This definition involves the notion of a flux of molecules to at least two targets. An odds ratio of 1 means that both isotopes have the same probability of being selected for that target.

Isotope dynamics can only be understood if mass dynamics do no longer have any secrets. So section 3.6 (and 4.7) can best be skipped at first reading.

All three basic fluxes, assimilation, dissipation and growth, have an anabolic and a catabolic aspect. In other words: substrates have a dual function; they serve as source for energy and building blocks. These functions are typically incompatible, because the use as energy source involves a decomposition into simple products that are excreted into the environment. Because of the difference in fate of substrate molecules, selection of molecules with particular isotopes can occur at the partitionning of anabolic and catabolic fluxes; if selection does not occur, we choose $\beta = 1$, which is just a special case.

We follow fluxes in C-moles, so for carbon in transformation k we can simply write $\dot{J}_{sk} = \kappa_k \dot{J}_{sk_a} + (1-\kappa_k)\dot{J}_{sk_c}$ for any $s \in \mathcal{S}$, where $\mathcal{S}$ is the set of all substrates in transformation k. Notice that κ_k does not depend on s, only on k. For element i we need to account for the chemical index, so $n_{is}\dot{J}_{sk} = \kappa_k n_{is}\dot{J}_{sk_a} + (1-\kappa_k)n_{is}\dot{J}_{ak_c}$. This does not add anything new, because the chemical indices of the anabolic and catabolic fluxes are identical. This does not hold for the isotopes, however. So the balance equation for the isotopes reads $n_{is}^{0k}\dot{J}_{sk} = \kappa_k n_{is}^{0k_a}\dot{J}_{sk_a} + (1-\kappa_k)n_{is}^{0k_c}\dot{J}_{ak_c}$, where $n_{is}^{0k_a} \neq n_{is}^{0k_c}$ if $\beta \neq 1$. Notice that the selection is different for the different transformations, so k appears in n_{is}^{0k}.

If we integrate time t over a time increment dt, the total number of 'balls' in our pool is $m = n_{is}\dot{J}_{sk}\,dt$, where $m_0 = n_{is}^{0k}\dot{J}_{sk}\,dt$ are 'white' and $m_1 = m - m_0$ are 'black'. In the anabolic flux we select $n = n_{is}\dot{J}_{sk_a}\,dt = \kappa_k n_{is}\dot{J}_{sk}\,dt$ 'balls' from this pool, where $n_0 = n_{is}^{0k_a}\dot{J}_{sk_a}\,dt = \kappa_k n_{is}^{0k_a}\dot{J}_{sk}\,dt$ are 'white' and $n_1 = n - n_0$ are 'black'.

We now use (3.25), substitute for $\beta = \beta_{is}^{0k_a}$, n, m_0 and m_1

$$\begin{aligned}
n_0 &= \frac{2c}{\sqrt{b^2-4ac}-b} \\
\kappa_k n_{is}^{0k_a}\dot{J}_{sk}\,dt &= \frac{2c}{\sqrt{b^2-4ac}-b} \\
n_{is}^{0k_a} &= \frac{2c}{\sqrt{b^2-4ac}-b}\,\frac{1}{\kappa_k\dot{J}_{sk}\,dt} \quad \text{with} \\
a &= \beta - 1 = \beta_{is}^{0k_a} - 1 \\
b &= n - m_1 - (m_0+n)\beta = (n+m_0)(1-\beta) - m \\
&= \left((\kappa_k + \frac{n_{is}^{0k}}{n_{is}})(1-\beta_{is}^{0k_a}) - 1\right) n_{is}\dot{J}_{sk}\,dt \equiv B n_{is}\dot{J}_{sk}\,dt
\end{aligned}$$

$$c \;=\; m_0 n\beta = \kappa_k \beta_{is}^{0k_a} \frac{n_{is}^{0k}}{n_{is}} (n_{is} \dot{J}_{sk}\, dt)^2$$

The expression for $n_{is}^{0k_a}$ can be simplified to

$$n_{is}^{0k_a} \;=\; \frac{2\beta_{is}^{0k_a} n_{is}^{0k}}{\sqrt{B^2 + 4(1-\beta_{is}^{0k_a})\beta_{is}^{0k_a}\kappa_k \frac{n_{is}^{0k}}{n_{is}}} - B}$$

Since $n_{is}^{0k} = \kappa_k n_{is}^{0k_a} + (1-\kappa_k) n_{is}^{0k_c}$, we have $n_{is}^{0k_c} = \frac{n_{is}^{0k} - \kappa_k n_{is}^{0k_a}}{1-\kappa_k}$. For $\beta_{is}^{0k_a} = 1$, we have $B = -1$ and $n_{is}^{0k_a} = n_{is}^{0k}$, so the process is unselective.

3.7 Synthesising Units

The concept of Synthesising Units comes back in DEB theory at all levels of organisation; it was implicitly applied already in Chapter 2 and will be applied explicitly in Chapter 4, comming back in all other chapters, such as in 7.1 and 7.6 on applications of SUs in pathway dynamics. At the molecular level SU dynamics in intrinsically stochastic, and since it is also used to model baheviour (which is notoriously stochastic), the stochastic behaviour of SUs comes back at the population level in 9.3.1. This is a reason to consider the stochastic aspects at the molecular level in more detail, although 11.2 argues that this world is more alien than generally recognised.

3.7.1 From substrate to product

The derivation of the simplest SU-mediated transformation $A \to B$, see Figure 3.6, is as follows. On the basis of an advection-diffusion argument, the association between substrate A and the SU is taken proportional to the concentration X_A of substrate A. This is also called the law of mass action. Let $\theta_.$ denote the fraction of SU's that can bind substrate A and θ_A the fraction that is already bound: $1 = \theta_. + \theta_A$. One can also think of a single SU where $\theta_.$ and θ_A stand for the the fractions of time that it is in the free and bounded state. This better illustrates that we here exploit the conservation law of time. Given the dissociation rate $\dot{k}_B$ and the association rate $\dot{b}_A$, the change in the fraction of enzyme in the various binding states is given by

$$\frac{d}{dt}\theta_. = \dot{k}_B \theta_A - \dot{b}_A X_A \theta_.$$

We now use a time scale separation argument and evaluate the steady state fraction $\theta_.^*$ for which $\frac{d}{dt}\theta_. = 0$. We find $\theta_.^* = \frac{\dot{k}_B}{\dot{k}_B + \dot{b}_A X_A}$ and $\theta_A^* = \frac{\dot{b}_A X_A}{\dot{k}_B + \dot{b}_A X_A}$. The flux of substrate A that disappears is $\dot{J}_A = \dot{b}_A X_A \theta_.^* = \frac{\dot{k}_B \dot{b}_A X_A}{\dot{k}_B + \dot{b}_A X_A}$. The flux of product B that is produced is $\dot{J}_B = \dot{k}_B \theta_A^* = \frac{\dot{k}_B \dot{b}_A X_A}{\dot{k}_B + \dot{b}_A X_A}$. No surprise that $\dot{J}_A = \dot{J}_B$. In the context of mass balances we might take $\dot{J}_A$ negative. This is the well-known Michaelis–Menten kinetics [591] or Holling II functional response [624]. If one molecule of A produces y_{BA} molecules of B, we need to multiply $\dot{J}_B$ by y_{BA}.

3.7.2 Derivation of (3.33)

Equations (3.30)-(3.32) can be written in matrix notation as

$$\frac{d}{dt}\begin{pmatrix}\theta_{..}\\ \theta_{A.}\\ \theta_{.B}\\ \theta_{AB}\end{pmatrix}=\begin{pmatrix}-\dot{b}_A X_A-\dot{b}_X X_B & \dot{k}_A & \dot{k}_B & \dot{k}_C\\ \dot{b}_A X_A & -\dot{k}_A-\dot{b}_B X_B & 0 & \dot{k}_B\\ \dot{b}_X X_B & 0 & -\dot{k}_B-\dot{b}_A X_A & \dot{k}_A\\ 0 & \dot{b}_B X_B & \dot{b}_A X_A & -\dot{k}_A-\dot{k}_B-\dot{k}_C\end{pmatrix}\begin{pmatrix}\theta_{..}\\ \theta_{A.}\\ \theta_{.B}\\ \theta_{AB}\end{pmatrix}$$

or

$$\frac{d}{dt}\boldsymbol{\theta}=\dot{\boldsymbol{k}}\boldsymbol{\theta}$$

Notice that the sum of all rows is zero for all columns, so $\mathbf{1}^T\dot{\boldsymbol{k}}=\mathbf{0}$ and $\dot{k}_{ii}=-\sum_{j\neq i}\dot{k}_{ij}$. The differential equation only specifies changes in state, not the state itself. We have the extra constraint $\mathbf{1}^T\boldsymbol{\theta}=1$, which, in combination, specifies the equilibrium, where we have $\mathbf{0}=\dot{\boldsymbol{k}}\boldsymbol{\theta}$. We now out-scale time using $\tau=t\dot{k}_B$, arriving at $\frac{d}{d\tau}\boldsymbol{\theta}=\boldsymbol{k}\boldsymbol{\theta}$ with

$$\boldsymbol{k}=\begin{pmatrix}-x_A k_A-x_B & k_A & 1 & k_C\\ x_A k_A & -k_A-x_B & 0 & 1\\ x_B & 0 & -1-x_A k_A & k_A\\ 0 & x_B & x_A k_A & -k_A-1-k_C\end{pmatrix}$$

We just divided all elements of $\dot{\boldsymbol{k}}$ by $\dot{k}_B$ and introduced the scaled variables with $x_A=X_A\dot{b}_A/\dot{k}_A$, $x_B=X_B\dot{b}_B/\dot{k}_B$, $k_A=\dot{k}_A/\dot{k}_B$, $k_C=\dot{k}_C/\dot{k}_B$. At equilibrium we have $\mathbf{0}=\boldsymbol{k}\boldsymbol{\theta}$ and $\mathbf{1}^T\boldsymbol{\theta}=1$. This is a system of 5 equations with 4 unknowns (namely the θ's), but these equations are not all independent. We replace the first of the set of 4 equations, namely

$$0=\begin{pmatrix}-x_A k_A-x_B & k_A & 1 & k_C\end{pmatrix}\boldsymbol{\theta}$$

by $1=\mathbf{1}^T\boldsymbol{\theta}$. We can write that again compactly in matrix form using a matrix $\boldsymbol{k}_*$ which equals matrix $\boldsymbol{k}$, but with a first row replaced one ones. The result is $(\,1\;\;0\;\;0\;\;0\,)^T=\boldsymbol{k}_*\boldsymbol{\theta}$. This can now be solved by left-multiplication with the inverse of $\boldsymbol{k}_*$, giving $\boldsymbol{k}_*^{-1}(\,1\;\;0\;\;0\;\;0\,)^T=\boldsymbol{\theta}$, which is (3.33).

3.7.2 Synthesising Units at molecular scale

Because a Synthesising Unit does not dissociate from substrates, it can be considered as a server, i.e. a unit handling particles. A large but fixed number of identical servers handle particles simultaneously, without interfering with each other, except by competing for the same particles (clients). The term 'server' stems from an extensive theory of applied probability calculus, known as queueing theory, which deals with this type of problem, e.g. [1241, 1321]. The extension of the previous derivation of the dynamics of the SU to include an arbitrary number of copies of an arbitrary number of substrates becomes complex, but this is still feasible if the derivation uses the servers' point of view.

In its simplest form, the Synthesising Unit (SU) is an enzyme or a complex of enzymes that binds a substrate molecule to deliver (synthesise) a product molecule or a set

of product molecules. For simplicity's sake, I assume that the substrate molecules arrive according to a Poisson process, that the binding occurs with a fixed probability ρ if the SU is in its binding stage, and that the production stage lasts an exponentially distributed time interval. The production stage corresponds with a kind of 'handling' time. During the production process, no substrate molecules are accepted by the SU, so the binding probability $\underline{\rho}$ for each arriving substrate molecule follows a renewal process [279], alternating between the values ρ and 0, when the SU is binding and producing, respectively. I call this SU a one substrate-one copy SU, which will be generalised to a multi substrate-multi copy SU.

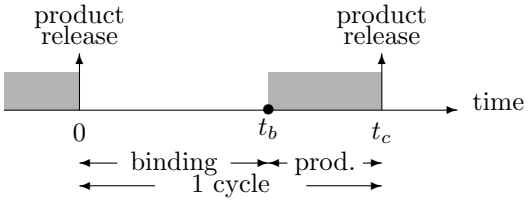

Let the binding and production periods, $\underline{t}_b$ and $\underline{t}_p$, be exponentially distributed random variables, with means $\dot{J}_{Xb}^{-1}$ and $\dot{J}_{Xm}^{-1}$, respectively. The substrate molecules arrive at rate $\dot{J}_{Xa} = \dot{J}_{Xb}/\rho$, where ρ denotes the binding probability per arriving substrate molecule. The cycle period of the SU, $\underline{t}_c = \underline{t}_b + \underline{t}_p$, catenates one binding period and the subsequent production period. The inverse of its expected value, $\dot{J}_X = 1/\mathcal{E}\underline{t}_c$, equals the mean production rate, which I will call the intensity of the production process; it is defined as the ratio of the cumulative number of events in a period to the length of the period, for a large period.

When substrate molecules are sent to a one substrate-one copy SU, according to a Poisson process with intensity $\dot{J}_{Xa}$, it returns a Poisson process of rejected substrate molecules, with an intensity that alternates between values $(1-\rho)\dot{J}_{Xa}$ and $\dot{J}_{Xa}$, and a renewal process of product molecules, with intensity $\dot{J}_X = (\dot{J}_{Xm}^{-1} + \dot{J}_{Xb}^{-1})^{-1}$. The mean intensity of the rejected substrate molecules amounts to $\dot{J}_{Xa} - \dot{J}_X$. Note that for very high intensities of the arrival process, the production process approximates the value $\dot{J}_{Xm}$.

The events of substrate rejection and production are mutually dependent, but I will not work out the structure in detail, because the practical interest is not in the performance of a single SU, but a large set of independently operating SUs. The central limit theorem for the addition of independent stochastic point processes implies that the rejected substrate molecules and the product molecules of a sufficiently large set of s independent SUs converge to independent Poisson processes with constant intensities $\dot{J}_{Xa} - \dot{J}_X$ and $\dot{J}_X = ((s\dot{J}_{Xm})^{-1} + \dot{J}_{Xb}^{-1})^{-1}$, respectively. An increase in the amount of SUs has the effect of decreasing the production period; the reduction of the intensity of arriving substrate molecules per SU cancels against the increase of the binding probability. Other implementations of the step to group performance are conceivable, but these require details of the SUs' spatial organization.

3.7.2 Multi substrate-multi copy SU

Suppose that the SU can be in a binding or in a production stage, and that it needs n copies of a single substrate X to produce a product molecule Y, while the moment at which the production stage of the SU is entered, $\underline{t}_b$, equals the moment of the n-th binding, $\underline{t}_n$, so $\underline{t}_b = \underline{t}_n$. Such a SU can be called a one substrate-multi copy SU, or n-SU. The binding period follows the Erlangian distribution $\phi_{\underline{t}_b}(t) = \frac{\dot{J}_X(\dot{J}_X t)^{n-1}}{(n-1)!}\exp\{-\dot{J}_X t\}$, which has a mean

value of $\mathcal{E}\underline{t}_b = n\dot{J}_X^{-1}$. It results from adding n independently exponentially distributed random variables with parameter $\dot{J}_X$. For a mean production period $\dot{J}_{Ym}^{-1}$, the appearance of Y molecules from a single SU is a renewal process with intensity $\dot{J}_Y = (\dot{J}_{Ym}^{-1} + n\dot{J}_X^{-1})^{-1}$. A large set of s SUs will produce a Poisson stream of Y molecules with intensity $\dot{J}_Y = ((s\dot{J}_{Ym})^{-1} + n\dot{J}_X^{-1})^{-1}$, and a Poisson stream of rejected substrate molecules of intensity $\dot{J}_X - y_{X,Y}\dot{J}_Y$, where $y_{Y,X}$ stands for the number of molecules of Y produced per processed molecule X.

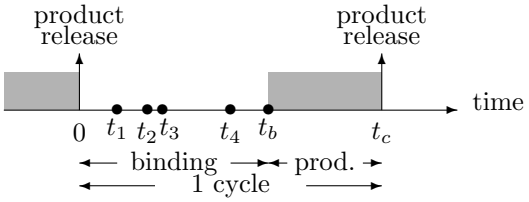

The model does not specify the details of the production process. The SU might have n different binding sites, or just a single one in combination with a fast process of precursor production while the precursor molecules remain in the local environment of the SU that is under its control.

Now we are ready for the more interesting multi substrate-multi copy SU, which requires n different substrate types for the production of a single molecule, or set of molecules, Y: the $n_1, n_2, \cdots, n_n$-SU. The kinetics of the production process is based on the idea that the SU can only enter the production stage if all required substrate molecules are bound.

3.7.3 Sequential processing

When the SU binds the different types of substrate sequentially, in a random order, the expected waiting time to the binding of n_i molecules of type i is $n_i\dot{J}_i^{-1}$. The order of the types is not relevant, but when the SU is binding type i it continues to do so until all required molecules for the production of one product molecule are bound. This directly leads to the expected binding period

$$\mathcal{E}\underline{t}_b = \sum_{i=1}^{n} \frac{n_i}{\dot{J}_i} \tag{3.1}$$

and the mean production rate $\dot{J}_X = (\dot{J}_{Xm}^{-1} + \sum_i n_i\dot{J}_i^{-1})^{-1}$.

The interest in this mechanism is mainly in its mathematical simplicity, and its interesting properties (M. P. Boer, pers. comm.) The parallel binding period is equal to the sequential binding period minus the gain in time (compare (3.1) and (3.5)). Suppose that the substrate fluxes are proportional to the substrate concentrations X_i, as a result of some convection or diffusion process. The production rate can then be rewritten as $\dot{J}_X = \dot{J}_{Xm}(1 + \sum_i X_{Ki}/X_i)^{-1} = \dot{J}_{Xm}f_n$, where X_{Ki} denotes the saturation constant, which quantifies the affinity of the SU for substrate i, including the transport rate from the (local) environment to the SU, and the factor f_n is the scaled functional response for n types of possibly limiting substrates, which takes values between 0 and 1. (The term 'functional response' originates from ecology, and stands for the feeding rate of a predator as function of the density of prey.) The recurrent relationship $f_n = \frac{X_n f_{n-1}}{X_n + X_{Kn} f_{n-1}}$ applies, for $f_0 = 1$ and $n = 1, 2, \cdots$, which leads to $f_n = \prod_i X_i (\prod_i X_i + \sum_i X_{Ki} \prod_{j \neq i} X_j)^{-1}$.

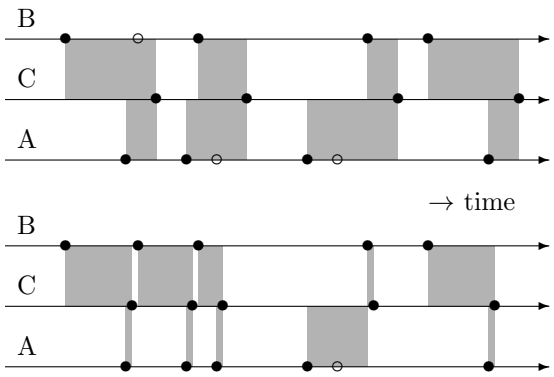

Figure 3.3: These pictures illustrate the production by a strongly binding relatively slow (upper) and a very fast (lower) 1,1-SU. The arrival events of substrate molecules A and B, and the production events of product molecules C are indicated with filled and open dots on three time-axes. Filled dots stand for acceptance, open ones for rejection. The grey areas indicate periods during which the SU is blocked for a substrate. Note that the fast SU still has substantial blocked periods.

3.7.3 Parallel processing

Suppose that the binding of one type of substrate does not interfere with that of another. The SU will not bind substrate i molecules, either if it already bound n_i molecules of that substrate, but still has to bind other types of substrate, or if the SU is in the production stage, see Figure 3.3. For application, one might think of a substrate-product conversion that is uphill, meaning that the chemical potential of the product is larger than that of the substrate, and must be coupled to another conversion that is downhill. Let $\underline{t}_{bi}$ denote the moment of the binding of the n_i-th molecule of substrate type i (so the binding is complete for that substrate), and $\underline{t}_b = \max_i\{\underline{t}_{bi}\}$ the moment when all required substrate molecules are bound, and the production stage is entered. The distribution function of the binding period $\underline{t}_b$ equals the product of the distribution functions of $\underline{t}_{bi}$, which are incomplete gamma functions

$$\Phi_{\underline{t}_b}(t) = \prod_{i=1}^{n} \Phi_{\underline{t}_{bi}}(t) = \prod_{i=1}^{n} \int_0^t \phi_{\underline{t}_{bi}}(t_1)\, dt_1 = \prod_{i=1}^{n} P(n_i, t\dot{J}_i) \tag{3.2}$$

where $P(n,t) = \frac{1}{\Gamma(n)} \int_0^t \exp\{-t_1\} t_1^{n-1}\, dt_1 = 1 - \exp\{-t\} \sum_{j=0}^{n-1} \frac{t^j}{j!}$ is the incomplete gamma function. The expected value of the binding period is

$$\mathcal{E}\underline{t}_b = \int_0^\infty \left(1 - \Phi_{\underline{t}_b}(t)\right)\, dt = \int_0^\infty \left(1 - \prod_{i=1}^{n} P(n_i, t\dot{J}_i)\right)\, dt \tag{3.3}$$

and the expected value of the cycle period is $\mathcal{E}\underline{t}_c = \dot{J}_{Xm}^{-1} + \mathcal{E}\underline{t}_b$. The mean production rate, therefore, occurs at intensity $\dot{J}_X = (\dot{J}_{Xm}^{-1} + \mathcal{E}\underline{t}_b)^{-1}$ for a single SU, and $\dot{J}_X = ((s\dot{J}_{Xm})^{-1} + \mathcal{E}\underline{t}_b)^{-1}$ for a set of s SUs. The intensity of the rejected substrate molecules of type i amounts to $\dot{J}_i/\rho_i - n_i\dot{J}_X$, where arriving substrate molecules of type i are bound with probability ρ_i if the SU is in the binding stage.

For two possibly limiting nutrients, so $n = 2$, (3.3) reduces to

$$\mathcal{E}\underline{t}_b = \frac{n_1}{\dot{J}_1} + \frac{n_2}{\dot{J}_2} - \sum_{i=0}^{n_1-1} \sum_{j=0}^{n_2-1} \frac{(i+j)!}{i!\, j!} \frac{\dot{J}_1^i \dot{J}_2^j}{(\dot{J}_1 + \dot{J}_2)^{i+j+1}} \tag{3.4}$$

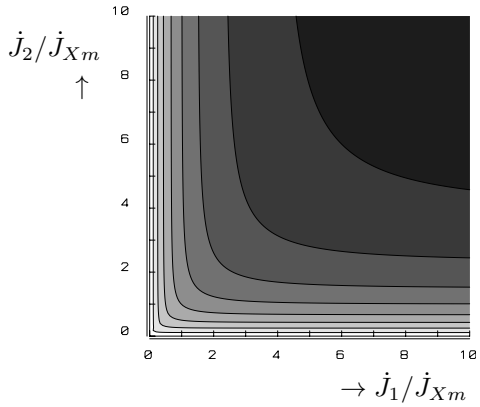

Figure 3.4: The 0.1(0.1)0.7 contours of the scaled production flux $\dot{J}_X/\dot{J}_{Xm}$ as function of the scaled substrate supply fluxes $\dot{J}_1' = \dot{J}_1/\dot{J}_{Xm}$ and $\dot{J}_2' = \dot{J}_2/\dot{J}_{Xm}$ for a 1,1-SU. The production flux for a 1,1-SU simplifies to $\dot{J}_X = \left(\dot{J}_{Xm}^{-1} + \dot{J}_1^{-1} + \dot{J}_2^{-1} - (\dot{J}_1 + \dot{J}_2)^{-1}\right)^{-1}$.

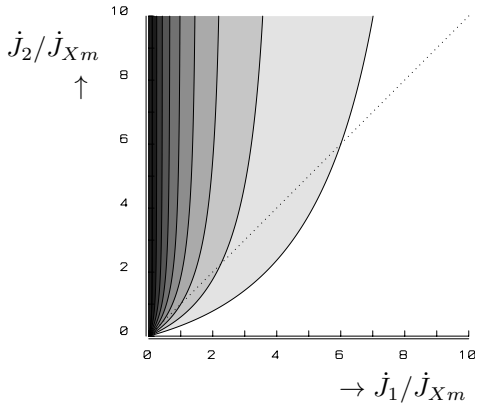

Figure 3.5: The 0.1(0.1)0.9 contours (right to left) of the flux control coefficients $\frac{\partial \ln \dot{J}_X}{\partial \ln \dot{J}_1'}$ of the substrate flux $\dot{J}_1'$ on the production flux $\dot{J}_X$ for a 1,1-SU. The flux control coefficients for substrate $\dot{J}_2$ can be obtained by interchanging the labels on the axes. The stippled line marks $\dot{J}_1 = \dot{J}_2$.

and for three possibly limiting nutrients

$$\mathcal{E}\underline{t}_b = \sum_{i=1}^{3} \frac{n_i}{\dot{J}_i} - \sum_{i_2>i_1=1}^{3} \sum_{i=0}^{n_{i_1}-1} \sum_{j=0}^{n_{i_2}-1} \frac{(i+j)!}{i!\,j!} \frac{\dot{J}_{i_1}^i \dot{J}_{i_2}^j}{(\dot{J}_{i_1} + \dot{J}_{i_2})^{i+j+1}} + \\ + \sum_{i_3>i_2>i_1=1}^{3} \sum_{i=0}^{n_{i_1}-1} \sum_{j=0}^{n_{i_2}-1} \sum_{k=0}^{n_{i_3}-1} \frac{(i+j+k)!}{i!\,j!\,k!} \frac{\dot{J}_{i_1}^i \dot{J}_{i_2}^j \dot{J}_{i_3}^k}{(\dot{J}_{i_1} + \dot{J}_{i_2} + \dot{J}_{i_3})^{i+j+k+1}} \tag{3.5}$$

from which it is obvious how this expression generalises for a larger number of possibly limiting substrates. There is no need to evaluate the integral in (3.3), when it comes to practical computations. Note that the first summation in the last (i.e. third) summation term in (3.5) only contains one element. The first summation in the middle summation term contains three elements.

Figure 3.4 illustrates that the 1,1-SU behaves very like a minimum operator for small substrate supply fluxes. This can be quantified using the Metabolic Control Analysis [584], which shows that the flux control coefficients $\frac{\partial \ln \dot{J}_X}{\partial \ln \dot{J}_i}$ rapidly decrease for increasing substrate concentrations, see Figure 3.5. The elasticity coefficients, which quantify the effect of a change in the SU concentration on the production flux, are $\frac{\partial \ln \dot{J}_X}{\partial \ln s} = \frac{\dot{J}_X}{s\dot{J}_{Xm}}$. When a 1,1-SU binds sequentially, the production rate is $\dot{J}_X = \left(\dot{J}_{Xm}^{-1} + \dot{J}_1^{-1} + \dot{J}_2^{-1}\right)^{-1}$, which is obviously lower than that obtained using parallel binding. An important implication of SUs behaving like a minimum operator is that abundant substrates do not matter, and only possibly limiting substrates need to be followed explicitly.

The supply fluxes of substrates to the SU can result from convection or diffusion processes, which makes it likely that they are proportional to the concentration X_i of substrate

in the local environment of the SU and the number of SUs. The 1-SU then behaves quantitatively according to the familiar MM-kinetics [591, 970]. Most texts on this kinetics [1280, 1281] assume a reversible binding to the enzyme, however. For the 1-SU such an extension hardly complicates the model. The 1,1-SU requires 9 binding and dissociation rates to quantify the production process [60, 966], but reversible binding becomes really complex for the multi substrate–multi copy enzymes. It requires the kinetics of all possible combinations of partially filled enzyme–substrate complexes to be specified [1200], which is not only cumbersome, but also involves a huge amount of parameters. The Carrier-Synthesising Unit complex allows reversible binding with relative ease, see below.

3.7.3 Production of generalised compounds

As might be expected, an increase in substrate concentration almost cancels against an increase in stoichiometric requirements, so $\dot{J}_X$ is rather insensitive to multiplication of both $\dot{J}_i$ and n_i by an arbitrary factor. This allows the use of SUs to quantify the production of generalised compounds. The product flux of a $\{n_i\}_1^n$-SU approximates that of a $1,1,\cdots,1$-SU, when we replace $\dot{J}_i$ by $\dot{J}_i/n_i$, resulting in

$$\dot{J}_X = \left(\dot{J}_{Xm}^{-1} + \sum_{i_1=1}^{n} \left(\frac{\dot{J}_{i_1}}{n_{i_1}} \right)^{-1} - \sum_{i_2>i_1=1}^{n} \left(\sum_{j=1}^{2} \frac{\dot{J}_{i_j}}{n_{i_j}} \right)^{-1} + \sum_{i_3>i_2>i_1=1}^{n} \left(\sum_{j=1}^{3} \frac{\dot{J}_{i_j}}{n_{i_j}} \right)^{-1} - \cdots \right.$$

$$\left. \cdots - (-1)^n \sum_{i_n>\cdots>i_1=1}^{n} \left(\sum_{j=1}^{n} \frac{\dot{J}_{i_j}}{n_{i_j}} \right)^{-1} \right)^{-1} \tag{3.6}$$

As is obvious from the derivation, the constraints $n_i \dot{J}_X < \dot{J}_i$ apply for all $i = 1, 2, \cdots n$.

Many applications of SUs not only involve generalised compounds, but also generalised enzymes that catalyse the transformation. They can be thought of as a set of enzymes that pass metabolites to each other, without accumulating pools of intermediary metabolites. The implication is that the transformation is halted instantaneously when one of the required substrate molecules is not (yet) available, and the SU ceases binding other substrates, until the generalised product molecule is delivered.

3.7.3 Mixed transformations

The four basic classes of transformations are sequential-substitutable (ss), sequential-complementary (sc), parallel-substitutable (ps) and parallel-complementary (pc). Mixed transformations can be written as weighted sums of these four basic types. The change in binding fractions is for $\dot{J}'_* = \rho_* \dot{J}_*$ and $\boldsymbol{\theta}^T = (\ \theta_{\cdot\cdot} \quad \theta_{A\cdot} \quad \theta_{\cdot B} \quad \theta_{AB}\ )$

$$\frac{d}{dt}\boldsymbol{\theta} \;=\; \dot{\boldsymbol{k}}\boldsymbol{\theta} \quad \text{with } \dot{\boldsymbol{k}} = w_{ss}\dot{\boldsymbol{k}}_{ss} + w_{sc}\dot{\boldsymbol{k}}_{sc} + w_{ps}\dot{\boldsymbol{k}}_{ps} + w_{pc}\dot{\boldsymbol{k}}_{pc}$$

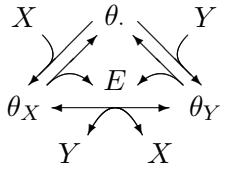

Figure 3.6: The conversion $X \to E$ and $Y \to E$ with interaction. θ_* indicates the fraction of Synthesising Units that is bound to substrate $*$.

$$\dot{\boldsymbol{k}} = \begin{pmatrix} -\dot{k}_{A\cdot,\cdot\cdot} - \dot{k}_{\cdot B,\cdot\cdot} & \dot{k}_{\cdot\cdot,A\cdot} & \dot{k}_{\cdot\cdot,\cdot B} & \dot{k}_{\cdot\cdot,AB} \\ \dot{k}_{A\cdot,\cdot\cdot} & -\dot{k}_{\cdot\cdot,A\cdot} - \dot{k}_{\cdot B,A\cdot} & 0 & \dot{k}_{A\cdot,AB} \\ \dot{k}_{\cdot B,\cdot\cdot} & 0 & -\dot{k}_{\cdot\cdot,\cdot B} - \dot{k}_{AB,\cdot B} & \dot{k}_{\cdot B,AB} \\ 0 & \dot{k}_{\cdot B,A\cdot} & \dot{k}_{AB,\cdot B} & -\dot{k}_{\cdot\cdot,AB} - \dot{k}_{A\cdot,AB} - \dot{k}_{\cdot B,AB} \end{pmatrix}$$

$$\text{with} \quad \begin{array}{lll} \dot{k}_{A\cdot,\cdot\cdot} = \dot{J}'_A w_{++} & \dot{k}_{\cdot B,A\cdot} = \dot{J}'_B(w_{++} - w_{ss}) & \dot{k}_{\cdot\cdot,AB} = \dot{k}_C w_{+c} \\ \dot{k}_{\cdot B,\cdot\cdot} = \dot{J}'_B(w_{++} - w_{sc}) & \dot{k}_{\cdot\cdot,\cdot B} = \dot{k}_B w_{+s} & \dot{k}_{A\cdot,AB} = \dot{k}_B w_{ps} \\ \dot{k}_{\cdot\cdot,A\cdot} = \dot{k}_A w_{+s} & \dot{k}_{AB,\cdot B} = \dot{J}'_A w_{p+} & \dot{k}_{\cdot B,AB} = \dot{k}_A w_{ps} \end{array}$$

The zeros in $\dot{\boldsymbol{k}}$ relate to the assumption that transformations are orderly processes: within a time increment, at most one event can occur. This covers all possibilities with the constraint $\frac{\dot{k}_{\cdot\cdot,A\cdot}}{\dot{k}_{\cdot\cdot,\cdot B}} = \frac{\dot{k}_{\cdot B,AB}}{\dot{k}_{A\cdot,AB}} = \frac{\dot{k}_A}{\dot{k}_B}$. This constraint relates to a symmetry relationship between A and B in binding to the SU, which is removed in the class of co-metabolic transformations. Notice that $\dot{\boldsymbol{k}}$ has 9 degrees of freedom that can be expressed as functions of 4 weight coefficients w, 2 arrival rates $\dot{J}$ and 3 dissociation rates $\dot{k}$, which amounts to 8 degrees of freedom; if we multiply all rates with a constant, but divide all weight coefficients by that constant, nothing changes.

3.7.4 Preference

Eqn. (3.35) corresponds to the situation where S_1 can bind to an SU-S_2 complex to become an SU-S_1 complex, releasing substrate S_2 untransformed. Unfortunately, Figure 3.8 corresponds to the situation where S_2 can replace S_1, as indicated in the legends.

The preference scheme of Figure 3.8 is a special case of the interaction scheme of Figure 3.6 of the comments. The change in binding fractions for substrates X and Y and product E are

$$\begin{aligned} \frac{d}{dt}\theta_\cdot &= \dot{k}_X\theta_X + \dot{k}_Y\theta_Y - (\dot{b}_X X + \dot{b}_Y Y)\theta_\cdot \\ \frac{d}{dt}\theta_X &= -\dot{k}_X\theta_X + \dot{b}_X X\theta_\cdot - \dot{b}_{YX} Y\theta_X + \dot{b}_{XY} X\theta_Y \\ \frac{d}{dt}\theta_Y &= -\dot{k}_Y\theta_Y + \dot{b}_Y Y\theta_\cdot + \dot{b}_{YX} Y\theta_X - \dot{b}_{XY} X\theta_Y \end{aligned}$$

with $1 = \theta_\cdot + \theta_X + \theta_Y$ and X and Y stand for the densities of substrates X and Y in moles per volume (or surface area). The pseudo steady state fractions are

$$\theta^*_X = \frac{\alpha_Y \dot{b}_X X - \beta_X \dot{b}_Y Y}{\alpha_X\alpha_Y - \beta_X\beta_Y}; \quad \theta^*_Y = \frac{\alpha_X \dot{b}_Y Y - \beta_Y \dot{b}_X X}{\alpha_X\alpha_Y - \beta_X\beta_Y}$$

with

$$\alpha_X = \dot{k}_X + \dot{b}_X X + \dot{b}_{YX} Y; \quad \alpha_Y = \dot{k}_Y + \dot{b}_Y Y + \dot{b}_{XY} X; \quad \beta_X = \dot{b}_X X - \dot{b}_{XY} X; \quad \beta_Y = \dot{b}_Y Y - \dot{b}_{YX} Y$$

The product flux amounts to $\dot{J}_E = y_{EX} M_X \dot{k}_X \theta_X^* + y_{EY} M_Y \dot{k}_Y \theta_Y^*$ and the fluxes of used substrates to $\dot{J}_X = M_X \dot{b}_X \theta_\cdot^* + M_X \dot{b}_{XY} \theta_Y^* - M_Y \dot{b}_{YX} \theta_X^*$ and $\dot{J}_Y = M_Y \dot{b}_Y \theta_\cdot^* + M_Y \dot{b}_{YX} \theta_X^* - M_X \dot{b}_{XY} \theta_Y^*$. In absence of interaction, $\dot{b}_{XY} = 0$ and $\dot{b}_{YX} = 0$, this transformations reduce to sequential processing of substitutable compounds. Notice the symmetry in X and Y of all expressions.

This interaction scheme can be used to model dynamic preferences as described in Subsection 5 of the comments for a 2-food, 2-reserve system. The concept of preference is closely linked to that of inhibition. Think, for instance, about the situation that an individual becomes a specialist of catching one type of prey species and ignores other species unless that species becomes very rare (meaning that the ingestion rates drops far below the maximum). It is as if the target species inhibits the catching of other species, a situation worked out in Section 7.9.4.

3.7.4 Derivation of Eq (3.39)

The derivation of demand kinetics , Eq (3.39), for 2 substrates-with-preference assumes that the supply kinetics which leads to Eq (3.36) still applies. The difference is that the dissociation rate parameters $\dot{k}_{S_1}$ and $\dot{k}_{S_2}$ are no longer constant, but depend on the fractions of SUs that are free, or bound to S_1 or S_2. This dependence is such that the delivery rate of product P, $\dot{k}_P$ is constant (as long as substrate supply allows). This product can be formed from substrate S_1, with yield y_{PS_1}, or from substrate S_2, with yield y_{PS_2}. So $j_P = y_{PS_1} j_{S_1}^+ + y_{PS_2} j_{S_2}^+$, where $j_{S_i}^+$ denotes the flux of substrate that is accepted by the SUs. The flux of substrate S_i that arrives is called j_{S_i}, but part of this flux is rejected because a fraction of the SUs was already bounded by substrate at the moment of arrival. The arriving flux equals the accepted flux plus the rejected flux: $j_{S_i} = j_{S_i}^+ + j_{S_i}^-$. The lowercase for the fluxes is used, rather than the upper case, because the fluxes depend on the number of SUs, which is taken to be constant in the derivation. The flux of product j_P in the demand-formulation is considered to be constant, so is in fact a model parameter. To express this difference in nature with the substrate fluxes (which depend on substrate availability), j_P is replaced by the parameter $\dot{k}_P$. So

$$\dot{k}_P = y_{PS_1} j_{S_1}^+ + y_{PS_2} j_{S_2}^+ = y_{PS_1} \dot{k}_{S_1} \theta_{S_1} + y_{PS_2} \dot{k}_{S_2} \theta_{S_2}$$

Both dissociation rates depend on the bound fractions, but we now further restrict freedom by assuming that ratio of the dissociation rates, $\rho_{S_2} = \dot{k}_{S_2} / \dot{k}_{S_1}$, remains constant, so ρ_{S_2} is a parameter. Substitution gives

$$\dot{k}_P = \dot{k}_{S_1} (y_{PS_1} \theta_{S_1} + \rho_{S_2} y_{PS_2} \theta_{S_2}) = \dot{k}_{S_1} \theta$$

for $\theta = y_{PS_1} \theta_{S_1} + \rho_{S_2} y_{PS_2} \theta_{S_2}$. From an application perspective it is important to know how much substrates is actually used per unit of time for product formation, i.e. j'_{S_i}. If

we know one of them, the other follows from the relationship $\dot{k}_P = y_{PS_1} j^+_{S_1} + y_{PS_2} j^+_{S_2}$, since $j^+_{S_i} = \dot{k}_{S_i}\theta_{S_i}$. The changes in the fractions is given in Eq (3.35) and we assume that the fractions are in pseudo steady state (i.e. $\frac{d}{dt}\theta_{S_i} = 0$ for $\theta_{S_i} = \theta^*_{S_i}$), using a time-scale separation argument. The equilibrium values get an $*$ to differentiate them from the time-varying fractions. Writing primes for multiplication by a (constant) binding probability upon arrival of a substrate molecule to a free SU, we get from Eq (3.36)

$$\theta^*_{S_1} = \frac{j'_{S_1}}{\dot{k}_{S_1} + j'_{S_1}} \quad \text{and} \quad \theta^*_{S_2} = \frac{\dot{k}_{S_1} j'_{S_2}}{(\dot{k}_{S_1} + j'_{S_1})(\dot{k}_{S_2} + j'_{S_1} + j'_{S_2})}$$

but the varying $\dot{k}_{S_i}$ values need to be replaced now using $\dot{k}_{S_1} = \dot{k}_P/\theta$ and $\dot{k}_{S_2} = \rho_{S_2}\dot{k}_{S_1}$. From the latter 2 equations we have $j^+_{S_2} = \rho_{S_2}\dot{k}_P\theta^*_{S_2}/\theta^*$. Substitution of $\theta^*_{S_2}$ and θ^* gives the equation $Ax^2+Bx+C = 0$, with $x = \frac{\theta^*_{S_1}}{\rho_{S_2} y_{PS_2} \theta^*_{S_2}}$, from which x can be solved. An alternative derivation, due to Jaap van der Meer, is to solve $\dot{k}_{S_1}$ from $\dot{k}_P = \dot{k}_{S_1}(y_{PS_1}\theta^*_{S_1} + \rho_{S_2} y_{PS_2}\theta^*_{S_2})$, which can be rewritten in the form $A\dot{k}^2_{S_1} + B\dot{k}_{S_1} + C = 0$, with $A = \rho_{S_1}(y_{PS_1} j'_{S_1} + y_{PS_2} j'_{S_2} - \dot{k}_P)$, $B = y_{PS_1} j'_{S_1}(j'_{S_1} + j'_{S_2}) - \dot{k}_P(\rho_{S_2} j'_{S_1} + j'_{S_1} + j'_{S_2})$, $C = -\dot{k}_P j'_{S_1}(j'_{S_1} + j'_{S_2})$. Back-substitute this value for $\dot{k}_{S_1}$ and $\dot{k}_{S_2} = \rho_{S_2}\dot{k}_{S_1}$ in $\theta^*_{S_2}$ and θ^*. The accepted flux of substrate S_2 again becomes $j^+_{S_2} = \rho_{S_2}\dot{k}_P\theta^*_{S_2}/\theta^*$.

3.7.5 Co-metabolism

The text discusses the situation where A as well as B can be transformed to C; Notice that the scheme in Figure 3.9 is more general: B is transformed to D. The situation that D is identical to C is a special case.

3.8 Metabolism

3.8.1 Trophic modes

The aphid *Acyrthosiphon pisum* can synthesise carotenoids with which, under favourable conditions, it can extract energy from light to drive ATP synthesis [1453]. The genes for this synthesis probably orinigate from bacteria or fungi; the carotenoids are not extracted from food. Green phenotypes could be selected from orange ones at 8 °C that were exceptionally rich in carotenoids; the green phenotype is heritable, supporting the hypothesis of epigenetic regulation, but fades away at 22 °C. The ability to synthesise carotenoids seems to be unique among animals.

Desulfobulbus forms colonies in the from of threads from the ocean bottom surface to a centimeter deep down to transport electrons. This distance is enough to link dioxygen-rich to hydrogen sulfide-rich environments to extract energy from H_2S oxydation, see Figure 3.7.

The sulphur bacterium *Achromatium oxaliferum* lives on freshwater sediments in steep dioxygen gradients, where it oxydises sulphur and iron and can fix inorganic carbon [1257].

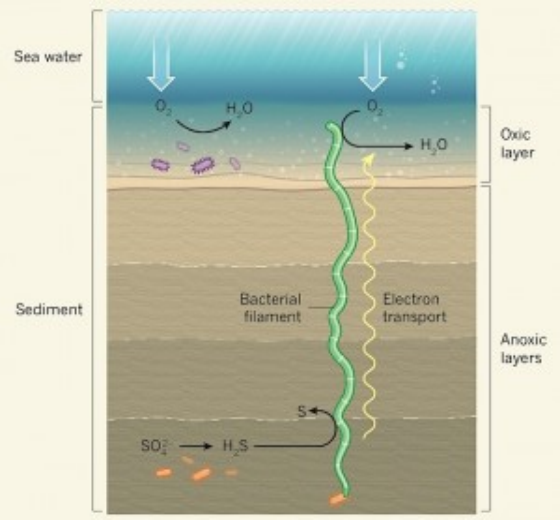

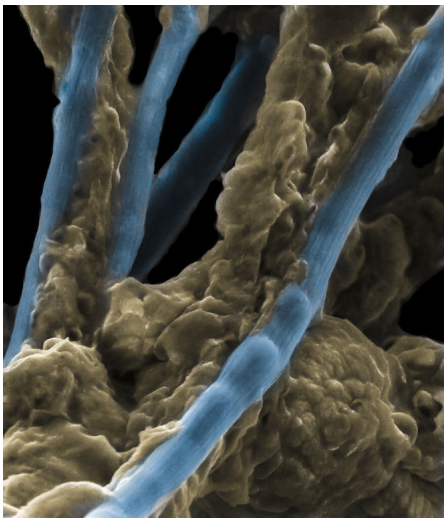

Figure 3.7: The bacterium *Desulfobulbus* forms multicellular threats to transport electons and extract energy from the oxydation of H_2S [1095].

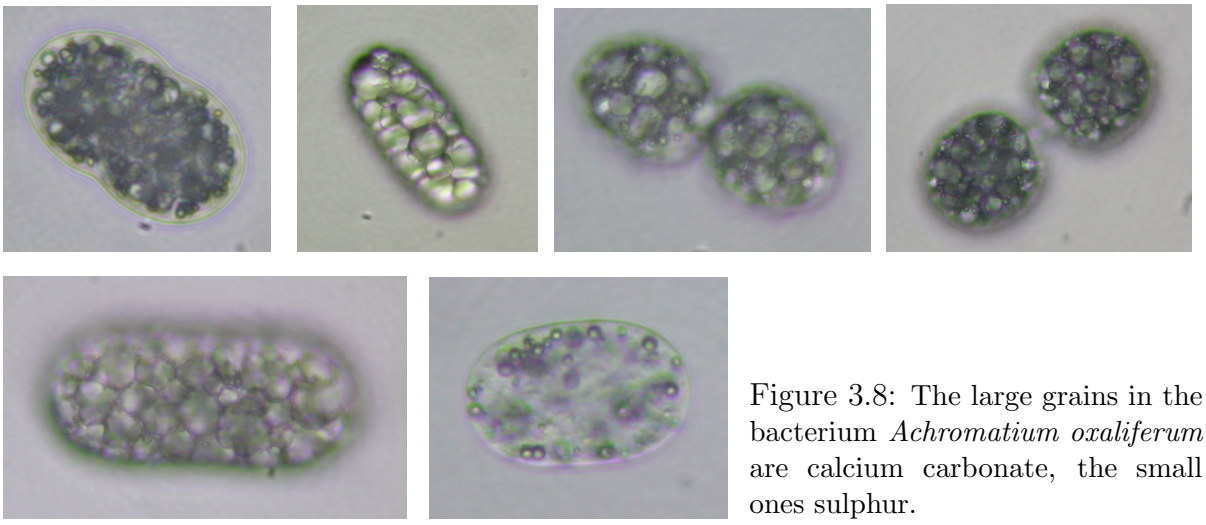

Figure 3.8: The large grains in the bacterium *Achromatium oxaliferum* are calcium carbonate, the small ones sulphur.

It only occurs in environments that are rich in dissolved Fe^{2+} and is the only organism known to store $CaCO_3$ intracellularly (large grains), see Figure 3.8; Coccolithophorans (a group of haptophyta) form carbonate platelets intracellularly, but then export them. *A.oxaliferum* does not store $CaCO_3$ in acidic environments, where CO_2 predominates HCO_3^-. Both iron and sulphur oxidation consume protons and so promotes HCO_3^- and $CaCO_3$ formation, reducing the flux of CO_2 to RuBiSCO for C-fixation. A possible candidate transformation that explains $CaCO_3$ and S accumulation is [517]:

$$2\,FeS + 2\,Ca^{2+} + 2\,CO_2 + O_2 \rightarrow 2\,S + 2\,CaCO_3 + 2\,Fe^{2+}$$

The anaerobic methanotroph *Methylomirabilis oxyfera* is able to oxidize methane anearobically while reducing nitrite and producing dioxygen and dinitrogen, without producing other nitrogen oxides [399]. This pathway for dioxygen production might have preceded that via oxygenic photosynthesis.

3.9 Auxiliary theory for the standard DEB model

The variables of the standard DEB model cannot be measured directly, only indirectly. Auxiliary theory deals with the relationships between quantities that can be measured and model variables. Its assumptions for the standard DEB model are

- A well-chosen physical length of the body is proportional to (volumetric) structural length; the proportionality constant is called the shape correction factor $\delta_{\mathcal{M}}$. It is constant because of the assumption of isomorphy in the standard DEB model.
- Volume, wet weight and dry weight have contributions from structure, reserve and the reproduction buffer.
- A unit of structure, reserve and reproduction buffer as a constant mass and occupied a constant volume on the basis of strong homeostasis. The specific chemical and physical properties on these three quantities are constant (chemical composition, chemical potential, specific entropy). Water might be an exception in some taxa (where water can replace decreasing reserve, for instance). The relationship between mass and volume can be more complex in terrestrial ecdysozoa (e.g. insects, where air can replace decreasing reserve).
- The chemical composition of juveniles growing at constant food levels remains constant. The comparison of the chemical composition of juveniles growth at different food levels gives access to the chemical composition of reserve and structure. The situation for adults is complicated by the role of the reproduction buffer.

Notice that the standard DEB model does not deal with fast pools, such as the digestive systems and blood (see Chapter 7). The time scale of the dynamics of the faster pools should be taken into account in the interpretation of data in the context of the standard DEB model. Gut content might contribute to weight in reality, but is ignored in the standard DEB model, so linking measurements to predictions by the standard DEB model should take this into account. A similar problem relates to the use of time. The standard DEB model

only recognises searching for food and handling of food. So everything an individual does (such as sleeping) should be classified into these two categories.

Future developments in the application of DEB theory might use chemical proxies for the amounts of reserve and stucture. Subsection 4.3.3 states that DNA belongs to structure and rRNA possibly belongs to reserve. Other proxies might be found as well; some of them might be taxon-specific. Further experience will learn to what extend such proxies are useful and give satisfactory results. Variables that are hidden at this moment not necessarily remain hidden in the future.

4

Univariate DEB models

4 Multiple-reserve as one-reserve systems

Organisms that take their various substrates from the environment independently of each other can, under particular conditions, still be modelled as one-reserve systems. So there is not always a need to include all reserves explicitly. This can be seen using the following argument and the notation is further developed in chapter 5.

If all rejected reserve fluxes are excreted, we have $\kappa_{E_i} = 0$ and in steady state $m_{E_i} = j_{E_iA}/\dot{k}_E$ (see (5.17) for $\frac{d}{dt} m_{E_i} = 0$), which means that m_{E_i} is constant if j_{E_iA} is constant, so if the concentration of the i-th nutrient in the medium is constant. The concentration of nutrients depend on the growth rate in a chemostat. If the concentration of the non-limiting nutrients is large relative to the half saturation constant, we have $j_{E_iA} \simeq j_{E_iAm}$ for i unequal to the limiting one, which is independent of the growth rate and the non-limiting reserves count as parts of the structure in the analysis of the chemical composition.

4.1 Changing feeding conditions

McCue [937] reviews starvation physiology and noticed that some small birds and mammals may tolerate only one day of starvation, some snakes and frogs two years, and the European eel *Anguilla anguilla* holds the record of surviving for 1594 d under non-hibernation conditions. He reports that the mean relative weight loss in endotherms is almost always higher than that of ectotherms, which is doubtlessly linked to the maintenance rate being body temperature dependent. Mass reductions during starvation by a factor 0.5 are no exception, but this differs between organs, probably linked to functional aspects. Some amphibians and fish are known to increase water content during starvation; the water content of reserve might be less than that of structure, but water might also escape the strong homeostasis rules. The very long survival times during starvation can only be understood from the ability to shut down maintenance costs. A satisfactory inclusion of this process involves considerable biochemical 'detail'.

4.1.4 Prolonged starvation

Atlantic hagfish (*Myxine glutinosa*), living in deep waters (120 till 1200 m), feed on carrion, e.g. dead mammals that sink to the ocean bottom in addition to small animals that share their muddy habitat. Both male and female gonads develop till near maturity, but then one of the types degenerate; functional hermaphrodites are being very rare and the female:male ratio in catches is 99:1. The incidence of egg resorption (atresia) is very high and the reproduction cycle is not synchronised. No method is presently available to access their age, so parameter values are speculative by necessity. Yet, using data of Scott Grant (pers. comm.) and assuming a reproductive cycle of a year, the estimated value of $\kappa = 0.76$ (see add_my_pet), while estimated ages at birth and puberty are $a_b = 131$ d and $a_p = 1082$ d at 5°C and abundant food for a typical value of the energy conductance $\dot{v} = 0.098\,\mathrm{cm\,d^{-1}}$ and the Arrhenius temperature $T_A = 8$ kK. This combination of values suggests that juveniles mainly feed on the low density of small-bodied fauna and the adult females use their reproduction buffer as an extended reserve. Large males may be rare because of the likely occurrence of large periods between finding carrion to feed on, while the density of small-bodies fauna is too low to cover their maintenance costs; the minimum food level for longer survival increases with size ($f = l_i$). The species probably have developed ways avoiding frequent death of adult males.

4.1.5 Shrinking during starvation

The derivation of (4.5) from (3.39) is on the basis of the following substitutions: $\dot{k}_P = j_{ES}$, $y_{PS_1} = 1$, $y_{PS_2} = j_{ES}/j_{VS}$, $\rho_{S_2} = \rho_V/y_{EV}$, $j'_{S_1} = \kappa j_{EC}$ and $j'_{S_2} = y_{EV} j_{VC}$. P has the interpretation of maintenance products, S_1 of reserve, S_2 of structure. The role of y_{EV} in the substitutions is on dimensional grounds: A, B and C are all squared specific fluxes of reserve.

The equivalent of (4.6) for allocation of energy from reserve and structure to somatic maintenance reads

$$[\dot{p}_S^E] = \min\{[\dot{p}_S], \kappa[\dot{p}_C]\} \quad \text{and} \quad [\dot{p}_S^V] = [\dot{p}'_S](1 - [\dot{p}_S^E]/[\dot{p}_S]) \tag{4.1}$$

where $[\dot{p}'_S] = [\dot{p}'_M] + \{\dot{p}'_T\}/L$ is the volume-specific somatic maintenance costs if fully paid from structure. A natural simplification is to assume that $[\dot{p}'_M]/[\dot{p}_M] = \{\dot{p}'_T\}/\{\dot{p}_T\}$. If maintenance would be an energy demand only (i.e. no building block aspects), a further simplification would be $[\dot{p}'_S] = [\dot{p}_S]$, where the energy is mobilised from the pool $\mu_V M_V = \mu_V [M_V] L^3$. The energy invested to create that pool was $[E_G] L^3 > \mu_V [M_V] L^3$, so paying maintenance from structure increases the somatic maintenance costs by a factor $\kappa_G^{-1} = \frac{[E_G]}{\mu_V [M_V]}$. The fraction κ_G has the intepretation of a growth efficiency. For $E_V = \mu_V M_V = \mu_V [M_V] L^3$, we have $\frac{d}{dt} E_V = \kappa_G \dot{p}_G$.

The specific mobilisation rate is given in (2.12): $[\dot{p}_C] = [E_m] e (\dot{v}/L - \dot{r})$. During shrinking we have $[\dot{p}_S^E] = \kappa[\dot{p}_C]$ and $[\dot{p}_S^V] = [\dot{p}'_S](1 - \kappa[\dot{p}_C]/[\dot{p}_S])$. This gives the shrinking rate implicitly

from $-\dot{r}\mu_V[M_V] = [\dot{p}'_S](1-\kappa[\dot{p}_C]/[\dot{p}_S])$. The (negative) specific growth rate then equals

$$\dot{r} = \frac{e\frac{\dot{v}}{L} - \frac{[\dot{p}_S]}{\kappa[E_m]}}{e + \frac{\mu_V[M_V]}{\kappa[E_m]}\frac{[\dot{p}_S]}{[\dot{p}'_S]}} = \dot{k}_M g \frac{e/l - 1 - l_T/l}{e + \frac{\mu_V[M_V]}{\kappa[E_m]}\frac{[\dot{p}_S]}{[\dot{p}'_S]}} \overset{[\dot{p}_S]=[\dot{p}'_S]}{=} \dot{k}_M g \frac{e/l - 1 - l_T/l}{e + \kappa_G g} \tag{4.2}$$

The last expression very much resembles the expression for positive specific growth rates, we just have to take $\kappa_G = 1$. Notice that $\dot{r} = 0$ if $\kappa[\dot{p}_C] = [E_m]e\dot{v}/L = [\dot{p}_S]$ or $e\dot{v}/L = (1 + l_T/l)g\dot{k}_M$ or $e = l + l_T$. Further discussion is given in [53].

If shrinking is allowed, we need a death-rule, e.g. death by starvation occurs if shrinking of structure exceeds a given fraction of the original structure (at the onset of ceasing growth). The planarian *Dugesia polychroa* can shrink form 15 to 3 mm and fully recover from this after resuming feeding [71]. Shrinking might be rather widespread, even among species with an internal skeleton. The Dehnel phenomenon was mentioned in Section 4.1.5 for shrews; Galápagos marine iguanas (*Amblyrhynchus cristatus*) can shrink 20% (6.8 cm) within 2 years [1541].

4.1.5 Rejuvenation during starvation

During prolonged starvation, not only structure, but also maturity can shrink if the allocated reserve to maturity maintenance plus maturation (or reproduction) is not sufficient to cover the maturity maintenance costs, $(1-\kappa)\dot{p}_C < \dot{k}_J E_H$. This is behind strategy 2 in section 4.1.4 when κ is increased when the allocation to maturation (or reproduction) is already ceased. This implies that the whole flux $(1-\kappa)\dot{p}_C$ is already allocated to maturity maintenance; Empirical support comes from [1417], as mentioned in section 2.5.3. Reserve can never be exhausted completely, thus the mobilisation rate $\dot{p}_C$ can never go down to zero, so there is always some maturity level that can be maintained; it amounts to $(1-\kappa)\dot{p}_C/\dot{k}_J$. The simplest implementation of the rejuvenation process is an exponential decay from E_H to this level at rate $\dot{k}'_J$, say, so

$$\frac{d}{dt}E_H = -\dot{k}'_J(E_H - (1-\kappa)\dot{p}_C/\dot{k}_J) \quad \text{or} \tag{4.3}$$

$$\frac{d}{dt}M_H = -\dot{k}'_J(M_H - (1-\kappa)\dot{J}_{EC}/\dot{k}_J) \tag{4.4}$$

If $\dot{k}'_J = \dot{k}_J$, decrease and increase of maturity follows the same expression. An extreme situation is that $\dot{k}'_J = 0$, and maturity maintenance is "voluntary". The general idea is that maturity maintenance includes ((bio)chemical) defence and this system is no longer 'updated' e.g. with the side effect that the hazard rate is taken proportional to the fraction of maturity that is not maintained, so $\dot{h} \propto (1 - \frac{(1-\kappa)\dot{p}_C}{\dot{k}_J E_H})_+$. Alternatively, the effect on the hazard can be linked to 'attack' events by pathogens. Like the situation of shrinking of structure, it seems realistic to install a death-rule e.g. death by starvation occurs if shrinking maturity exceeds a given fraction of the original maturity (at the onset of ceasing maturation).

For scaled maturity $v_H = \frac{E_H}{g[E_m]L_m^3(1-\kappa)}$, and $[\dot{p}_C] = [E](\dot{v}/L - \dot{r})$, and scaled time $\tau = t\dot{k}_M$, we have

$$\frac{d}{dt}v_H = -\dot{k}'_J(v_H - l^2e(\dot{k}_M - l\dot{r}/g)/\dot{k}_J) \quad \text{or} \tag{4.5}$$

$$\frac{d}{d\tau}v_H = -k'_J(v_H - l^2e(1 - lr/g)/k_J) \tag{4.6}$$

where $r = \dot{r}/\dot{k}_M$, $k'_J = \dot{k}'_J/\dot{k}_M$, $k_J = \dot{k}_J/\dot{k}_M$. Further discussion is given in [53].

Empirical support for rejuvenation in response to feeding stress not only comes from krill, see [1417] as discussed in subsection 2.5.3, but also from the beetle *Trogoderma glabrum*, [97]. Earthworms, *Dendrobaena octaedra*, loose their clitellum (which plays a role in reproduction) when cultured at high density (so low amount of food per individual), and get it back when better fed (much) later on (pers. comm Tjalling Jager). This is handy when juvenile individuals are required for bioassays. Starving fully mature medusae of the hydropolyp *Turritopsis nutricula* can even back-transform to colonial polyps and can completely reverse their life cycle [1106].

4.1.7 Dormancy

Food shortage coincides with low temperature in cold temperate seas, which is typically avoided by linking rates to temperature. Metabolic rates are then depressed compared to what can be expected on the basis of the Arrhenius relationship. Coma et al [266] report that benthic invertebrates in warm temperate seas have their resting phase in the summer, following a variety of strategies among bryozoans, bivalves, sponges, hydrozoans and ascidians. Most species in the temperate zone follow a year cycle, where some species are only active during spring, while others are during summer or winter. These patterns are the result of several factors, rather then the availability of a single nutrient; water, temperature, light, vectors for pollination or seed dispersal, a variety of nutrients can interactively influence when species peak their metabolism.

Lack of water (and so of food) is for many (terrestrial) species a trigger to switch to the torpor state. Lungfish, tenrecks, desert frogs and plants are familiar examples, but the phenomenon is widespread. Tardigrades master the art in extreme and can recover from torpor even after 120 years, if they have been able to store enough trehalose before entering [649]. Only during World War II it was discovered that baker's yeast, *Saccharomyces cerevisiae*, can only enter torpor by desiccation if nutrient, but not energy starved, in which case large amounts of trehalose accumulate, see Subsection 5.2.4 on damming up. Trehalose not only provides an energy storage, but also protects membranes during desiccation [649].

Geiser [473] delineates two types of torpor: by low temperature and by metabolic inhibition in combination with low temperature. He observes that endothermic hibernators (mammals and one bird species, *Phalaenoptlius nuttallii*) are typically small (10 to 1000 g) with a medium mass of 85 g.

4.1.8 Emergency reproduction

Myxobacteria (e.g. *Stigmatella*) respond to starvation by aggregation, the formation of a fruiting body which produces spores [588] in ways that are well-captured by DEB theory. This is an example of emergency reproduction. The life cycle of myxobacteria shares a lot of features with those of myxamoeba (cellular and acellular slime moulds, e.g. *Dictyostelium*) and the heterolobosean *Acrasis*.

4.2 Changing shapes

If individuals change in shape during growth, physical length is a poor quantifier for size, but volumetric structural length defined as $L = V^{1/3}$ is still useful. The shape coefficient $\delta_{\mathcal{M}}$, converting some physical length to volumetric length, see Section 1.2.3, changes with length if shape changes. The idea of the shape correction function $\mathcal{M}(V)$ is to multiply all 'per surface area'-parameters with it, to know how functions of those parameters behave for individuals that change in shape. The primary parameters are listed in Table 8.1, and only $\{\dot{F}_m\}$, $\{\dot{p}_{Am}\}$, $\{\dot{p}_T\}$ and $\dot{v}$ depend on surface area; dimension 'length' in $\dot{v}$ represents the ratio of a volume and a surface area. Maximum reserve density $[E_m] = \{\dot{p}_{Am}\}/\dot{v}$ is not affected by changes in shape, because $\{\dot{p}_{Am}\}$ and $\dot{v}$ are affected in the same way; so $e = [E]/[E_m]$ is also not affected. Maximum length $L_m = \frac{\dot{v}}{\dot{k}_M g} = \frac{\kappa\{\dot{p}_{Am}\}}{[\dot{p}_M]}$, however, should be multiplied by the shape correction function, since $\dot{k}_M$ and g, or κ and $[\dot{p}_M]$, are not affected.

An example of a function of parameters is the specific growth rate $\dot{r} = \dot{v}\frac{e/L - 1/L_m}{e+g} = \frac{\dot{v}e/L - g\dot{k}_M}{e+g}$, see (2.21) for isomorphs with $L_T = 0$. Isomorphs are V$\frac{2}{3}$-morphs and have shape correction function $\mathcal{M}(L) = 1$. The shape correction function of a V1-morph is $\mathcal{M}(L) = L/L_d$, see (4.11). So if we want to know the specific growth rate of V1-morphs, we find it from that of isomorphs by

$$\dot{r} = \frac{\mathcal{M}(L)\dot{v}e/L - g\dot{k}_M}{e+g} = \frac{e\dot{v}/L_d - g\dot{k}_M}{e+g} = \frac{e\dot{k}_E - g\dot{k}_M}{e+g}$$

for $\dot{k}_E = \dot{v}/L_d$, which is equivalent to (4.14) in the case that $\dot{J}_V^M = 0$ (no shrinking). Another example is the reserve residence time $t_E = \frac{1+e/g}{\dot{v}/L + \dot{k}_M}$ for an isomorph with $L_T = 0$, see Section 2.3 of the comments. For a V1-morph this becomes $t_E = \frac{1+e/g}{\dot{k}_E + \dot{k}_M}$. Notice that for constant e, both $\dot{r}$ and t_E are constant, i.e. independent of length, for V1-morphs. This 'trick' can be done for all properties that can be written as functions of states and parameters. Never do this for growth curves or cumulative reproduction, since changes in shape affect rates and these statistics integrate rates over time.

A nice confirmation of effects of changes in shape is found by White et al [1526] for encrusting bryozoans as dynamic mixtures of V0- and V1-morphs: just as expected their respiration is proportional to the square-root of mass and the diameter of the colonies is proportional to time in constant environments.

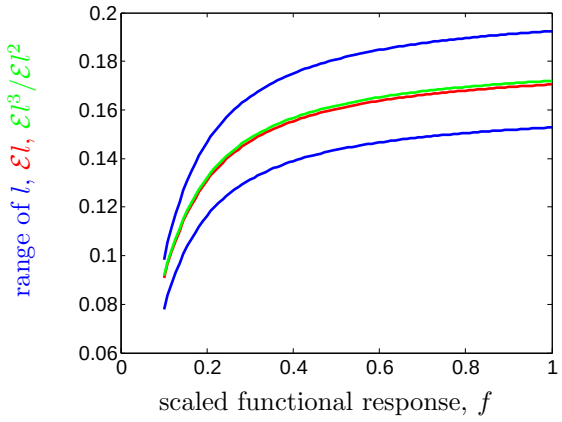

Figure 4.1: Scaled length at birth l_b and division l_d for an isomorph as function of scaled functional response, f, for $g = 1$, $k = 0.1$ and $v_H^d = 0.01$. The smallest f that allows division is 0.1. The mean length and the ratio of the mean volume and surface area are also indicated.

4.2.0 isomorphs

Although isomorphs, or V$\frac{2}{3}$-morphs, don't change shape during growth, this section is probably best to specify volume at division for dividing isomorphs, since chapter 2 deals with propagation via eggs or fetuses.

The volume at division should be found from $V_d = \int_{E_H^d/2}^{E_H^d} \frac{\frac{d}{dt}V}{\frac{d}{dt}E_H} dE_H$, with $\frac{d}{dt}V = \dot{r}V$, $\frac{d}{dt}E_H = (1-\kappa)\dot{p}_C - \dot{k}_J E_H$, $\dot{p}_C = e[E_m]V(\dot{v}/L - \dot{r})$ and $\dot{r} = \dot{v}\frac{e/L-1/L_m}{e+g}$. The initial condition $V(0) = V_d/2$ causes this equation for V_d to be an implicit one. Maturity density remains constant if $\dot{k}_J = \dot{k}_M$, from which follows $V_d = \frac{E_H^d/[E_m]}{(1-\kappa)g}$. This value can be used as an initial estimate in the case that $\dot{k}_J \neq \dot{k}_M$.

The number of parameters that are involved can be reduced by working with scaled quantities: scaled maturity $v_H = \frac{u_H}{1-\kappa}$ with $u_H = \frac{E_H}{g[E_m]L_m^3}$, scaled length $l = L/L_m$, maintenance ratio $k = \dot{k}_J/\dot{k}_M$. Just like (2.54), we have $\frac{d}{dv_H}l = \frac{(f-l)g/3}{fl^2(g+l)-kv_H(g+f)}$ and solve $l_d = \int_{v_H^b}^{v_H^d} \frac{dl}{dv_H} dv_H$ for $v_H^b = v_H^d/2$ and $l(v_H^b) = l_b = l_d 2^{1/3}$, starting from $l_d = (v_H^d)^{1/3}$. We now see that l_d only depends on k, g and v_H^d, while it only can exist if $f > l_d$. This lower boundary for f is $(kv_H^d)^{1/3}$, where we have $l_d = f$. DEBtool/alga/get_ld computes l_d and DEBtool/alga/get_ed_min computes the smallest f, see Figure 4.1.

The survivor function of the stable length distribution is given by (9.13) of the comments, so the probability density function is given by

$$\phi_{\underline{l}}(l) = -\frac{d}{dl}\Pr\{\underline{l} > l\} = \frac{2^{1+\ln\frac{f-l}{f-l_b}/\ln\frac{f-l_b}{f-l_d}}}{f-l}\frac{\ln 2}{\ln\frac{f-l_b}{f-l_d}}$$

DEBtool/alga/get_Eli computes, $\mathcal{E}l$, $\mathcal{E}l^2$ and $\mathcal{E}l^3$ at constant f.

4.2.0 V$\frac{1}{2}$-morphs

Euglena has a cylindrical cell that grows in diameter, not in length, and divides longitudinally. See Figure 4.2. Its surface area is (roughly) $2\pi L_r L_c$ and volume $\pi L_r^2 L_c$, where L_r is the changing cell radius and L_c the constant cell length. The cell tappers toward the ends, so the caps are not included in the surface area and L_c should be adjusted a little

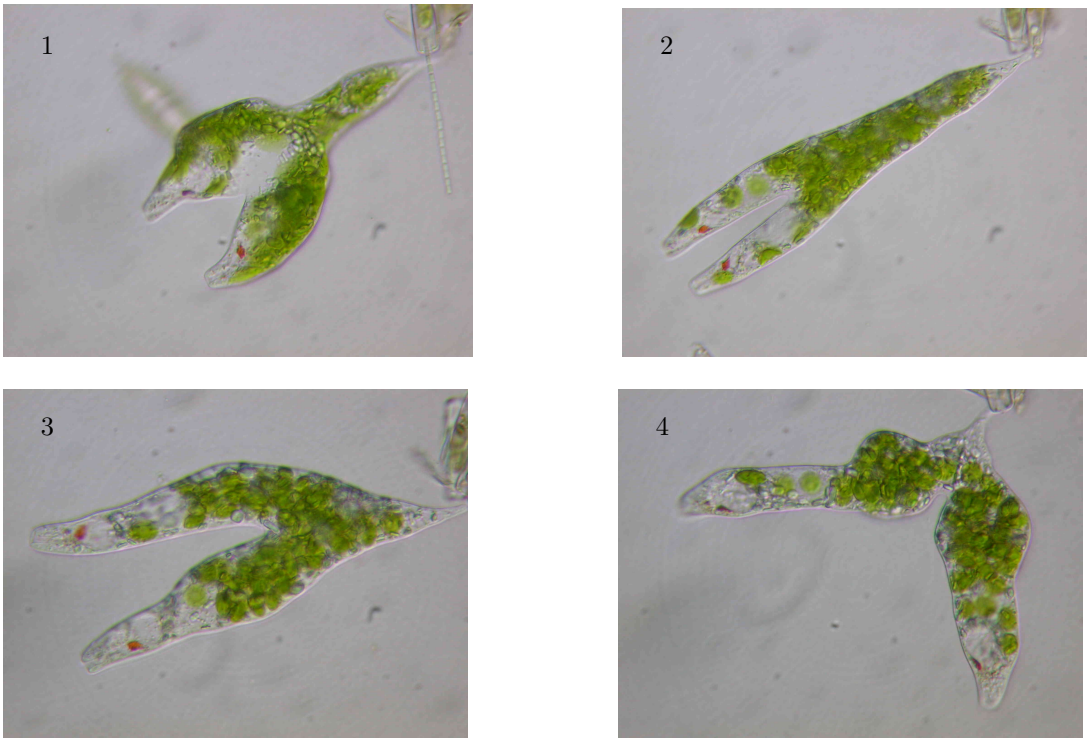

Figure 4.2: *Euglena* cells divide longitudinally and don't grow in length. They qualify as V$\frac{1}{2}$-morphs. The division process takes a full hour at 20°C. Schiermonnikoog, 2012/12/28.

to account for the shape difference with a cylinder. Cells can change shape dramatically within seconds, but these changes don't affect surface area or volume; amounts of outer membrane don't change that fast and water is not flowing in and out rapidly. Surface area is, therefore, proportional to volume to the power $\frac{1}{2}$, which classifies *Euglena* as a V$\frac{1}{2}$-morph, and the shape correction function is $\mathcal{M}(L) = (V/V_d)^{-1/6} = (L/L_d)^{-1/2}$. The specific growth rate amounts to $\dot{r} = \frac{\dot{v}e\sqrt{L_d/L^3} - \dot{k}_M g}{e+g} = \frac{\dot{k}_E e (L_d/L)^{3/2} - \dot{k}_M g}{e+g}$ for a cell of structural length L. The cell increases in volume by a factor 2 if the radius increases by a factor $\sqrt{2}$. The inter-division interval a_d can be found from $L_r(a_d) = L_d^\circ$, with $L_r(0) = L_d^\circ/\sqrt{2}$ and $\frac{d}{dt} L_r = L_r \dot{r}/3$. L_d serves the role of a reference value for the changing structural length L, as does L_d° for the cell radius. The (specific) population growth rate relates to the inter-division interval as $\dot{r} = a_d^{-1} \ln 2$, a result which helps to see how cell dimensions (L_c, L_d), metabolic properties ($\dot{v}$, $\dot{k}_M$, g) and substrate availability ($e = f$ if scaled functional response f is constant) affect population performance.

Figure 4.3 shows that the growth curves of V0-morphs are more convex than the von Bertalanffy one for isomorphs and that V$\frac{1}{2}$-morphs are in between.

	V0	V$\frac{1}{2}$	V$\frac{2}{3}$
$3(f+g)\ \frac{d}{d\tau}l\Big\vert_{l_b} + gl_b$	$fk_E l_b^{-2}$	$fk_E l_b^{-1/2}$	fk_E
$\frac{L_\infty}{L_d}$	$\left(\frac{fk_E}{g}\right)^{1/3}$	$\left(\frac{fk_E}{g}\right)^{2/3}$	$\frac{fk_E}{g}$

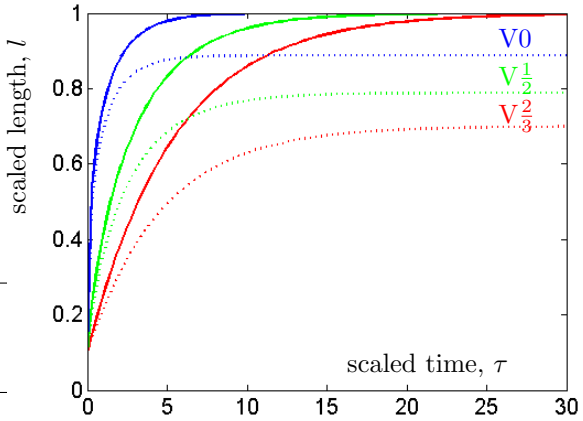

Figure 4.3: To compare growth of V0-, V$\frac{1}{2}$- and V$\frac{2}{3}$-morphs at constant substrate densities, we scale time as $\tau = \dot{k}_M t$ and length as L/L_d, where scaled length at birth is $l_b = L_b/L_d$, and scaled reserve turnover is $k_E = \dot{k}_E/\dot{k}_M$. Energy conductance is $\dot{v} = L_d\dot{k}_E$ by definition. Left: Growth at l_b and ultimate length. The table shows that all maximum lengths ($f = 1$) are equal if $g = k_E$. Right: Growth curves for scaled functional response $f = 0.7$ (stippled) and 1 (drawn). Parameters: $l_b = 0.1$, $g = k_E = 1.25$.

4.2.1 V0- versus iso-morphs

Figure 4.3 shows that the growth curves of V0-morphs are more convex than the von Bertalanffy one for isomorphs and that V$\frac{1}{2}$-morphs are in between.

4.2.2 V1- versus iso-morphs

Let us compare the performance of iso- and V1-morphs that are otherwise as equal as possible in terms of parameter values and state variables. The significance of this comparison is that the specification of population dynamics of dividing V1-morphs only requires ODE's, since all individuals have the same reserve densities (that might change in time) and only the total amount of structure of all individuals in the population is important, not the amount of structure for each individual. The population dynamics of dividing isomorphs, however, requires a formulation in PDE's, which are way more complex to integrate, or IBM's, which are also computationally intensive. If substrate density fluctuates in time in a spatially homogeneous environment, reserve densities of isomorphs scatter, since baby cells follow these fluctuations faster than mother cells while changing in time. This suggests to approximate the dynamics of a population of isomorphs with that of 'appropriate' V1-morphs. One way to define 'appropriate' is to consider the parameters of individual isomorphs in a time-length-mass frame:

$$K,\ y_{EX},\ \{\dot{J}_{EAm}\},\ \dot{v},\ \kappa,\ j_{EM},\ y_{VE},\ M_H^d,\ \dot{k}_J$$

or in a time-length-energy frame

$$K,\ \kappa_X,\ \{\dot{p}_{Am}\},\ \dot{v},\ \kappa,\ [\dot{p}_M],\ [E_G],\ E_H^d,\ \dot{k}_J$$

The parameters of the most appropriate V1-morph have the same values, except for $\{\dot{J}_{EAm}\}$ and $\dot{v}$, because the corresponding parameters for V1-morphs, $[\dot{J}_{EAm}]$ and $\dot{k}_E$ have different dimensions. Maturity at division M_H^d affects mean cell size, but this cell size does not affect population dynamics of V1-morphs, while it does affect that of isomorphs.

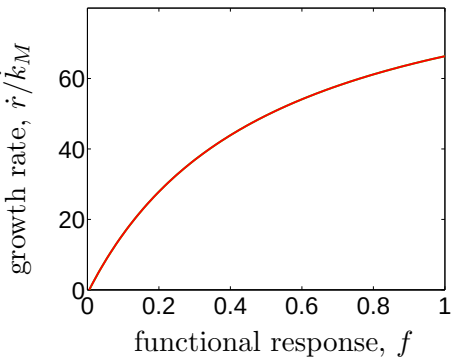

Figure 4.4: The scaled population growth rates for V1-morphs (red) and isomorphs (green, but invisible, because it is beneath the red curve) and V0-morphs (blue, but invisible, because it is also beneath the red curve), as function of the functional response, such that their growth rates at $f = 1$ are identical. Given the parameters $g = 0.5$ and $\dot{k}_E/\dot{k}_M = 100$, this happens for $L_d^*/L_d = 0.8929$ for isomorphs and $L_d^*/L_d = 0.7216$ for V0-morphs.

If the uptake capacities of the iso- and V1-morphs are equal at birth (just after division), the V1-morph can grow faster, because it can increase its surface area faster during the cell cycle. If, on the contrary, the uptake capacities are equal just prior to division, the isomorph can grow faster, because it has a larger surface area at birth. This illustrates the problem that the detailed way how we compare them really matters.

Resource acquisition depends on assimilation. For an isomorph, the surface area-specific assimilation rate $\{\dot{J}_{EAm}\} = \dot{J}_{EAm}/L^2$ is a constant and $[\dot{J}_{EA}] = \dot{J}_{EAm}/L^3 = \{\dot{J}_{EAm}\}/L$ is a variable. For a V1-morph $[\dot{J}_{EA}]$ is a constant and $\{\dot{J}_{EAm}\}$ is a variable. A similar relationship applies to the reserve mobilisation: the role of (varying) $\dot{v}/L$ for an isomorph is similar to that of (constant) $\dot{k}_E$ for a V1-morph.

For an isomorph, the reserve capacity is $[M_{Em}] = \frac{\{\dot{J}_{EAm}\}}{\dot{v}}$ and for a V1-morph $[M_{Em}] = \frac{[\dot{J}_{EAm}]}{\dot{k}_E}$. The uptake and mobilisation rate as well as the reserve capacity are all three equal for iso- and V1-morphs if $[\dot{J}_{EAm}] = \{\dot{J}_{EAm}\}\mathcal{E}L^2/\mathcal{E}L^3$ and $\dot{k}_E = \dot{v}\mathcal{E}L^2/\mathcal{E}L^3$. Since $\mathcal{E}L^i$ depends on the growth rate, so on the substrate concentration, it can vary in time. The idea of approximating the population performance of isomorphs by that of V1-morphs is to assume that the length distribution of individuals changes in pseudo-equilibrium and the scaled reserve density of V1-morphs equals to the mean scaled reserve density of isomorphs.

Notice that V_d depends on $\dot{r}$ that can change in time, , see 4.2.0 of the comments, and the parameters $[\dot{J}_{EAm}]$ and $\dot{k}_E$ should be evaluated for each time increment. Since changes in time are only slow, a continuation method using the Newton Raphson scheme is likely to be numerically very efficient. This strategy can be followed for all non-V1-morphs.

Furthermore, we can substantially reduce computations by equating $[\dot{J}_{EAm}] = \{\dot{J}_{EAm}\}\mathcal{E}L^2/\mathcal{E}L^3$ and $\dot{k}_E = \dot{v}\mathcal{E}L^2/\mathcal{E}L^3$ only for $f = 1$ and use these values for all food conditions. The relationship between population growth rate $\dot{r}$ and division interval a_d is $\dot{r} = \frac{\ln 2}{a_d}$. The division interval for an isomorph at constant food is $a_d = \dot{r}_B^{-1} \ln \frac{L_\infty - L_b}{L_\infty - L_d}$, where $L_b = 2^{-1/3} L_d$ for division into two parts at length L_d and $\dot{r}_B = \frac{\dot{k}_M/3}{1+f/g}$ and $L_\infty = \frac{f\dot{v}}{g\dot{k}_M}$, see (2.23). The specific growth rate for a V1-morph at constant food is $\dot{r} = \frac{\dot{k}_E f - \dot{k}_M g}{f+g}$, see (4.18). By equating these growth rates we can find L_d^* for $\dot{v}/L_d^* = \dot{k}_E$

$$\frac{L_d^*}{L_d} = \frac{\alpha - 2^{-1/3}}{\alpha - 1} \frac{g}{f k_E} \quad \text{with } \alpha = \exp\left(\frac{\ln 2}{3} \frac{1}{f k_E/g - 1}\right) \text{ and } k_E = \frac{\dot{k}_E}{\dot{k}_M}$$

The conclusion is that L_d^* depends (theoretically) on f, so a possibility is to select $f = 1$ as reference. In practice, however, for realistic values of the parameters, the population growth rate as function of the scaled functional response is almost identical for dividing iso- and V1-morphs, see Figure 4.4. Notice that the curve $\dot{r}(f)$ for isomorphs only depends on L_d via L_d^*/L_d (given that we replace $\dot{v}/L_d^*$ by $\dot{k}_E$ and $\{\dot{p}_{Am}\}/L_d^*$ by $[\dot{p}_A]$) and that the curve for V1-morphs does not depend on L_d at all. The role of κ remains hidden in g. For $\dot{k}_J \neq \dot{k}_M$, L_d depends on f, and the story becomes somewhat more complex. Because the $\dot{r}(f)$-curves are almost identical in practice, these developments would be of academic value only.

4.2.2 V1- versus V0-morphs

As we did for equating the population growth rates for V1- and isomorphs, we can equate the population growth rate for V1 and V0-morphs. From (4.10) we learn for constant $e = f$ that $V(t) = V_\infty - (V_\infty - V_b)\exp(-\frac{\dot{k}_M g}{f+g}t)$ for $V_\infty = fV_d^{2/3}V_m^{1/3}$ and $V_b = V_d/2$ and $V_m^{1/3} = \frac{\dot{v}}{\dot{k}_M g}$ as before. The inter-division interval a_d follows from $V(a_d) = V_d$ with the result that $a_d = \frac{f+g}{\dot{k}_M g}\ln\frac{V_\infty - V_d/2}{V_\infty - V_d}$, while $\dot{r} = \frac{\ln 2}{a_d}$. We are now looking for an $L_d^* = \dot{v}/\dot{k}_E$ such that the population growth rate of V0-morphs equals that of V1-morphs, $\dot{r} = \frac{\dot{k}_E f - \dot{k}_M g}{f+g}$, and find for $L_d = V_d^{1/3}$

$$\frac{L_d^*}{L_d} = \frac{\alpha - 2^{-1}}{\alpha - 1}\frac{g}{fk_E} \quad \text{with } \alpha = 2^{(fk_E/g-1)^{-1}} \text{and } k_E = \frac{\dot{k}_E}{\dot{k}_M}$$

4.2.2 Droop as special case of DEB

The demonstration that the one reserve - one structure DEB model for V1-morphs without maintenance or growth overhead reduces to the Droop model is as follows. The Droop equations [358] are:

$$\frac{d}{dt}Q = u - \mu Q \tag{4.7}$$
$$\mu/\mu'_m = 1 - k_Q/Q \tag{4.8}$$
$$u/u_m = s/(k_s + s) \tag{4.9}$$

quantity	Droop	DEB
specific growth rate	μ	$\dot{r}$
asymptotic growth rate	μ'_m	$\dot{k}_E$
cell nutrient quota	Q	$m_E + n_{XV}$
subsistence quota	k_Q	n_{XV}
specific uptake rate	u	j_{XA}
max spec uptake rate	u_m	j_{XAm}
half saturation constant	k_s	K
nutrient concentration	s	X

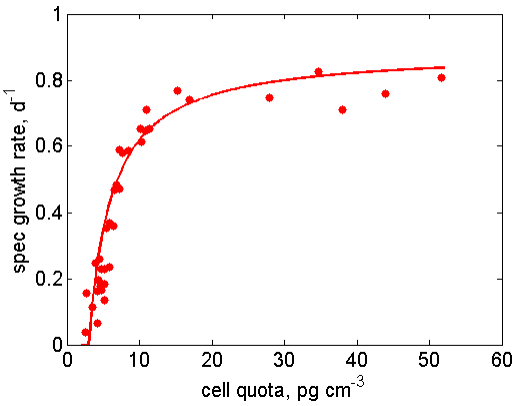

Figure 4.5: The specific growth rate $\dot{r}$ as function of the cell quota Q for vitamin B_{12} limited growth of *Pavlova lutheri*, as specified by Droop's model [357]. The data were copied from [833], but the curve $\dot{r}(Q) = \dot{r}_m(1 - Q_0/Q)$ was recalculated to remove the 'artistic freedom' that turned out to be included.

For internalised nutrient as reserve we have $j_{EAm} = y_{EX} j_{XAm}$ with $y_{EX} = 1$. Mobilised nutrient from reserve is built into structure without overhead, so $y_{VE} = n_{EV} = n_{XV}$. Since $\dot{k}_E = j_{XAm}/m_{Em}$, see {125}, the specific reserve dynamics (4.13) becomes

$$\frac{d}{dt} m_E = j_{EAm} f - \dot{k}_E m_E$$

Now, (4.9) shows that $u = j_{EAm} f$. To see that Droop's cell quota kinetics is equivalent to DEB reserve kinetics for zero maintenance costs, $\dot{k}_M = 0$, we need to demonstrate that μQ is equivalent to $\dot{k}_E m_E$, since $\frac{d}{dt} Q$ is equivalent to $\frac{d}{dt} m_E$. Multiplication of (4.8) with Q leads to $\mu Q = \mu'_m (Q - k_Q)$. Since $Q - k_Q$ is equivalent to m_E, we only need to demonstrate that μ'_m is equivalent to $\dot{k}_E$, where μ'_m is the specific growth rate at infinite reserve density. Since $\dot{r} = \dot{k}_e \frac{e - l_d}{e + g} = \frac{\dot{k}_E e - \dot{k}_M g}{e + g}$ with $e = m_E/m_{Em}$, see (4.14), we indeed have that $\dot{r} \to \dot{k}_E$ for $m_E \to \infty$ (which is obviously not possible in the cell since the maximum reserve density is $m_{Em} = j_{XAm}/\dot{k}_E$). A minor difference between the Droop and the DEB models is the use of units. Where DEB theory uses C-mol (because this is most handy when evaluating mass conservation), Droop's model is frequently applied on (dry) weights.

Droop aimed to relate cell quota to the specific growth rate as observed in chemostats in steady state, see Figure 4.5. He had no dynamic system in mind, and emphasised its empirical nature. To go from Droop to DEB, we need to split quota in subsistence quota and reserve, link subsistence quota to structure, translate the model that links quota to specific population growth rate into a model that specifies changes in reserve and structure, include the effect of maintenance, and separate effects of surface areas from that of volumes at the level if the individual, i.e. translate V1- to iso-morphs.

4.2.2 Growth at maximum yield

Eqn. (4.22) gives the (inverse) yield for V1-morphs as function of the growth rate at steady state. The maximum yield is found from $\frac{d}{d\dot{r}} Y = 0$ to be reached for specific growth rate

$$\dot{r}_Y = \dot{k}_M + \sqrt{\dot{k}_M (\dot{k}_M + \dot{k}_E)}$$

The maximum specific growth rate is given by (4.21): $\dot{r}_m = \frac{\dot{k}_E - \dot{k}_M g}{1 + g}$. Since maximum growth must be positive, a natural constraint on biologically reasonable parameters values

is $0 < g < \frac{\dot{k}_E}{\dot{k}_M}$. The growth rate for maximum yield $\dot{r}_Y$ can only be effectuated if $\dot{r}_Y < \dot{r}_m$; This translates to the condition $g < \frac{\dot{k}_E - \dot{r}_Y}{\dot{k}_M + \dot{r}_Y}$, which is thus more constraining than that for maximum growth. Since $g > 0$, at least we must have $\dot{k}_E > \dot{r}_Y$, so $\dot{k}_E > 3\dot{k}_M$. Since investment ratio $g = \frac{y_{EV}}{\kappa m_{Em}}$ (Table 3.3) and maximum reserve capacity $m_{Em} = j_{EAm}/\dot{k}_E$ (see (4.12)), we can further translate the condition to

$$\kappa j_{EAm} y_{VE} > \frac{\dot{k}_M + \dot{r}_Y}{1 - \dot{r}_Y/\dot{k}_E}$$

If this condition is not satisfied, the yield of structural biomass on substrate increases monotonically with the growth rate till the maximum growth rate is reached.

4.2.4 Crusts

The diameter of a crust of constant height L_h grows approximately linearly in time, $L_d = t\dot{v}_d/\delta_{\mathcal{M}}$, at constant food density. The conductance $\dot{v}_d$ depends on food density. Physical volume is $V_w = L_h L_d^2 \pi/4$, physical volumetric length $L_w = V_w^{1/3} = (L_h L_d^2 \pi/4)^{1/3}$, structural length $L = \delta_{\mathcal{M}} L_w$, so that the diameter relates to structural length as $L_d = \sqrt{\frac{4L^3}{\pi \delta_{\mathcal{M}}^3 L_h}}$. Structural volume grows as $V(t) = L^3(t) = \delta_{\mathcal{M}}^3 L_w^3(t) = \dot{v}_d^2 t^2 L_h \delta_{\mathcal{M}} \pi/4$.

The specific growth rate is given by $\dot{r} = V^{-1}\frac{d}{dt}V = \frac{2}{t} = \frac{2\dot{v}_d}{\delta_{\mathcal{M}} L_d} = \dot{v}_d\sqrt{\pi \delta_{\mathcal{M}} L_h/L^3}$. We further have for mobilisation C, assimilation A, maintenance M and growth G

$$\kappa \dot{p}_C \quad = \quad \dot{p}_M + \dot{p}_G = \kappa(\dot{p}_A - \dot{r}e[E_m]V); \quad \kappa[\dot{p}_A] = [\dot{p}_M] + \dot{r}[E_G](1 + e/g)$$

The shape correction function for crusts is

$$\mathcal{M}(V) = \frac{[\dot{p}_{Am}]L^3}{\{\dot{p}_{Am}\}L^2} = \frac{[\dot{p}_M]L^3 + [E_G](1 + 1/g)\dot{v}_{dm}\sqrt{\pi \delta_{\mathcal{M}} L_h L^3}}{\kappa\{\dot{p}_{Am}\}L^2} = \frac{L}{L_m} + \sqrt{\frac{L_1}{L}}$$

with $L_m = \frac{\kappa\{\dot{p}_{Am}\}}{[\dot{p}_M]} = \frac{\dot{v}}{\dot{k}_M g}$ and $L_1 = \pi \delta_{\mathcal{M}} L_h (1 + g)^2 \dot{v}_{dm}^2/\dot{v}^2$, where $\dot{v}_{dm}$ is the maximum value for $\dot{v}_d$ (i.e. for $f = 1$). The specific growth rate can also be found from (2.21) by multiplying $\dot{v}$ with $\mathcal{M}(V)$

$$\dot{r} = \frac{\mathcal{M}(L)\dot{v}e/L - g\dot{k}_M}{e + g} = \frac{e\dot{v}\sqrt{L_1/L^3} - (1 - e)g\dot{k}_M}{e + g} = \frac{(1 + g)e\dot{r}_m - (1 - e)g\dot{k}_M}{e + g}$$

with $\dot{r}_m = \dot{v}_{dm}\sqrt{\pi \delta_{\mathcal{M}} L_h/L^3}$ which reveals how $\dot{v}_d$ depends on $f = e$.

If maintenance represents the main contribution to dissipation, the use of dioxygen amounts to

$$\dot{J}_O = \eta_{OA}\dot{p}_A + \eta_{OD}\dot{p}_D + \eta_{OG}\dot{p}_G = \alpha V + \beta\sqrt{V}$$

The conclusion is that respiration increases with the square root of biomass for growing crusts at constant food, if the contribution of maintenance to respiration is relatively small.

4.3 Three basic fluxes

4.3.1 Assimilation

The matrix of chemical indices for the organics, $\boldsymbol{n}_{\mathcal{O}}$ as in (4.34) should generally include water. Excersize 3.1.1 shows how to convert indices for dry to that of wet organics. Only if the abundance of water, relative to carbon, in all organics is the same, we can also work with dry organics, see Section 3.2.1 of the comments.

μ_X stands for the chemical potential of X, so of food. $\mu_{AX} = \mu_E/y_{EX}$ stands for the energy per C-mole of food that is fixed in reserve, after the transformation. Using $\dot{J}_X = -\dot{J}_{XA}$ (food disappears so the flux $\dot{J}_X$ is taken to be negative), $\dot{p}_A = -\mu_{AX}\dot{J}_X = \mu_E\dot{J}_{EA} = -\mu_E y_{EX}\dot{J}_X$. The difference $\mu_X - \mu_{AX}$ went lost for the organism, so the assimilation efficiency can be written as $\kappa_X = \mu_{AX}/\mu_X = \{\dot{p}_{Xm}\}/\{\dot{p}_{Am}\}$, see {35}. Part of this difference is still conserved in the faeces, some of it sits in e.g. the carbon dioxide production and in heat production that are associated with assimilation. The notation in μ_{AX} is somewhat uneasy, because first the process (assimilation A) is identified, and then the compound (food X). The reason is in the relationship $\mu_{AX} = \eta_{XA}^{-1}$, which has nice notational properties.

For the assimilation process we can work out the balance as follows. We first define the matrix of mineral mass-energy couplers

$$\boldsymbol{\eta}_{\mathcal{M}} = \begin{pmatrix} \eta_{CA} & \eta_{CD} & \eta_{CG} \\ \eta_{HA} & \eta_{HD} & \eta_{HG} \\ \eta_{OA} & \eta_{OD} & \eta_{OG} \\ \eta_{NA} & \eta_{ND} & \eta_{NG} \end{pmatrix} \equiv \begin{pmatrix} \boldsymbol{\eta}_{\mathcal{M}A} & \boldsymbol{\eta}_{\mathcal{M}D} & \boldsymbol{\eta}_{\mathcal{M}G} \end{pmatrix}$$

The parameters $\boldsymbol{\eta}$ are given by $\boldsymbol{\eta}_{\mathcal{M}} = -\boldsymbol{n}_{\mathcal{M}}^{-1}\boldsymbol{n}_{\mathcal{O}}\boldsymbol{\eta}_{\mathcal{O}}$, where the organic mass-energy couplers $\boldsymbol{\eta}_{\mathcal{O}}$ are given in (4.37). So the mineral fluxes that are released in the environment in association with assimilation are $\dot{\boldsymbol{J}}_{\mathcal{M}A} = \dot{p}_A\boldsymbol{\eta}_{\mathcal{M}A}$. This represents an energy drain $\dot{p}_{\mathcal{M}A} = \boldsymbol{\mu}_{\mathcal{M}}^T\dot{p}_A\boldsymbol{\eta}_{\mathcal{M}A}$. The energy drain in product that is associated with assimilation (think e.g. of faeces for animals) amounts to $\dot{p}_{PA} = \dot{p}_A\mu_P\eta_{PA}$. The energy balance for assimilation process thus amounts to

$$\begin{aligned} -\mu_X\dot{J}_X &= \dot{p}_A + \dot{p}_{PA} + \dot{p}_{\mathcal{M}A} + \dot{p}_{TA} \\ &= \dot{p}_A(1 + \mu_P\eta_{PA} + \boldsymbol{\mu}_{\mathcal{M}}^T\boldsymbol{\eta}_{\mathcal{M}A}) + \dot{p}_{TA} \\ \mu_X &= \left(\mu_{AX}(1 + \mu_P\eta_{PA} + \boldsymbol{\mu}_{\mathcal{M}}^T\boldsymbol{\eta}_{\mathcal{M}A}) - \dot{p}_{TA}\right)/\dot{J}_X \end{aligned}$$

where $\dot{p}_{TA}$ is the heat that dissipates into the environment in association with the assimilation process; its amount follows from this energy balance. So the terms in the right argument stands for the energy flux fixed in reserve, product en minerals, followed by the dissipating heat. Only the reserve stays in the individual, the rest dissipates into the environment.

It is possible to express the basic powers as weighted sums of organic fluxes as

$$\begin{pmatrix} \dot{p}_A \\ \dot{p}_D \\ \dot{p}_G \end{pmatrix} = \begin{pmatrix} -\mu_{AX} & 0 & 0 & 0 \\ -\mu_{AX} & -\mu_{GV} & -\mu_E & 0 \\ 0 & \mu_{GV} & 0 & 0 \end{pmatrix} \begin{pmatrix} \dot{J}_X \\ \dot{J}_V \\ \dot{J}_E + \dot{J}_{E_R} \\ \dot{J}_P \end{pmatrix} \quad \text{or} \quad \dot{\boldsymbol{p}} = \boldsymbol{\eta}_{\mathcal{O}}^{-1} \dot{\boldsymbol{J}}_{\mathcal{O}}$$

for $\mu_{AX} = \eta_{XA}^{-1}$ and $\mu_{GV} = \eta_{VG}^{-1}$. If $\boldsymbol{n}_{\mathcal{O}}^{-1}$ exists, the basic powers can also be written as weighted sums of mineral fluxes: $\dot{\boldsymbol{p}} = -\boldsymbol{\eta}_{\mathcal{O}}^{-1} \boldsymbol{n}_{\mathcal{O}}^{-1} \boldsymbol{n}_{\mathcal{M}} \dot{\boldsymbol{J}}_{\mathcal{M}}$. This quantification is likely to be sensitive to inaccuracies.

Since $Y_{VX} = -\frac{\dot{J}_V}{\dot{J}_X} = \frac{\eta_{VG}\dot{p}_G}{\eta_{XA}\dot{p}_A} = \frac{\eta_{VG} j_{EG} \mu_E}{\eta_{XA} j_{EA} \mu_E} = \frac{\eta_{VG} y_{EV} \dot{r}}{\eta_{XA} y_{EX} j_{XA}} = \frac{\eta_{VG} \dot{r}}{\eta_{XA} j_{XA}} y_{VX}^{-1}$, we clearly see that $Y_{VX} \neq y_{VX}$. The first quantity is variable, the second one is fixed.

4.3.1 Product formation

Eqn. (4.37) is general for the product formation for the standard DEB system (one type of food, one reserve, one structure). In the case of faeces, we have $\eta_{PD} = \eta_{PG} = 0$, but one can also think of other products, such as hair, skin flakes, sweat etc. Goldfish produces e.g. ethanol at low dioxygen levels; organisms other than animals have an even wider set of possible products.

4.3.1 Anabolism & catabolism

Substrate and reserve serve a dual function; they are a sources of energy as well as building blocks. For this reason, assimilation, dissipation as well as growth can be partitioned into a catabolic and an anabolic flux, see Table 4.1 for aerobic metabolism. The table does not present the anabolic aspect of dissipation because the stuctural compounds are degraded and synthesized at the same rate with additional use of reserve, making that the overall stoichiometry is identical to the catabolic aspects. This turnover of structure complicates the behaviour of isotopes, however. In anaerobic metabolism dioxygen O is replaced by another electron acceptor, but otherwise the derivations are similar. If other than the mineral products are formed, such feaces for animals, we need extra information of how this product formation is linked to the catabolic and anabolic aspects to be able to partition the flux. In the catabolic aspect, substrates are transformed to extract energy and all the products are excreted. Since the catabolic aspect of growth concerns the use of reserve, just like maintenance, the stoichiometries of the two processes are identical, and different from the anabolic aspect of growth. In the anabolic aspect, some of the substrates are incorporated in biomass, others are excreted; anabolic processes typically require energy derived from catabolic processes. Since the anabolic aspect is a fixed fraction of the total flux (both for assimilation and for growth), this partitioning does not imply an extension of the number of independent fluxes in the total metabolism, which remains 3 (assimilation, dissipation and growth). Phosphates and other micro-nutrients are not included for simplicity's sake.

If we assemble a matrix of chemical indices $\boldsymbol{n}$, with 4 elements in the rows and 8 compounds in the columns, and a matrix of yield coefficients $\boldsymbol{Y}$, with 8 compounds in

Table 4.1: The yield coefficients (upper panel) and the chemical indices (lower panel) for the 8 compounds that are involved in the 5 transformations with one reserve and one structure; the energy and carbon substrates, X and S respectively, are frequently identical. Assimilation, dissipation and growth have a catabolic and an anabolic aspect; that of dissipation is discussed in the section on isotopes. The yield coefficients stand for

$Y^a_{CS} = 0$	$Y^a_{HS} = n_{HS}/2 - n_{HE}/2 - Y^a_{NS}3/2$	$Y^a_{OS} = n_{OS}/2 - n_{OE}/2 - Y^a_{HS}/2$	$Y^a_{NS} = n_{NS} - n_{NE}$
$Y^c_{C*} = n_{C*}$	$Y^c_{H*} = -n_{N*}3/2 + n_{H*}/2$	$Y^c_{O*} = -1 + n_{O*}/2 - Y^a_{H*}/2$	$Y^c_{N*} = n_{N*}$
$Y^a_{CE} = 0$	$Y^a_{HE} = n_{HE}/2 - n_{HV}/2 - Y^a_{NE}3/2$	$Y^a_{OE} = n_{OE}/2 - n_{OV}/2 - Y^a_{HE}/2$	$Y^a_{NE} = n_{NE} - n_{NV}$

Following microbiological tradition, substrate is chosen as reference in the yield coefficients for assimilation and reserve for dissipation and growth. The specific rates $j_{EA} = \dot{p}_A/\mu_E$, $j_{ED} = \dot{p}_D/\mu_E$ and $j_{EG} = \dot{p}_G/\mu_E$ are specified by the DEB theory (see Tables 3.5 and 3.6). The specific dissipation flux $j_{ED} = j_{EM}/\kappa$ for V1-morphs (or $j_{ED} = j_{EM}$ if $\kappa = 1$).

symbol	processes	C: carbon dioxide	H: water	O: dioxygen	N: ammonia	X: E-substrate	S: C-substrate	E: reserve	V: structure	specific rates
A_c	assim. (cat)	Y^c_{CX}	Y^c_{HX}	Y^c_{OX}	Y^c_{NX}	-1	0	0	0	$(y_{XE} - 1)j_{EA}$
A_a	assim. (ana)	0	Y^a_{HS}	Y^a_{OS}	Y^a_{NS}	0	-1	1	0	j_{EA}
D	dissipation	Y^c_{CE}	Y^c_{HE}	Y^c_{OE}	Y^c_{NE}	0	0	-1	0	j_{ED}
G_c	growth (cat)	Y^c_{CE}	Y^c_{HE}	Y^c_{OE}	Y^c_{NE}	0	0	-1	0	$(1 - y_{VE})j_{EG}$
G_a	growth (ana)	0	Y^a_{HE}	Y^a_{OE}	Y^a_{NE}	0	0	-1	1	$y_{VE}j_{EG}$
C	carbon	1	0	0	0	n_{CX}	1	1	1	
H	hydrogen	0	2	0	3	n_{HX}	n_{HS}	n_{HE}	n_{HV}	
O	oxygen	2	1	2	0	n_{OX}	n_{OS}	n_{OE}	n_{OV}	
N	nitrogen	0	0	0	1	n_{NX}	n_{NS}	n_{NE}	n_{NV}	

the rows and 5 transformations in the columns (Table 4.1 presents the transposed $\boldsymbol{Y}$ rather than $\boldsymbol{Y}$, for typographic reasons), then the conservation law for elements implies that $\boldsymbol{nY} = \boldsymbol{0}$; it takes only simple book keeping and some patience to solve these yield coefficients.

The assimilation flux of reserves depends on the concentrations of the complementary compounds substrates, dioxygen and ammonia. The SU rule for the assimilation rate of reserves j_{EA} for $x = X/K_X$, $s = S/K_S$, $o = O/K_O$, $n = N/K_N$ work out as follows:

$$j_{EA} = \frac{j_{EAm}}{1 + \sum_i A_i^{-1} - \sum_i B_i^{-1} + \sum_i C_i^{-1} - D^{-1}} \quad \text{with}$$
$$A_i = x,\ s,\ o,\ n; \quad B_i = x+s,\ x+o,\ x+n,\ s+o,\ s+n,\ o+n$$
$$C_i = x+s+o,\ x+s+n,\ x+o+n,\ s+o+n; \quad D = x+s+o+n$$

where X, S, O and N are the concentrations of energy substrate, carbon substrate, dioxygen and ammonia, K_X, K_S, K_O and K_N are the half saturation constants; j_{EAm} is the

maximum specific assimilation rate of reserves. The consumption of substrates, dioxygen and ammonia follow from the production of reserve via fixed coupling coefficients. A rather small range of concentrations of substrates, dioxygen and ammonia limit assimilation simultaneously. In many practical applications we have at abundant dioxygen and $x \ll n$ or $x \gg n$

$$j_{EA} \simeq \frac{j_{EAm}}{1 + x^{-1}} = \frac{j_{EAm} X}{K_X + X} \quad \text{or} \quad j_{EA} \simeq \frac{j_{EAm}}{1 + n^{-1}} = \frac{j_{EAm} N}{K_N + N}$$

This is the familiar standard formulation for single-substrate limitation. If energy and carbon substrate is identical, we should $s \to \infty$ to remove the extra limitation by carbon. This might seem to be counter intuitive, because we in fact have $x = s$. The explanation is that a single molecule is used for both energy and carbon, so we remove waiting time compared to the situation for two different molecules.

The specific rate of appearance of ammonia in association with maintenance, for instance, is $j_{NM} = n_{NE} j_{EM}$; that of dioxygen is $Y^c_{OE} j_{EM}$. If we assemble the rates in Table 4.1 in a 5-vector $\dot{\boldsymbol{k}}$, the 8-vector of specific rates of appearances or disappearances of compounds is given by $\boldsymbol{Y}\dot{\boldsymbol{k}}$, where each rate can be positive as well as negative.

Reserve density dynamics of V1-morphs is $\frac{d}{dt} m_E = j_{EA} - \dot{k}_E m_E$, where $\dot{k}_E$ is the reserve turnover rate. The specific maintenance flux of reserve is constant at rate $j_{EM} = y_{EV}\, \dot{k}_M$. The specific growth rate is $\dot{r} = \frac{m_E \dot{k}_E - j_{EM}}{m_E + y_{EV}}$, where $m_E \dot{k}_E - j_{EM}$ is the reserve flux that is released from the reserves minus the losses through maintenance; $m_E + y_{EV}$ are the specific costs for new reserve plus structure. So the growth rate depends on the reserve density m_E, not on the nutrient concentrations directly; growth ceases at reserve density $m_E = j_{EM}/\dot{k}_E$, where all mobilized reserves are used for maintenance. The flux of reserve associated with growth is $j_{EG} = y_{EV} \dot{r}$.

The assumption by [1343] that the specific entropy of a compound is constant directly translates in the entropy balance equation for compound $*$

$$\overline{s}_* = Y^c_{C*} \overline{s}_C + Y^c_{H*} \overline{s}_H + Y^c_{O*} \overline{s}_O + Y^c_{N*} \overline{s}_N$$

which gives the specific entropy of compound $*$, $\overline{s}_*$, given the specific entropies of C, H, O and N.

It is important to realize that the microchemical reaction equations are still far away from a detailed chemical description of metabolism. Compounds can be produced in one part of the pathway, and used in another part, and do not occur in the micro- or macro-chemical reaction equation.

[780] gives such a decomposition for methanotrophy and [174] for the anaerobic oxidation of ammonia (anammox). In the example of methanotrophy, the energy and carbon source are identical, in the anammox the are different. The example for anammox shows how additional biochemical information can be used in these decompositions and how the number of conserved quantities can be extended. Here with eletrical charge, but extensions with other chemical elements work out similarly.

4.3.1 Type I methanotrophy

The macro-chemical reaction equation for methanotrophs is

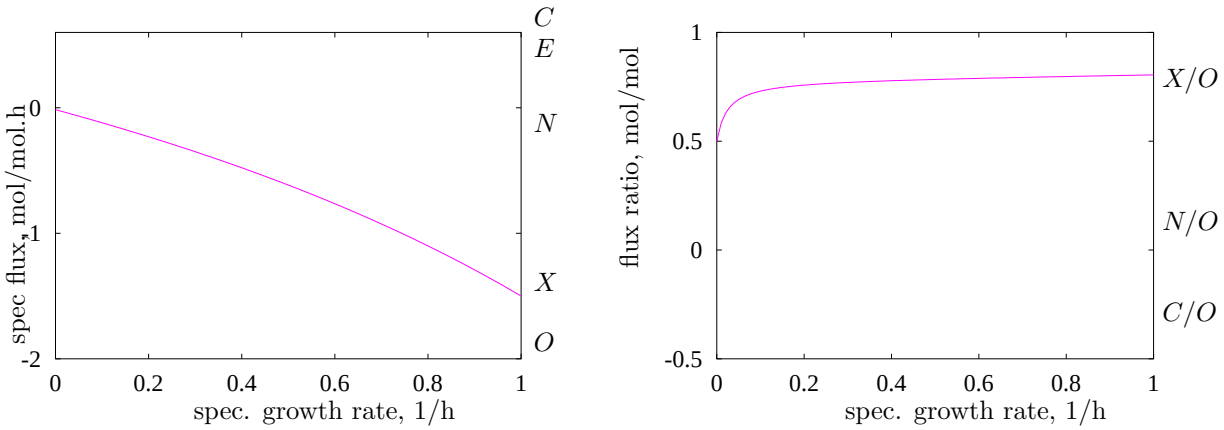

Figure 4.6: The specific fluxes (left graph) of (from top to bottom) carbon dioxide C, reserves E, ammonia N, methane X and dioxygen O as a function of the specific growth rate of a methanotroph. That of water and structure are not shown. The ratio of the fluxes (right graph) of methane (top curve), carbon dioxide (bottom curve) and ammonia (middle curve), with that of dioxygen. Parameters: max spec assimilation rate (of E) $j_{EAm} = 1.2$ mol/(h.mol), yield coefficients $y_{EX} = 0.8$ mol/mol and $y_{VE} = 0.8$ mol/mol, maintenance rate constant $\dot{k}_M = 0.01$ 1/h, reserve turnover rate $\dot{k}_E = 2.00$ 1/h. Chemical indices of reserve and structure: $n_{HE} = 1.8$; $n_{OE} = 0.3$; $n_{NE} = 0.3$; $n_{HV} = 1.8$; $n_{OV} = 0.5$; $n_{NV} = 0.1$.

$$\mathrm{CH_4} + Y_{CX}\,\mathrm{CO_2} + Y_{OX}\,\mathrm{O_2} + Y_{NX}\,\mathrm{NH_3} + Y_{HX}\,\mathrm{H_2O} \rightarrow Y_{WX}\,\mathrm{CH}_{n_{HW}}\mathrm{O}_{n_{OW}}\mathrm{N}_{n_{NW}}$$

Methanotrophs use methane (CH_4) as energy source; methane is the only carbon source in Type I methanotrophs, such as *Methylomonas*, *Methylomicrobium*, *Methylobacter* and *Methyloccus*, which use the monophosphate pathway to process formaldehyde (CH_2O), a metabolite of methane. Methane and carbon dioxide (CO_2) are carbon sources for Type II methanotrophs, such as *Methylosinus* and *Methylocystis*, which use the serine pathway to process formaldehyde. These organisms can also fix dinitrogen. I here selected type I methanotrophs to illustrate the stoichiometric principles because very simple compounds are involved only, see [780]. So we have $n_{CX} = n_{CS} = 1$, $n_{HX} = n_{HS} = 4$, $n_{OX} = n_{OS} = 0$ and $n_{NX} = n_{NS} = 0$.

Figure 4.6 gives the specific fluxes of compounds as functions of the specific growth rate. It also gives the ratio of the carbon dioxide and dioxygen fluxes, and that of ammonia and dioxygen. Many text books deal with these ratios as being proportional to the specific growth rate. This obviously does not apply here.

The result we obtained is that we can relate the yield coefficients and chemical indices of biomass to (varying) concentrations of nutrients in the environment, and to a (varying) reserve density, which involves a number of constant energy budget parameters. These constant parameters are the specific maintenance rate $\dot{k}_M$, the reserve turnover $\dot{k}_E$, the yield of structure on reserve y_{VE}, the chemical indices of reserve and structure, and the parameters of the assimilation process. Some text books mention that methanotrophs consume two methane molecules for each produced carbon dioxide molecule. Our analysis shows, however, that such a fixed relationship does not exist; it is very sensitive to environmental conditions.

Methane burning in assimilations' catabolic transformation should generate enough energy to drive assimilations' anabolic component. For the chemical potential μ_X of methane and μ_E of reserve, we have $\mu_X\, j^C_{XA} > (\mu_E - \mu_X) j^A_{XA}$ or $\mu_X(1 - y_{EX}) > (\mu_E - \mu_X) y_{EX}$ or $y_{EX} > \mu_E/\mu_X$.

Notice that ammonia is taken up as well as excreted; a phenomenon that only recently attracted attention in algal physiology. We know a priori that ammonium uptake always exceeds excretion at steady state.

4.3.1 Anammox

The anammox (anaerobic ammonia oxidation) process is only known from the chemolithotrophic planctomycete *Brocadia anammoxidans*. It generates energy from $NH_4^+ + NO_2^- \rightarrow N_2 + 2\,H_2O$, and fixes carbon from $CO_2 + 2\,NO_2^- + H_2O \rightarrow CH_2O + 2\,NO_3^-$. The measured macrochemical reaction equation at specific growth rate $\dot r = 0.0014\ h^{-1}$ is [1391]

$$1\,NH_4^+ + 1.32\,NO_2^- + 0.066\,HCO_3^- + 0.13\,H^+ \rightarrow \\ 1.02\,N_2 + 0.26\,NO_3^- + 0.066\,CH_2O_{0.5}N_{0.15} + 2.03\,H_2O$$

Also is known that N_2 comes from NH_4^+ and NO_2^- and that N in biomass comes from NH_4^+. The coefficients depend on the growth rate in a way that has been evaluated by Bernd Brandt [174] who also corrected and detailed the equation. We here extend the elemental balance equations with that for the electric charge. Table 4.2 presents the summary of the decomposition of the macrochanical reaction equation.

Figure 4.7 shows how the fluxes of the compounds that are involved in the anammox transformation depend on the growth rate. The chemical indices for biomass depend on the specific growth rate as $n_{iw} = \frac{n_{iV} + m_E n_{iE}}{1 + m_E}$ where the reserve density is given by $m_E = j_{EA}/\dot k_E = y_{EV}\frac{\dot k_M + \dot r}{\dot k_E - \dot r}$. The specific growth flux equals $j_{EG} = \dot r y_{EV}$ and the specific maintenance flux $\dot k_M y_{EV}$. For further discussion see [174].

4.3.1 Dioxygen flux

The standard DEB model assumes that dioxygen is abundantly available, or not at all for fermenting organisms. If dioxygen is co-limiting (together with food), multivariate formulations should be used. Suppose that the nitrogen waste is ammonia (NH_3), and faeces the only non-mineral product ($\eta_{PD} = \eta_{PG} = 0$). In that case we have

$$\boldsymbol{n}_{\mathcal{M}}^{-1} = \begin{pmatrix} 1 & 0 & 0 & 0 \\ 0 & 2^{-1} & 0 & 1.5 \\ -1 & -4^{-1} & 2^{-1} & 0.75 \\ 0 & 0 & 0 & 1 \end{pmatrix} \quad \text{and} \quad \boldsymbol{\eta}_{\mathcal{O}}\, \mathbf{diag}(\dot{\boldsymbol{p}}) = \begin{pmatrix} -\eta_{XA}\dot p_A & 0 & 0 \\ 0 & 0 & \eta_{VG}\dot p_G \\ \overline{\mu}_E^{-1}\dot p_A & -\overline{\mu}_E^{-1}\dot p_D & -\overline{\mu}_E^{-1}\dot p_G \\ \eta_{PA}\dot p_A & 0 & 0 \end{pmatrix}$$

The flux of the 4 minerals associated to the 3 powers is given by (4.38): $\dot{\boldsymbol{J}}_{\mathcal{M}*} = -\boldsymbol{n}_{\mathcal{M}}^{-1}\boldsymbol{n}_{\mathcal{O}}\boldsymbol{\eta}_{\mathcal{O}}\, \mathbf{diag}(\dot{\boldsymbol{p}})$, where the 4 minerals are in the rows, the 3 powers in the columns. The fluxes of dioxygen

Table 4.2: The yield coefficients (upper panel) and the chemical indices (lower panel) for the nine compounds that are involved in the five transformations by anammox bacteria. The yield coefficients are

$$Y^A_{CS} = -n^{-1}_{NE} \qquad Y^A_{H_1S} = Y^A_{CS}$$
$$Y^A_{HS} = (3 + Y^A_{CS}(n_{HE} - 2))/2 \qquad Y^A_{N_3S} = (3 - n_{OE})Y^A_{CS} + Y^A_{HS}$$
$$Y^M_{N_3E} = (-4 - n_{HE} + 2n_{OE} + 3n_{NE})/6 \qquad Y^M_{SE} = n_{NE} - Y^M_{N_3E}$$
$$Y^M_{H_1E} = 1 + Y^M_{N_3E} \qquad Y^M_{HE} = n_{OE} - 2Y^M_{N_3E} - 3$$
$$Y^G_{N_3E} = Y^M_{N_3E} - (-4 - n_{HV} + 2n_{OV} + 3n_{NV})/6 \qquad Y^G_{H_1E} = Y^G_{N_3E}$$
$$Y^G_{HE} = -2Y^G_{N_3E} + n_{OE} - n_{OV} \qquad Y^G_{SE} = -Y^G_{N_3E} + n_{NE} - n_{NV}$$

Following microbiological tradition, substrate is chosen as reference in the yield coefficients: ammonium for assimilation, and reserve for maintenance and growth. The yield coefficients follow from the conservation law for elements and electrical charge. The DEB theory provides the specific rates j_{EA}, j_{EM}, and j_{EG} (see text). Note that the yield coefficients for the catabolic aspect of growth equal those for maintenance.

symbol	processes	C: HCO_3^-	H_1: H^+	H: H_2O	S: NH_3	N: N_2	N_3: NO_2^-	N_5: NO_3^-	E: reserve	V: structure	specific rates
A_C	assim. (cat.)	0	–1	2	–1	1	–1	0	0	0	$(y_{SE} - n_{NE})j_{EA}$
A_A	assim. (ana.)	Y^A_{CS}	$Y^A_{H_1S}$	Y^A_{HS}	–1	0	$Y^A_{N_3S}$	$-Y^A_{N_3S}$	$-Y^A_{CS}$	0	$n_{NE}j_{EA}$
M	maintenance	1	$Y^M_{H_1E}$	Y^M_{HE}	Y^M_{SE}	0	$Y^M_{N_3E}$	0	–1	0	j_{EM}
G_C	growth (cat.)	1	$Y^M_{H_1E}$	Y^M_{HE}	Y^M_{SE}	0	$Y^M_{N_3E}$	0	–1	0	$(1 - y_{VE})j_{EG}$
G_A	growth (ana.)	0	$Y^G_{H_1E}$	Y^G_{HE}	Y^G_{SE}	0	$Y^G_{N_3E}$	0	–1	1	$y_{VE}\, j_{EG}$
C	carbon	1	0	0	0	0	0	0	1	1	
H	hydrogen	1	1	2	3	0	0	0	n_{HE}	n_{HV}	
O	oxygen	3	0	1	0	0	2	3	n_{OE}	n_{OV}	
N	nitrogen	0	0	0	1	2	1	1	n_{NE}	n_{NV}	
$+$	charge	–1	1	0	0	0	–1	–1	0	0	

$\dot{\boldsymbol{J}}_O^T = (\ \dot{J}_{OA} \quad \dot{J}_{OD} \quad \dot{J}_{OG}\ )$ are in the third row:

$$\dot{\boldsymbol{J}}_O^T = -\begin{pmatrix} -1 - n_{HX}/4 + n_{OX}/2 + 3n_{NX}/4 \\ -1 - n_{HV}/4 + n_{OV}/2 + 3n_{NV}/4 \\ -1 - n_{HE}/4 + n_{OE}/2 + 3n_{NE}/4 \\ -1 - n_{HP}/4 + n_{OP}/2 + 3n_{NP}/4 \end{pmatrix}^T \begin{pmatrix} -\eta_{XA}\dot{p}_A & 0 & 0 \\ 0 & 0 & \eta_{VG}\dot{p}_G \\ \overline{\mu}_E^{-1}\dot{p}_A & -\overline{\mu}_E^{-1}\dot{p}_D & -\overline{\mu}_E^{-1}\dot{p}_G \\ \eta_{PA}\dot{p}_A & 0 & 0 \end{pmatrix}$$

The dioxygen flux that is associated to growth is given in element 3, i.e.

$$\begin{aligned} \dot{J}_{OG} &= \dot{p}_G\left((-1 - n_{HE}/4 + n_{OE}/2 + 3n_{NE}/4)/\overline{\mu}_E - (-1 - n_{HV}/4 + n_{OV}/2 + 3n_{NV}/4)\eta_{VG}\right) \\ &= \dot{p}_G(-1 - n_{HE}/4 + n_{OE}/2 + 3n_{NE}/4)\left(\overline{\mu}_E^{-1} - \eta_{VG}\right) \quad \text{for} \begin{cases} n_{HV} = n_{HE} \\ n_{OV} = n_{OE} \\ n_{NV} = n_{NE} \end{cases} \end{aligned}$$

where the mass-energy coupler for growth is given by $\dot{J}_V = \eta_{VG}\dot{p}_G = \kappa_G\dot{p}_G/\mu_V$. So in absence of overhead costs of growth, i.e. $\eta_{VG} = \overline{\mu}_E^{-1}$ or $\mu_{GV} = \overline{\mu}_E$ or $\mu_V\dot{J}_V = \dot{p}_G$ or $\kappa_G = \mu_V[M_V]/[E_G] = 1$, and if the elemental composition of reserve and structure match, no dioxygen is used. In other words: all use of dioxygen that is linked to growth comes from the growth overheads, if the elemental composition of reserve and structure match.

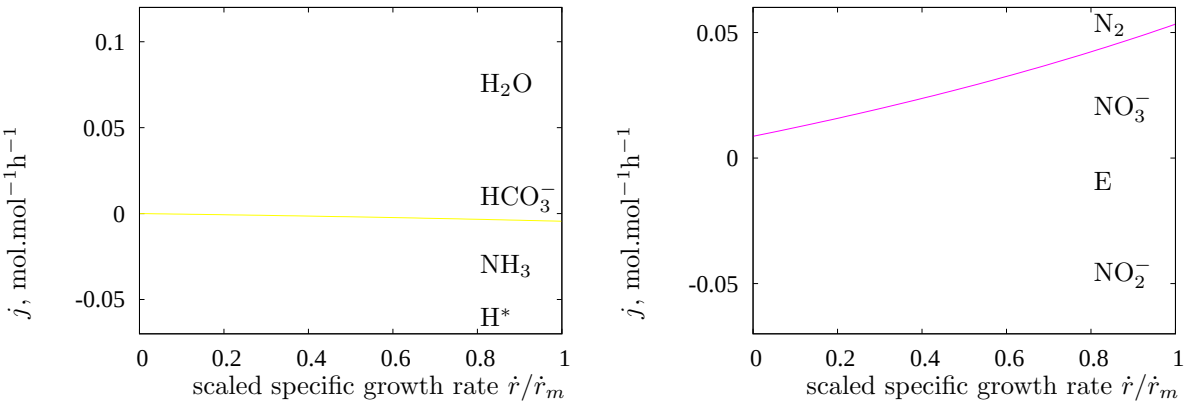

Figure 4.7: The specific fluxes of the compounds as a function of the specific growth rate as fraction of the maximum of $\dot{r}_m = 0.003$ h^{-1} of the anammox bacteria. DEB Parameters: $\dot{k}_E = 0.0127$ h^{-1}, $\dot{k}_M = 0.000811$ h^{-1}, $y_{SE} = 8.80$, $y_{VE} = 0.8$ C-mol/C-mol reserve. Composition parameters: $n_{HE} = 2$, $n_{OE} = 0.46$, $n_{NE} = 0.25$, $n_{HV} = 2$, $n_{OV} = 0.51$, $n_{NV} = 0.125$.

4.3.1 Stochastic mineral fluxes

Section 2.9 of the comments presents a natural stochastic version of the standard DEB model, where the stochasticity is in food searching and survival. How would that work out for the production of CO_2, H_2O and NH_3 and the consumption of O_2?

We first need to express the fluxes of compounds in terms of changes of scaled state variables e and l. For this purpose, we scale the organic fluxes $\boldsymbol{\jmath}_{\mathcal{O}} = \frac{\boldsymbol{j}_{\mathcal{O}}}{\dot{k}_M M_{Vm}}$ with $M_{Vm} = [M_V]L_m^3$ as function of scaled time $\tau = t\dot{k}_M$. Notice that these scaled fluxes are not dimensionless; their units are mol mol^{-1}

The scaled organic fluxes $\boldsymbol{\jmath}_{\mathcal{O}} = \begin{pmatrix} \jmath_X & \jmath_V & \jmath_E + \jmath_{E_R} & \jmath_P \end{pmatrix}^T$ are for f alternating stochastically from 0 to 1 and backwards

$$\begin{aligned}
\jmath_X &= -\frac{\dot{J}_{XA}}{\dot{k}_M M_{Vm}} = -\frac{y_{XE} f\{\dot{J}_{EAm}\} l^2 L_m^2}{\dot{k}_M [M_V] L_m^3} = -\frac{f l^2}{\kappa y_{VX}} \\
\jmath_V &= \frac{\dot{J}_V}{\dot{k}_M M_{Vm}} = \frac{[M_V] L_m^3}{\dot{k}_M M_{Vm}} \frac{d}{dt} l^3 = 3l^2 \frac{d}{d\tau} l \\
\jmath_E &= \frac{\dot{J}_E}{\dot{k}_M M_{Vm}} = \frac{\frac{d}{dt} E}{\mu_E \dot{k}_M M_{Vm}} = \frac{l^3 \frac{d}{d\tau} e + 3el^2 \frac{d}{d\tau} l}{g\kappa y_{VE}} = \frac{l^3 \frac{d}{d\tau} e + e\jmath_V}{g\kappa y_{VE}} \\
\jmath_{E_R} &= \frac{\dot{J}_{E_R}}{\dot{k}_M M_{Vm}} = \frac{M_E^0 \dot{R}}{\dot{k}_M M_{Vm}} = \frac{u_E^0 R}{\kappa y_{VE}} \\
\jmath_P &= \frac{\dot{J}_{PA}}{\dot{k}_M M_{Vm}} = \frac{y_{PX} \dot{J}_{XA}}{\dot{k}_M M_{Vm}} = -y_{PX} \jmath_X
\end{aligned}$$

We also scale the mineral fluxes $\boldsymbol{\jmath}_{\mathcal{M}} = \frac{\boldsymbol{j}_{\mathcal{M}}}{\dot{k}_M M_{Vm}}$. Using (4.35), the scaled mineral fluxes follow from the scaled organic fluxes: $\boldsymbol{\jmath}_{\mathcal{M}} = -\boldsymbol{n}_{\mathcal{M}}^{-1} \boldsymbol{n}_{\mathcal{O}} \boldsymbol{\jmath}_{\mathcal{O}}$. In summary, apart from the

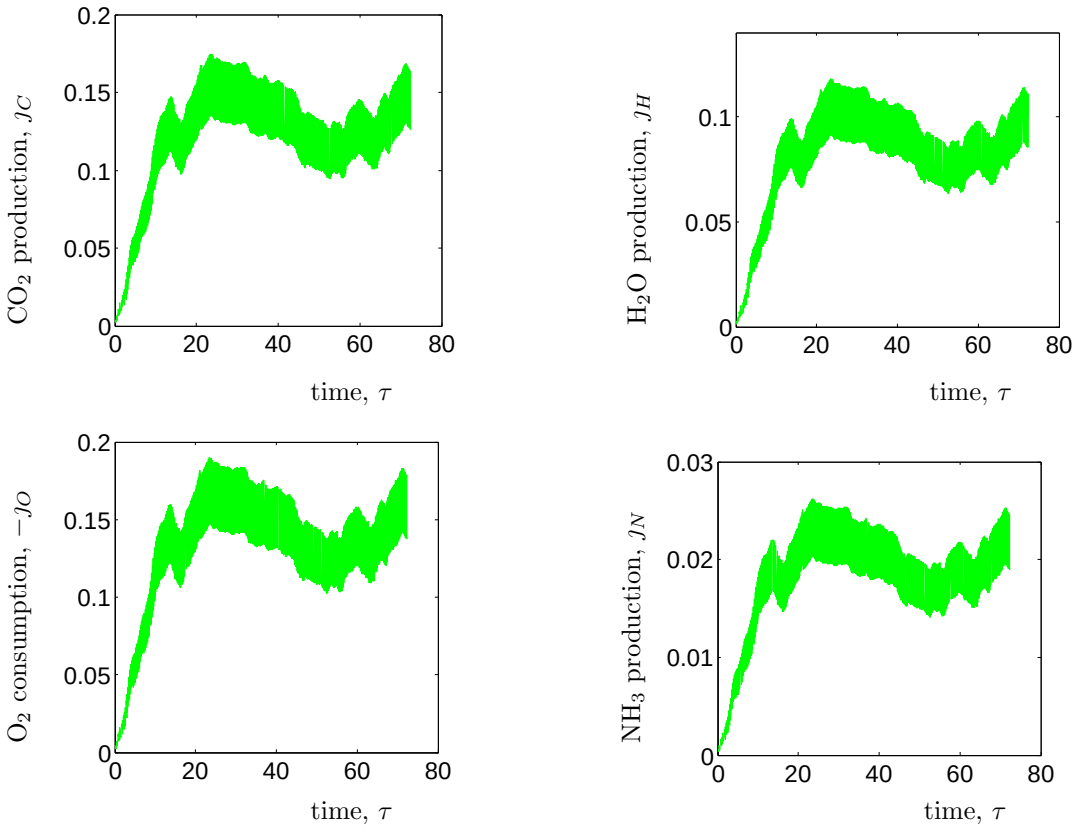

Figure 4.8: If searching follows a time-inhomogeneous Poisson process, the mineral fluxes behave stochastically as well, with a relatively large scatter. The stochastic standard DEB model, as well as the parameters, are as presented in Section 2.9 of the comments. The extra parameters for the mineral fluxes are: $y_{EX} = 0.8$, $y_{VE} = 0.8$, $y_{PX} = 0.1$, $\kappa = 0.8$. The latter parameter does not occur independently from the others, so does not count as extra.

chemical indices $\boldsymbol{n}_{\mathcal{M}}$ and $\boldsymbol{n}_{\mathcal{O}}$, we need 3 extra parameters for the scaled mineral fluxes: κy_{VE}, κy_{VE}, y_{PX}.

Figure 4.8 presents a simulated trajectory of the 4 mineral fluxes, where the minerals show more scatter than the state variables in figure 2.11. Part of this scatter will not appear in practice because the digestive system will smooth out some fluctuations of the assimilation. On the other hand, more sources of stochasticity can be expected, such as differences in particle sizes (so in handling times), in food quality, in temperature, in somatic maintenance (which includes behaviour), etc.

4.3.2 Derivation of (4.39) & (4.40)

The derivation is as follows, using Table 3.3 for conversions

$$\frac{d}{dt}l \;=\; \frac{d}{dt}(M_V/M_{Vm})^{1/3} = \frac{\frac{d}{dt}M_V}{3M_V^{2/3}M_{Vm}^{1/3}}$$

$$\begin{aligned} &= \frac{\dot{p}_G \eta_{VG}}{3M_V^{2/3} M_{Vm}^{1/3}} = \frac{\dot{p}_G \eta_{VG}}{3l^2 M_{Vm}} = \frac{\dot{p}_G}{3l^2 \mu_{GV} M_{Vm}} \\ &= \frac{\dot{p}_G}{3l^2 [E_G] M_{Vm}/[M_V]} = \frac{\dot{p}_G}{3l^2 [E_G] V_m} = \frac{\dot{p}_G}{3l^2 [E_G] E_m/[E_m]} \\ &= \frac{\dot{p}_G}{3l^2 \kappa g E_m} \end{aligned}$$

$$\begin{aligned} \frac{d}{dt}e &= \frac{d}{dt}\frac{M_E M_{Vm}}{M_V M_{Em}} = \frac{M_{Vm}}{M_{Em}}\frac{d}{dt}\frac{M_E}{M_V} = \frac{M_{Vm}}{M_{Em}}\left(M_V^{-1}\frac{d}{dt}M_E - \frac{M_E}{M_V^2}\frac{d}{dt}M_V\right) \\ &= \frac{M_{Vm}}{M_V M_{Em}}\left(\frac{d}{dt}M_E - \frac{M_E}{M_V}\frac{d}{dt}M_V\right) = \frac{M_{Vm}}{M_V M_{Em}}\left(\frac{\dot{p}_A - \dot{p}_C}{\mu_E} - \frac{M_E}{M_V}\dot{p}_G \eta_{VG}\right) \\ &= \frac{1}{l^3 M_{Em}}\left(\frac{\dot{p}_A - \dot{p}_C}{\mu_E} - \frac{M_E}{M_V}\dot{p}_G \eta_{VG}\right) = \frac{1}{l^3 \mu_E M_{Em}}\left(\dot{p}_A - \dot{p}_C - \dot{p}_G \frac{M_E}{M_V}\frac{\mu_E}{\mu_{GV}}\right) \\ &= \frac{1}{l^3 \mu_E M_{Em}}\left(\dot{p}_A - \dot{p}_C - \dot{p}_G\, e\, m_{Em}\frac{\mu_E}{\mu_{GV}}\right) = \frac{1}{l^3 \mu_E M_{Em}}\left(\dot{p}_A - \dot{p}_C - \dot{p}_G\, e\, \frac{y_{EV}}{\kappa g}\frac{\mu_E}{\mu_{GV}}\right) \\ &= \frac{1}{l^3 \mu_E M_{Em}}\left(\dot{p}_A - \dot{p}_C - \dot{p}_G \frac{e}{\kappa g}\right) = \frac{1}{l^3 E_m}\left(\dot{p}_A - \dot{p}_C - \dot{p}_G \frac{e}{\kappa g}\right) \end{aligned}$$

The maintenance process is here assumed to produce ammonia as single nitrogen waste. It is theoretically also possible that some dinitrogen is formed in this process. The results of [174] show that this hardly affect to macrochemical reaction equation.

4.3.3 Derivation of (4.41)

Notice that

$$\begin{pmatrix} w_E & w_V \end{pmatrix}\begin{pmatrix} e_0 & e_b l_b^3 \\ 0 & l_b^3 \end{pmatrix} = \begin{pmatrix} w_E e_0 & w_E e_b l_b^3 + w_V l_b^3 \end{pmatrix}.$$

If the write out the product with the factor $[M_{Em}]V_m$, we arrive at the initial wet weight $W_w(0) = [M_{Em}]V_m w_E e_0$, where $[M_{Em}]V_m e_0$ is the initial amount of C-moles of reserve. The wet weight at birth is $W_w(a_b) = [M_{Em}]V_m\,(w_E e_b l_b^3 + w_V l_b^3)$, where $[M_{Em}]V_m e_b l_b^3$ is the C-moles of reserve at birth and $[M_{Em}]V_m l_b^3$ is the C-moles of structure at birth. If we replace the molecular weights w_E and w_V, by those corresponding to dry-weights, we get the result in dry-weights, rather than wet weights.

4.3.3 Derivation of (4.43)

Notice that $[M_V]V_b$ stands for the C-moles of the structure of a neonate, so having volume V_b. Further, $E_0 - E_b$ is the energy that is used from the reserve during the incubation period, so $\mu_E^{-1}(E_0 - E_b)$ is the number of C-moles that is used from the reserve during this period.

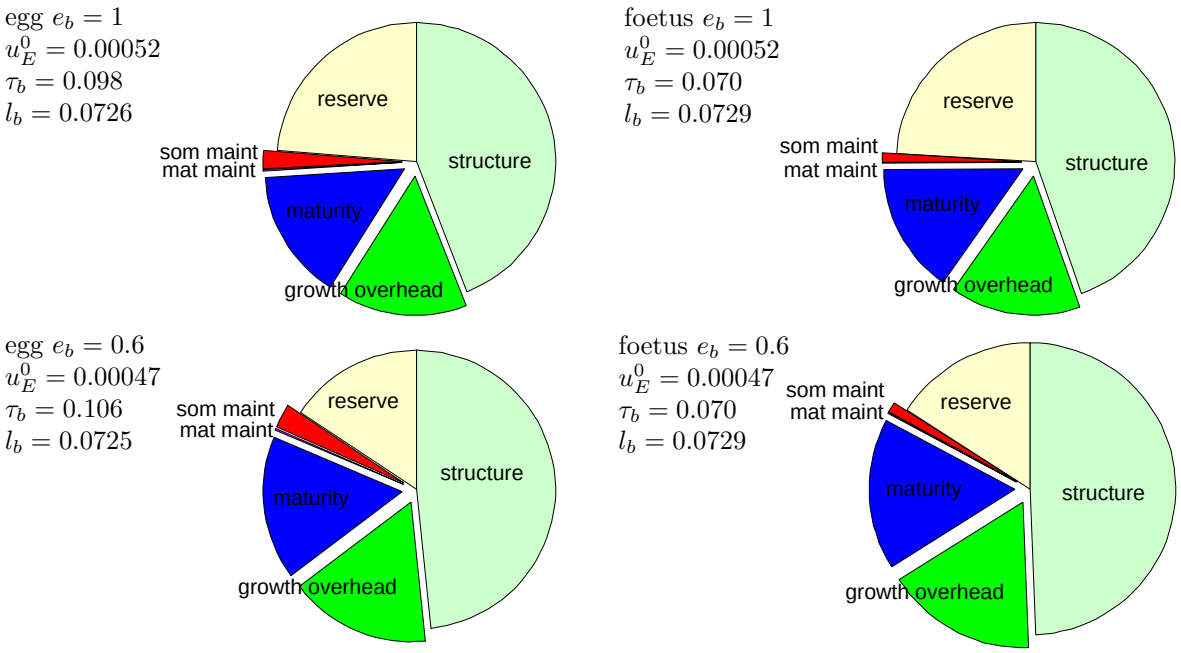

Figure 4.9: The fractions of cumulated energy investment at birth for an egg (left) and foetus (right) at $e_b = 1$ (top) and $e_b = 0.6$ (bottom). Foetal development does not suffer from the problem that reserve decreases during growth, so the age at birth and the cumulated maintenance losses are smaller. Egg development at $e_b = 1$ is faster than for $e_b = 0.6$, so the age at birth and the cumulated maintenance losses are smaller. The parameter values are those for the generalised animal, Table 8.1: $g = \frac{[E_G]\dot{v}}{\kappa\{\dot{p}_{Am}\}} = 3.11$, $k = \frac{\dot{k}_J[E_G]}{[\dot{p}_M]} = 0.311$, $v_H^b = \frac{E_H^b[\dot{p}_M]^3}{(1-\kappa)\kappa^2[E_G]\{\dot{p}_{Am}\}^3} = 0.0004$, $\kappa = 0.8$, $\kappa_G = \frac{\mu_V[M_V]}{[E_G]} = 0.747$.

4.3.3 Mass investment in neonates

At birth, the cumulative energy investment in somatic maintenance amounts to $E_M^b = \int_0^{a_b}[\dot{p}_M]L^3(a)\,da$, in maturity maintenance to $E_J^b = \int_0^{a_b}\dot{k}_J E_H(a)\,da$, in growth to $E_G^b = [E_G]L_b^3$, in maturity to E_H^b and energy in reserve E_b is left over from E_0 it initially had. The energy fixed in structure equals $\kappa_G E_G^b = \mu_V M_V^b$, while $(1-\kappa_G)E_G^b$ dissipated as growth overheads. So the energy content of the egg decreased from E_0 to $E_W^b = E_b + \kappa_G E_G^b$ at birth.

These various destinies of allocated energy can be expressed in a relative way as $e_M^b = \frac{E_M^b}{E_0} = \frac{u_M^b}{u_E^0}$, $e_J^b = \frac{E_J^b}{E_0} = \frac{u_J^b}{u_E^0}$, $e_G^b = \frac{E_G^b}{E_0} = \frac{u_G^b}{u_E^0}$ and $e_E^b = \frac{E_b}{E_0} = \frac{u_E^b}{u_E^0}$, with $1 = e_M^b + e_J^b + e_G^b + e_E^b$ and $u_* = \frac{E_*}{\{\dot{p}_{Am}\}}\frac{g^2\dot{k}_M^3}{\dot{v}^2}$, as before, see Table 2.1. Scaled initial reserve u_E^0, scaled length at birth l_b and scaled age at birth τ_b are functions of g, k, v_H^b and e_b. We also have $u_M^b = \kappa\int_0^{\tau_b} l^3(\tau)\,d\tau$ and $u_J^b = k\int_0^{\tau_b} u_H(\tau)\,d\tau$ and $u_G^b = \kappa l_b^3$ and $e_E^b = \frac{e_b l_b^3}{g}$. The evaluation of this relative budget involves, therefore, one new parameter, κ, and if we want to split out the growth overheads, we also need κ_G. The scaling shows that we don't need to know any rate parameter explicitly, since the energy fractions don't involve time, see Fig. 4.9. Notice that the pies have 5 degrees of freedom, which are determined by 5 parameters.

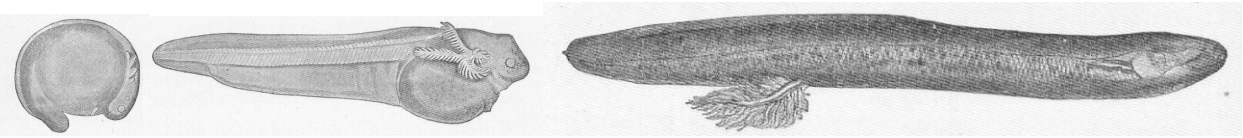

Figure 4.10: Embryo, 3 d before hatching (left), larva, 13 d after hatching (middle), and breeding male (right) of the South American lungfish, which shows the gills-like structures on the pelvic fin that work opposite to typical gills and provide offspring with dioxygen. From University of Washington Libraries.

4.4 Respiration

The South American lungfish, *Lepidosiren paradoxa*, lives in dioxygen-poor waters. When the male guards the brood in its 1.5 m long debris-filled burrow during the rainy season, his pelvic fins develop highly vascularized, gill-like, feathery structures that release dioxygen from the blood and take in carbon dioxide; the filaments disappear after the end of the breeding season [1110]. The neonates are equipped with external gills, which eventually disappear, see Figure 4.10.

4.4 Respiration: Derivation of (4.49)

We use (4.35) and (eqn:JO) to find $\dot{\boldsymbol{J}}_{\mathcal{M}} = -\boldsymbol{n}_{\mathcal{M}}^{-1}\boldsymbol{n}_{\mathcal{O}}\boldsymbol{\eta}_{\mathcal{O}}\dot{\boldsymbol{p}}$. The first element of this vector is the one that we need if we exclude assimilation by $\dot{p}_A = 0$ and product formation by $\eta_{PD} = \eta_{PG} = 0$. From (4.5) we find

$$\boldsymbol{\eta}\dot{\boldsymbol{p}} = (\ 0 \quad \eta_{VG}\dot{p}_G \quad -(\dot{p}_D + \dot{p}_G)/\mu_E \quad 0\ )^T$$

The first row of $\boldsymbol{n}_{\mathcal{M}}^{-1}\boldsymbol{n}_{\mathcal{O}}$ is for $n_{C*} = 1$, because we work in C-moles:

$$(\ 1 - n_{NX}\tfrac{n_{CN}}{n_{NN}} \quad 1 - n_{NV}\tfrac{n_{CN}}{n_{NN}} \quad 1 - n_{NE}\tfrac{n_{CN}}{n_{NN}} \quad 1 - n_{NP}\tfrac{n_{CN}}{n_{NN}}\ )$$

Minus the product of this first row and $\boldsymbol{\eta}\dot{\boldsymbol{p}}$ directly gives (4.49)

The significance of (4.49) is to demonstrate that, if respiration quotient is taken to be constant, which is frequently done in animal physiology, the implied assumption is that a very special relationship must exist between the elemental frequencies of reserve, relative to structure. It is a rather complex relationship, however. If we make a slightly stronger assumption, namely that urination and watering quotients are also constant, it in fact means that reserve and structure must have the same relative elemental frequencies. This is mentioned at the end of subsection 4.4.1. Reserve and structure can still differ in chemical composition, while having the same relative elemental frequencies. That RQ does not vary that much in animals is shown in Table , where lipids, carbohydrates and proteins in combination comprise most of biomass and differ only a little in relative frequencies of C, H and O, while N is confined to proteins. A large discrepancy between the relative elemental frequencies of reserve and structure would imply an inefficiency of the conversion from reserve to structure. Organisms that assimilate different nutrients independently have multiple reserves, which is why microbiologists never assume RQ to be constant. Respiration

is typically measured to quantify metabolic rate, which should be quantified as entropy dissipation, but, under aerobic conditions, is typically quantified as heat dissipation in practice. Calorimetry deals with the relationship between heat dissipation and respiration, see Section 4.8.2 of the comments.

4.4.1 Derivation of (4.52)

The definition of n is given in (4.36), where $n_{CN} = 0$ in case of ammonia as nitrogen waste.

4.4.2 Heat increment of feeding paid from mobilised reserve

In the standard DEB model, the heat increment of feeding (specific dynamic action) is paid as (fixed) part of the overhead costs for assimilation, directly from food; this is why these costs don't show up explicitly in the equations for growth or reproduction. The use of dioxygen actually rises in a very early phase of the digestion process. The standard DEB model assumes instantaneous digestion and conversion to reserve, so that 'detail' cannot be captured in the standard model; we need an explicit digestion module for this, cf. 7.3. What if we don't pay the heat increment of feeding as overhead of the assimilation process, but from the mobilised flux of reserve to the soma, $\kappa \dot{p}_C$? The energy costs are still proportional to the feeding rate, so we can assume that an energy flux of size $\dot{p}_F = \kappa_F \dot{p}_A$ is involved, where κ_F is a constant for a certain food type. So, using (2.12), we arrive for $[\dot{p}_S] = [\dot{p}_M] + \{\dot{p}_T\}/L$, $[\dot{p}_G] = [E_G]\dot{r}$, $[\dot{p}_F] = \kappa_F[\dot{p}_A]$ and $[\dot{p}_A] = f\{\dot{p}_{Am}\}/L$ at

$$\begin{aligned}
\kappa[\dot{p}_C] &= [\dot{p}_S] + [\dot{p}_G] + [\dot{p}_F] = \kappa[E](\dot{v}/L - \dot{r}) \\
\dot{r} &= \frac{[E]\dot{v}/L - [\dot{p}_S]/\kappa - [\dot{p}_A]\kappa_F/\kappa}{[E] + [E_G]/\kappa} \overset{[E]=f[E_m]}{=} \frac{(1-\kappa_F/\kappa)f\{\dot{p}_{Am}\}/L - [\dot{p}_S]/\kappa}{[E] + [E_G]/\kappa} \\
L_\infty &= \frac{\kappa[E]\dot{v} - \{\dot{p}_T\} - \kappa_F\{\dot{p}_{Am}\}f}{[\dot{p}_M]} \overset{[E]=f[E_m]}{=} f(\kappa - \kappa_F)\frac{\{\dot{p}_{Am}\}}{[\dot{p}_M]} - \frac{\{\dot{p}_T\}}{[\dot{p}_M]}
\end{aligned}$$

This evaluation shows that at constant food the payment of the heat increment of feeding from assimilation overhead or mobilised reserve have the same result, apart from a small change in the detailed interpretation of κ. In dynamic situations, however, where f changes in time, payment of the heat increment of feeding from mobilised reserve implies an extension of the specification of growth with an extra parameter. The difference only shows up if $\frac{d}{dt}f \gg \dot{v}/L$. Section 2.5.1 of the comments presents an argument to add the cost of the heat increment of feeding (if paid from mobilised reserve) to that of searching for food, and include it in the surface-linked maintenance costs. We then don't need extra parameters to quantify growth.

4.6 Water balance

Some terrestrial taxa, such as birds [1185], reptiles [1059] and terrestrial amphibians [982] show a decreasing water content in their tissues during embryo and early juvenile development. Altricial birds, which hardly have access to water in the nest as nestling, have

a higher water content as embryo than precocial ones, which supports the interpretation that water content, as provided by the mother, anticipates on the availability of water. Water shortage can affect development [1059, 172, 982, 608, 609]. This can be taken into account by delineating a state variable 'water content', apart from maturity, reserve and structure, and treat it as a chemical compound, see Chapter 6. The 'too little' range is here of interest, rather than the 'too much' range, but otherwise particular parameters can depend on the water content.

4.7 Isotope dynamics in the standard DEB model

4.7.1 Maintenance substrate

The implications of atoms of mobilised reserve having priority over that of mobilised structure to be build in into structure in the turnover of structure is that the reshuffling parameters of the dissipation transformation for nitrogen and carbon are

$$E + y_{VE}^{M_a} V \to y_{VE}^{M_a} V + C + n_{NE} N + \text{water} + \text{dioxygen}$$

is

$$\begin{aligned}
\alpha_{NE}^{ND} &= \frac{(n_{NE} - y_{VE}^{M_a} n_{NV})_+}{n_{NE}}; \quad \alpha_{VE}^{ND} = 1 - \alpha_{NE}^{ND} \\
\alpha_{NV}^{ND} &= 1 - \alpha_{VV}^{ND}; \quad \alpha_{VV}^{ND} = \frac{(y_{VE}^{M_a} n_{NV} - n_{NE})_+}{y_{VE}^{M_a} n_{NV}} \\
\alpha_{CE}^{CD} &= (1 - y_{VE}^{M_a})_+; \quad \alpha_{VE}^{CD} = 1 - \alpha_{CE}^{CD} \\
\alpha_{CV}^{CD} &= 1 - \alpha_{VV}^{CD}; \quad \alpha_{VV}^{CD} = \frac{(y_{VE}^{M_a} - 1)_+}{y_{VE}^{M_a}}
\end{aligned}$$

4.8 Enthalpy, entropy and free energy balances

4.8.1 Heat proportional to dioxygen flux

In microbiology, heat is frequently taken to be proportional to the dioxygen flux. We can now try to understand how this translates to constraints on biomass composition, and we can specify the proportionality factor in terms of DEB parameters.

Let

$$\boldsymbol{n}_{\mathcal{M}}^{-1} = \boldsymbol{u}_{\mathcal{M}} = \begin{pmatrix} \boldsymbol{u}_C \\ \boldsymbol{u}_H \\ \boldsymbol{u}_O \\ \boldsymbol{u}_N \end{pmatrix} = \begin{pmatrix} 1 & 0 & 0 & -\frac{n_{CN}}{n_{NN}} \\ 0 & 2^{-1} & 0 & -\frac{n_{HN}}{2n_{NN}} \\ -1 & -4^{-1} & 2^{-1} & \frac{n}{4n_{NN}} \\ 0 & 0 & 0 & n_{NN}^{-1} \end{pmatrix}; \quad n \equiv 4n_{CN} + n_{HN} - 2n_{ON}$$

and

$$\boldsymbol{n}_{\mathcal{O}} = \begin{pmatrix} n_{CX} & n_{CV} & n_{CE} & n_{CP} \\ n_{HX} & n_{HV} & n_{HE} & n_{HP} \\ n_{OX} & n_{OV} & n_{OE} & n_{OP} \\ n_{NX} & n_{NV} & n_{NE} & n_{NP} \end{pmatrix} = \begin{pmatrix} \boldsymbol{n}_X & \boldsymbol{n}_V & \boldsymbol{n}_E & \boldsymbol{n}_P \end{pmatrix}$$

and

$$\boldsymbol{\eta}_{\mathcal{O}} = \begin{pmatrix} -\eta_{XA} & 0 & 0 \\ 0 & 0 & \eta_{VG} \\ \mu_E^{-1} & -\mu_E^{-1} & -\mu_E^{-1} \\ \eta_{PA} & \eta_{PD} & \eta_{PG} \end{pmatrix} = \begin{pmatrix} \boldsymbol{\eta}_A & \boldsymbol{\eta}_D & \boldsymbol{\eta}_G \end{pmatrix}$$

The dioxygen flux can thus be written as $\dot{J}_O = -\boldsymbol{u}_O \boldsymbol{n}_{\mathcal{O}} \dot{\boldsymbol{J}}_{\mathcal{O}}$, see (4.3). Dissipating heat is given by

$$\begin{aligned} \dot{p}_{T+} &= -\boldsymbol{\mu}_{\mathcal{M}}^T \dot{\boldsymbol{J}}_{\mathcal{M}} - \boldsymbol{\mu}_{\mathcal{O}}^T \dot{\boldsymbol{J}}_{\mathcal{O}} \\ &= (\boldsymbol{\mu}_{\mathcal{M}}^T \boldsymbol{n}_{\mathcal{M}}^{-1} \boldsymbol{n}_{\mathcal{O}} - \boldsymbol{\mu}_{\mathcal{O}}^T) \dot{\boldsymbol{J}}_{\mathcal{O}} \end{aligned}$$

see (4.77) and (4.35). The question now translates as: under what constraints do we have $\dot{p}_{T+} = -\mu_{OT} \dot{J}_O$, and how does the constant μ_{OT} relate to parameter values? So we have that

$$\mu_{OT} = -\frac{\dot{p}_{T+}}{\dot{J}_O} = \frac{(\boldsymbol{\mu}_{\mathcal{M}}^T \boldsymbol{n}_{\mathcal{M}}^{-1} \boldsymbol{n}_{\mathcal{O}} - \boldsymbol{\mu}_{\mathcal{O}}^T) \dot{\boldsymbol{J}}_{\mathcal{O}}}{\boldsymbol{u}_O \boldsymbol{n}_{\mathcal{O}} \dot{\boldsymbol{J}}_{\mathcal{O}}} = \frac{(\boldsymbol{\mu}_{\mathcal{M}}^T \boldsymbol{u}_{\mathcal{M}} \boldsymbol{n}_{\mathcal{O}} - \boldsymbol{\mu}_{\mathcal{O}}^T) \boldsymbol{\eta}_{\mathcal{O}} \dot{\boldsymbol{p}}}{\boldsymbol{u}_O \boldsymbol{n}_{\mathcal{O}} \dot{\boldsymbol{\eta}}_{\mathcal{O}} \dot{\boldsymbol{p}}}$$

must be constant, while the three elements of $\dot{\boldsymbol{p}}$ can vary. This can only happen if this relationship applies to each of the three powers $\dot{\boldsymbol{p}}$:

$$\mu_{OT} = \frac{(\boldsymbol{\mu}_{\mathcal{M}}^T \boldsymbol{u}_{\mathcal{M}} \boldsymbol{n}_{\mathcal{O}} - \boldsymbol{\mu}_{\mathcal{O}}^T) \boldsymbol{\eta}_A}{\boldsymbol{u}_O \boldsymbol{n}_{\mathcal{O}} \boldsymbol{\eta}_A} = \frac{(\boldsymbol{\mu}_{\mathcal{M}}^T \boldsymbol{u}_{\mathcal{M}} \boldsymbol{n}_{\mathcal{O}} - \boldsymbol{\mu}_{\mathcal{O}}^T) \boldsymbol{\eta}_D}{\boldsymbol{u}_O \boldsymbol{n}_{\mathcal{O}} \boldsymbol{\eta}_D} = \frac{(\boldsymbol{\mu}_{\mathcal{M}}^T \boldsymbol{u}_{\mathcal{M}} \boldsymbol{n}_{\mathcal{O}} - \boldsymbol{\mu}_{\mathcal{O}}^T) \boldsymbol{\eta}_G}{\boldsymbol{u}_O \boldsymbol{n}_{\mathcal{O}} \boldsymbol{\eta}_G}$$

so

$$\boldsymbol{\mu}_{\mathcal{M}}^{T*} \boldsymbol{u}_{\mathcal{M}} \boldsymbol{n}_{\mathcal{O}} \boldsymbol{\eta}_{\mathcal{O}} = \boldsymbol{\mu}_{\mathcal{O}}^T \boldsymbol{\eta}_{\mathcal{O}} \quad \text{with } \boldsymbol{\mu}_{\mathcal{M}}^{T*} = \begin{pmatrix} \mu_C & \mu_H & \mu_O - \mu_{OT} & \mu_N \end{pmatrix}$$

If $\boldsymbol{\eta}_{\mathcal{O}}^{-1}$ exists, this further reduces to the constraint $\boldsymbol{\mu}_{\mathcal{M}}^{T*} \boldsymbol{u}_{\mathcal{M}} \boldsymbol{n}_{\mathcal{O}} = \boldsymbol{\mu}_{\mathcal{O}}^T$. It still depends on some coefficients η via μ_{OT}, which is in $\boldsymbol{\mu}_{\mathcal{M}}^{T*}$.

Faeces as only product

Suppose $\eta_{PD} = \eta_{PG} = 0$, while $\eta_{PA} \neq 0$. This situation occurs when faeces is the only product, as in animals; $\boldsymbol{\eta}_{\mathcal{O}}^{-1}$ does not exist. Substitution for dissipation gives

$$\mu_{OT} = \frac{\boldsymbol{\mu}_{\mathcal{M}}^T \boldsymbol{u}_{\mathcal{M}} \boldsymbol{n}_E - \mu_E}{\boldsymbol{u}_O \boldsymbol{n}_E}$$

which does not depend on any coefficient η. Let

$$\boldsymbol{\mu}^T = \boldsymbol{\mu}_{\mathcal{M}}^{T*} \boldsymbol{u}_{\mathcal{M}} \boldsymbol{\eta}_{\mathcal{O}} = \begin{pmatrix} \mu_1 & \mu_2 & \mu_3 & \mu_4 \end{pmatrix}$$

We then must have that $\mu_2 = \mu_V$, $\mu_3 = \mu_E$, and $\eta_{PA}\mu_4 - \eta_{XA}\mu_1 = \eta_{PA}\mu_P - \eta_{XA}\mu_X$.

No product

Suppose $\eta_{PA} = \eta_{PD} = \eta_{PG} = 0$ (no product; this situation can occur with bacteria). We now have $\mu_1 = \mu_X$, so the constraints no longer depend on coefficients η. Substitution of the η's gives

$$\begin{aligned} \mu_{OT} &= \frac{\boldsymbol{\mu}_{\mathcal{M}}^T \boldsymbol{u}_{\mathcal{M}} (\boldsymbol{n}_E - \mu_E \eta_{XA} \boldsymbol{n}_X) - \mu_E (1 - \mu_X \eta_{XA})}{\boldsymbol{u}_O (\boldsymbol{n}_E - \mu_E \eta_{XA} \boldsymbol{n}_X)} \\ &= \frac{\boldsymbol{\mu}_{\mathcal{M}}^T \boldsymbol{u}_{\mathcal{M}} \boldsymbol{n}_E - \mu_E}{\boldsymbol{u}_O \boldsymbol{n}_E} \\ &= \frac{\boldsymbol{\mu}_{\mathcal{M}}^T \boldsymbol{u}_{\mathcal{M}} (\boldsymbol{n}_E - \mu_E \eta_{VG} \boldsymbol{n}_V) - \mu_E (1 - \mu_V \eta_{VG})}{\boldsymbol{u}_O (\boldsymbol{n}_E - \mu_E \eta_{VG} \boldsymbol{n}_V)} \end{aligned}$$

or, for $\boldsymbol{n}_{\mathcal{O}} = \begin{pmatrix} \boldsymbol{n}_X & \boldsymbol{n}_V & \boldsymbol{n}_E \end{pmatrix}$ and $\boldsymbol{\mu}_{\mathcal{O}}^T = \begin{pmatrix} \mu_X & \mu_V & \mu_E \end{pmatrix}$

$$\begin{aligned} \boldsymbol{\mu}_{\mathcal{O}}^T &= \boldsymbol{\mu}_{\mathcal{M}}^{T*} \boldsymbol{u}_{\mathcal{M}} \boldsymbol{n}_{\mathcal{O}} = (\boldsymbol{\mu}_{\mathcal{M}}^T \boldsymbol{u}_{\mathcal{M}} - \mu_{OT} \boldsymbol{u}_O) \boldsymbol{n}_{\mathcal{O}} \\ \boldsymbol{u}_O \boldsymbol{n}_E \boldsymbol{\mu}_{\mathcal{O}}^T &= (\boldsymbol{\mu}_{\mathcal{M}}^T \boldsymbol{u}_{\mathcal{M}} \boldsymbol{u}_O \boldsymbol{n}_E - \boldsymbol{\mu}_{\mathcal{M}}^T \boldsymbol{u}_{\mathcal{M}} \boldsymbol{n}_E \boldsymbol{u}_O + \mu_E \boldsymbol{u}_O) \boldsymbol{n}_{\mathcal{O}} \\ &= \left(\boldsymbol{\mu}_{\mathcal{M}}^T \boldsymbol{u}_{\mathcal{M}} (\boldsymbol{u}_O \boldsymbol{n}_E - \boldsymbol{n}_E \boldsymbol{u}_O) + \mu_E \boldsymbol{u}_O \right) \boldsymbol{n}_{\mathcal{O}} \end{aligned}$$

Notice that $\boldsymbol{u}_O \boldsymbol{n}_E$ is a scalar and $\boldsymbol{n}_E \boldsymbol{u}_O$ a (4×4)-matrix. Although the result does not depend on the detailed dynamics of the DEB model, it does depend on an important property of the standard DEB model: all mass fluxes are weighted sums of assimilation, dissipation and growth.

Ammonia as N-waste

$n_{CN} = 0$, $n_{HN} = 3$, $n_{ON} = 0$ and $n_{NN} = 1$, so $n = 3$ and

$$\boldsymbol{u}_{\mathcal{M}} = \frac{1}{4} \begin{pmatrix} 4 & 0 & 0 & 0 \\ 0 & 2 & 0 & -6 \\ -4 & -1 & 2 & 3 \\ 0 & 0 & 0 & 4 \end{pmatrix}$$

This can be used to work out a numerical example.

4.8.2 Indirect calorimetry

Respiration, urination and watering quotients, as discussed in Section 4.4.1 and 4.5.1, deal with the relationships between mineral fluxes (CO_2, H_2O, O_2, NH_3). Calorimetry deals with the relationship between dissipating heat and these mineral fluxes. DEB theory assumes that parameter values are individual-specific, including the relative elemental frequencies of reserve and structure. So considerations about the possible variation of these quotients relate to ontogenetic comparisons, where the relative elemental frequencies are treated as constants. Inter-specific comparisons, however, also need to deal with variations in relative elemental frequencies. These variations can be considerable [1491, 1490], which come with the need to calibrate the coefficients that are used in indirect calorimetry.

The interpretation of respiration and heat dissipation in terms of metabolism needs considerable care. Most of the amazement in the literature that respiration frequently

scales approximately with body weight$^{3/4}$, known as Kleiber's law, see Section 11.1 of the comments, originates from the shaky assumption that respiration represents maintenance, if contributions from assimilation are excluded from the measurements by starving the subject. DEB theory shows that this interpretation is wrong. It also shows that reproduction represents the export of reserve that comes with little overhead costs, so hardly contributes to respiration. Although respiration and heat dissipation quantify metabolic activity, these measures do have their limitations. The existence of life in anaerobic environments and some (anaerobic) bacteria that consume rather than dissipate heat further illustrate this limitation.

Modern ecological literature is frequently very sloppy on the relationships between fluxes. Hirst et al. [611], for instance, group Rubner's surface law [1224] together with DEB theory as being ideas that link external surfaces of organisms to fluxes, to contrast it with MTE, see Section 11.1.1 of the comments, which links fluxes to internal tubing networks. Where DEB theory links food uptake to surface, Rubner links dissipating heat to surface, and Hirst et al. don't specify what flux they link to surface, mention excretion as example, and treat it as being proportional to respiration. Also MTE does not specify what flux they have in mind and also treat it as being proportional to respiration. Indirect calorimetry shows, however, that the fluxes are not all proportional to each other, and DEB theory explains why. If all these fluxes to and from an individual would be proportional to each other, it is impossible for the individual to follow a life cycle (embryo, juvenile and adult), where reproduction is initially absent and growth eventually ceases. Respiration is typically quantified in the ecological literature as an allometric function of body weight. The additive nature of the various contributions to respiration, which are different functions of body weight, is at odds, however, with any allometric function. Discussions on the precise value of the scaling exponent are bound to be unproductive. This additive nature is also at odds with any role for respiration to explain other metabolic functions, despite the many attempts in the literature to project such a role on respiration. See Section 11.1.1 of the comments for further discussions of ideas on respiration.

4.8.3 Equation (4.84)

The powers $\dot{\boldsymbol{p}}$ in Equation (4.84) are functions in scaled reserve density e and scaled length l of an individual V1-morph, in this case, while the heat that dissipates from a population of V1-morphs in a chemostat is evaluated. Assimilation, dissipation and growth all increase proportional to mass (i.e. cubed length) of an individual. So by evaluating the powers for $l^3 = 1$ and dividing by the maximum mass M_{Vm} of an individual we arrive at the mass-specific fluxes that are still a function of e. Multiplication with the total structural mass M_{V+} of all individuals in the chemostat gives the performance of the whole chemostat.

4.9 Otoliths as composite products

Like wood of plants and shells of molluscs, otoliths in fish can be considered as products which helps to convert observations from otoliths to expectations for growth and food

intake in the past (collaborative work with Laure Pecquerie). We assume that otoliths remain isomorphic, except at metamorphosis, where they make an instantaneous change from a disc-like shape to a more complex one. The shape correction function of otoliths can be quantified as $\mathcal{M}_\oslash(U_H) = \mathcal{M}^b_\oslash + (U_H > U^j_H)(\mathcal{M}^p_\oslash - \mathcal{M}^b_\oslash)$. So $\frac{d}{dt}\mathcal{M} = 0$, except at $U_H = U^j_H$. The physical otolith length $\mathcal{L}_\oslash$ relates to the volumetric otolith length $L_\oslash$ as $\mathcal{L}_\oslash = L_\oslash/\delta_{\mathcal{L}\oslash}$, where $\delta_{\mathcal{L}\oslash} = \delta^b_{\mathcal{L}\oslash}$ or $\delta^p_{\mathcal{L}\oslash}$, depending on U_H. The physical otolith surface area (which we need for the degradation process of otoliths) is proportional to the squared volumetric otolith length, but the proportionality factor makes a jump at metamorphosis.

Suppose that otoliths are products with volume $V_\oslash$ and volumetric length $L_\oslash = V_\oslash^{1/3}$. Like all product formation, change in otolith volume is a weighted sum of contributions from assimilation, dissipation and growth. The otolith is in the otosac and suppose that the otosac is isomorphic with volume $\delta_S V$, that the use of otolith material in the fluid in the otosac is proportional to the concentration of otolith material in this fluid and that the precipitation of utilized material is proportional to the volume of fluid in the otosac, relative to the volume of the otosac. The rest of mobilized otolith material is excreted into the environment. The change in otolith volume then becomes

$$\frac{d}{dt}V_\oslash = \left(\frac{\dot{p}_A}{[E_{\oslash A}]} + \frac{\dot{p}_D}{[E_{\oslash D}]} + \frac{\dot{p}_G}{[E_{\oslash G}]}\right)\left(1 - \frac{V_\oslash}{\delta_S V}\right)$$

The change in otolith volumetric length is $\frac{d}{dt}L_\oslash = \frac{1}{3}L_\oslash^{-2}\frac{d}{dt}V_\oslash$ and change in (body) volumetric length $\frac{d}{dt}L = \frac{1}{3}L^{-2}\frac{d}{dt}V = \frac{1}{3}L^{-2}\dot{p}_G/[E_G]$. So the change in volumetric length as function of the change in otolith volumetric length is

$$\begin{aligned}\frac{d\mathcal{L}}{d\mathcal{L}_\oslash} &= \frac{\delta_{\mathcal{L}\oslash}}{\delta_\mathcal{L}}\frac{\frac{1}{3}L^{-2}\dot{p}_G/[E_G]}{\frac{1}{3}L_\oslash^{-2}(\dot{p}_A/[E_{\oslash A}] + \dot{p}_D/[E_{\oslash D}] + \dot{p}_G/[E_{\oslash G}])(1 - L^3_\oslash/\delta_S L^3)}\\ &= \frac{\delta_{\mathcal{L}\oslash}}{\delta_\mathcal{L}}\frac{\dot{p}_G/[E_G]}{(\dot{p}_A/[E_{\oslash A}] + \dot{p}_D/[E_{\oslash D}] + \dot{p}_G/[E_{\oslash G}])(L^2/L^2_\oslash - L_\oslash/\delta_S L)}\end{aligned}$$

where

$$\begin{aligned}\dot{p}_A &= \{\dot{p}^*_{Am}\}fL^2; \quad \dot{p}_D = \dot{p}_M + \dot{p}_J + (1-\kappa_R)\dot{p}_R; \quad \dot{p}_M = [\dot{p}_M]L^3\\ \dot{p}_J &= \dot{k}_J E_H; \quad \dot{p}_R = (1-\kappa)\dot{p}_C - \dot{p}_J; \quad \dot{p}_G = \kappa\dot{p}_C - \dot{p}_M; \quad \dot{p}_C = [E]\frac{\dot{v}^* L^2 + \dot{k}_M L^3}{1 + \kappa[E]/[E_G]}\end{aligned}$$

with $f = 0$ for $U_H < U^b_H$, $\kappa_R = 0$ for $U_H < U^p_H$. Furthermore $\{\dot{p}^*_{Am}\} = \{\dot{p}_{Am}\}\mathcal{M}(L)$.

We can remove energies via division by $\{\dot{p}_{Am}\}$ at a reference temperature and maturity, i.e. $S_i = \dot{p}_i/\{\dot{p}_{Am}\}$, with $i = A, D, G, C, R, B, M, J$ with $\dim(S_i) = L^2$:

$$S_C = \frac{\dot{p}_C}{\{\dot{p}_{Am}\}} = \frac{L^2 e}{g+e}(\mathcal{M}(L)g + L/L_m); \quad S_M = \frac{\dot{p}_M}{\{\dot{p}_{Am}\}} = \frac{\kappa L^3}{L_m}; \quad S_J = \frac{\dot{p}_J}{\{\dot{p}_{Am}\}} = \dot{k}_J U_H$$

to obtain

$$\begin{aligned}\frac{d\mathcal{L}}{d\mathcal{L}_\oslash} &= \frac{\delta_{\mathcal{L}\oslash}}{\kappa g \delta_\mathcal{L}}\frac{\dot{v}S_G}{(\dot{v}_{\oslash A}S_A + \dot{v}_{\oslash D}S_D + \dot{v}_{\oslash G}S_G)(L^2/L^2_\oslash - L_\oslash/\delta_S L)}\\ \frac{d}{dt}\mathcal{L}_\oslash &= \frac{(\dot{v}_{\oslash A}S_A + \dot{v}_{\oslash D}S_D + \dot{v}_{\oslash G}S_G)(1 - L^3_\oslash/\delta_S L^3)}{3\delta_{\mathcal{L}\oslash}L^2_\oslash}\end{aligned}$$

with

$$S_A = \mathcal{M}(L) f L^2; \quad S_D = S_M + S_J + (1-\kappa_R) S_R; \quad S_G = \kappa S_C - S_M; \quad S_R = (1-\kappa) S_C - S_J$$

and

$$\dot{v}_{\oslash A} = \{\dot{p}_{Am}\}/[E_{\oslash A}]; \quad \dot{v}_{\oslash D} = \{\dot{p}_{Am}\}/[E_{\oslash D}]; \quad \dot{v}_{\oslash G} = \{\dot{p}_{Am}\}/[E_{\oslash G}]$$

Notice that $\dim(\dot{v}_i) = L/t$, with $i = \oslash A, \oslash D, \oslash G, \oslash$. The removal of energies from the equations comes with a reduction of one parameter, namely

$$U_H^b, U_H^j, U_H^p, \dot{k}_M, \dot{k}_J, g, \kappa, \dot{v}, \dot{v}_\oslash$$

combined with

$$[E_G], [E_{\oslash A}], [E_{\oslash D}], [E_{\oslash G}] \quad \textit{versus} \quad \dot{v}_{\oslash A}, \dot{v}_{\oslash D}, \dot{v}_{\oslash G},$$

given $f(t)$. If food density $X(t)$ is given, rather than scaled functional response $f(t)$, we need one extra parameter, the half saturation coefficient K. The conversion from the energy allocated to reproduction $\dot{p}_R$ to eggs involves the overhead factor $1 - \kappa_R$. The module for the buffer handling rule has additional parameters. The velocities $\dot{v}_i$ might be negative, provided that $L_\oslash > 0$ for all possible environmental scenario's for which the individual can survive. They do not depend on temperature, because we obtained them by via $\{\dot{p}_{Am}\}$ at a standardized temperature. Notice also that if $\dot{v}_{\oslash A} = \dot{v}_{\oslash D} = 0$ and δ_S large, we have $\frac{d\mathcal{L}}{d\mathcal{L}_\oslash} = \frac{\delta_{\mathcal{L}\oslash}}{\delta\mathcal{L}} \frac{L_\oslash^2}{\kappa g L^2} \frac{\dot{v}}{\dot{v}_{\oslash G}}$ and $\mathcal{L}^3 = \frac{\delta_{\mathcal{L}\oslash}}{\delta\mathcal{L}} \frac{\dot{v}}{\kappa g \dot{v}_{\oslash G}} \mathcal{L}_\oslash^3$ if $L_\oslash = 0$ when $L = 0$.

4.9 Otolith opacity

Otoliths typically have layers of transparent keratine-like protein, and opaque aragonite plus protein. This observed sequence of layers can be explained if the deposition on the otolith that is associated with growth and (possibly) assimilation has aragonite, and that linked to dissipation has not. Otoliths of embryos are opaque, and embryos don't have assimilation, so contribution from growth and/or maintenance must have aragonite. In winter, when food intake is so low that somatic maintenance costs is partly paid from the reproduction buffer and growth is ceased, otolith depositions have no aragonite, so the contribution from dissipation must be positive and must have no aragonite, while that of growth must also be positive and must have aragonite. If fully grown the deposition has no aragonite, so if the contribution of assimilation is positive, it can have no aragonite. On the assumption that degradation does not affect the opacity, opacity is given by

$$O(t) = \frac{\dot{v}_{\oslash A} S_A + \dot{v}_{\oslash G} S_G}{\dot{v}_{\oslash A} S_A + \dot{v}_{\oslash D} S_D + \dot{v}_{\oslash G} S_G}$$

which assumes value 1 if aragonite content is maximum, and 0 in complete absence of aragonite. The relative contributions of assimilation and growth linked depositions to opacity can be weighted unequally.

The color bands are used to assess growth. The human eye recognizes the band boundaries as maximum changes in color. Color change (in length of otolith) is given by

$$\frac{dO}{d\mathcal{L}_\oslash} = \frac{dO}{dt} \frac{dt}{d\mathcal{L}_\oslash} = \frac{\sum_k \dot{v}_{\oslash k} \frac{d}{dt} S_k - O \sum_i \dot{v}_{\oslash i} \frac{d}{dt} S_i}{(\sum_i \dot{v}_{\oslash i} S_i) \delta_{\mathcal{L}\oslash}^{-1} \frac{d}{dt} L_\oslash} \quad \text{for } i = A, D, G; \quad k = A, G$$

where we need

$$\begin{aligned}
\frac{d}{dt}S_A &= fL^2\frac{d}{dt}\mathcal{M} + \mathcal{M}L^2\frac{d}{dt}f + \mathcal{M}f2L\frac{d}{dt}L \\
\frac{d}{dt}\mathcal{M} &= (U_H > U_H^b)(U_H < U_H^j)(\frac{d}{dt}U_H/U_H^b)/(3\mathcal{M}^2) \\
\frac{d}{dt}f &= f^2\frac{K}{X^2}\frac{d}{dt}X \\
\frac{d}{dt}S_D &= \frac{d}{dt}S_M + \frac{d}{dt}S_J + (1-\kappa_R)\frac{d}{dt}S_R \\
\frac{d}{dt}S_G &= \kappa\frac{d}{dt}S_C - \frac{d}{dt}S_M \\
\frac{d}{dt}S_R &= (1-\kappa)\frac{d}{dt}S_C - \frac{d}{dt}S_J \\
\frac{d}{dt}S_C &= \frac{L}{g+e}(\mathcal{M}g + \frac{L}{L_m})(\frac{gL}{g+e}\frac{d}{dt}e + 2e\frac{d}{dt}L) + \frac{L^2e}{g+e}(g\frac{d}{dt}\mathcal{M} + \frac{d}{dt}\frac{L}{L_m}) \\
\frac{d}{dt}S_M &= \frac{3\kappa L^2}{L_m}\frac{d}{dt}L \\
\frac{d}{dt}S_J &= \dot{k}_J\frac{d}{dt}U_H
\end{aligned}$$

If $X(t)$ is described by a cubic spline or a Fourier series, the evaluation of $\frac{d}{dt}X$ is straightforward.

4.9 Isotopes in otoliths

To follow isotopes in otoliths, it is most convenient to work with masses, rather than energies or lengths. We also need more chemical detail. The chemical composition of the contributions from assimilation, dissipation and growth to the otolith can differ; the chemical indices are denotes by n_{ij}^k for $k = A, D, G$. Each C-mole contributes differently to volume, which makes that the otolith volume relates to the otolith mass as

$$V_\oslash = M_\oslash^A/[M_\oslash^A] + M_\oslash^D/[M_\oslash^D] + M_\oslash^G/[M_\oslash^G]$$

where the parameters $[M_\oslash^A]$, $[M_\oslash^D]$ and $[M_\oslash^G]$ are treated as constants. If $[M_\oslash^A] = [M_\oslash^D] = [M_\oslash^G] = [M_\oslash]$, the volume of the otolith simplifies to $V_\oslash = (M_\oslash^A + M_\oslash^D + M_\oslash^G)/[M_\oslash]$, which might be used as a first approximation to reduce the number of parameters.

Working with masses invites for working with yields, so we apply the relationships

$$[M_\oslash^A]\dot{v}_{\oslash A} = \{\dot{J}_{EAm}\}y_{\oslash E}^A; \quad [M_\oslash^D]\dot{v}_{\oslash D} = \{\dot{J}_{EAm}\}y_{\oslash E}^D; \quad [M_\oslash^G]\dot{v}_{\oslash G} = \{\dot{J}_{EAm}\}y_{\oslash E}^G.$$

Product formation, including otoliths, affects mineral fluxes. This can be avaluated by extending the sets of organic yields for assimilation, dissipation and growth with that on product formation, and the organic chemical indices with those of for otoliths, and obtain the mineral fluxes from the elemental balance equaltion. Since otoliths are very small, the correction is likely to be minute.

The changes in mass of otolith, the color, the chemical indices, the isotope indices and the isotope fractions of the otolith amount to

$$\begin{aligned}
\frac{d}{dt}M_{\oslash}^{A} &= y_{\oslash E}^{A}\dot{J}_{EA}\left(1-\frac{V_{\oslash}}{\delta_S V}\right)\\
\frac{d}{dt}M_{\oslash}^{D} &= -y_{\oslash E}^{D}\dot{J}_{ED}\left(1-\frac{V_{\oslash}}{\delta_S V}\right)\\
\frac{d}{dt}M_{\oslash}^{G} &= -y_{\oslash E}^{G}\dot{J}_{EG}\left(1-\frac{V_{\oslash}}{\delta_S V}\right)\\
O(t) &= \frac{y_{\oslash E}^{A}\dot{J}_{EA}-y_{\oslash E}^{G}\dot{J}_{EG}}{y_{\oslash E}^{A}\dot{J}_{EA}-y_{\oslash E}^{D}\dot{J}_{ED}-y_{\oslash E}^{G}\dot{J}_{EG}}\\
n_{i\oslash}(t) &= \frac{n_{i\oslash}^{A}y_{\oslash E}^{A}\dot{J}_{EA}-n_{i\oslash}^{D}y_{\oslash E}^{D}\dot{J}_{ED}-n_{i\oslash}^{G}y_{\oslash E}^{G}\dot{J}_{EG}}{y_{\oslash E}^{A}\dot{J}_{EA}-y_{\oslash E}^{D}\dot{J}_{ED}-y_{\oslash E}^{G}\dot{J}_{EG}}\\
n_{i\oslash}^{0}(t) &= \frac{n_{i\oslash}^{0A}y_{\oslash E}^{A}\dot{J}_{EA}-n_{i\oslash}^{0D}y_{\oslash E}^{D}\dot{J}_{ED}-n_{i\oslash}^{0G}y_{\oslash E}^{G}\dot{J}_{EG}}{y_{\oslash E}^{A}\dot{J}_{EA}-y_{\oslash E}^{D}\dot{J}_{ED}-y_{\oslash E}^{G}\dot{J}_{EG}}\\
\delta_{i\oslash}^{0}(t) &= \frac{n_{i\oslash}^{0}(t)}{n_{i\oslash}(t)}
\end{aligned}$$

with $\dot{J}_{EA}, \dot{J}_{EG} \leq 0$. Notice that the chemical indices n_{ij} and the isotope indices n_{ij}^0 are relative to carbon and that $n_{C\oslash}^{A} = n_{C\oslash}^{D} = n_{C\oslash}^{G} = n_{C\oslash} = 1$. Notice also that the otolith is not mixed, so we don't have dilution by growth of the otolith.

Several possibilities can be delineated for $n_{i\oslash}^{0k}$. The simplest set of possiblities is that no fractionation occurs at otolith formation, which we will examine in more detail. The isotope indices $n_{i\oslash}^{0k}$ are obtained from $n_{i\oslash}^{0k} = -\sum_s \alpha_{\oslash s}^{ik} n_{is}^{0k}/Y_{\oslash s}^{k}$, where for elements $i = C, H, N$ we have substrate $s = X$ for transformation $k = A$ and $s = E$ for $k = D, G$. For the element oxygen, $i = O$, we have two substrates, the second one being dioxygen, $s = O$. Since otoliths are very small, the effect of their production on the reshuffling parameters α will be minute, and we can link the isotope indices directly to that of reserve or structure. The contribution of dioxygen for oxygen in otoliths should be reconsidered. Since fractionation occurs at the anabolic/catabolic forks of the three fluxes, the allocation to otoliths can occur before or after the forks, so we have three possibilities per flux

$$\begin{aligned}
n_{i\oslash}^{0A} &= n_{i\oslash}^{A}\frac{n_{iX}^{0A}}{n_{iX}} \quad \text{or } n_{i\oslash}^{A}\frac{n_{iX}^{0A_a}}{n_{iX}} \quad \text{or } n_{i\oslash}^{A}\frac{n_{iX}^{0A_c}}{n_{iX}}\\
n_{i\oslash}^{0D} &= n_{i\oslash}^{D}\frac{n_{iE}^{0D}}{n_{iE}} \quad \text{or } n_{i\oslash}^{D}\frac{n_{iE}^{0D_a}}{n_{iE}} \quad \text{or } n_{i\oslash}^{D}\frac{n_{iE}^{0D_c}}{n_{iE}}\\
n_{i\oslash}^{0G} &= n_{i\oslash}^{G}\frac{n_{iE}^{0G}}{n_{iE}} \quad \text{or } n_{i\oslash}^{G}\frac{n_{iE}^{0G_a}}{n_{iE}} \quad \text{or } n_{i\oslash}^{G}\frac{n_{iE}^{0G_c}}{n_{iE}}
\end{aligned}$$

This does not exhaust all possibilities; part of the atoms in otoliths can originate from structure in the anabolic sub-flux of somatic maintenance. If we include the contribution from growth into the anabolic flux (the second option), we have $\kappa_G^a = y_{VE} + y_{\oslash E}^{G}$ and

$\kappa_G^c = 1 - \kappa_G^a$ and for assimilation $\kappa_A^a = y_{EX} + y_{\oslash E}^A$ and $\kappa_A^c = 1 - \kappa_A^a$. For dissipation the situation is simpler because κ_D^a is a free parameter, independent of other parameters.

With the presently available information, we can neglect the contribution from assimilation to otoliths, $y_{\oslash E}^A = 0$, but future work with biomarkers might change that.

Simulation results show that, even in absence of effects of temperature on the odds ratios, seasonal cycles in temperature result in a covariance of temperature and the isotope fractions in otoliths.

4.10 Parameter estimation

Parameters can be estimated from a collection of n data sets by minimizing the (dimensionless) loss function F_{sb}

$$F_{sb} = \sum_{j=1}^{n} \sum_{i=1}^{n_j} \frac{w_{ij}}{n_j} \frac{(d_{ij} - p_{ij})^2}{d_j^2 + p_j^2} \quad \text{with } p_j = n_j^{-1} \sum_{i=1}^{n_j} p_{ij} \text{ and } d_j = n_j^{-1} \sum_{i=1}^{n_j} d_{ij}$$

where data set j has n_j data points d_{ij} with predictions p_{ij} and w_{ij} are chosen weight coefficients (default $w_{ij} = 1$), see [911, 910]. This loss function is called 'symmetric bounded', because it is symmetric in the roles of data and predictions (so it punishes over- and under-estimation equally), while the contributions of infinitely large predictions to the loss function remain limited. In the practice of the Add_my_Pet (AmP) collection, some pseudo-data are added to the collection of data sets with small weights coefficients (default 0.1) to avoid ill-posedness, and to reduce the risk to arrive at nonsense values for parameters in a biological perspective. All pseudo-data is zero-variate (so just single numbers), see [856, 857].

The marginal confidence interval for parameter θ can be based on the profile of the loss function, $F_{sb}(\theta)$, where all parameters are estimated from the data, except θ, and θ is varied around its point-estimate θ^*, see [911]. The interval for confidence level p, with $0 < p < 1$, is defined as the set of values for θ for which $F_{sb}(\theta) < F_{sb}^p$. The cut-off value F_{sb}^p is subsequently found from a calibration-step using a Monte-Carlo simulation: Independently centered log-normally distributed random quantities, with a variation coefficient equal to the observed variation coefficient, are added to the predicted values for the data and the minimum of the loss function is determined for each Monte-Carlo run. In this way, a frequency distribution of minima is constructed and the p-level cut-off value F_{sb}^p determined. The resulting confidence interval was found to be very close to the one that results from a Maximum Likelihood method, for the simple case of a single data-set for the surviving fraction of individuals as a function of time [854]. The reasons why Maximum Likelihood methods cannot be used in the context of AmP are discussed in [911].

The survivor function $S(\theta)$ for the parameter θ can be found from a set of p-values, with $S(\theta^*) = 0.5$. Let θ_l^p be the lower boundary of the p-level confidence interval for θ, and θ_u^p be the upper boundary, so $S(\theta_l^p) - S(\theta_u^p) = p$ with $\theta_l^p < \theta^* < \theta_u^p$, while $\theta_l^0 = \theta^* = \theta_p^0$. For non-negative parameters we must have $\theta_l^1 = 0$, for unbounded parameters $\theta_l^1 = -\infty$, while $\theta_u^1 = \infty$. We also have $S(\theta_l^p) - S(\theta^*) = S(\theta_l^p) - 0.5 = p/2$, so $S(\theta_l^p) = (1 + p)/2$. Similarly $S(\theta^*) - S(\theta_u^p) = 0.5 - S(\theta_u^p) = p/2$, so $S(\theta_u^p) = (1 - p)/2$. This provides the recipe for

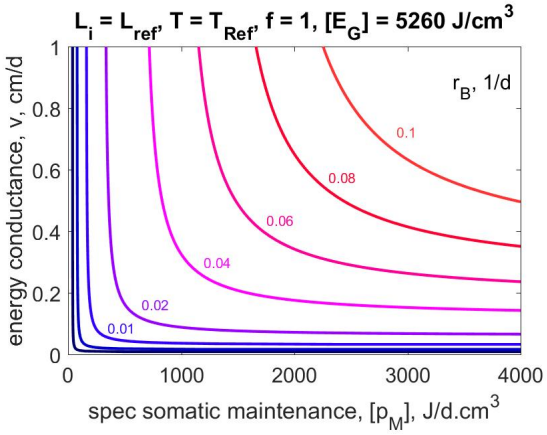

Figure 4.11: Lines of equal values for the von Bertalanffy growth rate $\dot{r}_B$ for $L_m = L_{\mathrm{ref}}$, $f = 1$, $T = T_{\mathrm{ref}}$, and $[E_G] = 5260\,\mathrm{J/cm^3}$ in the std model. The lines follow from the relationship $[\dot{p}_M] = 3\dot{r}_B([E_G] + \kappa\{\dot{p}_{Am}\}/\dot{v})$, while $[\dot{p}_M] = \kappa\{\dot{p}_{Am}\}/L_{\mathrm{ref}}$.

obtaining $S(\theta)$ from the loss function profile and the frequency distribution of minima of the loss function.

This method for estimation of parameters can be extended to multiple species [854], offering the opportunity to constrain similar parameters for n_s different species. The most obvious constraint is to choose some of them to be equal for all species. A less stringent constraint is to reduce the scatter of selected parameters among species by augmenting the loss function F_{sb} with the dimensionless term $\sum_{k=1}^{N} \frac{w_k \mathrm{var}(\theta_s^k)}{\mathrm{mean}(\theta_s^k)^2}$, where $k = 1, \cdots, N$ scans the parameters, w_k denotes chosen weights coefficients and θ_s^k parameter k for species s, for $s = 1, \cdots, n_s$. The constraint disappears for $w_k = 0$ (so the species are independent), while a high value for w_k forces the corresponding parameters to be equal for the different species. The general idea is to stepwise increase w_k, estimate parameters and observe the trait-off between the reduction of the variation coefficient for that parameter and the increase in the mean relative error of all predictions for all data sets for all species. The largest weight coefficient that does not spoil the mean relative error substantially is the value we are looking for: this separates the real biological variation in the parameter from the artificial one caused by ill-posedness of the parameter estimation.

Males differ from females in many AmP entries only by parameters $\{\dot{p}_{Am}\}$ and/or E_H^p, while all other parameters are taken equal. This can be seen as a special case of multi-species estimation. Likewise particular patterns in the co-variation of parameters among species can be taken into account in a sloppy by, i.e. not imposing such patterns in a hard way, but by reducing deviations from such patterns. We call this type of parameter estimation, including the notion of pseudo-data: 'estimation in context'.

4.10 Parameter estimation

If data includes time-length, so the von Bertalanffy growth rate $\dot{r}_B$ is well-fixed by the data, Fig. 4.11 shows that specific somatic maintenance $[\dot{p}_M]$ tends to correlate negatively with energy conductance $\dot{v}$ if L_∞ is fixed. For small $\dot{r}_B$, either $[\dot{p}_M]$ or $\dot{v}$ is poorly fixed. Incubation time and/or respiration data fix the energy conductance well, so in combination with time-length data, no problem is to be expected.

The ultimate reproduction rate (at constant food) is a hump-shaped function of κ, if all other parameters remain fixed. For high κ, little is allocated to reproduction and for

low κ little is allocated to growth, while feeding is coupled to size. For typical values of the parameters, the ultimate reproduction rate has a maximum around $\kappa = 0.45$ for supply species and $\kappa = 0.66$ for (extreme) demand species, see Section 10.5.5 of the comments, while values around $\kappa = 0.9$ most frequently occur, see Section 8.1.3 of the comments. This means that both a low and a high value of κ can predict a (relatively) low ultimate reproduction rate. If κ is decreased and $\{\dot{p}_{Am}\}$ is increased, such that their product remains constant (so g remains constant), growth is hardly affected. The maturity thresholds have to increase simultaneously to keep stage transitions at the same age and size, and other parameters have to be adjusted as well to correct for difference in the costs per eggs, which affect the reproduction rate. So both a low and a high value of κ can capture a particular growth and reproduction pattern, as illustrated in Table 4.3. The high value for κ (prediction H) represents a local minimum for the Weighted sum of Least Squares, but this is not sure for the low value of κ (prediction L). This depends on numerical details of the routines that compute the predictions. Prediction I here overestimates the length and weight at birth, which directly relates to maximum reproduction, which is estimated correctly. Notice that prediction L has a higher assimilation, but the same energy conductance, so more reserve relative to structure. The effect on predicted physical lengths is compensated by a lower shape coefficient.

4.10.0 Bijection between data and parameter space

Given a number of assumptions on (mainly) auxiliary parameters, a bijection (= one-one map) is possible between 9 parameters and 9 data points, see [855] and Table 4.4. Data are sensitive to environment conditions (food, temperature) and parameter values are individual-specific. The relationship between parameter space and data space has parallels with that between geno- and pheno-type. The required assumptions are

A1 temperature is constant and the reference temperature is $T_{\text{ref}} = 293\,\text{K}$. If the actual temperature differs, a_b, a_p, a_m and $\dot{R}_m$ must first be temperature corrected. A typical Arrhenius temperature is $T_A = 8\,\text{kK}$, which can be used for this purpose in absence of better information. The correction can be done by dividing the ages and multiplying the rate by temperature correction factor $\exp(T_A/T - T_A/T_{\text{ref}})$, see [775, Eq (1.2)].

A2 food is abundantly available. Feeding is not explicitly included here, meaning that we don't include digestion efficiency κ_X and maximum specific searching rate $\{\dot{F}_m\}$, which are two core parameters of the standard model.

A3 surface-linked somatic maintenance $\{\dot{p}_T\} = 0$. This primarily concerns investment into heating (for endotherms) and osmotic work (for freshwater organisms), which depends on environmental conditions. We thus assume that these conditions are such that our assumption holds.

A4 the chemical potentials of structure and reserve are $\mu_V = 0.5$ and $\mu_E = 0.55\,\text{MJ C-mol}^{-1}$. The bulk composition of dry biomass is a mixture of carbohydrates, proteins and fats [775, Table 4.2], which is species-specific, but the overall values are assumed

Table 4.3: Artificial and pseudo data at abundant food, except length at puberty at $f = 0.7$, and predictions based on two different parameter estimates. Reproduction is well-predicted for a low value of κ (pred. L), as well as for a high value of κ (pred. H). Data and parameters on feeding, ageing and temperature dependence have been omitted. Fixed parameter values: reproduction efficiency $\kappa_R = 0.95$, chemical potential for structure $\mu_V = 500\,\mathrm{kJ\,mol^{-1}}$, specific mass of structure $[M_V] = 4.2\,\mathrm{mmol\,cm^{-3}}$.

data	symbol	unit	value	pred. L	pred. H
age at birth	a_b	d	15.5	15.5	15.54
age at puberty	a_p	d	240	214	239.4
physical length at birth	L_w^b	cm	0.46	0.7482	0.4619
physical length at puberty	L_w^p	cm	2.2	2.096	2.19
– at $f = 0.7$	$L_{0.7}^p$	cm	2.1	2.018	2.102
ultimate physical length	L_w^∞	cm	6.25	6.176	6.26
dry weight at birth	W_b	g	6e-5	26.1e-5	6.023e-5
dry weight at puberty	W_p	g	0.0064	0.005738	0.0064
ultimate dry weight	W_∞	g	0.15	0.1467	0.15
ultimate reproduction rate	$\dot{R}_\infty$	$\#\,\mathrm{d^{-1}}$	2.1	2.153	2.107
energy conductance	$\dot{v}$	cm d−1	0.02	0.02182	0.02007
vol-spec. somatic maint.	$[\dot{p}_M]$	J d−1cm^{-3}	18	17.88	17.6
growth efficiency	κ_G	−	0.74	0.5693	0.7391

parameter	symbol	unit	estim. I	estim. II
spec max assimilation	$\{\dot{p}_{Am}\}$	$\mathrm{J\,d^{-1}cm^{-2}}$	343.07	21.98
shape coefficient	$\delta_{\mathcal{M}}$	−	0.09262	0.1606
energy conductance	$\dot{v}$	$\mathrm{cm\,d^{-1}}$	0.02182	0.02
allocation fraction to soma	κ	−	0.02981	0.808
vol-specific somatic maint.	$[\dot{p}_M]$	$\mathrm{J\,d^{-1}cm^{-3}}$	17.89	17.61
maturity maint. rate coeff.	$\dot{k}_J$	$\mathrm{d^{-1}}$	8.505e-4	8.968e-4
spec cost for structure	$[E_G]$	$\mathrm{J\,cm^{-1}}$	3676	2813
maturity at birth	E_H^b	J	40.93	0.2813
maturity at puberty	E_H^p	J	1145	40.48

Table 4.4: The combination of nine data (left) and parameters (right) that map to each other one-to-one on the basis of the standard DEB model with acceleration and ageing.

description	symbol	unit	unit	symbol	description
age at birth	a_b	d	J	E_H^b	maturity at birth
age at puberty	a_p	d	J	E_H^j	maturity at metam.
age at death	a_m	d	J	E_H^p	maturity at puberty
dry/wet weight ratio	δ_W	–	$\mathrm{J\,d^{-1}cm^{-2}}$	$\{\dot{p}_{Am}\}$	specific assimilation
wet weight at birth	W_b	g	$\mathrm{cm\,d^{-1}}$	$\dot{v}$	energy conductance
wet weight at metam.	W_j	g	-	κ	allocation fraction to soma
wet weight at puberty	W_p	g	$\mathrm{J\,d^{-1}cm^{-3}}$	$[\dot{p}_M]$	spec. somatic maintenance
ultimate wet weight	W_∞	g	$\mathrm{J\,cm^{-3}}$	$[E_G]$	specific cost for structure
max. reproduction rate	$\dot{R}_m$	$\#\,\mathrm{d^{-1}}$	$\mathrm{d^{-2}}$	$\ddot{h}_a$	ageing acceleration

to be insensitive for these variations. Chemical potentials of reserve and structure can be estimated from data on energy content of biomass at two (or more) food levels.

A5 ratios of chemical elements in dry structure as well as dry reserve is C:H:O:N = 1:1.8:0.5:0.15. This fixes the molecular weight of reserve and structure to $w_E = w_V = 23.9\ \mathrm{g\,C\text{-}mol^{-1}}$. Notice that similarity of elemental frequencies does not imply similarity in chemical composition. Avoidance of this assumption, including the similarity between structure and reserve, requires measured elemental frequencies of biomass at two (or more) food levels.

A6 only if the water content of reserve and structure are equal is the dry/wet weight ratio independent of nutritional conditions (as is the standard assumption in the ecological literature). We also make this assumption with the implication that the dry/wet weight ratio δ_W has a simple relationship with specific density of biomass d_W and the specific density of structure d_V, where the specific density of wet structure is $d_V^w = 1\,\mathrm{g\,cm^{-3}}$ and the specific density of reserve equals that of structure. The water content of structure and reserve can be estimated from data on dry and wet weight trajectories during starvation.

A7 we refrain from the detailed specification of the handling rules for the reproduction buffer and only consider maximum reproduction rate as a mean over several reproduction cycles for a fully grown adult female. To avoid this assumption, we need reproduction data as function of time. Buffer handling rules tend to be species-specific. Maximum weight as data point, see Table 4.4, is assumed to exclude the reproduction buffer.

A8 reproduction efficiency $\kappa_R = 0.95$, which stands for the fraction of reserve that is allocated to reproduction that ends up in offspring. In the case of reproduction by eggs this represents a conversion from reserve of the mother to that of eggs, so no chemical transformation is involved. This parameter can only be estimated if the full energy balance is available from data.

A9 growth efficiency $\kappa_G = 0.8$, which stands for the fraction of reserve that is allocated to growth (of structure) that ends up in structure. This involves a chemical transformation from reserve to structure. Growth efficiency can be estimated from e.g. growth data at two (or more) food levels. In cases where this parameter could be estimated, 0.8 turns out to be consistent with data.

A10 maturity maintenance rate coefficient $\dot{k}_J = 0.002\,\mathrm{d}^{-1}$, which stands for the maturity specific maintenance costs, if maturity is expressed in cumulative energy investment in maturation. Maturity itself does not have mass or energy. The parameter can only be estimated from data if reproduction is measured at several food levels. In cases where this parameter could be estimated, $0.002\,\mathrm{d}^{-1}$ turns out to be consistent with data.

A11 Gompertz stress coefficient $s_G = 10^{-4}$, which quantifies how fast ageing accelerates during ontogeny. The parameter can be estimated from data on relative survival frequency as function of age. For ectotherms acceleration is typically very low, for endotherms it can be in the order of 0.1 (steeper decline of survival probability as function of age). The value only affects survival by ageing and has no effect on the energy budget, but the energy budget affects ageing.

Assumptions A1 to A3 relate to restrictions on environmental conditions under which data has been collected. Assumptions A4 to A6 relate to body composition and assumptions A8 to A11 species properties. All these assumptions can be avoided, but this requires more complex data, frequently at several food levels, and more advanced parameter identification methods [856, 857]. This list of assumptions leaves nine degrees of freedom for the dynamic energy budgets as specified by the standard DEB model with acceleration and ageing. The analysis can be simplified by reducing the 9 dimensions to 7 by omitting $\ddot{h}_a$ and a_m, and obtaining $[E_G]$ directly from d_V, but this is not done because of future extensions to include the primary parameters $\{\dot{F}_m\}$, κ_G and $\dot{k}_J$.

The implied bijection in both directions has the following algorithm.

4.10.0.1 Map from parameters to data

P1 maintenance ratio $k = \frac{\dot{k}_J}{\dot{k}_M}$, with somatic maintenance rate coefficient $\dot{k}_M = \frac{[\dot{p}_M]}{[E_G]}$

P2 dry/wet weight ratio $\delta_W = \frac{d_V}{d_V^w}$, with specific density of structure $d_V = \kappa_G [E_G] \frac{w_V}{\mu_V}$

P3 energy investment ratio $g = \frac{[E_G]\dot{v}}{\kappa\{\dot{p}_{Am}\}}$ and maximum structural length $L_m = \frac{\kappa\{\dot{p}_{Am}\}}{[\dot{p}_M]}$

P4 scaled maturity $U_H^* = \frac{E_H^*}{\{\dot{p}_{Am}\}}$, $V_H^* = \frac{U_H^*}{1-\kappa}$ and $v_H^* = \frac{V_H^* g^2 \dot{k}_M^3}{\dot{v}^2}$ with $* = b, j, p$

P5 scaled length at birth l_b is solved from $\frac{x_b g v_H^b}{v(x_b) l_b^3} = \int_0^{x_b} \frac{g + l(x)}{v(x)}\, dx$ with $x_b = \frac{g}{1+g}$ and $v(x) = \exp\left(-\int_0^x \frac{k - x_1}{1 - x_1} \frac{l(x_1)}{g x_1}\, dx_1\right)$ and $l(x) = \left(\frac{1}{l_b}\left(\frac{x_b}{x}\right)^{1/3} - \frac{B_{x_b}(\frac{4}{3},0) - B_x(\frac{4}{3},0)}{3 g x^{1/3}}\right)^{-1}$, where $B_x(a,b)$ is the incomplete beta function

P6 scaled age at birth $\tau_b = 3\int_0^{x_b} \frac{dx}{(1-x)x^{2/3}(3gx_b^{1/3}/l_b - B_{x_b}(\frac{4}{3},0) + B_x(\frac{4}{3},0))}$

P7 scaled exponential growth rate $\rho_j = g\frac{1/l_b - 1}{1+g}$ (between birth and metamorphosis)

P8 scaled length at metamorphosis $l_j = l_b + \int_{v_H^b}^{v_H^j} \frac{d}{dv_H} l \, dv_H$ with $\frac{d}{dv_H} l = \frac{\rho_j l/3}{l^3(1/l_b - \rho_j/g) - k v_H}$ and $l(v_H^b) = l_b$

P9 scaled ultimate length $l_\infty = s_{\mathcal{M}}$ with acceleration factor $s_{\mathcal{M}} = l_j/l_b$

P10 scaled length at puberty $l_p = l_j + \int_{v_H^j}^{v_H^p} \frac{d}{dv_H} l \, dv_H$ with $\frac{d}{dv_H} l = \frac{\frac{g}{3}\frac{l_\infty - l}{g+1}}{l^2 \frac{gl_\infty + l}{g+1} - k v_H}$ and $l(v_H^j) = l_j$.

P11 scaled age at metamorphosis $\tau_j = \tau_b + 3\rho_j^{-1} \log s_{\mathcal{M}}$

P12 scaled von Bertalanffy growth rate $\rho_B = (3 + 3/g)^{-1}$ (after metamorphosis)

P13 scaled age at puberty $\tau_p = \tau_j + \rho_B^{-1} \log \frac{l_\infty - l_j}{l_\infty - l_p}$

P14 ages $a_* = \tau_*/\dot{k}_M$ with $* = b, p$

P15 structural lengths $L_* = l_* L_m$ with $* = b, j, p, \infty$

P16 wet weights $W_* = d_V^w L_*^3 \left(1 + \frac{[E_m] w_E}{d_V \mu_E}\right)$ with $* = b, j, p, \infty$ and $[E_m] = \frac{\{\dot{p}_{Am}\}}{\dot{v}}$

P17 maximum reproduction rate $\dot{R}_m = \frac{\kappa_R}{E_0}(\frac{1-\kappa}{\kappa}[\dot{p}_M] s_{\mathcal{M}}^3 L_m^3 - \dot{k}_J E_H^p)$ with initial reserve $E_0 = u_E^0 L_m^3 [E_G]/\kappa$ and initial scaled reserve $u_E^0 = \left(\frac{3g}{3gx_b^{1/3}/l_b - B_{x_b}(\frac{4}{3},0)}\right)^3$ and $x_b = \frac{g}{1+g}$

P18 age at death $a_m = \Gamma\left(\frac{4}{3}\right)\left(\frac{6}{g\dot{k}_M \ddot{h}_a}\right)^{1/3}$, where $\Gamma(x)$ is the gamma function.

The computation of scaled length at birth l_b in step 5 is by far the most demanding, but efficient routines based on [774] are available in software package DEBtool. Numerical integrations are required in l_j, l_p and τ_b as well, which reduces accuracy.

4.10.0.2 Map from data to parameters

D1 acceleration factor $s_{\mathcal{M}} = (W_j/W_b)^{1/3}$. For non-accelerating species: $W_j = W_b$ and $s_{\mathcal{M}} = 1$ and $a_j = a_b$

D2 scaled length at birth $l_b = \frac{L_b}{L_m} = s_{\mathcal{M}}\left(\frac{W_b}{W_\infty}\right)^{1/3}$, scaled length at metamorphosis $l_j = \frac{L_j}{L_m} = s_{\mathcal{M}}\left(\frac{W_j}{W_\infty}\right)^{1/3}$ and scaled length at puberty $l_p = \frac{L_p}{L_m} = s_{\mathcal{M}}\left(\frac{W_p}{W_\infty}\right)^{1/3}$ can be obtained from wet weights. Although structural lengths themselves cannot be accessed yet, their ratios can. Ultimate structural length $L_\infty = L_m s_{\mathcal{M}}$ and maximum structural length L_m be will given below when using ultimate wet weight W_∞. Maximum structural length L_m will be treated as a compound parameter and the interpretation only applies to non-accelerating species; ultimate structural length L_∞ exceeds L_m for accelerating species at abundant food

D3 age at metamorphosis $a_j = \frac{a_p \log s_{\mathcal{M}} + a_b \log s}{\log s_{\mathcal{M}} + \log s}$ with $s = \left(\frac{s_{\mathcal{M}} - l_j}{s_{\mathcal{M}} - l_p}\right)^{1/l_b - 1}$. This is based on the relationship between the exponential growth rate $\dot{r}_j = \frac{3 \log s_{\mathcal{M}}}{a_j - a_b}$ during acceleration between birth and metamorphosis and the von Bertalanffy growth rate $\dot{r}_B = \frac{1}{a_p - a_j} \log \frac{s_{\mathcal{M}} - l_j}{s_{\mathcal{M}} - l_p}$ after metamorphosis. Their links with DEB parameters at abundant food is $\dot{r}_j = \dot{k}_M \frac{1/l_b - 1}{1 + 1/g}$ and $\dot{r}_B = \frac{\dot{k}_M/3}{1 + 1/g}$, see [775, Eq (2.24)]. So $\dot{r}_B = \frac{r_j}{3/l_b - 3}$ and substitution gives the result

D4 cost for structure $[E_G] = \frac{\mu_V d_V}{w_V \kappa_G} = 26151\, \delta_V\, \mathrm{J\,cm^{-3}}$, given the assumptions. This directly follows from the definition of growth efficiency $\kappa_G = \frac{\mu_V d_V}{w_V [E_G]}$

D5 von Bertalanffy growth rate $\dot{r}_B = \frac{1}{a_p - a_j} \log \frac{1 - l_j}{1 - l_p}$, which directly follows from the definition $L(t) = L_\infty - (L_\infty - L_0) \exp(-\dot{r}_B t)$

D6 maximum reserve residence time $t_{Em} = \frac{L_m}{\dot{v}} = \frac{1}{g \dot{k}_M} = \frac{a_b}{3.7 l_b}$, where scaled length at birth l_b is given above. This is based on $\frac{d}{dt} L(0) = \dot{v}/3$ and the approximation that this holds during the full incubation time, leading to $L_b = \dot{v} a_b / 3$, see [775, Eq (2.47)]. However, reserve becomes depleted during incubation of eggs, increasing incubation time by a mean factor of 1.226 among species that are present in the collection. This value for t_{Em} is an approximation that will be replaced in step 9

D7 specific somatic maintenance cost $[\dot{p}_M] = \frac{3 \dot{r}_B [E_G]}{1 - 3 \dot{r}_B t_{Em}}$. This is based on the von Bertalanffy growth rate $\dot{r}_B = \frac{[\dot{p}_M]/3}{[E_G] + [\dot{p}_M] t_{Em}}$ at abundant food ([775, Eq (2.24)]) after metamorphosis. Since t_{Em} is an approximation, this value for $[\dot{p}_M]$ is also approximative (see next step)

D8 somatic maintenance rate coefficient $\dot{k}_M = [\dot{p}_M]/[E_G]$, from its definition, see [775, Section 2.5.1]. This value for $\dot{k}_M$ can be used as initial value for a numerical procedure to solve $\dot{k}_M$ from the exact value for $a_b = \tau_b / \dot{k}_M$, with τ_b given by [775, Eq (2.38)]. So $\dot{k}_M$ must be solved from $\dot{k}_M a_b = 3 \int_0^{x_b} \frac{(1-x)^{-1} x^{-2/3}\, dx}{\alpha_b - B_{x_b}(\frac{4}{3}, 0) + B_x(\frac{4}{3}, 0)}$, where $B_x(a, b)$ is the incomplete beta function, $\alpha_b = 3 g x_b^{1/3} / l_b$, $x_b = \frac{g}{e_b + g}$, $g = \frac{\dot{r}_B}{\dot{k}_M/3 - \dot{r}_B}$ (see D9), while $\dot{r}_B$ is given in D5, a_j in D3, l_b, l_j, l_p in D2 and $s_{\mathcal{M}}$ in D1. With this correct value for $\dot{k}_M$, we obtain $[\dot{p}_M] = \dot{k}_M [E_G]$ to replace the value obtained in step D7

D9 energy investment ratio $g = \frac{\dot{r}_B}{\dot{k}_M/3 - \dot{r}_B}$. This is based on the von Bertalanffy growth rate $\dot{r}_B = \frac{\dot{k}_M/3}{1 + 1/g}$, see [775, Eq (2.24)] and its definition $g = \frac{[E_G]}{\kappa [E_m]}$, see [775, Eq (2.21)]. The value for $t_{Em} = (g \dot{k}_M)^{-1}$ that was obtained in step 6 can now be replaced

D10 allocation fraction $\kappa = 1 - \dot{R}_m t_{Em} s_{\mathcal{M}}^{-3} l_b^3 (1.75 + g)/\kappa_R$, with $\kappa_R = 0.95$ as default. This is based on the maximum reproduction rate $\dot{R}_m = \frac{\kappa_R}{E_0} (\frac{1 - \kappa}{\kappa} \dot{k}_M [E_G] s_{\mathcal{M}}^3 L_m^3 - \dot{k}_J E_H^p)$, [775, Eq (2.58)], the costs per (foetal) offspring $E_0 = L_b^3 ([E_m] 7/4 + [E_G]/\kappa)$, see [775, Eq (2.51)] and neglecting maturity maintenance ($\dot{k}_J = 0$). The cost of an egg is slightly larger, due to retardation of development by the reserve becoming limiting,

which increases cumulative maintenance costs. Placental costs are ignored as well, assuming that most of it is recovered by eating the placenta after birth. Substitution gives $\dot{R}_m = \frac{(1-\kappa)\kappa_R \dot{k}_M}{1.75/g+1} \frac{s_M^3 L_m^3}{L_b^3}$. This value for κ will be replaced in step 15.

D11 reserve capacity $[E_m] = \frac{[E_G]}{\kappa g}$, based on the definition of the energy investment ratio $g = \frac{[E_G]}{\kappa [E_m]}$, see [775, Eq (2.21)]

D12 maximum structural length $L_m = s_M^{-1} \left(\frac{W_\infty}{d_V^w \left(1 + \frac{[E_m] w_E}{d_V \mu_E}\right)} \right)^{1/3}$ where the coefficients d_V^w, d_V, w_E and μ_E are specified by the assumptions. This is based on $W_\infty = d_V^w L_\infty^3 \left(1 + \frac{[E_m] w_E}{d_V \mu_E}\right)$, see [775, Eq (3.2)]. We now have access to $L_b = l_b L_m$, $L_j = l_j L_m$ and $L_p = l_p L_m$

D13 energy conductance $\dot{v} = L_m / t_{Em}$, which directly follows from $t_{Em} = L_m / \dot{v}$

D14 specific assimilation rate $\{\dot{p}_{Am}\} = \dot{v}[E_m] = [\dot{p}_M] L_m / \kappa$. This follows from the definition of reserve capacity $[E_m] = \{\dot{p}_{Am}\}/\dot{v}$, see Section 2.3.1, and from maximum structural length $L_m = \kappa \{\dot{p}_{Am}\}/[\dot{p}_M]$, see [775, Section 2.6]

D15 maturity level at birth $E_H^b = \frac{1-\kappa}{\kappa}[E_G] L_b^3$, metamorphosis $E_H^j = \frac{1-\kappa}{\kappa}[E_G] L_j^3$ and puberty $E_H^p = \frac{1-\kappa}{\kappa}[E_G] L_p^3$. This is based on $k = \dot{k}_J / \dot{k}_M = 1$, where maturity density does not change, see [775, Eq (2.32)]. The exact values can be obtained by integrating the ode's for reserve E and maturity E_H over structural length L. For that purpose the initial reserve $E(0) = E_0$ is obtained by step 9 of the previous subsection, while $E_H(0) = 0$. The value for κ can be used as initial value for a numerical procedure to solve κ from the exact value for $\dot{R}_m$, repeating steps 11 till 15 till conversion

D16 ageing acceleration $\ddot{h}_a = \frac{4.27}{a_m^3 \dot{k}_M g}$, for small Gompertz stress coefficient $s_G = 10^{-4}$. This is based on $a_m = \Gamma(4/3)/\dot{h}_W$, with $\dot{h}_W^3 = \frac{\ddot{h}_a \dot{v}}{6 L_m}$ and $\Gamma(4/3) = 0.893$, see [775, Eq (6.6)]

This series of 16 steps involves the solution of two implicit equations, each in one variable, step 8 and 15, where good initial values are available.

4.10.0.3 Boundaries of parameter space

The following formal constraints on parameter values apply at constant food at scaled function response f, with $0 < f \leq 1$. We assume a constant scaled food functional response, rather than $f = 1$, because we here consider constraints on parameter and data values. Parameter values are the result of natural selection, which occurs in the field, where food is not always abundant. Demand species have a high specific searching rate, $\{\dot{F}_m\}$, so a small half saturation constant K, meaning that $f = 1$ is approximated for a large range of fluctuating food densities. Supply species, however, have a large value for K, meaning that the mean f will generally be smaller than 1, and this affects selection for parameter values. So at first reading the sections on the boundaries of parameter and data space, you

can best assume $f = 1$, but at second reading you might want to consider $f < 1$, especially for supply-species.

BP1 All parameters, i.e. $\{\dot{p}_{Am}\}$, $\dot{v}$, κ, $[\dot{p}_M]$, $[E_G]$, E_H^b, E_H^j, E_H^p, $\ddot{h}_a$, must be positive. The specific costs for structure $[E_G] > d_V\mu_V/w_V$ follows from $\kappa_G < 1$.

BP2 Allocation fraction κ must be smaller than 1. Constraint BP6 is more restrictive, however.

BP3 The maturity levels must increase: $0 < E_H^b \leq E_H^j \leq E_H^p$;

BP4 Birth can be reached at f if $f > f_R$, where f_R is the scaled function response at which maturation ceases at birth. For $u_E = \frac{\kappa E}{[E_G]L_m^3}$ and $v_H = \frac{\kappa E_H}{(1-\kappa)[E_G]L_m^3}$ and $\tau = t\dot{k}_M$, we have $\frac{d}{d\tau}u_E = -u_E l^2 \frac{g+l}{u_E+l^3}$ and $\frac{d}{d\tau}v_H = u_E l^2 \frac{g+l}{u_E+l^3} - kv_H$ with $\frac{d}{d\tau}v_H(\tau_b) = 0$ for $f = f_R$. So $\frac{d}{d\tau}u_E(\tau_b) = -kv_H^b$ and $u_E^b = \frac{kv_H^b l_b^3}{l_b^3+gl_b^2-kv_H^b}$. Since $u_E^b = \frac{e_b l_b^3}{g}$, we have $f_R = \frac{gu_E^b}{l_b^3} = \frac{gkv_H^b}{l_b^3+gl_b^2-kv_H^b}$ and, for $x = \frac{g}{g+e}$, $x_b = \frac{g}{g+f_R} = \frac{l_b^3+gl_b^2-kv_H^b}{l_b^3+gl_b^2}$. Since $\frac{d}{d\tau}x = gx\frac{1-x}{l}$ and for $y = \frac{xe_H}{1-\kappa}$, $\frac{d}{dx}y = r(x) - ys(x)$ and $r(x) = g + l(x)$ and $s(x) = \frac{k-x}{1-x}\frac{l(x)}{gx}$. This ODE for y in x needs to be integrated from $(x, y) = (0, 0)$ to (x_b, y_b) with $y_b = gx_b v_H^b/l_b^3$, for $\frac{1}{l(x)} = \frac{1}{l_b}\left(\frac{x_b}{x}\right)^{1/3} - \frac{B_{x_b}(\frac{4}{3},0)-B_x(\frac{4}{3},0)}{3gx^{1/3}}$. From the boundary condition $y(x_b) = y_b$, l_b can be solved and f_R is found.

Birth can just be reached under the best feeding condition if $f_R = 1$. In that case $(g + 1)kv_H^b = l_b^3 + gl_b^2$. This cubic polynomial in l_b must have a real root between 0 and 1, which translates into $kv_H^b < 1$ or $E_H^b < \frac{(1-\kappa)\kappa^2\{\dot{p}_{Am}\}^3}{\dot{k}_J[\dot{p}_M]^2}$. If $\dot{k}_J < \dot{k}_M$, as found in all entries of the collection, shrinking occurs at f_R before birth.

Scaled length at birth l_b cannot exceed 1. This implies that, given energy investment ratio g and maintenance ratio k, scaled maturity v_H^b cannot be larger than the value discussed in section 2.6.2 of the comments.

BP5 Supply stress $s_s = \frac{\dot{k}_J E_H^p [\dot{p}_M]^2}{f^3 s_M^3 \{\dot{p}_{Am}\}^3} \leq \frac{2^2}{3^3}$, else allocation fraction κ cannot be between 0 and 1 (see BP1 and BP2).

BP6 Allocation fraction κ must satisfy $\kappa^2(1-\kappa) > s_s$, in other words, it must be between the two positive roots of $\kappa^2(1-\kappa) = s_s$. If κ is at one of the boundaries, maturity at puberty is only reached asymptotically, maximum reproduction $\dot{R}_m = 0$. If $s_s = \frac{2^2}{3^3}$, the two positive roots coincide and we have $\kappa = \frac{2}{3}$.

BP7 The constraint $a_p < a_m$ (see BD1) translates to $\ddot{h}_a < \Gamma\left(\frac{4}{3}\right)\frac{6}{g\dot{k}_M t_p^3}$. The detailed argument is a bit more complex because death by ageing is stochastic and not all individuals need to reach puberty.

Notice that BP4 concerns birth and BP5 puberty. These boundary conditions differ, but have relationships. If we focus on abundant food conditions, BP4 states that $kv_H^b < 1$. Given BP3, this condition is satisfied if $kv_H^p < 1$. Under abundant food conditions, again, s_s

relates to v_H^p as $s_s = \kappa^2(1-\kappa)kv_H^p s_{\mathcal{M}}^{-3}$. BP6 translates into the condition that $kv_H^p < s_{\mathcal{M}}^3$, where $s_{\mathcal{M}} = l_j/l_b \geq 1$. If species don't accelerate, $s_{\mathcal{M}} = 1$, the condition that it must be possible to reach puberty automatically implies that birth can be reached as well. For accelerating species, however, this no longer holds, and parameter combinations exist where puberty can be reached, but birth cannot.

4.10.0.4 Boundaries of data space

The following formal constraints on data values apply at constant food at scaled function response f, with $0 < f \leq 1$.

BD1 All data, i.e. d_V, a_b, a_p, a_m, W_b, W_j, W_p, W_m, $\dot{R}_m$, must all be positive

BD2 Ages must increase during the life-cycle: $0 < a_b \leq a_p < a_m$

BD3 Weights must increase during the life-cycle: $0 < W_b \leq W_j \leq W_p \leq W_\infty$.

BD4 A solution for $\dot{k}_M$ from D8 must exist, which translates for $\tau_b = a_b \dot{r}_B$ and $k_M = \dot{k}_M/\dot{r}_B$ and $\alpha_b = 3gx_b^{1/3}/l_b$ and $x_b = \frac{g}{1+g}$ and $g = \frac{3}{k_M - 3}$ into:

$$\lim_{k_M \downarrow 3} \frac{3}{k_M} \int_0^{x_b} \frac{(1-x)^{-1}x^{-2/3}\,dx}{\alpha_b - B_x(\frac{4}{3},0) + B_{x_b}(\frac{4}{3},0)} \leq \tau_b \leq \lim_{k_M \to \infty} \frac{3}{k_M} \int_0^{x_b} \frac{(1-x)^{-1}x^{-2/3}\,dx}{\alpha_b - B_x(\frac{4}{3},0) + B_{x_b}(\frac{4}{3},0)}$$

Numerical studies suggest that by approximation we must have

$$1.93\,10^{-6} l_b \leq \tau_b \leq l_b + l_b^2/4$$

BD5 Puberty can be reached if maximum reproduction $\dot{R}_m > 0$. Allocation fraction κ only has a solution if for $\dot{p}_M^m = s_{\mathcal{M}}^3 L_m^3 [\dot{p}_M]$ and $\dot{p}_J^m = \dot{k}_J E_H^p$ and $\dot{p}_R^m = E_0 \dot{R}_m/\kappa_R$

$$\dot{p}_R^m < \dot{p}_M^m \frac{1-\kappa}{\kappa} - \dot{p}_J^m \quad \text{for } \kappa \to 0$$

The quantities $s_{\mathcal{M}}$, $\dot{R}_m$, $[\dot{p}_M]$, $\dot{k}_J$, L_m, E_H^p and u_E^0 are treated here as functions of data (see algorithm of the bijection) and $E_0 = u_E^0 L_m^3 [E_G]/\kappa$. So for small κ the condition reduces to

$$u_E^0 [E_G] \dot{R}_m/\kappa_R < s_{\mathcal{M}}^3 [\dot{p}_M] - \dot{p}_J^m/L_m^3$$

Step D10 of the map from data to parameters shows that $\dot{R}_m t_{Em} l_b^3 (1.75 + g) < \kappa_R s_{\mathcal{M}}^3$ follows naturally from the approximative estimate for κ, but is an approximative constraint only.

In practice it sometimes occurs that W_j has not been measured and a_b is too large for application of the standard DEB model without acceleration. This large a_b might indicate acceleration, and one way to reconstruct W_j is to increase it incrementally from W_b (no acceleration), till a_b crosses the boundaries of the data space.

Table 4.5: Elasticity coefficients $\boldsymbol{e}_d$ for data, e.g. $\frac{\{\dot{p}_{Am}\}}{d_V}\frac{\partial d_V}{\partial \{\dot{p}_{Am}\}} = 0$ and $\boldsymbol{e}_p$ for parameters, e.g. $\frac{d_V}{\{\dot{p}_{Am}\}}\frac{\partial \{\dot{p}_{Am}\}}{\partial d_V} = 1$, in case of parameter and data values that map onto each other as indicated in the last columns. The second last column gives the relative error of mapping forward, followed by backward. The data-elasticities were obtained by extrapolating the numerical derivatives to zero perturbation; the parameter-elasticities were computed from the data-elasticities.

$\boldsymbol{e}_d$	$\{\dot{p}_{Am}\}$	$\dot{v}$	κ	$[\dot{p}_M]$	$[E_G]$	E_H^b	E_H^j	E_H^p	$\ddot{h}_a$	error	value $\boldsymbol{d}$
d_V	0	0	0	0	1	0	0	0	0	0	0.1
a_b	-0.060	-0.912	1.560	-0.048	-0.216	-0.324	0	0	0	3.1e-6	115.8 d
a_p	-0.254	0.759	1.435	-0.031	-0.053	0.230	-0.167	0.275	0	-3.8e-5	464.1 d
a_m	0.333	-0.333	0.333	-0.333	0	0	0	0	-0.333	-1.7e-4	1288 d
W_b	0.849	-0.726	4.820	-0.179	-1.630	0.959	0	0	0	9.1e-6	2.156 g
W_j	0.877	-0.709	4.770	-0.251	-1.572	-0.050	0.995	0	0	-1.7e-4	20.39 g
W_p	0.925	-0.648	4.630	-0.429	-1.404	-0.091	0.089	0.911	0	-2.4e-4	316 g
W_∞	3.870	-0.814	2.945	-3.070	-0.772	-1.010	0.995	0	0	-1.8e-4	55.7 kg
$\dot{R}_m$	2.286	0.691	-6.680	-1.945	0.650	-1.990	1.000	-0.002	0	-1.9e-4	7.23 d^{-1}

$\boldsymbol{e}_p$	d_V	a_b	a_p	a_m	W_b	W_j	W_p	W_∞	$\dot{R}_m$	error	value $\boldsymbol{p}$
$\{\dot{p}_{Am}\}$	1.004	4.131	-4.957	0	-0.013	-0.882	1.497	-0.265	0.181	2.8e-7	225 J $\mathrm{d}^{-1}\mathrm{cm}^{-2}$
$\dot{v}$	0	-3.529	2.464	0	0.526	4.438	-0.744	-0.111	-0.069	-1.1e-7	0.02 cm d^{-1}
κ	-0.003	0.067	-0.316	0	-0.286	0.028	0.095	0.162	-0.251	-3.8e-7	0.8
$[\dot{p}_M]$	1.006	6.338	-7.352	0	-0.783	-0.890	2.220	-0.541	-0.000	1.9e-16	18 J $\mathrm{d}^{-1}\mathrm{cm}^{-3}$
$[E_G]$	1	0	0	0	0	0	0	0	0	0	2615 J cm^{-3}
E_H^b	1.016	-5.476	6.466	0	2.744	0.806	-1.950	-0.599	1.050	1.1e-5	275 J
E_H^j	1.017	-5.156	6.117	0	1.701	1.778	-1.844	-0.633	1.049	-1.7e-4	2750 J
E_H^p	1.016	-4.107	4.986	0	1.584	0.555	-0.404	-0.731	1.047	-2.5e-4	50 kJ
$\ddot{h}_a$	-0.003	1.393	-0.392	-3.003	-0.043	-0.403	0.118	0.327	-0.001	5.0e-4	10^{-6} d^{-2}

4.10.0.5 Elasticities of the bijection

The bijection $\mathcal{P}$ from data $\boldsymbol{d} = (d_1, ., d_9)^T$ to parameters $\boldsymbol{p} = (p_1, ., p_9)^T$ has a differentiable inverse $\mathcal{D}$, so it classifies as a $\mathcal{C}^1$-diffeomorphism. In other words $\mathcal{P}(\mathcal{D}(\boldsymbol{p})) = \boldsymbol{p}$ and $\mathcal{D}(\mathcal{P}(\boldsymbol{d})) = \boldsymbol{d}$. A 9×9 matrix of elasticity coefficients $\boldsymbol{e}_p$ is associated to each point in the 9 dimensional parameter space and $\boldsymbol{e}_d$ to each point in the 9 dimensional data space.

Table 4.5 gives (9 dimensional) parameters and data that are connected by the bijection, including the relative error between $\boldsymbol{d}$ and $\mathcal{D}(\mathcal{P}(\boldsymbol{d}))$ and between $\boldsymbol{p}$ and $\mathcal{P}(\mathcal{D}(\boldsymbol{p}))$, respectively. The absolute relative errors vary from 0 till $1.8\,10^{-4}$. These errors reflect the accuracy of the numerical procedures that are used in the algorithm of the bijection, where numerical integration and root finding occurs. We randomly sampled the data and parameter space for mapping and noticed that the relative error could increase above 0.1 if $a_b < 0.5\,\mathrm{d}$ or $a_m > 10^4\,\mathrm{d}$ or $W_m > 1\,\mathrm{Mg}$. After filtering the random trials for these boundaries, the mapping in both directions had a typical relative error of 0.0005, but could occasionally increase till 0.05, while the errors in both directions correlated. These errors reflect accuracy settings in the numerical procedures in the mapping.

The product $\boldsymbol{e}_p\boldsymbol{e}_d = \boldsymbol{e}_d\boldsymbol{e}_p = \boldsymbol{I}$ must hold. Jean-Christophe Poggiale proved this as follows. Let $\boldsymbol{D} = \mathbf{diag}(\boldsymbol{d})$ and $\boldsymbol{P} = \mathbf{diag}(\boldsymbol{p})$. The elasticity matrices can now be written as $\boldsymbol{e}_d = \boldsymbol{D}^{-1}\frac{\partial}{\partial \boldsymbol{p}^T}\mathcal{P}(\boldsymbol{d})\boldsymbol{P}$ and $\boldsymbol{e}_p = \boldsymbol{P}^{-1}\frac{\partial}{\partial \boldsymbol{d}^T}\mathcal{D}(\boldsymbol{p})\boldsymbol{D}$. The inverse function theorem [35, p 372] learns that $(\frac{\partial}{\partial \boldsymbol{p}^T}\mathcal{P}(\boldsymbol{d}))^{-1} = \frac{\partial}{\partial \boldsymbol{d}^T}\mathcal{D}(\boldsymbol{p})$. As a result we have $\boldsymbol{e}_d^{-1} = (\boldsymbol{D}^{-1}\frac{\partial}{\partial \boldsymbol{p}^T}\mathcal{P}(\boldsymbol{d})\boldsymbol{P})^{-1} = \boldsymbol{P}^{-1}(\frac{\partial}{\partial \boldsymbol{p}^T}\mathcal{P}(\boldsymbol{d}))^{-1}\boldsymbol{D} = \boldsymbol{P}^{-1}\frac{\partial}{\partial \boldsymbol{d}^T}\mathcal{D}(\boldsymbol{p})\boldsymbol{D} = \boldsymbol{e}_p$. Likewise we have $\boldsymbol{e}_p^{-1} = \boldsymbol{e}_d$ and $\boldsymbol{e}_p\boldsymbol{e}_d = \boldsymbol{e}_d\boldsymbol{e}_p$. The elasticities for the parameters, $\boldsymbol{e}_p$, could not be obtained reliably by numerical differentiation; many values sensitively depend on the perturbation factor that was used,

specially for small factors. The values in Table 4.5 were obtained from those for $\boldsymbol{e}_d$. The values for $\boldsymbol{e}_d$ could only be obtained by plotting the numerical derivatives as function of the perturbation factor and graphically back-extrapolate to perturbation zero. Many values were approximately linear in the perturbation factor; not a good sign, but still workable. The determinant of the matrix for the data elasticities was found to be $\det(\boldsymbol{e}_d) = 0.447$ in this numerical example.

The position of the zeros indicate absence of information, so $\dot{R}_m$ has information for $\ddot{h}_a$, but $\ddot{h}_a$ has no information for $\dot{R}_m$. The reason is that, in the present simple implementation of the ageing module in the standard DEB model, energetics affects ageing, but ageing does not affect energetics. Since $[E_G]$ is proportional to d_V, the elasticity $\frac{d_V}{[E_G]} \frac{\partial [E_G]}{\partial d_V} = 1$, while that d_V does not affect any other parameter.

The most extreme elasticity is $\frac{a_p}{[\dot{p}_M]} \frac{\partial [\dot{p}_M]}{\partial a_p} = -7.4$, that of $[p_M]$ for a_p. The map from parameters to data is most sensitive to the parameter κ, with the weights and maximum reproduction to be affected the most. The map from data to parameters are sensitive mainly to the ages at birth and puberty, a_b and a_p, which affect all parameters except κ and $[E_G]$ (small elasticities).

4.10.0.6 Map from data to parameters for mammals

Mammals don't accelerate, but sport foetal development in combination with a delay of the start of development and weaning. The Gompertz stress coefficient is assumed to be given, but not necessarily small. To match the number of parameters to data types, we assume that time at start of development t_0 is known. Data that is typically available: t_b, t_x, t_p, t_m, δ_W, W_b, W_x, W_∞, $\dot{R}_m$. Parameters that must be estimated are: E_H^b, E_H^x, E_H^p, $\{\dot{p}_{Am}\}$, $\dot{v}$, κ, $[\dot{p}_M]$, $[E_G]$, $\ddot{h}_a$.

The map from data to parameters has the following steps

D1m Age at birth $a_b = t_b - t_0$, at weaning $a_x = a_b + t_x$, at puberty $a_p = a_b + t_p$, at death $a_m = a_b + t_m$.

D2m Scaled lengths $l_b = (W_b/W_\infty)^{1/3}$ and $l_x = (W_x/W_\infty)^{1/3}$.

D3m Von Bertalanffy growth rate $\dot{r}_B = \frac{1}{t_x} \log \frac{1-l_b}{1-l_x}$.

D4m Scaled length at puberty $l_p = 1 - (1 - l_b) \exp(-\dot{r}_B(t_p - t_b))$.

D5m Cost for structure $[E_G] = \frac{\mu_V d_V}{w_V \kappa_G} = 26151 \delta_V \, \mathrm{J \, cm^{-3}}$.

D6m We have $L_b = \dot{v} a_b/3$ and $L_m = \frac{\dot{v}}{\dot{k}_M g}$, so $l_b = a_b \dot{k}_M g/3$ and $\dot{k}_M g = \frac{3 l_b}{a_b}$.

D7m Further $\dot{r}_B = \frac{g}{1+g} \frac{\dot{k}_M}{3} = \frac{l_b/a_b}{1+g}$, so $g = \frac{l_b}{a_b \dot{r}_B} - 1$. Consequently from D6m: $\dot{k}_M = \frac{3 l_b}{g a_b}$. From this we can solve $[\dot{p}_M] = \dot{k}_M [E_G]$.

D8m Maximum reproduction $\dot{R}_m = \kappa_R \dot{k}_M \frac{1 - k v_H^p}{v_E^0}$ with $v_E^0 = \frac{u_E^0}{1-\kappa}$, $u_E^0 = u_E^b + l_b^3 + \frac{3}{4} \frac{l_b^4}{g}$ and $u_E^b = l_b^3/g$. So $u_E^0 = (1 + g + l_b 3/4) l_b^3/g$ and $\dot{R}_m = (1 - \kappa) \kappa_R \dot{k}_M (1 - k v_H^p)/u_E^0$. For

$\dot{k}_J = \dot{k}_M$, so $k = 1$, $kv_H^p = l_p^3$ and $\dot{R}_m = (1-\kappa)\kappa_R \dot{k}_M (1-l_p^3)/u_E^0$ and $\kappa = 1 - \frac{\dot{R}_m u_E^0}{\kappa_R \dot{k}_M (1-l_p^3)}$. This value of κ can be used as initial value for the exact solution from the equation for $\dot{R}_m$, where $v_H^p = \frac{u_H^p}{1-\kappa}$ is obtained like in step D11m.

D9m Maximum reserve capacity $[E_m] = \frac{[E_G]}{\kappa g}$ and maximum weight $W_\infty = L_m^3(1+\omega)$ with $\omega = \frac{w_E [E_m]}{\mu_E d_V}$. This gives $L_m = (W_\infty/(1+\omega))^{1/3}$ and $\dot{v} = \dot{k}_M g L_m$, while $\dot{k}_M g$ was obtained in D6m. The unscaled structural lengths are $L_b = l_b L_m$, $L_x = l_x L_m$, $L_p = l_p L_m$

D10m Specific assimilation $\{\dot{p}_{Am}\} = [E_m]/\dot{v}$.

D11m Scaled maturity at birth is $u_H^b = \int_0^{l_b} \frac{d}{dl} u_H \, dl$ with $\frac{d}{d\tau} u_H = (1-\kappa) l^2 (g+l) - k u_H$ and $\frac{d}{d\tau} l = g/3$ and $\frac{d}{dl} u_H = \frac{du_H}{d\tau} \frac{d\tau}{dl}$. Likewise scaled maturity at weaning is $u_H^x = u_H^b + \int_{l_b}^{l_x} \frac{d}{dl} u_H \, dl$ with $\frac{d}{d\tau} u_H = (1-\kappa) l^2 \frac{g+l}{g+1} - k u_H$ and $\frac{d}{d\tau} l = \frac{g}{3} \frac{1-l}{g+1}$. Scaled maturity at puberty is $u_H^p = u_H^b + \int_{l_b}^{l_p} \frac{d}{dl} u_H \, dl$. The unscaled maturity levels are $E_H^b = u_H^b g [E_m] L_m^3$, $E_H^x = u_H^x g [E_m] L_m^3$ and $E_H^p = u_H^p g [E_m] L_m^3$.

D12m Ageing acceleration $\ddot{h}_a$ must be solved from $a_m = \int_0^\infty \exp(\frac{6\dot{h}_W^3}{\dot{h}_G^3}(1 - \exp(\dot{h}_G t) + \dot{h}_G t + \dot{h}_G^2 t^2/2))\, dt$ with $\dot{h}_W^3 = \frac{\ddot{h}_a \dot{v}}{6 L_m} = \ddot{h}_a g \dot{k}_M / 6$ and $\dot{h}_G = s_G \dot{v}/L_m = s_G g \dot{k}_M$. One approach is to approximate $\Pr\{\underline{a}_\dagger > a_m\} = 0.5$, leading for $\tau_G = \dot{h}_G a_m$ to $-\ln 2 = \frac{6\dot{h}_W^3}{\dot{h}_G^3}(1 - \exp(\tau_G) + \tau_G + \tau_G^2/2)$ or $\ddot{h}_a = \frac{-s_G g^2 \dot{k}_M^2 \ln 2}{1 - \exp(\tau_G) + \tau_G + \tau_G^2/2}$

The delay t_0 can obviously not exceed the time at birth $t_b = a_b + t_0$. Moreover, $g > 0$, which translates with D7m to $a_b < l_b/\dot{r}_B$, so $t_b - l_b/\dot{r}_B < t_0 < t_b$. Age at birth is rather constrained since $L_b = \dot{v} a_b/3$ and $L_b < W_b^{1/3}$, because reserve contributes to weight. The parameters $[\dot{p}_M]$ and $\ddot{h}_a$ decrease as function of increasing t_0, while $\dot{v}$, E_H^b, E_H^x and E_H^p increase and $[E_G]$ is unaffected by t_0. The behaviour of the parameters $\{\dot{p}_{Am}\}$ and κ depends on the values of the other parameters. In most cases it will be possible to select t_0 such that $\dot{v} = 0.02\,\mathrm{cm\,d^{-1}}$.

4.11 Trajectory reconstruction

4.11.4 Reconstruction from otolith data

The available info about otolith opacity is now

$$\frac{dO}{dL_O} = \left(\dot{v}_{OG} \frac{d}{dt} S_G - O \sum_i \dot{v}_{Oi} \frac{d}{dt} S_i \right) \frac{3 O^2 L_O^2}{\dot{v}_{OG}^2 S_G^2 (1 - L_O^3/\delta_S L^3)} \quad \text{for } i = D, G$$

with

$$S_D = (S_M + (1 - (L > L_p)\kappa_R)(1-\kappa) S_G)/\kappa$$

$$
\begin{aligned}
S_G &= \kappa S_C - S_M \\
S_C &= L^2 e \frac{g + L/L_m}{g + e} \\
S_M &= \frac{\kappa L^3}{L_m} \\
\frac{d}{dt} S_D &= (\frac{d}{dt} S_M + (1 - (L > L_p)\kappa_R)(1 - \kappa) \frac{d}{dt} S_G)/\kappa \\
\frac{d}{dt} S_G &= \kappa \frac{d}{dt} S_C - \frac{d}{dt} S_M \\
\frac{d}{dt} S_C &= \frac{L}{g + e}(g + \frac{L}{L_m})(\frac{gL}{g + e} \frac{d}{dt} e + 2e \frac{d}{dt} L) + \frac{L^2 e}{g + e} \frac{d}{dt} \frac{L}{L_m} \\
\frac{d}{dt} S_M &= 3\kappa \frac{L^2}{L_m} \frac{d}{dt} L \\
\frac{d}{dt} e &= ((L > L_b) f - e) \dot{v}/L \\
\frac{d}{dt} L &= \frac{\dot{v}}{3} \frac{e - L/L_m}{e + g}
\end{aligned}
$$

We assume that T_{ref} and the 11 parameters T_A, L_b, L_p, κ, κ_R, g, $\dot{k}_M$, $\dot{v}$, $\dot{v}_{OD}$, $\dot{v}_{OG}$, δ_S are known.

5

Multivariate DEB models

5.1 Several substrates

5.1.3 Photo-synthesis, respiration and inhibition

The scheme in Figure 5.3 integrates the antenna system and the Calvin cycle into a single PSU. It results in the following dynamics for $j'_C = \dot{b}_C^{\cdot\cdot} X_C^{\mathrm{int}}$, where X_C^{int} is the intracellular molar concentration of carbon dioxide and $\dot{b}_C^{\cdot\cdot}$ the affinity for free PSUs, $j'_O = \dot{b}_O^{\cdot\cdot} X_O^{\mathrm{int}}$ the same for dioxygen, $j'_L = \rho_{\cdot\cdot} j_L$, where $\rho_{\cdot\cdot}$ is the binding efficiency of photons to free PSUs, $j''_C = \dot{b}_C^{L\cdot} X_C^{\mathrm{int}}$, $j''_O = \dot{b}_O^{L\cdot} X_O^{\mathrm{int}}$, $j''_L = \rho_{\cdot C} j_L = \rho_{\cdot O} j_L$, $j'''_L = \rho_{L\cdot} j_L$.

$$\begin{aligned}
\frac{d}{dt}\theta_{\cdot\cdot} &= \dot{k}_H \theta_{LC} + \dot{k}_C \theta_{LO} - (j'_C + j'_L + j'_O)\theta_{\cdot\cdot} \\
\frac{d}{dt}\theta_{LC} &= j''_L \theta_{\cdot C} + j''_C \theta_{L\cdot} - \dot{k}_H \theta_{LC} \\
\frac{d}{dt}\theta_{\cdot C} &= j'_C \theta_{\cdot\cdot} - j''_L \theta_{\cdot C} \\
\frac{d}{dt}\theta_{L\cdot} &= j'_L \theta_{\cdot\cdot} + \dot{k}_L \theta_{LL} - (j''_C + j''_O + j'''_L)\theta_{L\cdot} \\
\frac{d}{dt}\theta_{LL} &= j'''_L \theta_{L\cdot} - \dot{k}_L \theta_{LL} \\
\frac{d}{dt}\theta_{\cdot O} &= j'_O \theta_{\cdot\cdot} - j''_L \theta_{\cdot O} \\
\frac{d}{dt}\theta_{LO} &= j''_L \theta_{\cdot O} + j''_O \theta_{L\cdot} - \dot{k}_C \theta_{LO} \\
1 &= \theta_{\cdot\cdot} + \theta_{LC} + \theta_{\cdot C} + \theta_{L\cdot} + \theta_{LL} + \theta_{\cdot O} + \theta_{LO}
\end{aligned}$$

The specific flux of carbohydrates amounts to

$$\begin{aligned}
j_H &= \dot{k}_H \theta^*_{LC} - \dot{k}_C \theta^*_{LO} = \left(j'_C - j'_O + \frac{j''_C - j''_O}{j''_C + j''_O} j'_L \right) \theta^*_{\cdot\cdot} \qquad (5.1) \\
\frac{1}{\theta^*_{\cdot\cdot}} &= 1 + \frac{j'_C}{\dot{k}_H} + \frac{j'_C + j'_O}{j''_L} + \frac{j'_O}{\dot{k}_C} + \frac{j'_L}{j''_C + j''_O} \left(1 + \frac{j'''_L}{\dot{k}_L} + \frac{j''_C}{\dot{k}_H} + \frac{j''_O}{\dot{k}_C} \right)
\end{aligned}$$

where θ^*_{LC} and θ^*_{LO} are the steady state fractions of PSUs. The PSU density affects the binding probabilities ρ and affinities $\dot{b}$, and the yield of carbohydrate on photons are in the binding probabilities ρ. Notice that j'''_L and $\dot{k}_L$ only occur in the combination $j'''_L/\dot{k}_L$, which means that we can remove one parameter. The number of parameters can be further reduced by assuming $j''_L = j'_L$, $j''_C = j'_C$ and $j''_O = j'_O$, which leads to

$$\begin{aligned} j_H &= \frac{(j'_C - j'_O)(1 + \frac{j'_L}{j'_C + j'_O})}{1 + \frac{j'_C}{\dot{k}_H} + \frac{j'_C + j'_O}{j'_L} + \frac{j'_O}{\dot{k}_C} + \frac{j'_L}{j'_C + j'_O}\left(1 + \frac{j'''_L}{\dot{k}_L} + \frac{j'_C}{\dot{k}_H} + \frac{j'_O}{\dot{k}_C}\right)} \\ &= \frac{j'_C - j'_O}{1 + \frac{j'_C}{\dot{k}_H} + \frac{j'_O}{\dot{k}_C} + \frac{j'_L j'''_L/\dot{k}_L + (j'_C + j'_O)^2/j'_L}{j'_L + j'_C + j'_O}} \end{aligned} \tag{5.2}$$

If self-shading can be ignored, the arriving photon flux j_L can be taken proportional to light intensity and the proportionality factor can be included in ρ. The rate $\dot{k}_H$ has the interpretation of the specific maximum (net) rate of carbohydrate synthesis and $\dot{k}_C$ the specific maximum (net) rate of photorespiration.

If $O = 0$ (no photorespiration), (5.1) reduces to

$$\begin{aligned} j_H &= \frac{j'_C + j'_L}{1 + \frac{j'_C}{\dot{k}_H} + \frac{j'_C}{j''_L} + \frac{j'_L}{j''_C}\left(1 + \frac{j'''_L}{\dot{k}_L} + \frac{j''_C}{\dot{k}_H}\right)} \\ \overset{\substack{j''_C = j'_C \\ j''_L = j'_L}}{=} & \frac{j'_C + j'_L}{1 + \frac{j'_C}{\dot{k}_H} + \frac{j'_C}{j'_L} + \frac{j'_L}{j'_C}\left(1 + \frac{j'''_L}{\dot{k}_L} + \frac{j'_C}{\dot{k}_H}\right)} \end{aligned}$$

Notice that the present formulation has no photoinhibition if carbon dioxide is non-limiting; to implement that, we need a possible transition for θ_{CL} to a new inhibition state θ_{CLL}.

If $\rho_{L\cdot} = 0$ (no inhibition), (5.1) reduces to

$$\begin{aligned} j_H &= \frac{j'_C - j'_O + \frac{j''_C - j''_O}{j''_C + j''_O} j'_L}{1 + \frac{j'_C}{\dot{k}_H} + \frac{j'_C + j'_O}{j''_L} + \frac{j'_O}{\dot{k}_C} + \frac{j'_L}{j''_C + j''_O}\left(1 + \frac{j''_C}{\dot{k}_H} + \frac{j''_O}{\dot{k}_C}\right)} \\ \overset{\substack{j''_C = j'_C \\ j''_L = j'_L}}{=} & \frac{j'_C - j'_O}{1 + \frac{j'_C}{\dot{k}_H} + \frac{j'_O}{\dot{k}_C} + \frac{j'_C + j'_O}{j'_L} - \frac{j'_C + j'_O}{j'_C + j'_O + j'_L}} \end{aligned}$$

The latter expression is (5.10) for photorespiration.

If $\rho_{L\cdot} = 0$ and $O = 0$ (no respiration or inhibition), (5.1) reduces to

$$j_H = \frac{j'_C + j'_L}{1 + \frac{j'_C + j'_L}{\dot{k}^{LC}_H} + \frac{j'_C}{j''_L} + \frac{j'_L}{j''_C}} \overset{j''_L = j'_L}{=} \frac{1}{\frac{1}{\dot{k}_H} + \frac{1}{j'_C} + \frac{1}{j'_L} - \frac{1}{j'_C + j'_L}}$$

The latter expression is the one for parallel complementary compounds, as given in Figure 3.7.

The processed photon flux amounts to

$$\begin{aligned} j'^{+}_L &= j'_L(\theta^*_{..} + \theta^*_{.C} + \theta^*_{.O} + \theta^*_{L.}) = j'_L(1 + \frac{j'_C + j'_O}{j'_L} + \frac{j'_L}{j'_C + j'_O})\theta^*_{..} \\ &= \frac{j'_H}{j'_C - j'_O}\left(j'_L + \frac{(j'_C + j'_O)^2}{j'_L + j'_C + j'_O}\right) \end{aligned}$$

The photons that are captured by the antenna system, but not processed in the processes of photo-synthesis, respiration or inhibition must be removed to avoid harm to the assimilation machinery. Energy can be emitted (known as energy quenching) in the form of heat or emitted as chlorophyll fluorescence, which has links to the Mehler reaction. So the rate of the Mehler reaction is proportional to $j'^{-}_L = j'_L - j'^{+}_L$. Fluorescence yield is high when less energy is emitted as heat or used in photochemistry; the emitted light has a longer wavelength than the absorbed light. Chlorophyll fluorescence quantifies, therefore, the efficiency of photochemistry and non-photochemical quenching. The Mehler reaction consumes some dioxygen and produces some carbon dioxide. If the (ultimate) source of this carbon dioxide is carbohydrate reserve, the quantitative effect of the Mehler reaction will be difficult to separate from photo-respiration.

Let us now consider the C and O dynamics of the cell to determine j'_C and j'_O. Oxygenic photosynthesis amounts to the transformation $CO_2 + 2\,H_2O + \text{light} \rightarrow CH_2O + H_2O + O_2$, where water has been treated as non-limiting. The flux of hydrocarbon thus equals the flux of dioxygen and also minus the flux of carbon dioxide: $j_H = j_O = -j_C$. The rest of metabolism interacts via the (intracellular) concentrations of carbon dioxide and dioxygen.

Suppose that somatic maintenance only requires the carbohydrate reserve in the transformation $CH_2O + O_2 \rightarrow CO_2 + H_2O$. The specific O_2 consumption and the CO_2 production in association with maintenance both equal j_{HM}, which is a parameter.

Suppose, furthermore, that growth is possibly (co)-limited by nitrogen and that nitrogen is stored in the form of nitrate, NO_3^-, and that growth has no nitrogen overheads. The macro-chemical transformation of the growth process for carbohydrate reserve H and nitrogen reserve N reads for $y_{CV} = 1 - y_{VH}$ and $y_{OV} = y_{CV} - \frac{n_{HV} - 2n_{OV} + 6n_{NV}}{4}$:

$$y_{VH}^{-1}CH_2O + n_{NV}NO_3 + y_{OV}O_2 \rightarrow CH_{n_{HV}}O_{n_{OV}}N_{n_{NV}} + y_{CV}CO_2 + (y_{HV}^{-1} - \frac{n_{HV}}{2})H_2O$$

So the specific flux of CO_2 that is associated with growth amounts to $j_{CG} = \dot{r}y_{CV}$ and of O_2 to $j_{OG} = -\dot{r}y_{OV}$.

For a first-order exchange with the environment we get for environmental concentrations X_C and X_O

$$\begin{aligned} \frac{d}{dt}X_C^{\text{int}} &= \dot{k}_C^{\text{in}}X_C + (j_{HM} + \dot{r}y_{CV} - j_H)[M_V] - (\dot{k}_C^{\text{out}} + \dot{r})X_C^{\text{int}} \\ \frac{d}{dt}X_O^{\text{int}} &= \dot{k}_O^{\text{in}}X_O - (j_{HM} + \dot{r}y_{OV} - j_H)[M_V] - (\dot{k}_O^{\text{out}} + \dot{r})X_O^{\text{int}} \end{aligned}$$

The specific growth rate $\dot{r}$ is given in (5.14), and is a function of the reserve densities of carbohydrate and nitrate. It is likely that C and O don't accumulate, so $\dot{k}_C^{\text{in}} = \dot{k}_C^{\text{out}} = \dot{k}_C^{\text{env}}$

and $\dot{k}_O^{\text{in}} = \dot{k}_O^{\text{out}} = \dot{k}_O^{\text{env}}$. For the purpose of following growth, the internal concentrations can be set in pseudo-steady state, i.e. $\frac{d}{dt}X_C^{\text{int}} = \frac{d}{dt}X_O^{\text{int}} = 0$, which links net photosynthesis directly to the availability of light, carbon dioxide and dioxygen in the environment and to the metabolic acticity:

$$\begin{aligned} j'_C &= \frac{\dot{k}_C^{\text{env}} X_C + (j_{HM} + \dot{r} y_{CV} - j_H)[M_V]}{\dot{k}_C^{\text{env}} + \dot{r}} \dot{b}_C \\ j'_O &= \frac{\dot{k}_O^{\text{env}} X_O - (j_{HM} + \dot{r} y_{OV} - j_H)[M_V]}{\dot{k}_O^{\text{env}} + \dot{r}} \dot{b}_O \end{aligned}$$

This pseudo steady state assumption also avoids to problem of having to deal with the cells' spatial structure. The fluxes j'_C and j'_O need to be substituted in (5.2) of the comments and j_H needs to be solved numerically; this is dome in DEBtool using a Newton Raphson method with optional initial value and analytical derivative for j_H. This initial value is obtained by setting $j_H = 0$ in the expression for j'_C and $j''_L = j'_O = 0$ in the expression for j_H. The number of iteration steps is typically 2 till 4, so the conversion is fast indeed, but this might depend on parameter values.

Heterotrophic activity further modifies the dynamics of C and O and CO_2 concentration mechanisms can be considered where uptake from (and elimination to) the environment is not proportional to its concentration, but again controlled by SUs. Although the photosynthesis module has rather few parameters, quite a few other metabolic parameters modify the resulting rate of photosynthesis. A high light level gives a large drain in intracellular CO_2 and a high production of O_2, so a high photorespiration, which, in combination, can easily appear as photoinhibition.

The photo-synthesis and inhibition model discussed in [877] differs in several aspects. The antenna-system has been separated from the Calvin cycle and the inhibited state falls back to the free state, rather than the excited state.

5.1.3 Combined dioxygen and dihydrogen production

The unicellular diazotrophic cyanobacterium *Cyanothece* sp. ATCC 51142 (wildtype) can produce dihydrogen at rates as high as 465 μmol per mg of chlorophyll per hour in the presence of glycerol under aerobic conditions [78]. It does so while photosynthesing simultaneously. This dihydrogen production is mediated by an efficient nitrogenase system. Dinitrogen fixation and dihydrogen production are typically inhibited by dioxygen; how this bacterium manages to do it simultaneously and at high rates is yet unkown.

The mixture of dioygen and dihydrogen is known as knallgas and can be explosive. Knallgas-bacteria, including *Hydrogenobacter thermophilus*, *Hydrogenovibrio marinus*, and *Helicobacter pylori*, oxidize dihydrogen. There are both Gram positive and negative knallgas bacteria and grow best under microaerophilic conditions. This is because hydrogenase, which used in dihydrogen oxidation, is inhibited by dioxygen, but dioxygen is still needed as a terminal electron acceptor.

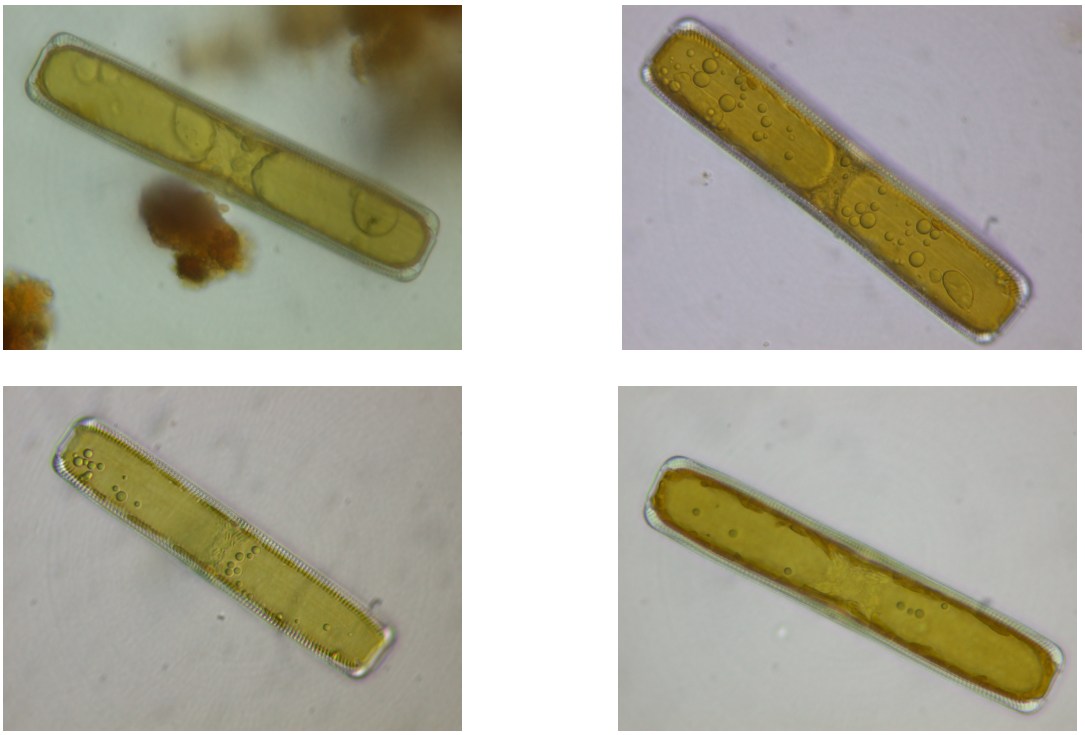

Figure 5.1: The unicellular diatom *Pinnularia* uses lipids as energy reserve. The interface between the lipid droplets and the structure is clearly visible and varies substantially, depending on the recent environmental trajectory. Stochasticity increases for decreasing spatial scale. Reserve dynamics follows from the requirement of weak homeostasis. A simple mechanism behind reserve dynamics is that mobilization is proportional to the surface area of the interface between reserve and structure.2 These pictures suggest that this surface area also shows considerable stochasticity.

5.2 Several reserves

Figure 5.1 shows lipid droplets in the diatom *Pinnularia* for several levels of lipid content. Diatoms are mixotrophs, but mainly phototrophs, and lipids represent only their carbon and energy reserve. These lipids consist mostly of triglycerides, monogalactosyl, digalactosyl and sulphoquinovosyl diglycerides, phosphatidyl glycerol, phosphatidyl choline (lecithin), and phosphatidyl ethanolamine [1053]. The major fatty acids, palmitoleic, palmitic, eicosapentaenoic and eicosate-traenoic acids [1053], are probably also in these droplets. The interphase between lipid reserve and structure is clearly defined and well visible.

5.2.1 Growth: Derivation of (5.14)

We here deal with the transformation $y_{E_1V}E_1 + y_{E_2V}E_2 \rightarrow V$, where E_1 and E_2 are complementary compounds. Figure 3.7 for parallel complementary compounds gives for $j_C = j_{VG}$

and large $\dot{k}_C$ and $j''_A = y_{VE_1} j_{E_1G}$ and $j''_B = y_{VE_2} j_{E_2G}$

$$\begin{aligned} j_{VG} &= \left((y_{VE_1} j_{E_1G})^{-1} + (y_{VE_2} j_{E_2G})^{-1} - (y_{VE_1} j_{E_1G} + y_{VE_2} j_{E_2G})^{-1}\right)^{-1} \\ &= \left(\left(\frac{j_{E_1G}}{y_{E_1V}}\right)^{-1} + \left(\frac{j_{E_2G}}{y_{E_2V}}\right)^{-1} - \left(\frac{j_{E_1G}}{y_{E_1V}} + \frac{j_{E_2G}}{y_{E_2V}}\right)^{-1}\right)^{-1} \end{aligned}$$

Notice that j_{VG} represents the gross specific synthesis of structure. It only equals the nett synthesis if no shrinking occurs simultaneously ($j^S_V = 0$).

5.2.7 2-substrate, 2-reserve, 1-structure isomorphs

Proteins can be used as energy source, but this use generates metabolites that can be become toxic at low concentrations. Carbohydrates and lipids are better sources for energy, while proteins are better sources for building blocks. Since maintenance represents a need for energy in the first place, the use of proteins for maintenance is probably avoided as much as possible. Growth requires energy and building blocks in a (more or less) fixed ratio. This subsection works out an extension of the standard DEB model for 2 types of food X and Y of constant composition, 2 reserves (protein standing for 'building block' reserve, 1, and non-protein for energy reserve, 2) and 1 structure for an isomorph. This formulation is loosely based on [815, 814]. Several choices are made that can be replaced by other choices.

nutrition We assume that the rules of Subsection 3.7.4 of the comments apply for sequential processing of substitutable substrates with interaction, where substrate is identified with food (as generalised compound) and product with reserve (again a generalised compound). Each food type contributes to both reserves, specified in yield coefficients that will here be treated as constant, but can vary in practice (depending on the nutritional condition of prey, for instance). So each assimilation process, defined as the input to a particular reserve from the environment, has to deal with both food types.

The dissociation rates relate to the maximum specific feeding rates as $\dot{k}_X = \{\dot{h}_{XAm}\}L^2$ and $\dot{k}_Y = \{\dot{h}_{YAm}\}L^2$, where L is the structural length of the individual and $\{\dot{h}_{XAm}\}$ the maximum specific feeding rate of food particles of type X in numbers per time.

The association rates relate to the maximum specific searching rates as $\dot{b}_X = \{\dot{F}_{Xm}\}L^2$ and $\dot{b}_Y = \{\dot{F}_{Ym}\}L^2$. A natural simplification is $\{\dot{F}_{Xm}\} = \{\dot{F}_{Ym}\} = \{\dot{F}_m\}$ in absence of an intrinsic preference for a food type.

The interaction affinities $\dot{b}_{XY}$ and $\dot{b}_{YX}$ are based on the deficits of the reserves defined as $s_i = \frac{m_{E_im} - m_{E_i}}{m_{E_im}}$, with 'maximum' reserve densities $m_{E_im} = \max(m^X_{E_im}, m^Y_{E_im})$ and $m^X_{E_im} = \frac{\{j^X_{E_iAm}\}}{\dot{v}[M_V]}$ and $m^Y_{E_im} = \frac{\{j^Y_{E_iAm}\}}{\dot{v}[M_V]}$. The maximal reserve densities are not real maxima because in 2-reserves systems these values can be exceeded due to the (partial) return of rejected allocations to growth. See further below under assimilation. These deficits thus stand for the relative 'reserve-space' that can still be filled

by the individual; it is indicated by a symbol that stands for stress on the basis of the idea that the individual wants to top up its reserves to maximum capacity. A possible specification of the specific interaction affinities for $\{\dot{b}_{XY}\} = \dot{b}_{XY}/L^2$ and $\{\dot{b}_{YX}\} = \dot{b}_{YX}/L^2$

$$\begin{aligned}\rho_{XY} = \frac{\{\dot{b}_{XY}\}}{\{\dot{F}_{Xm}\}} &= s_1\left(\frac{M_X}{M_Y}\frac{y_{E_1X}}{y_{E_1Y}} - 1\right)_+ + s_2\left(\frac{M_X}{M_Y}\frac{y_{E_2X}}{y_{E_2Y}} - 1\right)_+\\ \rho_{YX} = \frac{\{\dot{b}_{YX}\}}{\{\dot{F}_{Ym}\}} &= s_1\left(\frac{M_Y}{M_X}\frac{y_{E_1Y}}{y_{E_1X}} - 1\right)_+ + s_2\left(\frac{M_Y}{M_X}\frac{y_{E_2Y}}{y_{E_2X}} - 1\right)_+\end{aligned}$$

where index + stands for taking the maximum of 0 and the value between the braces. So $\dot{b}_{XY} = 0$ if a food particle M_Y has the same contribution to reducing the deficits in both reserves as a food particle M_X. This has as consequence that the individual will not change food particle X for Y. The better the potential to reduce the reserve deficits, the more likely the individual will feed on that type of food. The choice of adding the effects on the deficits is not well motivated and alternatives might be considered as well.

feeding Let $\{\dot{J}_{XAm}\} = M_X\{\dot{h}_{XAm}\}$ denote the feeding rate in mass per time, where M_X is the mass of a food particle of type X. The maximum specific assimilation rate for reserve i for food X is $\{\dot{J}^X_{E_iAm}\} = y_{E_iX}\{\dot{J}_{XAm}\}$, where y_{E_iX} is the yield of reserve i on food X and $i = 1, 2$ (protein and non-protein). These yields are treated as constants. The same we have for food Y (replace X by Y). The total assimilation rate for reserve i is $\{\dot{J}_{E_iA}\} = f_X\{\dot{J}^X_{E_iAm}\} + f_Y\{\dot{J}^Y_{E_iAm}\}$, where the scaled functional responses are $f_X = \{\dot{J}_{XA}\}/\{\dot{J}_{XAm}\}$ and $f_Y = \{\dot{J}_{YA}\}/\{\dot{J}_{YAm}\}$. The scaled functional responses f_X and f_Y are specified below. If the composition of food particles varies in time (because they themselves have reserves and structure, for instance), the yield coefficients y_{E_iX} and y_{E_iY} will vary in time.

assimilation Summing up: the specific assimilation rate for reserve i amounts to

$$\{\dot{J}_{E_iA}\} = y_{E_iX}\{\dot{J}_{XAm}\}f_X + y_{E_iY}\{\dot{J}_{YAm}\}f_Y$$

with

$$\begin{array}{ll} f_X = \frac{\dot{\alpha}_Y\{\dot{F}_{Xm}\}X - \dot{\beta}_X\{\dot{F}_{Ym}\}Y}{\dot{\alpha}_X\dot{\alpha}_Y - \dot{\beta}_X\dot{\beta}_Y}; & f_Y = \frac{\dot{\alpha}_X\{\dot{F}_{Ym}\}Y - \dot{\beta}_Y\{\dot{F}_{Xm}\}X}{\dot{\alpha}_X\dot{\alpha}_Y - \dot{\beta}_X\dot{\beta}_Y}\\ \dot{\alpha}_X = \{\dot{h}_{XAm}\} + \{\dot{F}_{Xm}\}X + \{\dot{b}_{YX}\}Y; & \dot{\alpha}_Y = \{\dot{h}_{YAm}\} + \{\dot{F}_{Ym}\}Y + \{\dot{b}_{XY}\}X\\ \dot{\beta}_X = \{\dot{F}_{Xm}\}X - \{\dot{b}_{XY}\}X; & \dot{\beta}_Y = \{\dot{F}_{Ym}\}Y - \{\dot{b}_{YX}\}Y \end{array}$$

The specific feeding rates are $\{\dot{J}_{XA}\} = \{\dot{J}_{XAm}\}f_X$ and $\{\dot{J}_{YA}\} = \{\dot{J}_{YAm}\}f_Y$. The rates at which particles X and Y disappear from the environment (in numbers per time) are $\{\dot{h}_{XA}\} = \{\dot{h}_{XAm}\}f_X$ and $\{\dot{h}_{YA}\} = \{\dot{h}_{YAm}\}f_Y$.

For increasing X and constant Y, we have $\dot{\alpha}_X \to \{\dot{F}_{Xm}\}X$, $\dot{\beta}_X \to (\{\dot{F}_{Xm}\} - \{\dot{b}_{XY}\})X$, $\dot{\alpha}_Y \to \{\dot{b}_{XY}\}X$, and $\dot{\beta}_Y$ remains constant. This amounts to $f_X \to 1$ and $f_Y \to 0$.

The results for increasing Y and constant X follow from symmetry, i.e. interchanging X and Y in all symbols. If both X and Y increase, both f_X and f_Y remain smaller than 1, with the implication that $\{\dot{J}_{E_iAm}\} = \max(y_{E_iX}\{\dot{J}_{XAm}\}, y_{E_iY}\{\dot{J}_{YAm}\}) = \max(\{\dot{J}^X_{E_iAm}\}, \{\dot{J}^Y_{E_iAm}\})$. If the rejected mobilized reserve fluxes in the growth process are excreted ($\kappa_{E_i} = 0$), the maximum reserve density becomes $m_{E_im} = \frac{\{\dot{J}_{E_iAm}\}}{\dot{v}[M_V]}$, as stated above and see under mobilization.

reserve dynamics The change in reserve density is given by (5.17) and amounts to

$$\frac{d}{dt} m_{E_i} = j_{E_iA} - j_{E_iC} + \kappa_{E_i} j_{E_iP} - \dot{r} m_{E_i}$$

where the specific mobilization flux j_{E_iC} and the specific rejection flux j_{E_iP} and the specific growth rate $\dot{r}$ are defined below. The mass-specific assimilation rate relates to the surface area-specific one as $j_{E_iA} = \frac{\{\dot{J}_{E_iA}\}}{[M_V]L}$, where $[M_V]$ is the volume-specific mass of structure, which is treated as a constant.

mobilization On the assumption that the energy conductances of both reserves are the same, specific reserve mobilization follows (5.13)

$$j_{E_iC} = m_{E_i}(\dot{v}/L - \dot{r})$$

where specific growth rate $\dot{r}$ still has to be determined.

At maximum structural mass $M_{Vm} = [M_V]L_m^3$, where $\dot{r} = 0$ and $\frac{d}{dt} m_{E_i} = 0$, specific assimilation equals specific mobilization, $j_{E_iA} = j_{E_iC} = m_{E_i}\dot{v}/L$. The maximum reserve density can now be solved: $m_{E_im} = \frac{j_{E_iAm}}{\dot{v}/L_m} = \frac{\dot{J}_{E_iAm}}{M_{Vm}\dot{v}/L_m} = \frac{\{\dot{J}_{E_iAm}\}L_m^2}{[M_V]L_m^3\dot{v}/L_m} = \frac{\{\dot{J}_{E_iAm}\}}{[M_V]\dot{v}}$.

allocation The κ-rule is applied to both mobilization rates, with the same value for κ.

growth Following (5.14), the i-th reserve sends a specific flux $j_{E_iG} = \kappa j_{E_iC} - j^S_{E_i}$ to the SU for growth of structure which leads to

$$j_{VG} = \dot{r} + j^S_V = \left(\sum_i \left(\frac{j_{E_iG}}{y_{E_iV}}\right)^{-1} - \left(\sum_i \frac{j_{E_iG}}{y_{E_iV}}\right)^{-1}\right)^{-1} \tag{5.3}$$

which determines $\dot{r}$ after having determined $j^S_{E_i}$ (see below). The specific shrinking rate $j^S_V = 0$ in the case that mobilization is sufficient to pay the maintenance costs or if the reproduction buffer is not empty. If the reproduction buffer is empty and somatic maintenance is (just) an energy requirement, we have $j^S_V = j_{E_iS}\frac{\mu_{E_i}}{\mu_V}\left(1 - \frac{j^S_{E_1}}{j_{E_1S}} - \frac{j^S_{E_2}}{j_{E_2S}}\right)_+$ with $j_{E_1S}\mu_{E_1} = j_{E_2S}\mu_{E_2}$.

The growth efficiency κ_G, defined as $\frac{d}{dt}E_V = \kappa_G \dot{p}_G$, is for the standard DEB model given by $\kappa_G = \frac{\mu_V[M_V]}{[E_G]} = \frac{\mu_V}{\mu_{GV}} = \frac{\mu_V y_{VE}}{\mu_E}$.

For two reserves, it becomes $\kappa_G = \frac{\mu_V j_{VG}}{\sum_i \mu_{E_i}(\kappa j_{E_iC} - j_{E_iS})}$, where $j_{VG} = \dot{r}$ by definition. Notice that κ_G relates to the growth SU, implying that the rejected fluxes can affect the reserve dynamics, but should not affect κ_G.

somatic maintenance Protein and non-protein reserves are substitutable for maintenance, with a strong preference for non-proteins, and binding is parallel. According to (4.5) where structure is now replaced by protein-reserve, the specific fluxes that are actually used for somatic maintenance are

$$j^S_{E_1} = \min\left(\kappa j_{E_1C}, \frac{2A\, j_{E_1S}}{2A + \sqrt{B^2 - 4AC} - B}\right); \quad j^S_{E_2} = \min\left(\kappa j_{E_2C}, j_{E_2S}(1 - j^S_{E_1}/j_{E_1S})\right)$$

with $A = \rho_1 j_{E_1C} j_{E_1S}$, $B = C + (j_{E_1C} + (1-\rho_1) j_{E_2C}) j_{E_2S}$, $C = -\kappa j_{E_2C}(j_{E_1C} + j_{E_2C})$. The parameter ρ_1 represents a preference for reserve 1 (which is close to 0 for proteins). The specific maintenance costs $j_{E_iS} = j_{E_iM} + \frac{\{j_{E_iT}\}}{[M_V]L}$, as given in (2.17), represents the somatic maintenance costs if all would have been paid from reserve i, while $j^S_{E_i}$ represents the costs that is actually paid from reserve i. Natural simplifications are $\frac{j_{E_1M}}{j_{E_2M}} = \frac{\{j_{E_1T}\}}{\{j_{E_2T}\}} = \frac{\mu_{E_1}}{\mu_{E_2}}$. Together with the expressions for growth and mobilization, this implicitly determines $\dot{r}$, $j^S_{E_i}$ and j_{E_iC}.

excretion A fixed fraction of the reserve fluxes that are rejected by the growth and maturation SUs are excreted, as specified by (5.15). The specific rejected flux is

$$j_{E_iP} = \kappa j_{E_iC} - j^S_{E_i} - y_{E_iV} j_{VG}$$

The flux $\kappa_{E_i} j_{E_iP}$ returns to the reserve, while the flux $(1-\kappa_{E_i}) j_{E_iP}$ is excreted. The book uses the notation j_{E_iR} for the rejected flux, but it does not consider rejection in combination with reproduction, a process that is already indicated by R. A better choice might be P for 'Product formation', although rejected fluxes are not necessarily excreted. The choice $\kappa_{E_i} = 1$ still excludes the problem of possible unbounded damming up of a reserve.

maturity maintenance Since the whole flux $(1-\kappa)\dot{J}_{E_iC}$ dissipates, it seems less natural to install a priority rule for the use of a particular reserve for maturity maintenance and allocate the rest to maturation. The simplest implementation of maturity maintenance is to pay the energy drain $\dot{p}_J = \dot{k}_J E_H$ from the summed mobilization fluxes $(1-\kappa)\sum_i \dot{p}^i_C$, with $\dot{p}^i_C = \mu_{E_i}\dot{J}_{E_iC}$. The (absolute) mobilization flux relates to the specific one as $\dot{J}_{E_iC} = j_{E_iC} M_V = j_{E_iC}[M_V]L^3$. This allocation means a drain of $\dot{J}_{E_iJ} = \dot{J}_{E_iC}\dot{p}_J / \sum_i \dot{p}^i_C$ from reserve i.

maturation The simplest implementation of maturation is to consider it as an energy allocation:

$$\begin{aligned} \frac{d}{dt}E_H &= (1-\kappa)\sum_i \dot{p}^i_C - \dot{k}_J E_H \quad \text{if positive, else} \\ &= -\dot{k}'_J(E_H - (1-\kappa)\sum_i \dot{p}^i_C/\dot{k}_J) \end{aligned}$$

The (absolute) flux that is allocated to maturation (or reproduction) relates to the specific one as $\dot{J}_{E_iR} = j_{E_iR}M_V = j_{E_iR}[M_V]L^3 = (1-\kappa)\dot{J}_{E_iC} - \dot{J}_{E_iJ}$.

Like in the standard model, maturation continues till $E_H = E_H^p$. If the reproduction buffer is not empty, rejuvenation can be delayed by draining this buffer to supplement maturity maintenance.

reproduction After $E_H = E_H^p$, further maturation is ceased and the flux $\dot{J}_{E_iR}$ is allocated to reproduction, i.e. filling a reproduction buffer that is (partially) emptied at spawning. The maternal effect is applied for both reserves independently: the reserve densities at birth equals those of the mother at egg formation (i.e. at spawning). The costs of an egg, in terms of the initial amounts for both reserves $M_{E_i}^0$, is obtained numerically (see below). The (standard) spawning rule is that as soon as enough reserves are available in the reproduction buffer, an egg is made and laid, which empties the reproduction buffer for one reserve. Some of the other reserve that is left over and is left in the reproduction buffer; this rule can come with a considerable accumulation of one of the reserves in the reproduction buffer. The mean reproduction rate amounts, according to (2.56), to

$$\dot{R} = \min(\kappa_R^1 \dot{J}_{E_1R}/M_{E_1}^0, \kappa_R^2 \dot{J}_{E_2R}/M_{E_2}^0)$$

for $E_H = E_H^p$, else $\dot{R} = 0$. A rather natural simplification is $\kappa_R^1 = \kappa_R^2$.

mineral fluxes The mineral fluxes must be found from $\mathbf{0} = \boldsymbol{n}_{\mathcal{M}}\dot{\boldsymbol{J}}_{\mathcal{M}} + \boldsymbol{n}_{\mathcal{O}}\dot{\boldsymbol{J}}_{\mathcal{O}}$ with

$$\dot{\boldsymbol{J}}_{\mathcal{O}} = \begin{pmatrix} \dot{J}_X & \dot{J}_Y & \dot{J}_V & \dot{J}_{E_1} + \dot{J}_{E_1R} & \dot{J}_{E_2} + \dot{J}_{E_2R} & \dot{J}_{P_X} & \dot{J}_{P_Y} \end{pmatrix}^T$$

$$\boldsymbol{n}_{\mathcal{O}} = \begin{pmatrix} n_{CX} & n_{CY} & n_{CV} & n_{CE_1} & n_{CE_2} & n_{CP_X} & n_{CP_Y} \\ n_{HX} & n_{HY} & n_{HV} & n_{HE_1} & n_{HE_2} & n_{HP_X} & n_{HP_Y} \\ n_{OX} & n_{OY} & n_{OV} & n_{OE_1} & n_{OE_2} & n_{OP_X} & n_{OP_Y} \\ n_{NX} & n_{NY} & n_{NV} & n_{NE_1} & n_{NE_2} & n_{NP_X} & n_{NP_Y} \end{pmatrix}$$

where P_X is faeces that is derived from prey X and P_Y that from prey Y; the production flux amounting to $\dot{J}_{P_X} = -y_{P_XX}\dot{J}_X$ with $\dot{J}_X = -\dot{J}_{XA}$ (negative because food X is disappearing). The inequality $y_{P_XX} + y_{E_1X} + y_{E_2X} < 1$ has apply to allow for CO_2 production in association with assimilation of X. Further $\dot{J}_V = j_{VG}M_V$ and $\dot{J}_{E_i} = (j_{E_iA} - j_{E_iC} + \kappa_{E_i}j_{E_iP})M_V$.

ageing The ageing process can be quantified approximately by substitution of

$$\frac{\dot{p}_C}{E_m} = \frac{j_{E_1C} - j_{E1P}}{m_{E_1}} + \frac{j_{E_2C} - j_{E2P}}{m_{E_2}} \quad \text{and} \quad L_m = \kappa \min\left(\frac{\{\dot{J}_{E_1Am}\}}{[\dot{J}_{E_1S}]}, \frac{\{\dot{J}_{E_2Am}\}}{[\dot{J}_{E_2S}]}\right)$$

in (6.1). The changes in ageing acceleration and hazard then become

$$\frac{d}{dt}\ddot{q} = \left(\ddot{q}\frac{L^3}{L_m^3}s_G + \dddot{h}_a\right)\frac{\dot{p}_C}{E_m} - \dot{r}\ddot{q}; \quad \frac{d}{dt}\dot{h} = \ddot{q} - \dot{r}\dot{h}$$

Figure 5.2: This spider wasp *Anoplius viaticus* just paralised the wolf spider *Arctosa leopardus* and carries it to its burrow that she dug in the sand, where she will lay an egg on it (left). The hatching juvenile will be able to complete its juvenile stage with the spider as food, pupate, emerge and feed on nectar as adult; here *Ammophila sabulosa* feeding on *Senecio inaequidens* (right). The pictures were taken in the dunes of Amsterdam near de Zilk.

maximum size Maximum structural length is reached at maximum assimilation, i.e.

$$\{\dot{J}_{E_iAm}\} = y_{E_iX}\{\dot{J}_{XAm}\} + y_{E_iY}\{\dot{J}_{YAm}\}$$

and the reserves are fully filled, i.e. $m_{E_im} = \frac{\{\dot{J}_{E_iAm}\}}{\dot{v}[M_V]}$. Maximum structural length L_m is now found from equating $\dot{r} = 0$ for these reserve densities. See function `DEBtool_M/iso_21/get_Lm_iso_21`.

This model captures the general 'stylised empirical fact' that young (fast growing) individuals prefer protein-rich food types, while fully-grown individuals tend to prefer food types with less protein. Think, for instance, of mammals, doves and flamingos, which feed on milk as baby. This trait is developed in a spectacular way in ichneumonid and sphecid wasps, such as *Anoplius* and *Ammophila*, see Figure 5.2, which feed on (protein rich) spiders and insects as juvenile and (carbohydrate rich) nectar as adult. Hatchlings of direct developing caecilians feed on the skin of their mother (dermatophagy), while the foetuses of viviparous caecilians feed intrauterine by scraping from the uterus epithelium. Hatchlings of the arrow frog *Dendrobatus* are fed by the mother with unfertilised eggs in bromelias high in the trees, those of the white shark *Carcharodon carcharias* in the uterus of the mother.

One 5th of all insects have endosymbiontic bacteria. Termites and cockroaches (which are closely related) have what is called a fat body in their abdomen, consisting of adipose tissue, with adipocytes (cells filled with lipid globules) and mycetocytes (cells packed with bacteria, *Blattabacterium* in the case of cockroaches). The cockroaches hardly excrete nitrogen waste but store it as uric acid crystals in their fat body, where the bacteria convert it, using the stored lipids, to all the 10 amino acids the cockroaches need as well as some vitamins. These bacteria cannot live outside the cockroach and the latter pass them to the next generation via its eggs. This symbiosis allows the cockroach to live on protein-poor diets.

5.2.7.1 Specific growth rate of 21-isomorphs

Since the specific growth rate $\dot{r}$ is specified implicitly, the change of the states of the individual comprises a set of Differential Algebraic Equations (DAEs). It is more efficient to make use to the properties of this model, rather than using a general method for solving such a system. The specific growth rate $\dot{r}$ of an isomorph with 2 reserves and 1 structure can be found using a Newton Raphson method with continuation, i.e. where the initial value $\dot{r}_0$ equals the result of the previous iteration: $\dot{r}_{i+1} = \dot{r}_i - H(\dot{r}_i)/\frac{d}{d\dot{r}}H(\dot{r}_i)$. The iteration is terminated if $|H(\dot{r}_i)| < 10^{-8}$. The function H is found using (5.3) of the comments:

$$\begin{aligned}
H(\dot{r}) &= \dot{r} + j_V^S - \left(\sum_i \left(\frac{j_{E_iG}}{y_{E_iV}}\right)^{-1} - \left(\sum_i \frac{j_{E_iG}}{y_{E_iV}}\right)^{-1}\right)^{-1} \\
\frac{d}{d\dot{r}}H(\dot{r}) &= 1 - j_{E_iS}\frac{\mu_{E_i}}{\mu_V}\left(\frac{j_{E_1}^{S\prime}}{j_{E_1S}} + \frac{j_{E_2}^{S\prime}}{j_{E_2S}}\right)(j_V^S > 0) - \\
&\quad \left(\dot{r} + j_V^S - H(\dot{r})\right)^2 \left(\sum_i \left(\frac{j_{E_iG}}{y_{E_iV}}\right)^{-2} \frac{j'_{E_iG}}{y_{E_iV}} - \left(\sum_i \frac{j_{E_iG}}{y_{E_iV}}\right)^{-2} \sum_i \frac{j'_{E_iG}}{y_{E_iV}}\right) \\
j'_{E_iG} &= -\kappa m_{E_i} - j_{E_i}^{S\prime} \\
j_{E_1}^{S\prime} &= j_{E_1}^S \left(\frac{A'}{A} - \frac{2A' + (B^2 - 4AC)^{-1/2}(BB' - 2A'C - 2AC') - B'}{2A + \sqrt{B^2 - 4AC} - B}\right) \\
&\quad \text{with } A' = -\rho_1 m_{E_1} j_{E_2S}^2 / j_{E_1S}; \quad B' = C' - (m_{E_1} + (1-\rho_1)m_{E_2}) j_{E_2S} \\
&\quad C' = \kappa m_{E_2}(j_{E_1C} + j_{E_2C}) + \kappa j_{E_2C}(m_{E_1} + m_{E_2}) \\
&\quad \text{for } j_{E_1}^S < \kappa j_{E_1C} \text{ else } j_{E_1}^{S\prime} = -\kappa m_{E_1} \\
j_{E_2}^{S\prime} &= -j_{E_1}^{S\prime} j_{E_2S}/j_{E_1S} \quad \text{for } j_{E_2}^S < \kappa j_{E_2C} \text{ else } j_{E_2}^{S\prime} = -\kappa m_{E_2}
\end{aligned}$$

If $j_{E_i}^S = j_{E_iC}$, however, we have $j_{E_i}^{S\prime} = j'_{E_iC} = -m_{E_i}$, The choice $\dot{r}_0 = 0$ can be used for the very first call this procedure. Even at constant food densities the ODE's need to be integrated numerically and $\dot{r}$ needs to be evaluated at each time increment. Typically the iteration for $\dot{r}$ requires very few steps (2 or 3) for convergence.

The specific growth rate needs special care for embryos, since $\dot{r} \to \infty$ for $L \downarrow 0$. To avoid numerical problems for the embryo state variables, it is better to work with the variable $\frac{d}{dt}L = \dot{r}L/3 = \dot{v}_B$ rather than $\dot{r}$ (for embryos at least; the notation refers to the concept of the generalized von Bertalanffy growth, as discussed in 2.4 of the comments.) Avoiding the pathological case of shrinking before birth, we have $j_V^S = 0$. We also have $j_{E_i}^S = j_{E_i}^M$, since $j_{E_iT} = 0$ for embryos. This leads, for $\dot{v}_{G_i} = y_{VE_i}(\kappa m_{E_i}(\frac{\dot{v}}{3} - \dot{v}_B) - j_{E_i}^M \frac{L}{3})$, to $\dot{v}_B$ as the root of

$$\begin{aligned}
H(\dot{v}_B) &= \dot{v}_B - \left(\sum_i \dot{v}_{G_i}^{-1} - \left(\sum_i \dot{v}_{G_i}\right)^{-1}\right)^{-1} \\
\frac{d}{d\dot{v}_B}H(\dot{v}_B) &= 1 - (\dot{v}_B - H(\dot{v}_B))^2 \left(\sum_i \frac{\theta_{G_i}}{\dot{v}_{G_i}^2} - \frac{\sum_i \theta_{G_i}}{\left(\sum_i \dot{v}_{G_i}\right)^2}\right) \\
\theta_{G_i} &= -y_{VE_i}(\kappa m_{E_i} + j_{E_i}^{M\prime})
\end{aligned}$$

$$\begin{aligned} j_{E_1}^{M\prime} &= j_{E_1}^{M}\left(\frac{A'}{A} - \frac{2A' + (B^2-4AC)^{-1/2}(BB' - 2A'C - 2AC') - B'}{2A + \sqrt{B^2-4AC} - B}\right) \\ & \text{with } A' = -\rho_1 m_{E_1}\frac{j_{E_2M}^2}{j_{E_1M}}; \quad B' = C' - (m_{E_1} + (1-\rho_1)m_{E_2})j_{E_2M} \\ & C' = \kappa m_{E_2}(j_{E_1C} + j_{E_2C}) + \kappa j_{E_2C}(m_{E_1} + m_{E_2}) \\ & \text{for } j_{E_1}^S < \kappa j_{E_1C} \text{ else } j_{E_1}^{S\prime} = -\kappa m_{E_1} \\ j_{E_2}^{M\prime} &= -j_{E_1}^{M\prime} j_{E_2M}/j_{E_1M} \quad \text{for } j_{E_2}^S < \kappa j_{E_2C} \text{ else } j_{E_2}^{S\prime} = -\kappa m_{E_2} \end{aligned}$$

Using a continuation method, again, the Newton Raphson scheme $\dot{v}_B^{i+1} = \dot{v}_B^i - H(\dot{v}_B^i)/\frac{d}{d\dot{v}_B}H(\dot{v}_B^i)$ will not give numerical problems.

5.2.7.2 Initial state of 21-isomorphs

At age zero we have $\frac{d}{dt}L(0) = \frac{\dot{v}}{3} = \dot{v}_B(0)$, see (2.47), also in the 2-reserve case, because reserves are initially not limiting growth. Going backwards in time we have $L \downarrow 0$, $m_{E_i} \uparrow \infty$, $\dot{v}_B \uparrow \dot{v}/3$ and $\dot{v}_G^i \uparrow y_{E_iV}\dot{v}_B$. Very shortly after the start of development, when maintenance is still negligible but reserve densities not very large, we have for small $t = a_b/100$, say

$$\begin{aligned} M_V(t) &= [M_V]L^3(t) \quad \text{with } L(t) = t\dot{v}/3 \\ M_{E_i}(t) &= M_{E_i}^0 - \frac{M_V(t)}{\kappa y_{VE_i}} \quad \text{and } m_{E_i}(t) = \frac{M_{E_i}^0}{M_V(t)} - \frac{1}{\kappa y_{VE_i}} \\ E_H(t) &= (1-\kappa)\sum_i \mu_{E_i}(M_{E_i}^0 - M_{E_i}(t)) = \frac{1-\kappa}{\kappa}M_V(t)\sum_i \frac{\mu_{E_i}}{y_{VE_i}} \end{aligned}$$

The application of this is to determine $M_{E_i}^0$, a_b and L_b of a 21-isomorph by a shooting method: (1) development is followed from an very early age till birth, using initial estimates for $M_{E_i}^0$, (2) maturity densities at birth $m_{E_i}^b$ are evaluated, compared with the target values and (3) estimates for $M_{E_i}^0$ are adapted and the procedure repeated till $m_{E_i}^b$ are at the target values. The initial guess values are: $L_b^3 = \frac{E_H^b}{[E_G]}\frac{\kappa}{1-\kappa} = \frac{M_V^b}{[M_V]}$, $a_b = \frac{3L_b}{\dot{v}}$, $M_{E_1}^0 = M_V^b(m_{E_1}^b + \frac{1}{\kappa y_{VE_1}})$, $M_{E_2}^0 = M_V^b(m_{E_2}^b + \frac{1}{\kappa y_{VE_2}} + \frac{j_{E_2M}a_b}{\kappa})$. These initial guesses under-estimate a_b, over-estimate L_b and possibly over-estimate maintenance losses in $M_{E_2}^0$ (by almost a factor 2 if the $m_{E_i}^b$'s are large). A (small) over-estimation of the start-values for the initial reserves is numerically better, however, than an under-estimation (to complete development properly). The initial reserves are also necessary to translate the reproduction buffer into numbers of eggs at spawning.

The idea behind the maternal effect in the standard model is that the reserve density does not change at constant food density after birth. This property does not necessarily hold for a 221-isomorph; the quality of her eggs (quantified as $M_{E_i}^0$) might change during the life cycle, even at constant food. This is partly caused by changes in food preference and by damming up of reserve.

5.2.7 Variable stoichiometry in iso_21 growth

As alternative for fixed stoichiometric requirements for both somatic maintenance and growth, we can consider a scheme where growth is split into in a building-block component (anabolic part) that is fueled by protein reserve only and an energy component (catabolic part) that is preferentially fueled by carbohydrate/lipid reserve E_2, but can also be fulled by protein reserve E_1 if necessary. The implication is that the mobilized E_1 flux is never rejected, $j_{E_1P} = 0$, and the E_2 flux only if more is mobilized than required for somatic maintenance plus the catabolic part of the growth process.

For simplicity's sake we assume that the preference for using E_2 for maintenance and growth overheads is absolute, so $\rho_1 = 0$, in which case the preference module reduces to the switch module:

$$j^S_{E_2} = \min(\kappa j_{E_2C}, j_{E_2S}); \quad j^S_{E_1} = \min\left(\kappa j_{E_1C}, j_{E_1S}(1 - j^S_{E_2}/j_{E_2S})\right)$$

We also assume that $\mu_{E_1} j_{E_1S} = \mu_{E_2} j_{E_2S}$, meaning that the somatic maintenance need represents an energy investment in the first place.

The yield y_{E_1V} specifies how many moles of E_1 are required to synthesize one mole of structure V, if no E_2 is used. The yield y_{E_2V} is not defined, because V cannot be synthesized from E_2 only and how much E_2 is used is variable. The energy that is fixed per mole of structure is μ_V and, if all structure is synthesized from E_1 only, the energy that is used per mole of structure is $\mu_{E_1} y_{E_1V}$, so the growth efficiency is $\kappa_G = y_{VE_1}\mu_V/\mu_{E_1}$, which must be less than 1. To ensure this, it seems best practice to specify κ_G and derive $y_{VE_1} = \kappa_G \mu_{E_1}/\mu_V$. Notice that y_{VE_1} under variable stoichiometry is not comparable with that under fixed stoichiometry. The growth efficiencies are comparable, but is variable under fixed stoichiometry.

To simplify the notation, we write $\dot{k}_E = \dot{v}/L$, but we have to remember that this is not a constant parameter.

mode 1 Suppose that the E_2 flux that is allocated to soma is more than can be used for somatic maintenance plus growth overheads, let us call this situation mode 1. No shrinking occurs, i.e. $j^S_V = 0$, $j^S_{E_1} = 0$, $j^S_{E_2} = j_{E_2S}$, $j_{VG} = \dot{r}$, $j_{E_1G} = \kappa j_{E_1C} = \kappa m_{E_1}(\dot{k}_E - \dot{r})$ and the specific growth $\dot{r}$ follows from $\mu_{E_1} j_{E_1G} = \mu_V j_{VG}$, which covers the anabolic part of growth. Notice that each carbon in E_1 coverts to in 1 in structure V by definition, since we here consider the anabolic part of growth only. The result is $\dot{r} = \frac{\kappa m_{E_1} \dot{k}_E}{\kappa m_{E_1} + \mu_V/\mu_{E_1}}$. The catabolic part of growth that needs to be covered by reserve E_2 is $j_{E_2G} = (1 - \kappa_G)\dot{r}\mu_V/\mu_{E_2}$. The rejected E_2 flux is $j_{E_2P} = \kappa j_{E_2C} - j_{E_2S} - j_{E_2G}$. This flux equals zero if $\kappa j_{E_2C} = j_{E_2S} + j_{E_2G}$ for $j_{E_2C} = m_{E_2}(\dot{k}_E - \dot{r})$. It implies a lower boundary of reserve density $m_{E_2} = \frac{j_{E_2S} + j_{E_2G}}{\kappa(\dot{k}_E - \dot{r})}$, below which reserve E_2 cannot cover all growth overheads and possibly also not all somatic maintenance. Maximum size is not well-defined in this mode, since m_{E_1} needs to be zero to avoid growth.

mode 2 Suppose now that the E_2 flux that is allocated to soma can cover all somatic maintenance, but not all growth overheads. The energy flux to growth that this flux can cover is $\mu_{E_2}(\kappa j_{E_2C} - j_{E_2S})$, while E_1 contributes $\mu_{E_1}\kappa j_{E_1C}$ to growth. No

rejection of E_2 occurs, $j_{E_2P} = 0$, nor shrinking, $j_V^S = 0$. For specific growth rate $\dot{r}$, the required investment is $\mu_V \dot{r}/\kappa_G = \dot{r}\mu_{E_1}/y_{VE_1}$, so $\dot{r} = \frac{\sum_i \mu_{E_i} m_{E_i} \kappa \dot{k}_E - \mu_{E_2} j_{E_2S}}{\mu_{E_1}/y_{VE_1} + \kappa \sum_i \mu_{E_i} m_{E_i}}$. The flux of E_2 to growth overheads is zero if $\kappa j_{E_2C} = j_{E_2S}$, which implies a lower boundary of reserve density $m_{E_2} = (j_{E_2S}/\kappa + \dot{r})/\dot{k}_E$, below which E_2 cannot cover not all somatic maintenance. Maximum size occurs when growth is zero, i.e. $L_\infty = \frac{\kappa \dot{v} \sum_i \mu_{E_i} m_{E_i}}{\mu_{E_2} j_{E_2S}}$

mode 3 If the E_2 flux cannot cover all somatic maintenance, but growth is still positive, some of the costs needs to be covered from E_1. The part of somatic maintenance that is contributed by E_2 is $j_{E_2}^S = \kappa j_{E_2C}$, so E_1 needs to contribute $j_{E_1}^S = j_{E_1S} - j_{E_2}^S \mu_{E_2}/\mu_{E_1}$. The specific growth rate follows from the balance $j_{E_1G} = \mu_V \dot{r}/\kappa_G = \kappa j_{E_1C} - j_{E_1}^S$, which results in $\dot{r} = \frac{(m_{E_1} + m_{E_2}\mu_{E_2}/\mu_{E_1})\kappa \dot{k}_E - j_{E_1S}}{\kappa + \kappa \mu_{E_2}/\mu_{E_1} + \mu_{E_1}/y_{VE_1}}$. Growth is zero if $m_{E_1} + m_{E_2}\mu_{E_2}/\mu_{E_1} = j_{E_1}^S/(\dot{k}_E \kappa)$, which implies lower boundaries of reserve densities m_{E_i}, below which shrinking occurs because not somatic maintenance can be covered. Maximum size occurs when growth is zero, i.e. $L_\infty = \frac{\kappa \dot{v} \sum_i \mu_{E_i} m_{E_i}}{\mu_{E_1} j_{E_1S}}$, like in mode 2, since $\mu_{E_1} j_{E_1S} = \mu_{E_2} j_{E_2S}$.

mode 4 The final situation is that the mobilized reserves can cover only part of the somatic maintenance costs, and the remaining part has to be covered from shrinking of structure. No nett growth occurs in this situation. We assume that structure first needs to be back-converted to reserve 1, before paying the remaining maintenance costs, and the reproduction buffer does not contribute. The reserves contribute to somatic maintenance with $\sum_i \mu_{E_i} j_{E_iC}$, while $\mu_{E_1} j_{E_1S}$ needs to be payed. Thus shrinking structure has to contribute $j_V^S = -\dot{r} = (\mu_{E_1} j_{E_1S} - \sum_i \mu_{E_i}(m_{E_i}\dot{k}_E - \dot{r}))/(\kappa_G \mu_V)$. The implied specific growth rate is $\dot{r} = -\frac{\mu_{E_1} j_{E_1S} - \sum_i \mu_{E_i} m_{E_i} \dot{k}_E}{\mu_V \kappa_G + \sum_i \mu_{E_i}}$. The mobilization fluxes are $j_{E_iC} = m_{E_i}(\dot{k}_E - \dot{r})$ and the allocation to somatic maintenance $j_{E_i}^S = \kappa j_{E_iC}$.

The state at birth follows from the maternal effect, which specifies that m_{E_i} at birth equals that of the mother at egg formation. The initial amounts of reserve must be obtained by a shooting method. Starting values can be based on the assumptions that all somatic maintenance and growth overheads are paid from reserve 2, embryo development follows the foetal pattern, so no retardation of growth, $\dot{r} = \dot{k}_E$ and $L(t) = \dot{v}t/3$, and maturity density does not change too much, $[E_H] = \frac{1-\kappa}{\kappa} \frac{\mu_V [M_V]}{\kappa_G}$, which gives $L_b^3 = \frac{\kappa}{1-\kappa} \frac{\kappa_G E_H^b}{\mu_V [M_V]}$, while $a_b = 3L_b/\dot{v}$. Structural mass at birth is $M_V^b = [M_V] L_b^3$ and required $M_{E_1}^G = [M_V] L_b^3 \mu_V/\mu_{E_1}$ moles of reserve 1 plus $M_{E_2}^G = \frac{1-\kappa_G}{\kappa_G} \frac{\mu_V}{\mu_{E_2}} [M_V] L_b^3$ moles of reserve 2 to make it. The maintenance of this structure during the embryo stage required $M_{E_1}^M = 0$ and $M_{E_2}^M = j_{E_2M}[M_V] \int_0^{a_b} L(t)^3 \, dt = j_{E_2M}[M_V] \frac{3}{4} \frac{L_b^4}{\dot{v}}$ moles of reserve 2. The reserves at birth are $M_{E_i}^b = m_{E_i}[M_V] L_b^3$, so a first guess for the initial amounts of reserve is $M_{E_i}^0 = M_{E_i}^b + (M_{E_i}^M + M_{E_i}^G)/\kappa$.

The shooting method requires the evaluation of reserve and structure during the embryo period. We might use the above-mentioned integration method with $y_{VE_1} = \frac{\mu_{E_1}}{\mu_V}$ and $y_{VE_2} = \frac{\kappa_G}{1-\kappa_G} \frac{\mu_{E_2}}{\mu_V}$.

5.2.7 Reduction of iso_221 to iso_111

To demonstrate that the iso_221 model can reduce to the iso_111 model, so the standard DEB model, we first focus on substrate uptake. It is easiest to assume that $\{\dot{J}_{YAm}\} = 0$ and $\{\dot{F}_{Ym}\} = 0$. Alternatively, we could also take X equal to Y in all respects (abundance, composition, yield coefficients, etc), but then we still have two substrate uptake routes, where we must assume that the sum of these uptakes equals the uptake of a single substrate and we have to account for this factor 2. So, for simplicity's sake, we don't do that. The consequence is that $\{\dot{J}^Y_{E_iAm}\} = 0$ and $m^Y_{E_im} = 0$, and $m_{E_im} = m^X_{E_im}$. The consequence of $\{\dot{F}_{Ym}\} = 0$ is that $\dot{b}_Y = 0$ and $\{\dot{b}_{YX}\} = 0$. Further, we take $M_Y = M_X$ and $y_{E_iY} = y_{E_iX}$, with the consequence that $\rho_{XY} = 0$ and $\{\dot{b}_{XY}\} = 0$ and $\{\dot{b}_{YX}\} = 0$. The next step is to take $\{\dot{h}_{YAm}\} = 0$, so $\{\dot{J}_{YAm}\} = 0$ and $\{\dot{J}^Y_{E_iAm}\} = 0$ and $\{\dot{J}_{E_iA}\} = f_X\{\dot{J}_{E_iAm}\} = f_X y_{E_iX}\{\dot{J}_{XAm}\}$. We now have $\alpha_X = \{\dot{h}_{XAm}\} + \{\dot{F}_{Xm}\}X$, $\alpha_Y = 0$, $\beta_X = \{\dot{F}_{Xm}\}X$, $\beta_Y = 0$, $f_X = \frac{\{\dot{F}_{Xm}\}X}{\{\dot{h}_{XAm}\}+\{\dot{F}_{Xm}\}X}$, $f_Y = 0$. The half-saturation coefficient is $K = \{\dot{h}_{XAm}\}/\{\dot{F}_{Xm}\}$ and $f_X = \frac{X}{K+X}$ We now reduced the uptake of 2 substrates to a single one.

Likewise we now omit reserve 2, by setting $y_{E_2X} = 0$ and $y_{VE_2} = 0$, with the consequence that $m_{E_2} = 0$ and $j_{E_2C} = 0$, and avoid excretion of rejected reserve 1 by setting $\kappa_{E_1} = 1$, κ_{E_2} becoming irrelevant. Alternatively, it is again possible to make both reserves identical, but again we have to deal with 2 mobilization fluxes, which we now avoid. The reserve dynamics reduces to $\frac{d}{dt}m_{E_1} = j_{E_1A} - j_{E_1C} + j_{E_1P} - \dot{r}m_{E_1}$. The implicit equation for the specific growth rate reduces to $j_{VG} = \dot{r} + j^S_V = \frac{j_{E_1G}}{y_{E_1V}} = y_{VE_1}j_{E_1G}$ and the growth efficiency to $\kappa_G = \frac{\mu_V}{\mu_{E_1}y_{VE_1}}$.

The maintenance flux follows from setting $\rho_1 = 1$, while $B = C = 0$, which reduces the somatic maintenance to $j^S_{E_1} = \min(\kappa j_{E_1C}, j_{E_1S})$ and $j^S_{E_1} = 0$.

5.3 Several structural masses

5.3.1 Growth of body parts

The growth of body parts directly follows from the extended κ-rule:

$$\begin{aligned}
[\dot{p}_C] &= \frac{g[E]}{g + [E]/[E_m]}(\dot{v}/L + \dot{k}_M(1 + L_T/L) \equiv \dot{k}_C[E_G]/\kappa \quad \text{from (2.12)} \\
\frac{d}{dt}V_H &= \frac{\kappa\kappa_H}{[E_{GH}]}\dot{p}_C - \frac{[\dot{p}_M]}{[E_{GH}]}V_H \quad \text{from (5.24)} \\
&= e_H\kappa_H\dot{k}_C - \dot{k}_{MH}V_H \\
\frac{d}{dt}V_R &= \frac{\kappa(1-\kappa_H)}{[E_G]}\dot{p}_C - \frac{[\dot{p}_M]}{[E_G]}V_R(1 + L_T/L_R) \quad \text{from (eqn:dVR)} \\
&= (1-\kappa_H)\dot{k}_C V_R - \dot{k}_M V_R(1 + L_T/L_R)
\end{aligned}$$

6

Effects of compounds on budgets

6.1 Gompertz stress

The ageing module of DEB theory has two components: the induction of damage inducing compounds by ROS derived from atmospheric dioxygen and the self-induction of these compounds. ROS production by affected mitochondria play an important role in the latter process. See Figure 6.1. The first route hardly depends on feeding level, because the enhanced respiration is approximately balanced by an increase dilution by growth. The second route depends on food level rather strongly because it is proportional to the mobilisation rate (metabolic activity). The importance of the second route is quantified by the Gompertz stress coefficient.

6.1.1 Mean age for short growth periods

Suppose that growth period is small relative to the life span. Eq (6.3) was obtained from Eq (6.2) by taking $\dot{r} = 0$ and setting $L = f * L_m = L_\infty$. The expression for $\dot{h}_W$, where a factor 6 was introduced, was motivated by the result in the second equation of Eq (6.3): the Weibull aging model is widely known and the term 'Weibull aging rate' was introduced to celebrate this milestone. The Gompertz aging model is also widely known; the term 'Gompertz aging rate' $\dot{h}_G$ was introduced as a natural counter-player of the Weibull aging rate. As far as I know, this is the first time where both well-known aging models appear as two sides of the same medallion: these models are not really different.

The mean age at death, as far as ageing is concerned, is $\mathcal{E}\underline{a}_\dagger = \int_0^\infty \Pr\{\underline{a}_\dagger > t\}\, dt$ with $\Pr\{\underline{a}_\dagger > t\}$ given in (6.5). The result must be obtained numerically, but a straightforward integration results in numerical instabilities. For $x = a\dot{h}_W$ and $h_G = \dot{h}_G/\dot{h}_W$,

$$\begin{aligned}
\mathcal{E}\underline{a}_\dagger &= \int_0^\infty \Pr\{\underline{a}_\dagger > a\}\, da \overset{\dot{h}_G \downarrow 0}{=} \int_0^\infty \exp\left(-(\dot{h}_W a)^3\right) da = \frac{\int_0^\infty \exp(-x^3)\, dx}{\dot{h}_W} = \frac{\Gamma(\frac{4}{3})}{\dot{h}_W} \\
&= \int_0^{a_m} \Pr\{\underline{a}_\dagger > a\}\, da + \int_{a_m}^\infty \Pr\{\underline{a}_\dagger > a\}\, da = \int_0^{a_m} \Pr\{\underline{a}_\dagger > a\}\, da + a_{\text{tail}} \\
&= \int_0^{a_m} \exp\left(\left(1 + \dot{h}_G a + \frac{\dot{h}_G^2 a^2}{2} - \exp(\dot{h}_G a)\right) \frac{6}{h_G}\right) da + a_{\text{tail}}
\end{aligned}$$

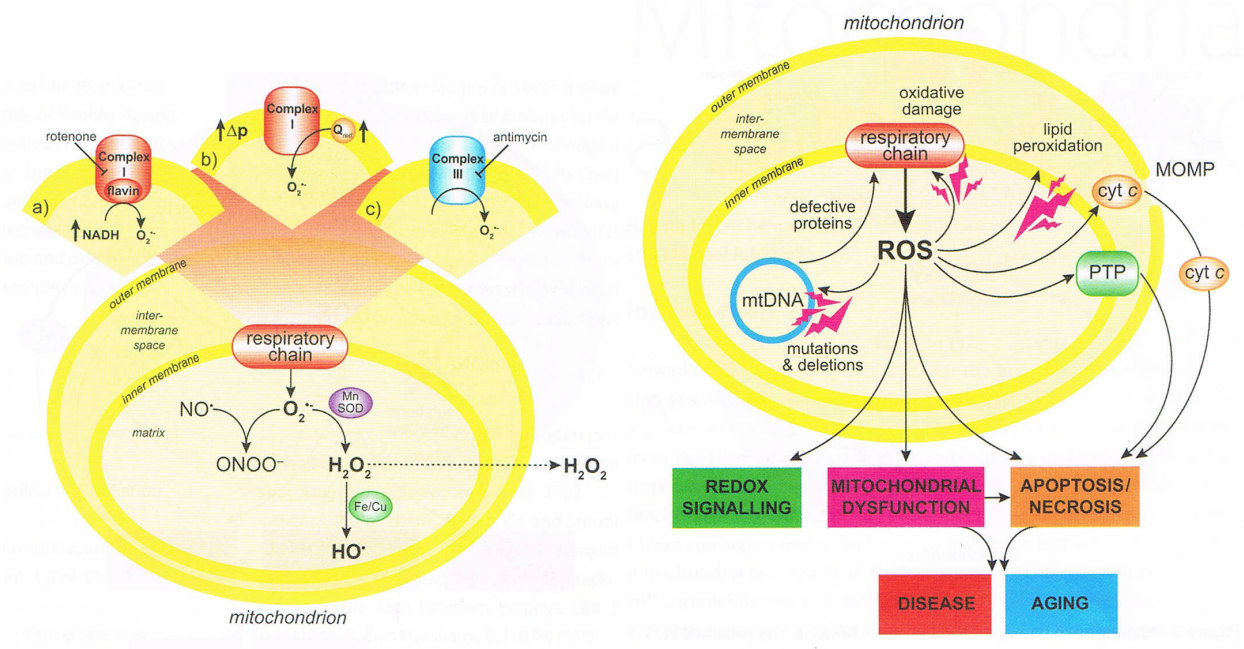

Figure 6.1: The proximal ROS produced by mitochondria is superoxide ($O_2^{\cdot-}$, left). Its production from the respiratory chain can be induced (a) from Complex I by adding the inhibitor rotenone in the presence of NADH, (b) under high $\Delta\rho$ and reduced coenzyme Q pool (Qred) that together favour reverse electron transport, (c) from Complex III by inhibitor antimycin. The less-damaging superoxide is rapidly converted into (1) less-damaging hydrogen peroxide by SOD-catalysed dismutation, which can form very damaging hydroxyl radical ($HO^{\cdot}$) (2) damaging peroxynitrite ($ONOO^{\cdot}$) by reacting with nitric oxide ($NO^{\cdot}$). Mitochondrial ROS can lead to oxidative damage to mitochondrial proteins, membranes and mtDNA (right). This leads to reduced activity of the TCA and urea cycles, fatty acid oxydation, amino acid and haem synthesis, iron-sufur-centre assembly. The outer and inner membranes of affected mitochondria become more permeable; the leak of cytochrome c to the cytosol via the outer membrane permeabilisation (MOMP) activates apoptosis. The increased permeability of transition pores (PTP) for small molecules leads to ischaemia/reperfusion injury. From [264].

$$
\begin{aligned}
&= \int_0^{a_m} \exp\left(-6\frac{\dot{h}_W^3}{\dot{h}_G^3}\sum_{i=3}^{\infty}\frac{(\dot{h}_G a)^i}{i!}\right) da + a_{\text{tail}} \\
&= \frac{1}{\dot{h}_W}\int_0^{a_m \dot{h}_W} \exp\left(-x^3\left(1+\frac{h_G x}{4}+\frac{h_G x}{4}\frac{h_G x}{5}+\frac{h_G x}{4}\frac{h_G x}{5}\frac{h_G x}{6}+\cdots\right)\right) dx + a_{\text{tail}}
\end{aligned}
$$

where age a_m is such that the rest term a_{tail} is small. For $\dot{h}_G < 0$, the expression with the series should not be used, but the standard formulation (6.5) does then give no problems.

For $\dot{h}_G > 0$ we require that $\exp(\dot{h}_G a_m) \gg 1 + \dot{h}_G a_m + \dot{h}_G^2 a_m^2$. For $\dot{h}_G a_m = 10$ is condition is satisfied. The rest term can be approximated by

$$
a_{\text{tail}} \simeq \int_{a_m}^{\infty} \exp\left(-6\frac{\dot{h}_W^3}{\dot{h}_G^3}\exp(\dot{h}_G a)\right) da = \frac{E_1\left(6\frac{\dot{h}_W^3}{\dot{h}_G^3}\exp(\dot{h}_G a_m)\right)}{\dot{h}_G}
$$

where the exponential integral is defined as $E_1(x) = \int_x^{\infty}\frac{\exp(-t)}{t}\,dt \simeq \frac{\exp(-x)}{x}\sum_{n=0}^{N-1}\frac{n!}{(-x)^n}$; it

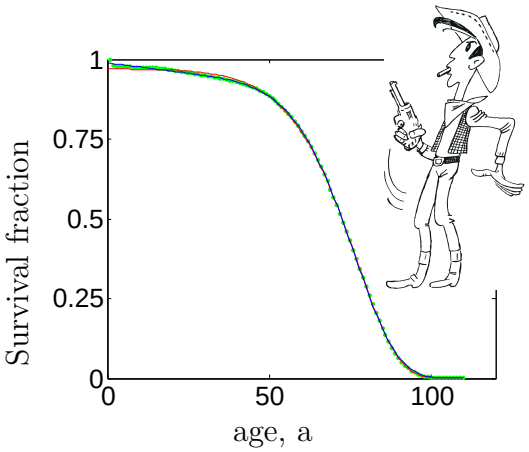

Figure 6.2: The Weibull model $S(t) = q\exp(-\dot{h}t - (\dot{h}_W t)^\beta)$ (blue), and the corresponding DEB model (6.5) (red) are fitted to the survival data from Elandt-Johnson and Johnson [383] for white USA males in the period 1969-1971. The data don't deviate from the Weibull model, which has probably been used to generate the data. Yet the DEB model also fits the data very well, despite the fact that the shape parameter deviates from 3. Parameter values Weibull model: $q = 0.989$, $\dot{h} = 0.0013\,\mathrm{a}^{-1}$, $\dot{h}_W = 0.01275\,\mathrm{a}^{-1}$, $\beta = 6.812$. Parameter values DEB model: $q = 0.980$, $\dot{h} = 0.3302\,\mathrm{a}^{-1}$, $\dot{h}_W = 0.00539\,\mathrm{a}^{-1}$, $\dot{h}_G = 0.0824\,\mathrm{a}^{-1}$.

is built in Matlab as expint.

For $\dot{h}_G < 0$ we require that $-\dot{h}_G a_m \gg 2$, the rest term can be approximated by

$$a_{\text{tail}} \simeq \int_{a_m}^{\infty} \exp\left(3\frac{\dot{h}_W^3}{\dot{h}_G^3}(\dot{h}_G a)^2\right) da = \frac{\operatorname{erfc}\left(\dot{h}_W a_m \sqrt{\frac{3\dot{h}_W}{-\dot{h}_G}}\right)}{2\dot{h}_W \sqrt{\frac{3\dot{h}_W}{-\pi\dot{h}_G}}}$$

the complementary error function is defined as $\operatorname{erfc}(x) = \frac{2}{\sqrt{\pi}} \int_x^\infty \exp(-t^2)\, dt$.

Let the median age a_{50} be such that $\Pr\{\underline{a}_\dagger > a_{50}\} = \frac{1}{2}$. As a rule of thump we have $\mathcal{E}\underline{a}_\dagger < a_{50}$ for $s_G \geq 0$ and $\mathcal{E}\underline{a}_\dagger > a_{50}$ for s_G sufficiently less than 0. For $s_G = 0$, we have $a_{50} = \frac{(\log(2))^{1/3}}{\dot{h}_W} = \frac{0.885}{\dot{h}_W}$ and $\mathcal{E}\underline{a}_\dagger = \frac{\Gamma(\frac{4}{3})}{\dot{h}_W} = \frac{0.893}{\dot{h}_W}$.

For numerical purposes it makes sense to scale variables, using scaled time $\tau = \dot{k}_M t$, see Eq (2.26-28), and section 2.9 of the comments. Scaled specific growth amounts, from (2.21), to $r = \frac{\dot{r}}{\dot{k}_M} = \frac{e/l - 1 - l_T/l}{\kappa_G + e/g}$, with $\kappa_G = 1$ if $r \geq 0$. Changes in scaled acceleration and hazard become $\frac{d}{d\tau}q = e(ql^3 s_G + h_a)(g/l - r) - rq$ and $\frac{d}{d\tau}h = q - rh$. This set works well after birth, but at the start of development r and e are infinitely large and is it easier to work with $u_E = el^3/g$, since $u_E(0) = u_E^0$ giving $\frac{d}{d\tau}q = gu_E(qs_G + h_a/l^3)(g/l - r) - rq$. We have $q(0) = 0$, $\frac{d}{d\tau}q(0) = 0$, since $\lim_{t\downarrow 0} r \to g/l$, and $h(0) = 0$, $\frac{d}{d\tau}h(0) = 0$

6.1.1 Empirical Weibull curves

Figure 6.2 shows survival data of white USA males, as presented in [383], and the fitted empirical Weibull model as well as the DEB model. The data seems too smooth to be real observations, and they were probably generated with the Weibull model. This has been the reason not to include them in the book any longer. I still show it here to demonstrate that the DEB model can be very similar to the general Weibull model, even when the shape coefficient is much higher than 3. We can conclude that the DEB model can span the full range of shapes of survival curves for the general Weibull and Gompertz models, but also shows how aging is linked to nutrition.

6.2 Temperature stress

Metabolic rates, including the ageing process, depend on temperature. The 1-parameter Arrhenius model let the rate increase with temperature (in a particular way), while the 5-parameter Arrhenius model let the rate decrease outside the temperature tolerance range, linked to how far the temperature is beyond the temperature boundaries.

Apart from this effect of temperature on metabolic rates, temperature can also have a lethal effect outside the temperature tolerance range, which can be called temperature stress. Although this range for temperature stress does not need to coincide with that for effects on rates, for simplicity's sake we here assume it does. The modeling strategy is the same as for effects of toxicants: the stress increases proportional to the difference of (absolute) temperature with the temperature boundaries, while the target parameter is the hazard rate. So the hazard rate associated with temperature stress amounts to $\dot{h}_T = \dot{h}_{TL}(1 - T/T_L)$ for $T < T_L$, $\dot{h}_T = 0$ for $T_L < T < T_H$ and $\dot{h}_T = \dot{h}_{TH}(T/T_H - 1)$ for $T > T_H$. The idea behind this approach is the same as for toxicants: only small stress levels have biological significance and, therefore, we can locally linearize using a Taylor argument. If there is no low or high temperature stress, or there is no need to model it, we have $\dot{h}_{TL} = 0$ or $\dot{h}_{TH} = 0$.

Assuming that the temperature stress, ageing and other causes of death (such as accidental death, or effects of toxicants) are all independent, we can add the associated hazards, so for the first two causes we have $\dot{h}(a) = \dot{h}_a(a) + \dot{h}_T$. The survival probability as function of age a is, as usual, $S(a) = \int_0^a \exp(-\dot{h}(t)t)\,dt$ and the mean age at death is $\int_0^\infty S(a)\,da$.

6.2 Toxins and toxicants

The Amazonian climber *Strychnos* produces spherical seeds with a hard shell and tasty flesh. The easy-to-damage soft skin of its seed is, however, loaded with deadly strychnine. *Ateles* monkeys learned to eat these seeds by removing the hard shell and swallow the fruit in one piece. Their digestive system digests the fruit flesh, but leaves the poisonous skin of the seed untouched; when defecating simultaneously in the early morning as a group, scarab beetles fly in and bury the faeces with the seeds. This not only provides the seeds with good growth conditions, but also protects them. A beautiful example of co-evolution.

The maned rat, *Lophiomys imhausi*, chews on the toxic bark of the apocynacean *Acokanthera schimperi* to extract acovenoside A and ouabaïne and smear his long hairs on the back with these poisons for protection against predators.

6.4 Energetics affects toxicokinetics

6.4.2 Derivation of (6.28)

We start from the simple one-compartment model (6.9), but first write it in changes of the number of molecules in the compartment: import to the compartment is proportional to the concentration in the water c_d and export from the compartment proportional to the

number of molecules in the compartment M_Q

$$\frac{d}{dt}M_Q = \dot{\alpha}^* c_d - \dot{\beta}^* M_Q$$

where $\dot{\alpha}^*$ and $\dot{\beta}^*$ are parameters. The one-compartment model rests on advective-diffusive transport, with a leading role for concentrations (moles per volume) in homogeneous space (applies to environment and compartment).

Now we make explicit how this kinetics depends on the size of the compartment. We consider a compartment of length L and compare compartments of different lengths, but of the same shape, for instance a sphere. Import is proportional to the surface area of the compartment, because transport in 3 dimensions is across 2 dimensions. So we substitute $\dot{\alpha}^* = \dot{\alpha} L^2$, for some parameter value $\dot{\alpha}$. The molecules are homogeneously distributed in the compartment, but only those very near to the outer surface can leave the compartment in a short period. They represent a fraction of the molecules in the compartment that is proportional to the ratio of the surface area and the volume, so inversely proportional to the length of the compartment. Think, for instance, of a sphere again. If the length L represents the radius, it has surface area $4\pi L^2$ and volume $\frac{4}{3}\pi L^3$, so the surface area-volume ratio is $3/L$. This ratio is thus inversely proportional to L. So we substitute $\dot{\beta}^* = \dot{\beta}/L$, for some parameter value $\dot{\beta}$.

Let us consider the dimensions: $\dim(\frac{d}{dt}M_Q) = \dim(\dot{\alpha}L^2 c_d) = \dim(M_Q\dot{\beta}/L) = \#\,\mathrm{time}^{-1}$, where # stands for number of molecules in the compartment. So, given $\dim(M_Q) = \#$, $\dim(L) = \mathrm{length}$, $\dim(\dot{\beta}) = \mathrm{length}\,\mathrm{time}^{-1}$. This means that we can write $\dot{\beta} = L_{\mathrm{ref}}\dot{k}_e$, where $\dim(L_{\mathrm{ref}}) = \mathrm{length}$ and $\dim(\dot{k}_e) = \mathrm{time}^{-1}$. We have this freedom because $\dot{\beta}$, L_{ref} and $\dot{k}_e$ are all numbers and we can choose $\dot{k}_e$ always such that the substitution is valid for any given L_{ref}. Likewise, given $\dim(c_d) = \#\,(\mathrm{length\ of\ environment})^{-3}$, $\dim(\dot{\alpha}) = (\mathrm{length\ of\ environment})^3\mathrm{length}^{-2}\,\mathrm{time}^{-1}$ and we can write $\dot{\alpha} = \dot{k}_e P^*_{Vd} L_{\mathrm{ref}}$, with $\dim(P^*_{Vd}) = (\mathrm{length\ of\ environment})^3\mathrm{length}^{-3}$. We have this freedom because $\dot{\alpha}$ and P^*_{Vd} are numbers and we can choose P^*_{Vd} always such that the substitution is valid for any given L_{ref} and $\dot{k}_e$. So we now arrive at

$$\begin{aligned}
\frac{d}{dt}M_Q &= c_d\dot{\alpha}^* - M_Q\dot{\beta}^* \\
&= c_d L^2\dot{\alpha} - M_Q\dot{\beta}/L \\
&= c_d L^2\dot{k}_e P^*_{Vd} L_{\mathrm{ref}} - M_Q\dot{k}_e L_{\mathrm{ref}}/L \\
&= (c_d L^3 P^*_{Vd} - M_Q)\dot{k}_e L_{\mathrm{ref}}/L \\
\frac{d}{dt}[M_Q] &= (c_d P^*_{Vd} - [M_Q])\dot{k}_e/l
\end{aligned}$$

for $[M_Q] = M_Q/L^3$ and $l = L/L_m$ and $L_{\mathrm{ref}} = L_m$. We are free to select a reference length and selecting the maximum structural length of an animal is one of the possibilities. The parameter $\dot{k}_e$ has the interpretation of an elimination rate for a compartment of length L_{ref}; it controls the rate at which the concentration in the compartment follows the concentration in the environment (which might change in time). L_{ref} just serves as a reference value for $\dot{k}_e$ and does not need to have the interpretation of a maximum structural length of an

animal. We see that P^*_{Vd} has the interpretation of a bioconcentration coefficient, since $P^*_{Vd} = [M^*_Q]/c_d$, where $[M^*_Q]$ is the value of $[M_Q]$ at equilibrium. After this observation, we can drop $*$ and substitute P_{Vd} for P^*_{Vd}.

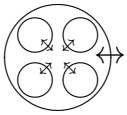

Let us now partition the compartment into reserve E and structure V, such that reserve represents blobs in a matrix of structure and compound Q freely travels between E (the collection of blobs) and V (the matrix), but the compartment exchanges Q with the environment via V, not E. The mass of Q is thus partitioned as $M_Q = M_{QV} + M_{QE}$, the volume of the compartment as $V_W = V + V_E$ with $V = L^3$. (The latter equality specifies how we choose our length-measure.) Structure has mass M_V, reserve M_E. (I avoid introducing the mass of the whole compartment, because V and E might differ in chemical composition and M's are quantified as C-moles. Moles of different compounds cannot be added in a meaningful way; their weights can.)

Transport of Q from V to E is proportional to $[M_{QV}] = M_{QV}/V$, that from E to V proportional to $M_{QE}/V_E = c_E$. Let us ignore, for a while, the transport of Q between V and the environment, so $\frac{d}{dt}M_Q = 0$ and

$$\frac{d}{dt}[M_{QV}] = (c_E P^*_{VE} - [M_{QV}])\dot{k}^*_e/l$$

where P^*_{VE} is the partition coefficient between reserve and structure on the basis of volume. Notice the similarity with $\frac{d}{dt}[M_Q]$, which we already derived; reserve now plays the role of environment and structure the role of the compartment. We just nested the same reasoning. Suppose now that $\dot{k}^*_e \gg \dot{k}_e$, so that the distribution of Q over V and E is in pseudo-equilibrium with $[M^*_{QV}] = c_E P^*_{VE}$. This leads for $M_{QE} = M_Q - M_{QV}$ to $M_Q = M_{QV}(1 + P^*_{EV}[V_E])$. We now convert the partition coefficient P^*_{EV} on the basis of volumes to the partition coefficient P_{EV} on the basis of C-moles, to avoid dealing with the variable $[V_E]$:

$$P^*_{EV} = \frac{\frac{\text{mol } Q \text{ in } E}{V_E}}{\frac{\text{mol } Q \text{ in } V}{V}} = \frac{\frac{\text{mol } Q \text{ in } E}{M_E}}{\frac{\text{mol } Q \text{ in } V}{M_V}} \frac{V}{V_E}\frac{M_E}{M_V} = P_{EV}\frac{1}{[V_E]}\frac{[M_E]}{[M_V]} = \frac{P_{EV}}{[V_E]}\frac{e[M_{Em}]}{[M_V]}$$

(Using P_{Vd} and P_{EV}, while their dimensions differ, is an abuse of DEB notation. The motivation is that their interpretations as partition coefficients are very related and we need to keep the number of symbols to a minimum.) Substitution of the result gives $M_Q = M_{QV}\left(1 + e\frac{[M_{Em}]}{[M_V]}P_{EV}\right) = M_{QV}P_{WV}$ or $M_{QV} = M_Q P_{VW}$. This should be read as a definition of P_{WV} and the observation that $P_{VW} = 1/P_{WV}$. Extension of the scaled reserve density e with a possible reproduction buffer e_R gives (6.27). The next step is to replace $[M_Q]$ in the right-hand side of $\frac{d}{dt}[M_Q]$ by $[M_{QV}]$ and arrive at

$$\frac{d}{dt}[M_Q] = (c_d P_{Vd} - [M_Q]P_{VW})\dot{k}_e/l$$

If the volume of the compartment is changing, we need to account for dilution by growth:

$$\frac{d}{dt}[M_Q] = (c_d P_{Vd} - [M_Q]P_{VW})\dot{k}_e/l - [M_Q]\dot{r}$$

with specific growth rate $\dot{r} = \frac{d}{dt} \ln l^3$. The last step to arrive at (6.28) is to account for uptake via food. Since food uptake is proportional to surface area as well, we can substitute $c_d + f c_X$ for c_d.

6.5 Toxicants affect energetics

6.5.2 Hormesis

Two additional routes to hormesis have been found in the context of DEB theory in terms of changes of parameter values. An small increase in costs for structure, $[E_G]$, can substantially increase the reproduction rate, see [774], and this small change in costs can be difficult to detect directly. A second route is a decrease in the specific somatic maintenance, $[\dot{p}_M]$, in species that sport metabolic acceleration, see [777]. The route of decreasing somatic maintenance is more likely in cases where specific somatic maintenance is high. Species that waste a lot, i.e. have a high value for $[\dot{p}_M]$, were found to have a small NEC, so are sensitive to toxicants, see [59] and Section 8.2.1 of the comments. Such species are popular for use in toxicity experiments, since their fast growth and reproductions combines well with economic reasons for keeping experiments as short as possible. No wonder that hormesis is frequently found in practical toxicity testing.

6.5.4 Direct effect on reproduction

Chlorpyrifos reduces reproduction (and survival) in the springtail *Folsomia candida*, without affecting growth [658] at low concentrations. See Figure 6.3; the highest tested concentration was $20\,\mathrm{mg\,kg^{-1}_{food}}$. Effects on growth, without effects on reproduction would be much more difficult to understand in the context of DEB theory, since size is coupled to assimilation.

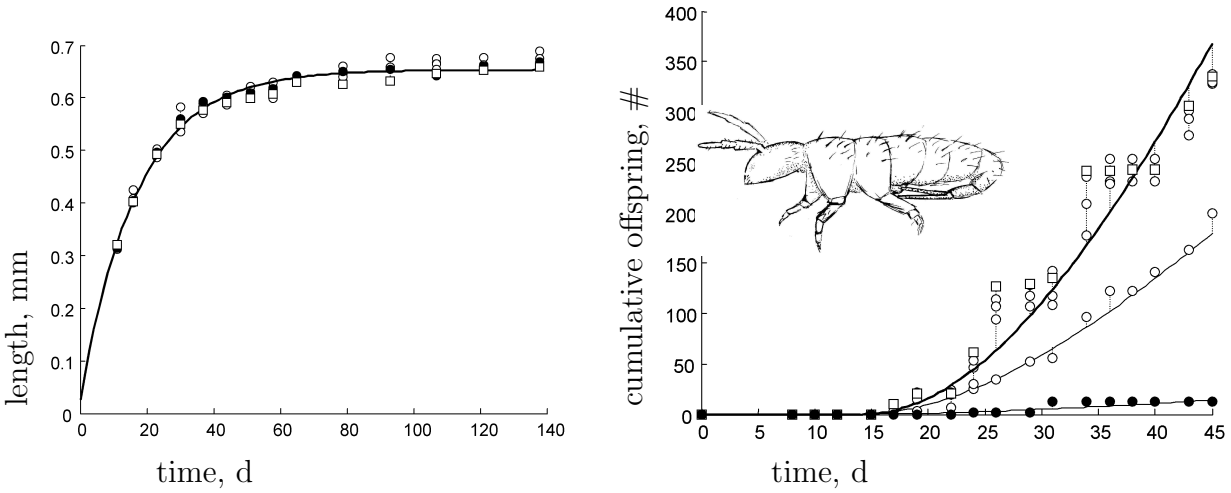

Figure 6.3: Effect of chlorpyrifos on *Folsomia candida*, from Jager et al. [658]. Parameters $\dot{r}_B = 0.058\,\mathrm{d}^{-1}$, $L_m = 0.653\,\mathrm{mm}$, $L_p = 0.418\,\mathrm{mm}$, $\dot{R}_m = 26.2\,\mathrm{eggs/d}$, $\dot{k}_e = 10\,\mathrm{d}^{-1}$, $c_{0R} = 0.0107$ -, $c_R = 6.77\,10^{-3}$ -, $\dot{b}_{fn} = 1.21\,10^{-3}\,\mathrm{mg\,kg}_{\mathrm{food}}^{-1}\mathrm{d}^{-1}$ $\dot{r}_{nf} = 0.672\,\mathrm{d}^{-1}$

7

Extensions of DEB models

7.2 Feeding

7.2.2 Food or nutrient intake after starvation

The Morel [994] model is in DEB notation

$$j_{XA}(X, m_E) = f\left(j^h_{XAm} - (j^h_{XAm}/j^l_{XAm} - 1)m_E\dot{k}_E/y_{EX}\right) \quad \text{with} \quad f = \frac{X}{K+X} \tag{7.1}$$

$$\frac{d}{dt}m_E = y_{EX}fj^h_{XAm} - (1 - f + fj^h_{XAm}/j^l_{XAm})m_E\dot{k}_E \tag{7.2}$$

$$m^*_E = \frac{y_{EX}fj^h_{XAm}/\dot{k}_E}{1 - f(1 - j^h_{XAm}/j^l_{XAm})} = \frac{Xy_{EX}j^l_{XAm}/\dot{k}_E}{X + Kj^l_{XAm}/j^h_{XAm}} \tag{7.3}$$

The maximum reserve density is $m_{Em} = y_{EX}j^l_{XAm}/\dot{k}_E$. If nutrients are just internalized, rather than transformed, we typically have $y_{EX} = 1$. For $j^h_{XAm} \to j^l_{XAm}$, the standard food intake is recovered. A change in assimilation does not affect the way how growth depends on reserve (density), so $\dot{r} = \frac{m_E\dot{k}_E - j_{EM}/\kappa}{m_E + y_{EV}/\kappa}$. This extension of Droop's model is not consistent with DEB theory. Therefore, it was slightly modified in the DEB book.

Andersen [29] proposed the algal growth model

$$v = v_i - v_e = \alpha'\frac{Q' - Q}{Q'' - Q'}(S - S')$$

$$\frac{\mu}{\mu'} = 1 - \frac{Q'}{Q} \quad \text{and} \quad \frac{\mu''}{\mu'} = 1 - \frac{Q'}{Q''} \quad \text{and} \quad \frac{d}{dt}Q = v - \mu Q$$

where the symbols are given in Table 7.1. Nutrients not only enter cells but also leave cells at rate v_e; this leak is not further specified, but serves to motivate the existence of the parameter S'. He mentions the problem this model gives for low S and high Q, which he 'solves' by taking $\max(0, \mu)$ for growth and neglecting the effect of leaking nutrients on S in these situations.

Like Droop, he considers simple nutrients (such as phosphate and nitrate) and follows in fact chemical elements, neglecting any overheads. In DEB terms this means that $y_{EX} = 1$,

Table 7.1: Symbols of the model by Anderson [29] and the DEB equivalents

v	j_{XA}	nutrient uptake	S	X	nutrient concentration
v_e	$y_{XE}\, j_{EM}/\kappa$	maintenance losses	S'		nutrient conc at $v = 0$
α'	$\dot{F}_m/M_V$	affinity			
Q	$m_E + y_{EV}$	cell quota	μ	$\dot{r}$	specific growth rate
Q'	y_{EV}	subsistence quota	μ'	$\dot{k}_E$	μ at $Q = \infty$
Q''	$m_{Em} + y_{EV}$	max cell quota	μ''	$\dot{r}_m$	μ at $Q = Q''$

$\kappa = 1$ and $y_{VE} = 1/n_{EV}$ where X and E now stand for some chemical element. Table 7.1 gives the link with DEB theory, where m_{Em} and $\dot{r}_m$ now only mean the maximum of m_E and $\dot{r}$, and the expressions found for them no longer apply. The interpretation that v_e relates to maintenance losses is mine; Andersen thought about an analogy with one-compartment kinetics. I will here avoid problems with negative uptake and growth rates assuming that $v_e = 0$ and $S' = 0$ and $\kappa = 1$.

The model in DEB notation reads for $j_{EM} = 0$ and $\dot{f}_m = \dot{F}_m/M_V$

$$\begin{aligned} j_{XA}(X, m_E) &= \dot{f}_m(1 - m_E/m_{Em})X \\ \frac{d}{dt}m_E &= y_{EX}j_{XA} - \dot{k}_E m_E \quad \text{and} \quad \dot{r} = \frac{\dot{k}_E}{1 + y_{EV}/m_E} \end{aligned}$$

where m_{Em} is a parameter, like $\dot{f}_m$, $\dot{k}_E$ and y_{EV}. We also have $\dot{r}_m = \frac{\dot{k}_E}{1+y_{EV}/m_{Em}}$.

At steady state we must have for $y_{XE} = 1/y_{EX}$

$$y_{EX}\dot{f}_m(1 - m_E^*/m_{Em})X = \dot{k}_E m_E^* \quad \text{or} \quad m_E^* = \left(m_{Em}^{-1} + y_{XE}\dot{k}_E(\dot{f}_m X)^{-1}\right)^{-1}$$

The specific nutrient uptake at constant X amounts for $j_{EAm} = y_{EX}j_{XAm}$ to

$$j_{XA}^*(X) = \left((m_{Em}y_{XE}\dot{k}_E)^{-1} + (\dot{f}_m X)^{-1}\right)^{-1} \quad \text{so} \quad m_{Em} = j_{EAm}/\dot{k}_E$$

where j_{XAm} is the maximum of j_{XA}^* as function of X. To avoid the use of m_{Em}, we can also write

$$j_{XA}(X, m_E) = (\dot{f}_m - y_{XE}m_E\dot{k}_E/K)X$$

for half-saturation constant $K = j_{XAm}/\dot{f}_m$.

The parameters are $\dot{f}_m$, j_{XAm}, $\dot{k}_E$, y_{EV} and $y_{EX} = 1$; I still include the latter parameter for dimensional purposes. The relationship $j_{XA}^*(S') = j_{XM}$, or $j_{XM}^{-1} = j_{XAm}^{-1} + (\dot{f}_m S')^{-1}$, gives perhaps the best map of Andersen's parameter S' to DEB concepts, but this map is not free of problems. (Notice that $j_{XM} = j_{EM}y_{XE}$.)

In summary, Andersen's model only deviates from the DEB model for V1-morphs in the uptake rate (which depends on reserve in his model) and in the way maintenance is implemented (by subtracting the costs from assimilation, and avoiding the inherent problems); his reserve dynamics is identical to (4.13) and his growth dynamics to (4.14). His focus on simple nutrients makes that $y_{EX} = 1$ (nutrients are internalised, not transformed) and no growth overhead costs are paid and, as consequence, no nutrients are released to the environment in association with growth. As a consequence Anderson's model inherits most of the nice DEB properties on homeostasis.

Figure 7.1: These talking gouramis, *Trichopsis vittatus*, come from the same brood and therefore are the same age. They also grew up in the same aquarium. The size difference resulted from competition for a limited amount of food chunks, which amplified tiny initial size differences. This illustrates that age cannot serve as a satisfactory basis for the description of growth and food intake should be included explicitly.

7.2.4 Feeding: Size variation via food intake

We here focus on spatially homogeneous situations, and create ourselves a stochastic model for feeding of a single individual on a single type of food particles. We then extend the model to more individuals and see how social interaction can amplify size differences. This section is meant to present a mechanism behind the phenomenon depicted in Figure 7.1.

The stochastic feeding model is constructed such that the expected feeding rate is $\dot{J}_{XA} = f\{\dot{J}_{XAm}\}L^2$ with $f = X/(K+X)$, where $\dot{J}_{XA}$ is quantified as mass of particles per time and food density X and saturation constant K as mass of food particles per volume. The mass of a food particle is M_X (in C-mole). In number of food particles, we write $\dot{h}_X = f\{\dot{h}_{Xm}\}L^2$ with $\{\dot{J}_{XAm}\} = -\{\dot{h}_{Xm}\}M_X$, and $f = X_\#/(K_\# + X_\#)$, with $X = X_\# M_X$ and $K = K_\# M_X$. (Notice that $\dot{J}_{XA} < 0$ and $\dot{h}_X > 0$.) At high food density $X_\#$, for $f = 1$, searching takes a negligible amount of time, and the mean time it takes to handle a single food item is $t_h = 1/\dot{h}_{Xm} = \{\dot{h}_{Xm}\}^{-1}L^{-2}$. Since $\dot{h}_X = (t_s + t_h)^{-1}$, the time for searching is

$t_s = 1/\dot{h}_X - 1/\dot{h}_{Xm} = K_\#\{\dot{h}_{Xm}\}^{-1} X_\#^{-1} L^{-2}$.

Suppose that the food particles at a given time are randomly distributed in space with mean density $X_\#$. The probability that the nearest food particle is at a distance larger than L from an individual at a random site is

$$\text{Prob}\{\underline{L}_d > L\} = \exp(-X_\# L^3 \pi 4/3)$$

So, the nearest food particle is at mean distance

$$\mathcal{E}\underline{L}_d = \int_0^\infty \text{Prob}\{\underline{L}_d > L\}\, dL = \Gamma(4/3)(X_\# \pi 4/3)^{-1/3} = a X_\#^{-1/3}$$

with $a = \Gamma(4/3)(\pi 4/3)^{-1/3} \simeq 0.554$. Traveling at speed $\dot{S}$, the time to reach this particle is $t_s = \mathcal{E}\underline{L}_d/\dot{S} = a X_\#^{-1/3}/\dot{S}$, so the speed is $\dot{S} = a X_\#^{-1/3}/t_s = a K_\#^{-1}\{\dot{h}_{Xm}\} X_\#^{2/3} L^2 = \dot{b} X_\#^{2/3} L^2$ for $\dot{b} = a K_\#^{-1}\{\dot{h}_{Xm}\}$.

We now construct a feeding process of a single individual in a unit cube of habitat on the basis of the following rules

R1 a new food particle appears at a random site within the cube at the moment one of the resident particles disappears. It stays on this site till it disappears; the total number of food particles remains constant.

R2 a food particle disappears at a constant probability rate μ, or because it is eaten by the individual.

R3 the individual travels in a straight line to the nearest visible food particle at speed $\dot{S} = \dot{b} X_\#^{2/3} L^2$, eats the particle upon arrival and waits at this site for a time $t_h = \{\dot{h}_{Xm}\}^{-1} L^{-2}$. The individual changes direction if the food particle at which it is aiming disappears or a nearer new one appears. It changes speed because of changes in length.

R4 the individual grows following the DEB rules for an isomorph, i.e. the food particle converts to reserve instantaneously; the scaled reserve density e of an individual of structural volume L^3 makes a jump from e to $e + (L_X/L)^3$ upon feeding; scaled reserve density is used for metabolism at rate $\frac{d}{dt}e = -e\{\dot{h}_{Xm}\} L_X^3/L$; reserve converts to structure and the length changes at rate $\frac{d}{dt}L = \frac{\{\dot{h}_{Xm}\} L_X^3 e - L\dot{k}_M g}{3(e+g)}$. At time $t = 0$ the length is $L = L_b$, and the reserve density $e = f$.

R5 all food particles are visible.

We now extend the rules for N individuals that interact not only by competition, but also by social intimidation using the following rule that replaces R5

R5 a food particle becomes invisible for an individual of length L_1, if an individual of length L_1 is within a distance $L_s(L_2/L_1)^2$ from the food particle, irrespective of being aimed at.

Notice that even for the intimidation length $L_s \to 0$ the individuals interact (weakly) by competition because the mean traveling distance will increase, despite the replacement of disappearing food particles. The differences in length will amplify for increasing intimidation length.

The interpretation of the food length L_X is $L_X^3 = M_X y_{EX}/[M_{Em}]$, which makes that $L_m = \frac{-\{\dot{J}_{XAm}\} y_{EX}}{k_M g [M_{Em}]} = \frac{\kappa\{\dot{J}_{EAm}\}}{j_{EM}[M_V]} = -\frac{\kappa\{-\dot{J}_{XAm}\}}{j_{XM}[M_V]}$ (cf {122} Table 3.4). Notice that by increasing

mass M_X, while keeping $\{\dot{J}_{XAm}\}$ constant, the maximum length will increase as well. Keeping $\{\dot{J}_{XAm}\}$ constant, however, will result in an increase in variance. The speed can be made independent of food density and proportional to length, rather than squared length, by inserting more detail in the feeding process (especially in the visibility module). We here want to minimize the number of parameters that needs to be specified.

The food density X and the particle disappearance rate μ are environmental parameters. Although our food particles do not move, the replacement scheme has the effect as if the particles move at infinite speed to another random location at random points in time. The mean distance between two random points on a unit edge is $1/3$, on a unit square it is 0.521405, and on a unit cube it is 0.65853. So the mean speed of a food particle in a cube with edge L_D is $0.65853 L_D \mu$. If this is in the same order of magnitude as the speed of the organism, it strongly affects the feeding process; if it is much larger, the individuals will starve to death.

We have two different spatial units, that of the individual (in $\{\dot{h}_{Xm}\}$, L_b and L_X) and of the environment (in X, K and L_s), here chosen as cm and m, respectively. Speed is primarily controlled by the saturation constant K. The social interaction increases with decreasing number of food particles per individual. The variance increases with food length L_X, but decreases in time because of the smoothing capacity of the individual increases with size (the catabolic flux is inversely proportional to a length measure).

We have 8 parameters $X_\#$, $K_\#$, L_b, L_X, $\{\dot{h}_{Xm}\}$, $\dot{k}_M$, g, μ for feeding and growth of a single individual with state variables scaled reserve density e and structural length L, and one extra parameter, L_s, for the feeding and growth of N individuals. Notice that $\{\dot{h}_{Xm}\}L_X^3$ plays the role of the energy conductance $\dot{v}$ in the standard DEB formulation, which does not account for stochasticity and the discreteness of food particles. This stochastic extension, therefore, does not come with an increase in the number of parameters, while we need a single parameter to introduce social interaction. We can out-scale one parameter, if our interest is in relative length $l = L/L_m$ with $L_m = \{\dot{h}_{Xm}\}L_X^3/\dot{k}_M g$, and another one by choosing the spatial scale such that $K_\# = 1$, and a final one if we out-scale time, e.g. by choosing the maintenance rate coefficient $\dot{k}_M^{-1}$ as unit of time. The core of the problem of how the variance in length builds up as function of time t, food density X, number of interacting individuals N and the intimidation length L_s has thus 6 parameters.

Figure 7.2 illustrates simulation results; notice that both individuals have exactly the same parameter values, although they seem to follow different growth curves! Stochastic growth is retarded relative to the deterministic expectations because of the border effects (which increase the traveling distances), and the stochastic displacements of food particles. Even in the single individual case, the variance behaves different, compared to the random telegraph process, as described in section 4.1.1 and Figure 4.1. Notice also how effectively reserve smooths out stochastic fluctuations in food availability.

7.6 Organelle-cytosol interactions

I here use the link between two levels of organisation to extract information about cells regulatory activities for a univariate V1-morph.

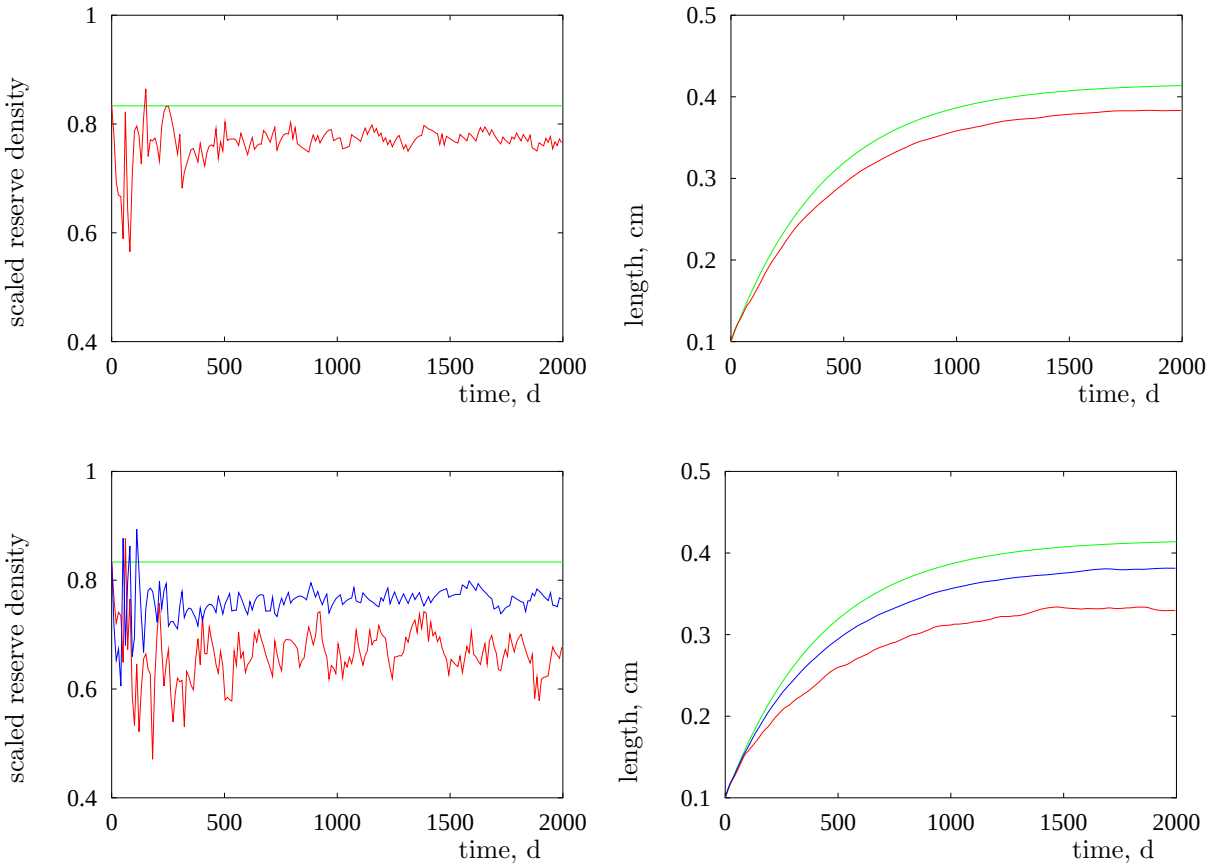

Figure 7.2: The scaled reserve density e and the length L, in the single (top) and the two (bottom) individual situation. The green lines give the deterministic expectation without interaction. Parameters: $\mu = 2\,\mathrm{d}^{-1}$, $X_\# = 10\,\mathrm{m}^{-3}$, $K_\# = 2\,\mathrm{m}^{-3}$, $\{\dot{h}_{Xm}\} = 10\,\mathrm{d}^{-1}\mathrm{cm}^{-2}$, $L_b = 0.1\,\mathrm{cm}$, $L_X = 0.1\,\mathrm{cm}$, $\dot{k}_M = 0.01\,\mathrm{d}^{-1}$, $g = 2$, $L_s = 0.2\,\mathrm{m}$.

7.6.1 Varying cellular needs for products from the pathway

Mitochondria serve a wide range of functions in eukaryotic cells. The mitochondrion also houses the tricarboxylic acid (TCA) cycle, cf {109}. The nine transformations of this linear metabolic pathway amount to the oxidation of the acetyl group of acetyl-CoA to CO_2:

$$C_2H_3O\text{-SCoA} + 3\,NAD^+ + FAD + GDP^{3-} + P_i^{2-} + 2\,H_2O \rightarrow$$
$$2\,CO_2 + 3\,NADH + FADH_2 + GTP^{4-} + 2\,H^+ + H\text{-SCoA}$$

The H-SCoA re-binds to pyruvate or fatty acid for the next cycle; the reduced co-enzymes NADH and $FADH_2$ are re-oxidised by dioxygen in a multi-step transformation of the respiratory chain. The free energy is used to convert ADP and P_i to ATP via a proton gradient across the mitochondrial inner membrane, as is well known. What is usually less emphasised in text books is that the intermediary metabolites (e.g. citrate, succinate, fumarate, malate) are also used as building blocks. So not all the pyruvate that is passed to mitochondria should be combusted completely. Cells' need for building blocks, relative to that for ATP, depends on the growth rate, and hence on the rate of pyruvate allocation to mi-

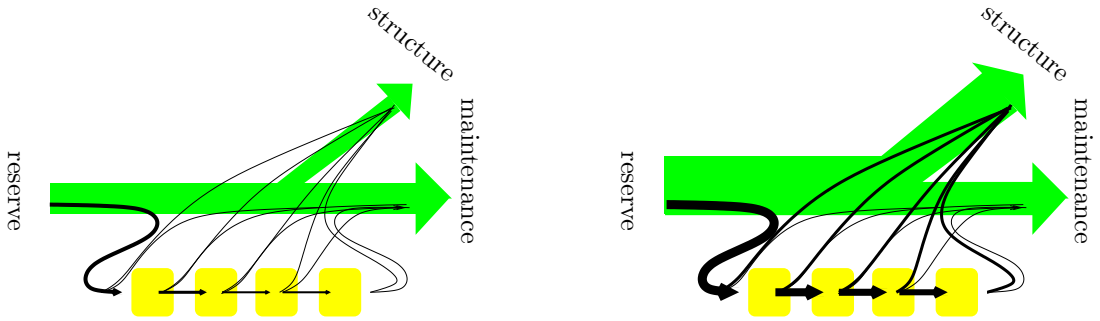

Figure 7.3: The resources that are mobilised from the reserve by the catabolic flux are allocated to maintenance and growth, i.e. increase in structure. When the reserve density increases, the catabolic flux and the allocation to growth increase, but not the allocation to maintenance (right panel; widths of arrows indicate the sizes of fluxes). The flux of substrate to the enzymatic pathway is proportional to the catabolic flux. The mixture of products and intermediary metabolites that are released from a linear pathway and allocated to maintenance (or growth) is constant. This paper solves the problem of how the non-linear dynamics of the pathway should be organised to fulfil this complex task.

tochondria. The six non-membrane-bound enzymes of the TCA cycle are released from the gel-like mitochondrial matrix by gentle ultrasonic vibration as a very large multi-protein complex [869]. This spatial organisation suggests interactions between the enzymes that might be responsible for the regulation of the proper ATP/building blocks ratio.

Consider an n-step linear metabolic pathway, as illustrated in Figure 7.3, which is mediated by enzymes $S_1, \cdots, S_n$ with the following i-th step:

$$X_{i-1} \to y_{X_i X_{i-1}} X_i + y_{P_i X_{i-1}} P_i \quad \text{with } i = 1, \cdots, n. \tag{7.4}$$

A molecule of intermediary metabolite X_{i-1} is transformed into $y_{X_i X_{i-1}}$ molecules of another intermediary metabolite X_i and $y_{P_i X_{i-1}}$ molecules of product. Other substrate molecules might be involved as well, but their availability is assumed to be such that they do not limit the rate of transformation. The product P_i might actually be composed of a set of (possibly different) molecules, rather than a single molecule. Products are, therefore, taken to be generalised compounds. Without loss of generality we can identify the last intermediary metabolite X_n with the last product P_n. The substrate flux $J_{X_0 A}$ to the pathway is given by a model for the whole cell and might vary (slowly) in time. If all intermediary metabolites would follow the full pathway (which they generally do not), we have the overall transformation

$$X_0 \to \sum_{i=1}^{n} y_{P_i X_0} P_i \quad \text{with } y_{P_i X_0} = y_{P_i X_{i-1}} \Pi_{j=1}^{i-1} y_{X_j X_{j-1}} \quad \text{for } i = 2, \cdots, n \tag{7.5}$$

Now consider the situation where some intermediary metabolites follow only part of the pathway and step out of the transformation process at the various nodes of the pathway and become available for two cellular functions: maintenance and growth of structure, see

Figure 7.3. Cellular maintenance and growth require the intermediary metabolites X_i and products P_i in possibly different relative amounts:

$$\sum_i y_{X_i X_M} X_i + \sum_i y_{P_{i+1} X_M} P_{i+1} \to X_M; \quad \sum_i y_{X_i X_G} X_i + \sum_i y_{P_{i+1} X_G} P_{i+1} \to X_G \tag{7.6}$$

where X_M and X_G are taken to be generalised compounds that are involved in the maintenance and growth process, respectively, and the yield coefficients y are taken to be stoichiometric constants (i.e. fixed constants whose values follow are constraint by mass conservation). This latter requirement yields the important conclusion that all products and intermediary metabolites that are released from the pathway depend linearly on the growth rate. To see this, note that the released material at growth rate zero is allocated to maintenance. If more material is released than is needed for maintenance, the extra material is allocated to growth. If, for example, the growth rate is doubled, then twice as much material per unit of time is needed for growth, provided that structure does not change in composition. Maintenance has priority over growth. Accordingly, the flux ratio $\dot{J}_{X_G}/\dot{J}_{X_M}$ depends on the flux $\dot{J}_{X_0}$ in a very special way, as will be discussed below.

The problem now is that the mass balance at the whole-cell level forces us to assume that the chemical composition of the mixture of metabolites and products that is allocated to maintenance is constant. The same applies to the mixture that is allocated to growth, while the composition of both mixtures will differ. This mass balance does not and cannot account for leaks from a pathway, where leaks are defined to be fluxes that are not associated to maintenance or growth (or any other process that the whole-cell model specifies). What does this imply for the dynamics of the pathway? How is pathway kinetics linked to cellular requirements for particular compounds? The cell has many pathways and if each pathway produced compounds that are not allocated to maintenance or growth, any model at the cellular level would be problematic, unless the cellular model incorporated the details of the then (very large) set of models for all different pathways. Such a complex model would hardly contribute to further insight concerning cellular metabolic functions and would be highly impractical in most applications. Consequently, we here discuss a consistency issue between a whole-cell model and model for the dynamics of a pathway.

Pathway model

The cellular requirements can be expressed in the overall transformation

$$X_0 \to Y_{X_M X_0} X_M + Y_{X_G X_0} X_G \tag{7.7}$$

where the variable stoichiometric coefficients Y depend on the flux of substrate $J_{X_0 A}$ to the pathway. Both these coefficients and the flux must be specified by a model for the whole cell, which we will now specify.

To make a clear notational distinction between the two levels of organisation (pathway and cell), we will mark all yield coefficients (i.e. mass-mass couplers) that link the levels with $\circ$.

Substrate X_0 is released from the reserve as part of the catabolic flux, so

$$\dot{J}_{X_0} = y^\circ_{X_0 E} \dot{J}_{E,C} \quad \text{or for } j_{X_0 A} = \dot{J}_{X_0}/M_V \quad j_{X_0 A} = y^\circ_{X_M E} j_{EC} \tag{7.8}$$

Generalised compound X_M participates in the maintenance flux, so

$$\dot{J}_{X_M} = y^\circ_{X_M E} \dot{J}_{E,M} \quad \text{or for } j_{XM} = \dot{J}_{X_M}/M_V \quad j_{XM} = y^\circ_{X_M E} j_{EM} \tag{7.9}$$

while generalised compound X_G is used for building structure, so

$$\dot{J}_{X_G} = y^\circ_{X_G V} \dot{J}_{V,G} \quad \text{or for } j_{X_G} = \dot{J}_{X_G}/M_V \quad j_{X_G} = y^\circ_{X_G V} \dot{r} \tag{7.10}$$

Compound X_G differs from the structure X_V by the inclusion of compounds that are used in the overhead of growth and by that fact that more than one pathway will deliver compounds that are used in growth. For $y_{X_M X_0} = y^\circ_{X_M E}/y^\circ_{X_0 E}$ and $y_{X_G X_0} = y^\circ_{X_G V}/(y^\circ_{X_0 E} y_{EV})$, the variable yield coefficients required in (7.7) can now be expressed in terms of DEB fluxes as

$$Y_{X_M X_0} = \frac{\dot{J}_{X_M}}{\dot{J}_{X_0}} = \frac{y_{X_M X_0}}{1 + y_{EV}\dot{r}/j_{EM}} \quad \text{and} \quad Y_{X_G X_0} = \frac{\dot{J}_{X_G}}{\dot{J}_{X_0}} = \frac{y_{X_G X_0}}{1 + j_{EM}/(y_{EV}\dot{r})} \tag{7.11}$$

The enzymes that are involved in the metabolic pathway are, by definition, part of the reserve and/or structure since these two components constitute the whole cell in an univariate system. So the amount of the i-th enzyme, M_{S_i}, can be written as weighted sums of reserve and structure:

$$M_{S_i} = n_{S_i E} M_E + n_{S_i V} M_V = (n_{S_i E} m_E + n_{S_i V})\, M_V \quad \text{with} \quad m_E = \frac{j_{EM} + \dot{r} y_{EV}}{\dot{k}_E - \dot{r}}, \tag{7.12}$$

The costs for synthesis of the enzymes appear in the yield coefficients for assimilation and growth:

$$y_{XE} = 1/y_{EX} = y^\circ_{XE} + \sum_i n_{S_i E}\, y_{X S_i} \tag{7.13}$$

$$y_{EV} = y^\circ_{EV} + \sum_i n_{S_i V}\, y_{E S_i} \tag{7.14}$$

Turnover costs of enzymes that are part of the structure should be included in the specific maintenance costs as

$$j_{EM} = j^\circ_{EM} + \dot{k}_{S_i}\, n_{S_i V}\, y^*_{E S_i} \tag{7.15}$$

where $y^*_{E S_i} = y_{E S_i}$ if no reserve components are saved from the decomposition of enzyme S_i; generally we have $y^*_{E S_i} \leq y_{E S_i}$. The turnover of enzymes that are part of the reserve is implied by the reserve turnover. If both $n_{S_i E} > 0$ and $n_{S_i V} > 0$, we must have that $\dot{k}_{S_i} = \dot{k}_E$ to avoid a distinction between enzyme molecules that are part of the reserve and of the structure.

Notice that the intermediary metabolites of the metabolic pathway, X_i, don't appear in the reserve or structure; they only occur in fluxes, not in pools. Strict consistency requires that their amounts are negligibly small, and no need exists to evaluate their concentrations in the highly spatially structured internal environment of the cell. The maintenance compound X_M will be excreted in one form or another, just like part of the growth compound X_G, while another part of X_G will be included in the structure X_V. This completes the placement of our dual function problem in the context of the DEB theory

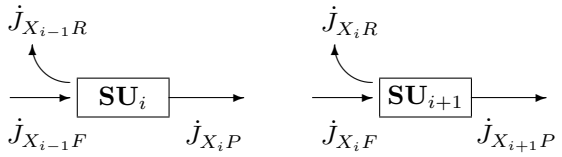

Figure 7.4: The arrival (F, for "feeding"), rejection (R) and production (P) fluxes for two Synthesising Units that are involved in a metabolic pathway. In a linear pathway for $i = 1, \cdots, n$ we have that $\dot{J}_{X_i,P} = \dot{J}_{X_i,F}$.

for we now have defined and related the various fluxes at the cellular level that specify the fluxes and the variable yield coefficients in (7.7).

We now specify the fluxes through the linear metabolic pathway as a function of the arrival flux of substrate to the pathway, including the branches of rejected fluxes of intermediary metabolites and products. We need interaction between SUs in the pathway, because without interaction, some intermediate metabolites always escape further transformation, while the cell might not need them for maintenance or growth. For this purpose we introduce $n-1$ handshaking parameters α_i, $0 \leq \alpha_i \leq 1$, that affect the release of product and the binding of substrate between SU i and $i+1$. The unbound fraction of the i-th SU changes such that if the handshaking parameter $\alpha_i = 0$, the handshaking is *open*, cf {251}, and the SUs operate independently. If $\alpha_i = 1$, however, the handshaking is *closed*, cf {250}, and no intermediary metabolites X_i are released if the binding probability $\rho_i = 1$; an SU only releases its product if the receiving neighbour SU is in the binding state. This coordinates the activities of all the SUs in the pathway and quantifies the distributed release of products and intermediary metabolites. If the handshaking parameter α_i is set to zero, all control is "bottom up" because the SUs do not interact and the behaviour of the whole follows (in complex ways) from the behaviour of the units. If the handshaking parameters are increased, the control becomes increasingly "top down", cf [1282] since the behaviour of the whole feeds back to the behaviour of the units. If the handshaking is closed for all SUs in the pathway, $\alpha_i = 1$ for $i = 1, \cdots, n-1$, and binding is sure, $\rho_i = 1$ for $i = 1, \cdots, n$, then the full pathway acts as if it is just a single SU (see appendix) and all metabolites X_0 that are processed are transformed into products. The behaviour of the units is then fully controlled by the behaviour of the whole.

We use a time scale argument to derive the arrival (F), rejection (R) and production (P) fluxes of intermediary metabolites in terms of the steady state binding fractions of the SUs. (We use F for "feeding" to indicate arrival rates to avoid confusion with assimilation, which we also need; when a metabolite flux is "fed" to an SU, it does not mean that all will be "eaten"). All intermediary metabolites X_i that are produced by the i-th SUs, arrive at the $i+1$-th SUs, so $J_{X_iF} = J_{X_iP}$. The pathway kinetics (cf 7.1.2) amounts for $i = 1, \cdots, n-1$ to the following changes of unbound fractions, θ_i, of SUs:

$$\frac{d}{dt}\theta_i = (1 - \alpha_i(1-\theta_{i+1}) - \theta_i)\, k_i - (\theta_i + \alpha_{i-1}(1-\theta_i))\, \rho_i J_{X_{i-1}F}/M_{S_i} \tag{7.16}$$

$$\frac{d}{dt}\theta_n = (1-\theta_n)k_n - (\theta_n + \alpha_{n-1}(1-\theta_n))\, \rho_n J_{X_{n-1}F}/M_{S_n} \tag{7.17}$$

Setting the change in the fractions, (7.16, 7.17) equal to zero, we obtain for the unbound

fractions of the i-th SUs at steady state (denoted by *) as

$$\theta_i^* = \frac{(1-\alpha_i+\alpha_i\theta_{i+1}^*)k_i - \alpha_{i-1}\rho_i J_{X_{i-1}F}/M_{S_i}}{k_i + (1-\alpha_{i-1})\rho_i J_{X_{i-1}F}/M_{S_i}} \quad \text{for } i = 1,\cdots,n-1 \tag{7.18}$$

$$\theta_n^* = \frac{k_n - \alpha_{n-1}\rho_n J_{X_{n-1}F}/M_{S_n}}{k_n + (1-\alpha_{n-1})\rho_n J_{X_{n-1}F}/M_{S_n}} \tag{7.19}$$

where the arrival flux J_{X_0F} of substrate to the pathway is given. Since SU i exists in M_{S_i} copies, and produces $y_{X_iX_{i-1}}$ intermediary metabolites X_i from each molecule X_{i-1}, the production fluxes are

$$J_{X_iP} = (1-\alpha_i(1-\theta_{i+1})-\theta_i)\, k_i\, y_{X_iX_{i-1}} M_{S_i} \quad \text{for } i = 1,\cdots,n-1 \tag{7.20}$$

$$J_{X_nP} = (1-\theta_n) k_n\, y_{X_nX_{n-1}} M_{S_n} \tag{7.21}$$

The set of equations (7.18–7.21) determine the unbound fractions θ_i and arrival rates J_{X_iF} for all SUs. Since mass conservation implies that the rejection fluxes equal the difference between the arrived and the processed fluxes, the rejection fluxes are

$$J_{X_iR} = J_{X_iP}\,(1-(\theta_{i+1}+\alpha_i(1-\theta_{i+1}))\,\rho_{i+1}) \tag{7.22}$$

$$= J_{X_iP} - J_{X_{i+1}P}/y_{X_{i+1}X_i} \quad \text{for } i = 0,\cdots,n-1 \tag{7.23}$$

$$J_{X_nR} = J_{X_nP} \tag{7.24}$$

Note that, if $\alpha_i = \rho_i = 1$, no rejection of X_i, $i = 0,\cdots,n-1$, occurs, so $J_{X_iR} = 0$. This is how closed handshaking is constructed. A nice property of this construction is that more than once a particular enzyme turns out to be a consortium of several smaller ones. As long as the members of the consortium pass metabolites by direct channeling (i.e. the enzyme-product complex does not release the product molecule into the liquid environment, but the molecule is directly bound to a neighbouring enzyme molecule in a enzyme-substrate complex), such a discovery has no consequence for the pathway model. Constraints apply to parameter values; the handshaking parameters restrict the maximum flux that can be processed. With an open handshaking protocol all excess flux is simply rejected, but that possibility becomes increasingly restricted by gradually closing the handshaking. The physical impossibility to allocate more than can be processed leads to unbound fractions outside the interval (0,1). Any choice of parameter values should be tested for its validity.

This completes the model specification of cells' regulatory functions in terms of the handshaking and the binding parameters. The fluxes and bound fractions can be obtained analytically for $n = 2$, but you don't want to see the result. The result is of little relevance for our purpose, fortunately, because the DEB model already specifies the fluxes. Our interest is in the implied constraints; the next section shows that these can be obtained without explicitly solving for the fluxes.

7.6.3 Matching the pathway and the DEB model

We specified the flux of substrate to the pathway (7.8), and the (variable) yield coefficients (7.11), while the maintenance flux $\dot{J}_{EM} \equiv j_{EM} M_V$ and the growth flux $\dot{J}_{E,G} = y_{EV}\dot{r}M_V$

are given in (4.14) and (4.16). Together they quantify the transformation at the cellular level. We also specified how the fluxes of substrates for maintenance and growth (7.20 – 7.24) as released by the pathway depend on the flux of substrate to the pathway.

The specific flux of substrate X_0 to the pathway equals by equations $\dot{J}_{E,C} \equiv j_{EC} M_V = (\dot{k}_E - \dot{r}) M_E$ and (7.8)

$$j_{X_0F} = n_{X_0E}\, j_{EC} = n_{X_0E}(j_{EM} + \dot{r} y_{EV}) = n_{X_0E}(\dot{k}_E - \dot{r}) m_E = n_{X_0E} \frac{j_{EM} + \dot{k}_E y_{EV}}{1 + y_{EV}/m_E} \quad (7.25)$$

where the specific growth rate $\dot{r}$ and the reserve density m_E can vary in time. We now equate the release of intermediary metabolites and products from the pathway to their use by the cell. Given (7.6), (7.9) and (7.10), the specific required fluxes of intermediary metabolites and products are,

$$\begin{aligned} j_{X_iP} &= j_{P_i}/y_{P_iX_i} = y^P_{X_iE}\, j_{EM} + y^P_{X_iV}\, \dot{r} \quad \text{for } i = 1, \cdots, n \quad (7.26) \\ &\quad \text{with } y^P_{X_iE} = y_{P_iX_M}\, y^\circ_{X_ME}/y_{P_iX_i} \quad \text{and} \quad y^P_{X_iV} = y_{P_iX_G}\, y^\circ_{X_GV}/y_{P_iX_i} \\ j_{X_iR} &= j_{X_i} = y_{X_iE}\, j_{EM} + y_{X_iV}\, \dot{r} \quad \text{for } i = 0, \cdots, n-1 \quad (7.27) \\ &\quad \text{with } y_{X_iE} = y_{X_iX_M}\, y^\circ_{X_ME} = y^P_{X_iE} - y^P_{X_{i+1},E}/y_{X_{i+1}X_i} \\ &\quad \text{and } y_{X_iV} = y_{X_iX_G}\, y^\circ_{X_GV} = y^P_{X_iV} - y^P_{X_{i+1}V}/y_{X_{i+1}X_i} \end{aligned}$$

The first equality sign in (7.26), and in (7.27), is a consequence of the following considerations for the links between the fluxes that are required by the cell and those released by the pathway. The released intermediary metabolites X_i, $i = 0, \cdots, n-1$, are the rejected fluxes $\dot{J}_{X_i,R}$; the released products P_i, $i = 1, \cdots, n$, are linked to the production fluxes of the metabolites one step earlier. Since both intermediate metabolite X_i and product P_i are stoichiometrically linked to X_{i-1}, product P_i is linked to X_i with yield coefficient $y_{P_iX_i} = y_{P_iX_{i-1}}/y_{X_iX_{i-1}}$.

We must have that $j_{X_iP} > j_{X_iR}$ for all growth rates $\dot{r}$, which implies from (7.26) and (7.27) that $y_{P_iX_M} > y_{P_iX_i}\, y_{X_iX_M}$ and $y_{P_iX_G} > y_{P_iX_i}\, y_{X_iX_G}$. It turned out that j_{X_iP} and j_{X_iR} cannot be exactly linear in the specific growth rate $\dot{r}$ [797] for $i = 1, \cdots, n$, but numerical studies of (7.18–7.21) reveal that, given values for $\dot{k}_i$, the values for α_i, ρ_i, n_{S_iE}, and n_{S_iV} can be chosen such that linearity is almost perfect.

The conclusion is that to match the products of pathways to the varying needs of the cell, we need an appropriate mix between open and closed handshaking protocols and an appropriate link of the abundance of the enzymes to reserve and structure. All required information on the fate of the products of the pathway is then contained in the flux of substrate to the pathway. Applied to mitochondria this means that if the amount of (active) mitochondria is linked appropriately to reserve and structure, they can deliver the required mixture of ATP and intermediary metabolites using the flux of pyruvate to the mitochondria as only control; the composition of the mixture depends on the flux of pyruvate.

The significance of this result is that if the reserve is omitted from the cell model, and/or no enzyme is associated with reserve, $n_{S_iE} = 0$, production and rejection fluxes deviate from linearity in the specific growth rate and the pathway model does not match the cell

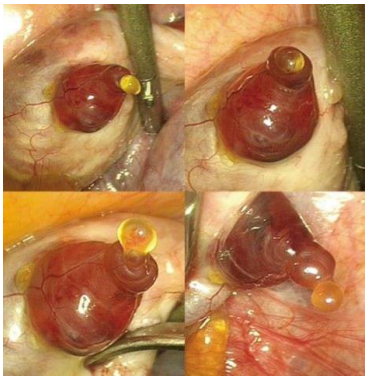

Figure 7.5: This is how humans lay eggs, from [880].

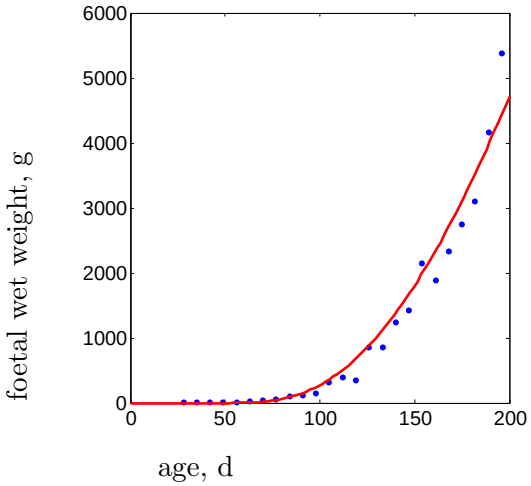

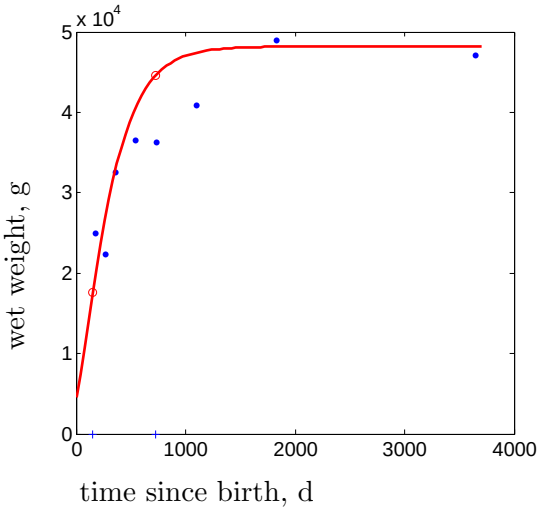

Figure 7.6: The pre- (left) and post-embryonic (right) development of the male impala *Aepyceros melampus*. Data from [401, 402]. The curves have been estimated simultaneously, assuming slow development, and the energy conductance was estimated to be $\dot{v} = 0.35\,\mathrm{cm\,d^{-1}}$ at 20°C, using an Arrhenius temperature of 8 kK and a body temperature of 39.5°C. The start of development was 53.2 d after fertilization. The observed ages and expected weights at weaning and puberty are indicated. Add_my_pet gives further details.

model. The Marr-Pirt model, for instance, which is a limiting case of the DEB model for vanishing reserve, has a consistency problem with this pathway model. We believe that this result is rather general, and applies to a large class of acceptable pathway models. Cyclically organised pathways turn out to behave very similar to the linear ones that are discussed above [797], which further supports the generality of this conclusion.

7.7 Mother–foetus system

At birth of the baby, the human mother produces 3500 g baby, 900 g placenta and 900 g amniotic fluid, while she increased her blood volume with 2000 g, her body fluids with 1500 g, her uterine with 900 g and her breasts with 500 g; the latter in preparation of milk production. This all on top of an increase in reserve, so more than three times the mass of the baby is involved in pregnancy.

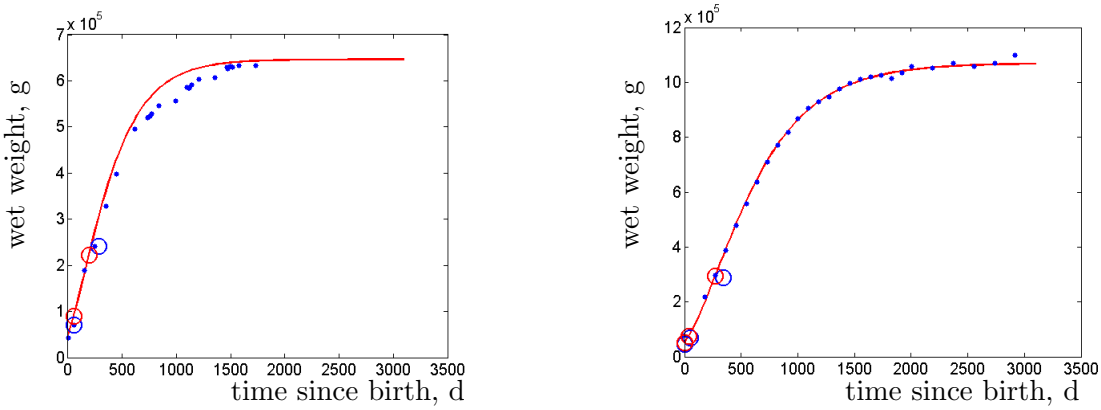

Figure 7.7: Post-embryonic development of the female (left) and male (right) cow *Bos primigenius* Holstein. Data from [105]. The observed and predicted age and weight at birth, weaning and puberty are indicated. The gestation time is 277 d with a body temperature of 38 °C, but the start of development was estimated to be 215 d (female) or 163 d (male). Add_my_pet gives further details.

Figure 7.6 shows that foetal development and milk production do not affect growth in the impala. Moreover the initiation of foetal growth is only at 25% of the gestation time; this period is probably used for placental growth and hormonal preparation of the body. The less-than-perfect fit for post-embryonic growth probably relates to the scatter in environmental conditions. This interpretation is confirmed by the post-embryonic growth of the related cow *Bos primigenius* under controlled conditions: almost all scatter is gone, especially in the bull data, see Figure 7.7. I have presently no explanation for why the times at the start of the development is different for female and male embryos, while the weights at birth are equal. Section 8.1.1 of the comments gives further details.

The simplest implementation of foetal development is to work with an mean allocation to foetal development $\dot{p}_R$ across reproductive cycles, see Section 2.6.2 of the comments. Work with Jess Roberts and Mike Kearney suggests a more detailed implementation of foetal development of the reproduction buffer in combination with an explicit allocation to milk production and an up-regulation of the assimilation (and intake) of the mother. The mammalian reproduction rate is to some extend constraint by $\dot{R} = (t_0 + a_x)^{-1}$, where t_0 is the time at first development. The rate must be multiplied by the litter size N, but let us assume that $N = 1$ for simplicity's sake.

The allocation to the foetus, including reproduction overheads, at scaled functional response f is $\dot{p}_R = f\{\dot{p}_{Am}\}L_F^2/\kappa_R$ during pregnancy and $\dot{p}_L = f\{\dot{p}_{Am}\}L_F^2/\kappa_R^L$ during lactation in the form of milk, see Section 2.6.2 of the comments. No up-regulation occurs during the juvenile period.

Let us here suppose that allocation to the reproduction buffer just covers the costs for foetal development till birth, but not lactation, and that milk production is paid from extra (= up-regulated) assimilation. At the end of a reproduction cycle, the reproduction buffer is just emptied. If this extra assimilation input does not end up in reserve, but directly

in the reproduction buffer, the lactation has no interaction with growth or maintenance (somatic or maturity) of the mother. This seems consistent with observations so far.

The extra assimilation of the lactating mother is converted into milk from the reproduction buffer as a buffer handling rule. The cumulative milk production for a single baby from birth till weaning is $E_L = \frac{f\{\dot{p}_{Am}\}}{\kappa_R^L \kappa_L} \int_{a_b}^{a_x} L_F^2(a)\, da$, where κ_L is the conversion efficiency from milk to baby reserve. For constant food availability, we have $\int_{a_b}^{a_x} L_F^2(a)\, da = L_\infty^2(a_x - a_b) - \frac{L_x - L_b}{\dot{r}_B}\left(L_\infty + \frac{L_b + L_x}{2}\right)$. The extra mean amount of food that is eaten by the lactating mother is $\dot{p}_L^+/\kappa_X$, while it actually increases during lactation till weaning. The (mean) energy investment into milk production by the mother is $\dot{p}_L^+ = E_L \dot{R}$, where $\dot{R}$ stands for the reproduction rate. The assimilation rate has to be up-regulated by this flux to cover the energy costs for milk production. The next reproduction cycle typically starts directly after weaning. The relative up-regulation, i.e. up-regulated relative to standard assimilation, is highest just prior to weaning (structural length of the baby is largest) of mother's first baby (structural length of the mother is smallest).

The placenta consists of a foetal part (chorion frondosum) and a maternal part (decidua basalis). Mammalia typically eat their placenta (and most of the umbilicus) and neonates directly start feeding on milk. After birth, allocation to milk production by the mother takes over from allocation to foetal development; the overhead might differ, but otherwise the dynamics is the same till weaning. Initially milk is the only water source for the neonate; baby's water intake gradually increases during lactation, while milk becomes less watery. Milk consumption reaches a peak when the baby reaches a maturity threshold E_H^s, which coincides with permanent pouch exit in marsupials. The preference for milk decays till zero at weaning, i.e. when the baby reaches another maturity threshold level E_H^j and food intake of the mother is not longer up-regulated. If milk and solid food are considered as substitutable parallely processed substrates and the specific searching is linked linearly to the maturity levels at peak milk intake and at weaning, we arrive at

$$\{\dot{J}_{EA}\} = y_{EX}\{\dot{J}_{XAm}\} f_X + y_{EY}\{\dot{J}_{YAm}\} f_Y$$

with

$$f_X = \frac{\{\dot{F}_{Xm}\}X}{\{\dot{h}_{XAm}\} + \{\dot{F}_{Xm}\}X + \{\dot{F}_{Ym}\}Y}; \quad f_Y = \frac{\{\dot{F}_{Ym}\}Y}{\{\dot{h}_{YAm}\} + \{\dot{F}_{Xm}\}X + \{\dot{F}_{Ym}\}Y}$$
$$\{\dot{F}_{Xm}\} = \frac{E_H^j - E_H}{E_H^j - E_H^s}\{\dot{F}_{Xm}^s\} \qquad \{\dot{F}_{Ym}\} = \frac{E_H - E_H^s}{E_H^j - E_H^s}\{\dot{F}_{Ym}^j\}$$

Milk production is not always done by the mother in mammals; the Dayak fruit-eating bat *Dyacopterus spadiceus* sports paternal lactation. The masked stingaree *Trygonoptera personata* feeds their offspring with uterine milk; many pigeons do this with gastric milk.

The composition of (cow) milk, c.f. Table 4 is

compound	formula	g/g-wet milk	kJ/g	g/mol	mol/mol-dry milk
carbohydrate	CH_2O	0.046	17.2	30	0.38
lipid	$CH_{1.92}O_{0.12}$	0.015	38.9	15.84	0.24
protein	$CH_{1.61}O_{0.33}N_{0.28}$	0.035	17.6	22.81	0.38
mineral		0.007	0		0
water	H_2O	0.877	0	18	0

which amounts to $2\,\mathrm{kJ\,g^{-1}}$ wet milk or $16.26\,\mathrm{kJ\,g^{-1}}$ dry milk or $4\,\mathrm{mmol\,g^{-1}}$ wet milk and

an overall formula of $CH_{1.83}O_{0.53}N_{0.11}$ for dry milk. The water content typically decreases during the lactation period, which motivates to work in dry milk and consider water balances separately. We need this to evaluate respiration during lactation. To that end, the organic fluxes $\dot{\boldsymbol{J}}_{\mathcal{O}}$ are extended with $\dot{J}_L$ as

$$\dot{\boldsymbol{J}}_{\mathcal{O}}^T = \begin{pmatrix} \dot{J}_X & \dot{J}_V & \dot{J}_E & \dot{J}_P & \dot{J}_L \end{pmatrix}$$

and the chemical indices with a new column

$$\boldsymbol{n}_{\mathcal{O}} = \begin{pmatrix} n_{CX} & n_{CV} & n_{CE} & n_{CP} & n_{CL} \\ n_{HX} & n_{HV} & n_{HE} & n_{HP} & n_{HL} \\ n_{OX} & n_{OV} & n_{OE} & n_{OP} & n_{OL} \\ n_{NX} & n_{NV} & n_{NE} & n_{NP} & n_{NL} \end{pmatrix}$$

and the basic powers with

$$\dot{\boldsymbol{p}}^T = \begin{pmatrix} \dot{p}_A & \dot{p}_D & \dot{p}_G & \dot{p}_L \end{pmatrix}$$

and the mass-energy couplers $\boldsymbol{\eta}_{\mathcal{O}}$ with a new row and column

$$\boldsymbol{\eta}_{\mathcal{O}} = \begin{pmatrix} -\eta_{XA} & 0 & 0 & 0 \\ 0 & 0 & \eta_{VG} & 0 \\ \overline{\mu}_E^{-1} & -\overline{\mu}_E^{-1} & -\overline{\mu}_E^{-1} & 0 \\ \eta_{PA} & 0 & 0 & 0 \\ 0 & 0 & 0 & \eta_{LL} \end{pmatrix}$$

were $\eta_{LL} = 2\,\mu\text{mol}\,\text{J}^-1$. Notice that $\dot{J}_{E_r} = 0$ during lactation. The mineral fluxes now follow from (4.35) and (4.37).

7.8 Extra life–stages

Subsection 7.8.1 assumes that you have had a glance at subsection 7.8.2 on acceleration, an odd consequence of following the (sub)sections of the DEB book.

7.8.1 The abp and sbp model for copepods

Copepods have sexual reproduction in last copepodite stage. They moult 11 times: 5 naupliar stages and 6 copepodite stages. The naupliar and copepodite stages differ substantially in morphology, so the transition can be called metamorphosis. In cyclopoids, the last copepodite stage is carnivore, younger copepodites are omnivore, and the nauplii are herbivore. This feeding pattern suggests that only the last copepodite stage allocates to reproduction, so has to be classified as adult, in the context of DEB theory, and the other copepodite and nauplii stages as juvenile. The need for proteins for copepodite relates allocation to reproduction, where embryos are in need for protein-rich reserve. Length versus time curves show a clear upcurving till the final stage, where growth ceases.

The abp model

The simplest DEB model that captures this pattern is that the embryo follows the standard model without acceleration, the juvenile the standard model with type $\mathcal{M}$ acceleration. The adult increases somatic maintenance such that growth ceases. Another way to cease growth is that κ switches $\kappa_a = \frac{[\dot{p}_M]L_p}{\{\dot{p}^*_{Am}\}e}$, where $\{\dot{p}^*_{Am}\} = \{\dot{p}_{Am}\}s_{\mathcal{M}}$. The end of acceleration coincides with puberty, so $L_j = L_p$ and $s_{\mathcal{M}} = L_p/L_b$. Expressed in the specific assimilation at birth, κ of adults amounts to $\kappa_a = \frac{[\dot{p}_M]L_b}{\{\dot{p}_{Am}\}e}$, which changes in time because scaled reserve density e does. The juvenile is growing exponentially at constant food density, with specific growth rate $\dot{r}_j = \frac{\kappa\dot{p}_A - \dot{p}_M}{f[E_m]+[E_G]} = \dot{v}\frac{f/L_b - 1/L_m}{f+g}$, so $L(t) = L_b \exp(\dot{r}_j t/3)$, where t is time since birth. During the adult stage, where $\dot{r} = 0$, the reserve mobilisation rate amounts to $\dot{p}_C = \dot{v}^* E/L_p = \dot{v}E/L_b$, where $v^* = vs_{\mathcal{M}}$. See Eq (2.12) for $\dot{r} = 0$. No allocation to growth, as long as reserve allows, and allocation to the reproduction buffer is $\dot{p}_R = (1 - \kappa_a)\dot{p}_C - \dot{k}_J E^p_H = \dot{p}_C - \dot{p}_M - \dot{k}_J E^p_H$. The mean reproduction rate amounts to $\dot{R} = \kappa_R \dot{p}_R/E_0$, as before.

Since food quality changes during ontogeny, it is at this moment not sure that $\{\dot{p}_{Am}\}$ remains constant and that $\{\dot{p}_{Xm}\}$ and κ_X are changing. Unless contra-evidence shows up, we make that assumption, however, meaning that assimilation amounts to $\dot{p}_A = f\{\dot{p}_{Am}\}L^3/L_b$, where L grows from L_b to L_p during the juvenile period, after which it remains constant at L_p.

If dilution be growth can be neglected in the ageing process, we have the cubed Weibull aging rate $\dot{h}^3_W = \frac{\ddot{h}_a e\dot{v}}{6L_b}$ and the Gompertz ageing rate $\dot{h}_G = \frac{s_G e\dot{v}L^3_p}{L_b L^3_m}$, while the survival probability Eq (6.5) still applies. For small s_G, so small $\dot{h}_G$, the mean age at death is approximately $\Gamma(4/3)/\dot{h}_W$, as before.

Copepods differ from insects, metabolically, by the larval stages being juvenile, rather than adult. Moults are triggered by maturity levels in copepods, but this cannot be the case in insects since maturity no longer increases during the adult stage. Notice that cladocerans don't accelerate and do grow as adult; quite a difference with copepods. May be that spiders, scorpions and ostracods also follow the copepod pattern.

The sbp model

Calanus sinicus was found to follow the standard DEB model without acceleration till puberty, where growth ceases, like in the abp-model. So the κ no longer applies after puberty.

Both the abp and the sbp model suffer from the property that asymptotic length is not observable, which substantially complicates the estimation of $[\dot{p}_M]$ and κ.

7.8.1 The hep model for ephemeropterans

Nymphs of ephemeropterans transform into flying subimagos, which subsequently transform into imagos withing minutes till 3 days (depending on species and temperature). Imagos live several days, and, like subimagos, don't feed, implying that nymphs allocate to reproduction. Ephemeropterans are presently the only insects that moult (once) while

having wings. The hep model also applies to Odonata and possibly some other groups as well.

To capture this pattern the hep model assumes that type $\mathcal{M}$ acceleration occurs between birth (event b) and puberty (event p), and transformation to subimago occurs when reproduction buffer exceeds a threshold (event j), called $[E_R^j]$. So (isomorphic) growth occurs in the adult nymph, but not in the (sub)imago. We assume that the heating length is zero, i.e. $L_T = 0$, so $l_T = 0$ as well.

Allocation to reproduction at constant food amounts to $\frac{d}{dt}E_R = \dot{p}_R = (1-\kappa)\dot{p}_C - \dot{p}_J$, with reserve mobilisation $\dot{p}_C = [E_m]L^3(\frac{\dot{v}s_{\mathcal{M}}}{L} + \dot{k}_M)\frac{eg}{e+g}$, maturity maintenance $\dot{p}_J = \dot{k}_J E_H^p$, acceleration factor $s_{\mathcal{M}} = L_p/L_b = l_p/l_b$. If emergence would not kick in, $L \to L_\infty = s_{\mathcal{M}} f L_m$ and the reproduction buffer density grows at constant rate $\frac{d}{dt}[E_R] \to \frac{1-\kappa}{\kappa}[\dot{p}_M] - \frac{\dot{p}_J}{L_\infty^3}$. The change in reproduction buffer density is $\frac{d}{dt}[E_R] = [\dot{p}_R] - 3\dot{r}_B(L_\infty/L - 1)[E_R]$. Since reproduction buffer density starts at zero at event p, we are sure that it hits any finite threshold, but we need to find the first event as long as $(1-\kappa)[\dot{p}_M]L_\infty^3 > \kappa\dot{p}_J$, to allow for puberty to be reached. In the hex model (see next section), the reproduction buffer density has a maximum, due to acceleration, and therefore does not hit a threshold value for sure.

At constant food density, scaled length changes in scaled time as $\frac{d}{d\tau}l = r_B(l_\infty - l)$ or $l(\tau) = l_\infty - (l_\infty - l_p)\exp(r_B\tau)$ with scaled $r_B = (3 + 3f/g)^{-1}$ and $l_\infty = s_{\mathcal{M}} f$. The dimensionless scaled reproduction buffer density $v_R = \frac{\kappa}{1-\kappa}\frac{[E_R]}{[E_G]}$ changes as $\frac{d}{d\tau}v_R = \frac{fgs_{\mathcal{M}}/l + f}{g+f} - \frac{kv_H^p}{l^3} - 3r_B v_R(fs_{\mathcal{M}}/l - 1)$. So scaled time at emergence is $\tau_j = \int_0^{v_R^j} \frac{d}{dv_R}\tau$ and $l(0) = l_p$ and $l(\tau_j) = l_j$ with $v_R^j = \frac{\kappa}{1-\kappa}\frac{[E_R^j]}{[E_G]}$. The number of eggs at emergence is $N = \kappa_R[E_R^j]L_j^3/E_0 = (1-\kappa)\kappa_R v_R^j l_j^3/u_E^0$

7.8.1 The hex model for holometabolic insects

Work with James Maino and Mike Kearney on holometabolic insects shows that insect larvae, like copepods, most fish and molluscs, sport metabolic acceleration [796, 778] (i.e. behave as V1-morphs). So energy conductance $\dot{v}$ and specific maximum assimilation $\{\dot{J}_{EAm}\}$ and searching $\{\dot{F}_m\}$ rates are increasing with length between birth (event b) and metamorphosis (event j), while the embryo (in the egg) and the imago (in the pupa) grow isomorphically; growth ceases after emergence.

Some insect taxa don't feed as imago (e.g. ephemeropterans), meaning that allocation to reproduction must have taken place during the larval stage, which classifies larvae as adults. Insects thus skip the juvenile stage and directly go from embryos to adults, like *Oikopleura*, see 2.7.1, and maturity remains constant during the larval stages. Maturity is linked to structure and larval structure transforms to reserve in the pupa, so maturity of that structure becomes irrelevant and maturity of the imago builds up from zero till emergence.

Thysanura, the most basal insect order continues moulting till death, like Collembola (also hexapods, but not insects); the total number of moults amounting from 17 to 66. The ephemeropterans sport some 45 moults, the anisopterans some 8 till 18 moults (avaraging

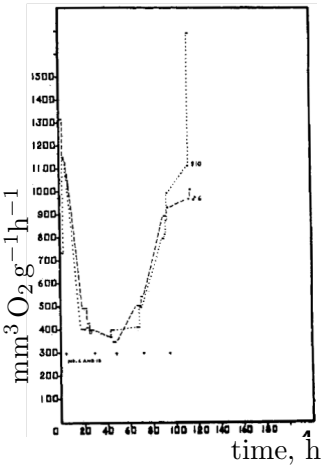

Figure 7.8: Dioxygen consumption in the blowfly *Phormia regina* at 20-24 °C. From Taylor [1406]

at 12.5 moults [276]). These two taxa comprise the Palaeoptera (which develop wings gradually and cannot fold them), while other insects are classified as Neoptera (which develop wings in the transition to the final moult only and can fold them). The neopterans are subsequently divided in the hemi- and holo-metabolic insects. The number of moults in the holo-metabola, the most advanced neopterans is around 6 (and also sport pupae and some endothermy), revealing a dramatic reduction of the number of moults in insect evolution.

Moulting occurs when the surface area of the gut (which grows continuously and controls food digestion) exceeds that of the head (which remains fixed during each instar and controls food acquisition) by some threshold value, so when $L^2(t)/L_i^2 > s_i$, where L_i is set to $L(t)$ at moulting. The idea is that food acquisition and processing (digestion) need to be in balance, a practical problem for ecdysozoans. Ephemeropterans are unique among insects by having an instar in the imago stage, that can fly but not eat; this moult must be triggered differently.

Reserve mobilisation during the larval stages amounts to $\dot{p}_C = E(\dot{k}_E - \dot{r})$, while $[E_G]\frac{d}{dt}V = [E_G]\dot{r}V = \kappa p_C - [\dot{p}_M]V$, so $\dot{r} = \frac{\kappa[E]\dot{k}_E - [\dot{p}_M]}{\kappa[E]+[E_G]} = \frac{e\dot{k}_E - g\dot{k}_M}{e+g} = g\dot{k}_M\frac{e/l_b - 1}{e+g}$. Reserve turnover $\dot{k}_E$ relates to energy conductance of the embryo $\dot{v}$ as $\dot{k}_E = \dot{v}/L_b$. Notice that $\frac{\dot{k}_E}{g\dot{k}_M} = \frac{1}{l_b}$. At constant food, we have $e = f$ and structural length grows as $L(a_b) = L_b\exp(t\dot{r}/3)$ for t is time since birth. So the first moult occurs at $L^2 = L_b^2\exp(t_1\dot{r}2/3) = s_1L_b^2$, i.e. time $t_1 = \frac{3\log(s_1)}{2\dot{r}}$ after birth. The second moult occurs at time $t_2 = \frac{3\log(s_2)}{2\dot{r}}$ after the first one, etc. The values s_i will probably don't differ very much, so the inter-moult period remains constant, like the ratio of surface areas (and lengths and volumes); the detailed nature of the moulting trigger only reveals by comparing different feeding levels. The moulting triggers are not part of the DEB model. Since L_b depends on the nutritional status via the maternal effect, all lengths at moulting do. Feeding actually ceases around moulting, which modifies the growth trajectory; this is here treated as a modifying 'detail'. Shrinking will probably hardly occur in insects, since the reproduction buffer only becomes depleted if starvation is really extreme.

Metamorphosis (pupation, event j) occurs when the reproduction buffer per amount of structure exceeds the value $[E_R^j]$. This trigger also induces spawning in molluscs, see

Section 2.7.2. Allocation to reproduction amounts to $\dot{p}_R = (1-\kappa)\dot{p}_C - \dot{p}_J$, with constant $\dot{p}_J = \dot{k}_J E_H^b$, and the reproduction buffer builds up as $E_R(t) = \int_{a_b}^t \dot{p}_R(s)\,ds$. So at constant food, where $e = f$ and $\dot{r}$ are constant, we have for time t since birth

$$\begin{aligned} E_R(t) &= (1-\kappa)(\dot{k}_E - \dot{r})f[E_m]\int_0^t V(s)\,ds - t\dot{p}_J \\ &= (1-\kappa)E_b\frac{g+l_b}{e-l_b}(\exp(\dot{r}t)-1) - t\dot{p}_J \quad \text{with} \quad E_b = f[E_m]V_b \end{aligned}$$

Pupation occurs when $E_R(t)/V(t) = [E_R^j]$, a time which has to be evaluated numerically. This time decreases for decreasing f, but the size at metamorphosis, and so the number of eggs, decrease as well. The maximum value $[E_R]$ can take for increasing $V(t)$ is $[E_R^m] = (1-\kappa)f[E_m](\dot{k}_E/\dot{r} - 1) = (1-\kappa)f[E_m]\frac{g+l_b}{f-l_b}$, which is reached asymptotically only. It might be useful to define the stress value $s_j = [E_R^j]/[E_R^{\mathrm{ref}}]$, with $[E_R^{\mathrm{ref}}] = (1-\kappa)[E_m]g\frac{\dot{k}_E+\dot{k}_M}{\dot{k}_E - g\dot{k}_M} = (1-\kappa)[E_m]\frac{g+l_b}{1-l_b}$, which is $[E_R^m]$ for $f = 1$, as parameter. The maximum reproduction buffer density at f thus becomes $[E_R^m] = [E_R^{\mathrm{ref}}]f\frac{1-l_b}{f-l_b}$. This rule for metamorphosis, i.e. metamorphosis occurs when $[E_R] = s_j[E_R^{\mathrm{ref}}]$, allows that the number of instars can depend on food density.

Stress s_j has a simple relationship with scaled reproduction buffer density: $v_R^j = \frac{[E_R^j]}{[E_G]}\frac{\kappa}{1-\kappa} = s_j\frac{1+l_b/g}{1-l_b}$. Scaled time since birth at pupation, $\tau_j = t_j\dot{k}_M$, can be found from $v_R^j = \frac{f}{g}\frac{g+l_b}{f-l_b}(1-\exp(-r\tau_j)) - \tau_j k v_H^b \exp(-\tau_j r)/l_b^3$ with $r = \frac{\dot{r}}{\dot{k}_M} = \frac{f/l_b - 1}{f/g+1}$. A decrease of food availability, f from 1 to l_b decreases allocation to reproduction, but even more to growth, with the effect that pupation is reached earlier, but at a smaller size. The lowest scaled function response $f_{\min}$ for which pupation is possible, $\tau_j < \infty$, satisfies the condition $\frac{f_{\min}-l_b}{1-l_b} = \frac{f_{\min}}{s_j}$, so $f_{\min} = \frac{s_j l_b}{s_j - 1 + l_b}$, while $f_{\min} > l_b$ must apply to start development.

The simplifying assumption that the chemical composition of the structures of imago and lava are equal in terms of relative elemental frequencies seems to be rather natural. The measured respiration of pupae follows the pattern that can be expected on the basis of DEB theory, see Figure 7.8. We see an initial decline during the final stages of the transformation of structure of the juvenile to reserve, followed by an increase when the structure of the adult builds up. This once more demonstrates that reserve does not require maintenance. More in particular the mineral fluxes of the pupa simplify to $\mathbf{0} = \boldsymbol{n}_{\mathcal{M}}\dot{\boldsymbol{J}}_{\mathcal{M}} + \boldsymbol{n}_{\mathcal{O}}\dot{\boldsymbol{J}}_{\mathcal{O}}$ with $\boldsymbol{n}_{\mathcal{O}}^T = \begin{pmatrix} n_{CV} & n_{HV} & n_{OV} & n_{NV} \\ n_{CE} & n_{HE} & n_{OE} & n_{NE} \end{pmatrix}$ and $\dot{\boldsymbol{J}}_{\mathcal{O}}^T = \begin{pmatrix} \dot{J}_V & \dot{J}_E \end{pmatrix}$,

$$\begin{aligned} \dot{J}_V &= -M_V^l\dot{k}_E^l + M_V\dot{r} \quad \text{with } \frac{d}{dt}M_V^l = -\dot{k}_E^l M_V^l \text{ and } \frac{d}{dt}M_V = \dot{r}M_V \\ \dot{J}_E &= y_{EV}^l M_V^l \dot{k}_E - \dot{J}_{EC} \quad \text{with } \dot{J}_{EC} = M_E(\dot{v}_j/L - \dot{r}) \text{ and } \kappa J_{EC} = y_{EV}\dot{r}M_V + j_{EM}M_V \end{aligned}$$

where $M_V^l(t)$ and y_{EV}^l refer to the larval structure and M_E, M_V, L to the reserve and structure of the imago; $\dot{v}_j = \dot{v}L_j/L_b$ is the elevated energy conductance, where L_b and L_j are the lengths are birth and metamorphosis. A simplifying assumption is $\dot{k}_E = \dot{k}_E^l$, although the substrates for both transformations differ. Since maturity builds up, no allocation to

reproduction occurs during the pupal stage. Applications of the model should reveal if the reproduction buffer that has been build up during the larval stages remains separate from the reserve in the pupa, or that they merge; merging leads to earlier emergence and a reduction of effects of nutritional condition on emergence. The inverse yield for structure (of the image) on reserve $y_{EV}^{-1} = y_{VE}$ must be smaller than y_{VE}^{l} if structure of larva and imago are chemically identical, else the interconversion to reserve would be without overhead.

Although the gradual decay of larval structure is important to capture the U-shaped profile of pupal respiration in time, for the state at emergence we can simplify by assuming that the conversion is instantaneous. In that case, reserve at pupation (excluding the reproduction buffer) amounts to $E_j = y_{EV}^{l} M_V^j \mu_E + E(t_j)$, where M_V^j is larval structure at pupation and $E(t_j)$ larval reserve at pupation. So the pupa evolves from $(L, E, E_H) = (0, E_j, 0)$ to (L_e, E_e, E_H^e), where E_H^e is a parameter. The method to derive L_e and E_e differs from that of egg development, because egg initial reserve was unknown, but reserve density at birth was. The changes in u_E, l and u_H given in (2.26-28) still apply, where the start now has label j, and 'birth' label e. The scaled quantity $v_H = \frac{u_H}{1-\kappa}$ changes as $\frac{d}{d\tau} v_H = -\frac{d}{d\tau} u_E - k v_H$ and the scaled time since pupation is given by $\tau_e = \int_0^{v_H^e} \frac{d\tau}{dv_H}$ with $\frac{d}{d\tau} u_E = -u_E l^2 \frac{g+l}{u_E+l^3}$ and $\frac{d}{d\tau} l = \frac{1}{3} \frac{g u_E - l^4}{u_E + l^3}$ and $u_E(0) = l_j^3(\kappa\kappa_V + f/g)$ with $\kappa_V = y_{EV}^{l}/y_{EV}$ is the conversion efficiency from larval reserve to larval structure, back to imago reserve.

The weight at emergence has contributions from structure, reserve and reproduction buffer; the latter is the same as at pupation. Substitution gives $W_w^e = V_e d_V^w + (E + E_R)\frac{d_V^w w_E}{d_E \mu_E} = d_V^w L_m^3 (l_e^3 + \frac{[E_G] w_E}{\kappa d_E \mu_E}((1-\kappa) v_R^j l_e^3 + u_E^e))$ with typically $d_V^w = 1\,\mathrm{g\,cm^{-3}}$.

Reserve mobilisation in imagos is at a constant rate to fuel (somatic plus maturity) maintenance, while the reproduction buffer is also mobilised at a constant rate to production of batches of eggs. Metabolic history prior to pupation can dominate reproductive output after emergence (such as in ephemeropterans) and buffer handling rules can be species specific; The steady state reproduction rate, where assimilation balances mobilisation, is $\dot{R} = (\dot{p}_X^e \kappa_X - \dot{p}_J^e - \dot{p}_M^e)/E_0$, where $\dot{p}_X^e = f\{\dot{p}_{Xm}\} L_e^2$ is the feeding rate (in $\mathrm{J\,d^{-1}}$), $\dot{p}_J^e = \dot{k}_J E_H^e$ is the (constant) maturity maintenance rate of the imago, $\dot{p}_M^e = [\dot{p}_M] L_e^3$ is the (constant) somatic maintenance rate and E_0 the energy cost of an egg at f. Since food of larvae and imagos is very different, the specific assimilation rates might differ as well. Imagos typically heat their body before and during flying [583], so somatic maintenance is temporarily increased. Since the reproduction buffer is also used for maintenance if reserve mobilisation is not sufficient, it hardly makes sense to separate reserve from the reproduction buffer in imagos. Like larvae, imagos don't change in maturity.

Given the reasoning of ageing, it is likely that larvae live too short for ageing to be important and that ageing is reset at pupation. On the assumption that ageing acceleration does not occur ($s_G = 0$) and that ageing during pupation can be neglected and given that growth is ceased after emergence ($\dot{r} = 0$), (6.1) reduces to $\frac{d}{dt} m_Q = \eta_{QC} \frac{\dot{p}_C}{M_V}$ and $\frac{d}{dt} m_D = \dot{k}_W y_{DQ} m_Q$. For constant $\dot{p}_C$ and $m_Q(0) = 0$ and $m_D(0) = 0$, this leads to $m_Q(t) = \eta_{QC} \frac{\dot{p}_C}{M_V} t$ and $m_D(t) = \dot{k}_W y_{DQ} \eta_{QC} \frac{\dot{p}_C}{2M_V} t^2$. The result is that the hazard rate equals $\dot{h}(t) = 3\dot{h}_W t^2$ and the mean time since emergence at death is $t_m = \Gamma(\frac{4}{3})/\dot{h}_W$.

Hibernation can occur in all stadia and impressive migratory movements are known in

a variety of insect species [843].

This model differs from the standard DEB model with acceleration by the acceleration that here occurs during the adult stage; the end of acceleration is not triggered by a maturity threshold by a threshold of $[E_R]$. Moreover larval structure is transformed to reserve, maturity is reset at pupation and growth of the imago is ceased at emergence. For comparative reasons it might be of interest to derive a maturity threshold at pupation if maturation would continue during larval development. With $\dot{r} = \frac{f\dot{k}_E - g\dot{k}_M}{f+g}$ and $\dot{p}_C = f[E_m]Vg\frac{\dot{k}_E+\dot{k}_M}{f+g}$, maturity would change as $\frac{d}{dt}E_H = (1-\kappa)\dot{p}_C - \dot{k}_J E_H$, which amount to $E_H(t) = E_H^b \exp(-\dot{k}_J t) + \frac{1-\exp(-(\dot{r}+\dot{k}_J)t)}{\dot{r}+\dot{k}_J}(1-\kappa)\dot{p}_C(t)$ for t is time since birth.

Josef Koch demonstrated that holometabolic insects exist that do not allocate to reproduction as larva or early imago. This calls for an alternative pupation trigger: reserve density at pupation equals reserve density at emergence. Assuming that the pupa still resets maturity and converts larval structure to reserve instantaneously, the equivalent of the maternal rule for embryo development specifies the pupation trigger. This trigger has a lot in common with a maturation trigger for pupation, but differs in the specification of the reserve density at emergence. With the maturation trigger for both pupation and emergence, reserve density at emergence is a complex function of these maturity levels and other parameters. The Matlab function `DEBtool_M/animal/get_tj_holo` has the maturity level at pupation as output. The larva grows exponentially at constant food as $L(t) = L_b \exp(t\dot{r}_j/3)$ with $\dot{r}_j = \dot{k}_M(f/l_b - 1)/(f/g + 1)$. The larva-derived reserve of the early pupa is $E_j^E = f[E_m]L_j^3$. The energy in larval structure is $E_V^j = L_j^3[M_V]\mu_V$, which contributes to pupal reserve with $E_j^V = \kappa_V L_j^3[M_V]\mu_V$ with a conversion efficiency of κ_V from larval structure to pupal reserve. The contribution of larval structure to early pupal scaled reserve u_E^j is $u_E^{jV} = \frac{\kappa_V L_j^3[M_V]\mu_V}{g*[E_m]*L_m^3} = l_j^3\kappa_V\kappa\mu_V[M_V]/[E_G] = l_j^3\kappa_V\kappa\kappa_G = l_j^3\omega_j$ for $\omega_j = \kappa_V\kappa\kappa_G$ The total reserve $E_j = E_j^E + E_j^V$ should be just enough to cover the costs of the pupa to develop to emergence with structure L_e and reserve $f[E_m]L_e^3$ and maturity E_H^e. At constant food, maturity from birth to pupation amounts for t is time since birth to $E_H(t) = (1-\kappa)f[E_m]L_b^3(\frac{\dot{v}}{L_b} - \dot{r}_j)\frac{\exp(\dot{r}_j t)-\exp(-\dot{k}_J t)}{\dot{r}_j+\dot{k}_J} + E_H^b \exp(-\dot{k}_J t)$. The scaled maturity at pupation $v_H^j = \frac{E_H^j}{(1-\kappa)g[E_m]L_m^3}$ amounts for τ_j is scaled time since birth at pupation to $v_H^j = fl_b^2(1-\rho_j l_b/g)\frac{\exp(\rho_j\tau_j)-\exp(-k\tau_j)}{\rho_j+k} + v_H^b \exp(-k\tau_j)$. After emergence, maturity changes at constant food as $\frac{d}{dt}E_H = (1-\kappa)\dot{p}_C - \dot{k}_J E_H$, with $\dot{p}_C = fs_M\dot{v}[E_m]L_e^2$. For t is time since emergence, $E_H(t) = E_H^\infty - (E_H^\infty - E_H^e)\exp(-\dot{k}_J t)$ with $E_H^\infty = (1-\kappa)\dot{p}_C/\dot{k}_J$. Puberty is reached for $E_H(t_p) = E_H^p$, i.e. for time since emergence $t_p = \dot{k}_J^{-1}\log(\frac{E_H^\infty - E_H^e}{E_H^\infty - E_H^p})$. Scaled time since emergence to puberty is $\tau_p = k^{-1}\log(\frac{v_H^\infty - v_H^e}{v_H^\infty - v_H^p})$, with $v_H^\infty = fs_M kl_e^2$. The reproduction rate after puberty at constant food is $\dot{R} = \kappa_R((1-\kappa)fs_M\dot{v}[E_m]L_e^2 - \dot{k}_J E_H^p)/E_0$. The larval feeding rate at constant food is $\dot{p}_X = fs_M\{\dot{p}_{Am}\}L^2/\kappa_X$ with $s_M = L/L_b$ and $L(t) = L_b\exp(t\dot{r}_j/3)$ for $L < L_j$, so $\dot{p}_X(t) = \frac{f\{\dot{p}_{Am}\}L_b L_j}{\kappa_X}\exp(t\dot{r}_j)$ and the cumulative amount of food in energy becomes $E_X(t) = \frac{f\{\dot{p}_{Am}\}L_b L_j}{\kappa_X\dot{r}_j}(\exp(t\dot{r}_j) - 1)$. If we want to have it in grams wet weight, we have to multiply with $\frac{w_X}{\mu_X d_X}$. The change in acceleration and hazard in the

imago at constant food is $\frac{d}{dt}\ddot{q} = (\ddot{q}l_e^3 s_G + \ddot{h}_a) f \dot{k}_M g / l_e$ and $\frac{d}{dt}\dot{h} = \ddot{q}$. If the hazard rate is small at emergence, this results in $\dot{h}(t) = \frac{6\dot{h}_W^3}{\dot{h}_G}(\exp(\dot{h}_G t) - 1 - \dot{h}_G t)$ with $\dot{h}_W^3 = \frac{\ddot{h}_a f \dot{k}_M g}{6 l_e}$ and $\dot{h}_G = s_G f \dot{k}_M g l_e^2$. The mean time since emergence at death is $\Gamma(4/3)/\dot{h}_W$ for small $\dot{h}_G$.

7.8.1.1 Pupa dynamics in hex and hax models

Dina Lika composed to following derivation of pupa-dynamics as used in `DEBtool_M\animal\get_tj_hex` and `get_tj_hax`.

Decay of larval structure:

$$\frac{dV^l}{dt} = -\dot{k}_E^l V \tag{7.28}$$

Increase of pupa structure:

$$\frac{dV}{dt} = \dot{r} V \tag{7.29}$$

Reserve dynamics:

$$\frac{dE}{dt} = \kappa_V \dot{k}_E^l V - \dot{p}_C \tag{7.30}$$

Changes in maturity

$$\frac{dE_H}{dt} = (1-\kappa)\dot{p}_C - \dot{k}_J E_H \tag{7.31}$$

where $\dot{p}_C = E\frac{[E_G]\dot{v}_j/L + [\dot{p}_M]}{\kappa[E] + [E_G]}$ with $\dot{v}_j = \dot{v} L_j / L_b$. $\dot{v}$ is the energy conductance at birth, L_b and L_j the length at birth and pupation, respectively.

A simplifying assumption is that $\dot{k}_E^l = \dot{k} = \dot{v}/L_b$. To simplify further, we assume that the conversion of V^l to E is instantaneous. So, initial energy in reserve $E_0 = E(t_j) + \kappa_V [M_V] V_j \mu_V$.

Next we introduce scaled variable to arrive in a non-dimensional form of equations 8.1 and 7.30

Set $v_H = \frac{E_H/(1-\kappa)}{g[E_m]L_m^3}$, $u_E = \frac{E}{g[E_m]L_m^3}$ and $l = \frac{L}{L_m}$, with $g = \frac{[E_G]}{\kappa[E_m]}$, $\dot{k}_M = \frac{[\dot{p}_M]}{[E_G]}$, $[E_m] = \frac{\{\dot{p}_{Am}\}}{\dot{v}}$, and $L_m = \frac{\dot{v}}{g\dot{k}_M}$. Note that $\dot{v}$ is the energy conductance before acceleration.

Reserve dynamics:

$$\begin{aligned} \tfrac{d}{dt}E &= -\dot{p}_C = -E\tfrac{[E_G]\dot{v}_j/L + [\dot{p}_M]}{\kappa[E] + [E_G]} \\ &= -E\tfrac{[E_G]\dot{v}_j L^2 + [\dot{p}_M]L^3}{\kappa E + [E_G]L^3} \\ &= -EL^2\tfrac{[E_G]\dot{v}_j + [\dot{p}_M]L}{\kappa E + [E_G]L^3} \end{aligned} \tag{7.32}$$

In scaled form:

$$\begin{aligned} \tfrac{d}{dt}u_E &= -u_E l^2 L_m^2 \tfrac{\frac{[E_G]\dot{v}_j}{g[E_m]L_m^3} + \frac{[\dot{p}_M]L}{g[E_m]L_m^3}}{\kappa u_E + \frac{[E_G]L^3}{g[E_m]L_m^3}} \\ &= -u_E l^2 \tfrac{\frac{\kappa\dot{v}_j}{L_m} + \frac{[\dot{p}_M]l}{g[E_m]}}{\kappa u_E + \kappa l^3} \\ &= -u_E l^2 \tfrac{\dot{v}_j/L_m + \dot{k}_M l}{u_E + l^3} \\ &= -u_E l^2 \tfrac{\dot{v} s_M/L_m + \dot{k}_M l}{u_E + l^3} \\ &= -u_E l^2 \tfrac{g\dot{k}_M s_M + \dot{k}_M l}{u_E + l^3} \end{aligned} \tag{7.33}$$

Table 7.2: The different types of acceleration, the variables and/or parameter values that change, the approximate events of start and end of changes and the observable changes (decrease in blue, increase in red), relative to the standard DEB model.

type	variable	period	regulation
R	κ	h - j	$\dot{J}_O$, $\frac{d}{dt}E_H$, $\frac{d}{dt}W$, a_b, a_j, a_p, W_j, W_p
X	X	b - ∞	$\dot{J}_O$, $\dot{R}_m$, $\frac{d}{dt}W$, W_j, W_p, W/L^3, a_j, a_p
A	$\{\dot{p}_{Am}\}$	b - p	$\dot{J}_O$, $\dot{R}_m$, $\frac{d}{dt}W$, W_j, W_p, W/L^3, a_j, a_p
$\mathcal{M}$	$\{\dot{p}_{Am}\}$, $\dot{v}$	b - j	$\dot{J}_O$, $\dot{R}_m$, $\frac{d}{dt}W$, W_j, W_p, a_b, a_j, a_p
T	$\{\dot{p}_{Am}\}$, $\dot{v}$, $\dot{k}_J$, $[\dot{p}_M]$	0 - b	$\dot{J}_O$, $\dot{R}_m$, $\frac{d}{dt}W$, a_b, a_j, a_p

Note that in the third step $\dot{v}_j$ was set equal to $\dot{v}s_M$, with $s_M = L_j/L_b$.
If we set $t = \tau/\dot{k}_M$, equation 7.33 becomes

$$\frac{d}{d\tau}u_E = -u_E l^2 \frac{gs_M + l}{u_E + l^3} \tag{7.34}$$

Changes in the scaled length:

$$\begin{aligned} \frac{d}{d\tau}l &= \frac{1}{L_m \dot{k}_M}\frac{dL}{dt} \\ &= \frac{1}{L_m \dot{k}_M}\frac{\dot{r}}{3}L \\ &= \frac{\dot{r}}{3\dot{k}_M}l \end{aligned} \tag{7.35}$$

with $\dot{r} = \frac{[E]\dot{v}_j/L - [\dot{p}_M]/\kappa}{[E] + [E_G]/\kappa} = \frac{\kappa E \dot{v}s_M - [\dot{p}_M]L^4}{\kappa E + [E_G]L^3}\frac{1}{L} = \frac{u_E g s_M - l^4}{u_E + l^3}\frac{\dot{k}_M}{l}$.
Therefore,

$$\frac{d}{d\tau}l = \frac{1}{3}\frac{u_E g s_M - l^4}{u_E + l^3} \tag{7.36}$$

Finally

$$\frac{d}{d\tau}v_H = u_E l^2 \frac{gs_M + l}{u_E + l^3} - k v_H \tag{7.37}$$

At the start of pupal development $\{v_H, u_E, l\} = \{0, u_E^j, 0\}$ with $u_E^j = l_j^3(\frac{f}{g} + \kappa\kappa_V\kappa_G) = l_j^3(\frac{f}{g} + \omega_j)$ for $\omega_j = \kappa\kappa_V\kappa_G$. The scaled reserve density at emergence is $e_e = g u_E^e / l_e^3$.

7.8.2 Metabolic acceleration

Metabolic acceleration is defined as a long-term increase in respiration, relative to expectation based on the standard DEB model. Table 7.2 presents 5 types of metabolic acceleration that have been found, as discussed in [776]. The maturation type does not concern an increase in specific feeding, assimilation or mobilisation, only in change in allocation. The 4 other types do involve such an increase and concern an increasing number of parameters.

7.8.2.1 Maturation

An illustrative and remarkable form of acceleration of maturation has been observed in the Australian myobatrachid *Crinia georgiana*, compared to *Pseudophryne bibronii* [1002],

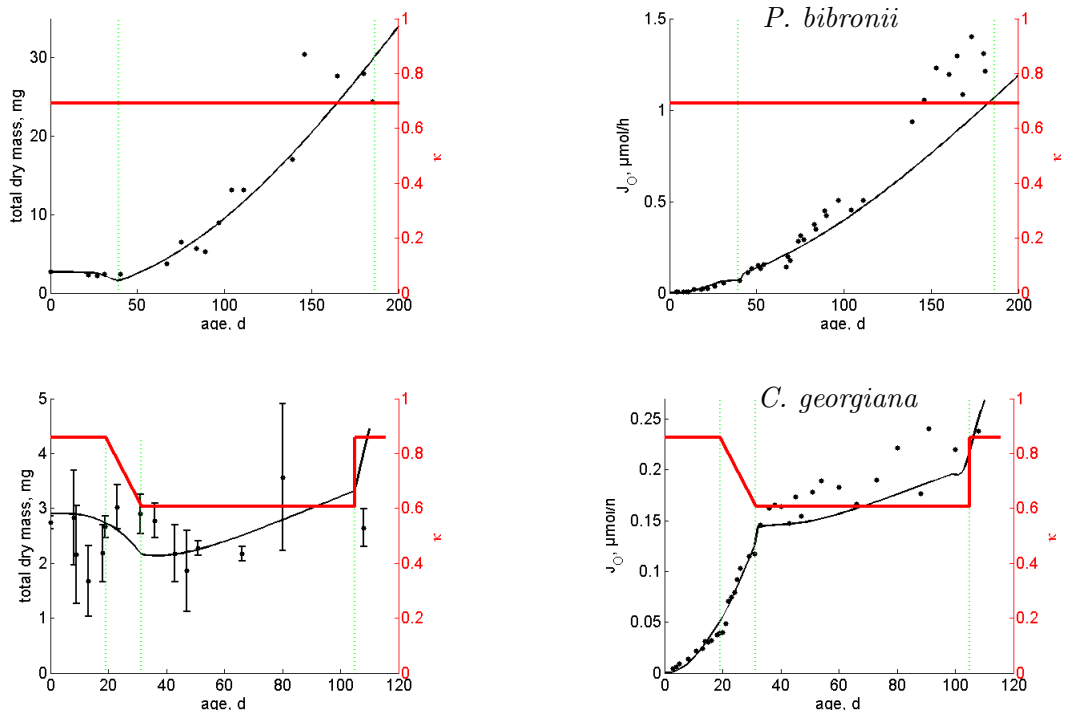

Figure 7.9: Dry weight (left) and dioxygen consumption (right) of two similar myobatrachid frogs *P. bibronii* (top) and *C. georgiana* (bottom) at 12 ∘C. Both sport indirect development, via a tadpole stage. Hatching, birth and metamorphosis are indicated, but the first two coincide in *P. bibronii*. The tadpoles of this species live in permanent pools, while that of *C. georgiana* in temporary ones that dry up, soon after their metamorphosis. *C. georgiana* accelerates maturation by lowering κ temporarily, as indicated, which also reduces growth. In this way it can leave the pond at the age of 110 days, while *P. bibronii* needs 200 d. *C. georgiana* is 4 mg at metamorphosis, *P. bibrionii* 35 mg dry, while the maximum weights are 500 and 200 mg, respectively. Both frogs have a (constant) specific somatic maintenance rate of some $400\,\mathrm{J\,d^{-1}cm^{-3}}$. The curves are based on DEB theory and have been estimated simultaneously per species [1002]. The step-up in respiration at birth is due to the onset of assimilation. The egg sizes differ by a factor 2 $E_0 = 65$ and 144 J, while the maximum adult sizes of these frogs differ by a factor 10, $W_d = 0.15$ and 1.2 g for *P. bibronii* and *C. georgiana*, respectively. Some parameters are for *P. bibronii*: $E_H^b = 9\,\mathrm{J}$, $E_H^j = 314\,\mathrm{J}$, $E_H^p = 2103\,\mathrm{J}$, $v = 0.040\,\mathrm{cm\,d^{-1}}$, $\kappa = 0.69$, $[\dot{p}_M] = 491\,\mathrm{J\,d^{-1}cm^{-3}}$. And for *C. georgiana*: $E_H^h = 1.5\,\mathrm{J}$, $E_H^b = 8\,\mathrm{J}$, $E_H^j = 71\,\mathrm{J}$, $E_H^p = 1686\,\mathrm{J}$, $v = 0.056\,\mathrm{cm\,d^{-1}}$, $\kappa_h = 0.86$, $\kappa_b = 0.61$, $[\dot{p}_M] = 369\,\mathrm{J\,d^{-1}cm^{-3}}$.

see figure 7.9. *Crinia* sports developmental acceleration, *Pseudophryne* does not. Their maximum body weights are similar, but *Crinia* has larger eggs. They both have a free-swimming tadpole stage, but we also found the pattern in species with direct development.

When *Crinia* hatches, before it starts feeding, and the water table in their pond is low, it decreases allocation fraction κ steadily till birth. Between birth and metamorphosis κ remains constant at a low level, and is reset after metamorphosis. This has several coordinated effects: respiration is increased, growth is decrease and maturation increased. In view of growth overheads, a decrease of growth might expected a decrease in respiration. But that does not happen: all reserve that embryos and juveniles allocate to the $(1 - \kappa)$ branch of mobilised reserve is spend on maturity maintenance and maturation, and eventually ends up as carbon doixide, water and N-waste, which comes with the use of dioxygen. The ecological significance is that they reach metamorphosis much earlier and smaller, allowing them to leave their pond before it dried out. It seems that the rate at which reserve is mobilized, which depends on the amounts of reserve and structure, is not changed. That is, the absolute mobilised flux steadily increases, and the one relative to structure steadily decreases. Mobilisation also does not change during the late embryo stage when the acceleration of maturation occurs. So respiration increases, but mobilisation does not.

Acceleration of maturation is remarkable, because it demonstrates the trait off between growth and maturation. Acceleration is achieved by changing κ, while it typically remains constant during the full life cycle [859]. The fact that it occurs in direct as well as indirectly developing frogs shows that the mode of development has nothing to do with acceleration of maturation.

In summary, the diagnostic characteristics of this type of acceleration are

- no change in size-specific feeding or mobilisation
- a temporary decrease in allocation fraction κ, with the effect of
  - a decrease of growth
  - an increase in maturation,
  - a reduction of the size at stage transitions
  - an increase in respiration

Since this type of acceleration is only found in embryos and juveniles, and the change in κ is only temporary, effects on reproduction are probably minor.

7.8.2.2 Intake

A rather frequently occurring form of acceleration is an increase in feeding rate combined with shifts in food preference. The feeding capacity just increases with squared structural length, but the amount of food and/or the food quality increases faster for some period and remains higher. Acceleration type X stands for 'food', and differs from other acceleration types because the parameters of the individual remain constant. The individual as a dynamic system does not change, only the interaction with the environment (food).

Neonates need high-quality food to cover their relatively high growth needs, compared to later stages that mainly need to cover maintenance needs. Fed with the same type of food, neonates do less well and can sport retarded growth. Taxa like fish are born tiny and change in food preference to bigger prey while growing. Not only because they are bigger themselves, but they also can swim faster. This can sometimes lead to an extra increase in food intake.

When some large individuals of perch *Perca fluviatilis* become cannibalistic, they grow into giants [1086]. The conversion efficiency from fish to fish is higher than from zooplankton to fish.

An increase in food availability means an increase in growth rate. Such a cause can be detected by comparing different diets and food availability levels. If the amount of upcurving of length-at-age is sensitive to such changes, this indicates for a type X acceleration. When fed with abundant food of high quality, length, or the cubic root of weight, increases linearly for neonates and incubation times are be well-predicted by the standard DEB model. So acceleration disappears in such situations. Although actual intake is increased, intake capacity is not.

In summary, the diagnostic characteristics of this type of acceleration are

- an increase in size-specific feeding and assimilation
- no increase in size-specific maximum assimilation

  an increase of growth, maturation and reproduction

  little change in size at stage transitions

  an increase in respiration
- acceleration disappears if high quality food is provided and incubation time is then predicted well by the standard model

7.8.2.3 Assimilation

Type A acceleration concerns in increase in surface area-specific assimilation capacity at some stage in development. This acceleration does not disappear at abundant high-quality food. Males of the longfin inshore squid seem to make this step-up at birth, see Figure 7.10, the southern elephant seal at puberty, see Figure 7.11. The curve for the male elephant seal assumes that puberty is an event; the data shows that puberty takes a period rather than an event, but this 'detail' is omitted for simplicity's sake. Food intake matches this capacity increase, since if not, we would not notice the increase. Where type X acceleration typically concerns a shift in food preference, type A acceleration is a step-up in the assimilation rate and with a constant digestion efficiency this goes with a step-up in the feeding rate. When assimilation is increased, but not reserve mobilisation (see next acceleration type), reserve capacity increases. As a consequence of the increase of reserve density (the amount of reserve per structure), mobilisation increases but not as a result of an increase in mobilisation capacity. This step-up in reserve capacity comes with a decrease of growth rate and an increase in capacity to survive starvation.

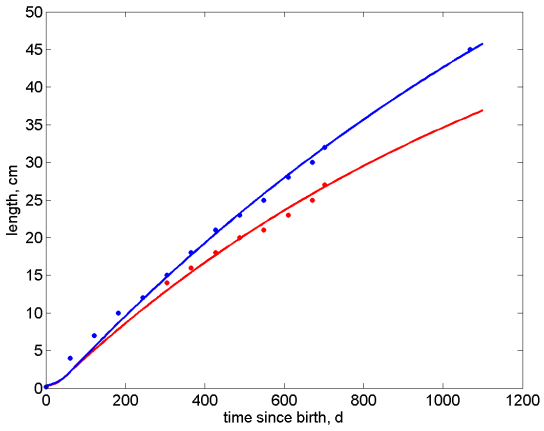

Figure 7.10: Length-at-time since birth of male (blue) and female (red) longfin inshore squid *Doryteuthis pealei*. Data from [1395]. The fits assume that the mean temperature was 15 °C. The parameters of both sexes are identical, except for the maximum specific assimilation rate $\{\dot{p}_{Am}\}$. The measured and predicted age at birth are

temperature (°C)	measured (d)	predicted (d)
22	10.71	11.14
18	18.54	17.35
15	26.75	25.83

Data from [944]

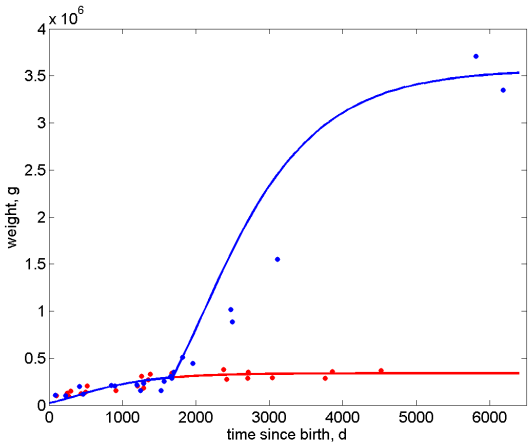

Figure 7.11: Weight-at-time since birth of male (blue) and female (red) southern elephant seal *Mirounga leonina*. Data from [213]. The fits assume that the body temperature was 38.1 °C. The parameters of both sexes are identical, except for the maximum specific assimilation rate $\{\dot{p}_{Am}\}$ of the male makes an instantaneous jump up at puberty.

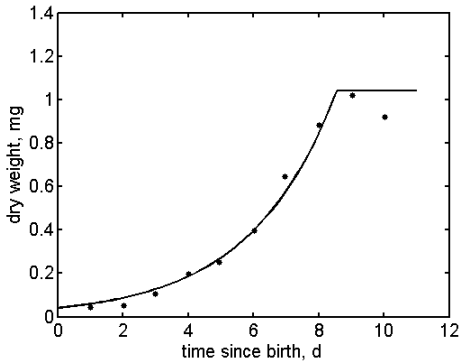

Figure 7.12: The pea aphid *Acyrthosiphon pisum* accelerates, like other insects, till the final moult, where growth is ceased. Data from [1287].

The function of this sex-dimorphy is probably social. So far, I don't know of examples of type A acceleration that affects both sexes.

In summary, the diagnostic characteristics of this type of acceleration are

- change in size-specific feeding and assimilation, but not mobilisation
- change in reserve structure ratio during acceleration at constant food

  an increase in growth, maturation, reproduction and respiration

  on effect on size at stage transitions

  an increase in respiration
- acceleration does not disappear if high quality food is provided
- incubation time is predicted well by the best fitting standard model

7.8.2.4 Mobilisation

A different and much more common form of acceleration is by the simultaneous increase of surface-area specific assimilation rate and energy conductance during the period between birth and metamorphosis [796]. The increase is proportional to structural length. The factor with which these parameters at birth are multiplied to arrive at those at (metabolic) metamorphosis, the acceleration factor, depends on feeding conditions. At high feeding levels, acceleration is larger than at low ones. So two individuals might be identical in terms of parameters and state variables (amounts of reserve and structure) at birth, might be in different environments during the early juvenile period, and remain different for the rest of their lives, even when exposed to the same environment. This pattern can be captured concisely in DEB theory by assuming that the embryo, late juvenile and adult stages behave as isomorphs, while the early juvenile stage increases its surface area proportional to structural volume, rather than volume to the power 2/3. Since assimilation and mobilisation increase simultaneously, reserve turnover increases, but reserve density is unaffected. Acceleration type $\mathcal{M}$ stands for 'morph', and differs from type A acceleration by the involvement of the energy conductance and by taking place between birth and metamorphosis. Metabolic metamorphosis is defined as the moment of switching back to

the isomorphic state and might, or might not, correspond with a sudden morphological change. This type of acceleration can be recognised by an up-curving of length-at-time since birth at constant food, an incubation time that is longer than expected without acceleration, and reserve density is unaffected.

Type $\mathcal{M}$ acceleration was first discovered in anchovy *Engraulis encrasicolus* [1079, 1080], bluefin tuna *Thunnus orientalis* [680] and zebrafish *Danio rerio* [49]. Acceleration has now been found in many ray-finned fish (actinopterygii) at scattered places, but not in cartilage fish (chondrichthyes), although all orders of this class are represented in the collection [792]. Ray-finned fish produce tiny eggs, compared to cartilage fish, and many (but not all) species first elongate their body as neonate and later become more bulky. When they elongate their body, they change in shape in the way described above. Quite a few other taxa, e.g. annelids, bivalves, echinoderms, have larval stages that have a very different morphology, compared to the late juvenile and adult stages. These larval stages develop slower than the late juvenile and adult stages. Other taxa, e.g. cephalopods, don't have deviating morphology of early juveniles, but still show acceleration. Figure 7.10 shows this for squid *Dorytheutis*. Although the acceleration is rather small in this example, and the up-curving of length-at-age is not really visible in the data (although it is in several other cephalopod species in the add_my_pet collection), type $\mathcal{M}$ acceleration is still detectable in squid because of the long incubation times. Without type $\mathcal{M}$ acceleration, the parameters that would describe post-embryonic growth correctly, would under-estimate incubation times considerably. Figure 7.12 gives an example of an insect, which sport extreme acceleration. The collembola *Folsomia* (enthognatha) represents a transition stage, where acceleration clearly occurs in the neonate till puberty, but most growth (after puberty) is of the von Bertalanffy type, so without acceleration. Insects evolved from crustations, according to many workers. It is remarkable that none of the 13 species of branchiopods in the collection have acceleration and all 4 species of maxillopods have it. Maxillopods have nymph stadia with a deviating morphology, which branchiopods don't have.

Figure 7.13 gives an overview of where type $\mathcal{M}$ acceleration has been found. It evolved at least 5 times in animal kingdom. We cannot be sure that accelerating metabolism is the original mode in animals and that it is lost in many taxa. Although species with larval stages typically accelerate, not all accelerating species have larval stages. Starting metabolism slowly seems to be more general than having larval forms. Larval development it thought to have evolved many times independently [538]. It is likely, therefore, that metabolic acceleration also evolved many times independently.

Big-bodied species typically get big-bodied offspring. The co-variation rules of DEB parameters specify that maturity at birth (and puberty) increase proportional with maximum structural volume. When we compare species of very different maximum body sizes, it is natural to compare them on the basis of maturity density: the ratio of maturity and maximum structural volume. Maturity density at birth and puberty have no clear relationship with acceleration, see Figure 7.14. The figure also illustrates that relative size at birth is taxon-specific, the lophotrochozoans, that is mostly the molluscs and specifically the bivalves, have really small neonates.

What could be the function of type $\mathcal{M}$ acceleration? The patterns for Actinopterygii, where relative length at birth hardly depends on ultimate length, suggest and neonates

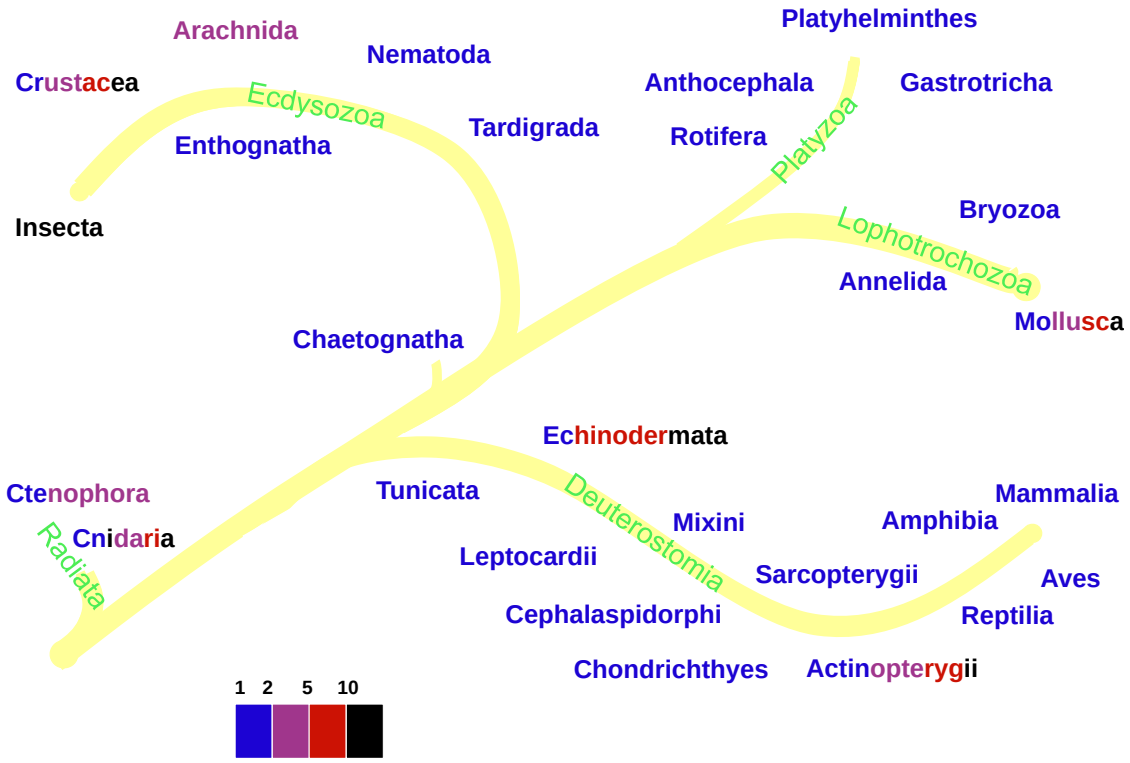

Figure 7.13: The distribution of acceleration in animal taxa. The colour of the font refers to the value of the acceleration coefficient. Taxa can have more or less accelerating species, which is why colours can vary within a word. The acceleration coefficient refers to the factor with which the specific assimilation and energy conductance for neonates have to be multiplied to arrive at values for late juveniles and adults.

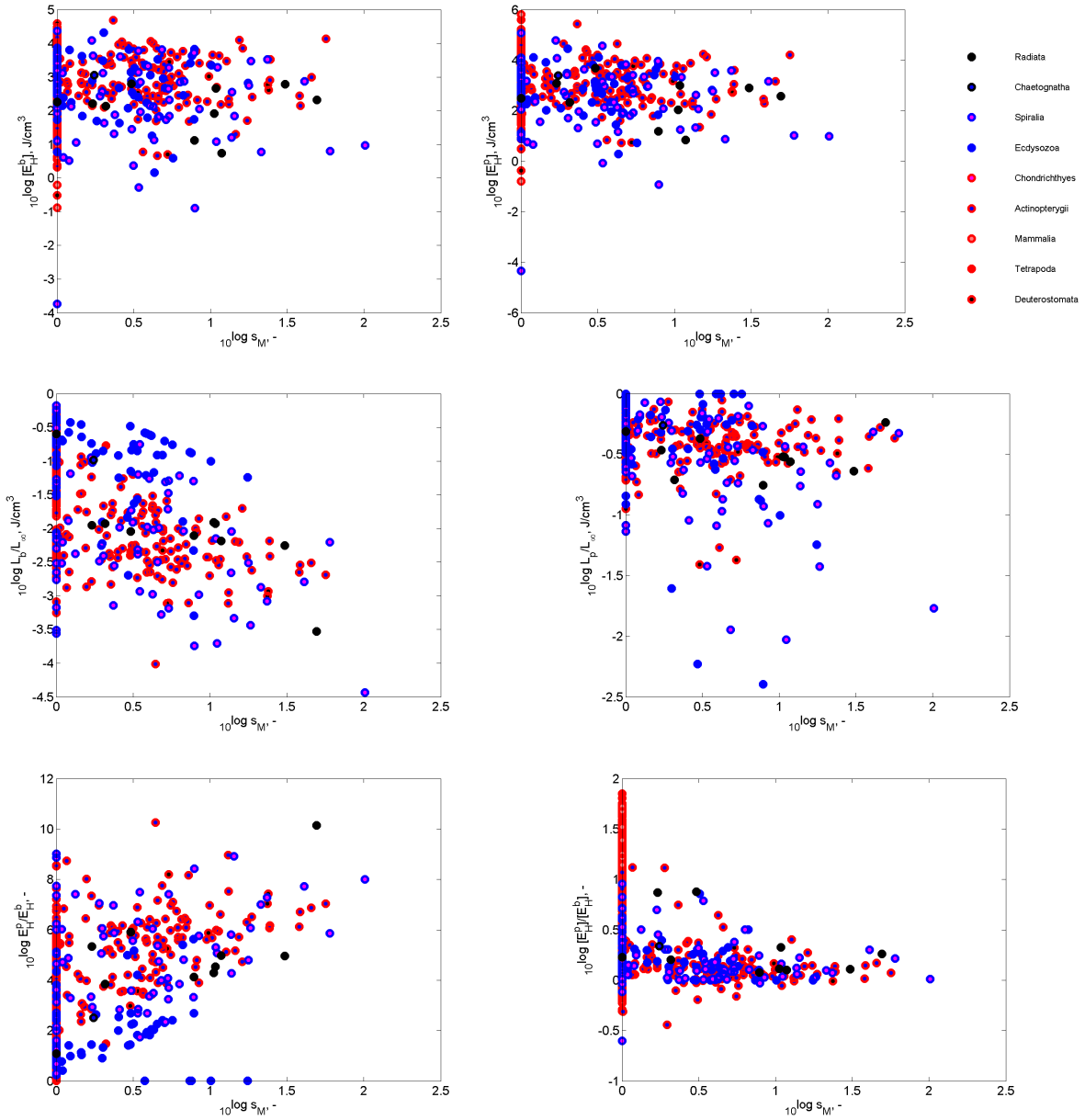

Figure 7.14: Maturity density at birth and puberty hardly depend on acceleration. Relative length at birth decreases with the acceleration factor, but length at puberty hardly so. As a consequence, maturity ratio $s_H^{pb} = E_H^p/E_H^b$ increases with the acceleration factor, but $[E_H^p]/[E_H^b]$ hardly so. Data for 785 species of the add_my_pet collection, sampling date 2017/05/14

need to have a particular small size to stay very close to the surface, where algae and small-bodied grazers are, which serve as food. Large-bodied fish species accelerate more to reduce the time to reach puberty. This seems to be an adaptation to the problem that their food are predators of their offspring. They try to super-saturate the predators of their neonates, by reducing the spawning period, and meeting in relatively small spawning grounds. This reminds of the strategy of bamboos, which suffer from chickens that feed on their seed. They synchronize flowering, skipping years, to avoid that these birds can build up high population densities.

Species range from supply to demand systems. Supply-species 'eat what is available' and demand-species 'eat what they need'. Insects and cnidarians are more to the supply end of the spectrum, bird and mammals to the demand end. The standard DEB model has a supply-organisation for growth and maturation (or reproduction) and a demand-organisation for maintenance. This set-up already reveals that no species are at the extremes of the spectrum. Independent of where species are in the spectrum, there must always be a balance between acquisition and use of resources.

Figure 8.9 shows the energy conductance as function of maximum structural length before and after acceleration. The scatter is large and there is no really clear pattern to discover for acceleration species. They do not have a low energy conductance before acceleration, combined with a typical one after, nor do they have a typical energy conductance before acceleration, combined with a larger one after. The figure does confirm the expectation of the co-variation rules of DEB theory that energy conductance does not depend on maximum structural length. When we look at the maturity levels at birth, metamorphosis and puberty, the pattern is much more clear: accelerating species have lower values than non-accelerating species, but the differences decrease from birth to puberty. Although size at birth, metamorphosis and puberty not only depend on parameter values, but also on food availability, generally size increases with maturity level. Figure 7.15 shows that the absolute neonate growth is larger for non-acceleration species, but at puberty it is smaller. Relative neonate growth is independent of acceleration, but accelerating species grow relatively faster at puberty. The difference between absolute and relative growth is caused by neonate accelerating species are relatively smaller than non-accelerating ones, see Figure 7.14.

A low metabolic rate at birth allows for more time to learn finding and selecting food, capturing it and digesting it. The specific somatic maintenance costs for accelerating and non-accelerating species turn out to be the same (not illustrated). So in terms of demand, a small size means less need for resources, which is thus less for accelerating species when young. Digestion frequently involves a gut flora that first needs to settle and might need time to function well in interaction with the host. The host supports gut flora by secreting polysaccharides into the gut, which might not only support the flora, but might also select for particular species. This illustrates the need of fine tuning between host and gut flora. A low level of metabolism only requires a low assimilation rate to support it. Endotherms have a high metabolic rate, because of their high body temperature, and don't sport acceleration. They do have advanced forms of parental care, however, and mammals typically feed milk to their neonates. Milk composition beautifully matches the needs of the neonate and changes dynamically with the needs. Kangaroos can have new neonates, while

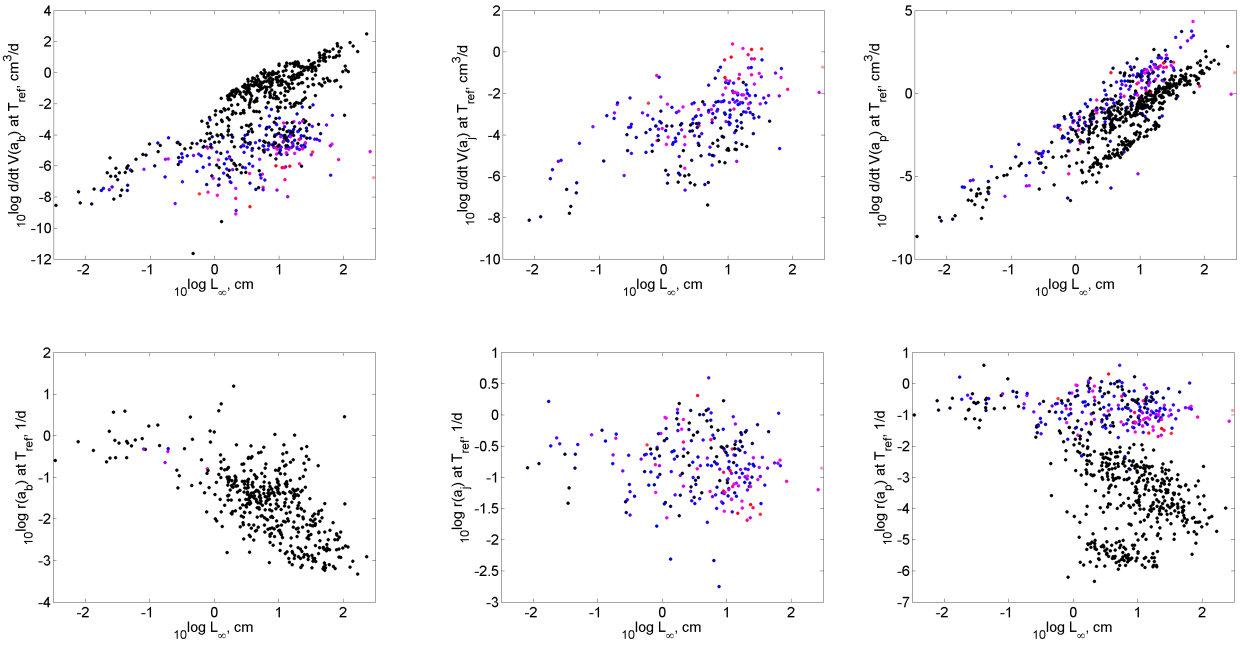

Figure 7.15: The growth rate (first row) at birth (left), metamorphosis (middle) and puberty (right), and the specific ones (second row) at 20 °C as functions of maximum structural length. Colours relate to acceleration: black = no acceleration, via blue and red, to white = max acceleration. Birth and metamorphosis coincide for non-accelerating species. Data from the add_my_pet collection, sampling date 2017/05/05 at 784 species.

the joey of the previous reproductive cycle still suckles, but from different nipples that give milk of different composition. Both birds and mammals typically inoculate the gut flora of their neonates via saliva. So here the parents assist in covering the metabolic need of the neonates; the consideration on acceleration helps to understand why parental care evolved in endotherms. These examples serve to illustrate that the initiation of assimilation is a delicate process and point to the functionality of starting slowly.

Since all species with larval forms have acceleration, and larvae thus have a lower metabolic rate before, compared to after metamorphosis, the suggested function of acceleration is in nice harmony with the idea of Garstang on the function of marine larvae as a mechanism for dispersal [465]. Slow metabolism allows for more dispersal time, especially in situations where dispersal rate is not metabolically controlled, but depend on water or air transport, for instance.

Not all larvae feed, while DEB theory defines birth as the onset of assimilation (potential), not as hatching. This classifies non-feeding larvae as embryos; they may represent transition to direct development, where the larval stage is completely taken out of the life cycle. With the reduction of the larval period, the embryo needs to increase metabolic rate, or the juvenile and adult need to decrease metabolic rate to avoid a sudden step up. Few data on metabolic rate of embryos and juveniles are available. Most data are consistent with the idea that acceleration of metabolism is initiated at birth. Data on early larval development of the Japanese oyster *Crassostrea gigantea* shows that acceleration only starts after birth and ceases at settlement. This pattern might be more general, and probably applies to most bivalves and possibly to many other taxa as well. The pondsnail *Lymnaea stagnalis* still has a trochophora larval stage, but it passes through this stage inside the egg. It even seems to start feeding inside the egg (pers. comm. Elke Zimmer), but continues to accelerate after hatching. Both examples show different cases of uncoupling between larval stage and acceleration.

In summary, the diagnostic characteristics of this type of acceleration are

- change in size-specific feeding and assimilation and mobilisation
- no change in reserve structure ratio during acceleration at constant food

  an increase in growth, maturation, reproduction and respiration

  on effect on size at stage transitions

  an increase in respiration
- acceleration does not appear if high quality food is provided
- incubation time is predicted well by the best fitting standard model

7.8.2.5 Temperature

Endotherms can accelerate during ontogeny due to an increase in body temperature, which stands for type T. Birds and mammals are ectotherms as embryo, and many need maternal care to keep body temperature in a healthy range. Since embryos are kept relatively warm by their parents, metabolism is high, so is heat generation, which increases with size.

Although this rest-heat is not sufficient to maintain a constant body temperature, it does elevate body temperature, also because surface area per volume decreases. While growing, their capacity to maintain a constant body temperature increases, which is visible as an acceleration of growth [765]. This is why (sigmoid) Gompertz curves and logistic curves have been used to describe size-at-age for birds, see Section 4.11.2. Measured and predicted the body temperature and growth curve of the guillemot match perfectly, see [775, Figure 4.28]. Such a cause can be detected by studying growth at sufficiently high environmental temperatures, such that body temperature is constant, even if the capacity to heat the body is less than adequate. This does not always work, however, because some species need a lower temperature and a temperature gradient during embryo development. Brunnich's guillemot seems to need a 40 °C temperature difference between one side of the egg and the other to develop [1173].

7.8.2 Derivation of Eq. (7.84)

All surface areas should be divided by the shape correction function $\mathcal{M}(V)$ during the juvenile I stage. Since the dimension length in the energy conductance $\dot{v}$ is the ratio of a volume and a surface area, $\dot{v}$ should be replaced by $\dot{v}^* = \dot{v}\mathcal{M}(V)$. The maximum specific searching rate $\{F_m\}$ and the maximum feeding rate $\{\dot{J}_{XAm}\}$ are both multiplied by the shape correction function, which implies that half saturation coefficient $K = \{\dot{J}_{XAm}\}/\{F_m\}$ remains constant; for constant food density X, the scaled functional response $f = \frac{X}{K+X}$ remains constant as well. The equation for $\frac{d}{dt}e$ is given in Eq. (2.11), where $\dot{v}$ is replaced by $\dot{v}^*$.

The specific growth rate for the standard DEB model is given in Eq. (2.21): $\dot{r} = \dot{v}\frac{e/L-(1+L_T/L)/L_m}{e+g}$. Since $g = \frac{[E_G]\dot{v}}{\kappa\{\dot{p}_{Am}\}}$, and $\dot{v}$ as well as $\{\dot{p}_{Am}\}$ are affected by the changes in shape during the juvenile I stage in the same way, g is not affected. Since $L_m = \frac{\kappa\{\dot{p}_{Am}\}}{[\dot{p}_M]} = \frac{\dot{v}}{\dot{k}_M g}$, L_m is affected and should be replaced by L_m^*. The replacement of $\dot{v}$ by $\dot{v}^*$ gives the result for $\dot{r}$. The equation for $\frac{d}{dt}L$ is given above Eq. (2.23); notice that $\dot{v}$ should be $\dot{r}$, as mentioned in the errata.

The equation for $\frac{d}{dt}U_H$ found from that for $\frac{d}{dt}E_H$ given in Eq. (2.5.2), that for $\dot{p}_C$ given in Eq. (2.12) and that for $\dot{p}_J$ given in Eq. (2.19). The substitutions for the standard model for juveniles amount to

$$\begin{aligned}
\frac{d}{dt}E_H &= (1-\kappa)E(\frac{\dot{v}}{L} - \dot{r}) - \dot{k}_J E_H && (7.38)\\
&= (1-\kappa)eL^3\frac{\{\dot{p}_{Am}\}}{\dot{v}}(\frac{\dot{v}}{L} - \dot{r}) - \dot{k}_J E_H && (7.39)\\
&= (1-\kappa)eL^2\{\dot{p}_{Am}\}\frac{g + (L+L_T)/L_m}{e+g} - \dot{k}_J E_H && (7.40)
\end{aligned}$$

where L_T is set equal to zero. In this equation $\{\dot{p}_{Am}\}$ should be replaced by $\{\dot{p}_{Am}\}^*$ and L_m by L_m^* for changing shape during the juvenile I stage. Now we divide by the left and right hand sides by $\{\dot{p}_{Am}\}$ to remove energy, $U_H = E_H/\{\dot{p}_{Am}\}$, but this assimilation power

$\{\dot{p}_{Am}\}$ only serves as a reference to eliminate the dimension energy, and should not be replaced. The result is

$$\frac{d}{dt}U_H = (1-\kappa)eL^2\frac{\{\dot{p}_{Am}\}^*}{\{\dot{p}_{Am}\}}\frac{g+L/L_m^*}{e+g} - \dot{k}_J U_H \tag{7.41}$$

$$= (1-\kappa)eL^2\frac{g^*+L/L_m}{e+g} - \dot{k}_J U_H \tag{7.42}$$

which is given in Eq. (7.84).

7.8.2 Metamorphosis at constant food

The amount of metabolic acceleration of type $\mathcal{M}$ at abundant food can be quantified by acceleration factor $s_{\mathcal{M}} = \mathcal{M}(V_j) = L_j/L_b$. The end of acceleration, an event called metamorphosis j, can, or cannot, be linked to an abrupt change in morphology. The use of physical length measures is problematic when shapes are changing. Generally the shape coefficient before, $\delta^b_{\mathcal{M}}$, and after, $\delta^j_{\mathcal{M}}$, acceleration can differ. Although no strict rules exist for how to link physical to structural length during acceleration, a natural choice for a shape coefficient is $\delta_{\mathcal{M}}(L) = w_b\delta^b_{\mathcal{M}}\delta^b_{\mathcal{M}} + (1-w_a)\delta^j_{\mathcal{M}}$, with $w_a = \mathcal{M}(L^3)$.

If food density is constant, and $e = f$, the juvenile I is growing exponentially at specific growth rate $\dot{r}_j$, say, where $\mathcal{M}(V) = L/L_b$ increases from $\mathcal{M}(V_b) = 1$ to $\mathcal{M}(V_j) = L_j/L_b = s_{\mathcal{M}}$. Type $\mathcal{M}$ metabolic acceleration is assumed to affect $\{\dot{F}_m\}$, $\{\dot{p}_{Am}\}$, $\dot{v}$ and $\{\dot{p}_T\}$ before acceleration by a factor $s_{\mathcal{M}}$ after the end of acceleration.

Work with Starrlight Augustine and Goçalo Marques showed the following simplifications. At metamorphosis length growth switches to von Bertalanffy growth in a smooth way, with the implication that $L_j = \frac{L_\infty}{1+\frac{\dot{r}_j}{3\dot{r}_B}}$. $L_m = \frac{\dot{v}}{\dot{k}_M g}$ does not have the interpretation of the maximum length. We have for $L(a_b) = L_b$ and $L(a_j) = L_j$ and $L_T = \frac{\{\dot{p}_T\}}{[\dot{p}_M]} < eL_m - L_b$, where $\{\dot{p}_T\}$ is the value at birth, while $\{\dot{p}_T\} = 0$ before birth.

$$\begin{aligned}
\frac{d}{da}L &= L\dot{r}_j/3 \quad \text{with } \dot{r}_j = \dot{v}\frac{e/L_b - (1+L_T/L_b)/L_m}{e+g} \overset{L_T=0}{=} \dot{k}_M\frac{eL_m/L_b - 1}{1+e/g} \text{ for } a_b \le a < a_j\\
L(a) &= L_b\exp\left(\dot{r}_j(a-a_b)/3\right) \quad \text{for } a_b \le a < a_j\\
\frac{d}{da}L &= \dot{r}_B(L_\infty - L) \quad \text{with } \dot{r}_B = \frac{\dot{k}_M/3}{1+e/g} \text{ and } L_\infty = eL_m s_{\mathcal{M}} - L_T s_{\mathcal{M}} \text{ for } a \ge a_j\\
L(a) &= L_\infty - (L_\infty - L_j)\exp\left(-\dot{r}_B(a-a_j)\right) \text{ for } a \ge a_j
\end{aligned}$$

The specific growth rate $\dot{r}$ relates to the von Bertalanffy growth rate $\dot{r}_B$ as $L\dot{r}/3 = \dot{r}_B(L_\infty - L)$, which leads to

$$\dot{r} = 3\dot{r}_B\frac{L_\infty - L}{L} = \frac{\dot{k}_M}{1+e/g}\frac{eL_m s_{\mathcal{M}} - L_T s_{\mathcal{M}} - L}{L} = \frac{\dot{v}}{e+g}\frac{es_{\mathcal{M}} - (L + L_T s_{\mathcal{M}})/L_m}{L}$$

with $\dot{r} = \dot{r}_j$ for $L = L_j$.

To find length at metamorphosis L_j given maturity at metamorphosis E_H^j, we first need the mobilisation rate from Eq. (2.12) and then the change in maturity from Eq. (2.18)

$$\begin{aligned} \dot{p}_C &= e[E_m]L^3(\dot{v}s_{\mathcal{M}}/L - \dot{r}) \overset{L=L_j}{=} f[E_m]L_j^3(\dot{v}/L_b - \dot{r}_j) \\ \frac{d}{da}E_H &= (1-\kappa)\dot{p}_C - \dot{k}_J E_H \quad \text{or} \quad \frac{d}{da}U_H = (1-\kappa)eL^3(1/L_b - \dot{r}/\dot{v}) - \dot{k}_J U_H \end{aligned}$$

starting from the state at birth $(a, e, L, E_H) = (a_b, f, L_b, E_H^b)$. The length at metamorphosis is found by integration of

$$\frac{d}{dE_H}L = \frac{\dot{r}_j L/3}{(1-\kappa)\dot{p}_C - \dot{k}_J E_H} \quad \text{with } L(E_H^b) = L_b \text{ and } L(E_H^j) = L_j = \int_{E_H^b}^{E_H^j} \left(\frac{d}{dE_H}L\right) dE_H$$

An alternative way to find L_j is to solve the ODE for E_H first. For t being the time since birth, $t = a - a_b$

$$E_H(t) = (1-\kappa)f[E_m]L_b^3(\dot{v}/L_b - \dot{r}_j)\frac{\exp(\dot{r}_j t) - \exp(-\dot{k}_J t)}{\dot{r}_j + \dot{k}_J} + E_H^b \exp(-\dot{k}_J t)$$

Now we should solve $E_H(t_j) = E_H^j$ and the solution for t_j must be found numerically. Finally we have $L_j = L_b \exp(\dot{r}_j t_j/3)$.

The change in length just before and after metamorphosis are equal, but the change of these changes, so the acceleration, makes a jump. These second derivatives, for $L_T = 0$, are given by $\frac{d^2}{dt^2}L\big|_{L\uparrow L_j} = \frac{\dot{r}_j^2}{3^2}L_j$ and $\frac{d^2}{dt^2}L\big|_{L\downarrow L_j} = -\dot{r}_B^2(L_\infty - L_j)$, and their ratio is $-(eL_m/L_b - 1)^3$. Although this ratio is independent of L_j, $L_\infty = eL_m s_{\mathcal{M}}$ still depends on L_j.

In scaled quantities, for $u_E = \frac{E}{g[E_m]L_m^3}$, $v_H = \frac{E_H}{(1-\kappa)g[E_m]L_m^3}$, $l = \frac{L}{L_m}$, $\tau = t\dot{k}_M$ (where t is time since birth), $k = \frac{\dot{k}_J}{\dot{k}_M}$, $r_B = \frac{\dot{r}_B}{\dot{k}_M}$, $r_j = \frac{\dot{r}_j}{\dot{k}_M}$, $q = \frac{\ddot{q}}{\dot{k}_M^2}$, $h_a = \frac{\ddot{h}_a}{\dot{k}_M^2}$, $h = \frac{\dot{h}}{\dot{k}_M}$ we have the following. The scaled specific growth rates r during and after acceleration amount for $l_\infty = s_{\mathcal{M}}(f - l_T)$ and $r = 3r_B(l_\infty/l - 1)$ to

$$r_j = \frac{g}{f+g}\frac{f - l_T - l_b}{l_b} \quad \text{and} \quad r = \frac{g}{f+g}\frac{fs_{\mathcal{M}} - l_T s_{\mathcal{M}} - l}{l} \quad \text{while} \quad r_B = \frac{g/3}{f+g}$$

where $r_j = r$ for $l = l_j$. Or in terms of $u_E = el^3/g$ rather than $f = e = gu_E/l^3$

$$r_j = \frac{gu_E l_b^{-1} - l^3 l_T/l_b - l^3}{u_E + l^3} \quad \text{and} \quad r = \frac{gu_E l^{-1} s_{\mathcal{M}} - l^2 l_T s_{\mathcal{M}} - l^3}{u_E + l^3}$$

Given $(\tau, e, l, v_H) = (\tau_j, f, l_j, v_H^j)$ at metamorphosis and assuming $v_H^j < v_H^p$

$$\begin{aligned} \frac{d}{d\tau}l &= lr_j/3 \quad \text{or} \quad lr/3 = r_B(l_\infty - l) \quad \text{before or after } j \\ \frac{d}{d\tau}u_E &= fl^3/l_b - u_E(g/l_b - r_j) \quad \text{or} \quad fs_{\mathcal{M}}l^2 - u_E(gs_{\mathcal{M}}/l - r) \quad \text{before or after } j \end{aligned}$$

$$\begin{aligned}
\frac{d}{d\tau}v_H &= el^3(1/l_b - r_j/g) - kv_H \quad \text{or} \quad el^2(s_{\mathcal{M}} - lr/g) - kv_H \quad \text{before or after } j\\
\frac{d}{d\tau}q &= (ql^3 s_G + h_a)e(s_{\mathcal{M}} g/l - r) - rq\\
\frac{d}{d\tau}h &= q - rh\\
\frac{d}{dv_H}l &= \frac{r_j l/3}{el^3(1/l_b - r_j/g) - kv_H} \quad \text{or} \quad \frac{rl/3}{el^2(s_{\mathcal{M}} - lr/g) - kv_H} \text{ with}
\end{aligned}$$

$$l(v_H^b) = l_b; \quad l(v_H^j) = l_j = \int_{v_H^b}^{v_H^j} \left(\frac{d}{dv_H}l\right) dv_H; \quad l(v_H^p) = l_p = \int_{v_H^j}^{v_H^p} \left(\frac{d}{dv_H}l\right) dv_H$$

Scaled maturity during acceleration ($\tau < \tau_j$) amounts to

$$v_H(\tau) = fl_b^3 \frac{1/l_b - r_j/g}{k + r_j}(\exp(r_j\tau) - \exp(-k\tau)) + v_H^b \exp(-k\tau)$$

with $v_H(\tau_j) = v_H^j$, $l(\tau_j) = l_j = l_b \exp(\tau_j r_j/3)$ or $\exp(\tau_j r_j) = (l_j/l_b)^3 = s_{\mathcal{M}}^3$ and $\exp(-k\tau_j) = s_{\mathcal{M}}^{-3k/r_j}$. Substitution gives

$$v_H^j = fl_b^3 \frac{1/l_b - r_j/g}{k + r_j}(s_{\mathcal{M}}^3 - s_{\mathcal{M}}^{-3k/r_j}) + v_H^b s_{\mathcal{M}}^{-3k/r_j}$$

from which $s_{\mathcal{M}}$, and so l_j, can be solved numerically. Change in scaled maturity after acceleration ($\tau \geq \tau_j$) is $\frac{d}{d\tau}v_H = fl^2(s_{\mathcal{M}} - \frac{l_\infty - l}{f+g}) - kv_H = b_2 l^2 + b_3 l^3 - kv_H$ for $b_2 = fs_{\mathcal{M}} - b_3 l_\infty$ and $b_3 = \frac{f}{f+g}$. Scaled maturity as function of scaled time since metamorphosis becomes

$$v_H(\tau) = \left(v_H^j + \sum_{i=0}^{3} a_i\right) e^{-k\tau} - \sum_{i=0}^{3} a_i e^{-ir_B\tau}$$

with

$$\begin{aligned}
a_0 &= -(b_2 + b_3 l_\infty) l_\infty^2/k\\
a_1 &= -(2b_2 + 3b_3 l_\infty) l_\infty l_\delta/(r_B - k)\\
a_2 &= (b_2 + 3b_3 l_\infty) l_\delta^2/(2r_B - k)\\
a_3 &= -b_3 l_\delta^3/(3r_B - k)
\end{aligned}$$

$$\begin{aligned}
\tau_p &= \tau_j + \frac{1}{r_B}\ln\frac{l_\infty - l_j}{l_\infty - l_p}\\
l_\delta &= l_\infty - l_j\\
l_\infty &= s_{\mathcal{M}}(f - l_T)
\end{aligned}$$

from with l_p can be solved numerically, while $v_H(\tau_p) = v_H^p$.

The reproduction rate $\dot{R}$ as function of length L can be found from Eq. (2.55)

$$\begin{aligned}
\dot{p}_C &= e[E_m]L^3(\dot{v}s_{\mathcal{M}}/L - \dot{r})\\
&= \{\dot{p}_{Am}\}\frac{eL^2}{e+g}(gs_{\mathcal{M}} + (L + L_T s_{\mathcal{M}})/L_m) = \{\dot{p}_{Am}\}S_C\\
\dot{R} &= \frac{\kappa_R}{E_0}\dot{p}_R = \frac{\kappa_R}{E_0}\left((1-\kappa)\dot{p}_C - \dot{k}_J E_H^p\right) = \frac{\kappa_R}{U_E^0}\left((1-\kappa)S_C - \dot{k}_J U_H^p\right)
\end{aligned}$$

The gonado-somatic index (4.89) at time t_1 since emptying the reproduction buffer amounts to

$$Q = \frac{M_{E_R}}{M_E + M_V} = \frac{t_1 \dot{p}_R}{E + L^3[M_V]\mu_E} = \frac{t_1 \dot{p}_R}{L^3(f[E_m] + [E_G]y_{VE})}$$

For a fully grown individual, with $\{\dot{p}_T\} = 0$ and $\dot{r} = 0$ and $L = fL_m s_{\mathcal{M}} = L_\infty$ and $e = f$, the mobilisation rate reduces to $\dot{p}_C = e[E_m]L_\infty^2 s_{\mathcal{M}} \dot{v} = f^3[E_m]L_m^2 s_{\mathcal{M}}^3 \dot{v}$ and the allocation to reproduction to $\dot{p}_R = (1-\kappa)\dot{p}_C - \dot{k}_J E_H^p = (1-\kappa)f^3[E_m]L_m^2 s_{\mathcal{M}}^3 \dot{v} - \dot{k}_J E_H^p$. The gonado-somatic index becomes

$$Q = \frac{t_1 \dot{k}_M g/f^3}{f + \kappa g y_{VE}} \left((1-\kappa) f^3 - \frac{\dot{k}_M^2 g^2}{s_{\mathcal{M}}^3 \dot{v}^2 \{\dot{p}_{Am}\}} \dot{k}_J E_H^p \right)$$

This reduces to (4.89) for $s_{\mathcal{M}} = 1$.

If food is constant, $e = f$, and the growth period is short, relative to the life span, $\dot{r} \simeq 0$, $L \simeq e s_{\mathcal{M}} L_m - L_T$ or $r \simeq 0$, $l \simeq f s_{\mathcal{M}} - l_T$. Further, for $l_T = 0$, we have $\frac{d}{d\tau} q = q f^3 s_{\mathcal{M}}^3 s_G g + h_a g$, $\frac{d}{d\tau} h = q$ and $h_W^3 = \frac{h_a g}{6}$, $h_G = s_G s_{\mathcal{M}}^3 f^3 g$. Substitution gives $\frac{d}{d\tau} q = q h_G + 6 h_W^3$ and $q(\tau) = \frac{6 h_W^3}{h_G} (\exp(h_G \tau) - 1)$. Since $\frac{d}{d\tau} S = -hS$, so $S(\tau) = \exp(-\int_0^\tau h(\nu)\, d\nu) = \exp(-q(\tau))$. For $S(\tau_m) = 2^{-1}$ or $q(\tau_m) = \log 2$ or the median life span τ_m is the root of $0 = \log(2) + \frac{6 h_W^3}{h_G^3} (1 - \exp(\tau_m h_G) + \tau_m h_G + \tau_m^2 h_G^2/2)$, see Eqn (6.5) of DEB3. For $s_G \to 0$, this equation reduces and can be solved, leading to $\tau_m = \left(\frac{\log 2}{h_W^3} \right)^{1/3}$.

7.8.2 Maturation ceasing at puberty

The minimum scaled functional response to reach puberty in the case of acceleration at constant food, is found from the conditions that both growth and maturation cease eventually. Growth ceases if $L_\infty = L_p$, which leads to $l_p = (f - l_T) s_{\mathcal{M}}$. Maturation ceases if $(1-\kappa)\dot{p}_C = \dot{k}_J E_H^p$, with $\dot{p}_C$ at $L = L_p$ and $\dot{r} = 0$ equals $\dot{p}_C = f[E_m] L_p^2 \dot{v} s_{\mathcal{M}}$. Substitution gives $k v_H^p = f(f - l_T)^2 s_{\mathcal{M}}^3$. In absence of acceleration, we have $s_{\mathcal{M}} = 1$ and the condition reduces to the one that is found in Section 2.6.3 of the comments. Section 4.10.0.3 of the comments states that supply stress at constant food amounts to $s_s = \kappa^2 (1-\kappa) k v_H^p s_{\mathcal{M}}^{-3}$. Substitution in the minimum f condition learns that f can also be found from $s_s = \kappa^2 (1-\kappa) f (f - l_T)^2$.

7.8.2 Acceleration of metabolism at birth

Type $\mathcal{M}$ acceleration amounts to the insertion of a V1-morphic stage between birth and metamorphosis, which has the effect that $\{\dot{p}_{Am}\}$ and $\dot{v}$ increase during this period [796]. The effect on growth is illustrated in Figure 7.16. The transition from the V1- to the iso-morphic stage is smooth, since the growth rate depends on reserve mobilisation, so on the amounts of reserve and structure, and the amounts don't change suddenly. The resulting exo-von Bertalanffy curve has 4 parameters. The smooth transition between the exponential and von Bertalanffy stages implies $\dot{r}_j = 3\dot{r}_B(e L_m / L_j - 1)$. Apart from

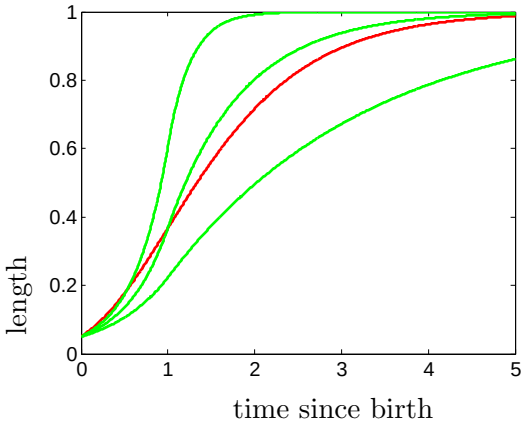

Figure 7.16: Length as function of time at constant food during acceleration. Time is scaled such that the inclination point (i.e. transition from V1- to iso-morphic stage) is at value 1. Length is scaled such that the asymptote has value 1. The green curves represent expo-von Bertalanffy-curves, for different choices of maximum growth rates, the red curve is the Gompertz one.

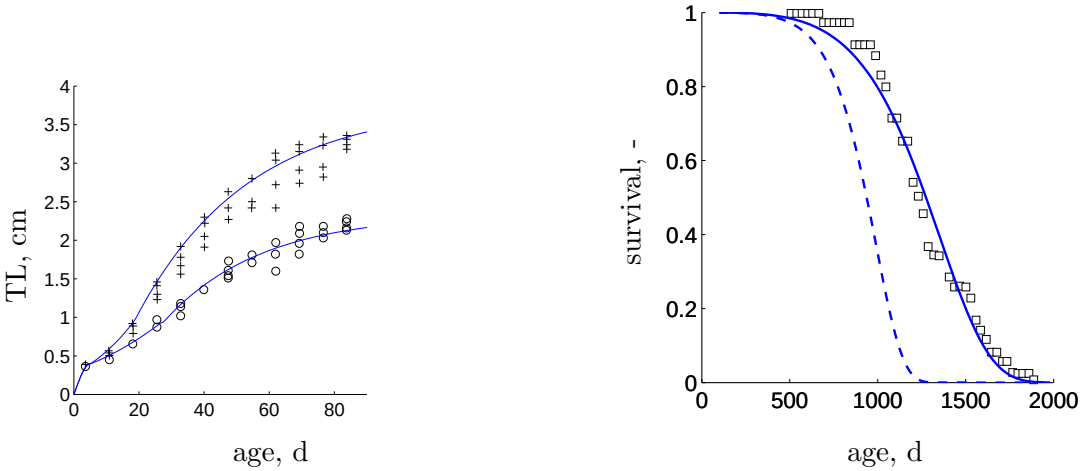

Figure 7.17: Total Length (snout till end of caudal fin, left) and survival probability (right) as functions of age for the zebrafish *Danio rerio*. From [49], based on data from [830, 479].

anchovy *Engraulis encrasicolus* [1079], this also has been found for Pacific bluefin tuna *Thunnus orientalis* [680], zebrafish *Danio rerio* [49], copepods, crabs and quite a few other species, see Figure 7.13. A remarkable implication is that if two identical neonates are exposed to different temperature and/or food conditions, their values for $\{\dot{p}_{Am}\}$ and $\dot{v}$ differ at metamorphosis and remain different, even if they experience the same conditions after metamorphosis. Figures 7.17 and 7.18, show a small sub-sample of the zebrafish data that have been used to estimate parameter values (see the add_my_pet collection. The acceleration by a factor $l_j/l_b = 3$ is clearly visible in the growth data of [830]. The parameters, as given in Figure 7.18 can be used to obtain the maturity levels at the various life stages, see Tables 7.3 and 7.4.

During the V1-morphic early juvenile stage, assimilation, dissipation and growth are all proportional to weight at constant food, so respiration is proportional to weight. This is exactly what [1123, 713, 992] found for prior to metamorphosis in seven species of fish: common carp (*Cyprinus carpio*), rainbow trout (*Oncorhynchus mykiss*), red sea bream (*Pagrus major*), ocean pout (*Macrozoarces americanus*), lumpfish (*Cyclopterus lumpus*),

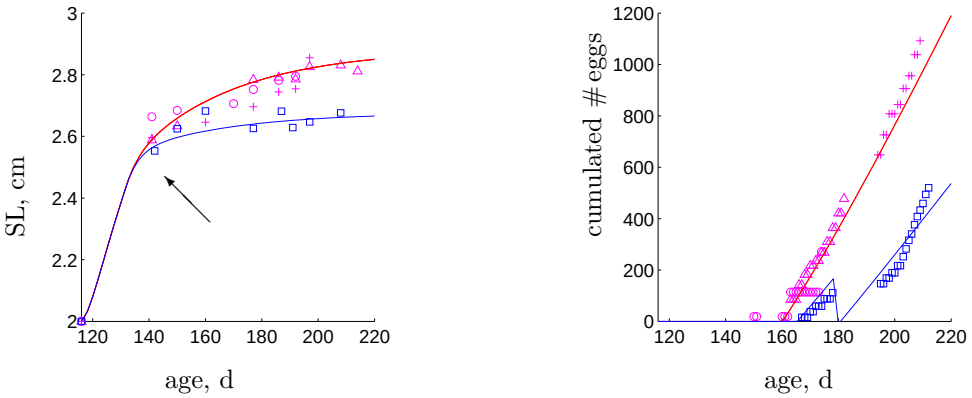

Figure 7.18: Observations, the symbols refer to the different individuals, and model predictions, solid lines, for growth (left) and reproduction (right) during 82 days of caloric restriction at two feeding levels which are estimated at $f_1 = 0.74$ and $f_2 = 0.69$. Animals are 116 d of age and 2 cm standard length SL (tip of snout till base of caudal fin) at arrival. They are acclimated to laboratory conditions for two weeks. Caloric restriction is initiated at age 132 d (arrow). From [49]. The shape coefficient during the acceleration was assumed to decrease linearly in length: $\delta_{\mathcal{M}}(L) = \delta^b_{\mathcal{M}} + (\delta^j_{\mathcal{M}} - \delta^b_{\mathcal{M}})\frac{L_j - L}{L_j - L_b}$. In combination with data illustrated in Figure 7.17 and other data, the parameters were estimated to be: $\{\dot{p}_{Am}\} = 246.3\,\mathrm{J\,d^{-1}cm^{-2}}$ (for the embryo), $\dot{v} = 0.0278\,\mathrm{cm\,d^{-1}}$ (for the embryo), $\kappa = 0.437$, $\kappa_X = 0.5$ (for Tetramin), $\kappa_R = 0.95$, $[\dot{p}_M] = 500.9\,\mathrm{J\,d^{-1}cm^{-3}}$, $\dot{k}_J = 0.0166\,\mathrm{d^{-1}}$, $[E_G] = 4652\,\mathrm{J\,cm^{-3}}$, $E^b_H = 0.54\,\mathrm{J}$, $E^j_H = 19.66\,\mathrm{J}$, $E^p_H = 2062\,\mathrm{J}$, $T_A = 3000\,\mathrm{K}$, $\ddot{h}_a = 1.96\,10^{-9}\,\mathrm{d^{-2}}$, $s_G = 0.0405$, $\delta^b_{\mathcal{M}} = 0.1325$ (for TL of embryo), $\delta^j_{\mathcal{M}} = 0.1054$ (for TL after metamorphosis).

Table 7.3: Maturity levels for the embryonic developmental milestones of the zebrafish *D. rerio*. Developmental stages and ages (28.5 °C) are as defined by [714]. Ages are presented in hours post fecundation, hpf. The ages depend on temperature and food conditions, the maturity levels do not.

	Stage	**Age** hpf	E_H mJ
	2-cell	0.75	0.01
	4-cell	1	0.02
	8-cell	1.25	0.02
	16-cell	1.5	0.02
	32-cell	1.75	0.02
	64-cell	2	0.03
	128-cell	2.25	0.03
	256-cell	2.5	0.04
	512-cell	2.75	0.05
	1k-cell	3	0.07
	High	3.33	0.088
	Oblong	3.66	0.11
	Sphere	4	0.14
	Dome	4.33	0.171
	30%-epiboly	4.66	0.20
	50%-epiboly	5.25	0.27
	Germ-ring	5.66	0.33

	Stage	**Age** hpf	E_H mJ
	Shield	6	0.38
	75%-epiboly	8	0.71
	90%-epiboly	9	0.96
	Bud	10	1.3
	3-somite	11	1.7
	6-somite	12	2.1
	14-somite	16	4.6
	21-somite	19.5	8.0
	26-somite	22	11.2
	Prim-6	25	16.0
	Prim-16	31	29.5
	Prim-22	35	41.4
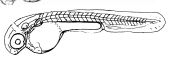	High-pec	42	68.9
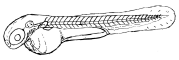	Long-pec	48	99.6
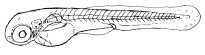	Pec-fin	60	180
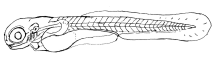	Protruding-mouth	72	280

Table 7.4: Maturity levels for post embryonic developmental milestones of the zebrafish *D. rerio*. Standard length SL (tip of snout till base of caudal fin), developmental stages and names as given in [1069]. Ages, in days post fecundation (dpf), at $f = 0.63$ and $f = 1$ as well as SL at $f = 1$ are model predictions at 28.5 °C. Birth corresponds with stage pSB+; metamorphosis is just before stage PR; puberty corresponds with stage A. The ages and lengths depend on temperature and food conditions, the maturity levels do not.

	Stage	**age** dpf	**SL** cm	**age** dpf	**SL** cm	E_H J
		f=0.63		f=1		
	pSB+ swim bladder inflation	4.5	3.8	4.0	3.7	**0.5**
	Fle early flexion	7.2	4.5	6.3	4.6	**1.1**
	CR caudal fin ray	8.9	4.9	7.4	5.1	**1.6**
	AC anal fin condensation	10.5	5.4	8.5	5.9	**2.3**
	DC dorsal fin condensation	12.3	5.7	9.6	5.8	**3.3**
	MMA metamorphic melanophore app.	12.9	5.9	10.0	6.0	**3.8**
	AR anal fin ray appearance	14.2	6.2	10.9	6.3	**5**
	DR dorsal fin ray appearance	15.0	6.4	11.4	6.5	**5.9**
	PB+ following pelvic fin bud app.	18.7	7.6	13.8	7.7	**12.7**
	PR pelvic fin ray appearance	21.3	8.5	15.5	8.5	**21.9**
	PR+ following pelvic fin ray app.	22.5	9.2	16.3	9.3	**27.9**
	SP onset of posterior squamation	23.8	9.8	17.2	9.8	**34.9**
	SA onset of anterior squamation	25.0	10.4	17.9	10.5	**42.3**
	J juvenile	26.2	11.0	18.7	11.0	**50.9**
	J+ following juvenile	30.8	13.0	21.6	13.2	**91.7**
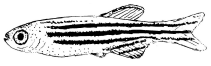	J++ following juvenile	40.7	16.0	27.5	16.4	**221.6**
 	A adults	218	26.0	59.9	30.6	**2061**

shorthorn sculpin (*Myoxocephalus scorpius*), yellowtail kingfish (*Seriola lalandi*). After metamorphosis, respiration was found to be less than proportional to weight, again as expected.

Acceleration has the effect that the residence time of molecules in the reserve does not change during acceleration, see Section 2.3 of the comments, while it would increase with length in absence of acceleration. The maximum reserve residence time $t_{Em} = L_m/\dot{v}$ is unaffected by acceleration. The mean value of energy conductance $\dot{v}$ at 20 °C before and after acceleration are 0.05 and 0.11 cm d^{-1} and the corresponding coefficients of variation are 1.2 and 2.1, respectively. So both in mean and in variation coefficient, this means a step-up of a factor 2 for all species together. Species that accelerate have a mean $\dot{v}$ before and after acceleration of 0.035 and 0.26 cm d^{-1}, while species that don't accelerate have 0.055 cm d^{-1}. Species that accelerate start with a relatively low $\dot{v}$ and end-up with a substantially larger one.

Bivalves vary on the acceleration scheme by accelerating at a later stage: the embryo and early juvenile stages follow the standard model, the V1-morphic phase is around metamorphosis, after which they follow the standard model again. The jump up in $\{\dot{p}_{Am}\}$ and $\dot{v}$ is around a factor 10 for *Crassostrea*, compared to pre-metamorphosis, as is beautifully illustrated in its mydata-file. The reserve capacity $[E_m] = \{\dot{p}_{Am}\}/\dot{v}$ is unaffected by the acceleration.

The Gompertz growth curve

$$L(t) = L_\infty \exp(-\exp(\delta_G - \dot{r}_G t))$$

where $\delta_G = \ln(\ln(L_\infty/L_b))$ and t is time since birth, is frequently used to describe growth empirically. It has 3 parameters, while the expo-von Bertalanffy curve has 4, so that latter has more plasticity in shape. We can compare both curves on the basis of the same values for length at birth $L_b = L(0)$, ultimate length $L_\infty = L(\infty)$ and moment of inclination, t_j. The Gompertz curve reaches maximum growth at $t_j = \delta_G/\dot{r}_G$, with $L_j = L(t_j) = L_\infty/e$ and $\frac{d}{dt}L(t_j) = L_\infty \dot{r}_G/e$. The expo-von Bertalanffy curve has $\frac{d}{dt}L(t_j) = L_j\dot{r}_j$ and $\dot{r}_j = 3\dot{r}_B(fL_m/L_j - 1)$.

Writing $l = L/L_\infty$, so $\delta_G = \ln(-\ln(l_b))$, and $\tau = t/t_j$, the Gompertz curve reduces to $l(\tau) = \exp(-\exp(\delta_G(1-\tau)))$ and the expo-von Bertalanffy curve to $l(\tau) = l_b \exp(\tau r_j/3)$ for $\tau < 1$ or $l(\tau) = 1 - (1 - l_j)\exp(-r_B(\tau - 1))$ for $\tau > 1$, where $r_j = \dot{r}_j t_j$, $r_B = \dot{r}_B t_j = \frac{r_j t_j}{3/l_j - 3}$ and $l_j = l_b \exp(r_j/3)$. To compare both curves, we now require that the latter equals the one for the Gompertz curve, $l_j = \exp(-1)$, from which follows $r_j = -3 - 3\ln l_b$. Figure 7.16 compares both curves. The scaled Gompertz curve has a scaled maximum growth rate of $\frac{d}{d\tau}l(1) = \frac{\delta_G}{\exp(1)}$ and the scaled expo-von Bertalanffy one of $\frac{d}{d\tau}l(1) = -\frac{1+\ln l_b}{\exp(1)}$. The latter is larger.

7.8.3 Programmed shrinking

Fish of the superorder Elopomorpha and of the order Ophidiiformes and several other scattered taxa, such as the paradoxal frog *Pseudis paradoxa* and the midwife toad *Alytes obstetricans*, show substantial programmed shrinking at some point during their juvenile

period, during which they cease feeding. This coincides with substantial changes in morphology, so it can be called metamorphosis. Unfortunately little is known about details of their embryo and early juvenile development, relative to later development. For the moment we assume that these events only affect shape and size, but its basis is lack of better knowledge.

To quantify their development, the assumptions are that they generally follow the standard model (for isomorphs). When maturity hits threshold E_H^s, shrinking starts at event called s, with specific rate $\dot{k}_E$, which lasts some period t_0. Structure, reserve and maturity shrink in harmony, so reserve density and maturity density do not change during this period of programmed shrinking. At event called j, the process is completed and the standard model is followed again with the same parameters. So if the state variables V_s, E_s and E_H^s apply at event s, the values at event j are $V_j = \delta_{sj} V_s$, $E_j = \delta_{sj} E_s$ and $E_H^j = \delta_{sj} E_H^s$, where $\delta_{sj} = \exp(-\dot{k}_E t_{sj})$. Like all rates and times, t_{sj} and $\dot{k}_E$ depend on temperature.

7.9 Changing parameter values

As discussed in subsection 2.5.2 of the comments, some frogs accelerate maturation by temporarily lowering κ. Some fish species insert a V1-morphic stage between birth and metamorphosis, and bivalves do this at metamorphosis, as discussed in subsection 7.8.2 of the comments.

7.9.2 Suicide reproduction

The occurrence of suicide reproduction is remarkably distributed among taxa, suggesting that it evolved many times independently. The lampreys (*Hyperoartia*) sport suicidal reproduction, but the hagfishes (*Myxini*) not. Like in eel and salmon, suicidal reproduction is coupled to spawning and an early development in freshwater and marine existence in between.

The North Pacific giant octopus *Enteroctopus doflein* reproduces only once at an age of 5 till 7 years when it can weigh some 70 kg. The mother lays some 10^5 eggs in a burrow and guards and cares for half a year without feeding. She dies when the eggs hatch. Although the temperature is low, such long starvation times are only possible for large-bodied species.

7.10 Summary

Add_my_Pet has 10 related DEB models, which specification can be summarized as follows, where the environmental variables, temperature $T(t)$ and food density $X(t)$, can change in time t. All models are variations on the standard (std) model and all models deal with environmental variables in the same way:

Effect of temperature on any rate $\dot{k}$:

Basic: $\frac{\dot{k}(T)}{\dot{k}(T_{\mathrm{ref}})} = \exp\left(\frac{T_A}{T_{\mathrm{ref}}} - \frac{T_A}{T}\right)$

Extended: $\frac{\dot{k}(T)}{\dot{k}(T_{\mathrm{ref}})} = \exp\left(\frac{T_A}{T_{\mathrm{ref}}} - \frac{T_A}{T}\right) \frac{1+\exp\left(\frac{T_{AL}}{T_{\mathrm{ref}}} - \frac{T_{AL}}{T_L}\right)_+ + \exp\left(\frac{T_{AH}}{T_H} - \frac{T_{AH}}{T_{\mathrm{ref}}}\right)_+}{1+\exp\left(\frac{T_{AL}}{T} - \frac{T_{AL}}{T_L}\right)_+ + \exp\left(\frac{T_{AH}}{T_H} - \frac{T_{AH}}{T}\right)_+}$

Effect of food on assimilation:

if $E_H < E_H^b$, $\dot{p}_X = 0$, else $\dot{p}_X = f\{\dot{p}_{Xm}\}L^2$ with $f = \frac{X}{K+X}$ and $K = \frac{\{\dot{J}_{Xm}\}}{\{\dot{F}_m\}}$ and $\{\dot{p}_{Xm}\} = \{\dot{p}_{Am}\}/\kappa_X$

7.10.1 s-models

s-models assume isomorphy throughout the full life cycle.

7.10.1.1 std model

The std-model follows from the assumptions as listed in Table 2.4.
Within the family of DEB models, the std-model can be seen as a canonical form.

Main characteristics:

- 1 type of food X, 1 type of structure V, 1 type of reserve E, 1 type of feces P
- 4 minerals (carbon dioxide C, water H, dioxygen O, N-waste N); O is not limiting
- 3 life stages (embryo, juvenile, adult) triggered by maturity thresholds
  - birth is defined as start of assimilation via food uptake
  - puberty as end of maturation and start of allocation to reproduction
- If mobilisation is not fast enough to cover maturity and/or somatic maintenance, rejuvenation and/or some shrinking can occur, but only after use of the reproduction buffer
- The reproduction buffer is continuously converted to a spawning buffer, which is instantaneously converted to exported eggs, if the spawning buffer exceeds a density threshold

Parameters:

Temperature: T_A, T_L, T_H, T_{AL}, T_{AH}

Hazard: $\ddot{h}_a$, s_G, δ_L, $\dot{h}_J$, $\dot{h}_0$, $\dot{h}_0^e$

Life stage: E_H^b, E_H^p

Core: $\{\dot{F}_m\}$, $\{\dot{p}_{Am}\}$, $[\dot{p}_M]$, $\{\dot{p}_T\}$, $\dot{k}_J$, $\dot{k}'_J$, $\dot{v}$, $[E_G]$, κ, κ_X, κ_P, κ_R, $[E_R^s]$

Chemical: $[M_V]$, $\boldsymbol{d}_{\mathcal{O}} = (\ d_X \quad d_V \quad d_E \quad d_P\ )$, $\boldsymbol{\mu}_{\mathcal{O}} = (\ \overline{\mu}_X \quad \overline{\mu}_V \quad \overline{\mu}_E \quad \overline{\mu}_P\ )$, $\boldsymbol{n}_{\mathcal{M}}$, $\boldsymbol{n}_{\mathcal{O}}^d$, where the chemical coefficients for minerals and (dry) organic compounds are

$$\boldsymbol{n}_{\mathcal{M}} = \begin{pmatrix} 1 & 0 & 0 & n_{CN} \\ 0 & 2 & 0 & n_{HN} \\ 2 & 1 & 2 & n_{ON} \\ 0 & 0 & 0 & n_{NN} \end{pmatrix} \text{ and } \boldsymbol{n}_{\mathcal{O}}^d = \begin{pmatrix} 1 & 1 & 1 & 1 \\ n_{HX}^d & n_{HV}^d & n_{HE}^d & n_{HP}^d \\ n_{OX}^d & n_{OV}^d & n_{OE}^d & n_{OP}^d \\ n_{NX}^d & n_{NV}^d & n_{NE}^d & n_{NP}^d \end{pmatrix}.$$

If the N-waste is ammonia, we have $n_{CN} = 0$, $n_{HN} = 3$, $n_{ON} = 0$, $n_{NN} = 1$.

Help quantities (for the specification of changes in state):

wet/dry mass: The chemical coefficients of wet organic mass $n^w_{*_1*_2}$ relate to that of dry mass $n^d_{*_1*_2}$ for $*_1 \in \{H, O\}$ and $*_2 \in \{X, V, E, P\}$ as $n^w_{H*_2} = 2x_{*_2} + n^d_{H*_2}$ and $n^w_{O*_2} = x_{*_2} + n^d_{O*_2}$, while $n^w_{C*_2} = n^d_{C*_2}$ and $n^w_{N*_2} = n^d_{N*_2}$, where $x_{*_2} = \frac{1-d^d_{*_2}/d^w_{*_2}}{18}$, while $d^w_{*_2} \simeq 1\,\mathrm{g/cm^3}$.

mass fluxes: $\dot{\boldsymbol{J}}_{\mathcal{O}} = (\ \dot{J}_X \quad \dot{J}_V \quad (\dot{J}_E + \dot{J}_{E_R}) \quad \dot{J}_P\ )$ relate to energy fluxes $\dot{\boldsymbol{p}} = \begin{pmatrix} \dot{p}_A & \dot{p}_D & \dot{p}_G \end{pmatrix}$, as $\dot{\boldsymbol{J}}_{\mathcal{O}} = \boldsymbol{\eta}_{\mathcal{O}} \dot{\boldsymbol{p}}$ with $\boldsymbol{\eta}_{\mathcal{O}} = \begin{pmatrix} -\frac{1}{\kappa_X \overline{\mu}_X} & 0 & 0 \\ 0 & 0 & \frac{\kappa_G}{\overline{\mu}_V} \\ \frac{1}{\overline{\mu}_E} & -\frac{1}{\overline{\mu}_E} & -\frac{1}{\overline{\mu}_E} \\ \frac{\kappa_P}{\kappa_X \overline{\mu}_P} & 0 & 0 \end{pmatrix}$ and $\kappa_G = \overline{\mu}_V \frac{[M_V]}{[E_G]}$

assimilation: $\dot{p}_A = \kappa_X \dot{p}_X$

somatic maintenance: $\dot{p}_S = [\dot{p}_S] L^3$. If $E_H < E^b_H$, $[\dot{p}_S] = [\dot{p}_M]$, else $[\dot{p}_S] = [\dot{p}_M] + \{\dot{p}_T\}/L$

maturity maintenance: if $(1-\kappa)\dot{p}_C > \dot{k}_J E_H$ (no rejuvenation), $\dot{p}_J = \dot{k}_J E_H$, else $\dot{p}_J = \dot{k}'_J E_H$

mobilization: $\dot{p}_C = E(\dot{v}/L - \dot{r})$. If $[E] \geq \frac{[\dot{p}_S] L}{\dot{v}\kappa}$ (no shrinking), $\dot{r} = \frac{[E]\dot{v}/L - [\dot{p}_S]/\kappa}{[E] + [E_G]/\kappa}$, else if $E_R > 0$, $\dot{r} = 0$, or if $E_R \leq 0$, $\dot{r} = \frac{[E]\dot{v}/L - [\dot{p}_S]/\kappa}{[E] + [E_G]\kappa_G/\kappa}$ (shrinking)

growth: $\dot{p}_G = \kappa \dot{p}_C - \dot{p}_S$, but if $\kappa \dot{p}_C < \dot{p}_S$ and $E_R > 0$: $\dot{p}_G = 0$

maturation/reproduction: $\dot{p}_R = (1-\kappa)\dot{p}_C - \dot{p}_J$, but if $(1-\kappa)\dot{p}_C < \dot{p}_J$ and $E_R > 0$: $\dot{p}_R = 0$

dissipation: if $E_H < E^p_H$, $\dot{p}_D = \dot{p}_S + \dot{p}_J + \dot{p}_R$, else $\dot{p}_D = \dot{p}_S + \dot{p}_J + (1-\kappa_R)\dot{p}_R$

Initial states: $L(0) = 0$, $E_H(0) = 0$, $E_R(0) = 0$, $\ddot{q}(0) = 0$, $\dot{h}_A(0) = 0$ and $E(0) = E_0$ such that $[E](a_b)$ equals that of mother at egg production

Changes in state:

structure: $\frac{d}{dt} L = L\dot{r}/3$. So, initial change is $\frac{d}{dt} L(0) = \dot{v}/3$

reserve: If $E_H < E^b_H$ (embryo), $\frac{d}{dt}[E] = -[E]\dot{v}/L$, else $\frac{d}{dt}[E] = (\{\dot{p}_{Am}\} f - [E]\dot{v})/L$

maturity: If $E_H < E^p_H$ (embryo or juvenile), $\frac{d}{dt} E_H = \dot{p}_R$, else $\frac{d}{dt} E_H = 0$. However, if $\dot{p}_J < 0$ and $E_R = 0$ (rejuvenation), $\frac{d}{dt} E_H = \dot{p}'_J$ with $\dot{p}'_J = \min(0, \dot{p}_J \dot{k}'_J / \dot{k}_J)$

buffer: If $E_H = E^p_H$ (adult), $\frac{d}{dt} E_R = \dot{p}_R - \dot{p}'_J - \dot{p}'_G$, else $(E_H < E^p_H)$ $\frac{d}{dt} E_R = 0$. If adult and $E_R > 0$, $\dot{p}'_G = \max(0, [\dot{p}_S] L^3 - \kappa \dot{p}_C)$, else $(E_R \leq 0)$ $\dot{p}'_J = 0$ and $\dot{p}'_G = 0$. The buffer is partitioned as $E_R = E^0_R + E^1_R$, where E^0_R converts, for positive E^0_R, to E^1_R at rate $\dot{p}^{\max}_R = \frac{1-\kappa}{\kappa} L^3 \frac{[E_G]\dot{v}/L + [\dot{p}_S]}{1+g} - \dot{p}_J$ and $g = \frac{[E_G]\dot{v}}{\kappa\{\dot{p}_{Am}\}}$.

hazard: $\dot{h} = \dot{h}_A + \dot{h}_X + \dot{h}_B + \dot{h}_P$

- aging: $\frac{d}{dt}\ddot{q} = (\ddot{q}\frac{L^3}{L^3_m} s_G + \ddot{h}_a) e(\frac{\dot{v}}{L} - \dot{r}) - \dot{r}\ddot{q}$; $\quad \frac{d}{dt}\dot{h}_A = \ddot{q} - \dot{r}\dot{h}_A$

- starving (food): If $E_H < E_H^b$, $\dot{h}_X = 0$, else if $\dot{p}_C < \frac{\dot{k}_J E_H}{1-\kappa}$, $\dot{h}_X = \dot{h}_J(1 - \frac{\dot{p}_C(1-\kappa)}{\dot{k}_J E_H})$.
  Let L_0 be the length at which $\dot{r} = 0$ for the last time.
  If $L = \delta_L L_0$, $h_X\, dt = \infty$ (instant death due to shrinking)
- accidental (background): If $E_H < E_H^b$, $\dot{h}_B = \dot{h}_B^{0b}$, else $\dot{h}_B = \dot{h}_B^{bi}$; both constant
- thinning (predation): If $E_H \geq E_H^b$, $\dot{h}_P = \frac{2}{3}\dot{r}$, else $\dot{h}_P = 0$

Input/output fluxes:

food: $\dot{J}_X = \frac{\dot{p}_A}{\kappa_X \overline{\mu}_X}$

feces: $\dot{J}_P = \frac{\kappa_P \dot{p}_A}{\kappa_X \overline{\mu}_P}$

eggs: If $E_R^1 = [E_R^s]L^3$: $\dot{R}\, dt = \kappa_R[E_R^s]L^3/E_0$ eggs are produced and E_R^1 is set to 0

minerals: $\dot{\boldsymbol{J}}_{\mathcal{M}} = -\boldsymbol{n}_{\mathcal{M}}^{-1}\boldsymbol{n}_{\mathcal{O}}^{w}\dot{\boldsymbol{J}}_{\mathcal{O}}$, where $\dot{\boldsymbol{J}}_{\mathcal{M}} = (\ \dot{J}_C \quad \dot{J}_H \quad \dot{J}_O \quad \dot{J}_N\ )$

heat: $\dot{p}_{T+} = -\overline{\boldsymbol{\mu}}_{\mathcal{O}}^T \dot{\boldsymbol{J}}_{\mathcal{O}}$

death: at death, $[M_V]L^3$ moles of structure and $(E+E_R)/\overline{\mu}_E$ moles of reserve become available in the environment

7.10.1.2 stf-model

Like the std-model but with

◦ fetal development (rather than egg development, see also the stx-model)

Budding, as found in cnidarians and salps has, metabolically, similarities with fetal propagation: no assimilation by buds during development. This type of fetal development is found in e.g. some cartilaginous and ray-finned fish, Peripatus.

The deviation from the standard model amounts for the fetus, which has $E_H < E_H^b$, to $E(0) = 0$ and $\frac{d}{dt}[E] = (\{\dot{p}_{Am}\}f - [E]\dot{v})/L$, where f equals the value of the mother. For the mother, the deviation amounts to $\frac{d}{dt}E_R = \dot{p}_R - n\{\dot{p}_{Am}\}fL_e^2$, where L_e is the structural length of the fetus, n the number of fetuses, such that $\dot{p}_R a_b = nf\{\dot{p}_{Am}\}\int_0^{a_b} L_e^2(t)\, dt$. The effect is that $E_R = 0$ at the end of the gestation period.

7.10.1.3 stx-model

Like the stf-model but with

◦ fetal development (rather than egg development) that first starts with a preparation stage and then sparks off at a time, t_0, that is an extra parameter

◦ a baby stage (for mammals) just after birth, ended by weaning, where the juvenile switches from feeding on milk to solid food at maturity level E_H^x. Weaning is between birth and puberty, so $E_H^b \leq E_H^x \leq E_H p$.

In its simplest form, it is a two parameter extension of std-model at abundant food. Food quality and up-regulation of assimilation can involve more parameters. This life history is found in placentalia. Milk production is from up-regulated feeding/assimilation.

7.10.1.4 ssj-model

Like the std-model but with

- a non-feeding stage between events s and j during the juvenile stage that is initiated at a particular maturity level, E_H^s and lasts a particular time, t_{sj}. Substantial metabolically controlled shrinking occurs during this period, with specific rate $\dot{k}_E$, faster than can be explained by starvation.

It is a three parameter extension of the std-model. This life history is found in Elopiformes, Albuliformes, Notacanthiformes, Anguilliformes, Ophidiiformes, some Anura and Echinodermata. The comments on Section 7.8.3 give more background.

Given $V = V_s$, $E = E_s$, $E_H = E_H^s$ at time t, $V = \delta_{sj} V_s$, $E = \delta_{sj} E_s$ and $E_H = \delta_{sj} E_H^s$ at time $t + t_{sj}$, with $\delta_{sj} = \exp(-\dot{k}_E \delta_{sj})$, while $\dot{p}_X = 0$ for $t \in (t, t + t_{sj})$.

7.10.1.5 sbp-model

Like the std model but with

- growth ceases at puberty, meaning that the κ-rule is not operational in adults.

It has the same parameters as the std-model, and is similar to the abp-model, which differs by acceleration. This life history is found in Calanus, while other copepods accelerate.

At puberty, growth ceases. so $\dot{p}_G = 0$, and the κ-rule no longer applies. Mobilisation after puberty is $\dot{p}_C = \dot{v} E / L_p$, and allocation to reproduction is $\dot{p}_R = \dot{p}_C - \dot{p}_M - \dot{p}_J$, with $\dot{p}_J = \dot{k}_J E_H^p$.

7.10.2 a-models

a-models also assume isomorphy, but during part of the life cycle metabolism accelerates following the rules for V1-morphy.

7.10.2.1 abj-model

The DEB model with type $\mathcal{M}$ acceleration is like std-model, but

- acceleration between birth b and metamorphosis j
- before and after acceleration: isomorphy

Metamorphosis is before puberty and occurs at maturity E_H^j, so $E_H^b \leq E_H^j \leq E_H p$, which might or might not correspond with changes in morphology. Type $\mathcal{M}$ acceleration has never been found in cartilaginous fish, amphibians, reptiles, birds or mammals, and typically occurs in taxa with larval stages.

The abj-model is a one-parameter extension of std-model and reduces to the std-model for $E_H^j = E_H^b$. During metabolic acceleration, $\{\dot{p}_{Am}\} = \{\dot{p}_{Am}^b\} L / L_b$ and $\dot{v} = \dot{v}^b L / L_b$, where $\{\dot{p}_{Am}^b\}$ and $\dot{v}^b$ refer to the values at birth. At j, acceleration ceases: $\{\dot{p}_{Am}\} = \{\dot{p}_{Am}^b\} s_{\mathcal{M}}$ and $\dot{v} = \dot{v}^b s_{\mathcal{M}}$, with acceleration factor $s_{\mathcal{M}} = L_j / L_b$.

7.10.2.2 asj-model

The DEB model with delayed type M acceleration is like abj-model, but

- start of acceleration is delayed till maturity level E_H^s and lasts till metamorphosis at maturity level E_H^j
- Before and after acceleration: isomorphy

Metamorphosis is still before puberty, so $E_H^b \leq E_H^s \leq E_H^j \leq E_H p$ and the acceleration factor is $s_{\mathcal{M}} = L_j/L_s$. This model is a one-parameter extension of the abj-model and reduces to the std-model for $E_H^b = E_H^s = E_H^j$. This life history is found in Mnemiopsis, Crassostrea and Aplysia. Further improvement of data might require a change from abj- to asj-models for quite a few species.

7.10.2.3 abp-model

The DEB model with type M acceleration is like model-abj, but

- acceleration between birth and puberty
- before acceleration: isomorphy
- after acceleration: no growth, so no κ-rule

Metamorphosis can occur before puberty and occurs at maturity E_H^j, but only affects morphology, not metabolism. This model has the same number of parameters as the std-model. The acceleration factor is $s_{\mathcal{M}} = L_p/L_b$. It is similar to the sbp-model, which has no acceleration. It applies to copepods, may be also to ostracods, spiders and scorpions.

At puberty, growth ceases, so $\dot{p}_G = 0$, and the κ-rule no longer applies. Mobilisation after puberty is $\dot{p}_C = s_{\mathcal{M}} \dot{v} E/L_p = \dot{v} E/L_b$, and allocation to reproduction is $\dot{p}_R = \dot{p}_C - \dot{p}_M - \dot{p}_J$, with $\dot{p}_J = \dot{k}_J E_H^p$.

7.10.3 h-models

h-models also assume isomorphy, but during part of the life cycle metabolism accelerates following the rules for V1-morphy

7.10.3.1 hep-model

The DEB for ephemeropterans, odonata and possibly other insect groups. Its characteristics are

- morphological life stages: egg, larva, (sub)imago; functional stages: embryo, juvenile, adult, imago
- the embryo still behaves like the std-model
- acceleration starts at birth and ends at puberty

- puberty occurs during the larval stage
- emergence of the imago occurs when reproduction buffer density, $E_R/L^3 = [E_R^j]$, hits a threshold
- the (sub)imago does not grow or allocate to reproduction. It mobilizes reserve to match constant (somatic plus maturity) maintenance

The model is discussed in the comments for Section 7.8. The difference with the abp-model is that growth continues at puberty, ceasing of growth uses on another trigger and imago's don't allocate to reproduction.

Between p and j, allocation to reproduction is $\dot{p}_R = (1-\kappa)\dot{p}_C - \dot{p}_J$. After j, mobilisation is $\dot{p}_C = \dot{p}_M + \dot{p}_J$, allocation to reproduction is $\dot{p}_R = 0$.

7.10.3.2 hex-model

The DEB model for holometabolic insects (and some other hexapods). Its characteristics are

- morphological life stages: egg, larva, (pupa), imago; functional stages: embryo, adult, (pupa), imago
- the embryo still behaves like the std-model
- the larval stage accelerates (V1-morph) and behaves as adult, i.e. no maturation, allocation to reproduction and $E_H^b = E_H^p$.
- pupation occurs when reproduction buffer density hits a threshold, $E_R/L^3 = [E_R^j]$
- pupa behaves like an isomorphic embryo of the std-model, emergence occurs at $E_H = E_H^e$ Larval structure rapidly transforms to pupal reserve just after start of pupation, and sets $E_H = 0$ at j.
- the reproduction buffer remains unchanged during the pupal stage
- the imago does not grow or allocate to reproduction. Imago's reserve mobilisation matched somatic plus maturity maintenance $\dot{p}_C = \dot{p}_M + \dot{p}_J$.

Hemi-metabolic insects skip the pupal stage, don't convert larval structure to reserve. Imago structure equals larval structure when reproduction buffer density hits a threshold. The model is discussed in the comments for Section 7.8.

For $\dot{k}_E = \dot{v}/L_b$, reserve mobilisation prior to pupation (i.e. during acceleration) is $\dot{p}_C = E(\dot{k}_E - \dot{r})$ with $\dot{r} = \frac{\kappa[E]\dot{k}_E - [\dot{p}_M]}{\kappa[E]+[E_G]} = g\dot{k}_M \frac{e/l_b - 1}{e+g}$. The larva allocates to reproduction as $\dot{p}_R = (1-\kappa)\dot{p}_C - \dot{p}_J$, with $\dot{p}_J = \dot{k}_J E_H^p$. $[E_R]$ has a maximum at $[E_R^m] = [E_R^{\mathrm{ref}}] f \frac{1-l_b}{f-l_b}$ with$[E_R^{\mathrm{ref}}] = (1-\kappa)[E_m]\frac{g+l_b}{1-l_b}$, so pupation occurs when $[E_R] = s_j[E_R^{\mathrm{ref}}]$, with $s_j = [E_R^j]/[E_R^{\mathrm{ref}}]$.

Reserve mobilisation of the imago is $\dot{p}_C = \dot{p}_M^e + \dot{p}_J^e$, where $\dot{p}_M^e = [\dot{p}_M]L_e^3$ and $\dot{p}_J^e = \dot{k}_J E_H^e$.

7.10.3.3 hax-model

The hax model is a hybrid between the hep and hex models: the hep-rules are followed till $[E_R] = [E_R^j]$, then pupation follows, with an emergence and an imago stage which might or might not feed. An example of a hax model with a non-feeding imago-stage is the harlequin fly *Chironomus riparius*.

8

Co-variation of parameter values

Genetic markers show that the quaking aspen, *Populus tremuloides*, is possibly the biggest organism on earth. A giant individual, called pando or the trembling giant, in south-central Utah (US), weighs 6 Gg, lives on 43 ha and has 4e4 truncs. The mean life span of a trunc is estimated at 130 yr, of the root at 8e4 yr, see Wiki.

8.1 Intra-specific parameter variations

8.1.1 Intra-specific effects of selection

Several animal species have been domesticated and selected for particular types of production, for instance chickens has been selected for meat or egg production, cows for meat and milk production. Tables 8.1 and 8.2 compare three races of each.

The red jungle fowl (RJ) is the wild race, while the White Leghorn (WL) has been selected for egg-laying and the Indian River (IR) for meat production. Little information was available to estimate the Arrhenius temperature; the used value of about $T_A = 20$ kK resulted in typical values for specific maintenance cost $[\dot{p}_M] = 18\,\mathrm{J\,d^{-1}cm^{-2}}$. The expected life span for RJ is much larger than for WL than for IR; that for IR is really short indeed. The males are bigger than the females; the female-to-male ratio of the zoom factors z for JF, WH and IR are 0.8305, 0.9597 and 0.6822, respectively. Compared to original RF, selection of egg-laying increased, and for meat production decreased relative female size while WH and IR are both much bigger than RF, WH being the largest.

The maximum specific assimilation rate $\{\dot{p}_{Am}\}$ of female IR remained the same, compared to the wild type RJ, but that of WL decreased. For the males it decreased for WL, and even further in IR. It is remarkable that selection on production did not increase specific assimilation, although it did increase maximum size.

The energy conductance $\dot{v}$ did not change much, that of IR males is a bit larger, meaning a faster metabolism. All are half the typical value $0.02\,\mathrm{cm\,d^{-1}}$. The implied shorter survival time in absence of food is compensated with their lower specific somatic maintenance costs. Both WL and IR have lower specific somatic maintenance $[\dot{p}_M]$ than JR, which might relate to the shorter life spans (less turnover of structure). It is less likely that enforced lack of movement in IR and WL plays an important direct role in the

Table 8.1: The parameters of the standard DEB model estimated for the male (m) and female (f) chicken *Gallus gallus* of the races Red Jungle fowl (RJ), the egg-chicken White Leghorn (WL), and the meat-chicken Indian River broiler (IR). The parameters were estimated using data from [1274]; see add_my_pet. The parameter are given for 20 °C, using an Arrhenius temperature $T_A = 19794$ K. The reproduction efficiency has been set at $\kappa_R = 0.95$ and the Gompertz stress coefficient at $s_G = 0.1$ for all cases. The dry-wet-weight ratio was set to $d_V = d_E = 0.38$ for RJ and WL and to 0.30 for IR. The feeding parameters has not been given here, due to lack of adequate data.

parameter	symbol	unit	RJ, f	RJ, m	WL, f	WL, m	IR, f	IR, m
zoom factor	z	-	4.97	5.984	8.649	9.012	8.391	12.3
spec. assimilation rate	$\{\dot{p}_{Am}\}$	J/d.cm^2	427	372	270	301	435	178
energy conductance	$\dot{v}$	cm/d	0.0083	0.0090	0.0113	0.0111	0.00965	0.0155
fraction to soma	κ	-	0.2486	0.4317	0.5051	0.4306	0.3492	0.6734
spec som. maint. cost	$[\dot{p}_M]$	J/cm^3	21.38	26.82	15.79	14.39	18.09	9.739
mat. maint. rate coeff.	$\dot{k}_J$	1/d	0.0025	0.0039	0.0020	0.0020	0.0020	0.0011
spec. cost structure	$[E_G]$	J/cm^3	9918	9864	9948	9947	7709	10600
maturity at birth	E_H^b	J	8.99e4	4.61e4	8.14e4	9.72e4	9.12e4	7.43e4
maturity at puberty	E_H^p	J	2.67e6	1.65e6	2.87e6	3.68e6	6.53e6	2.69e6
aging acceleration	$\ddot{h}_a$	1/d^2	2.72e-49	1.32e-45	2.32e-22	1.41e-21	5.24e-21	8.69e-22

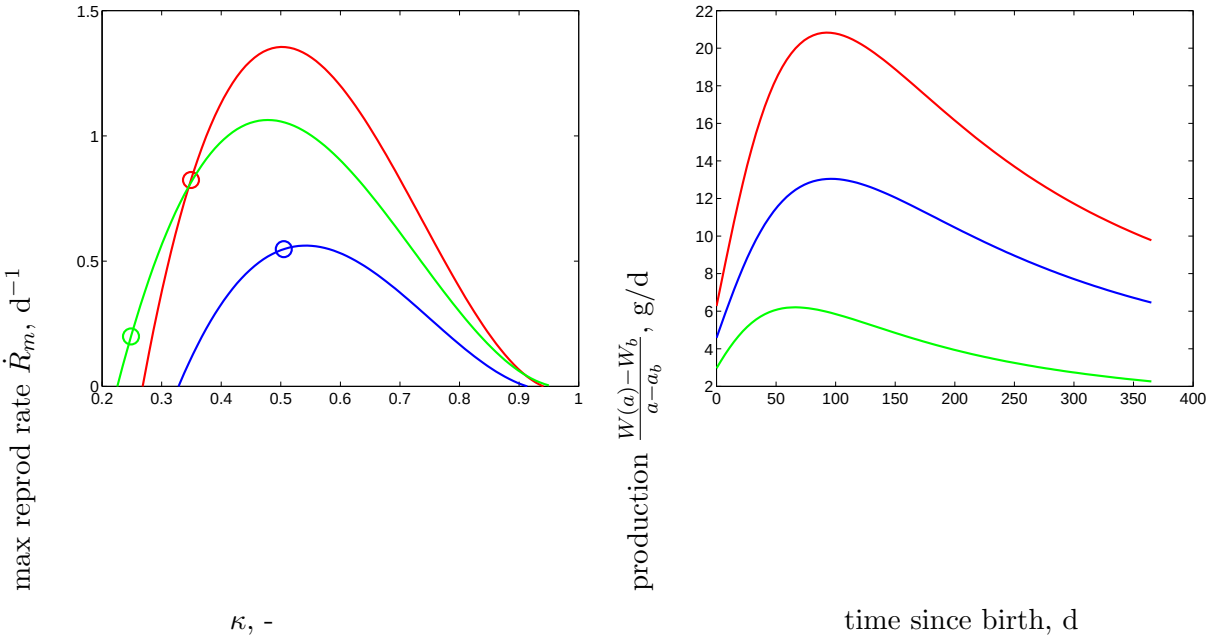

Figure 8.1: The maximum reproduction rate as function of κ (left) and the weight increase since birth function of time since birth (right), for three races of chicken, using the parameters of Table 8.1. The estimated values for κ are indicated.

lowering of $[\dot{p}_M]$, but possibly indirectly. It would be of significant scientific importance to find the reasons for this. The specific costs for structure $[E_G]$ reflects the dry-to-wet weight ratio, which was set to somewhat lower to IR, due to their meat being water-rich; adequate data were lacking, however. All has a growth efficiency κ_G around 0.8, but males IR had 0.6 only, despite the fact that they are the biggest. Allocation to sperm production in males was assumed to equal that to egg production in females (in absence of adequate data); yet, due to males' larger size, this allocation represents a relatively small fraction of the mobilisation flux, and κ for RJ and IR males is much bigger than that of females. Figure 8.1 shows that κ is much smaller than the typical for animals, which is around 0.8. It is smallest for RJ and largest for WL.

Several parameters affect how maximum reproduction rate depends on κ, but the maximum is reached but about $\kappa = 0.5$ and this is the value found for female WL, which was selected for maximizing reproduction. This is remarkable, because the maximum reproduction rate is typically only 25% of the optimized value, where κ is allowed to vary, keeping all other parameters fixed; RJ being no exception. It seems, therefore, that if selection is on maximizing reproduction, κ assumes the optimal value; the fact that κ is typically far from optimal means that selection is in different directions and/or that optimal κ comes with drawbacks that are not yet fully understood. Another remarkable feature is the cumulative growth rate, defined as the weight increase since birth over time since birth. Meat chickens are typically harvested when this reaches is peak, around 70 d. This growth rate is lowest for RJ, and (by far) highest for IR. The difference in practice is even much bigger, since IR is fed abundantly with a food type that gives a scaled functional response f over about 2; f is only confined to the interval (0,1) comparing different quantities of food of the same quality. Particular experimental conditions can only lead to 'overeating', i.e. eating more than typical at abundant food.

The $\log_{10}$ of the maturity ratio $s_H^{pb} = E_H^p/E_H^b$, see Section 2.5.2 of the comments, for RJ, WL and IR females are 1.47, 1.54, 1.66, and or males 1.55, 1.58, 1.56, respectively. All are close to 1.5, but the female IR is clearly more altricial than RJ.

Table 8.2 give the parameter values for three races of cows; all were selected for production, the wild type went extinct. Little information was available to estimate the Arrhenius temperature; the used value of $T_A = 12\,\mathrm{kK}$ resulted in typical values for specific maintenance cost $[\dot{p}_M] = 18\,\mathrm{J,d^{-1}cm^{-2}}$. Again, the males are larger than the females, but the specific assimilation rates of the females are larger than those of the males; in the case of the milk-cow Holstein even close to a factor 2. the female-to-male ratio of the zoom factors z for Ho, An and Br are 0.88, 0.82 and 0.80, respectively.

The energy conductances are larger for females than for the males, so they have less reserve, for Holstein and Angus this amounts to a factor 2. The values for the males are about double the typical value for animals. The specific maintenance cost $[\dot{p}_M]$ for the female Holstein is remarkably low; she is also the largest of the three females. This is doubtlessly connected with her very low value of κ, but the mechanistic coupling is not yet clear; milk production is from the $(1-\kappa)$ branch of the reserve mobilisation flux. The $\log_{10}$ of the maturity ratio $s_H^{pb} = E_H^p/E_H^b$ for Ho, An and Br females are 0.77, 1.49, 1.06, and for males 0.71, 0.88, 1.58, respectively. Holstein is most precocial. The difference between females and males seem to increase with altriciality.

Table 8.2: The parameters of the standard DEB model estimated for the male (m) and female (f) cow *Bos primegenius* of the races milk-cow Holstein (Ho), the meat-cow Agus (An) and the zebu Brahman (Br). The parameters were estimated using data from [105], see add_my_pet. The parameter are given for 20 °C, using an Arrhenius temperature $T_A = 12\,\mathrm{kK}$. The reproduction efficiency has been set at $\kappa_R = 0.95$ and the Gompertz stress coefficient at $s_G = 0.1$ for all cases. The dry-wet-weight ratio was set to $d_V = d_E = 0.3$. The feeding parameters has not been given here, due to lack of adequate data.

parameter	symbol	unit	Ho, f	Ho, m	An, f	An, m	Br, f	Br, m
zoom factor	z	-	51.71	58.83	46.68	57.06	47.18	58.64
spec. assimilation rate	$\{\dot{p}_{Am}\}$	J/d.cm^2	2206	1211	1755	1108	1625	1132
energy conductance	$\dot{v}$	cm/d	0.087	0.0413	0.0748	0.0368	0.0421	0.0367
fraction to soma	κ	-	0.326	0.971	0.618	0.96	0.552	0.966
spec som. maint. cost	$[\dot{p}_M]$	J/cm^3	13.9	20.0	23.3	18.7	19.0	18.6
mat. maint. rate coeff.	$\dot{k}_J$	1/d	0.0010	0.0040	0.00016	0.0049	0.0019	0.00028
spec. cost structure	$[E_G]$	J/cm^3	8307	7829	7825	7842	7844	7692
maturity at birth	E_H^b	J	2.00e8	1.72e6	4.49e7	1.42e6	3.37e7	2.58e6
maturity at puberty	E_H^p	J	1.19e9	8.74e6	1.40e9	1.09e7	3.87e8	9.96e7
aging acceleration	$\ddot{h}_a$	1/d^2	3.51e-15	1.12e-12	1.16e-14	1.89e-12	4.79e-13	2.12e-12

8.1.3 Allocation strategies

Species in the collection can roughly be classified as sub-optimal, optimal and supra-optimal on the basis of the maximum reproduction rate (of a fully grown adult at abundant food), relative to the value at optimal κ [792]. The 'optimal' value of κ is here defined as the value that maximized maximum reproduction rate. Optimal species have a maximum reproduction rate that is at least 80% of the maximum possible one for a species with that parameters while varying κ. Sub-optimal species have a lower maximum reproduction and a κ that is smaller than the one that maximizes reproduction; supra-optimal species have also a lower maximum reproduction, but a larger value for κ. Table 8.3 lists the optimal and sub-optimal species, of the 240 species studied, Figure 8.2 presents the κ values and Figure 8.3 the maximum reproduction rates as fraction of their optimized maximum. The κ values appear to follow a beta-distribution, in terms of approximate empirical description with mean 0.812 and variance 0.0442. (The survivor function of the beta distribution is given by $S(\kappa) = 1 - I_\kappa(a, b)$, where $I_\kappa(a, b)$ is the incomplete beta function.) Although the collection grew by a factor 4 since [857] at 2018/01/01, this hardly affected the frequency distribution of κ and the fit for 1000 species is even better. The explanation is that, for fully grown individuals, κ equals the somatic maintenance as fraction of assimilation, and assimilation equals somatic plus maturity maintenance plus reproduction investment [**?**]. These fluxes appear to follow Weibull distributions, with the mathematical consequence that the ratio follows a beta distribution to a very good approximation. The reason why these fluxes follow a Weibull distribution is, probably, because many factors contribute to their value. This is the same reason why allometric functions frequently fit scatter clouds in log-log plots very well. The result resembles a well-known property of gamma distributions: If x and y are independently gamma-distributed random variables, then $\frac{x}{x+y}$ follows (exactly) a beta distribution. This also holds for Weibull-distributed random variables to a very good

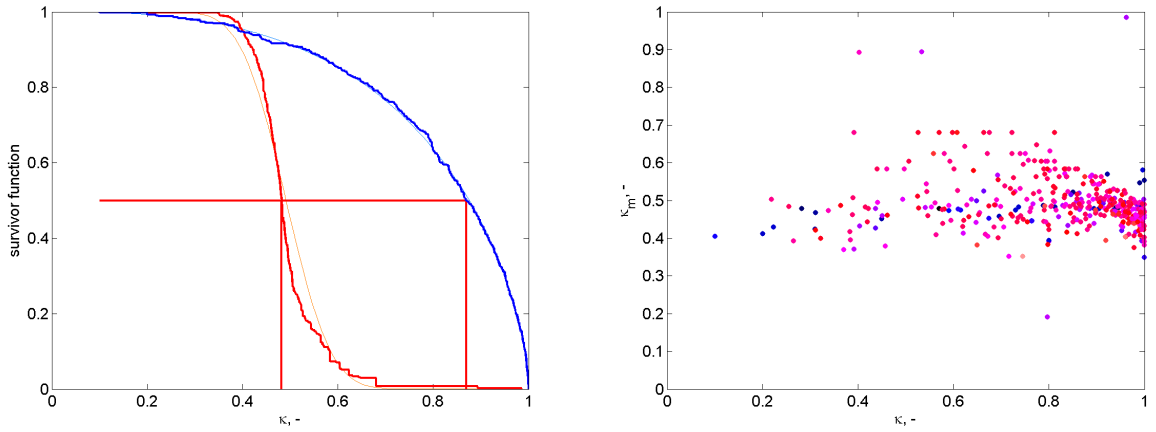

Figure 8.2: Left: The survivor function for κ among the 420 animal species in the add_my_pet collection (blue; sampling date 2016/10/24)) and that for the value that maximizes reproduction rate (red). The survivor functions for the beta distribution are also shown. Right: The value of κ that maximizes reproduction rate as function of κ. Colours indicate maximum structural length from small (black) to large (white).

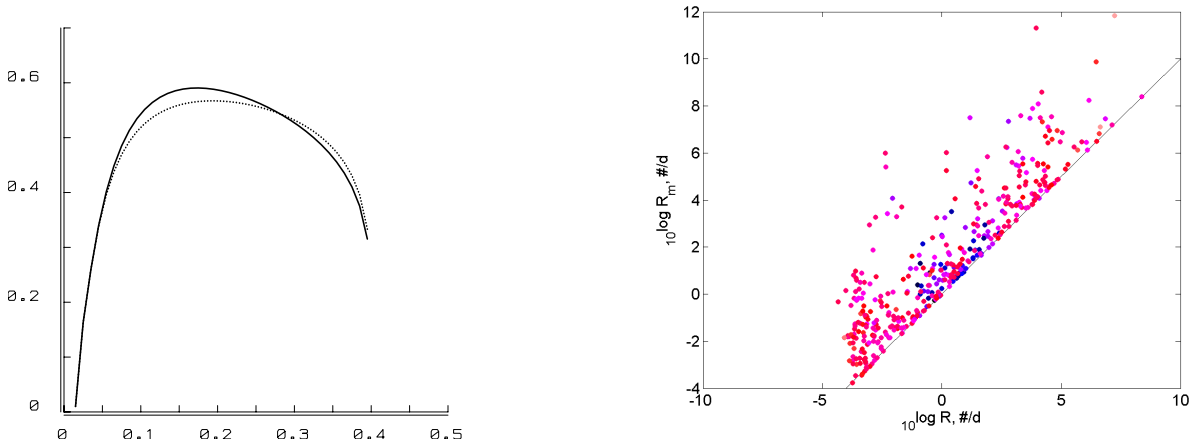

Figure 8.3: Left: The survivor function for maximum reproduction as fraction of the optimized maximum among the 420 animal species in the add_my_pet collection (sampling date 2016/10/24). Right: Maximum reproduction at optimal value of κ as function of the actual maximum reproduction. Colours indicate maximum structural length from small (black) to large (white).

approximation. The optimal κ values also seem to be beta distributed with mean 0.482 and variance 0.0034, very different from the actual values. The rare coelacanth *Latimeria* is among the optimal species, so being optimal does not imply great abundance.

Table 8.1 suggests that if selection is for maximizing reproduction, κ becomes optimal. So the conclusion is that natural selection is not maximizing reproduction.

Some species might have a low κ to reduce body size; maximum structural length is proportional to κ. The (huge) ocean sunfish *Mola* illustrates that a low κ does not imply small body size, but it would be even larger with a larger value of κ. The minimum food density that allows survival increases with body size, so does the risk of not finding enough food. The logic directly relates to the 'waste-to-hurry' hypothesis [777], that says that the specific somatic maintenance costs is (greatly) increased in species that live of blooming resources to boost production (growth and reproduction) and remain small, with a short life cycle as implication. This hypothesis helps to understand why the specific maintenance costs of copepods and daphnids is around $1400\,\mathrm{J\,d^{-1}\,cm^{-3}}$, while that of equally small aphids and tardigrades is much closer to the typical value of $20\,\mathrm{J\,d^{-1}\,cm^{-3}}$ at 20°C. While in a bloom, food availability is not a problem. If resources are not blooming, increase of maintenance is not a smart strategy, since food is typically not abundant. Species that live of resources that are more constant in time might reduce their κ to reduce the minimum food level that they require, while still running their metabolism economically.

Why then do other species have a large κ, close to 1? A possible reason is to increase body size to avoid size-dependent predation or increase the ability to average resource availability in space and time [792]. Large body size comes with large reserve capacity to smooth out temporary variation, large home ranges and a reduction of predation risk. The first two effects directly follow from the co-variation rules that are implied by DEB theory. Yet, the difference between a large value for κ and a very large one (= even more close to 1; the frequency distribution of Figure 8.2 shows that there are many of them), is hardly felt for maximum body size, but greatly for reproduction. The more important reason for a very large κ might be to reduce reproduction, avoiding exhaustion of resources via intra-specific competition of offspring. Survival of bleak periods might be a much stronger selection criterion than maximization of reproduction; not-exhausting the environment and so reducing the length of bleak periods might be part of this survival strategy. Predator-prey systems might co-evolve in terms of parameter settings, κ being one of them, where stability and robustness might be more important than absolute numbers. Frequent ecological disasters with introduced species point into that direction. Supporting observations for a reduction of reproduction are that the created pinguin *Eudyptes*, see Section 2.6.4, and the shoebill *Balaeniceps rex* produce two eggs per season (in a single clutch), while they can raise a single young only. The second one only serves as backup and is discarded as soon as the first one proves to be vital. So the limiting factor is not in egg production, but in raising offspring. This possibly applies to most species with parental care.

Discussions on allocation strategies easily make use of optimisation arguments. DEB theory hardly uses such arguments.

Table 8.3: Species of the add_my_pet collection that have a sub-optimal κ (left) and the optimal one (right). All other of the 240 species have a supra-optimal κ. The maximum reproduction rate is given as fraction of the one it would have with optimal κ. If this fraction is less than 0.8, a species is either sub- or supra-optimal.

sup-optimal species	$\dot{R}/\dot{R}_m$
Asplanchna girodi	0.1642
Folsomia candida	0.6213
Oikopleura longicauda	0.6373
Thalia democratica	0.2823
Hippocampus whitei	0.6953
Pleuronectes platessa	0.7097
Mola mola	0.3198
Geocrinia vitellina	0.6538
Gallus gallus IR	0.6776
Gallus gallus RJ	0.1875
Melopsittacus undulatus	0.0651
Myrmecophaga tridactyla	0.6402
Bos primigenius Holstein	0.7891

optimal species	$\dot{R}/\dot{R}_m$
Chironex fleckeri	0.9979
Hydra viridissima	0.9657
Pelagia noctiluca	1
Beroe ovata	0.8913
Sagitta hispida	0.9684
Aspidiophorus polystictos	0.9249
Crassostrea gigas	0.8595
Daphnia hyalina	0.9305
Diaphanosoma brachyurum	0.9507
Oikopleura dioica	0.8676
Eptatretus stoutii	0.8399
Lampetra planeri	0.914
Chiloscyllium plagiosum	0.9699
Thymallus thymallus	0.9995
Clupea harengus	0.9626
Danio rerio	0.9825
Pimephales promelas	0.9124
Trisopterus luscus	0.9648
Sparus aurata	0.8367
Zoarces viviparus	0.8587
Thunnus thynnus	0.9561
Latimeria chalumnae	0.9979
Crinia nimbus	0.9911
Heteronotia binoei	0.9552
Sceloporus undulatus	0.8697
Gallus gallus WL	0.975
Phocoena phocoena	0.9193

8.1.3.1 Small versus large eggs

There is a link between structural volume at birth, V_b, and maturity at birth, E_H^b. In case of a maintenance ratio of $k = 1$, this link is even a direct proportionality. Plant champion in mass of seed is the coco de mer palm *Lodoicea maldivica*, with seeds of 25 kg and 50 cm diameter. It grows on poor soils and their leaves seem to collect nutrients around the tree via rain, which might help offspring [378]. This is doubtlessly a more general strategy among plants on poor soils. Another aspect is that most of the weight of these seeds is not reserve, but floating material for traveling the sea, an adaptation to life on small islands. The parallel with the coelacanth *Latimeria chalumnae* is striking, which also lives in oligotrophic environments and make eggs of 325 g. Most fish make very small eggs. The coelacanth is ovoviviparous, however, and their large birth size of 50 cm long might be an adaptation to the type of food eaten by neonates.

Most optimization arguments lead to the uninspiring result that reproduction rate or population growth rate is maximized by producing an infinitely large number of infinitesimally small young. No energy argument seems to forbid this possibility. It is hard to understand why it pays to produce (few) large eggs. One possibility is in accounting for a changing spatially heterogeneous environment. Reproduction is usually synchronized with a favourable season, which is usually short. The reason why the crossbill breeds in midwinter in Scotland, for instance, is that it feeds its young with spruce seeds, which are mature early in spring. This habitat is not always favourable for them; if the seeds are finished, they have to move out. The same holds for ducks breeding in Iceland, where the adult starts to incubate while there is still snow. When the chicks hatch, food is available, but not for long; soon after they are able to fly, the conditions grow worse and they are forced to migrate to the sea. These examples are obvious, but the principle is probably quite common. The selection constraint is, therefore, a maximum period for completing development up to a stage allowing for migration.

It is consistent with the structure of the DEB model that such a stage can be tied to a certain body volume. That the time needed to reach such a volume is strongly reduced by laying large eggs is obvious from the expression for the juvenile period. The fact that birds with large eggs, such as shearwaters and the kiwi, also have long incubation times does not devalue the argument. The DEB model shows that the time taken for the chick to reach a certain size would be even longer if the eggs were smaller. This insight is one of the gains of formalized reasoning, where all relevant variables can be considered at the same time. Another aspect to consider for endotherms is that small young have a hard time maintaining a high body temperature.

A direct link exists between relative egg size and position in the altricial-precocial spectrum. In order to hatch in a late stage of development, eggs of precocial species must be relatively large to allow sufficient maturation at birth. This might give problems in terrestrial species, since nitrogen waste accumulates in the eggs, and the original one, ammonia, is rather toxic. Aquatic species hardly suffer from this problem, since ammonia is well-soluble. Most terrestrial species made the switch from ammonium secretion (ammonotely), to the somewhat less toxic, but also more expensive, but still well-soluble, urea (ureotely); the tadpoles of amphibia sport ammonotely, but most switch to ureotely at metamorpho-

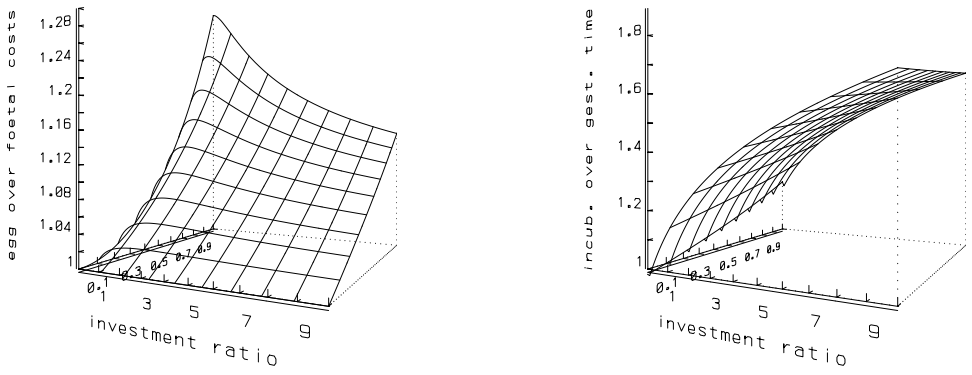

Figure 8.4: The energy costs of producing an egg relative to that of a foetus (left) and incubation time relative to gestation time (right), as a function of the investment ratio g and scaled length at birth l_b (plotted on the y-axis) at high energy density at birth, $e_b = 1$.

sis. Reptiles and birds even made the switch to uric acid (uritely), which is much less toxic, much less soluble, but also more expensive than urea [1547]. Some bird species with water-rich and nitrogen-poor food sport facilitative ammonotely [819], probably to reduce energy costs. This allowed the birds, and their ancestral dinosaurs, to make relatively large eggs, hatching into precocial neonates that hardly require parental care. All paleognaths (e.g. ostriches and tinamus) are precocial, only 'advanced' neoaves are altricial. The long incubation times of eggs of the dinosaurs Protoceratops and Hypacrosaurus (2.8–5.8 months) [394] suggest that they did not breed their eggs, so poorly developed parental care. The nests of oviraptor, the colonies of maiasaurs and the close association of an adult Psittacosaurus with many small juveniles, on the other hand, do suggest some form of parental care in dinosaurs, like found in contemporary crocodiles and ground-nesting precocial birds. Only after the development of flight, dinosaurs started to breed in trees as birds. The evolution of altricialy in (advanced) neoaves, and especially the songbirds (Passeriformes), can be seen as an adaptation to life in (deciduous) trees, which started to dominate the terrestrial environment around the time that the big dinosaurs disappeared (and might have contributed to their disappearance). Quite a few traits are coupled in this adaptation of life in trees, such as

- small maximum body weight of less than a kilo (extremes are the raven and the ground-dwelling lyrebird; small twigs cannot carry heavy weight)
- altriciality, combined with the demand-position in the supply-demand spectrum
- advanced parental care with adaptation of the nesting in the form of

  bright colours of the inner mouth and yellow swollen gape lining

  faecal sacs of nestlings, to facilitate sanitation [643]

  vocabulary and begging behaviour

- a high water content of neonate tissues (since water can be in short supply in a nest high in a tree),
- anisodactyl feet (perching), not requiring active muscle contraction for gripping branches
- short rounded wings and maneuverable tail, allowing sharp turns when slowly flying between branches
- advanced singing, including the development of a syrinx (a bony structure at the bottom of the trachea), since the leaves hamper visual signals
- high body temperature for flying vertically and fast manoeuvrings (songbirds are hot among birds)

So dinosaurs developed from precocial to altricial, just reverse, compared to mammals [51]. Mammals sport uerotely and evolved in parallel with the dinosaurs. They originated some 310 Ma ago, but lead eggs till some 30 Ma ago [180]. Ureotely probably prevented an early evolution of relatively large eggs in mammals and they were forced to the altricial condition till the invention of foetal development, where the foetus can use the draining system of the mother to get rid of its nitrogen waste. The precocial condition evolved much later in placental mammals; the (still egg-laying) monotremes and marsupials (with tiny neonates) are extremely altricial. Since they provided milk to their babies, right from their origin [180], the early mammals probably did also breed their eggs, so parental care was well developed, which combines well with the altricial condition.

8.1.3.2 Egg versus foetus

The ratio of the energy costs of egg to foetus production is shown in Figure 8.4 in the case of high reserve density at birth, $e_b = 1$. This figure also shows the ratio of the incubation and gestation time. For very small investment ratios, g, the latter ratio becomes

$$\frac{\sqrt{2}e_b u^3}{l_b}\left(\frac{1}{2}\ln\frac{u^2+u\sqrt{2}+1}{u^2-u\sqrt{2}+1}+\arctan\frac{u\sqrt{2}}{1-u^2}\right)$$

with $u \equiv (4e_b/l_b - 1)^{-1/4}$. For very small scaled lengths at birth, this ratio becomes $B_{x_b}(\frac{1}{3},0)x_b^{-1/3}/3$, with $x_b \equiv \frac{g}{e_b+g}$. The development of the embryo in an egg is somewhat retarded at the end of incubation, because of the diminishing reserves. This means that the incubation period is somewhat longer than the corresponding gestation period and that the cumulative costs at birth of an egg are somewhat higher than those of a foetus. This comparison assumes that all parameters are equal. Another difference is that, when breeding, the incubating individual is more restricted in its freedom than the pregnant mother.

8.1.3.3 Versatility versus specialization

Bacteria as a group are much more diverse in their metabolism than eukaryotes. Within the α-subgroup of the purple non-sulphur bacteria, there is a wide variety of complex

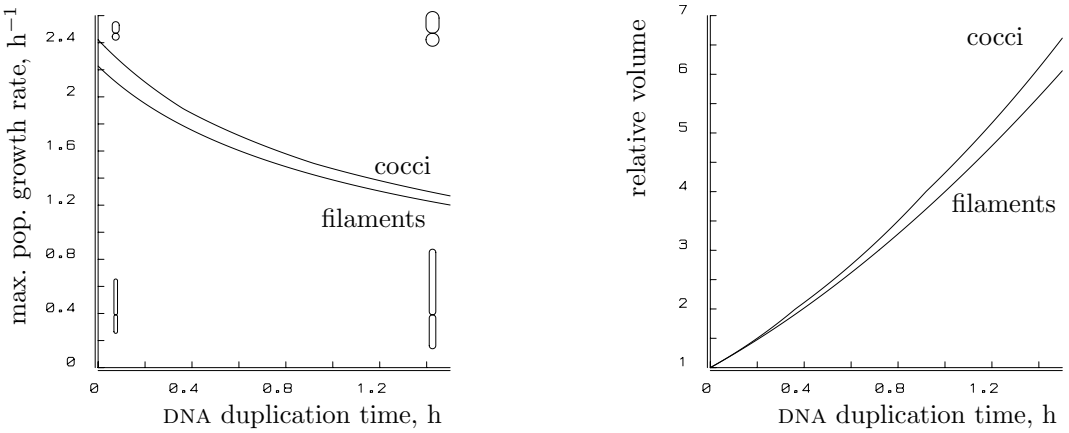

Figure 8.5: Maximum population growth rate decreases for increasing DNA duplication times. The curves are for aspect ratio $\delta = 0$, and 0.6. The aspect ratio is specified just prior to division and is fixed. Cell shape and relative size are indicated just before and after division for $\delta = 0.1$ and 0.6, at a doubling time of 0 and 1.5 h. Cell volume at division relative to the volume that triggers DNA duplication, V_d/V_p, is given in the right figure. Numerical studies show that the figure is independent of parameter values for l_p, g and k_M, given maximum population growth rate.

metabolic pathways, each involving a considerable number of genes [1380]. This can only be understood by assuming that the ancestor of this group possessed all the pathways for, for example denitrification, aerobic and anaerobic photosynthesis, methylotrophy, etc. During evolution, most species lost one or more of these traits; this brings us to the problem of understanding why it can be beneficial for species to cut out DNA that is not used in a particular environment rather than leaving it unused.

As shown in Figure 8.5, the DEB model offers an explanation; the population growth rate decreases for increasing DNA duplication time t_D, particularly at high substrate levels. As the growth process continues during DNA duplication, the cell becomes larger the longer the DNA duplication period, if DNA duplication is triggered once the cell reaches a certain specific size. Since the uptake of substrate relates to surface area, and the surface-area/volume ratio grows worse the larger the cell, the cell is better off reducing the time required to duplicate DNA. The effect of the DNA duplication time on the population growth rate is less at low substrate levels, because the division intervals are extended under these circumstances.

The evolutionary significance of a high population growth rate is probably found in the spatial and temporal heterogeneity of the environment. Useful substrates for heterotrophs are usually rare. If a plant or animal dies, the locally present microbes will grow at a high rate over a short period. If the subsequent selection processes thin randomly, the most abundant species has the best opportunity of surviving until the next time substrate becomes available. Since the ratio of the numbers grows exponentially at a rate equal to the difference in the population growth rates, small differences can be significant for long growth periods.

8.1.3.4 Growth versus reproduction: determinate growth

The relative amount of effort spent on reproduction differs from one species to another. Even within a species, it can depend on environmental conditions. Based on work with Dina Lika [858], this subsection compares the consequences of two allocation strategies in animals: indeterminate growth, where growth continues during the reproductive stage, and determinate growth, where growth is stopped during the reproductive stage. Both animals are otherwise similar, and have no differences during the embryonic stage, when no food uptake occurs, and the juvenile one, when no allocation to reproduction occurs. Both strategies frequently occur, even among rather closely related species: cladocerans sport indeterminate growth (*Daphnia magna* can grow by a factor two in length, that is a factor eight in volume, during the reproductive period), while copepods sport determinate growth.

8.1.3.5 Embryo and juvenile stages

The age at birth a_b and the energy costs per egg E_0 vary somewhat with the food density, because the reserve density at birth is taken to equal that of the mother: $[E_b] = f[E_m]$ at steady state. This applies to both allocation strategies that are compared. For simplicity's sake, I here take a_b constant and neglect maintenance costs during the embryonic stage, which results in the energy costs per egg $E_0 = ([E_G] + [E_m]f)V_b$. Up to the age at puberty a_p, the determinate animal is identical to the indeterminate one. At constant food density the volume $V(a)$ is given by

$$V(a) = \left(V_\infty^{1/3} - (V_\infty^{1/3} - V_b^{1/3}) \exp\{-\dot{r}_B a\}\right)^3 \tag{8.1}$$

with $\dot{r}_B = (3[E_G] + 3\kappa f[E_m])^{-1}[\dot{p}_M]$ and $V_\infty^{1/3} = fV_m^{1/3}$ and $V_m^{1/3} = \frac{\kappa\{\dot{p}_{Am}\}}{[\dot{p}_M]}$, where κ is the fraction of catabolic power that is allocated to somatic maintenance plus growth, as opposed to maturity maintenance plus maturation or reproduction.

The age at puberty a_p is reached when the cumulative investment in maturation exceeds a threshold value: $E_p = \int_{a_b}^{a_p} ((1-\kappa)\dot{p}_C(a) - [\dot{p}_J]V(a))\, da$, where E_p is the threshold value for energy invested in maturation, $\dot{p}_C$ the catabolic power and $[\dot{p}_J]$ is the specific maturation maintenance cost. The catabolic power is defined as the power that is released from the reserves to fuel metabolism. Substitution gives

$$E_p = (1-\kappa)f\left(\{\dot{p}_{Am}\}\int_{a_b}^{a_p} V^{2/3}(a)\, da - [E_m]\,(V(a_p) - V_b)\right) - [\dot{p}_J]\int_{a_b}^{a_p} V(a)\, da \tag{8.2}$$

If $[\dot{p}_J] = \frac{1-\kappa}{\kappa}[\dot{p}_M]$, the relationship (8.2) reduces to $E_p = [E_G](V(a_p) - V_b)\frac{1-\kappa}{\kappa}$, which reveals that $V(a_p)$ does not depend on the scaled functional response f. The stage transition occurs when cumulative investment in maturation exceeds a fixed threshold, while at the same time structural mass exceeds a fixed threshold; age at puberty a_p does depend on f, however. For other values of $[\dot{p}_J]$, $V(a_p)$ does depend on f, and κ, and stage transition no longer occurs at a fixed structural mass.

Figure 8.6 illustrates how the age and length at puberty depend on the scaled functional response f and the partitioning fraction κ. The value of κ for which the length at puberty

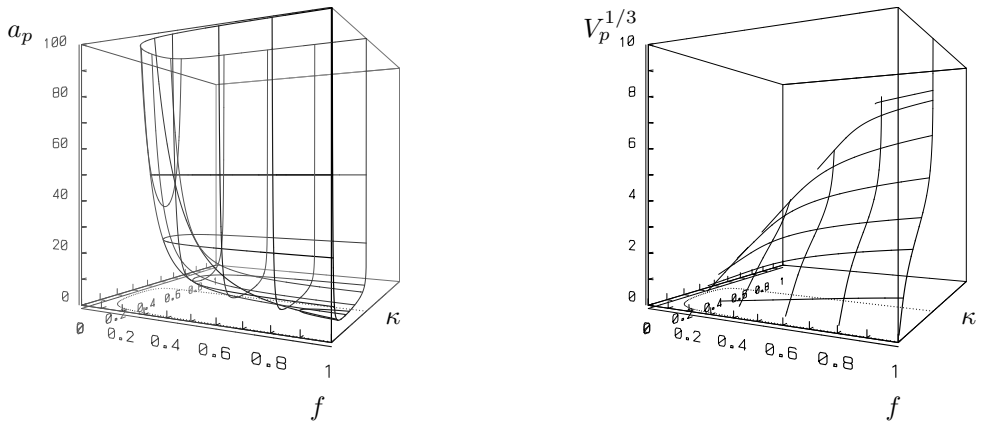

Figure 8.6: The age at puberty a_p (left) and length at puberty $V(a_p)^{1/3}$ (right) as functions of scaled functional response f, and partition coefficient κ. The parameter values are $V_b^{1/3} = 0.8\,\mathrm{mm}$, $[\dot{p}_M]/[E_m] = 0.1\,\mathrm{d}^{-1}$, $[\dot{p}_J]/[E_m] = 0.15\,\mathrm{d}^{-1}$, $E_p/[E_m] = 10\,\mathrm{mm}^3$, $\{\dot{p}_{Am}\}/[E_m] = 2.5\,\mathrm{mm\,d}^{-1}$, $[E_G]/[E_m] = 0.02$.

does not depend on the feeding rate is $\kappa = (1+[\dot{p}_J]/[\dot{p}_M])^{-1} = 0.4$, which is just outside the range for which maturity can be reached for this parameter combination (see also Figure 8.7). The volume at puberty can differ up to a factor of 6 from the ultimate volume at indeterminate growth for this choice of parameter values.

8.1.3.6 Adult stage

The hazard rate has a direct relationship with energetics, and relates to mean life span through $\mathcal{E}\underline{a}_\dagger = \int_0^\infty \Pr\{\underline{a}_\dagger > a\}\,da = \int_0^\infty \exp\{-\int_0^a \dot{h}(t)\,dt\}\,da$. For a reproduction rate $\dot{R}(a)$, the life span reproduction amounts to

$$N_R = \int_{a_p}^\infty \dot{R}(a) \Pr\left\{\underline{a}_\dagger > a\right\} da \tag{8.3}$$

Constant fraction allocation

In the constant fraction allocation strategy, a constant fraction κ of catabolic energy is allocated to somatic maintenance plus growth during all life stages. During the embryonic and juvenile stage, a constant fraction is allocated to maturity maintenance plus maturation; the investment in maturation switches to reproduction after the cumulated energy investment in maturation exceeds a certain threshold E_p. Maturity maintenance does not increase after the switch, but is proportional to volume before the switch. Somatic maintenance is always proportional to volume.

The reproduction rate is

$$\dot{R}(a) = \frac{\kappa_R}{E_0}\left(\frac{(1-\kappa)f}{\kappa f/[E_G] + 1/[E_m]}\left(\frac{\{\dot{p}_{Am}\}}{[E_m]}V^{2/3}(a) + \frac{[\dot{p}_M]}{[E_G]}V(a)\right) - [\dot{p}_J]V(a_p)\right) \tag{8.4}$$

while the volume $V(a)$ is given by (8.1).

If the aging acceleration is small enough, such that the period of substantial growth is short with respect to the life span, the hazard rate and the survival probability can be approximated by

$$\dot{h}(a) = \frac{\ddot{h}_a[\dot{p}_M]}{2\kappa[E_G]}(a-a_p)^2; \quad \Pr\{\underline{a}_\dagger \geq a\} = \exp\left\{-\frac{\ddot{h}_a[\dot{p}_M]}{6\kappa[E_G]}(a-a_p)^3\right\}$$

for $a \geq a_p$.

The mean life span equals

$$\mathcal{E}\underline{a}_\dagger = a_p + \Gamma\left(\frac{1}{3}\right)\left(\frac{6\kappa[E_G]}{27\ddot{h}_a[\dot{p}_M]}\right)^{1/3} \simeq a_p + 1.62\left(\frac{\kappa[E_G]}{\ddot{h}_a[\dot{p}_M]}\right)^{1/3} \tag{8.5}$$

Bang-bang allocation

The bang-bang allocation strategy is the same as the fixed-fraction allocation one, but growth is ceased at certain volume V_p; all catabolic energy is then allocated to maintenance (somatic plus maturity) plus reproduction. This leads to the reproduction rate

$$\dot{R} = \frac{\kappa_R}{E_0}\left(f\{\dot{p}_{Am}\}V^{2/3}(a_p) - ([\dot{p}_M] + [\dot{p}_J])V(a_p)\right) \tag{8.6}$$

If the aging acceleration is small enough, such that survival to puberty is almost sure, the hazard rate and the survival probability for the determinate animal can be approximated for $a \geq a_p$ by

$$\dot{h}(a) = \frac{\ddot{h}_a\{\dot{p}_{Am}\}f}{2[E_G]V^{1/3}(a_p)}(a-a_p)^2; \quad \Pr\{\underline{a}_\dagger \geq a\} = \exp\left\{-\frac{\ddot{h}_a\{\dot{p}_{Am}\}f}{6[E_G]V^{1/3}(a_p)}(a-a_p)^3\right\}$$

The mean life span is

$$\mathcal{E}\underline{a}_\dagger = a_p + \Gamma\left(\frac{1}{3}\right)\left(\frac{6[E_G]V^{1/3}(a_p)}{27\ddot{h}_a\{\dot{p}_{Am}\}f}\right)^{1/3} \simeq a_p + 1.62\left(\frac{[E_G]V^{1/3}(a_p)}{\ddot{h}_a\{\dot{p}_{Am}\}f}\right)^{1/3} \tag{8.7}$$

and the life span reproduction simplifies to $N_R = \dot{R}(\mathcal{E}\underline{a}_\dagger - a_p)$.

8.1.3.7 Comparison of reproduction and life span

Assuming that aging allows, the reproduction rate of the fully grown indeterminate animal exceeds that of the determinate one if

$$(1-\kappa)V_\infty - V_\infty^{1/3}V^{2/3}(a_p) + \kappa V(a_p) \geq 0 \tag{8.8}$$

Somatic maintenance costs can only be paid by the neonate if $V_\infty \geq V_b$. Maturity can only be maintained by the neonate if $V_\infty \geq V_b\left(\frac{\kappa}{1-\kappa}\frac{[\dot{p}_J]}{[\dot{p}_M]}\right)^3$. Reproduction is only initiated if $V_\infty > V(a_p)$. For very low feeding rates, the ultimate size can drop below the size at birth, as implied by the model assumptions. Figure 8.7 illustrates that the reproduction

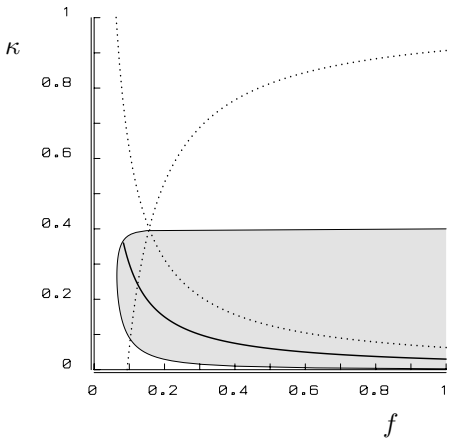

Figure 8.7: The grey area indicates the combination of values for the scaled functional response f and the partitioning fraction κ, for which the adult state is reached; the age at puberty is infinitely large at its border. The fat curve represents values for f and κ where the reproduction rate of the determinate animal equals that of a fully grown indeterminate one. The dotted curves represent boundaries for which the neonate just can pay somatic and maturity maintenance costs. Parameter values: see Figure 8.6.

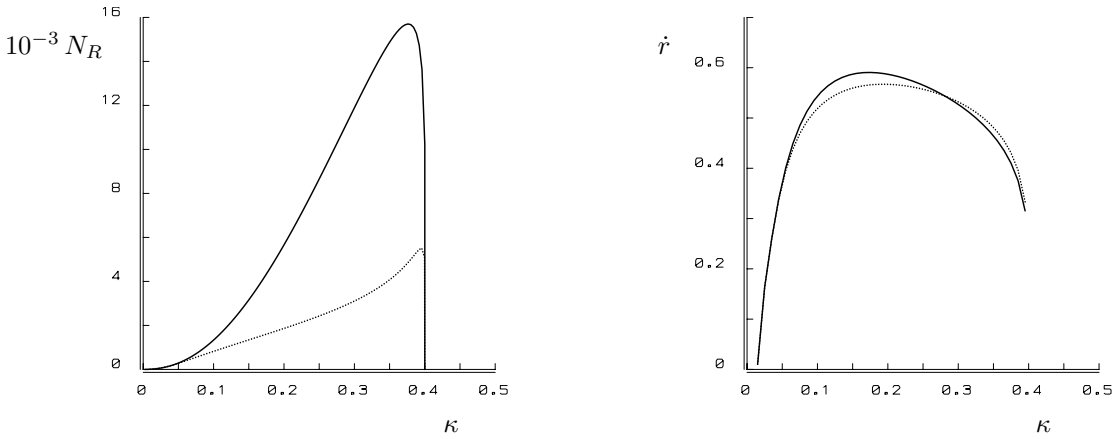

Figure 8.8: The life span reproduction N_R (left) and the population growth rate $\dot{r}$ (right) of the indeterminate (solid) and the determinate (dotted) animals as a function of the partitioning fraction κ at abundant food ($f = 1$). Parameters: see Figure 8.6, and $\kappa_R = 1$, $\ddot{h}_a = 5\,10^{-7}\,\mathrm{d}^{-1}$.

rate of a fully grown indeterminate animal exceeds that of the determinate one for all biologically meaningful combinations of f and κ, given the parameter values. The area left of the concave (upper-left to lower-right) dotted curve is less relevant, because this is where the ultimate size is below that of the neonate. The area left of the convex (lower-left to upper-right) dotted curve represents values for f and κ where neonates cannot maintain their state of maturity.

Comparison of (8.5) and (8.7) shows that the life span of the indeterminate animal exceeds that of the determinate one if $V_\infty > V(a_p)$, which is always the case. The reason is in the decreasing specific oxygen consumption for increasing body size. The assumption that death by aging is negligibly small before puberty obviously breaks down when the juvenile period becomes excessively large.

Figure 8.8 gives the life span reproduction and the population growth rate as a function of the partition coefficient at abundant food ($f = 1$), and shows that the differences between both allocation rules are substantial for the life time reproduction, but small for

the population growth rate, given this choice of parameter values.

The bang-bang allocation will probably lead to larger population growth rates for high death rates, because reproduction is larger just after maturation and the contribution of the early offspring to the population growth rate is more important than that made by later offspring. This is because the early offspring will reproduce earlier as well, the interest upon interest principle. Selection for high population growth rates can be expected in situations of alternating periods of food abundance, followed by starvation with random thinning.

The difference between determinate and indeterminate growth disappears if the switch to the adult stage is outside the growth period, so the body size at puberty is close to the ultimate body size. Copepods, which cannot grow once they start reproduction, in fact follow the von Bertalanffy growth curve quite well. The difference with daphnids, which keep their growth potential, only becomes apparent if the animals are continuously exposed to low food densities during their juvenile stage, and then exposed to high food densities during the adult stage. This might be a rather artificial situation, with little relevance to field ecology. Holometabolic insects cannot grow after the pupal stage, and juveniles and adults feed on different diets; the coupling of energetic properties between adults and juveniles still awaits further study in the context of the DEB theory.

8.2 Inter-specific parameter variations

8.2.1 Primary scaling relationships

The value $[E_G] = 2800\,\mathrm{J\,cm^{-3}}$ in Table 8.1 corresponds with a wet-over-dry weight ratio of 10, a chemical potential for structure of $\mu_V = 560\,\mathrm{kJ\,C\text{-}mol^{-1}}$, a growth efficiency of $\kappa_G = 0.8$ and the molecular weight for structure of $w_V = 24.6\,\mathrm{g\,C\text{-}mol^{-1}}$, so $[M_V] = d_V/w_V = 4\,\mathrm{mmol\,cm^{-3}}$. The growth efficiency κ_G is the energy fixed in new structure as fraction of the energy invested in growth. It is likely to vary somewhere between 0.75 and 0.9. The chemical potential is somewhere between 616 (for lipids) and 401 (for proteins) $\mathrm{kJ\,C\text{-}mol^{-1}}$, Table 4. The molecular weight is determined by the chemical indices as given in Figure 4.15, on the assumption that the chemical elements C, H, O and N comprise (almost) all of the mass. Although structure might differ from reserve in chemical composition, it is less likely that it will differ much in terms of elemental frequencies. The cost for structure is given by $[E_G] = \frac{\mu_V d_V}{\kappa_G w_V}$. Its most variable component is the specific density d_V. Assuming that the specific density for wet mass is close to $d_V = 1\,\mathrm{g\,cm^{-3}}$, that for dry mass will vary from $d_V = 0.01\,\mathrm{g\,cm^{-3}}$ for gelatinous taxa (cnidaria, ctenophores, appendicularians, tunicates) to $0.3\,\mathrm{g\,cm^{-1}}$ for vertebrates (birds, mammals), a variation by an order of magnitude. The variation in $[E_G]/d_V$ is found to be really small in the add_my_pet library, see Figure 8.9, but the role of κ_G as pseudo data point needs further evaluation.

Although most primary parameters depend on L_m as expected, see Figure 8.9, some noticeable deviations exist (see below). Accelerating species have a small maturity at birth, metamorphosis and puberty, given maximum structural length, but the differences with non-accelerating species decrease from birth to puberty. These seem to catch up with

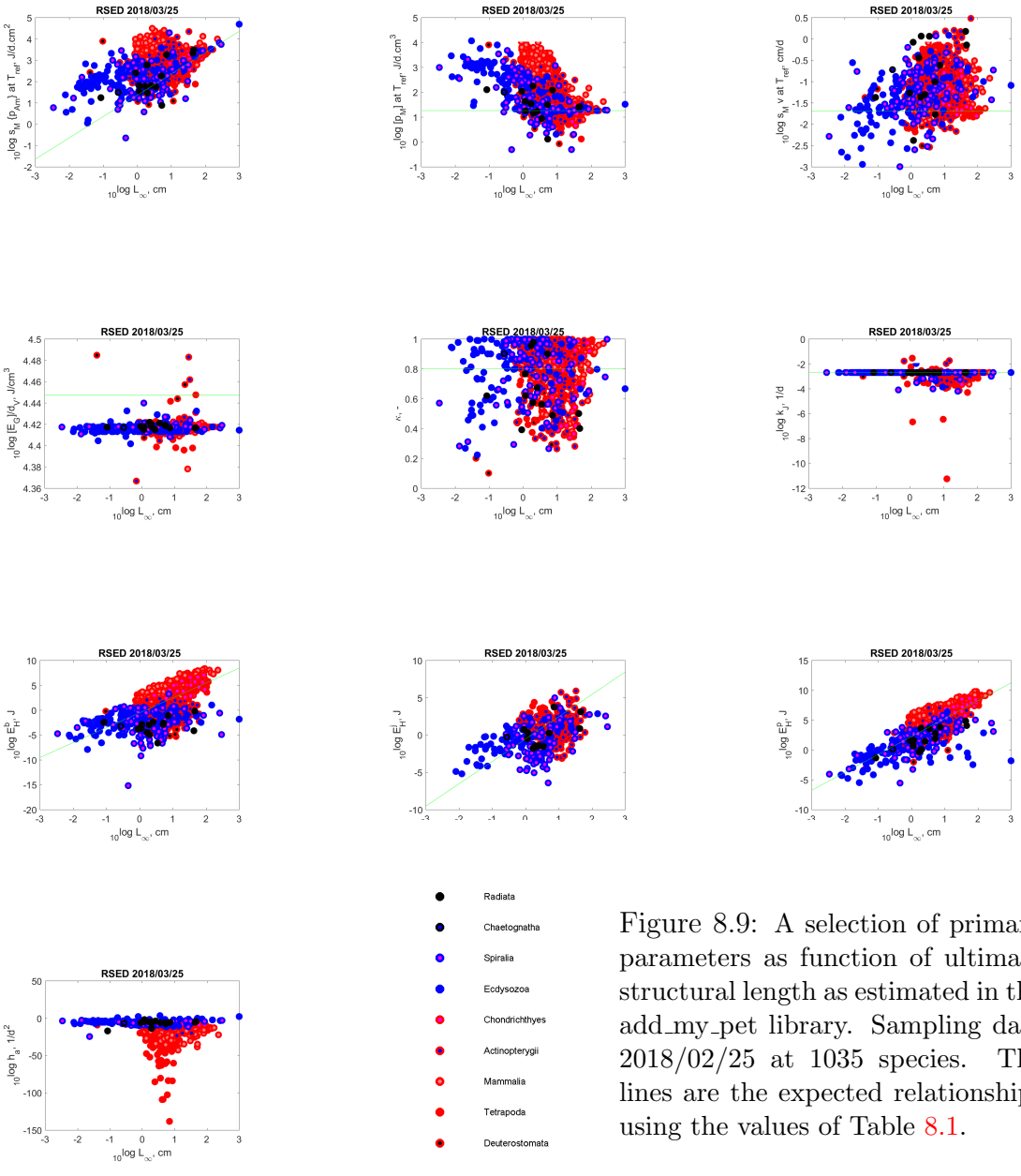

Figure 8.9: A selection of primary parameters as function of ultimate structural length as estimated in the add_my_pet library. Sampling date 2018/02/25 at 1035 species. The lines are the expected relationships using the values of Table 8.1.

Table 8.4: Extreme estimates for the specific somatic maintenance costs $[\dot{p}_M]$ in $\mathrm{J\,d^{-1}cm^{-3}}$, for the 130 species in the add_my_pet collection, corrected for a temperature of 20 °C. The cladocerans and copepods comprise *Chydorus sphaericus*, *Ceriodaphnia pulchella*, *Daphnia cucullata*, *Daphnia hyalina*, *Daphnia magna*, *Daphnia pulex*, *Scapholeberis mucronata*, *Simocephalus serrulatus*, *Diaphanosoma brachyurum*, *Acanthocyclops robustus*, *Cyclops vicinus*, *Mesocyclops leukarti*, *Eurytemora affinis*.

	$[\dot{p}_M] < 10\,\mathrm{J\,d^{-1}cm^{-3}}$		$[\dot{p}_M] > 1000\,\mathrm{J\,d^{-1}cm^{-3}}$
3	*Eunectus murinus*	1300	*Oikopleura longicauda*
4	*Boa constrictor*	1400	daphnids, copepods
5	*Andrias japonicus*	1450	*Caenorhaditis elegans*
7	*Callorhinus ursinus*	2100	*Bosmina coregoni, B. longirostris*
8	*Esox lucius*	2300	*Oikopleura dioica*
10	*Acipenser ruthenus*	8100	*Thalia democratica*

non-accelerating species during ontogeny.

8.2.1 Waste to hurry

Some small-bodied species have a very high specific somatic maintenance and assimilation rates (the two are coupled given a value for L_m). Other, medium-sized, species have low values [777]. Table 8.4 gives extremes in the add_my_pet collection; the champion is *Thalia democratica* with $8\,\mathrm{kJ\,cm^{-3}d^{-1}}$, which forms blooms that can be seen on satellite images. The tadpole shrimp *Triops longicaudatus* has a specific somatic maintenance of $4\,\mathrm{kJ\,cm^{-3}d^{-1}}$ at 20 °C; it needs to complete its life cycle during the short period that its pool lasts, to negotiate the subsequent long dry period as egg. The taxa with high values are all adapted to follow temporary peaks in local food abundance rapidly with population numbers; for most of these species resting stages are known to survive periods with starvation. This suggests that these species waste energy to stay small. Wasting energy is very well known in the micro-biological and biochemical literature as futile cycles [1140, 1366, 1367]. The pathway of destroying ATP is known, but its function was not. What is new is the effect that this can have, in combination with high intake, on growth and reproduction at the level of the individual, thanks to the κ-rule: somatic maintenance competes with growth and reproduction is a parallel process.

Figure 8.10 shows that specific somatic maintenance actually decreases for increasing ultimate length, and is about proportional to maximum specific growth and to squared specific investment into reproduction: the waste-to-hurry principle.

Figure 8.11 shows that the fact that $[\dot{p}_M]$ decreases with L_∞ is due to the fact that it increases with $\{\dot{p}_{Am}\}$ post-metamorphosis: $s_{\mathcal{M}}\{\dot{p}_{Am}\} \propto [\dot{p}_M]^x$ with $x \simeq 0.8$, [**?**]. Given that ultimate structural length at abundant food is $L_\infty = \kappa\{\dot{p}_{Am}\}/[\dot{p}_M]$, where $\{\dot{p}_{Am}\}$ is the value after acceleration for accelerating species, we then have $[\dot{p}_M] \propto L_\infty^{\frac{1}{x-1}}$ and $\{\dot{p}_{Am}\} \propto L_\infty^{\frac{x}{x-1}}$. Both these exponents are negative for $0 < x < 1$. Maximum assimilation is $\dot{p}_{Am} = \{\dot{p}_{Am}\}L_\infty^2 \propto L_\infty^{2+\frac{x}{x-1}}$. For $x = 0.8$ the exponent amounts to -2. The co-variation

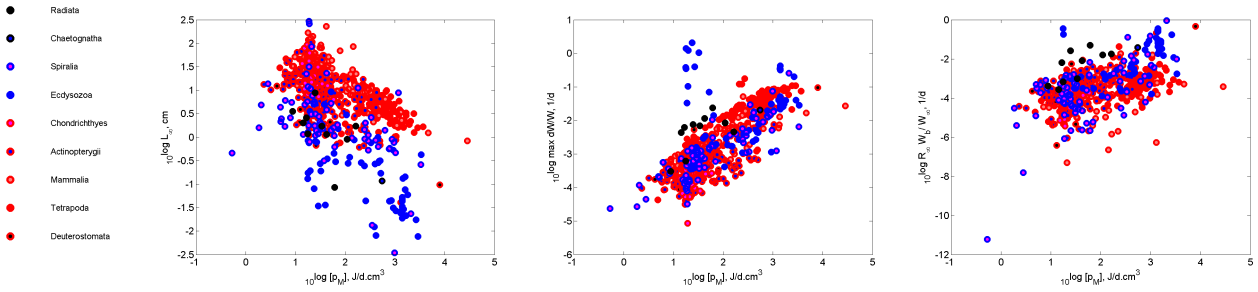

Figure 8.10: Ultimate length decreases for increasing specific somatic maintenance, while maximum growth rate and ultimate reproduction rate increases. Data from the AmP collection, sampling date 2017/05/23 at 685 species.

rules expect that $\dot{p}_{Am} \propto L_\infty^3$, so very different indeed! The consequence of $\{\dot{p}_{Am}\} \propto [\dot{p}_M]^{0.8}$ is, thus, that large-bodied species would have less to assimilate than small-bodied ones, which is clearly impossible. This explains why big-bodied species have problems to evolve the waste-to-hurry strategy. They cannot increase both (specific) assimilation and (specific) somatic maintenance to boost growth and reproduction, and are bound to be efficient, by having a low specific somatic maintenance. This problem comes on top of the problem that periods of food abundance do not last long, while juvenile period and life span increase with body size. Small-bodied species need to combine the waste-to-hurry strategy, i.e. increase both specific assimilation and specific somatic maintenance, with torpor or migration to survive starvation periods. Waste-to-hurry strategists are better in increasing specific somatic maintenance, than specific assimilation (hence the power 0.8). Yet, reserve density increases with specific somatic maintenance, caused by an increase of specific assimilation with specific somatic maintenance, while energy conductance is independent.

The combination of large body size and high specific somatic maintenance is not possible. The range of specific somatic maintenance values among species dramatically increases for decreasing maximum body size. The waste-to-hurry phenomenon has great ecological importance since it enhances the mass and energy flow from phyto-plankton to the food chain, where the fast-eating small-bodied grazers are at the bottom. Without this enhanced input, food pyramids would be much smaller in aquatic habitats.

A high specific somatic maintenance goes with a low no-effect concentration (NEC) for toxic chemicals [59], see Figure 8.12. Many agricultural pest species live under conditions that favor waste-to-hurry: the large food supply, so no selection for efficiency, but only available for a short time (at least the typical crops). This makes these pest species thus more vulnerable for pesticides (as general pattern).

8.2.1 Ageing acceleration

Another deviation in the trends in parameter values concerns the ageing acceleration $\ddot{h}_a$, which is expected to be proportional to the zoom factor, but found to be inversely proportional to it. This is caused by the waste-to-hurry phenomenon again, where small-bodied

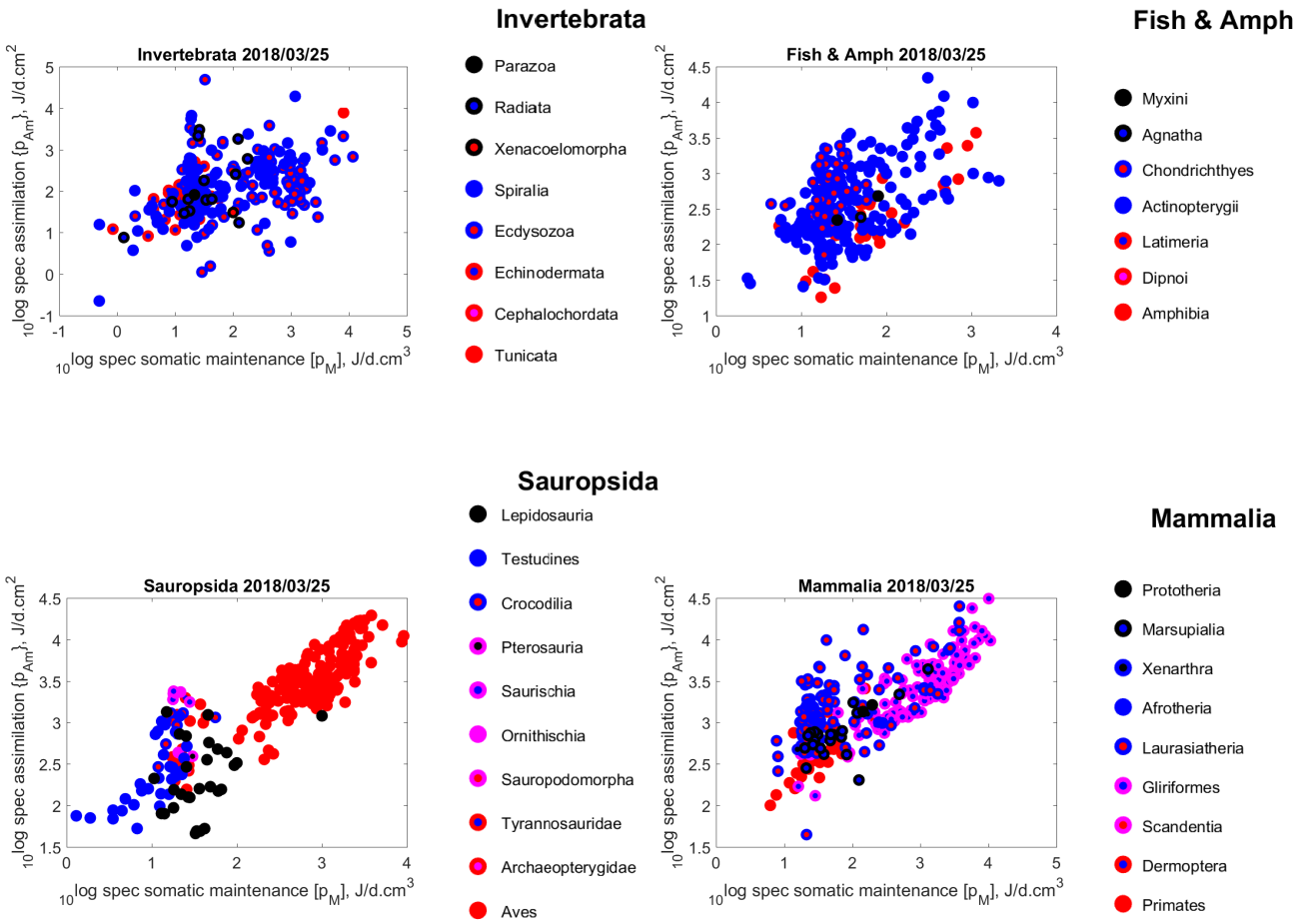

Figure 8.11: Maximum specific assimilation after acceleration as function of specific somatic maintenance at the reference temperature of 20 °C among animal taxa. The parameters come from the AmP collection at 2017/12/27, when it had 913 entries. The lines are eyeball fitted, see Table **??**

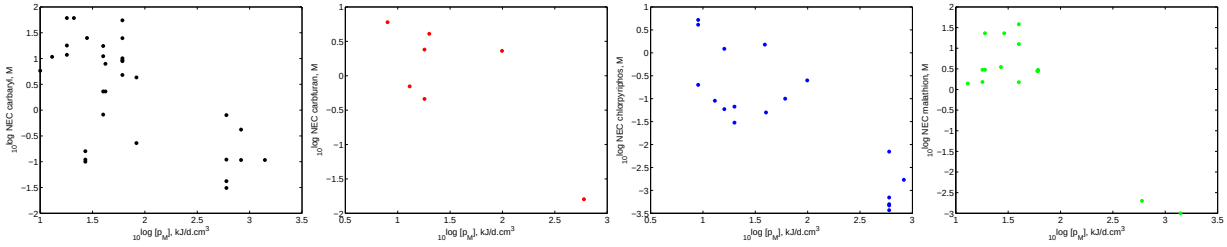

Figure 8.12: The No Effect Concentration as function of the specific somatic maintenance for 4 pesticides. Data from [59].

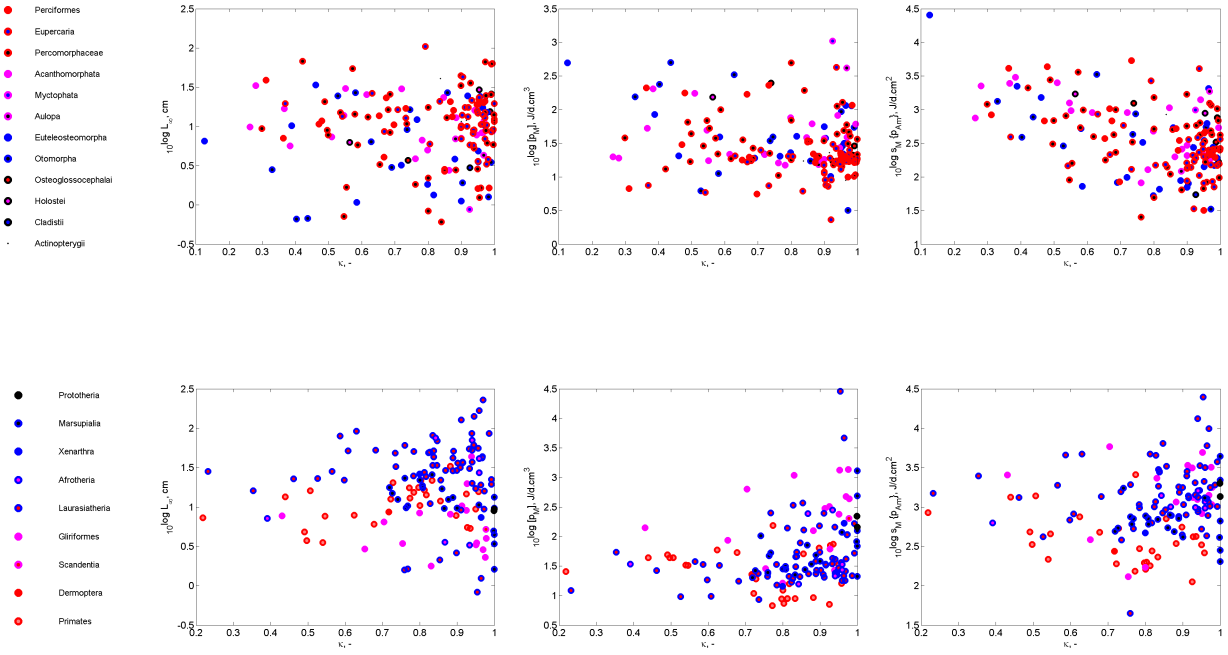

Figure 8.13: Ultimate length in Actinopterigii is independent of κ, because assimilation capacity decreases with κ. Ultimate length in Mammalia is also independent of κ, but now because specific maintenance increases with κ.

species have a very high maintenance, which affects how the ageing acceleration depends on maximum structural length.

8.2.1 Assimilation capacity

The primary parameters κ, $\{\dot{p}_{Am}\}$ and $[\dot{p}_M]$ are thought to be independent of each other. This would imply that ultimate length $L_\infty = \kappa s_\mathcal{M}\{\dot{p}_{Am}\}/[\dot{p}_M]$ would increase with κ. Although scatter obscures relationships, L_∞ does not always clearly behave like that in plots. In mammals, which have $s_\mathcal{M} = 1$, L_∞ seems independent of κ, because $[\dot{p}_M]$ tends to increase with it. In actynoperygii L_∞ seems independent of κ, because $s_\mathcal{M}\{\dot{p}_{Am}\}$ tends to decrease with it, see Figure 8.13.

Since $s_\mathcal{M}\dot{v}$ seems independent of κ for them, the implication is that reserve capacity $[E_m]$ decreases with κ and $g = \frac{[E_G]}{\kappa[E_m]}$ is again independent of κ.

8.2.2 Secondary scaling relationships

Length at birth is independent of ultimate length, $L_\infty = s_\mathcal{M} f L_m$, in the class Actinopterigii. This probably relates to adaption of feeding on plankton as neonates, and staying in surface waters without much effort, being transported by stream in these waters.

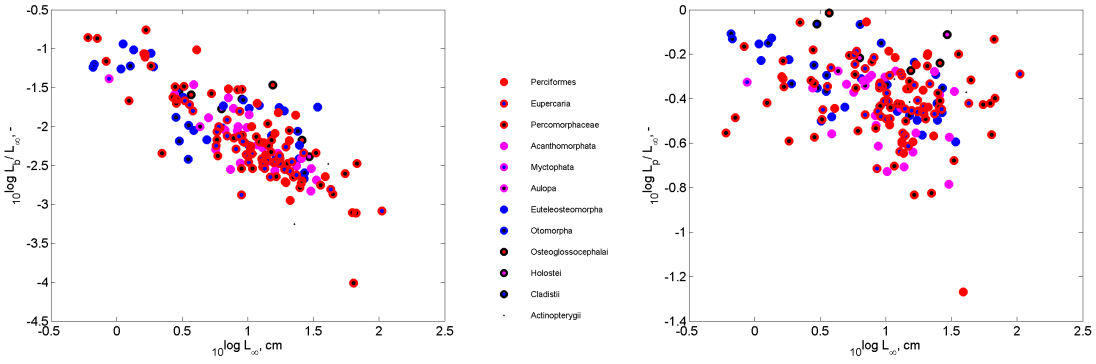

Figure 8.14: While length at puberty is proportional to ultimate length in Actinopterigii, as typical, length at birth is independent of ultimate length in this class.

8.2.2 Respiration

Only three key features of DEB theory matter to understand why weight-specific respiration decreases with maximum body weight of species [853]:

1 food is converted to a temporary metabolic pool called 'reserve' (a process called assimilation), and reserve is mobilized for metabolism (see [859] for a detailed discussion)

2 a fraction κ of mobilized reserve is allocated to somatic maintenance and growth (the κ-rule)

3 somatic maintenance is proportional to the permanent metabolic pool, referred to as 'structure'. So reserve does not require maintenance (see [762, 774] for a detailed discussion)

This is all one needs to know, since respiration, defined as dioxygen flux, follows from the mass balance.

If specific somatic maintenance increases, all else being equal, the ultimate body mass decreases and the weight-specific respiration increases since somatic maintenance dominates respiration in fully-grown individuals. If, on the other hand, specific assimilation increases, ultimate body mass increases, as does maximum reserve density, and the weight-specific respiration decreases as consequence.

These two changes in volume-specific somatic maintenance and surface area-specific assimilation underlie why weight-specific respiration generally decreases with body size. The understanding of why respiration behaves like this is directly linked to the understanding of why specific assimilation and/or specific maintenance would vary among species. Although these implications of DEB theory have been known for some time [760], the question of how or why assimilation and maintenance vary among species seems very different from the question of how respiration depends on body size, but in a DEB context they are actually the same questions.

type	quality	1	2	3	4	5	6	7	8
eye	closed	+	+	-	-	-	-	-	-
plumage	naked	+	-	-	-	-	-	-	-
	down	-	+	+	+	+	+	+	+
	contour	-	-	-	-	-	-	±	+
activity	motor	-	±	+	+	+	+	+	+
	locomotor	-	-	-	+	+	+	+	+
behaviour	stay in nest	+	+	+	-	-	-	-	-
	fed by parents	+	+	+	+	+	-	-	-
	follow parents	-	-	-	-	+	+	+	-
	search alone	-	-	-	-	-	±	+	+
	no interaction	-	-	-	-	-	-	-	+

score	label
1	altricial
2	semialtrical 2
3	semialtrical 1
4	semiprecocial
5	precocial 4
6	precocial 3
7	precocial 2
8	precocial 1

Table 8.5: Scores from altricial (1) to precocial (8) in neonate birds based on Nice [1030], according to Starck & Ricklefs[1356, 1357].

8.2.2 Respiration-reproduction coupling

Empirical relationships between parameter values suggest that the maximum neonate mass production rate is proportional to maximum respiration, with proportionality factor 10 g/mol. This relationship can be used in cases where we have uncertainty about the reproduction rate, and estimate κ from this relationship.

The maximum neonate mass production rate amounts to $\dot{J}^\infty_{W^b_w} = W^b_w \dot{R}_m = W^b_w \kappa_R * (1-\kappa) * \dot{k}_M * (s_\mathcal{M} * (s_\mathcal{M} - l_T)^2 - k * v_H p)/u_E 0$, cf Eq (2.58) of DEB3. The maximum respiration rate is the third element in $\dot{\boldsymbol{J}}_\mathcal{M} = -\boldsymbol{n}^{-1}_\mathcal{M} \boldsymbol{n}_\mathcal{O} \dot{\boldsymbol{J}}_\mathcal{O}$, see Eq (4.35), where $\dot{\boldsymbol{J}}_\mathcal{O} = (\ \dot{J}^\infty_X \quad \dot{J}^\infty_V \quad \dot{J}^\infty_E + \dot{J}^\infty_{E_R} \quad \dot{J}^\infty_P\ )^T$ and $\dot{J}^\infty_X = s_\mathcal{M}\{\dot{p}_{Am}\} \frac{L^2_m (s_\mathcal{M} - l_T)^2}{\mu_X \kappa_X}$, $\dot{J}^\infty_V = 0$, $\dot{J}^\infty_E = 0$, $\dot{J}^\infty_{E_R} = \frac{E_0 \dot{R}_m}{\kappa_R \mu_E}$ and $\dot{J}^\infty_P = \kappa_P s_\mathcal{M} \{\dot{p}_{Am}\} \frac{L^2_m (s_\mathcal{M} - l_T)^2}{\mu_P \kappa_X}$. The initial reserve is $E_0 = u^0_E g [E_m] L^3_m$. Given parameters, we can predict $w_R = dot J^\infty_{W^b_w} / \dot{J}^\infty_O$ and minimize the difference with the expected value of 10 g/mol. This can be seen as a constraint on parameter values, which involves many parameters, but is very sensitive for κ.

8.2.2 Altriciality index

The concept of the altricial-precocial spectrum typically applied to birds and mammals only. A semi-quantitive scoring method exists for birds, see Table 8.5.

Birds and mammals are described as altricial if born in an early state of development (no feather or fur, eyes closed) or as precocial if born in an advanced state (directly capable of running around, searching for food). A natural altriciality index is the maturity ratio $s^{pb}_H = E^p_H / E^b_H$, see Figure 8.15. *Oikopleura* (and insects) score lowest ($s^{pb}_H = 0$) by skipping the juvenile period and directly allocate to reproduction at birth. Endotherms are more precocial, while placentals are more precocial than marsupials and birds. See Section 8.1.3.1. of the comments for links between neonate size and nitrogen waste, and the explanation for why birds evolved from precocial to altricial, while mammals in the opposite direction. See Section 8.1.1 of the comments for intra-specific difference in altriciality for

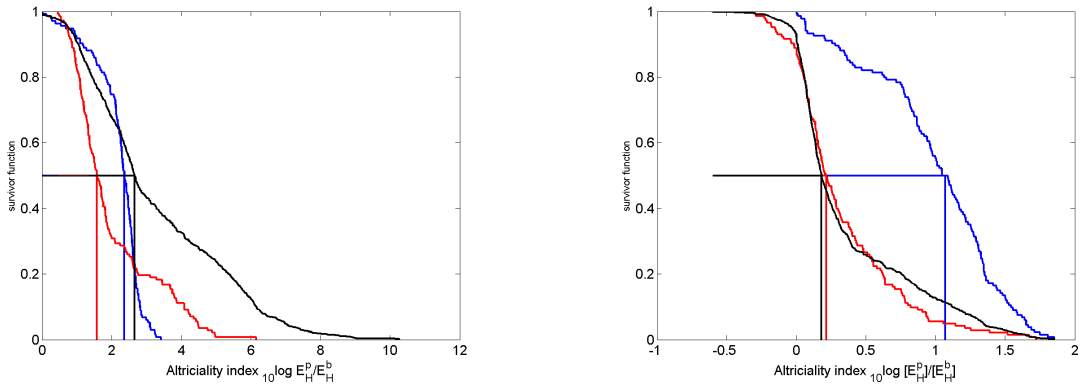

Figure 8.15: The survivor function of the $\log_{10}$ maturity ratio s_H^{pb} (left), and the corresponding one on the basis of maturity densities (right) of the species in the add_my_pet collection. Sampling animals (

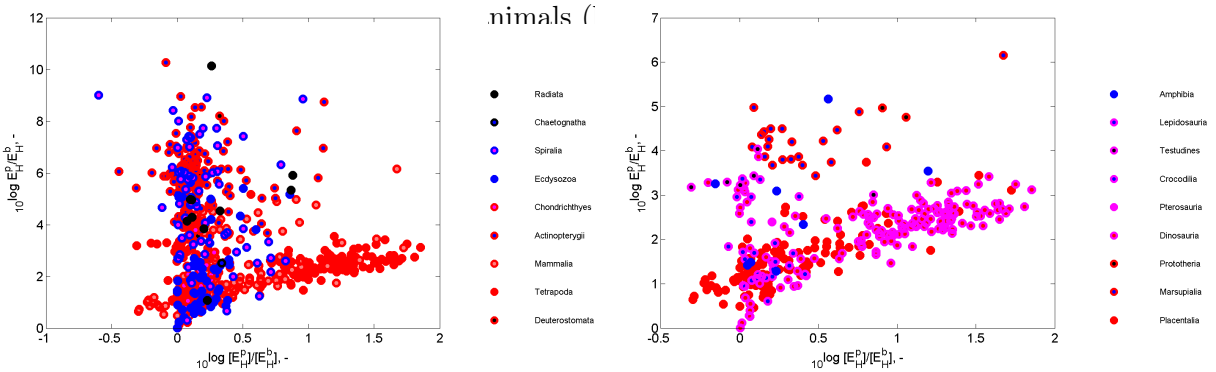

Figure 8.16: The alternative altriciality coefficients show little correlation, except for the Tetrapods; E_H^p/E_H^b for the marsupials scores higher than that of the placentalia, but still correlates well.

chickens and cows.

Figure 8.17 shows that the maturity ratio is proportional to L_∞^4 in ray-finned fish. If $E_H^p \propto L_p^3$ and $L_p \propto L_\infty$, while $E_H^b \propto L_b^3$ and $L_b \propto L_\infty^0$, we would expect an exponent of 3. See Figure 8.14. But it is found to be 4, due to the behaviour of E_H^p in ray-finned fish.

Figure 8.16 shows how the maturity ratio $s_H^{pb} = E_H^p/E_H^b$ relates to the maturity density ratio $s_{HL}^{pb} = [E_H^p]/[E_H^b]$.

8.2.2 Maximum reproduction

The reproduction rate is expected to decrease with maximum (structural) length among species. Maximum structural length, i.e. the cubic route for maximum structural volume, equals $L_m = \kappa\{\dot{p}_{Am}\}/[\dot{p}_M]$. Apart from contributions by reserve and reproduction buffer, maximum structural volume is the maximum volume of an individual. Maturity at birth is expected to be proportional to cubed maximum length, which leads to a constant relative

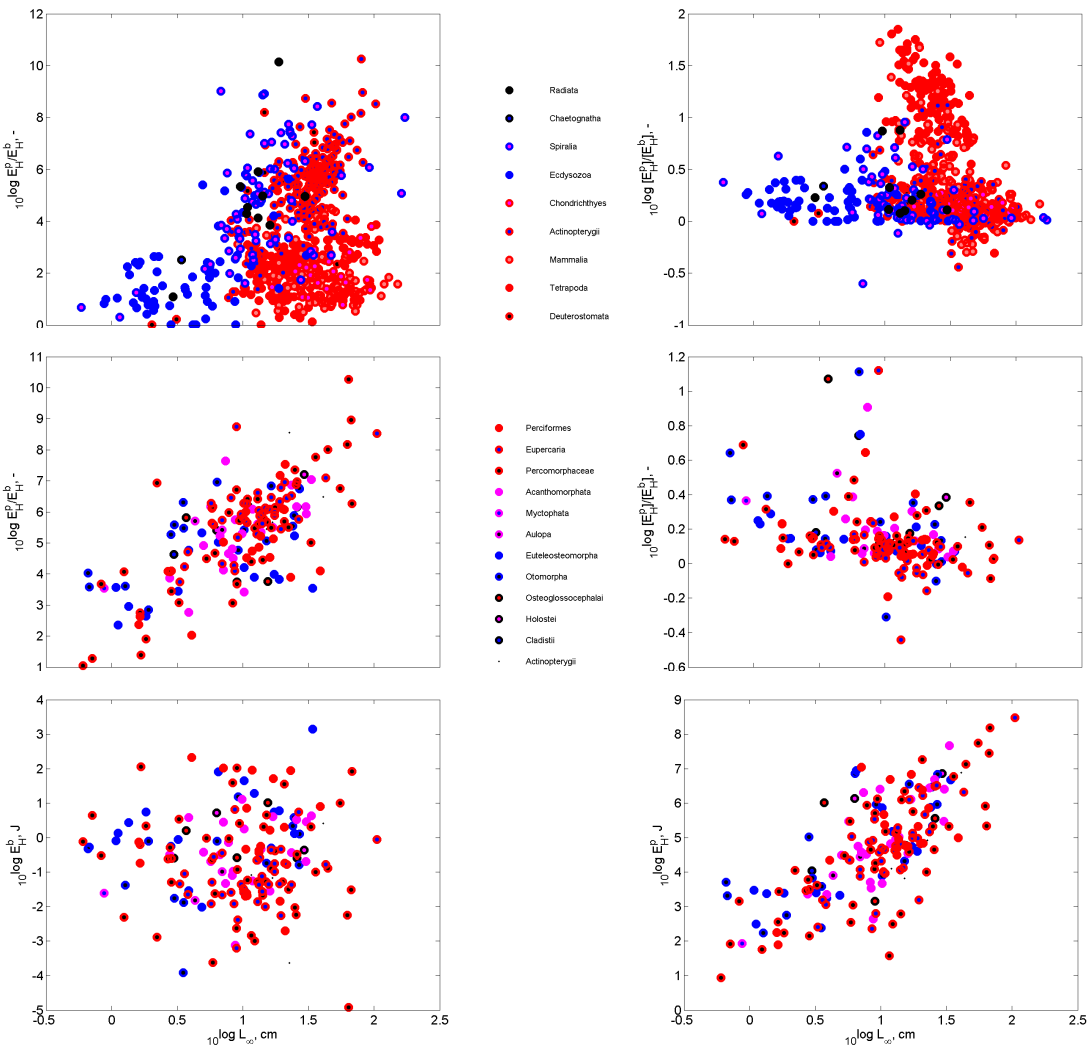

Figure 8.17: The maturity ratio $s_H^{pb} = E_H^p/E_H^b$ tends to increase in scatter with ultimate body length. It is about proportional to L_∞^4 for Actinopterygii, but not for other taxa. Maturity at birth is independent of ultimate body length in Actinopterygii, but increases with L_∞^4 at puberty. The maturity density ratio hardly depends on ultimate body length.

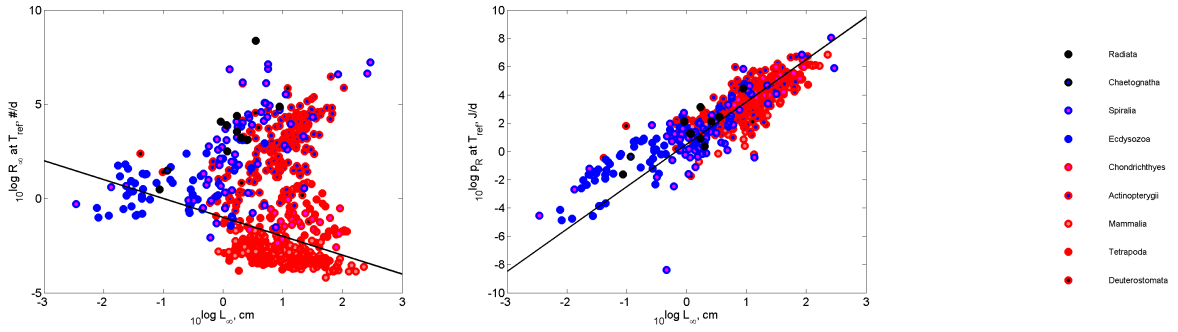

Figure 8.18: Left: The expected maximum reproduction rate (left) and investment in reproduction (right) at 20 °C as function of the maximum structural length among the 684 entries in the add_my_pet collection, sampling data 2017/05/08. The line, with slope −1 (left) or 3 (right), is based on simple physical and chemical expectations.

length at birth. Figure 8.18, updated from [792], shows that the tendency for reproduction is actually present in the add_my_pet collection, but large deviations occur. This is mainly due to species of fish, echinoderms and bivalves that have a (relatively) large body size, but tiny and many eggs. The ocean sunfish *Mola mola*, for example, has a maximum weight of 2.3 Mg and produces some $3\,10^{10}$ eggs per year. Endotherms (birds and mammals) have relatively large offspring. The cost per egg (or foetus) scales with structural length to the power 4 [762, 775], so the product of the reproduction rate and the cost per offspring, the energy investment in reproduction, should scale with cubed length and is not sensitive for relative size of offspring. Figure 8.18 confirms that beautifully and the scatter is much smaller.

A related quantifier is the investment into reproduction as fraction of assimilation at constant food for ultimate size, i.e. $e = l = f$. $\kappa_R^A = \frac{\dot{p}_R^\infty}{\dot{p}_A^\infty} = \frac{(1-\kappa)\dot{p}_C^\infty - \dot{p}_J^\infty}{\dot{p}_A^\infty} = \frac{(1-\kappa)\dot{p}_A^\infty - \dot{p}_J^\infty}{\dot{p}_A^\infty} = 1 - \kappa - \frac{\dot{p}_J^\infty}{\dot{p}_A^\infty} = 1 - \kappa - \frac{\dot{k}_J [E_H^p] f^3 L_m^3}{f^3 \{\dot{p}_{Am}\} L_m^2} = 1 - \kappa - \dot{k}_J [E_H^p] \frac{\kappa \{\dot{p}_{Am}\}/[\dot{p}_M]}{\{\dot{p}_{Am}\}} = 1 - \kappa - \kappa k \frac{[E_H^p]}{[E_G]} = 1 - \kappa - k u_H^p / f^3 = 1 - \kappa(1 + \frac{[\dot{p}_J^p]}{[\dot{p}_M]}) = 1 - \kappa - s_s/\kappa^2$, with $u_H^p = \frac{E_H^p}{g[E_m]L_m^3} = \kappa f^3 \frac{[E_H^p]}{[E_G]}$ for $[E_H^p] = \frac{E_H^p}{f^3 L_m^3}$ and $[\dot{p}_J^p] = [E_H^p]\dot{k}_J$ and supply stress $s_s = \frac{\dot{p}_J^\infty}{\dot{p}_A^\infty}\kappa^2 = \frac{\dot{p}_J^\infty \dot{p}_M^{\infty 2}}{\dot{p}_A^{\infty 3}}$. A natural constraint is $\kappa_R^A \geq 0$, which implies a lower and upper limit for κ that corresponds with the constraint that the supply stress must be between the 2 roots of $s_s = \kappa^2(1-\kappa)$ for positive reproduction. The value for κ, called κ^{opt}, that maximizes κ_R^A amounts to $\kappa^{\text{opt}} = \frac{(2\dot{p}_J^p [\dot{p}_M]^2)^{1/3}}{\{\dot{p}_{Am}\} f} = (2s_s)^{1/3}$ and $\kappa_R^{A\text{opt}} = 1 - \frac{3}{2}\kappa^{\text{opt}} = 1 - \frac{3}{2}(2s_s)^{1/3}$. Fig 8.19 illustrates how κ_R^A depends on κ and Fig. 8.20 shows how κ, s_s and κ_R^A co-vary among vertebrates in the AmP collection.

8.2.2 Overall reproduction efficiency

The energy allocation to reproduction is E_0/κ_R per offspring, while $L_b^3[M_V]\mu_V$ of that energy is fixed in neonate structure and $L_b^3[E_m]$ in neonate reserve, at abundant food. So the overall reproduction efficiency $\kappa_R^{\text{tot}} = \kappa_R([M_V]\mu_V + [E_m])L_b^3/E_0$ quantifies the fraction

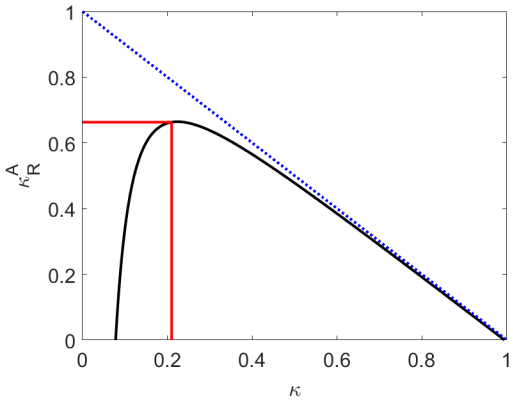

Figure 8.19: The allocation to reproduction as fraction of assimilation at ultimate size, κ_R^A as function of the allocation fraction of mobilised reserve to soma, κ. Parameters $E_H^p = 7e4\,\mathrm{J}$; $\dot{k}_J = 0.002\,\mathrm{d}^{-1}$; $[\dot{p}_M] = 200\,\mathrm{J/d.cm^3}$; $\{\dot{p}_{Am}\} = 1000\,\mathrm{J/d.cm^2}$; $f = 1$.

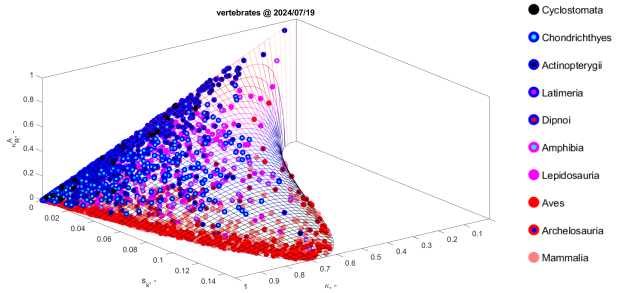

Figure 8.20: A plot for κ, supply-stress s_s and κ_R^A at $f = 1$ for the 4016 vertebrates in the AmP collection. The mesh is the surface defined by $\kappa_R^A = 1 - \kappa - s_s/\kappa^2$. All points are on that surface.

of energy allocated to reproduction that is fixed in neonate mass. It accounts for the losses in the conversion of reproduction buffer to embryo reserve, maturation and maturation maintenance of the embryo, somatic maintenance and growth overheads of the embryo. All costs after birth are taken care of by the neonate itself, apart from parental care.

8.2.2 Acceleration

Species with no metabolic acceleration have $E_H^b = E_H^j$. Figure 8.9 shows that species with metabolic acceleration have a relatively low E_H^p, E_H^j and E_H^p for their size, independent of the ultimate size. This is a remarkable feature that might link to the nature of metabolic acceleration. Section 2.6.4 of the comments on twinning discusses an intriguing implication: the yolkiness of eggs turns out the be proportional to metabolic acceleration.

8.2.2 von Bertalanffy growth rate

An interesting application of the scaling of the von Bertalanffy growth rate with body size is in speculations about the body temperature of dinosaurs. It relates to the question of whether or not dinosaurs were endotherms, which is still a topic of considerable controversy [408]. The blood vessels in bones [68], the bone structure [82], and predator/ prey ratios [407] resemble those of birds and mammals, the general morphology points to a very active life style [67], all indications that dinosaurs were endotherms [323]; the absence of respiratory turbinates in dinosaurs is taken as evidence that they were ectotherms with no need to recover water from their breath [1223], the micro-distribution of oxygen isotope in bones led some to conclude that the body temperature varied considerably in a 5-Mg *Tyrannosaurus* [977], and many speculations about growth and reproduction rates of dinosaurs are based on the low ectothermic levels [235]. The problem of sufficient heat loss

in big dinosaurs in hot mesozoic climates was stressed by others. Although some dinosaurs weighed up to 100 Mg [37], big dinosaurs were not born big, not all of them were big as adults and they also roamed in cold climates [219]. Studies by Alexander [16] showed that the body temperature of small dinosaurs would exceed the environmental temperature by a few degrees only.

Maiasaurs fit the von Bertalanffy growth curve very well, see Figure 8.21. This indicates that the body temperature was constant during their life span. If the shape coefficient would be $\delta_{\mathcal{M}} = 0.09$, while the maximum length is 7.6 m, with $\dot{k}_M = 400\,\mathrm{a}^{-1}$ and $\dot{v} = 300\,\mathrm{a}^{-1}$, the expected value is $\dot{r}_B = 0.146\,\mathrm{a}^{-1}$ at 25 °C, while the observed value is $0.347\,\mathrm{a}^{-1}$. Using an Arrhenius temperature of $T_A = 6$ kK, this leads to an estimated body temperature for the maiasaur of $6(\frac{6000}{298} - \ln\frac{0.347}{0.146})^{-1}$ kK or 38.3 °C. This has been recently confirmed independently by isotope data [371], cf Section 3.6 of the comments..

It would be most interesting to have data for smaller species and/or species in cold climates, but this will probably remain a wish.

8.3 Elimination rate as a function of partition

Another examples of the scaling of the elimination rate are given in Fig. 8.22 and 8.23. Both examples support the conclusion that the elimination rate is inversely proportional to the square root of the octanol-water partition coefficient.

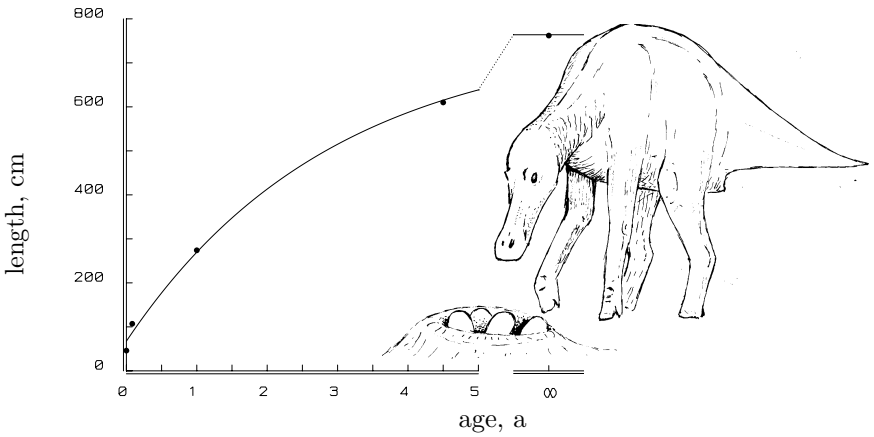

Figure 8.21: The measured length-at-age for the maiasaur (data by Horner, based on age estimates from bone structure [1137]) and the fitted von Bertalanffy growth curve (ultimate length 7.6 m, von Bertalanffy growth rate 0.347 a^{-1}). This suggests a body temperature of 38.3 °C, see text.

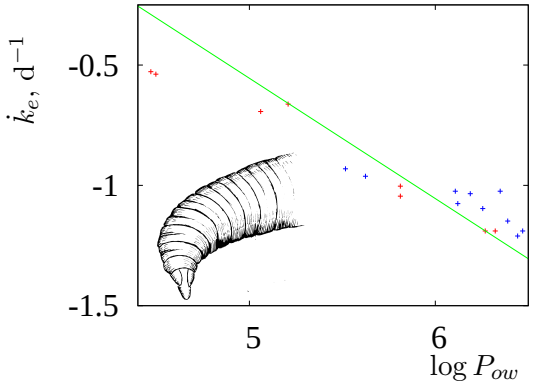

Figure 8.22: The elimination rate in *Eisenia fetida* is approximately proportional to $1/\sqrt{P_{ow}}$ for polycyclic aromatic compounds at 22 °C. Data from Matscheko *et al.* [924].

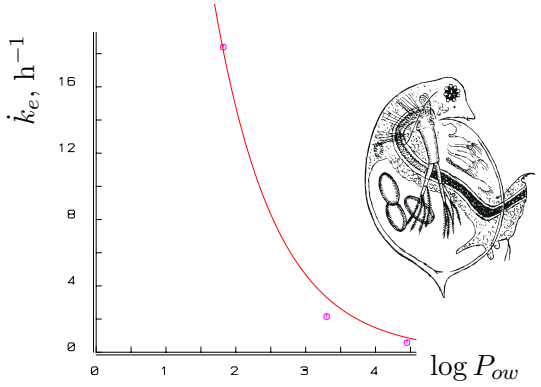

Figure 8.23: The elimination rate in *Daphnia pulex* is approximately proportional to $1/\sqrt{P_{ow}}$ for the compounds isoquinoline, acridine, and benz(a)acridine at 21 °C. Data from Southworth *et al.* [1345].

9

Living together

9.1 Trophic interactions

9.1.2 Syntropy: direct transfer

The constraints for weak homeostasis can be derived as follows. The first observation is that $\dot{r}_1 = 0$ if $f = g_1 \dot{k}_M^1 / \dot{k}_E^1$, and $\dot{r}_2 = 0$ if

$$\frac{M_V^1}{M_V^2} = \frac{g_2}{g_1} \frac{\dot{k}_M^2}{\dot{k}_M^1} \frac{j_{PAm}^2}{\dot{k}_E^2} \frac{1}{\zeta_{PM} + \zeta_{PA}} \tag{9.1}$$

This constraint can be substituted into the expression for $\dot{r}_2$ and allows $\dot{r}_1 = \dot{r}_2$ for $f = g_1 \frac{\dot{k}_M^1 + \dot{r}_1}{\dot{k}_E^1 - \dot{r}_1}$, to be written as

$$(1 + \dot{r}_1/\dot{k}_M^2)\dot{k}_M^1 g_1 (\zeta_{PM} + \zeta_{PA}) = (1 - \dot{r}_1/\dot{k}_E^2) j_P \tag{9.2}$$

Substitution of j_P shows that this constraint can be re-written as a third-order polynomial in $\dot{r}_1$ being equal to zero, which only holds if all coefficients are equal to zero.

Pitcher plants *Nepenthes* offer nice examples of mutual syntrophic relationships. *N. lowii* and *N. macrophylla* excrete carbohydrates at the underside of the lid that hags above to pitch that attracts the maintain tree shrew *Tupaia montana* to come to lick it and drops its nitrogen-rich faecal pellets in the pitch during the act. The plants lives too high in Borneo mountains to attract insects, like many of the other 150 pitcher plants species do. *N. rajah* catches both insects and droppings, also from the summit rat *Rattus baluensis*. *N. hemsleyana* offers housing to one or two tiny Hardwicke's woolly bats *Kerivoula hardwickii* to collect their droppings and ecto-parasites. These bats can locate the pitchers by their extra-high sonar, well above 250 kHz, which is well-reflected by the parabolic rear wall of the upper pitchers. The Black-spotted Sticky Frog *Kalophrynus pleurostigma* develops inside pitchers, profiting from the cached insects.

9.1.2 Derivation of (9.2)

The ratio M_{V1}/M_{V2} can be derived as follows: We are looking for conditions under which M_{V1}/M_{V2} remains constant, and is independent of the specific growth rate $\dot{r}$. So if M_{V1} is

growing at rate $\dot{r}$, M_{V2} must also grow at that rate. This must hold for all rates, so also for $\dot{r} = 0$. If $f = g_1\dot{k}_{M1}/\dot{k}_{E1}$, we have that $\dot{r}_1 = 0$ (see formula for $\dot{r}_1$ and set numerator equal to zero) and $j_P = \zeta_{PM}\dot{k}_{M1}g_1 + \zeta_{PA}\dot{k}_{E1}f = \dot{k}_{M1}g_1(\zeta_{PM} + \zeta_{PA})$ (see below the formulas for $\dot{r}_1$ and $\dot{r}_2$). We set the numerator of $\dot{r}_2$ equal to zero and obtain $\frac{\dot{k}_{E2}j_P}{j_{P,Am2}}\frac{M_{V1}}{M_{V2}} = \dot{k}_{M2}g_2$. Substitution of j_P and rearranging terms gives

$$\frac{M_{V1}}{M_{V2}} = \frac{g_2}{g_1}\frac{\dot{k}_{M2}}{\dot{k}_{M1}}\frac{j_{P,Am2}}{\dot{k}_{E2}}\frac{1}{\zeta_{PM} + \zeta_{PA}}$$

which is the formula that is presented. Equating the polynomial coefficients in $\dot{r}_1$ to zero, as explained in the text, we have $\frac{\zeta_{PM}}{\zeta_{PA}}\left(\frac{\dot{k}_{M1}}{\dot{k}_E} + \frac{\dot{k}_{M1}}{\dot{k}_{M2}}\right) = 1 - \frac{\dot{k}_{M1}}{\dot{k}_{M2}}$. Rearrangement of terms gives $\zeta_{PM} = \zeta_{PA}\frac{\dot{k}_{M1}^{-1} - \dot{k}_{M2}^{-1}}{\dot{k}_E^{-1} + \dot{k}_{M2}^{-1}}$, so $\zeta_{PM} + \zeta_{PA} = \zeta_{PA}\frac{\dot{k}_{M1}^{-1} + \dot{k}_E^{-1}}{\dot{k}_E^{-1} + \dot{k}_{M2}^{-1}}$. Substitution into the equation for M_{V1}/M_{V2} directly gives the result in the last line. The formula for M_{E1}/M_{E2} can be derived from the observations that $M_E = M_V m_{Em} f$ (from Table 3.4 at {122}), and the scaled functional response f of the recipient is $\frac{j_P}{j_{P,Am2}}\frac{M_{V1}}{M_{V2}}$. This gives $\frac{M_{E1}}{M_{E2}} = \frac{M_{V1}}{M_{V2}}\frac{m_{Em1}}{m_{Em2}}f\frac{j_{P,Am2}}{j_P}\frac{M_{V2}}{M_{V1}} = \frac{m_{Em1}}{m_{Em2}}\frac{j_{P,Am2}}{j_P}f$. We now substitute j_P, which reduces for $\zeta_{PG} = 0$ and $\dot{k}_{E1} = \dot{k}_E$ to $j_P = \zeta_{PM}\dot{k}_{M1}g_1 + \zeta_{PA}\dot{k}_E f = f\dot{k}_E\zeta_{PA}\left(1 + \frac{\dot{k}_{M2} - \dot{k}_{M1}}{\dot{k}_{M2} + \dot{k}_E}\frac{g_1}{f}\right)$. The latter follows after substitution of ζ_{PM} for the value obtained above. Substitution of $\frac{m_{Em1}}{m_{Em2}} = \frac{M_{Em1}}{M_{Em2}}\frac{M_{V2}}{M_{V1}}$ directly leads to the formula for M_{E1}/M_{E2} that is presented on the bottom line.

9.1.3 Symbiontic relationships

The number of known symbiontic relationships continues to increase. Mites and collemboles turn out to play a key role in the fertilization of mosses [287].

The flagellate *Hatena* (*Katablepharidophyta*) has the (single) symbiont *Nephroselmis* (*Prasinophyceae, Viridiplantae*). The symbiont retains its nucleus, mitochondria, plastid, and occasionally the Golgi body, but the flagella, cytoskeleton and endomembrane system are lost. Its eye-spot, which is inside the plastid, is always near the apex of the host and the host use it for phototaxis. When the host divides, a one daughter gets the symbiont, and the other develops a feeding apparatus to engulf a new symbiont, after which the feeding apparatus degenerates [1045].

The opistobranch *Phyllodesmium* feeds on soft symbiontic corals and houses coral's algal symbionts in its complex midgut. The zooanthellae not only remain active photosynthesically, but also give the slug exactly the same color as its coral prey, which makes it difficult to detect [1082]. The opistobranch *Elysia* harbors the chloroplast of its prey *Vaucheria* (*Xanthophyta*). Since *Elysia* parents don't pass the chloroplasts to their offspring, the acquisition of chloroplasts is the first thing to do in its 10-month life. It seems that *Elysia chlorotica* integrates genes for chorophyll production in its genome after eating *Vaucheria* chloroplasts for the first time [975], but it can't pass these genes to its offspring.

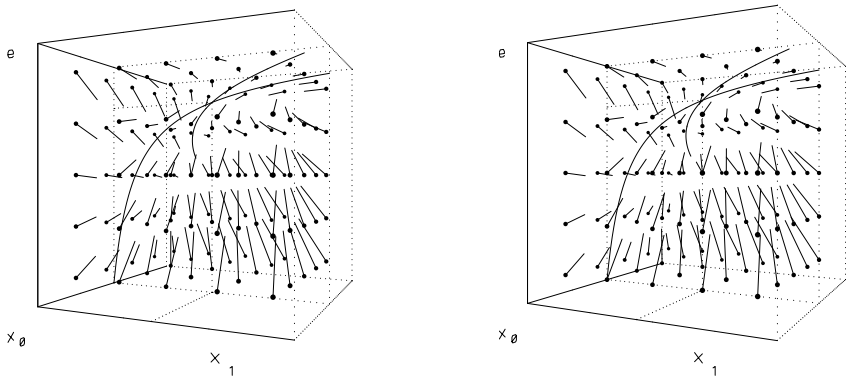

Figure 9.1: Stereo view of the direction field and isoclines for the DEB model for V1-morphs in a chemostat. The parameter values are the same as in Figure 9.2 and the projection of this direction field on the x, y-plane reduces to the direction field given in Figure 9.2, where the reserves are set at equilibrium.

9.2 Population dynamics

9.2.1 Expologistic growth; derivation of (9.17)

Notice that the general strategy of the chapter is to start on ground that should be familiar to microbiologists and step by step more DEB elements are introduced. So we have to show that (9.17) reduces to (9.12) by removing DEB elements. The first step is to exclude aging, so $\dot{h}_a = 0$. The second step is to remove reserve, so $[E_m] \to 0$. We work here with compound parameters, rather than with primary ones, so we have to study each of the compound parameters to evaluate the consequences. We have $g = \frac{[E_G]}{\kappa [E_m]}$, so $g \to \infty$. We also have $l_d = \frac{\dot{k}_M g}{\dot{k}_E} = \frac{[\dot{p}_M]}{\kappa [\dot{p}_{Am}]}$, so l_d remains fixed. The implementation of these changes in (9.17) results in $\frac{d}{d\tau} x_1 = Y_g \jmath_{Xm} (f - l_d) x_1 - x_1 = Y_g \frac{f - l_d}{f} \jmath_{Xm} f x_1 - x_1 = Y \jmath_{Xm} f x_1 - x_1$ with $Y = Y_g \frac{f - l_d}{f}$. This latter relationship is given in the table at the bottom of {315} for the Marr-Pirt model. Notice the absence of dots in the equations, because we work in scaled time, that is dimensionless.

The direction field of the model (9.17) is given in Figure 9.1. Mortality is excluded, $\dot{h}_a = 0$, to facilitate comparison with the situation where reserves are in equilibrium; see Figure 9.2.

9.2.1 Time scale separation

Simplifying approximations for batch dynamics by Jean-Christophe Poggiale. Assume that we have the following model for V1-morphs in a batch reactor (Figure 9.2)

$$\begin{aligned} \frac{d}{d\tau} x_0 &= I - j_{Xm} f x_1 \\ \frac{d}{d\tau} e &= k_E \left(f - e \right) \end{aligned}$$

Table 9.1: Definition, values and units of the parameters.

Symbol	Parameter Name	Value	Unit
$\dot{I}$	input rate of substrate	1	$\mathrm{mM\,h^{-1}}$
j_{Xm}	maximum specific uptake rate	0.125	$\mathrm{mM\,h^{-1}}$
K_x	half-saturation constant for uptake	5	mM
$\dot{k}_E$	Reserve turnover rate	0.925	$\mathrm{h^{-1}}$
$\dot{k}_M$	Maintenance turnover rate	0.04	$\mathrm{h^{-1}}$
g	Investment ratio	0.5	-

$$\frac{d}{d\tau}x_1 = \frac{k_E e - k_M g}{e+g}x_1$$

Let us assume that e is a fast variable with respect to x_0 and x_1. It follows that e reaches a quasi-steady state value f, which is a function of the slow variables:

$$f(x_0) = \frac{x_0}{K_x + x_0}$$

We can thus replace e by f in the third equation, which leads to the two dimensional model (Figure 9.3):

$$\begin{aligned}\frac{d}{d\tau}x_0 &= I - j_{Xm} f x_1 \\ \frac{d}{d\tau}x_1 &= \frac{(k_E - k_M g)\,x_0 - k_M g K_x}{x_0\,(1+g) + g K_x}x_1\end{aligned}$$

Furthermore, if we assume that x_0 is also fast with respect to x_1, then x_0 also reaches a quasi-steady state value obtained by vanishing the first equation. We thus get $f = \frac{I}{j_{Xm}x_1}$. Finally, we can replace f by its value in the third equation and we consequently a one-dimensional model (Figure 9.4):

$$\frac{d}{d\tau}x_1 = \frac{k_E I}{I + g j_{Xm} x_1}\left(1 - \frac{k_M g j_{Xm}}{k_E I}x_1\right)x_1 = r(x_1)\left(1 - \frac{x_1}{K}\right)x_1$$

where

$$r(x_1) = \frac{k_E I}{I + g j_{Xm} x_1} \quad \text{and} \quad K = \frac{k_E I}{k_M g j_{Xm}}$$

9.2.1 Derivation of (9.13)

The first step in the derivation of (9.13) from (9.12) is the determination of the equlibrium. To this end we start with the equation $\frac{d}{d\tau}x_1 = 0$, and learn for $f = \frac{x_0}{x_0+1}$ that $f^* = (Y j_{XAm})^{-1}$ and $Y j_{XAm} x_0^* = x_0^* + 1$, so that the equilibrium value for x_0 is $x_0^* = (Y j_{XAm} - 1)^{-1}$. We find the equilibrium value for x_1 from $\frac{d}{d\tau}x_0 = 0$ and obtain $x_1^* = \frac{x_r - x_0^*}{j_{XAm} f^*}$.

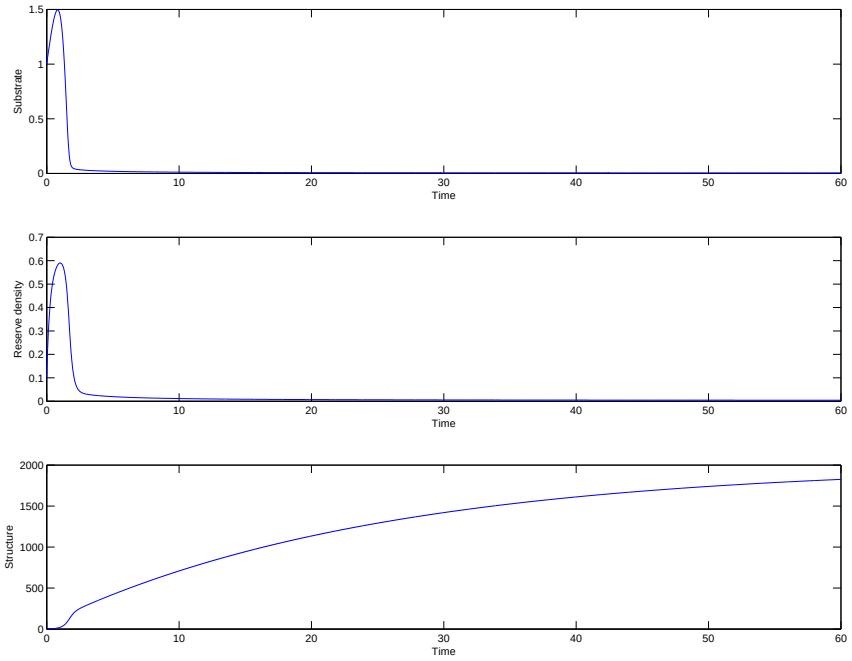

Figure 9.2: This figure shows the dynamics of the standard DEB - model

The second step is the linearisation of (9.12) around the equilibrium $\boldsymbol{x}^* = (x_0^* \; x_1^*)^T$, where linearisation means the two-term Taylor approximation of $\boldsymbol{H}$ in $\boldsymbol{x}^*$, where we re-write (9.12) as $\frac{d}{d\tau}\boldsymbol{x} = \boldsymbol{H}(\boldsymbol{x})$. The expression $\frac{d}{d\boldsymbol{x}^T}\boldsymbol{H}(\boldsymbol{x}^*)$ is known as the Jacobian matrix. We find for constant $Y = Y_g$

$$
\begin{aligned}
\frac{d}{d\tau}\boldsymbol{x} &= \boldsymbol{H}(\boldsymbol{x}) = \begin{pmatrix} H_1(\boldsymbol{x}) \\ H_2(\boldsymbol{x}) \end{pmatrix} = \begin{pmatrix} x_r - \jmath_{XAm} f x_1 - x_0 \\ Y_g \jmath_{XAm} f x_1 - x_1 \end{pmatrix} \\
&= \boldsymbol{H}(\boldsymbol{x}^*) + \left(\frac{d}{d\boldsymbol{x}^T}\boldsymbol{H}(\boldsymbol{x}^*) \right)(\boldsymbol{x} - \boldsymbol{x}^*) \quad \text{with } \boldsymbol{H}(\boldsymbol{x}^*) = \boldsymbol{0} \\
&= \begin{pmatrix} \frac{d}{dx_0}H_1(\boldsymbol{x}^*) & \frac{d}{dx_1}H_1(\boldsymbol{x}^*) \\ \frac{d}{dx_0}H_2(\boldsymbol{x}^*) & \frac{d}{dx_1}H_2(\boldsymbol{x}^*) \end{pmatrix}(\boldsymbol{x} - \boldsymbol{x}^*) \\
&= \begin{pmatrix} \frac{d}{dx_0}(x_r - \jmath_{XAm} f^* x_1^* - x_0^*) & \frac{d}{dx_1}(x_r - \jmath_{XAm} f^* x_1^* - x_0^*) \\ \frac{d}{dx_0}(Y_g \jmath_{XAm} f^* x_1^* - x_1^*) & \frac{d}{dx_1}(Y_g \jmath_{XAm} f^* x_1^* - x_1^*) \end{pmatrix}(\boldsymbol{x} - \boldsymbol{x}^*) \\
&= \begin{pmatrix} -\frac{\jmath_{XAm} x_1^*}{(1+x_0^*)^2} - 1 & -\jmath_{XAm} f^* \\ \frac{Y_g \jmath_{XAm} x_1^*}{(1+x_0^*)^2} & Y_g \jmath_{XAm} f - 1) \end{pmatrix}(\boldsymbol{x} - \boldsymbol{x}^*) \\
&\quad \text{with } \jmath_{XAm} f^* x_1^* = x_r - x_0^* \quad \text{and } Y_g = (f^* \jmath_{XAm})^{-1} \\
&= \begin{pmatrix} -\frac{x_r + x_0^{*2}}{x_0^* + x_0^{*2}} & -\frac{1}{Y_g} \\ \frac{x_r - x_0^*}{\jmath_{XAm} x_0^{*2}} & 0 \end{pmatrix}(\boldsymbol{x} - \boldsymbol{x}^*)
\end{aligned}
$$

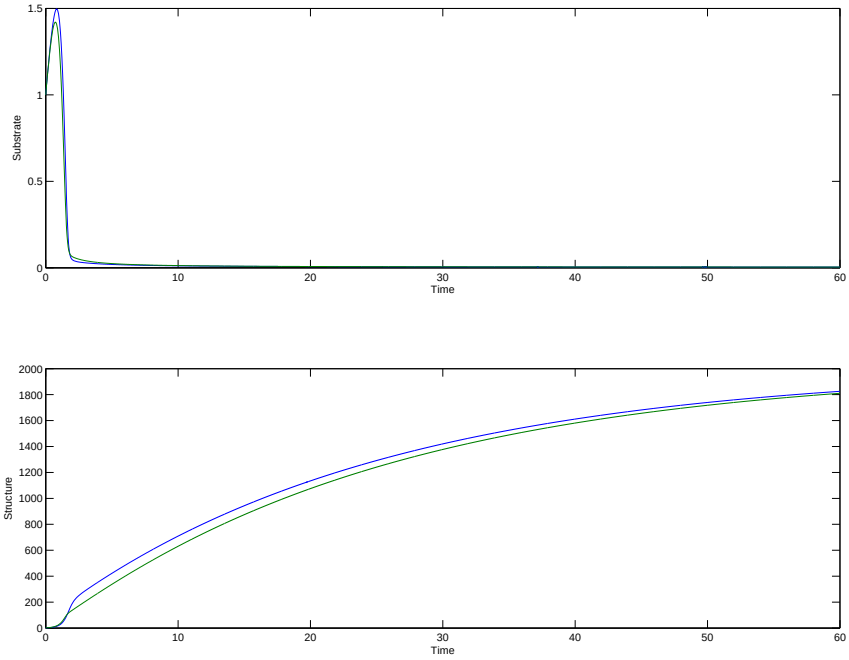

Figure 9.3: This figure compares the 2D-model dynamics to that of the DEB - model.

9.2.2 Structured population dynamics

I took the sections on stable age and size distribution out of the main text, because lack of space, and the general concepts behind these distributions can be found in many text books.

9.2.2.1 Stable age distributions

If food density is constant or high (with respect to the saturation coefficient), the distribution of individual states in the population, such as age and volume, stabilises, while the numbers grow exponentially. This distribution can be evaluated in a relatively simple way, which makes it possible to evaluate statistics such as the mean volume and its variance, mean life span, etc. Situations may occur where the individual states change cyclically, so that such a stable distribution does not exist. The distribution of individual states has a limited practical value, because it only holds at prolonged constant food densities. How long food density must remain constant for state distributions to stabilise is hard to tell in specific cases and impossible in general. The main value of stable distributions lies in finding practical approximations for the behaviour of population models based on individuals. The derivation of stable state distributions is easiest when looking at the stable age distribution, which I will explain briefly. More extensive treatment is given by Frauenthal [443].

Let $\phi_N(a,t)\,da$ denote the number of females at time t aged somewhere in the interval $(a, a+da)$, where da is an infinitesimally small time increment. The total number of individuals is thus $N(t) = \int_0^\infty \phi_N(a,t)\,da$. Individuals that have age a at t must have been

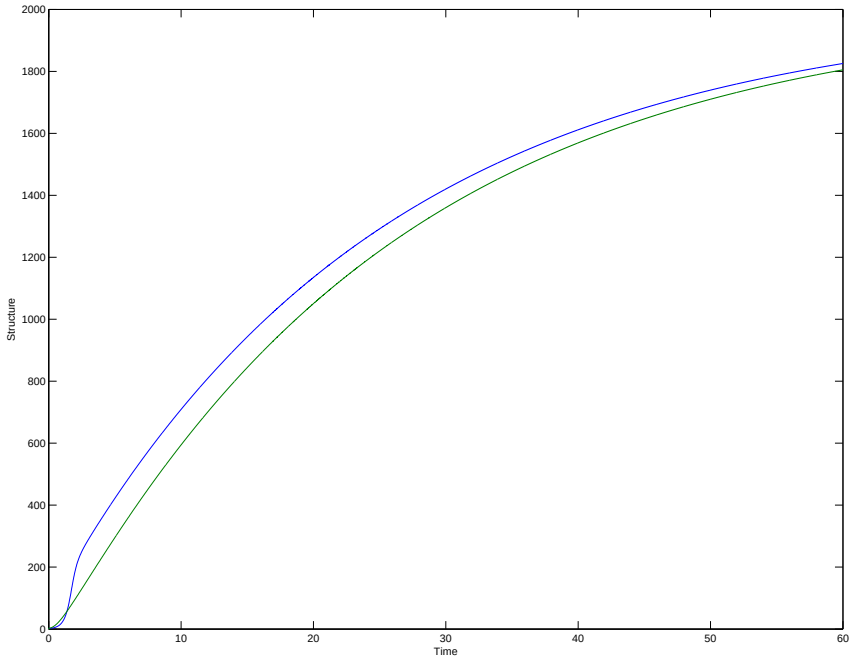

Figure 9.4: This figure compares the logistic-like growth dynamics to that of the DEB - model.

born at $t-a$ and must be still alive to be counted in N, so we have the recursive relationship $\phi_N(a,t) = \phi_N(0,t-a)\Pr\{\underline{a}_\dagger > a\}$, where $\phi_N(0,t)\,da$ denotes the number of births in $(t, t+da)$. The birth rate relates to the reproduction rate as $\phi_N(0,t) = \int_0^\infty \phi_N(a,t)\dot{R}(a)\,da$, where $\dot{R}(a)$ is the reproduction rate of an individual of age a. If we substitute the birth rate into the recursive relationship, we arrive at the integral equation

$$\phi_N(0,t) = \int_0^\infty \phi_N(0,t-a)\Pr\{\underline{a}_\dagger > a\}\dot{R}(a)\,da \tag{9.3}$$

Rather than specifying the number of births before the start of the observations at $t = 0$, we specify the founder population $\phi_N(a,0) = \phi_0(a)$ and write

$$\phi_N(0,t-a) = \phi_0(a-t)/\Pr\{\underline{a}_\dagger > a-t\} \quad \text{for } a > t \tag{9.4}$$

The integral in (9.3) can now be partitioned and gives what is known as the renewal equation

$$\phi_N(0,t) = \int_0^t \phi_N(0,t-a)\Pr\{\underline{a}_\dagger > a\}\dot{R}(a)\,da + \int_t^\infty \frac{\Pr\{\underline{a}_\dagger > a\}}{\Pr\{\underline{a}_\dagger > a-t\}}\phi_0(a-t)\dot{R}(a)\,da \tag{9.5}$$

The second term thus relates to the contribution of the individuals that were present in the founder population. Depending on the survival probability and age-dependent reproduction rate, its importance decreases with time. Suppose that it is negligibly small at some time t_1 and that the solution of (9.5) is of the form $\phi_N(0,t) = \phi_N(0,0)\exp\{\dot{r}t\}$, for

some value of $\dot{r}$ and $\phi_N(0,0)$. Substitution into (9.5) gives for $t > t_1$

$$\phi_N(0,0)\exp\{\dot{r}t\} = \int_0^{t_1} \phi_N(0,0)\exp\{\dot{r}(t-a)\}\Pr\{\underline{a}_\dagger > a\}\dot{R}(a)\,da \quad \text{or} \tag{9.6}$$

$$1 = \int_0^{t_1} \exp\{-\dot{r}a\}\Pr\{\underline{a}_\dagger > a\}\dot{R}(a)\,da \tag{9.7}$$

The latter equation is known as the characteristic equation. It is possible to show that, under some smoothness restrictions on reproduction as a function of age, this equation has exactly one real root for the population growth rate $\dot{r}_1$. The other roots are complex and have a real part smaller than $|\dot{r}_1|$. The general solution for $\phi_N(0,t)$ is a linear combination $\sum_i \phi_i(0,0)\exp\{\dot{r}_i t\}$. For large t, the exponential $\exp\{\dot{r}_1 t\}$ will be dominant, so the asymptotic solution will be $\phi_{N1}(0,0)\exp\{\dot{r}_1 t\}$; because the other roots are of little practical interest, the index will be dropped and $\dot{r}$ is thus taken to be the dominant root. The smoothness restrictions on $\dot{R}(a)$ are violated if, for instance, reproduction is only possible at certain ages. In this case, the information about the age distribution of the founder population is not lost.

The stable age distribution – i.e. the distribution of the ages of a randomly taken individual, $\underline{a}$ – is defined by $\phi_{\underline{a}}(a)\,da \equiv \phi_N(a,t)\,da/N(t)$ for $t \to \infty$. As before, we have for large t

$$\phi_N(a,t) = \phi_N(0,t-a)\Pr\{\underline{a}_\dagger > a\} = \phi_N(0,0)\exp\{\dot{r}(t-a)\}\Pr\{\underline{a}_\dagger > a\} \tag{9.8}$$

As $N(t) \equiv \int_0^\infty \phi_N(a,t)\,da$ serves only to normalise the distribution, we get the simple relationship between the age distribution and the survivor probability of the individuals

$$\phi_{\underline{a}}(a) = \frac{\exp\{-\dot{r}a\}\Pr\{\underline{a}_\dagger > a\}}{\int_0^\infty \exp\{-\dot{r}a_1\}\Pr\{\underline{a}_\dagger > a_1\}\,da_1} \tag{9.9}$$

Note that $\underline{a}$ is defined for the population level, while $\underline{a}_\dagger$ is the age at which a particular individual dies, so it is defined for the individual level. For a stable age distribution, the adage 'older and older, rarer and rarer' always holds. The mean age in the population is thus

$$\mathcal{E}\underline{a} = \int_0^\infty a\phi_{\underline{a}}(a)\,da = \frac{\int_0^\infty a\exp\{-\dot{r}a\}\Pr\{\underline{a}_\dagger > a\}\,da}{\int_0^\infty \exp\{-\dot{r}a\}\Pr\{\underline{a}_\dagger > a\}\,da} \tag{9.10}$$

9.2.2.2 Stable size distributions

Volume distribution is intimately related with the growth of dividing individuals, as has been widely recognised [265, 330, 561, 913, 1476]. It can most easily be expressed in terms of its survivor function. If death plays a minor role, (9.9) gives the stable age distribution for $\Pr\{\underline{a}_\dagger > a\} = (a < a_d)$ with $a_d = \dot{r}^{-1}\ln 2$. For dividing individuals aged between 0 and a_d, the stable age distribution is given by $\phi_{\underline{a}}(a)\,da = 2\dot{r}\exp\{-\dot{r}a\}\,da = \frac{2\ln 2}{a_d}2^{-a/a_d}\,da$. For reproducing immortal individuals, the stable age distribution is $\phi_{\underline{a}}(a)\,da = \dot{r}\exp\{-\dot{r}a\}\,da$. The expected value of scaled length to the power i amounts to $\mathcal{E}\underline{l}^i = \int \phi_{\underline{a}}(a)l(a)^i\,da$.

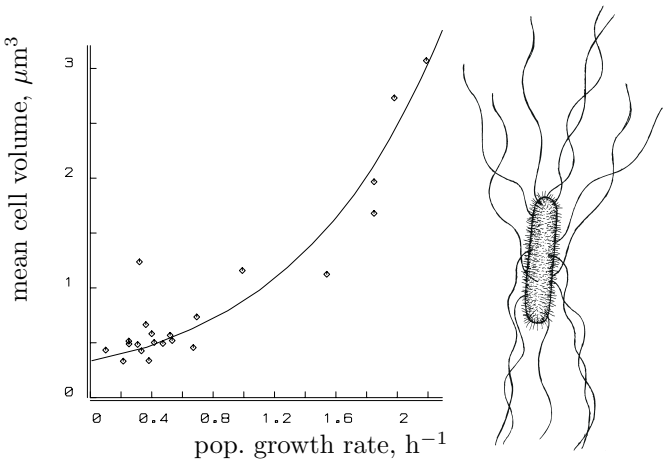

Figure 9.5: The mean volume of *E. coli* as a function of population growth rate at 37 °C. Data from Trueba [1442]. For a chosen aspect ratio $\delta = 0.28$, a maintenance rate coefficient $\dot{k}_M = 0.05\,\mathrm{h}^{-1}$ and an investment ratio $g = 1$, the least-squares estimates of the volume at the start of DNA replication is $V_p = 0.454\,\mu\mathrm{m}^3$, the time required for division is $t_D = 1.03\,\mathrm{h}$ and the energy conductance $\dot{v} = 31.3\,\mu\mathrm{m\,h}^{-1}$.

The mean length increases less steeply with increasing substrate density or $\dot{r}$ than length at division, because the mean age reduces. Figure 9.5 shows that the mean volume of rods depends on population growth rate in the predicted way.

The survivor function of the stable age distribution is thus: $\Pr\{\underline{a} > a\} \equiv \int_a^{a_d} \phi_{\underline{a}}(a_1)\,da_1 = (a < \dot{r}^{-1}\ln 2)(2\exp\{-\dot{r}a\} - 1)$. The stable age distribution only exists at constant food densities, where volume increases if age increases. It was first derived by L. Euler in the eighteenth century [736]. The remarks on the need for scatter for stability of age distributions also apply to size distributions. See Diekmann *et al.* [328, 329] for a more technical discussion.

If growth is deterministic and division occurs at a fixed size and the baby cells are of equal size, no stable age distribution exists. If there is some scatter in size at division, a stable age distribution exists, unless growth is exponential [102], because the information about the age distribution of the founder populations never gets lost. If sisters are not exactly the same size, a stable age distribution exists, even if growth is exponential. The age distribution has a weaker status, that of an eigenfunction: if the founder population has this particular age distribution, the age distribution will not change, while all other age distributions for the founder population will change cyclically with period a_d. In practice, however, scatter in growth rate and the size of baby cells will be more than sufficient for a rapid convergence to the stable age distribution.

The survivor function of the stable volume distribution is

$$\Pr\{\underline{V} > V\} = \Pr\{\underline{a} > t(V)\} = 2\exp\{-\dot{r}t(V)\} - 1 \quad \text{for } V \in (V_d/2, V_d] \tag{9.11}$$

where $t(V)$ is the age at which volume V is reached. The probability density is thus

$$\phi_{\underline{V}}(V)\,dV = (V \geq V_d/2)(V \leq V_d)2\dot{r}\exp\{-\dot{r}t(V)\}\,dt \tag{9.12}$$

For isomorphs, $t(V)$ is given in (2.23). Since scaled length, l, has a monotonous relationship with volume; we have $\Pr\{\underline{l} > l\} = \Pr\{\underline{V} > V\}$. The survivor function of the stable length distribution for isomorphs that divide at scaled length l_d becomes

$$\Pr\{\underline{l} > l\} = 2^{1+\ln\frac{f-l}{f-l_b}/\ln\frac{f-l_b}{f-l_d}} - 1 \tag{9.13}$$

The same can be done for rods, which leads to

$$\Pr\{\underline{l} > l\} = 2^{\ln \frac{1-l_d/f}{(1-l_d/f-\delta/3)(l/l_d)^3+\delta/3} / \ln \frac{2(1-l_d/f)}{1-l_d/f+\delta/3}} - 1 \tag{9.14}$$

and for V1-morphs

$$\Pr\{\underline{l} > l\} = (l_1/l)^3 - 1 \tag{9.15}$$

These relationships can be important for testing assumptions about the growth process using the stable length distribution. Actual stable length distributions reveal that the scaled length at division, l_d, is not identical for all individuals, but has some scatter, which is close to a normal distribution [737]. It is assumed that the size-age curve does not depend on the size of the baby cell. As soon as a small baby cell has grown to the size of a larger baby cell, the rest of their growth curves are indistinguishable. Let $\phi_{\underline{V}_b}$ denote the probability density of the number of baby cells of volume V, i.e. cells of an age less than an arbitrarily small period Δt, and $\phi_{\underline{V}_d}$ the probability density of the number of mother cells of volume V, i.e. cells which will divide within the period Δt. A practical way to determine $\phi_{\underline{V}_b}(V)\,dV$ and $\phi_{\underline{V}_d}(V)\,dV$ empirically is to make photographs at t and $t+\Delta t$ of the same group of cells and select cells that are divided at $t+\Delta t$, but not at t. The photograph at t can be used to obtain $\phi_{\underline{V}_d}(V)\,dV$ and that at $t+\Delta t$ to obtain $\phi_{\underline{V}_b}(V)\,dV$. When N denotes the total number of cells in the population, the number of cells with a volume in the interval $(V, V+dV)$ is $N\phi_{\underline{V}}(V)\,dV$. Painter and Marr [1064] argued that the change in this number is given by

$$\frac{d}{dt}N\phi_{\underline{V}} = 2\frac{d}{dt}N\phi_{\underline{V}_b} - \frac{d}{dt}N\phi_{\underline{V}_d} - N\frac{\partial}{\partial V}\left(\phi_{\underline{V}}\frac{dV}{dt}\right) \tag{9.16}$$

The first term stands for the increase caused by birth, the second one for loss attributed to division and the third term for loss due to growth. Since the stable volume distributions do not depend on time and $\frac{d}{dt}N = \dot{r}N$, some rearrangement of terms gives

$$\frac{\partial}{\partial V}\left(\phi_{\underline{V}}\frac{dV}{dt}\right) = \dot{r}\left(2\phi_{\underline{V}_b} - \phi_{\underline{V}_d} - \phi_{\underline{V}}\right)$$

This is a linear inhomogeneous differential equation in $\phi_{\underline{V}}(V)$, with solution

$$\phi_{\underline{V}}(V) = \frac{dt}{dV}\dot{r}\exp\{-\dot{r}t(V)\}\int_{V_{\min}}^{V}\exp\{\dot{r}t(V_1)\}(2\phi_{\underline{V}_b}(V_1) - \phi_{\underline{V}_d}(V_1))\,dV_1 \tag{9.17}$$

where $V_{\min}$ is the smallest possible cell volume and, since $\phi_{\underline{V}}(V_{\max}) = 0$, $\dot{r}$ satisfies [1476]

$$\int_{V_{\min}}^{V_{\max}}\exp\{\dot{r}t(V_1)\}(2\phi_{\underline{V}_b}(V_1) - \phi_{\underline{V}_d}(V_1))\,dV_1 = 0 \tag{9.18}$$

The connection with the previous deterministic rules for division can be made as follows. When mother cells divide into two equally sized baby cells, we have $\phi_{\underline{V}_b}(V) = 2\phi_{\underline{V}_d}(2V)$. So, $\phi_{\underline{V}_b}(V)\,dV = (V = V_d/2)$ and $\phi_{\underline{V}_d}(V)\,dV = (V = V_d)$ when division always occurs at V_d. Substitution into (9.17) gives (9.12) and into (9.18) gives $t_d^{-1}\ln 2$, as before. When

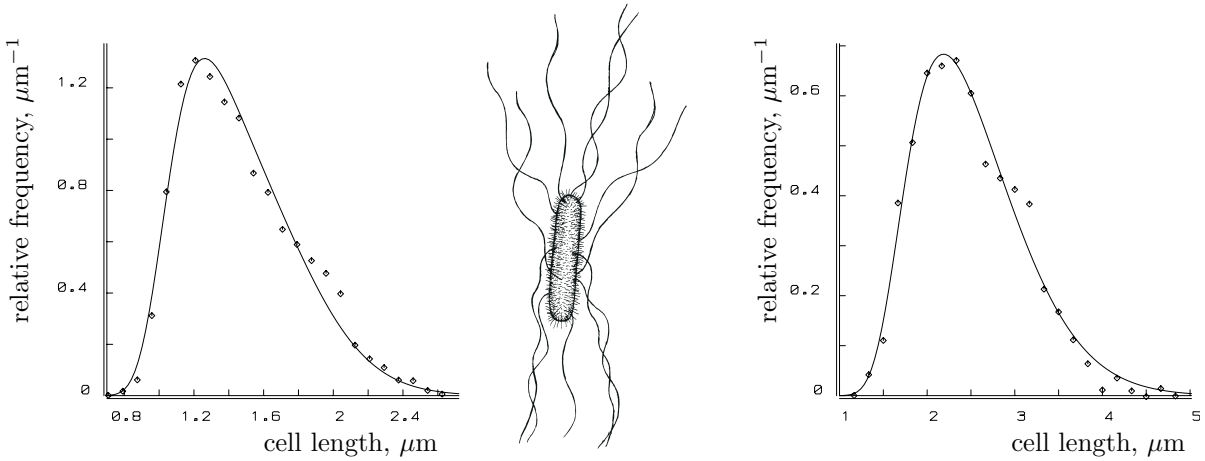

Figure 9.6: The probability density of the length of *E. coli* B/r A (left) and K (right) at a population growth rate of 0.38 and 0.42 h^{-1} respectively at 37 °C. Data from Koppes *et al.* [801]. For an aspect ratio of $\delta = 0.3$, the three parameters are $V_d = 0.506\,\mu m^3$, $V_\infty = -0.001\,\mu m^3$ and $\sigma^2 = 0.026$ and $V_d = 2.324\,\mu m^3$, $V_\infty = -1\ \mu m^3$ and $\sigma^2 = 0.044$. Because of the relatively large variance of the volume at division, these frequency distributions give poor access to the single parameter that relates to the growth process V_∞.

division always occurs at V_d, so $\phi_{\underline{V}_d}(V)\,dV = (V = V_d)$, and the sizes of the baby cells are V_a and V_p, we have $\phi_{\underline{V}_b}(V)\,dV = (V = V_a)/2 + (V = V_p)/2$ with $V_a + V_p = V_d$ and $V_a < V_p$. Substitution into (9.17) gives

$$\phi_{\underline{V}}(V)\,dV = (V \geq V_a)(V \leq V_d)\dot{r}\exp\{\dot{r}(t(V_a) + t(V_p)(V \geq V_p) - t(V))\}\,dt$$

and substitution into (9.18) gives $1 = \exp\{-\dot{r}t_{da}\} + \exp\{-\dot{r}t_{dp}\}$.

Figure 9.6 gives the stable length distribution for *Escherichia coli*, together with the model fit with a log-normal distribution for the length at division. Since the curves approach the x-axis very closely for large cell lengths, the approximation $\dot{r} = t_d^{-1}\ln 2$ is appropriate. Although the goodness of fit is quite acceptable and only three parameters occur, the one relating to the growth process, V_∞, is not well fixed by the data. Again, the conclusion must be that this population response is consistent with what can be deduced from the individual level, but that the population behaviour gives poor access to that of individuals.

9.2.2.3 Discrete individuals

The derivation of (9.22) is via

$$1 = \sum_{i=1}^{\infty}\exp\{-\dot{r}(a_p + i/\dot{R})\} = \exp\{-\dot{r}/\dot{R} - \dot{r}a_p\}\left(1 - \exp\{-\dot{r}/\dot{R}\}\right)^{-1} \tag{9.19}$$

9.2.2.4 Population growth rates and division intervals

Substitution of the expressions for age at division gives the expressions for the population growth rates at constant substrate densities and for their relative values with respect to the

Figure 9.7: The population growth rate $\dot{r}$ for dividing organisms as it simplifies when expressed as a fraction of its maximum $\dot{r}_m$ and small maintenance costs $[\dot{p}_M]$ and/or storage capacity $[E_m]$. The last three rows in the 'V1-morphs' column correspond to the models by Marr–Pirt, Droop and Monod. These models are graphically compared with the DEB model for V1-morphs in the figure below. The symbols l_1 and V_1 stand for l_d and V_d for $f = 1$.

	isomorphs	rods	V1-morphs
$\dot{r}$	$\frac{g\dot{k}_M}{f+g} \frac{\frac{1}{3}\ln 2}{\ln \frac{f-l_d 2^{-1/3}}{f-l_d}}$	$\frac{(1-\delta/3)f/l_d-1}{(f+g)/g\dot{k}_M} \frac{\ln 2}{\ln \frac{2(1-l_d/f)}{1-l_d/f+\delta/3}}$	$\frac{f/l_d-1}{(f+g)/g\dot{k}_M}$
$\frac{\dot{r}}{\dot{r}_m}$	$\frac{1+g}{f+g} \frac{\ln \frac{1-l_1 2^{-1/3}}{1-l_1}}{\ln \frac{f-l_d 2^{-1/3}}{f-l_d}}$	$\frac{1+g}{f+g} \frac{(1-\delta/3)f/l_d-1}{(1-\delta/3)/l_1-1} \frac{\ln \frac{2(1-l_1)}{1-l_1+\delta/3}}{\ln \frac{2(1-l_d/f)}{1-l_d/f+\delta/3}}$	$\frac{1+g}{f+g} \frac{f/l_d-1}{1/l_1-1}$
$\frac{\dot{r}}{\dot{r}_m} \Big\vert [E_m] \to 0$	$\frac{\ln \frac{1-l_1 2^{-1/3}}{1-l_1}}{\ln \frac{f-l_d 2^{-1/3}}{f-l_d}}$	$\frac{(1-\delta/3)f/l_d-1}{(1-\delta/3)/l_1-1} \frac{\ln \frac{2(1-l_1)}{1-l_1+\delta/3}}{\ln \frac{2(1-l_d/f)}{1-l_d/f+\delta/3}}$	$\frac{f/l_d-1}{1/l_1-1}$
$\frac{\dot{r}}{\dot{r}_m} \Big\vert [\dot{p}_M] \to 0$	$f \frac{1+g}{f+g} (\frac{V_1}{V_d})^{1/3}$	$f \frac{1+g}{f+g} (\frac{V_1}{V_d})^{1/3}$	$f \frac{1+g}{f+g}$
$\frac{\dot{r}}{\dot{r}_m} \Big\vert [E_m], [\dot{p}_M] \to 0$	$f(\frac{V_1}{V_d})^{1/3}$	$f(\frac{V_1}{V_d})^{1/3}$	f

maximum population growth rates, which are collected in Figure 9.7. The scaled length at division, l_d, is a function of f, because of the fixed period required to duplicate DNA. It has to be solved numerically from (7.69), but, for most practical purposes, it can probably be treated as a constant. For small aspect ratios, δ, the expressions for rods reduce to that for V1-morphs, while for an aspect ratio of $\delta = 0.6$ rods resemble isomorphs. The table in Figure 9.7 therefore illustrates how the population growth rate of dividing DEB isomorphs reduces stepwise to well known classic models. It also illustrates why many microbiologists do not like models that explicitly deal with substrate density; the saturation coefficient for uptake is usually very small for most combinations of micro-organisms and substrate types, and the saturation coefficient for population growth is even smaller, so that problems arise in measuring such low densities. Natural populations of micro-organisms tend either to grow at the maximum rate, or not to grow at all. This on/off behaviour is a major obstacle in the analysis of population dynamics.

The functions in Figure 9.7 are used to obtain Figure 9.9.

9.2.2.5 Generalized reactor: a semi-structured model

A well-stirred generalized reactor has a food input, and each component can leave the reactor at its own rate. The purpose of this section is to reduce the complex dynamics of DEB individuals in a generalized reactor to a small set of ODE's, by assuming that the stable age distribution applies at each point in time (which is obviously a crude approximation, since it typically takes a long time with constant conditions). This reduced formulation

can then be compared with more complete ones. The survivor function of the stable age distribution is

$$S_a(a) = \frac{\int_a^\infty \exp(-\dot r_N t) S(t)\, dt}{\int_0^\infty \exp(-\dot r_N t) S(t)\, dt}$$

where $\dot r_N$ is the (unknown) specific population growth rate (which varies in time, see below). The survival probability is approximated by

$$S(a) = \exp\left(\frac{6\dot h_W^3}{\dot h_G^3}\left(1 - \exp(\dot h_G a) + \dot h_G a + \dot h_G^2 a^2/2\right) - \dot h_B a\right),$$

see Eq (6.5), for background hazard $\dot h_B$ and approximated Gompertz aging hazard $\dot h_G = \dot k_M g s_G f^3$ and Weibull aging hazard $\dot h_W^3 = \ddot h_a \dot k_M g/6$. A typical maximum ages is $a_m = \Gamma(4/3)/\dot h_W$.

We partition the total number of individuals per volume, N, in embryo, juvenile and adult densities $N = N_{0b} + N_{bp} + N_{pi}$. Only 'average' lengths are delineated for the three stages: $L_{0b} = L_b/2$ and $L_{bp} = L_b/2 + L_p/2$ and $L_{pi} = L_p/3 + L_\infty * 2/3$ (since most of the time L will be close to L_∞). The lengths L_b, L_p and L_∞ depend on f and are updated for each time step. We further assume that reserve is in instantaneous equilibrium, $e = f$, and the reproduction rate is taken to be a continuous flux, while the cost per egg is always for $f = 1$: $\dot R = \left(\frac{f l_{pi}^2}{f+g}(g + l_{pi}) - k v_H^p\right)\frac{\kappa_R(1-\kappa)\dot k_M}{u_E^0}$ and scaled length $l_{pi} = L_{pi}/L_m$, see Eq (2.56). The specific population growth rate $\dot r_N$ is (implicitly) approximated by $\exp(-(\dot r_N + \dot h_B)a_p) = \exp((\dot r_N + \dot h_B)/\dot R) - 1$, cf Eq (9.22).

The dynamics of the number densities is

$$\frac{d}{dt}N_{0b} = \dot R N_{pi} - \dot h_{0b} N_{0b} - \dot k_b N_{0b}; \quad \frac{d}{dt}N_{bp} = \dot k_b N_{0b} - \dot h_{bj} N_{bj} - \dot k_p N_{bp}; \quad \frac{d}{dt}N_{pi} = \dot k_p N_{bp} - \dot h_{pi} N_{pi}$$

The flux $\dot k_b = \frac{\exp(-\dot r_N a_b) S(a_b)}{\int_0^{a_b} \exp(-\dot r_N t) S(t)\, dt} \simeq (\dot r_N + \dot h_B)\frac{\exp(-(\dot r_N + \dot h_B)a_b)}{1 - \exp(-(\dot r_N + \dot h_B)a_b)}$ is from embryo to juvenile and $\dot k_p = \frac{\exp(-\dot r_N a_p) S(a_p)}{\int_{a_b}^{a_p} \exp(-\dot r_N t) S(t)\, dt} \simeq \frac{(\dot r_N + \dot h_B)\exp(-(\dot r_N + \dot h_B)a_p)}{\exp(-(\dot r_N + \dot h_B)a_b) - \exp(-(\dot r_N + \dot h_B)a_p)}$ from juvenile to adult, assuming that aging plays a minor role till puberty. The stage-dependent hazards are approximated by $\dot h_{0b} = \frac{1 - S(a_b)}{a_b}$, $\dot h_{bp} = \frac{S(a_b) - S(a_p)}{a_p - a_b}$ and $\dot h_{pi} = \frac{S(a_p)}{a_m - a_p}$.

The dynamics of scaled food density $x = X/K$ in the reactor amounts to

$$\frac{d}{dt}x = \frac{\dot J_{XI}}{V_X K} - \dot h_X x - f\frac{\{\dot J_{XAm}\}}{K}(N_{bp} L_{bp}^2 + N_{pi} L_{pi}^2)$$

for half saturation coefficient K, scaled functional response $f = \frac{x}{1+x}$, food input to the reactor $\dot J_{XI}$, reactor volume V_K, hazard rate for food $\dot h_D$, specific feeding rate $\{\dot J_{XAm}\}$.

This completes the specification of the reactor dynamics. For $\dot h_B = \dot h_X$, the reactor behaves as a chemostat.

When starting with a freshly laid egg, initial food density matters more than with EBT and CPM, since embryos convert to juveniles directly. Fig 9.8 compares the trajectories for this semi structured model, the cohort projection model and the escalator boxcar train, for the same species and reactor parameters.

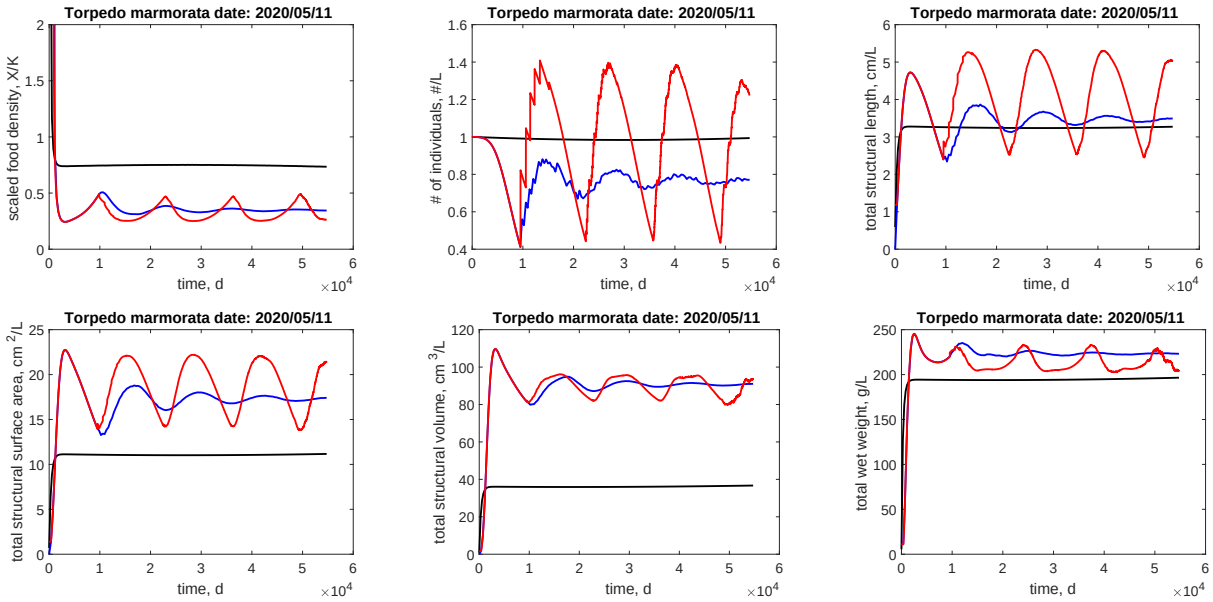

Figure 9.8: Population trajectories of *Torpedo marmorata* in a well-stirred reactor of volume $V_X = 1000\, L_m^3\,\mathrm{L}$, food hazard $\dot{h}_X = 0.1\,\mathrm{d}^{-1}$, $\dot{h}_B = 0\,\mathrm{d}^{-1}$, food supply $\dot{J}_{XI} = 0.03\, V_X\,\mathrm{mol/d}$ at 15°C, starting with a freshly laid egg and $x(0) = 10$. Trajectories are shown for the semi structured model (black), the cohort projection model (blue) and the escalator boxcar train (red). The period between reproduction events in the cohort projection model is 365 d.

9.2.2.5 Population growth rates for semelparous reproduction

If reproduction is semelparous, where N eggs are laid shortly before dying at age a_m, where survival probability is $S(a_m) = S_m$, the reproduction rate reduces to a Dirac delta function: $\dot{R}(a) = 0$ for $a < a_m$ and $\dot{R}(a_m) = \infty$ for $a = a_m$, while $\dot{R}(a_m)\, da = N$. In this case, the characteristic equation for specific population growth rate $\dot{r}_N$ reduces to $1 = S_m N \exp(-\dot{r}_N a_m)$ or $\dot{r}_N = a_m^{-1} \log(S_m N)$.

9.3 Food chains and webs

9.3.1 Asymptotic behaviour of trophic chains: bifurcation analysis

When the number of loosely coupled variables is sufficiently large in a system, the system is likely to have very complex asymptotic behaviour, including the occurrence of multiple attractors, possibly of the chaotic type. This is almost independent of the specific model; the behaviour has been observed in several models for tri-trophic food chains. Bifurcation analysis deals with qualitative changes in the asymptotic behaviour of the system, when a parameter is varied in value. Table 9.2 gives the possible bifurcation types, which all have been found in tri-trophic food chains. The bifurcation type depends on the value of the eigenvalue of the Jacobian matrix evaluated at the equilibrium and the Floquet multiplier, which is an eigenvalue of the Poincaré next-return map. If all complex values

Table 9.2: List of basic local bifurcations for ODEs: $dx/dt = f(x, \alpha)$, and maps: $y_{n+1} = f(y_n, \alpha)$ with normal forms. The bifurcation point is $\alpha = 0$. λ is the eigenvalue of the Jacobian matrix evaluated at the equilibrium ($\frac{d}{dt}x = 0$ and $y_{n+1} = y_n$) and μ is the Floquet multiplier evaluated at the limit cycle. The bifurcation type depends on the real (Re) parts of these characteristic exponents. With food web dynamics, a stable positive attractor originates at a supercritical transcritical bifurcation (superscript $+$) and an unstable positive equilibrium or limit cycle at a subcritical transcritical bifurcation (superscipt $-$). Superscript $\pm$ refers to supercritical and subtritical.

symbol	bifurcation	normal form	characteristic exponents
T_e	Tangent, of equilibrium	$\frac{d}{dt}x = \alpha - x^2$	Re $\lambda = 0$
T_c	Tangent, of limit cycle	$y_{n+1} = y_n + \alpha - y_n^2$	Re $\mu = 1$
$TC_e^{\pm}$	Transcritical, of equilibrium	$\frac{d}{dt}x = \alpha x \pm x^2$	Re $\lambda = 0$
$TC_c^{\pm}$	Transcritical, of limit cycle	$y_{n+1} = (1+\alpha)y_n \pm y_n^2$	Re $\mu = 1$
$H^{\pm}$	Hopf	$\frac{d}{dt}x = -y + x(\alpha \pm (x^2+y^2))$	
		$\frac{d}{dt}y = x + y(\alpha \pm (x^2+y^2))$	Re $\lambda_{1,2} = 0$
$F^{\pm}$	Flip	$y_{n+1} = -(1+\alpha)y_n \pm y_n^3$	Re $\mu = -1$

of the Floquet multipliers are within the unit circle, the dynamic system's orbit converges to a limit cycle.

9.3.1.1 Methods

The analysis of bifurcation behaviour must be done numerically, using specialised software: LOCBIF [712] and AUTO [340] can calculate bifurcation diagrams using continuation methods. The theory is documented in [817]. The analyses cannot be done on a routine basis, however, and the user must have a fairly good idea of what to expect and what to look for. Although the software is rapidly improving in quality, at present it is still deficient in computing certain types of global bifurcations, for instance, and one has to rely on 'in-house' software to fill in the gaps, see [151].

Results of bifurcation analyses are frequently reported in the form of bifurcation diagrams. These diagrams connect points where system's asymptotic behaviour changes in a similar way when the bifurcation parameters are varied. So, the system has similar asymptotic behaviour for values of bifurcation parameters within one region. The construction of such diagrams is only feasible if there are just one or two of such parameters. Many food chain studies take parameters that represent properties of species which cannot be changed experimentally. When the organisms live in a chemostat, two natural bifurcation parameters are the throughput rate and the concentration of substrate in the feed. Diagrams with these parameters are called operating diagrams.

9.3.1.2 Bifurcation diagrams for bi- and tri-trophic chains

Figure 9.9 shows the bifurcation diagram, as computed by Bob Kooi and Martin Boer for bi- and tri-trophic chains living in a chemostat. The reserve capacity is reduced to zero

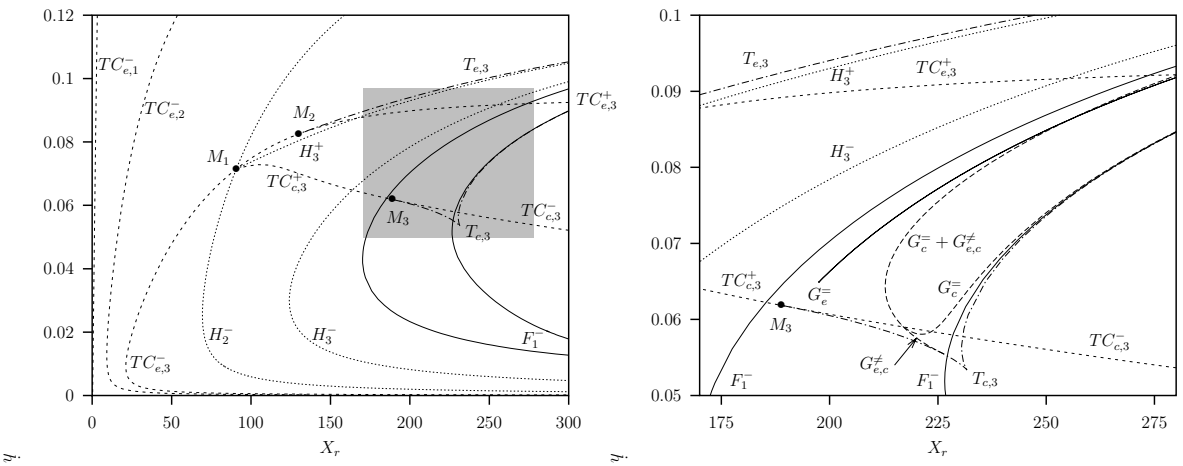

Figure 9.9: Bifurcation diagrams for Marr-Pirt model of bi- and tri-trophic chains. The right figure is a detail of the left one. The transcritical bifurcation curves $TC_{e,1}$, $TC_{e,2}$ and the supercritical Hopf bifurcation curve H_2^- relate to both bi- and tri-trophic chains, all others only to tri-trophic chains. The bifurcation parameters are the dilution rate $\dot{h}$ and the substrate concentration in the reservoir X_r. Left of the $TC_{e,2}^-$ curve, the predator is washed out; between this curve and the H_2^- curve, the bi-trophic chain has a stable equilibrium, and right of the curve H_2^- it has a stable limit cycle. The curves $TC_{e,3}^-$ and H_3^- mark similar regions for the tri-trophic chain. Within the folded (closed) flip-bifurcation curve F_1^- the limit cycle is unstable. Homoclinic $G_e^=$, $G_c^=$ and heteroclinic $G_{e,c}^{\neq}$ bifurcation curves denote global bifurcations to multiple attractors.

Parameters:

i	1	2	3	
K	8	9	10	$\mathrm{mg\,l^{-1}}$
j_{XAm}	1.25	0.33	0.25	$\mathrm{h^{-1}}$
Y_g	0.4	0.66	0.6	
$\dot{k}_M$	0.025	0.01	0.0027	$\mathrm{h^{-1}}$

for all species, so they follow the Marr–Pirt model. The system amounts to

$$\begin{aligned}
\frac{d}{dt}X_0 &= (X_r - X_0)\dot{h} - j^1_{XAm} f_{0,1} X_1 \\
\frac{d}{dt}X_1 &= (j^1_{XAm} f_{0,1} Y^1_g - \dot{k}^1_M - \dot{h})X_1 - j^2_{XAm} f_{1,2} X_2 \\
\frac{d}{dt}X_2 &= (j^2_{XAm} f_{1,2} Y^2_g - \dot{k}^2_M - \dot{h})X_2 - j^3_{XAm} f_{2,3} X_3 \\
\frac{d}{dt}X_3 &= (j^3_{XAm} f_{2,3} Y^3_g - \dot{k}^3_M - \dot{h})X_3
\end{aligned}$$

where j^i_{XAm} is the maximum specific feeding rate of species i; $f_{i,j} = (1 + K_j/X_i)^{-1}$ is the scaled function response; Y^i_g is the 'true' yield coefficient, $\dot{k}^i_M$ the maintenance rate coefficient. The bifurcation parameters are X_r and $\dot{h}$.

The bi-trophic chain has simple asymptotic behaviour only. If the species are not washed out, they can either coexist in a single stable equilibrium, or in a single limit cycle. A supercritical Hopf bifurcation separates the corresponding parameter regions. The diagram beautifully illustrates the paradox of enrichment, which is the observed induction of oscillatory behaviour that follows an increase in resource levels [1217].

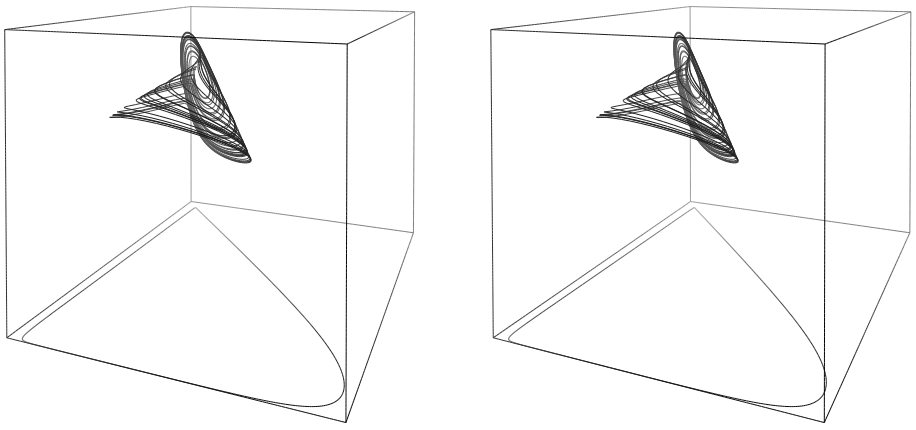

Figure 9.10: Stereo view of part of the orbit of the three trophic levels (x_1, x_2 and x_3 in the x-, y-, z-direction, respectively) of the Monod model for a food chain on a chaotic attractor (throughput rate $\dot{h} = 0.08732\,\mathrm{h}^{-1}$ and substrate level $X_r = 200\,\mathrm{mg\,l}^{-1}$).

Figure 9.9 illustrates that the bifurcation diagram of the tri-trophic chain is very complex in a small part of the parameter space. A detailed discussion is given in [751]. The diagram has an 'organising centre' M_1, which is a codimension-two point; the transcritical curves $TC_{e,3}$ and $TC_{c,3}$ for equilibrium and limit cycles, where $X_3 = 0$, originate here. The points M_2 and M_3 on these curves are the origins of the tangent bifurcation curves $T_{e,3}$ and $T_{c,3}$ for equilibria and limit cycles. A pair of interior equilibria or limit cycles disappears simultaneously as the two bifurcation parameters passes a tangent bifurcation curve. The latter tangent bifurcation curve $T_{c,3}$ has a cusp bifurcation point N. This type of bifurcation is often associated with a so-called catastrophe.

Figure 9.10 presents part of the orbit of the three trophic levels in a chemostat, using the Monod model. The bifurcation parameters are in the chaotic region of the bifurcation diagram. The bifurcation diagram for the tri-trophic chain on the basis of the full DEB model for V1-morphs resembles that of the Marr–Pirt model [750].

9.3.1.3 Closed nutrient-producer-consumer system

Figures 9.11 and 9.13 show the asymptotic dynamics of the system, while Figure 9.12 gives typical orbits. We observe that it shows the typical paradox of enrichment: the system starts oscillating above a certain nutrient level. If consumers require the reserve of the producers, it also has a lower bound for the nutrient level, due to the maintenance costs of the consumer and the system has an upper boundary for nutrient, above which it cannot exist. If the consumers do not require the reserve of the producers, both the homoclinic and the tangent bifurcation points disappear. This means, the upper bound for the nutrient level disappears (the larger the nutrient level, the larger the amplitude of the oscillations, cf [1038]) with unrealistic low minima. The lower bound also disappears in the sense that the system goes extinct at very low nutrient levels by a gradual decrease of the consumer population. Notice that consumers cannot invade the producer population with a very small inoculum size in the case of co-limitation by producers' reserve, but it can in absence of this co-limitation; see Figure 9.11. We can conclude that the nutritional details of the

producer/consumer interaction affect their kinetics in a qualitative way. Muller et al [1007] discuss a very similar producer-consumer model, which deviates slightly in the specification of consumers' growth (implementation of maintenance and of maximum growth).

9.3.1.4 Canonical map for tri-trophic chains

Many aspects of the bifurcation pattern of continuous-time systems can be understood from discrete-time systems, where the variables at time point $n+1$ are taken to be functions of those at time point n. These systems are called maps. Martin Boer [151] showed that the bifurcation behaviour of a tri-trophic chain of the Marr–Pirt and Monod type can be understood from the one-dimensional map

$$x_{n+1} = f_{\alpha,\beta}(x_n) = 16\beta x_n^3 - 24\beta x_n^2 + 9\beta x_n - \beta + \alpha \tag{9.20}$$

where x is an abstract variable, and α and β bifurcation parameters; $f_{\alpha,\beta}$ is thus a cubic polynomial in x_n, which is not invertable. There are two critical points, $c_1 = \frac{1}{4}$ and $c_2 = \frac{3}{4}$; $f(c_1) = \alpha$ is a local maximum, and $f(c_2) = \alpha - \beta$ is a local minimum. The map does not have a corresponding one-dimensional continuous system, and the equivalence is abstract, involving a Poincaré next-return map, where subsequent intersections of the dynamic system's orbit are compared with a plane chosen at a suitable location in the state space. All the points of intersection appear to lie close to a single curve when plotted against the preceding points, as occurs in the Lorenz system [878]. The shape of this curve resembles a cubic polynomial. A useful way to construct such a map is to select the local minima of the highest trophic level and to plot subsequent values against each other. The significance of identifying this one-dimensional map as a canonical form of the multi-dimensional system is in the powerful mathematical theory that exists for one-dimensional maps [959, 324, 894, 1318, 1388].

Figure 9.14 gives the map $f_{\alpha,\beta}$ for $\alpha = \beta = 0.8$, for which the map has three fixed points, $p_1 < p_2 < p_3$, and is invariant on the interval $[p_1, p_3]$. The fixed points p_1 and p_3 are repellors, since $\frac{d}{dx}f(p_i) > 1$. Then with $q \in (p_1, c_1)$ we have $\lim_{n\to-\infty} f^n_{0.8,0.8}(q) \to p_1$ and with $r \in (c_2, p_3)$ we have $\lim_{n\to-\infty} f^n_{0.8,0.8}(r) \to p_3$, where superscript n denotes the number of times the map f is applied.

An orbit starting at a point $q \in (p_1, c_1)$ is called *homoclinic* if there exists an $n > 0$ such that $f^n(q) = p_1$. This homoclinic orbit is called degenerated if $\frac{d}{dx}f^n(q) = 0$, which is the case in Figure 9.14. An orbit starting at a point $r \in (c_2, p_3)$ is called *heteroclinic* if there exists an $n > 0$ such that $f^n(r) = p_1$. The heteroclinic orbit in Figure 9.14 is also degenerated, since $\frac{d}{dx}f^n(r) = 0$. For further background, see for instance [324].

Figure 9.15 shows a one-parameter bifurcation diagram with bifurcation parameter α, for $\beta = 0.8$. It is symmetrical with respect to the point $(\alpha, x) = ((1+\beta)/2, 1/2) = (0.9, 0.5)$. The unstable equilibrium values p_1 and p_3 are plotted.

At the tangent bifurcation point T, at $\alpha \approx 0.2255$, the heteroclinic orbits disappear, together with the basin of attraction and the fixed points p_1 and p_2. In the region between this tangent bifurcation T and homoclinic bifurcation point $G^=$ ($\alpha \approx 0.5361$), the bifurcation diagram resembles the well-known bifurcation diagram of the (unimodal, with one critical point) logistic map $y_{n+1} = ry_n(1 - y_n)$ for $r \in [1, 4]$ discussed in [930].

For increasing α the fixed point becomes unstable and a cascade of period doubling leads to chaotic dynamics. As with the unimodal logistic map for $r = 4$, the strange attractor disappears suddenly at a homoclinic bifurcation point. In the interval $\alpha \in [0.8, 1.0]$ there is chaotic dynamics with abrupt destruction of the chaotic attractor and its basin of attraction at the end points of this interval in $\alpha = 0.8$ and $\alpha = 1.0$. Here homoclinic orbits to the equilibria p_1 and p_3, respectively, degenerate at the global bifurcation point (see Figure 9.14). With $\alpha = (1 + \beta)/2$ the equilibria p_3 and p_1 switch roles.

In the one-parameter bifurcation diagram of Figure 9.15 points on a heteroclinic orbit between p_3 and p_1 are plotted in the interval $\alpha \in [\approx 0.2255, 0.8]$. At the global bifurcation point $G^{\neq}$, the heteroclinic orbits between points p_3 and p_1 become degenerate. Figure 9.15 also gives the basin of attraction. In the absence of heteroclinic orbits, $\alpha \in [0.8, 1.0]$, the basin is connected. However, with heteroclinic orbits $\alpha \in [\approx 0.2255, 0.8]$ convergence to a positive attractor for $\alpha \in [\approx 0.2255, 0.5361]$ occurs in disconnected intervals with end points on heteroclinic orbits, and the basin boundary has a complex geometry close to the equilibrium p_3. In the 'hole' in the chaotic region there is convergence only for the countable points at the homoclinic and heteroclinic orbits and otherwise there is no convergence. At the tangent bifurcation point T the boundary basin is a vertical line where α is constant, that is the basin of attraction disappears abruptly at the tangent bifurcation together with the fixed points p_1 and p_2.

Figure 9.16 illustrates the next minimum map for the Monod model for a tri-trophic chain in the chemostat, and the one-parameter bifurcation diagram for the throughput rate. Both the map and the diagram have striking similarities with the canonical map given in Figures 9.14 and 9.15. A full analysis of the two-parameter bifurcation diagram can be found in [151].

9.3.1.5 Stochastic producer-consumer models

Trajectories for the producer and consumer populations at different values for the total amount of nutrient in the system are given in Figure 9.17 to show the vanishing role of the Hopf bifurcation point.

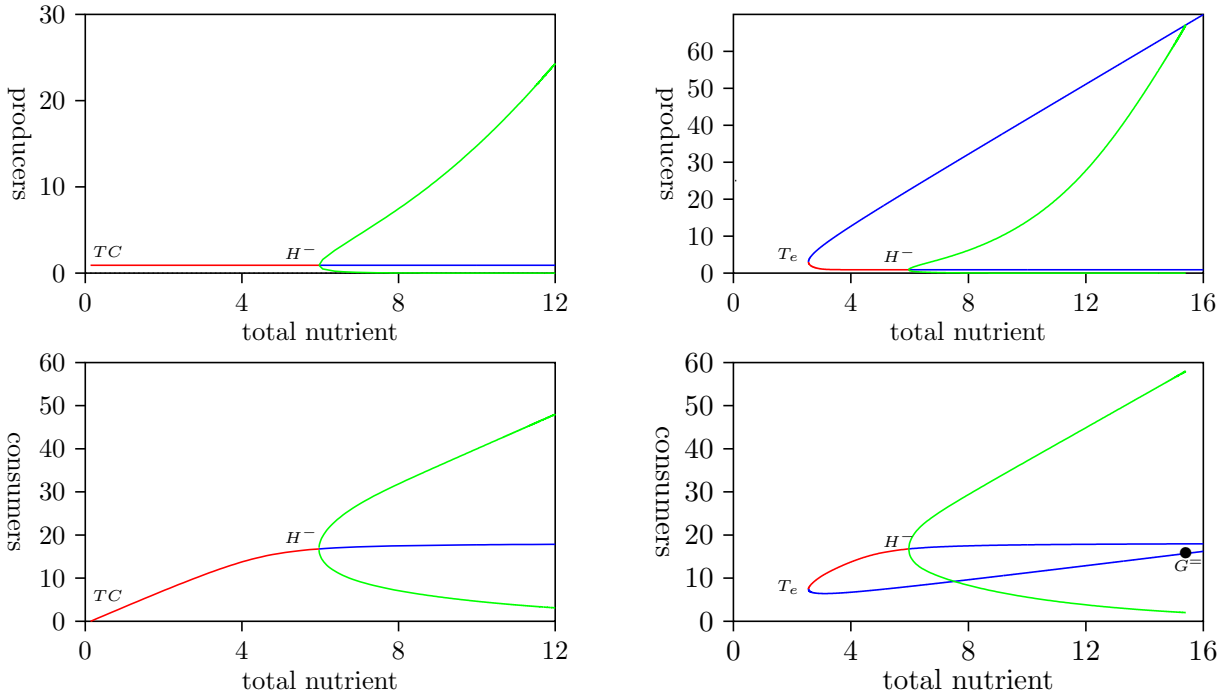

Figure 9.11: The bifurcation diagrams for the producer (top) and the consumer (bottom) dynamics in a closed system, using the total amount of nutrient as bifurcation parameter. The producer follows Droop's kinetics, the consumer follows Marr-Pirt's kinetics and has a constant hazard rate; there is no free nutrient in the environment. Left: The consumer is not limited by producers' reserve, so $\dot{r}_C = \dot{r}_{CP}$. Right: Producers' reserve and structure are complementary for consumers. At very low nutrient levels, the system cannot exist. At intermediary nutrient levels, the system has a point attractor. A transcritical (TC, left) or tangent (T_e, right) and a Hopf bifurcation point (H^-) mark the boundaries of these intermediary nutrient levels. At larger nutrient levels, the system oscillates with increasing amplitude. A homoclinic bifurcation point ($G^=$, right) marks the upper boundary of this interval; the system cannot exist at higher nutrient levels (right), while producers' minima become extremely small for growing nutrients levels (left). Parameters: $\dot{h} = 0.005\,\mathrm{h}^{-1}$, $n_{NP} = 0.15\,\frac{\mathrm{mol}}{\mathrm{mol}}$, $n_{NC} = 0.25\,\frac{\mathrm{mol}}{\mathrm{mol}}$, $y_{CN} = 5.5\,\frac{\mathrm{mol}}{\mathrm{mol}}$, $y_{CP} = 2\,\frac{\mathrm{mol}}{\mathrm{mol}}$, $K = 10\,\mathrm{mM}$, $j_{PAm} = 0.15\,\frac{\mathrm{mol}}{\mathrm{mol\ h}}$, $\dot{k}_N = 0.25\,\mathrm{h}^{-1}$, $\dot{k}_M^P = 0.02\,\mathrm{h}^{-1}$, $\dot{k}_M^N = 0.01\,\mathrm{h}^{-1}$.

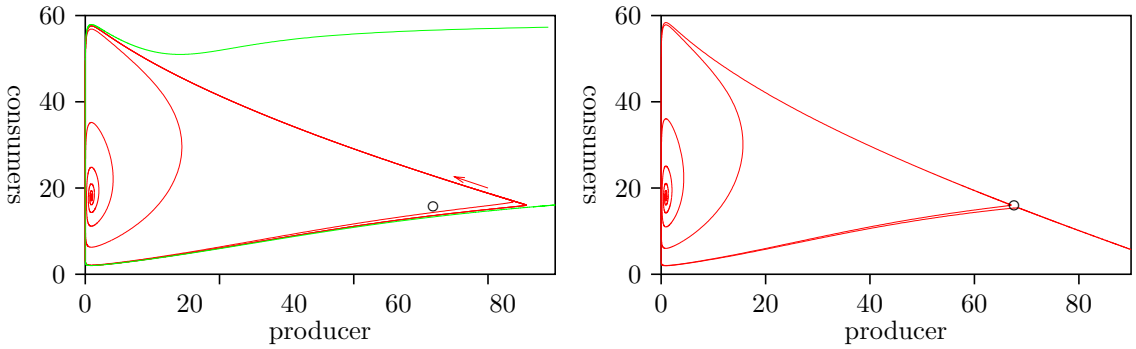

Figure 9.12: Orbits of the producer-consumer system of Figure 9.11 for nutrient levels just below (left, $N = 15.3\,\mathrm{mM}$) and above (right, $N = 15.5\,\mathrm{mM}$) the homoclinic bifurcation point. Orbits that start within the stippled separatrix of the top figure result in a stable oscillation (one such an orbit is indicated), while other orbits lead to extinction. This separatrix breaks open for higher nutrients levels (right figure), and all orbits lead to extinction (one such an orbit is indicated). The saddle point, and the spiral source are indicated.

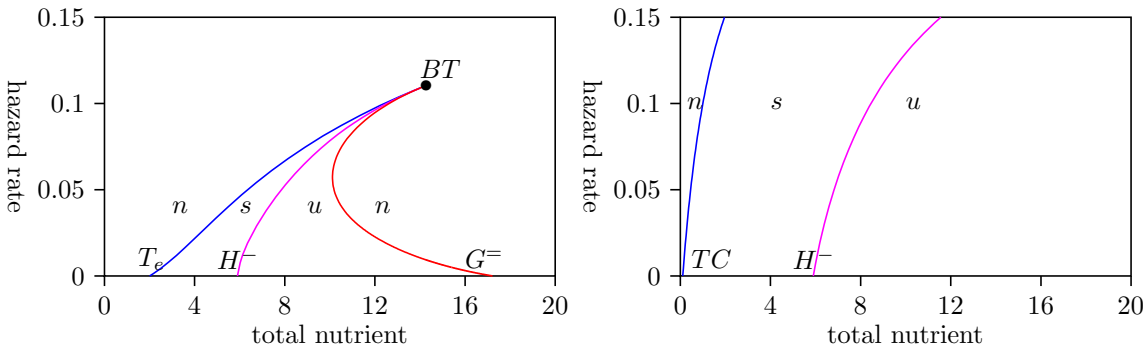

Figure 9.13: The two-dimensional bifurcation diagram for the producer-consumer system as in Figure 9.11, using the total nutrient level and consumers' hazard rate as bifurcation parameters. The consumer requires producers' structure *and* reserve (left) or producers' structure only (right). Three areas are indicated: n no co-existence, s stable co-existence, u unstable co-existence (oscillations). The tangent (T_e), Hopf (H^-) and Homoclinic ($G^=$) bifurcation curves meet in a Bagdanov-Takens point in the top figure; the transcritical (TC) and Hopf (H^-) bifurcation curves diverge in the bottom figure.

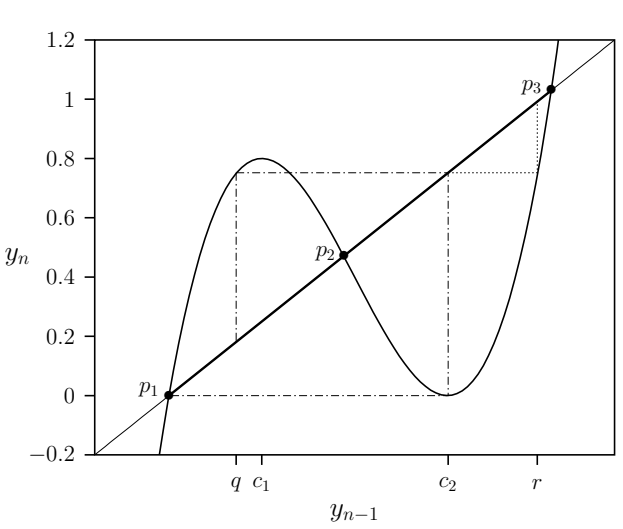

Figure 9.14: The function $f_{\alpha,\beta}$ for $\alpha = 0.8$ and $\beta = 0.8$. The points p_1, p_2 and p_3 are fixed points, and c_1 and c_2 are critical points. At point q a degenerate homoclinic orbit starts ($f^2_{0.8,0.8}(q) = p_1$ and $\lim_{n\to-\infty} f^n_{0.8,0.8}(q) \to p_1$ for $q \in (p_1, c_1)$). At point r a degenerate heteroclinic orbit starts ($f^2_{0.8,0.8}(r) = p_1$ and $\lim_{n\to-\infty} f^n_{0.8,0.8}(r) \to p_3$ for $r \in (c_2, p_3)$). The solid interval on the diagonal is the basin of attraction.

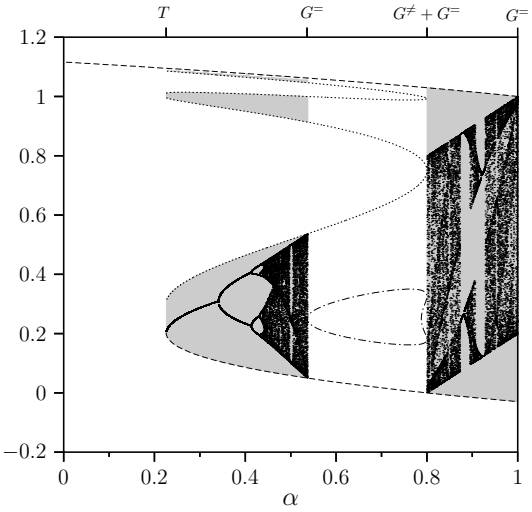

Figure 9.15: One-parameter bifurcation diagram of the canonical map for $\beta = 0.8$. The dashed curves indicate the repellors p_1 and p_3. The points on the dotted curves lie on a heteroclinic orbit. The points on the dashed-dotted curve lie on a homoclinic orbit. The attractors are plotted as points. The grey regions are the basin of attraction of these attractors. This diagram is point-symmetrical with respect to point $(0.9, 0.5)$.

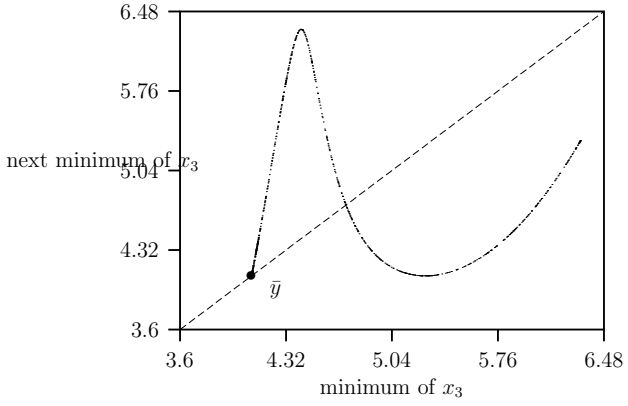

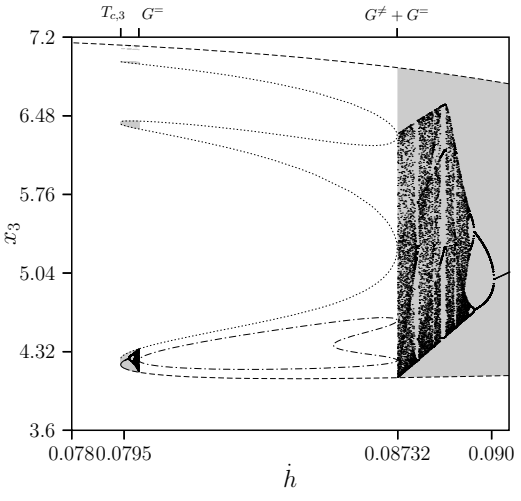

Figure 9.16: The left figure shows the next minimum of x_3 as a function of the current minimum for the Monod model, with dilution rate $\dot{h} = 0.08732\,\mathrm{h}^{-1}$ and concentration substrate in the feed $X_r = 200\,\mathrm{mg\,l}^{-1}$. The resulting map resembles the canonical cubic map with two critical points. The point $\overline{y}$ is the minimum of a limit cycle of the saddle type. The right figure shows the one-parameter bifurcation diagram of the Monod model, which again shows striking similarities with that of the canonical cubic map.

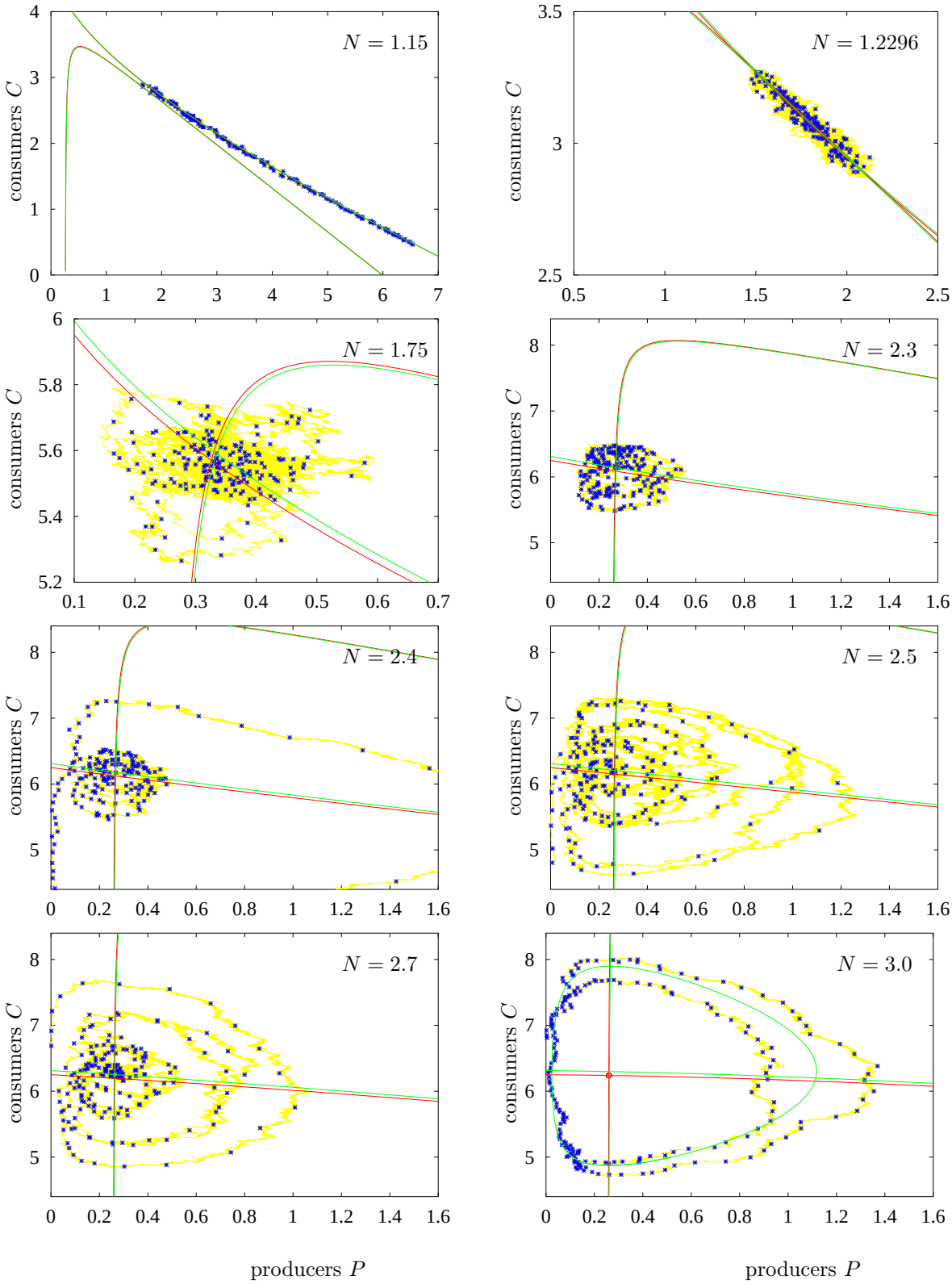
N = 1.15
N = 1.2296
N = 1.75
N = 2.3
N = 2.4
N = 2.5
N = 2.7
N = 3.0
consumers C
producers P

Figure 9.17: The trajectory of the stochastic model for different values for the total amount of nutrient N. The fat dots are the linearly interpolated values with equal time units apart. For low N-values, the start is at the stable equilibrium of the expected value of stochastic model, which is at the intersection of the $\frac{d}{dt}P = 0$ and the $\frac{d}{dt}C_h = 0$ isoclines (while $\frac{d}{dC_h}C_s = 0$; solid curves). For large N-values ($N = 2.7, 3.0$), the start is at a random point of the limit cycle of the NTS-model. The isoclines of the deterministic model are plotted as well (stippled). Notice that for $N = 2.3$ few points of the S-model are at the mean, because of its tendency to cycle. For $N < 2.6$ 1000 time units are used, and 5000 for $N > 2.6$. The various bifurcation points for the total amount of nutrient are:

	tangent	focus	Hopf	global
deterministic	1.217	1.520	3.165	7.11
stochastic	1.229	1.535	2.801	6.96

10

Evolution

10.1 Life orginated anaerobically

The frequency of the various types of amino acids in proteins of archaea, eubacteria and eukarya strongly suggests that the last universal common ancestor (LUCA) was an anaerobic organism, as were the ancestors of archaea and eubacteria, whereas the ancestor of eukarya was an aerobe [494]. The presence of DNA topoisomerase IB in Thaumarchaeota, eubacteria and eukarya suggests that LUCA had DNA [189].

10.3 Evolution of the individual as a dynamic system

10.3.3 Constant cell size at division

Recently some progress has been made to understand mechanisms that control the cell size at division of animals cells [1448].

10.3.4 Simplification and integration

10.3.4 Out of the sea

The idea that the ancestors of animals and fungi (Opisthokonts, notably the chytrids) left the sea well before the animals did (some 0.5 billion years ago), was recently supported by the discovery of fossilised eukaryotic cells in a 1.2 billion year old lake sediment in Scotland [1390]. The cyanobacteria, which evolved 2.7 billion years ago did so probably in a freshwater habitat, where they still have their largest diversity. Since they are mixotrophic, with heterotrophic origins, this habitat must have been rich in organic matter of bacterial origin.

10.3.4 Modular recombination

Lake [822] argued that all double-membrane prokaryotes form a natural group that originated from the merging of an Actinobacterium and a Clostridium; the Bacilli and the

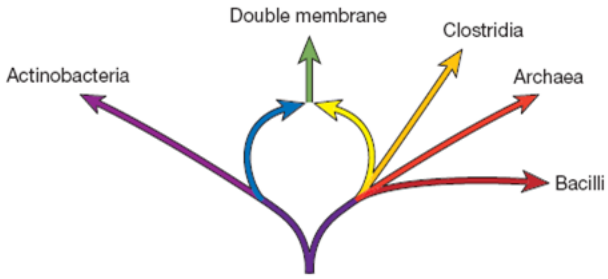

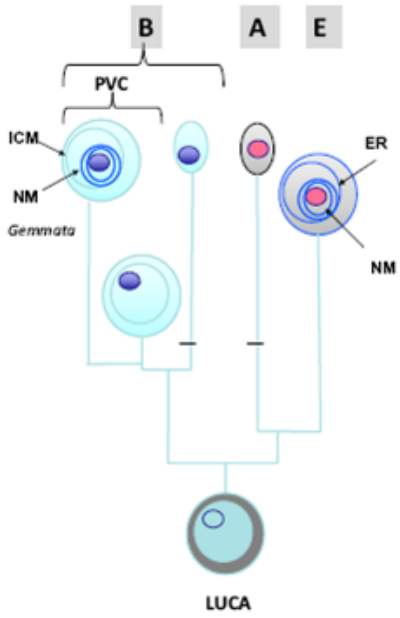

Figure 10.1: Two scenarios for the relative phylogenetic position of the Bacteria (B) Archaea (A) and Eukarya (E). In the above scenario from [822], all double-membrane organisms are grouped together, although the Bacteria have no membrane coat proteins, except those of the PVC superphylum. In the right scenario from [439], the double membrane and membrane coat proteins are thought to be present in the Last Universal Common Ancester (LUCA).

Archaea making up group 4 and 5, see Figure 10.1. It would explain the distribution of phototrophy (confined to Clostridia and these double-membrane prokaryotes) and of two slowly evolving indels in enzymes involved in pyrimidine- and histidine-biosynthesis, PyrD and HisA; these indels are shared by Actinobacteria and double-membrane prokaryotes.

An more promising alternative hypothesis was formulated after the recent discovery that *Gemmata*, a Planctomycete, so a member of the Planctomycetes-Verrucomicrobia-Chlamydiae (PVC) superphylum, not only has a nuclear membrane, but is also capable of endocytosis [876, 1243]; until very recently this property was thought to be confined to the Eukarya. If the required membrane coat proteins of PVC-bacteria and Eukarya have a common origin, a possible scenario is that Eukarya originated on the inclusion of an archaeal symbiont in a PVC-bacterium that subsequently lost its cell membrane and its genome somehow entered the nuclear membrane [439]. Alternatively, the LUCA was already compartmentalised and had already membrane coat proteins, see Figure 10.1. This would also explain the ability of some Archaea to produce methane, by adding 2 enzymes to the 16 that PVC-bacteria use to detoxify formalin. If the LUCA had it all, subsequent scenarios become simple, but the explanation of the acquisition of these properties become more complex.

10.3.4 Plastids and the storage of polysaccharides

The plastids of the Glaucophyta still contain the peptidoglycan wall of the cyanobacterial ancestors. See Figure 10.2. Secondary plastids typically have 4 membranes, rather than 2, as a result of the phagocytotic entering of the host. The biochemical properties of these membranes reveal their evolutionary origins. 'Algae' (= phototrophic eukaryotes) can be classified as α-glucan (glycogen, starch, i.e. a mixture of amylose and amylopectin) or β-glucan (paramylon, laminarans) accumulators. Starch is restricted to the Archaeplastida,

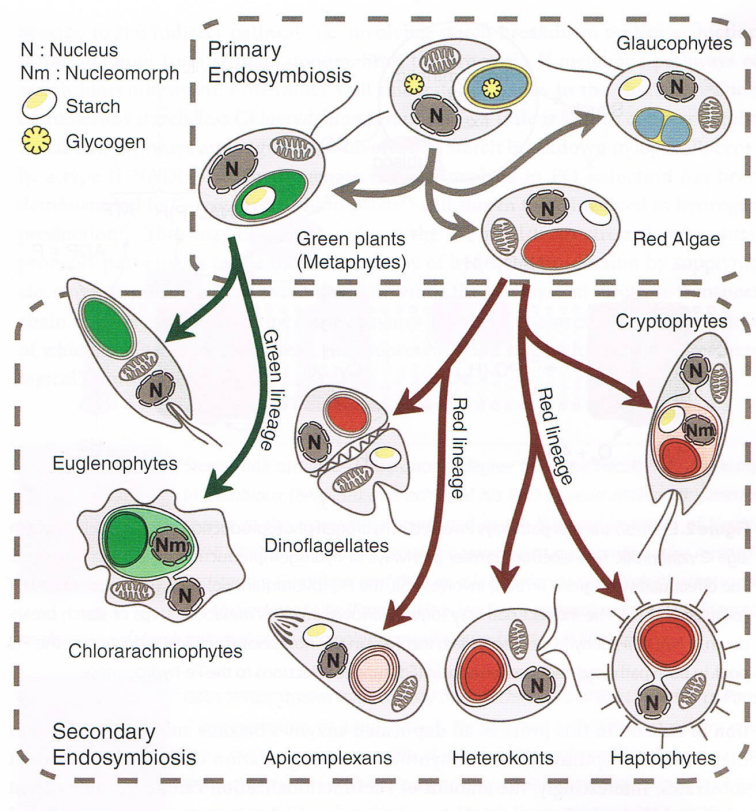

Figure 10.2: A heterotrophic ancestor of the Archaeplastida possibly included a cyanobacterium only once, an event followed by multiple secondary and tertiary endosymbioses of descending Chlorophytes and Rhodophytes in other heterotrophic taxa. The number of secondary inclusons is controversial. Some plastids lost phototrophy, as in the parasitic Apicomplexans. From [73]

.

to their secondary endosymbiosis derivatives and to a particular subgroup of unicellular nitrogen-fixing cyanobacteria. Rhodophytes and Glaucophytes synthesise starch in the cytoplasm, but Chlorophytes in their plastids. Rhodophytes posses the complete set of 12 genes for eukaryotic glycogen metabolism, but only a few genes originating from cyanobacterial pathways. Chlorophytes (including plants) have over 40 genes for starch metabolism, largely orginating from gene duplication of the Rhodophyte genes. Starch accumulation in plastids had 3 stages [73]: a small pool of malto-oligosaccharides, a larger pool of glycogen and then a big pool of starch. Apart from the early plastids, a more recent cyanobaterial endosymbiont evolved, see Figure 10.3; many symbiontic relationships between cynanobacteria and eukaryotes evolved independently, but their integration with the host metabolism is less intense.

10.5 Multicellularity and body size

10.5.5 From supply to demand systems

Species can be ranked according to a supply-demand spectrum that roughly reflects where the controls of energetics are: from environmental to internal, see [855]. The use of resources is 'pre-programmed' in demand-species and the individual tries hard to match this demand by eating enough. Supply-species hardly have such a program, or modify it in a flexible way, according to the possibilities offered by the environment. Table 10.1 compiles

Table 10.1: Stylised eco-physiological properties that relate to the position of a species in the supply-demand spectrum

Supply	**Demand**
eat what is available	eat what is needed
large half saturation coefficient	small half saturation coefficient
rather passive, simple behaviour	rather active, complex behaviour
little parental care	advanced parental care
sensors less developed	sensors well developed
can handle large range of intake	can handle small range of intake
low peak metabolic rate	high peak metabolic rate
open circulatory system	closed circulatory system
iso- & centro-lecithal eggs	a- & telo-lecithal eggs
typically ectothermic	typically endothermic
reserve density varies strongly	reserve density varies little
large range of ultimate sizes	small range of ultimate sizes
survives some shrinking well	survives shrinking badly
survives rejuvenation well	survives rejuvenation poorly
energetic birth control	behavioural birth control
no upregulation for reproduction	upregulation for reproduction
no acceleration of ageing	acceleration of ageing
evolutionary original	evolved from supply systems
has demand components (maintenance)	has supply components (some food must be available)

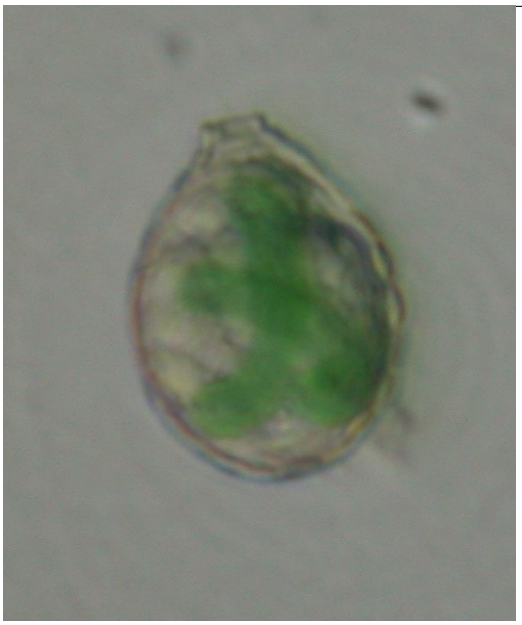

Figure 10.3: The thecate amoeba *Paulinella chromatophora* (*Cercozoa, Euglyphidae*) has an cyanobacterial symbiont that still has its full genome, including genes coding for nitrogen fixation. This symbiont is related to *Prochlorococcus* and *Synechococcus* [1572], while plastids are related to *Gloeobacter* and/or *Pseudanabaena* [1024]. Since *P. chromatophora* is closely related to the heterotrophic *P. ovalis*, and the endosymbiont hardly lost genes, *Paulinella* acquired its endosymbiont probably recently. Picture taken in Leeuwin-Naturaliste National Park, Western Australia, at 2014/12/12.

stylised eco-physiological properties of species that link to their position in the spectrum. No species are at the extremes of the spectrum, as indicated in the table. There is a lot coherence between these properties.

Demand species have less metabolic flexibility to handle starvation in terms of shrinking and rejuvenation, but they compensate that by a higher talent for finding the last food item (= low half saturation constant), for which they need complex behaviour and good memory and sensors. The half saturation constant is in fact the ratio of the (specific) ingestion and searching rates, meaning that demand species have a large specific food searching rates. High peak metabolic activity, relative to the standard one, is part of the skills they need to capture (fast) prey and is connected to searching rate. Capillaries (in a closed circulatory system) make that an increase in heart beat is felt in all corners of the body (where muscles contract), which explains the link with a high peak metabolic rate. Only annelids, cephalopods and vertebrates have capillaries, all other animal species work with open circulatory systems, where an increase in heart beat has less consequences for tissues that are further away from the heart. Annelids probably have them to build up pressure when pushing their body through soil; without capillaries muscle contraction would transport fluid inside the body too easily and does not have the effect that the body is pushed forward. We see this as an adaptation to life in soils that has little to do with the evolution from supply to demand systems. Cephalopods and vertebrates have telolecithal eggs, which possibly relates to their closed circulatory system with which they mobilise yolk. The embryo being on the outside of yolk facilitates access to environmental dioxygen and allows for high metabolic rates, compared to iso- or centro-lecithal eggs. Mammals have alecithal eggs, which probably relates to their foetal development.

Demand systems have (food) acquisition homeostasis, with thermal homeostasis as pinnacle. Many species (insects, reptiles) developed in the direction of thermal homeostasis via behaviour (sitting in sun or shade), some species (insects, tunas, sharks) sport metabolic heating (endothermy), but mammals and birds have fully mastered this art (after birth). Endothermy induces timing problems of ageing relative to maturation; food availability

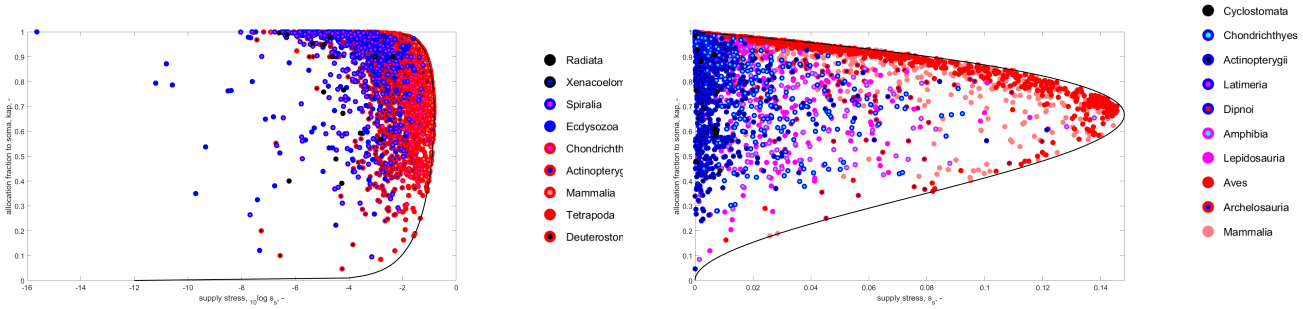

Figure 10.4: Allocation fraction κ as function of supply stress s_s for the species of the add_my_pet collection. Sampling date 2023/11/25 at 4237 entries. Modified from [855]. Notice that ecdysozoans are extreme supply species and endotherms (birds, mammals) extreme demand species. The points in both plots are identical, only the colour-coding is different and the abscissa is logarithmically transformed (left) to expose extreme supply species.

has seasonal controls and life cycles must fit seasonal cycles. If an endothermic mouse and an ectothermic lizard of the same body size and energy budget parameters would also have same ageing parameters, the (warmer) mouse would live too short. Endotherms accelerate ageing (Gompertz stress coefficient $s_G > 0$), starting with an extra-low ageing rate. This gives age-dependent survival probabilities that are high for a long time, and then suddenly drop. Survival curves of ectotherms drop much more gradually, as far as ageing is concerned [775, Chapter 6]. Notice that many factors affect survival and ageing is rarely the most important one in field conditions. Birds and mammals also sport upregulation of metabolism before egg laying or during pregnancy and lactation: maximum feeding rate is temporarily increased [775]. The rationale of this pattern is discussed below. Zoo keepers (and farmers) know that most birds can be stimulated to lay more eggs by removing freshly-laid eggs, which shows that egg-production is not energy limited. Offspring production in birds is typically limited by parental care just before fledging, when food requirement is at maximum [792].

Because supply stress $s_s = \frac{\dot{k}_J E_H^p [\dot{p}_M]^2}{f^3 s_{\mathcal{M}}^3 \{\dot{p}_{Am}\}^3} = \frac{k v_H^p}{f^3 s_{\mathcal{M}}^3}(1-\kappa)\kappa^2 = \frac{\dot{p}_J \dot{p}_M^2}{\dot{p}_A^3} = \frac{\dot{p}_J}{\dot{p}_A}\kappa^2$, as introduced in the boundaries of the data and parameter spaces in Section 4.10.0 of the comments, relates assimilation (supply) to maintenance (demand), it quantifies the distance to the supply-end in the classification of species in the supply-demand spectrum and as consequence $s_d = 2^2/3^3 - s_s$ the distance to the demand-end of the spectrum [855]. The width of the supply-demand spectrum is thus $s_s + s_d = 4/27$. Figure 10.4 also shows that κ is frequently very close to the upper boundary for zero reproduction, but not to the lower boundary. This is further discussed in [792]. Although maximum reproduction is around $\kappa = 0.45$ for supply-species [792], κ approaches 2/3 for demand-species. Hexapods are extreme supply species because they skip the juvenile stage and directly after birth allocate to reproduction. This has the consequence that $\dot{p}_J$ is very small for them. Notice that most points are near maximum κ, and few near minimum κ, especially for low s_s.

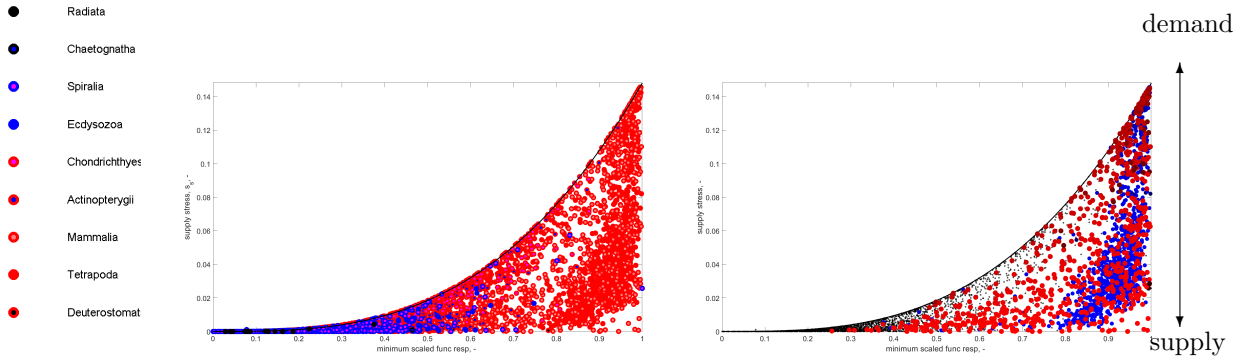

Figure 10.5: The supply stress as function of the minimum scaled functional response that is required to reach puberty. Figure updated from [855] for the add_my_pet collection, sampling date 2023/11/25 at 4237 entries. The curve is $s_s^{\max}(f_{\min}) = f_{\min}^3 4/27$. Left: Colour coding as in Figure 10.4. All supply species hide in the lower left corner of the figure. Right: As left, but only endotherms are highlighted, the rest only as small dots. The red-level for mammals (bigger dots) and the blue-level for birds (smaller dots) are proportional to κ; the closer to black, the lower κ, while the highest values of κ occur at low values for $f_{\min}$ and s_s.

If $f = 1$, $e = 1$ and $L = L_m$, we have $\dot{p}_A = \dot{p}_M + \dot{p}_J + \dot{p}_R$, while $\dot{p}_M/\dot{p}_A = \kappa$, $\dot{p}_J/\dot{p}_A = s_s/\kappa^2$ and $\dot{p}_R/\dot{p}_A = 1 - \kappa - s_s/\kappa^2$. So $\dot{p}_J/\dot{p}_M = s_s/\kappa^3$, while $\dot{p}_J = \dot{k}_J E_H^p$ and $\dot{p}_M = \dot{k}_M [E_G] s_{\mathcal{M}}^3 L_m^3$, so $\frac{s_s}{\kappa^3} = \frac{k E_H^p}{[E_G] s_{\mathcal{M}}^3 L_m^3}$. The significance of this relationship is that s_s rather strongly depends on taxonomy, while $\dot{k}_J$, so k, is poorly determined by data.

Maturity density $E_H^p/s_{\mathcal{M}}^3 L_m^3 = l_p^3(1-\kappa)g[E_m]$ for $k = 1$ while the relationship holds approximately for $k < 1$. Maturity ratio then reduces to $k \simeq \frac{s_s/\kappa^2}{(1-\kappa)l_p^3} = f_{\min}^3/l_p^3$, where scaled length at puberty l_p quantifies determinateness. Since $\kappa = \frac{4}{27}$ maximizes $(1-\kappa)\kappa^2$, we must have $s_s < l_p^3 4/27$, and, of course, $l_p < 1$. This translates to $k < \frac{3^6/2^2}{3^2-2^2} = 7.9$, which is uninformative since $k < 1$ must apply to avoid that maturity density increases over ontogeny. This relationship demonstrates that species that grow considerably as adult, i.e. during reproduction, are supply species. Fish frequently have $l_p = 0.5$, which translates to $s_s < 0.02$ if $k = 1$.

This interpretation of s_s is confirmed by Figure 10.5, which presents it as function of the minimum functional response, i.e. the food ingestion rate as fraction of the maximum one of an individual of that size, that is required to reach puberty. It amounts to $f_{\min} = \left(\frac{\dot{k}_J E_H^p [\dot{p}_M]^2}{\kappa^2(1-\kappa) s_{\mathcal{M}}^3 \{\dot{p}_{Am}\}^3}\right)^{1/3} = \left(\frac{f^3 s_s}{\kappa^2(1-\kappa)}\right)^{1/3}$ and has a minimum for $\kappa = 2/3$ for non-accelerating species. For $k = 1$ the minimum functional response reduces to $f_{\min} = f^3 l_p^3$. The figure also shows, in general, that $s_s^{\max}(f_{\min}) = f_{\min}^3 4/27$, which directly follows from the previous expression for $f = 1$ and $\kappa^2(1-\kappa) > s_s$ and $s_s < 4/27$.

Figure 10.6 shows that all points in a 3D-plot $(\kappa, f_{\min}, s_s)$ are on or very near a simple (curved) surface for $f = 1$. Given that $f_{\min}$ satisfies $k v_H^p = f_{\min}(f_{\min} - l_T)^2 s_{\mathcal{M}}^3$, and

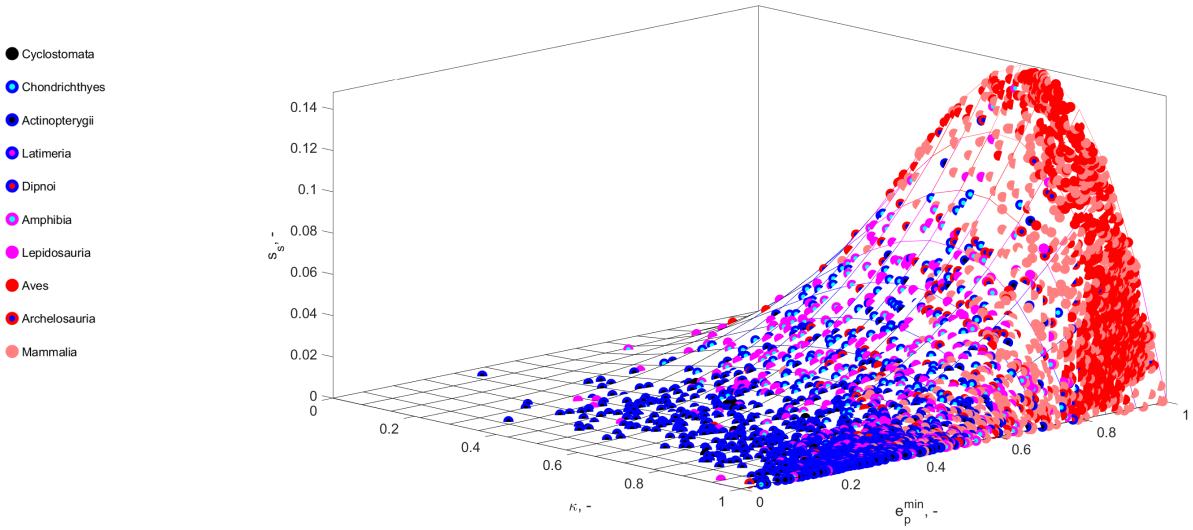

Figure 10.6: Supply stress s_s, allocation fraction to soma κ and minimum scaled functional response to reach puberty $f_{\min}$ are on, or very close to, the surface $s_s(\kappa, f_{\min}) = f_{\min}(f_{\min} - l_T)^2\kappa^2(1-\kappa)$ at $f = 1$. Deviations from this surface are due to the fact acceleration factor $s_{\mathcal{M}}$ depends on the scaled functional response if $s_{\mathcal{M}} > 1$. Data from the add_my_pet collection, sampling date 2023/11/25 at 4237 entries.

$f_{\min}^3 = \frac{s_s}{\kappa^2(1-\kappa)}$ with $s_s = \frac{kv_H^p}{s_{\mathcal{M}}^3}(1-\kappa)\kappa^2$, deviations from this surface can only occur for large $s_{\mathcal{M}}$ in combination with small $f_{\min}$, due to the fact that $s_{\mathcal{M}}$ depends on f. The figure clearly shows that supply species can reach puberty for a much broader range of food intake levels, compared to demand species. Some mammals and birds have a minimum scaled functional response for reaching puberty close one. This explains why these taxa have upregulation of metabolism linked to reproduction. This upregulation is an extra module in DEB models, that is not part of the standard DEB model.

Figure 10.5 shows that endotherms with low values for $f_{\min}$ and s_s have a high value for κ. The coupling between κ and s_s follows from the increase of the possible range of κ with s_s. Yet it is remarkable that none of the endotherms in the add_my_pet collection have a low supply stress s_s in combination with a low κ. These couplings require further investigation.

Another strong confirmation for the interpretation of s_s comes from taxa that have a large value of s_s: these are exactly the taxa that can considered to be demand species on the basis of the criteria of Table 10.1: all invertebrates have a small supply stress s_s, but vertebrates have higher values. While Myxini and Actinopterygii are close to the supply end of the spectrum, Chondrichthyes tend to be closer to the demand end. One species of Sarcopterygii, the coelanth, turns out to be a supply species, while the Australian lungfish has demand tendencies. This strategy is probably open to lungfish, because they can switch off maintenance (torpor, although the non-Australian species can do this better). Lampreys, Cephalaspidomorphi, seem to have some demand tendencies, which possibly relates to their life style of 'milking' fish. Only the European brook lamprey is presently in the collection; more species are required for confirmation. Bony fish, Actinopterygii,

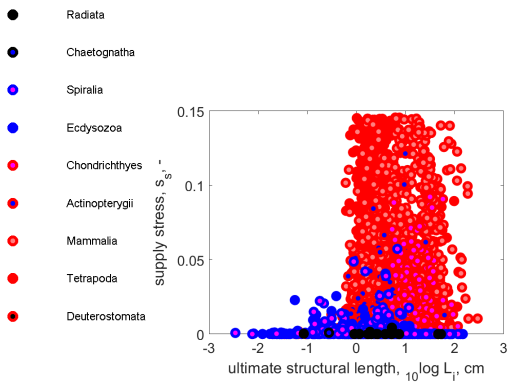

Figure 10.7: Supply stress as function of ultimate structural length. Data from the add_my_pet collection, sampling data 2023/11/25 at 4237 entries.

tolerate a very wide range of food levels [773], which confirms their classification as supply species.

Birds and mammals are close to the demand end, where food intake is primarily controlled by metabolic needs, while most invertebrates are close to the supply end, where food intake is primarily controlled by food availability. Cnidarians are possibly the most extreme supply species with extreme capacity of shrinking and rejuvenation in response to starvation: some medusea can even rejuvenate till polyps [1106]. Because cephalopods have a closed blood circulation system, telolecithal eggs, high peak metabolic rate, complex behaviour and superb vision, we expected to see tendencies for demand species in this taxon. Yet their s_s values are small, which probably relates to their life style of suicide reproduction. They don't die by ageing and their size at death is considerably smaller than their asymptotic size, while most species approximate that size (insects being an exception, [776]). This means that their value for $s_{\mathcal{M}}\{\dot{p}_{Am}\}$ is relatively very large for species with that size at death, so s_s is small; their range in body sizes at death is quite large.

Figure 10.7 shows supply-stress s_s as function of ultimate structural length of species. It shows that vertebrates, and especially endotherms are demand species and typically have a relatively large body size.

The values of the supply-stress follows a scaled beta distribution very closely, see Figure 10.8 and [853]. The explanation is that supply-stress is a product of three ratio's of fluxes; each of these ratio's follows a beta distribution, so does the product. The reason why each ratio follows a beta distribution is the same as why $\kappa = \dot{p}_M^\infty / \dot{p}_A^\infty$ follows a beta distribution: the fluxes themselves follow a Weibull distribution, and this is because many factors contribute. Products of independently beta-distributed variables are again beta-distributed. The three ratios are not mutually independent, however, two of them being even identical. Yet Monte-Carlo studies confirm that the approximation is close to perfect in the neighborhood of the parameter values as found. The reason why the survivor functions for somatic maintenance and assimilation are that close is because their ratio, κ, is close to 1, and because their ranges are huge, since the collection has tiny as well as huge bodied species. Figure 10.8 also presents support for why the Weibull distribution fits that of fluxes well: Maturity maintenance at birth fits the Weibull distribution rather well, but the one at puberty fits perfectly. Environmental scatter (including food availability)

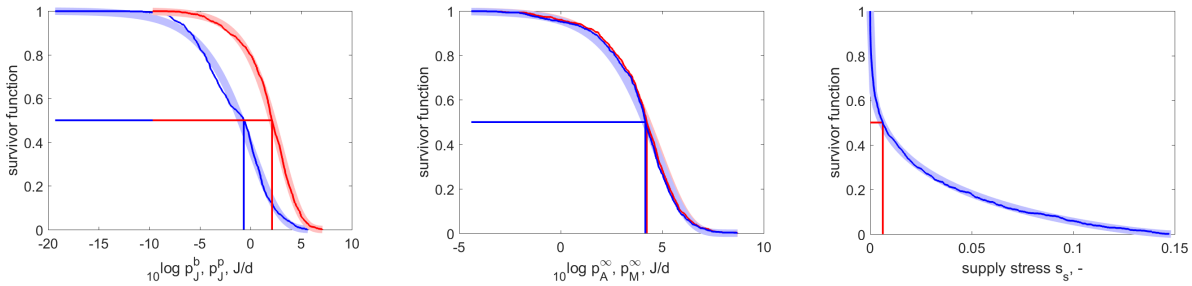

Figure 10.8: The survivor functions of maturity maintenance at birth and puberty (left), assimilation and somatic maintenance (middle) and supply stress (right). They are plotted on top of the best fitting Weibull distributions (left and middle) or beta distribution (right), scaled between 0 and $2^2/3^3$. Notice that $\dot{p}_J^p$ fits the Weibull distribution better than $\dot{p}_J^b$ and that $\dot{p}_J^p = \dot{p}_J^\infty$. Data from the add_my_pet collection, sampling date 2023/11/25 at 4237 entries.

during the juvenile period when maturity builds up, is the most likely cause.

11

Evaluation

11.1 Historic setting

Many of the questions around energy budgets are far from new. R. Boyle, R. Hooke and J. Mayow in the seventeenth-century were among the first to relate respiration to combustion, according to McNab [949]. The first measurements of the rate of animal heat production were made by A. Crawford in 1779, and A.L. Lavoisier and P.S. de Laplace in 1780 aimed to relate it to dioxygen consumption and carbon dioxide production [949]. The concept of energy was first proposed by Thomas T. Young in 1807, according to Blaxter [147]. It means something like 'the ability to do work', which primarily consists of driving chemical reactions against the direction of their thermodynamic decay. Interest in how metabolic rate, measured as dioxygen consumption rate, depends on body size goes back at least as far as the work of Sarrus and Rameaux [1246] in 1839. They were the first to find rates proportional to surface area for warm-blooded animals [125]. Later this became known as the Rubner's surface law [1224]. The casual way A.R. Wallace mentioned this idea in a note to E.B. Poulton (appendix 3 in [423]: *'Supposing organisms ever existed that had not the power of natural reproduction, then since the absoptive surface would not only increase as the square of the dimensions while the bulk to be nourished and renewed would increase as the cube, there must soon arrive a limit of growth'*) suggests that its roots go back to before 1865; he probably knew the work of Sarrus and Rameaux. As far as I know, Pütter [1139] is the first who restated this bright insight in a mathematical model, which he applied to fish. The fact that the surface law was based on work with warm-blooded animals, generated a lot of criticism. Pütter saw growth as the difference between build-up and break-down. The processes of build-up, which later became known as anabolic processes, were linked directly to the metabolic rate, which was assumed to follow the surface law. The processes of break-down, now known as catabolic processes, were assumed to proceed at a constant rate per unit of volume. Volume was thought to be proportional to weight; the growth rate then results from a weighted difference between surface area and volume. Pütter took the rate, that later became known as the von Bertalanffy growth rate, inversely proportional to ultimate length on the basis of a toxicity argument, see Section 2.4 of these comments. More data were generated with improved methods of measurement; invertebrates were also covered. Krogh [808] was the first in

1916 to fit general allometric curves to respiration as function of body weight, i.e. one of the type $y = \alpha x^{\beta}$, where y is a variable dependent on another variable x. Kleiber [725] found in 1932 that metabolic rates are proportional to weight to the power 0.75 and this became known as Kleiber's law. Extensive studies undertaken by Brody [192] confirmed this proportionality. Von Bertalanffy [125] saw anabolic and catabolic rates as special cases of the allometric relationship. He viewed this as a simplified approximation that could be applied to almost all types of metabolic rates, including the anabolic and the catabolic, but the constant β varies somewhat with the tissue, physiological conditions and experimental procedure. The growth curve proved to be rather insensitive to changes in β for catabolism, so, like Pütter, von Bertalanffy took the value one and classified species on the basis of the value for β of anabolism. The surface law was just one of the possibilities for von Bertalanffy.

Although von Bertalanffy [124] was the genius behind the ideas of general systems theory, he never included the feeding process in his ideas about growth. I do not know why, because mass balance equations are now always bracketed together with dynamic systems. I think that the use of allometric equations, which is a step away from mechanistic explanations towards meaningless empirical regressions, obstructs new ideas in metabolic control. The idea of allometry goes back to Snell [1337] in 1891 and, following the work of Huxley [642], it became widely known. Both Huxley and von Bertalanffy were well aware of the problems connected with allometric equations, and used them as first approximations. Now, a century later, it is hard to find a study that involves body size and does not use them.

The von Bertalanffy growth rate as function of ultimate length works out in the same way inter- and intra-specifically (for larger body sizes, see below), as does the respiration rate as function of body weight (approximately). These two facts might have contributed to the omission to distinguish between these two very different ways of comparison in the quest for broad patterns that characterises that period; an omission that did send the whole field into a Gordian knot for more than a century. Zeuthen [1575] was the first to point to the necessity of distinguishing between size differences within a species and between species, but these wise words did not land.

The condition index (weight over cubed length) was proposed by Heincke in 1908 [582] in the context of fisheries research. Since then, this index is widely used in animal ecology. It is key to the weak homeostasis of DEB theory, which fully specifies reserve mobilisation.

11.1 Metabolic Theory of Ecology

The problem of the scaling of respiration is still discussed actively [740, 7, 567] and many explanations have been suggested, such as the minimization of transport costs in fractally branching tube-systems assuming that all individuals have equal blood flow in their capillaries [1516]. The fact that only a minute fraction of the species have a closed circulatory system (and so capillaries) and the assumption that the flow in the main veins equals that in the capillaries (while in fact it differs by several orders of magnitude) are just two arguments from a list that renders this line of thinking unproductive [952, 34, 1342]. On top of

that, Brown himself exposed inconsistencies in their model assumptions [77], generalised it and concluded that all scaling exponents between 2/3 and 1 could be understood from the structural design of distributing networks. The central argument is that sites that need maintenance are connected by tubes that don't need it, and the larger the size, the large the relative mass of tubes. Empirical evidence does not support this view (whale biomass does not consist mainly of tubes, as is very well known in Japan), and it is not clear why these tubes, i.e. living tissue, would not require maintenance. Mysteriously enough, the explanation does not seem to apply to embryos in eggs, which initially hardly respire. Capillaries still playing a key-role in e.g. bird eggs. The fact that capillaries are found in demand systems that sport high peak over standard metabolic rate ratios, see Section 1.2.5, and distribution networks have to deal with peak metabolic rates, questions to what extent the design of these networks constrains standard metabolic rates. Demand systems need closed circulatory systems for peaking their metabolism; a higher hart beat directly results in an increased transport near all cells. The effect of increasing hart beat in open circulatory systems on transport at the periphery is much less. West et al [1516] suggested in error that branching tubing systems are really wide-spread and were fussy about what is transported in what systems for what function. They mentioned tracheal tubes in insects, but these tubes cannot branch because the inner lining is attached to the moult; this moulting system would be impossible with branched tubes. They even mentioned micro-organisms, but branching systems in micro-organisms still need to be discovered; the endoplasmatic reticulum is organised very differently from blood circulation systems and has no pump. The hart-beat of organisms has a complex relationship with body size [258], which makes it unlikely that minimisation of transport costs result in a 3/4-scaling. Encrusting bryozoans respire proportional to weight$^{0.5}$ [1526], as correctly predicted by DEB theory, see Section 4.2.4 of the comments. So there is no fundamental reason why the range of exponents is between 2/3 and 1. Embryos in eggs reduce weight over time combined with an increase in respiration. They clearly demonstrate that explanations for respiration should not focus on values of scaling exponents at all; the use of allometric regression should cease.

The West-Brown-Enquist (WBE) model [1517] used a very different argument to arrive at the 3/4-scaling for plants; plants would consist of a bundle of (non-branching) capillaries that would taper in a very special way towards the top and the minimisation of transport costs would lead to the scaling relationship. Such tapering has never been documented empirically. What is transported from where to where and how that relates to respiration remains unclear (including the definition of respiration itself). Price [1131] changed the argument, but confusingly still calls it the WBE-model. Respiration would be proportional to the number of petioles that are located at the tips of a fractally branching tubing network, similar to animals. The sum of the surface areas of the cross-sections remains constant, as well as the sum of the volumes of spheres of a diameter that equals the length of a branch, for each branching level. The first argument gives a constant flow rate through all branch levels, the second argument is not given further motivation. This review paper is silent about roots, both in terms of weight and contribution to respiration. This description of shape does not do right to the actual morphology and morphological diversity of plants. Many plant families have both trees and herbs. Wood is a product that does not respire

but in this respiration-weight relationship dominates weight. It is really doubtful that the 3/4-relationship applies to trees, where wood is included in the weight; no data are known.

All the many attempts to explain Keiber's 3/4-rule for respiration implicitly or explicitly consider respiration as THE key process behind metabolism. Once we would understand that, we understand it all. This idea is also behind the allometric patterns collected by Peters [1089] where all scaling exponents are compared with value 3/4. Respiration is typically identified with THE metabolic rate, where heat or CO_2 production or O_2 consumption are all considered as equivalent. One only has to think of organisms living in anearobic environments to realise that only entropy production can possibly quantify metabolic rate. One needs DEB theory (or an equivalent alternative theory that fully species all energy fluxes, but see Section 11.4 of these comments), however, to quantify entropy of living systems. Section 4.8.1 discusses that one first needs energy balances to obtain entropy balances, and for energy balances one needs mass balances. So one has to know quite a bit about the studied system to quantify entropy production. Many workers identify respiration of resting individuals with maintenance. DEB theory shows that respiration cannot be identified with maintenance and that biomass cannot be treated as a single variable and that respiration does and will not explain all metabolism. Section 4.4.1 shows that if heat or CO_2 production and O_2 consumption would be all proportional to each other, strong constraints on biomass composition would apply that lack empirical support. Reproduction, for instance, can be a substantial energy flux that hardly contributes to respiration, since reproduction concerns the export of reserve. The conversion of food into that reserve might have occurs quite some time before the respiration measurement. Respiration has contributions from several interacting processes and this interaction comes with the need to study all contributing processes simultaneously. In a DEB context, it makes no sense to study growth, but not food uptake or reproduction or maturation. Likewise, it makes no sense to study ageing or effects of chemical compounds without studying energetics. Some workers complain about the many parameters the standard DEB model would have [1585], but the number of parameters *per process* is really small (one or two). (Zuo et al [1585] state that the DEB model would have 17 variables; they just counted the number of entries in a symbol table in [1340].) The basic difference with alternative metabolic studies is that DEB theory studies all processes simultaneously, and others do it one by one, ignoring the interactions.

West et al [1518] proposed a growth model on the basis of the explanation for respiration, which became together with the Arrhenius relationship for temperature dependence, the pillars of the popular metabolic theory of ecology (MTE) [206]. Growth is taken to be a function of size only, and parameters depend on temperature. The embryo stage is ignored as well as reproduction or maturation (despite its name 'ontogentic growth model'). I don't see how an individual can grow incrementally while keeping the diameter and the flux in its capillaries constant and maintaining a fractally branching tubing transport system (it can only grow with jumps of a constant factor and has to restructure its transport system with each jump). The model ignores the huge body of empirical evidence that growth depends on food. This model also suffers from the absence of growth overheads, as pointed out in [952], which was later 'repaired' by including overheads only [630], but not the costs for new tissue [953]. The model was supported empirically by the argument that normalized

growth has a maximum at relative mass of 0.316, which is realistic for growth at abundant food, but Sousa et al [1342] correctly pointed out that this cannot be distinguished from the value 0.296 that results for von Bertalanffy growth at abundant food. Growth applies to a specific individual, while the respiration argument of [1516] does not distinguish between intra- and inter-specific comparisons. This discrepancy causes fundamental methodological problems that cannot be repaired. I fully agree with Zeuthen [1575] that all explanations of respiration that fail to distinguish between intra- and inter-specific comparisons are bound to fail, including all constructs that build on such explanations.

The recent growth model by Sibly et al. [1302] suffers from the same problem: growth is independent of food and the model does not specify what happens if food availability is not enough for the needs; reproduction is not specified. It has reserve, which somehow solves problems in case of starvation, but in some miraculous way it does not contribute to body weight and its dynamics is not specified. Although Sibly's motivation to develop an alternative for the standard DEB model was to simplify it, his model has more parameters. An even more fundamental problem of both these and other MTE-based growth models is that they start with the observation that respiration is an allometric function of weight. This idea cannot be combined with the notion that respiration has additive contributions from underlying processes, such as maintenance, growth overheads and specific dynamic action. These additive terms simply don't add up to an allometric function of body mass, especially because growth is fast in neonates but ceases later on in the life cycle. All such models have a problem with relating respiration to other metabolic activities of the individual, and cannot respect energy balances. Later Sibly et al realised that the von Bertalanffy growth model is incompatible with respiration scaling with weight$^{3/4}$ [1300], and argued that fish biologists should have filed parameters of the 'ontogenetic' growth model for that link. This is incorrect for two reasons, first DEB theory demonstrates that they are compatible (but one needs reserve for that), second the 'ontogenetic' growth model is incompatible with the scaling of respiration, as explained. Still later, Sibly and Brown proposed yet another growth model [1301], but it suffers from basic dimension errors and, therefore, does not count as a model.

Sibly et al were surprised that the von Bertalanffy growth rate turned out to scale with weight$^{-1/3}$ intra-specifically (in rayfinned fish), although the inventor of that statistic, August Pütter [1139], already pointed that out some 95 years ago, and he even presented a mechanism for that; see section 2.4 of these comments. They were also surprised to find that the von Bertalanffy growth rate turned out to scale with weight$^{-0.23}$ inter-specifically (in rayfinned fish). Yet they did not fit any data and just took reported values in Fishbase at 30 September 2014 and produced log-log plots. If they would have done this, they would have discovered that the von Bertalanffy growth curve does not fit well at all for accelerating species, section see 7.8.2 of these comments, and many rayfinned fish species do accelerate as shown by the add_my_pet collection. This is why fish biologists fit the Gompertz curve to the early stages of these fish species. The DEB explanation for why the von Bertalanffy growth rate seems to scale with weight$^{-0.23}$, rather than weight$^{-1/3}$ inter-specifically directly follows from [775, (8.5)], which shows that the von Bertalanffy growth rate is not an allometric function of body weight and the deviation builds up for decreasing body sizes.

The κ-rule was criticized by Johnston et al [669] as being at odds with the principles of physiological ecology, that state that growth and reproduction compete in terms of energy allocation. This is a misunderstanding of the κ-rule. Since DEB theory respects energy conservation, energy allocated to growth is not allocated to reproduction and vice verse. So these targets do compete, also in DEB theory. As explained in [859], it is always possible in models where food is first converted to reserve and reserve is mobilised for use in metabolism, to write allocation to growth plus somatic maintenance as fraction of mobilised reserve. This itself does not pose any restrictions. The simplifying assumption that κ is constant obviously does pose restrictions. We did find evidence for cases where κ did change temporarily, see [1002]. Changes in κ do not give theoretical complications in DEB theory, but it complicates applications. Section 5.3.2 on dynamic generalisations of the κ-rule discusses the interactive control of κ, which is necessary to understand particular details of allocation to body parts. Subsection 2.4 of the comments discusses arguments and empirical evidence for why a constant κ is generally a reasonable simplifying assumption. The mean relative error of 0.07 for DEB models applied to over 2000 animal species in the AmP collection further supports this. The explanation that the κ-rule provides for the waste-to-hurry phenomenon that emerged from the AmP collection is possibly the strongest argument in favor of a constant κ.

The default parameter value for the reproduction efficiency $\kappa_R = 0.95$ was criticized by Ginther et al [492], especially for mammals. They conclude that almost all allocation to mammal reproduction is lost in overheads, where DEB theory would assume trivial losses. They illustrate their claims by comparing pregnant sheep with non-pregnant ones, see Fig. 11.1. Several things went wrong here; the evaluation of reproduction efficiency cannot do without a model for embryos. They misunderstood that κ_R quantifies the conversion efficiency from the reproduction buffer to embryo reserve. This efficiency is high, because it only includes the wrapping of reserve into an egg; while the chemical composition of the reproduction buffer is very similar to the initial egg content. Foetal development is very similar to egg development, and some fish genera have species with aplancental oviviparous as well as placental viviparous development. Ginther et al 'stylised' the heat trajectory to a linear increase since copulation, and say it "was well supported by our data and was conservative". Fig. 11.1 shows that their claims are simply flawed and they must have known this. It turned out that the data source Brockway et al [191] used a 50 kg ewe, while AmP parameters result in a heat production that is a bit lower than the Brockway et al one and the ultimate weight of the AmP ewe is 86 kg (which might be the reason); the figure also shows foetal values that are corrected for this difference in ewe values. Notice that the DEB predictions are based on the AmP data for sheep, not on the presented heat data, and that they do not depend on the criticized parameter κ_R. The difference between DEB predictions and Brockway's data might be due to a difference in race of sheep; the mean relative error of predictions for the AmP entry is 0.04, which has both pre-natal and post-natal development. The integrated costs for reproduction overheads is 252 MJ for Ginther et al method, while 60.5 MJ was measured, and the DEB predictions amount to 64.6 MJ, or 79.4 MJ. So the DEB-based indirect costs are almost spot on (especially when the negative parts in the empirical trajectory are excluded), and Ginther's predictions were not. When they were pointed to this mismatch (see e-letter published with [492]), they simply waved

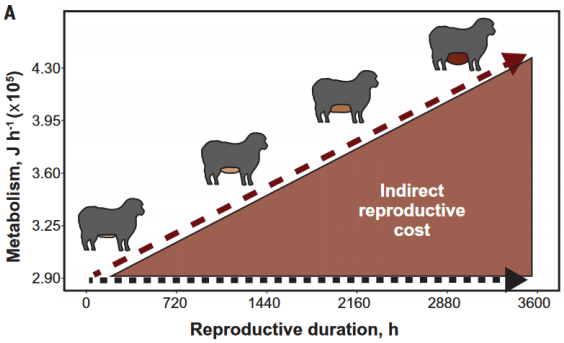

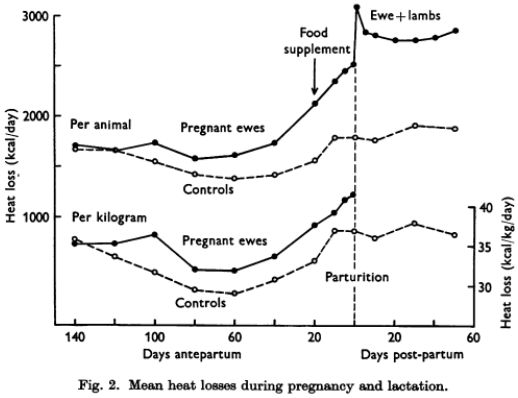

Fig. 2. Mean heat losses during pregnancy and lactation.

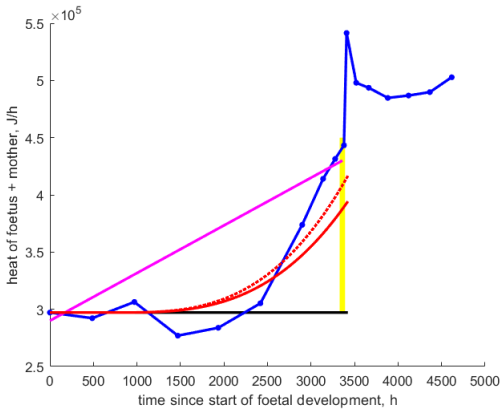

Figure 11.1: Upper left: Heat dissipation in a pregnant, *Ovis aries*, according to Ginther et al [492] as published in Science 2024. They 'stylised' the heat trajectory into a linear increase, using the upper right figure as data source from Brockway et al 1963 [191], which mentiones that it was a 50 kg ewe. Left: The same according to DEB theory (red), using the parameter values of the AmP collection, with the source data of Brockway (blue) and the 'stylised' tractory of Ginther (magenta). The AmP ewe has an ultimate weight of 86 kg and at 50 kg it generates 0.242 MJ/h, while the Brockway ewe generates 0.297 MJ/h. The red stippled curve 'corrects' the DEB predictions for the difference. Birth is indicated by the yellow line. Ginther arrives at the estimate $3600 \times (4.3e5 - 2.9e5)/2 = 252$ MJ for the indirect costs of reproduction, the measured costs are 60.5 MJ, while the DEB equivalent is 64.6 MJ and corrected 79.4 MJ.

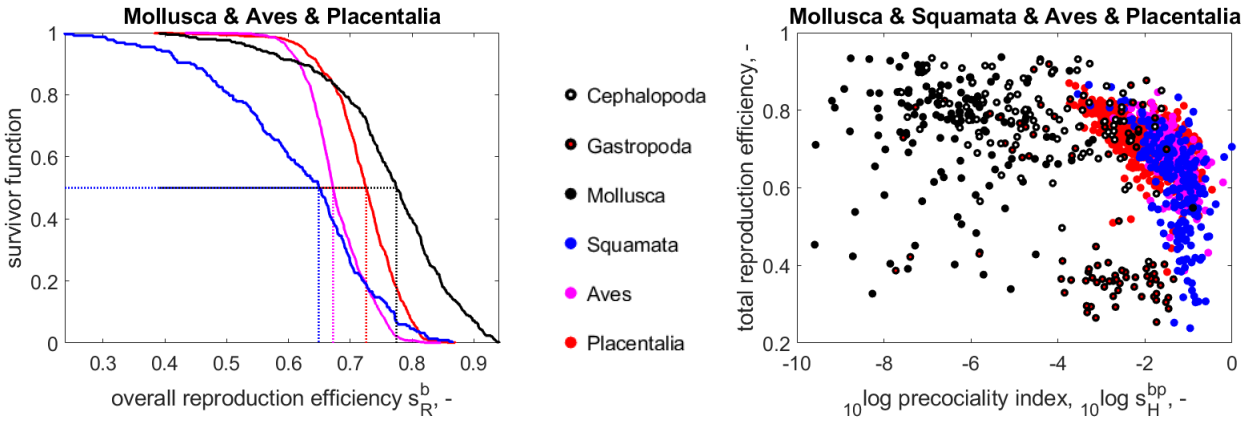

Figure 11.2: The overall reproduction efficiency $s_R^b = L_b^3([M_V]\mu_V + [E_m])\kappa_R/E_0$ for the molluscs, squamates, birds and mammals in the AmP collection. The deviating behaviour of the molluscs is caused by the many simultaneous hermaphrodites. They lay very small eggs, so suffer less from embryonic maintenance costs, and pay the bill after birth, where the multi-million offspring reduces to 1 or 2 during the life time of the mother (which can differ from less than a year to centuries).

Figure 11.3: The overall reproduction efficiency as function of the precociality index $s_H^{bp} = E_H^b/E_H^p$ for the same taxa. The cephalopods have a high overall reproduction efficiency and the gastropods a low one, but no clear link was found for them with the precociality index. Very unlike the three vertebrate taxa, where the overall reproduction efficiency decreases sharply for increasing precociality index.

it away with the remark that a non-linear increase in heat production did not improve the fit significantly above a linear one; they did not specify the assumptions made in this statistical testing. The rest of their rebuttal is an accumulation of misunderstandings of DEB theory and of metabolic costs, which resulted from the lack of a modeling framework in their analysis. By including the embryo development overheads, as Ginther et al do in their assessment, it seems that they actually aim at a overall efficiency measure, which would be $L_b^3([M_V]\mu_V + [E_m])\kappa_R/E_0$, where E_0/κ_R is the investment into a single offspring and $L_b^3[M_V]\mu_V$ is fixed in structure at birth and $L_b^3[E_m]$ in reserve, both at abundant food. The embryo overheads include somatic and maturity maintenance, growth overheads and maturation. If the step from food is included, the total efficiency should be multiplied by the digestion efficiency κ_X (typical range 0.1-0.8), which obviously depends on the type of food. Total foetal weight is about twice the actual foetal weight in mammals, where fluids that surround the foetus, the placenta, the increased uterus and milk accumulation (in the later stages of the pregnancy) contribute to the extra weight. Most of the fluids become lost, the increased uterus shrinks after birth, and the placenta is typically eaten by the mother; the latter two factors recover part of the costs. Milk production is typically paid via up-regulation of assimilation. These complications modify the total efficiency a bit. In their discussion of life history and evolutionary implications, they ignore that males also allocate to reproduction, with a comparable intensity relative to females, but hardly anything of this investment ends up in offspring tissue. Quite a few species are simultaneous hermaphrodites; the AmP collection takes this into account by halving the

value for κ_R.

Fig. 11.2 shows that the overall reproduction efficiency ranges from 0.65 to 0.75, based on assimilation energy (not food energy). Many species sport absorption of eggs, and/or canabalism among siblings, which reduces efficiency, as discussed in [52] for the Greenland shark. Fig. 11.3 shows that the reproduction efficiency decreases sharply for increasing precociality index for tetrapods. This is in part because energy allocated to maturity dissipates. Another reason is that more cumulative maintenance is paid in precocial species because they have relatively large offspring with a correspondingly long development time. The relationship was not found for molluscs, which have tiny altricial offspring.

As I see it, DEB theory is a very simple theory for a very complex network of interactive processes that together define how an individual develops from starting egg cell to death my aging in interaction with its environment. My personal surprise as biologist is not to find deviations from predictions in some cases, but that these simplistic assumptions generally do a great job in practice. This means that DEB theory meets to fine balance of accommodating the huge biodiversity and still has the required simplicity to allow practical applications. An exciting application of the theory is in its support to understand cases where the theory does not seem to work. When Barneche et al [81], for instance, conclude that present theories (including DEB theory) fail to match their empirical finding that fish fecundity scales hyperallometrically with body weight in field data, my first reaction is: DEB theory only gives hypoallometric predictions if you assume that food density is constant. Since fish grow from tiny fry to much larger sizes, they change food selection while growing. It is easy to get hyperallometric relationships with slightly more complex scenarios for food availability. This type of mismatch is not due to the structure of the theory in the first place, but to the simplifying assumptions about the environment. See also [700].

11.1 Criteria for general models

Table 11.1 presents criteria for general explanatory models for the energetics of individuals.

Models implied by DEB theory meet all 6 criteria for being general and explanatory.

ad 1 The theory consists of a list of coherent and consistent assumptions, as summarised in Table 2.4 for the standard DEB model. Practical applications require the derivation of specific mathematical models from these assumptions. Originally I thought that these assumptions could easily be replaced by others in the process of testing the implications against experimental data. Later it turned out difficult, if not impossible, to replace any of them without creating inconsistencies. This points to the possible existence of a smaller set of deeper assumptions, from which these assumptions follow. Many parts of the theory were originally more complex. As is typical in science, simplicity does not come naturally, but must be acquired with hard work.

ad 2 DEB theory has an explanation for each of the empirical stylized facts as presented in Table 11.2, Section see 11.1 of the comments. Table 11.1 gives an overview of the many empirical models that turn out to be special cases of DEB models, or very

Table 11.1: Criteria for general explanatory models for the energetics of individuals, modified from Sousa et al. [1341].

1	The models must be based on explicit assumptions that are consistent with physics and (geo)chemistry.
2	The assumptions should be consistent in terms of logic, but also with empirical patterns; see Table 11.2.
3	The taxa to which the model applies should be delineated by explicit criteria.
4	Different models for the various taxa should be consistent with an explicit evolutionary scenario.
5	The assumptions should cover the full life cycle of the individual, from initiation of development to death, and quantify all possible uses of substrates (to allow mass and energy balancing).
6	The predictions should be testable in practice, which typically constrains its maximum complexity substantially (quantified in terms of number of variables and parameters).

good numerical approximations; the list continued to grow over the years. Many of them are quite old and together they concern very different aspects of life; none of the original authors could be aware of the coherence of these empirical models. This in itself is for me already a most rewarding side-result of DEB theory. DEB theory reveals how they all follow from simple physical and chemical phenomena; this helps to understand under what conditions these models will probably not work that well. Each of these models was created because it described experimental data well. Using all this evidence, and the results of some 200 man-year of research by the group working on DEB theory, I dare to state that, at present, DEB theory is the best tested quantitative theory in biology.

ad 3 DEB theory deals with all organisms, i.e. micro-organisms, animals and plants. It is not only biologically but also chemically implicit; species and compounds only receive names in applications DEB theory meets the objective restriction criterium by including all taxa. The standard DEB model, which deals with isomorphs with one reserve and one structure feeing on one type of food, is supposed to apply to animals, i.e. organisms that feed on other organisms; micro-algae need several reserves, plants also need two structures (roots and shoots).

ad 4 An explicit evolutionary scenario has been worked out for the models of DEB theory. The applicability to all species restricts the possible structure of DEB theory substantially, because we know that most organisms evolved from the merging of ancestors. Think for instance of mitochondria and chloroplasts that once had an independent existence, and of the many symbioses (e.g. corals) that exist. The constraint that two taxa follow some set of energetic rules, and the merged taxon again follows the same set of rules restricts how this set of rules can potentially look like; see the discussion on partitionability and mergeability of reserve dynamics.

ad 5 DEB theory specifies the fluxes of all chemical compounds, using conservation laws for chemical elements (and their isotopes). It also exploits the conservation of energy and time and uses the state variable maturity to trigger qualitative changes in metabolism, and reserve to explain why embryos can grow (i.e. increase structure) without feeding.

ad 6 The core theory deals with the logic of quantitative aspects of metabolic organisation; the set-up has not been constrained by the necessity to test against experimental data. It turned out that quantities that play key roles in DEB theory (maturity, reserve(s), structure(s)) cannot be measured directly, only indirectly. This calls for elaborate auxiliary theory to relate DEB quantities to quantities that can be measured (lengths, weights, composition, performance in various situations). This auxiliary theory relates sets of different types of measurements to sets of several DEB quantities.

11.1 Empirical evidence

Table 11.2 presents (stylized) empirical facts, and Tables 11.3 and 11.4 show how DEB theory explains these facts. The patterns are used to test topological alternatives for the standard DEB model in Table 11.5, see Section 11.3 of the comments.

11.2 Number of free protons

The derivation of the probability distribution of the number of free protons is as follows. We can safely neglect the decrease of the number of water molecules, say N, due to dissociation. If $P_n(t)$ denotes the probability that the number of protons at time t equals n, we have for $n = 1, 2, \cdots$

$$\begin{aligned} P_n(t+\Delta t) &= k_2(n+1)^2\,\Delta t\,P_{n+1}(t) + k_1 C\,\Delta t\,P_{n-1}(t) + \\ &\quad + [1-(k_2 n^2 + k_1 C)\,\Delta t]P_n(t) + o(\Delta t) \end{aligned} \tag{11.1}$$

where $o(\Delta t)$ refers to the probability that more than one event (i.e. dissociation or binding) occurs during a time increment Δt. If we bring the term $P_n(t)$ to the left, divide by Δt and let Δt approach to zero, we arrive at

$$P_n'(t) = k_2(n+1)^2 P_{n+1}(t) + k_1 C P_{n-1}(t) - (k_2 n^2 + k_1 C)P_n(t) \tag{11.2}$$

where $P_n'(t)$ denotes the derivative of $P_n(t)$ with respect to the time. For $n = 0$ we have

$$P_0(t+\Delta t) = k_2\,\Delta t\,P_1(t) + [1 - k_1 C\,\Delta t]P_0(t) + o(\Delta t) \tag{11.3}$$

and so

$$P_0'(t) = k_2 P_1(t) - k_1 C\,\Delta t\,P_0(t) \tag{11.4}$$

Table 11.2: Stylized and empirical facts, modified from Sousa et al. [1340]

Feeding

F1 Many species (almost all animals and plants) have an embryo stage that does not feed

F2 During starvation, organisms are able to reproduce, grow and survive for some time

F3 At abundant food, the feeding rate is at some maximum, independent of food density

Growth

G1 Growth of isomorphic organisms at abundant food is well described by the von Bertalanffy; at constant food density, no substantial shrinking occurs independent of ageing

G2 The inverse von Bertalanffy growth rate increases linearly with ultimate length both intra-specifically (or different constant food levels) and inter-specifically for large body sizes

G3 Foetuses increase in weight approximately proportional to cubed time

Reproduction

R1 Many species (almost all animals and plants) have a juvenile stage that does not reproduce

R2 Reproduction increases with size intra-specifically, but decreases with size inter-specifically

R3 A range of constant low food levels exists at which an individual can survive, but not reproduce

R4 Growth can be simultaneous with reproduction, but growth can also cease long before reproduction is initiated

R5 Allocation to reproduction can continue during starvation

Respiration

O1 Animal eggs and plant seeds initially hardly use dioxygen

O2 The use of dioxygen increases with decreasing mass in embryos and increases with mass in juveniles and adults

O3 The use of dioxygen by isomorphs scales approximately with body weight raised to a power close to 0.75

O4 Animals show a transient increase in metabolic rate after ingesting food (heat increment of feeding)

Stoichiometry

S1 The chemical composition of organisms depends on the nutritional status (starved vs well-fed)

S2 The chemical composition of organisms at constant food density becomes constant during growth

Energy

E1 Some energy always dissipates, also in absence of dioxygen

E2 Dissipating heat for heterotrophic isomorphs under aerobic conditions is a weighted sum of three mass flows: carbon dioxide, dioxygen and nitrogenous waste

Ageing

A1 Mean life span typically increases inter-specifically with maximum body length in endotherms, but hardly depends on body length in ectotherms

A2 Survivor curves for life span terminated by ageing are typically well described by the Weibull and Gompertz models

Table 11.3: Explanations for the stylized facts listed in Table 11.2 as offered by DEB theory; see also Table 11.4.

F1 The embryo is considered as a non-feeding juvenile that starts its development with zero maturity and structure and an amount of reserve such that the reserve density at birth equals that of the mother at egg formation, see Subsection 2.6.2.

F2 Growth and reproduction are fuelled by mobilised reserve, not by feeding directly. Death by starvation occurs if shrinking of structure exceeds a threshold or when rejuvenation progresses, see Subsection 4.1.4 of the book and Subsections 4.1.5 and 4.1.5 of the comments.

F3 Feeding is at maximum if all time is allocated to the processing of food, see Section 2.1.

G1 The von Bertalannfy growth model is a special case of the standard DEB model, see Subsection 2.6.1.

G2 As August Pütter already noted, see Section 2.4 of the comments, the inverse von Bertalanffy growth rate increases linearly in ultimate length. This is implied by DEB theory, see Subsection 2.6.1, and is an important argument for why the allocation fraction κ to soma remains constant during development, see Section 2.4 of the comments. The von Bertalanffy growth rate of different species decreases almost linearly with the maximum body length due to the increase of the (maximum) reserve capacity, see Subsection 8.2.2.

G3 Huggett and Widdas (1951) already observed that foetuses increase in weight approximately proportional to cubed time, see Table 11.1; Their model is a special case of the standard DEB model, see Subsection 2.6.2.

R1 Allocation to reproduction is initiated when maturity reaches the puberty threshold, see Subsection 2.5.2.

R2 Reproduction increases intra-specifically between a squared and a cubed length, see Section 2.7, but inter-specifically it decreases approximately proportional to length, see Subsection 8.2.2.

R3 Due to the existence of maturity maintenance, individuals can survive, but not reproduce, in a certain range of low food densities, see Subsection 2.5.3 of the comments. Figure 9.13 of the DEB book beautifully demonstrates this. Moreover, if maturity maintenance would not exist, the supply stress would be zero for all species and they cannot be ranked in a supply-demand spectrum. See Subsection 10.5.5.

R4 At constant food, reproduction increases with length, see Section 2.7. Growth is competing with somatic maintenance, reproduction with maturity maintenance; both are parallel processes, due to the κ-rule for allocation, see Section 2.4.

Table 11.4: Table 11.3 continued.

O1 Since only structure requires somatic maintenance and the embryo starts at zero structure, it initially hardly use dioxygen, see Section 2.6.2.

O2 The use of dioxygen increases with decreasing mass in embryos because it looses (dry)mass (namely reserve) during development, while its structure is growing, see Section 2.6.2. Respiration increases with mass in juveniles and adults because reserve density remains constant at constant food, due to the assumption of weak homeostasis, see Subsection 1.2.2, and their increasing structure requires maintenance.

O3 The weight-specific use of dioxygen decreases during the life cycle because investment in growth decreases (and growth-overheads contribute to respiration), see Section 4.4. Fully grown adults of different species have a reserve density that increases with maximum length, see Section 8.2.2, while only structure requires maintenance.

O4 The conversion cost from food to reserve is paid from food, see Subsection 4.4.2 and Subsection 2.5.1 of the comments.

S1 The chemical composition of reserve and structure can differ, and reserve density depends on the nutritional status, see Section 2.3, the chemical composition of the body can vary.

S2 Due to the weak homeostasis assumption, see Section 1.2.2, the chemical composition of organisms at constant food density becomes constant during growth.

E1 The delineation of an explicit dissipating flux, see Section 2.5, and overhead costs in all transformations ensure that some energy is always dissipating; the flux of dioxygen is obtained from the oxygen balance, heat from the energy balance, see Subsection 4.3.1 and Sections 4.4 and 4.8.

E2 The method of indirect calorimetry by Lavoisier 1780, see Table 11.1, assumes that dissipating heat is a weighted sum of the fluxes of carbon dioxide, dioxygen and nitrogenous waste. This is a special case of the standard DEB model, see Subsection 4.8.2.

A1 If the Gompertz stress coefficient is close to zero, as holds for most ectotherms, life span hardly depends on maximum body size, but if it is positive, as is typical for endotherms, it increases with maximum length, see Section 6.1 and Subsection 8.2.2.

A2 Both the Weibull and the Gompertz models are special cases of the DEB module for ageing, see Section 6.1.

which is a special case of (11.2) when we make the appointment that $P_{-1}(t) = 0$. So, (11.2) represents the stochastic model for the number of 'free' protons.

By comparison, the corresponding deterministic model would be

$$n'(t) = k_1 C - k_2 n^2(t)$$

Separation of variables and integration gives

$$\frac{n(t) - m}{n(t) + m} = \frac{n(0) - m}{n(0) + m} e^{-t/\tau},$$

where m denotes the equilibrium number of 'free' protons in the deterministic model, which is given by $m = \sqrt{Ck_1/k_2}$, and τ the relaxation time, which is given by $\tau = 1/\sqrt{4Ck_1k_2}$. At 25°C, $k_1 = 2.4\,10^{-5}\,\mathrm{s}^{-1}$ and $k_2 = 10^3\,\mathrm{ion}^{-1}\,\mathrm{s}^{-1}$ (in ice, k_2 is faster!). This gives a relaxation time of some 36 μs.

We now continue with a further analysis of the stochastic model. As long as we are interested in processes with relaxation times much longer than 36 μs, we can confine ourselves to the limiting probability distribution of n for large t, where we have that $P_n'(\infty) = 0$. When we divide by k_2, call $Ck_1/k_2 = m^2$, as before, and abbreviate $P_n(\infty)$ to P_n, (11.2) reduces in the limit to

$$(n+1)^2 P_{n+1} + m^2 P_{n-1} - (n^2 + m^2) P_n = 0 \tag{11.5}$$

Starting with $P_1 = m^2 P_0$, and using (11.5) in the form

$$P_{n+1} = \left((n^2 + m^2) P_n - m^2 P_{n-1}\right)(n+1)^{-2},$$

we find by induction that $P_n = (m^n/n!)^2 P_0$. This relation determines the probabilities up to an arbitrary factor. Obviously, we must have that $\sum_{n=0}^{\infty} P_n = 1$. The series $I_0(x) = \sum_{i=0}^{\infty} (x/2)^{2i} (i!)^{-2}$ is well known as the modified Bessel function. So $\sum_{n=0}^{\infty} (m^n/n!)^2 = I_0(2m)$. We therefore arrive at

$$P_n = (m^n/n!)^2 I_0^{-1}(2m) \tag{11.6}$$

This probability distribution relates to the Poisson distribution by just squaring the Poisson probabilities and renormalizing to assure that the sum of the probabilities remains 1. The normalizing constant $I_0^{-1}(2m)$ in (11.6) compares with e^{-m} in the Poisson distribution.

Since $I_0'(x) = (2/x) \sum_{i=0}^{\infty} i (x/2)^{2i} (i!)^{-2}$, so $\sum_{n=0}^{\infty} n (m^n/n!)^2 = m I_0'(2m)$, the expected number of protons equals $\mu = m I_0'(2m)/I_0(2m)$. This is lower than the value m, which should be expected on the basis of the deterministic model. This is obvious when we obtain the variance by summing (11.5) for $n = -1, 0, 1, \cdots$. It is found to be $\sigma^2 = m^2 - \mu^2 = m^2 \left(1 - (I_0'(2m)/I_0(2m))^2\right)$. Although it is less than the variance of a Poisson distribution with the same mean it is still considerable for small m.

The lifetime of a randomly selected water molecule, a hydroxylion and a hydronium ion follow an exponential distribution with mean k_1^{-1}, i.e. some $4.16\,10^4\,\mathrm{s} = 11.55\,\mathrm{h}$, for water and k_2^{-1}, i.e. some $10^{-3}\,\mathrm{s}$, for both ions at 25°C. Diffusion causes these particles to displace

in time, t, over a mean distance of $\sqrt{2Dt}$, where D denotes the diffusion coefficient. For H_2O, OH^- and H^+, the latter is 2.26, 5.3 resp. $9.31\,10^{-5}\,cm^2s^{-1}$ at 25°C. The mean total lifetime displacement in an unbounded body of pure water is thus 1.37 cm, 3.26 μm and 4.32 μm, as a crow flies. This means that the limited size of a cell is likely to influence the transport, even apart from influences exercised by, e.g. the membrane.

11.3 Basal Metabolic Rate

Ricklefs *et al* [1187] partition the energy budget (in Joules per day) into the following modules

BMR Basal metabolic rate: the rate of energy metabolism of a non-growing individual ($\dot{p}_G = 0$) at rest under post-absorptive conditions ($\dot{p}_A = 0$) in a thermo-neutral environment ($\dot{p}_T = 0$).

DEE Daily energy expenditure: the rate of energy metabolism of an active individual. DEE = FMR (Field Metabolic Rate) when measured on free-living animals.

ACT Activity metabolism: ACT = DEE − BMR metabolic expenditures for activity.

As a rule of thump, they suggest that DEE $\simeq$ 4 BMR in birds and mammals, but the factor varies between 2 and 7. They found no correlation between DEE and BMR in 28 species of birds, but a strong correlation in 15 species of mammals. In an attempt to explain these differences they propose a (conceptual) 'shared pathway model', where the high rates in active individuals replace those of a passive one (leading to absence of correlation between DEE and BMR) and a 'partitioned pathway model', where activity is added to BMR (leading to positive correlations). All this concerns inter-specific comparisons.

BMR is not easy to address in a DEB context; allocations to maturation and/or reproduction need to be considered. Digestion can continue long after feeding is ceased, shrinking and rejuvenation can occur if digestion is ceased for too long. The growth period in birds is typically shorter than that in mammals, relative to the life span. Since growth is asymptotic and contributions from growth can affect the results (even if actual growth per day is negligibly small). Fully grown individuals can suffer from ageing, which typically reduces metabolic rates (quantified as effects of damage compounds on parameter values). Last but not least, differences in nutritional conditions can easily dominate the results. DEE is typically measured using the method of double labelled water, which makes strong assumptions. Inter-species comparisons involve variations in parameter values among species, which can easily obscure the more subtle patterns in budgets.

11.4 Topological alternatives

Apart from production and assimilation models, intermediate models can be formulated, as well as models of a different type. Lika and Kooijman [859] delineate the following classes of models that are topological alternatives of the standard DEB model

4 κ-models have branching first (κ stands for partitioning of energy fluxes). The lower left index refers to the branch of E, lower right to the branch of S (0 indicates S before E), and upper right to the branch of J (1 indicates J after E).

4 A-models have E first as destination of assimilates (A stands for assimilation). The lower right index refers to the branch of S, upper right to the branch of J.

3 P-models have allocation to $S+J$ first (P stands for production). The lower left index refers to the branch of E.

5 S-models have allocation to S first (S stands for somatic maintenance). The lower left index refers to the branch of E and upper right to the branch of J (0 and 1 indicate J before and after E).

5 J-models have allocation to J first (J stands for maturity maintenance). The lower left index refers to the branch of E and lower right to the branch of S (0 and 1 indicate S before and after E).

The standard DEB model classifies as A_G^R, the model by [860] as ${}_RP$, ${}_RS^{R0}$ or ${}_RS^{R1}$ (which all turn out to have the same properties, cf Table 11.5). Figure 11.4 illustrates the models.

The specification of the models for juveniles and adults can be done similar to the standard DEB model (see below), with the generalisation of the reserve density dynamics $\frac{d}{dt}[E] = (\kappa_w f[E_m] - [E])\dot{v}/L$, where κ_w equals 1, κ or $1-\kappa$, depending on the model, such that the mobilisation rate does not depend on assimilation.

All models have the same variables and parameters and also the same assimilation rate as function of body size, yet their properties are very different. The models for which E, S and/or J are on the same axis (main, $G-$ or $R-$axis), their sequence does not matter; so the models $A = P = S = J$ and $J_G = A_G$ and $S^R = A^R$ and ${}_R\kappa_{G0}^R = {}_R\kappa_{G1}^R$ and ${}_R\kappa_G^{R0} = {}_R\kappa_G^{R1}$ and ${}_RS^{R0} = {}_RS^{R1}$ and ${}_GJ_{G0} = {}_GJ_{G1}$ in terms of growth and reproduction; this leaves 12 different models. The models A, P, S, J and A_G^R are symmetric in allocation, relative to the G- and R-branches; the 16 other models are asymmetric.

For some models only a fraction κ of assimilation matters for ultimate length. Somatic maintenance controls ultimate length in all models, but for some models also maturity maintenance matters. Some models do not allow existence at low food levels, even if size is very small.

Table 11.5 compares the capacity to capture 8 general empirical patterns for all models. The standard DEB (A_G^R) model with constant κ is the only one that passes all our tests successfully [859]. Only A-models can naturally accommodate embryo development. The ${}_G\kappa_{G0}^R$-model passes most tests, but has maturation and reproduction directly from food. So embryos have to do this differently and reproduction is prohibited during starvation as observed, for instance, in baleen whales. The κ, ${}_RP$, ${}_GP$, ${}_RS^{R0}$ ${}_RS^{R1}$, ${}_GS^R$, ${}_GJ_{G0}$ and ${}_GJ_{G1}$-models have problems with weak homeostasis when κ is varying. [859] observed that models can be identical in their growth and reproduction behaviour, but different in the implied mineral fluxes.

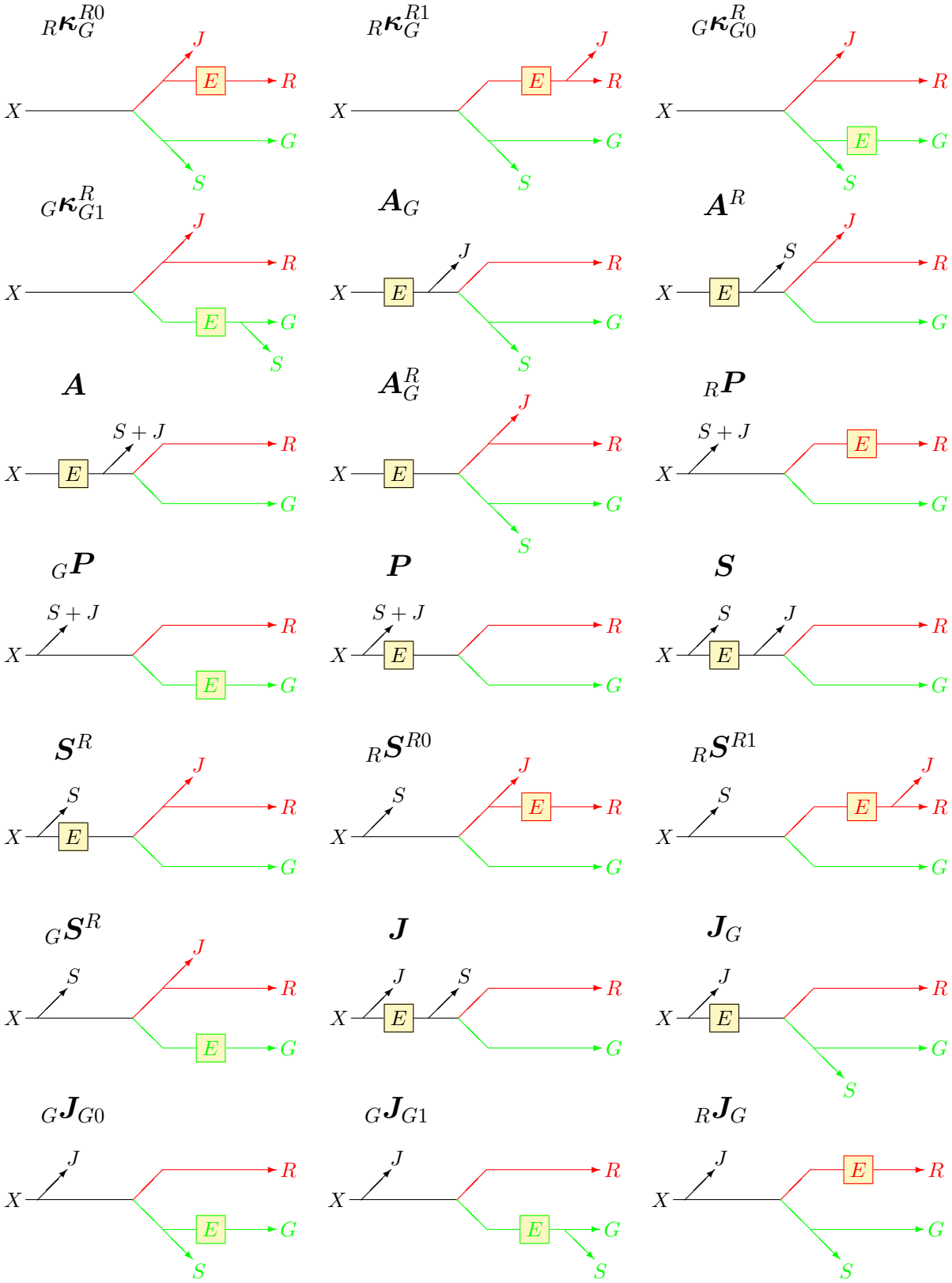

Figure 11.4: The 21 possible allocation schemes, excluding (S, R) and (J, G) combinations, from [859].

Table 11.5: Tests of the capacity to capture 8 patterns of Table 11.2 at constant food for the 21 energy budget models of Figure 11.4. Symbols: + means 'yes', − means 'no', ? means that numerical analysis is required. Where two marks are given, the first refers to constant κ, the second to variable κ. The test for the inverse generalised von Bertalanffy growth rate (pattern G2) is done for intra- and inter-specific comparisons; in the case of '?', the relationship is non-linear, the degree of curvature must be analysed numerically. From [859].

model	F2	G1	G2	R2	R3	R4	R5	S1
${}_R\boldsymbol{\kappa}_G^{R0}$	−	+	−/−	+	+	+	+	+/−
${}_R\boldsymbol{\kappa}_G^{R1}$	−	+	−/−	+	+	+	+	+/−
${}_G\boldsymbol{\kappa}_{G0}^{R}$	+	+	+/−	+	+	+	−	+/−
${}_G\boldsymbol{\kappa}_{G1}^{R}$	+	+	+/−	+	+	+	−	+/−
$\boldsymbol{A}_G$	+	+	−/−	+	+	+	+	+/+
$\boldsymbol{A}^R$	+	+	+/+	−	+	+	+	+/+
$\boldsymbol{A}$	+	+	?/?	−	+	−	+	+/+
$\boldsymbol{A}_G^R$	+	+	+/−	+	+	+	+	+/+
${}_R\boldsymbol{P}$	−	+	−/−	−	+	−	+	+/−
${}_G\boldsymbol{P}$	+	+	−/−	−	+	+	−	+/−
$\boldsymbol{P}$	+	+	?/?	−	+	−	+	+/+
$\boldsymbol{S}$	+	+	?/?	−	+	−	+	+/+
$\boldsymbol{S}^R$	+	+	+/+	−	+	+	−	+/+
${}_R\boldsymbol{S}^{R0}$	−	+	−/−	−	+	−	+	+/−
${}_R\boldsymbol{S}^{R1}$	−	+	−/−	−	+	−	+	+/−
${}_G\boldsymbol{S}^R$	+	+	+/+	−	+	+	−	+/−
$\boldsymbol{J}$	+	+	?/?	−	+	−	+	+/+
$\boldsymbol{J}_G$	+	+	−/−	+	+	+	+	+/+
${}_G\boldsymbol{J}_{G0}$	+	+	−/−	+	+	+	−	+/−
${}_G\boldsymbol{J}_{G1}$	+	+	−/−	+	+	+	−	+/−
${}_R\boldsymbol{J}_G$	−	+	−/−	+	+	+	+	+/−

11.4.1 Detailed specification per model with fixed and variable κ

In the expressions for specific influx into the reserve compartment $[\dot{p}_A^E]$, specific reserve mobilisation rate $[\dot{p}_C]$, specific growth rate $\dot{r}$ and specific maturation (or reproduction investment) $[\dot{p}_R]$, the fixed fraction to soma κ can be replaced by the variable $\kappa = 1 - L/L_\kappa$. Where only one expression for ultimate length L_∞ or inverse generalized von Bertalanffy growth rate $\dot{r}_B^{-1}$ is given, it is independent of κ, else the value for fixed κ is given first, followed by that of variable κ. The ultimate length L_∞ is for several models given implicitly only, and needs to be solved as root of a cubic polynomial in L_∞ (a built-in routine in Matlab and Octave). In the case of variable κ, length L can never exceed L_κ, which poses constraints on the value of L_κ: $L_\kappa > L_\infty$. Further: specific assimilation rate $[\dot{p}_A] = f\{\dot{p}_{Am}\}/L$, specific somatic maintenance rate $[\dot{p}_S] = [\dot{p}_M]$ (for $\{\dot{p}_T\} = 0$), specific maturity maintenance rate $[\dot{p}_J] = \dot{k}_J E_H/L^3$, specific growth rate $\dot{r} = \frac{d}{dt} \ln V$ (with $V = L^3$), change in reserve density $\frac{d}{dt}[E] = [\dot{p}_A^E] - [\dot{p}_C] - \dot{r}[E]$, change in maturity $\frac{d}{dt}E_H = [\dot{p}_R]L^3$ for $E_H < E_H^p$, else $\frac{d}{dt}E_H = 0$. $[\dot{p}_R]$ represents energy investment into reproduction, rather than maturation, for $E_H = E_H^p$ Parameters: specific maximum assimilation rate $\{\dot{p}_{Am}\}$, energy

conductance $\dot{v}$, specific somatic maintenance rate $[\dot{p}_M]$, specific maturity maintenance rate coefficient $\dot{k}_J$, specific costs for structure $[E_G]$, allocation fraction κ, maturity threshold at puberty E_H^p, length parameter for allocation L_κ. Input: scaled functional response f (a dimensionless function of food density between 0 and 1). Finally: $L \to L_\infty$ for $\dot{r} \to 0$.

κ-models

${}_R\kappa_G^{R0}$-model

$$\begin{aligned}
[\dot{p}_A^E] &= (1-\kappa)[\dot{p}_A] - [\dot{p}_J]; \quad [\dot{p}_C] = [E](\dot{v}/L - \dot{r}) - [\dot{p}_J] \\
\frac{d}{dt}[E] &= (1-\kappa)[\dot{p}_A] - [E]\dot{v}/L; \quad \dot{r} = \frac{\kappa[\dot{p}_A] - [\dot{p}_S]}{[E_G]} \\
\dot{r}_B^{-1} &= \frac{3[E_G]}{[\dot{p}_M]} \quad \text{or} \quad \dot{r}_B^{-1} = \frac{3[E_G]}{[\dot{p}_M]}\left(1 - \frac{L_\infty}{L_\kappa}\right) \\
L_\infty &= \frac{\kappa f\{\dot{p}_{Am}\}}{[\dot{p}_M]} \quad \text{or} \quad L_\infty = \frac{f\{\dot{p}_{Am}\}}{f\{\dot{p}_{Am}\}/L_\kappa + [\dot{p}_M]} \\
[\dot{p}_R] &= [E](\dot{v}/L - \dot{r}) - [\dot{p}_J]
\end{aligned}$$

${}_R\kappa_G^{R1}$-model

$$\begin{aligned}
[\dot{p}_A^E] &= (1-\kappa)[\dot{p}_A]; \quad [\dot{p}_C] = [E](\dot{v}/L - \dot{r}) \\
\frac{d}{dt}[E] &= (1-\kappa)[\dot{p}_A] - [E]\dot{v}/L; \quad \dot{r} = \frac{\kappa[\dot{p}_A] - [\dot{p}_S]}{[E_G]} \\
\dot{r}_B^{-1} &= \frac{3[E_G]}{[\dot{p}_M]} \quad \text{or} \quad \dot{r}_B^{-1} = \frac{3[E_G]}{[\dot{p}_M]}\left(1 - \frac{L_\infty}{L_\kappa}\right) \\
L_\infty &= \frac{\kappa f\{\dot{p}_{Am}\}}{[\dot{p}_M]} \quad \text{or} \quad L_\infty = \frac{f\{\dot{p}_{Am}\}}{f\{\dot{p}_{Am}\}/L_\kappa + [\dot{p}_M]} \\
[\dot{p}_R] &= [E](\dot{v}/L - \dot{r}) - [\dot{p}_J]
\end{aligned}$$

${}_G\kappa_{G0}^{R}$-model

$$\begin{aligned}
[\dot{p}_A^E] &= \kappa[\dot{p}_A] - [\dot{p}_S]; \quad [\dot{p}_C] = [E](\dot{v}/L - \dot{r}) - [\dot{p}_S] \\
\frac{d}{dt}[E] &= \kappa[\dot{p}_A] - [E]\dot{v}/L; \quad \dot{r} = \frac{[E]\dot{v}/L - [\dot{p}_S]}{[E_G] + [E]} \\
\dot{r}_B^{-1} &= \frac{3[E_G]}{[\dot{p}_M]} + \frac{3L_\infty}{\dot{v}} \quad \text{or} \quad \dot{r}_B^{-1} = \frac{3[E_G]}{[\dot{p}_M]}\left(1 - \frac{L_\infty}{L_\kappa}\right) + \frac{3L_\infty}{\dot{v}} \\
L_\infty &= \frac{\kappa f\{\dot{p}_{Am}\}}{[\dot{p}_M]} \quad \text{or} \quad L_\infty = \frac{f\{\dot{p}_{Am}\}}{f\{\dot{p}_{Am}\}/L_\kappa + [\dot{p}_M]} \\
[\dot{p}_R] &= (1-\kappa)[\dot{p}_A] - [\dot{p}_J]
\end{aligned}$$

${}_G\kappa^R_{G1}$-model

$$
\begin{aligned}
[\dot{p}_A^E] &= \kappa[\dot{p}_A]; \quad [\dot{p}_C] = [E](\dot{v}/L - \dot{r}) \\
\frac{d}{dt}[E] &= \kappa[\dot{p}_A] - [E]\dot{v}/L; \quad \dot{r} = \frac{[E]\dot{v}/L - [\dot{p}_S]}{[E_G] + [E]} \\
\dot{r}_B^{-1} &= \frac{3[E_G]}{[\dot{p}_M]} + \frac{3L_\infty}{\dot{v}} \quad \text{or} \quad \dot{r}_B^{-1} = \frac{3[E_G]}{[\dot{p}_M]}\left(1 - \frac{L_\infty}{L_\kappa}\right) + \frac{3L_\infty}{\dot{v}} \\
L_\infty &= \frac{\kappa f\{\dot{p}_{Am}\}}{[\dot{p}_M]} \quad \text{or} \quad L_\infty = \frac{f\{\dot{p}_{Am}\}}{f\{\dot{p}_{Am}\}/L_\kappa + [\dot{p}_M]} \\
[\dot{p}_R] &= (1-\kappa)[\dot{p}_A] - [\dot{p}_J]
\end{aligned}
$$

A-models

A_G-model

$$
\begin{aligned}
[\dot{p}_A^E] &= [\dot{p}_A]; \quad [\dot{p}_C] = [E](\dot{v}/L - \dot{r}) \\
\frac{d}{dt}[E] &= [\dot{p}_A] - [E]\dot{v}/L; \quad \dot{r} = \frac{[E]\dot{v}/L - [\dot{p}_S]/\kappa - [\dot{p}_J]}{[E_G]/\kappa + [E]} \\
\dot{r}_B^{-1} &= \frac{3L_\infty}{\dot{v}} + \frac{3[E_G]/[\dot{p}_M]}{1 + \frac{\kappa \dot{k}_J E_H^p}{[\dot{p}_M]L_\infty^3}} \quad \text{or} \quad \dot{r}_B^{-1} = \frac{3L_\infty}{\dot{v}} + \frac{3(1 - L_\infty/L_\kappa)[E_G]/[\dot{p}_M]}{1 + \left(1 - \frac{L_\infty}{L_\kappa}\right)\frac{\dot{k}_J E_H^p}{[\dot{p}_M]L_\infty^3}} \\
\frac{[\dot{p}_M]}{\kappa} &= \frac{f\{\dot{p}_{Am}\}}{L_\infty} - \frac{\dot{k}_J E_H^p}{L_\infty^3} \quad \text{or} \quad \frac{[\dot{p}_M]}{1 - L_\infty/L_\kappa} = \frac{f\{\dot{p}_{Am}\}}{L_\infty} - \frac{\dot{k}_J E_H^p}{L_\infty^3} \\
[\dot{p}_R] &= (1-\kappa)([E](\dot{v}/L - \dot{r}) - [\dot{p}_J])
\end{aligned}
$$

A^R-model

$$
\begin{aligned}
[\dot{p}_A^E] &= [\dot{p}_A]; \quad [\dot{p}_C] = [E](\dot{v}/L - \dot{r}) \\
\frac{d}{dt}[E] &= [\dot{p}_A] - [E]\dot{v}/L; \quad \dot{r} = \frac{[E]\dot{v}/L - [\dot{p}_S]}{[E_G]/\kappa + [E]} \\
\dot{r}_B^{-1} &= \frac{3[E_G]}{\kappa[\dot{p}_M]} + \frac{3L_\infty}{\dot{v}} \quad \text{or} \quad \dot{r}_B^{-1} = \frac{3[E_G]}{[\dot{p}_M]} + \frac{3L_\infty}{\dot{v}} \\
L_\infty &= \frac{f\{\dot{p}_{Am}\}}{[\dot{p}_M]} \\
[\dot{p}_R] &= (1-\kappa)([E](\dot{v}/L - \dot{r}) - [\dot{p}_S]) - [\dot{p}_J]
\end{aligned}
$$

A-model

$$
\begin{aligned}
[\dot{p}_A^E] &= [\dot{p}_A]; \quad [\dot{p}_C] = [E](\dot{v}/L - \dot{r}) \\
\frac{d}{dt}[E] &= [\dot{p}_A] - [E]\dot{v}/L; \quad \dot{r} = \frac{[E]\dot{v}/L - [\dot{p}_S] - [\dot{p}_J]}{[E_G]/\kappa + [E]}
\end{aligned}
$$

$$
\begin{aligned}
\dot{r}_B^{-1} &= \frac{3L_\infty}{\dot{v}} + \frac{3[E_G]}{\kappa[\dot{p}_M]}\left(1+\frac{\dot{k}_J E_H^p}{[\dot{p}_M]L_\infty^3}\right)^{-1} \quad \text{or} \quad \dot{r}_B^{-1} = \frac{3L_\infty}{\dot{v}} + \frac{3[E_G]}{[\dot{p}_M]}\left(1+\frac{\dot{k}_J E_H^p}{[\dot{p}_M]L_\infty^3}\right)^{-1} \\
[\dot{p}_M] &= \frac{f\{\dot{p}_{Am}\}}{L_\infty} - \frac{\dot{k}_J E_H^p}{L_\infty^3} \\
[\dot{p}_R] &= (1-\kappa)([E](\dot{v}/L - \dot{r}) - [\dot{p}_S] - [\dot{p}_J])
\end{aligned}
$$

A_G^R-model

$$
\begin{aligned}
[\dot{p}_A^E] &= [\dot{p}_A]; \quad [\dot{p}_C] = [E](\dot{v}/L - \dot{r}) \\
\frac{d}{dt}[E] &= [\dot{p}_A] - [E]\dot{v}/L; \quad \dot{r} = \frac{\kappa[E]\dot{v}/L - [\dot{p}_S]}{[E_G] + [E]\kappa} \\
\dot{r}_B^{-1} &= 3\left(\frac{[E_G]}{[\dot{p}_M]} + \frac{L_\infty}{\dot{v}}\right) \quad \text{or} \quad \dot{r}_B^{-1} = 3\left(\frac{[E_G]}{[\dot{p}_M]} + L_\infty\left(\frac{1}{\dot{v}} - \frac{[E_G]}{L_\kappa[\dot{p}_M]}\right)\right) \\
L_\infty &= \frac{\kappa f\{\dot{p}_{Am}\}}{[\dot{p}_M]} \quad \text{or} \quad L_\infty = \left(\frac{[\dot{p}_M]}{f\{\dot{p}_{Am}\}} + \frac{1}{L_\kappa}\right)^{-1} \\
[\dot{p}_R] &= (1-\kappa)[E](\dot{v}/L - \dot{r}) - [\dot{p}_J]
\end{aligned}
$$

P-models

${}_RP$-model

$$
\begin{aligned}
[\dot{p}_A^E] &= (1-\kappa)([\dot{p}_A] - [\dot{p}_S] - [\dot{p}_J]); \quad [\dot{p}_C] = [E](\dot{v}/L - \dot{r}) - (1-\kappa)([\dot{p}_S] + [\dot{p}_J]) \\
\frac{d}{dt}[E] &= (1-\kappa)[\dot{p}_A] - [E]\dot{v}/L; \quad \dot{r} = \frac{[\dot{p}_A] - [\dot{p}_S] - [\dot{p}_J])}{[E_G]/\kappa} \\
\dot{r}_B^{-1} &= \frac{3[E_G]}{\kappa[\dot{p}_M]}\left(1+\frac{\dot{k}_J E_H^p}{[\dot{p}_M]L_\infty^3}\right)^{-1} \quad \text{or} \quad \dot{r}_B^{-1} = \frac{3[E_G]}{[\dot{p}_M]}\left(1+\frac{\dot{k}_J E_H^p}{[\dot{p}_M]L_\infty^3}\right)^{-1} \\
[\dot{p}_M] &= \frac{f\{\dot{p}_{Am}\}}{L_\infty} - \frac{\dot{k}_J E_H^p}{L_\infty^3} \\
[\dot{p}_R] &= [E](\dot{v}/L - \dot{r}) - (1-\kappa)([\dot{p}_S] + [\dot{p}_J])
\end{aligned}
$$

${}_GP$-model

$$
\begin{aligned}
[\dot{p}_A^E] &= \kappa([\dot{p}_A] - [\dot{p}_S] - [\dot{p}_J]); \quad [\dot{p}_C] = [E](\dot{v}/L - \dot{r}) - \kappa([\dot{p}_S] + [\dot{p}_J]) \\
\frac{d}{dt}[E] &= \kappa[\dot{p}_A] - [E]\dot{v}/L; \quad \dot{r} = \frac{[E]\dot{v}/L - \kappa([\dot{p}_S] + [\dot{p}_J])}{[E_G] + [E]} \\
\dot{r}_B^{-1} &= \frac{3L_\infty}{\kappa\dot{v}} + \frac{3[E_G]}{\kappa[\dot{p}_M]}\left(1+\frac{\dot{k}_J E_H^p}{[\dot{p}_M]L_\infty^3}\right)^{-1} \quad \text{or} \quad \dot{r}_B^{-1} = \frac{3L_\infty}{\dot{v}} + \frac{3[E_G]}{[\dot{p}_M]}\left(1+\frac{\dot{k}_J E_H^p}{[\dot{p}_M]L_\infty^3}\right)^{-1} \\
[\dot{p}_M] &= \frac{f\{\dot{p}_{Am}\}}{L_\infty} - \frac{\dot{k}_J E_H^p}{L_\infty^3} \\
[\dot{p}_R] &= (1-\kappa)([\dot{p}_A] - [\dot{p}_S] - [\dot{p}_J])
\end{aligned}
$$

P-model

$$
\begin{aligned}
[\dot{p}_A^E] &= [\dot{p}_A] - [\dot{p}_S] - [\dot{p}_J]; \quad [\dot{p}_C] = [E](\dot{v}/L - \dot{r}) - [\dot{p}_S] - [\dot{p}_J] \\
\frac{d}{dt}[E] &= [\dot{p}_A] - [E]\dot{v}/L; \quad \dot{r} = \frac{[E]\dot{v}/L - [\dot{p}_S] - [\dot{p}_J]}{[E_G]/\kappa + [E]} \\
\dot{r}_B^{-1} &= \frac{3L_\infty}{\dot{v}} + \frac{3[E_G]}{\kappa[\dot{p}_M]}\left(1 + \frac{\dot{k}_J E_H^p}{[\dot{p}_M]L_\infty^3}\right)^{-1} \quad \text{or} \quad \dot{r}_B^{-1} = \frac{3L_\infty}{\dot{v}} + \frac{3[E_G]}{[\dot{p}_M]}\left(1 + \frac{\dot{k}_J E_H^p}{[\dot{p}_M]L_\infty^3}\right)^{-1} \\
[\dot{p}_M] &= \frac{f\{\dot{p}_{Am}\}}{L_\infty} - \frac{\dot{k}_J E_H^p}{L_\infty^3} \\
[\dot{p}_R] &= (1-\kappa)([E](\dot{v}/L - \dot{r}) - [\dot{p}_S] - [\dot{p}_J])
\end{aligned}
$$

S-models

S-model

$$
\begin{aligned}
[\dot{p}_A^E] &= [\dot{p}_A] - [\dot{p}_S]; \quad [\dot{p}_C] = [E](\dot{v}/L - \dot{r}) - [\dot{p}_S] \\
\frac{d}{dt}[E] &= [\dot{p}_A] - [E]\dot{v}/L; \quad \dot{r} = \frac{[E]\dot{v}/L - [\dot{p}_S] - [\dot{p}_J]}{[E_G]/\kappa + [E]} \\
\dot{r}_B^{-1} &= \frac{3L_\infty}{\dot{v}} + \frac{3[E_G]}{\kappa[\dot{p}_M]}\left(1 + \frac{\dot{k}_J E_H^p}{[\dot{p}_M]L_\infty^3}\right)^{-1} \quad \text{or} \quad \dot{r}_B^{-1} = \frac{3L_\infty}{\dot{v}} + \frac{3[E_G]}{[\dot{p}_M]}\left(1 + \frac{\dot{k}_J E_H^p}{[\dot{p}_M]L_\infty^3}\right)^{-1} \\
[\dot{p}_M] &= \frac{f\{\dot{p}_{Am}\}}{L_\infty} - \frac{\dot{k}_J E_H^p}{L_\infty^3} \\
[\dot{p}_R] &= (1-\kappa)([E](\dot{v}/L - \dot{r}) - [\dot{p}_S] - [\dot{p}_J])
\end{aligned}
$$

S^R-model

$$
\begin{aligned}
[\dot{p}_A^E] &= [\dot{p}_A] - [\dot{p}_S]; \quad [\dot{p}_C] = [E](\dot{v}/L - \dot{r}) - [\dot{p}_S] \\
\frac{d}{dt}[E] &= [\dot{p}_A] - [E]\dot{v}/L; \quad \dot{r} = \frac{[E]\dot{v}/L - [\dot{p}_S]}{[E_G]/\kappa + [E]} \\
\dot{r}_B^{-1} &= \frac{3[E_G]}{\kappa[\dot{p}_M]} + \frac{3L_\infty}{\dot{v}} \quad \text{or} \quad \dot{r}_B^{-1} = \frac{3[E_G]}{[\dot{p}_M]} + \frac{3L_\infty}{\dot{v}} \\
L_\infty &= \frac{f\{\dot{p}_{Am}\}}{[\dot{p}_M]} \\
[\dot{p}_R] &= (1-\kappa)([E](\dot{v}/L - \dot{r}) - [\dot{p}_S]) - [\dot{p}_J]
\end{aligned}
$$

${}_R S^{R0}$-model

$$
[\dot{p}_A^E] = (1-\kappa)([\dot{p}_A] - [\dot{p}_S]) - [\dot{p}_J]; \quad [\dot{p}_C] = [E](\dot{v}/L - \dot{r}) - (1-\kappa)[\dot{p}_S] - [\dot{p}_J]
$$

$$\begin{aligned}
\frac{d}{dt}[E] &= (1-\kappa)[\dot{p}_A] - [E]\dot{v}/L; \quad \dot{r} = \frac{[\dot{p}_A] - [\dot{p}_S]}{[E_G]/\kappa} \\
\dot{r}_B^{-1} &= \frac{3[E_G]}{\kappa[\dot{p}_M]} \quad \text{or} \quad \dot{r}_B^{-1} = \frac{3[E_G]}{[\dot{p}_M]} \\
L_\infty &= \frac{f\{\dot{p}_{Am}\}}{[\dot{p}_M]} \\
[\dot{p}_R] &= [E](\dot{v}/L - \dot{r}) - (1-\kappa)[\dot{p}_S] - [\dot{p}_J]
\end{aligned}$$

${}_RS^{R1}$-model

$$\begin{aligned}
[\dot{p}_A^E] &= (1-\kappa)([\dot{p}_A] - [\dot{p}_S]); \quad [\dot{p}_C] = [E](\dot{v}/L - \dot{r}) - (1-\kappa)[\dot{p}_S] \\
\frac{d}{dt}[E] &= (1-\kappa)[\dot{p}_A] - [E]\dot{v}/L; \quad \dot{r} = \frac{[\dot{p}_A] - [\dot{p}_S]}{[E_G]/\kappa} \\
\dot{r}_B^{-1} &= \frac{3[E_G]}{\kappa[\dot{p}_M]} \quad \text{or} \quad \dot{r}_B^{-1} = \frac{3[E_G]}{[\dot{p}_M]} \\
L_\infty &= \frac{f\{\dot{p}_{Am}\}}{[\dot{p}_M]} \\
[\dot{p}_R] &= [E](\dot{v}/L - \dot{r}) - (1-\kappa)[\dot{p}_S] - [\dot{p}_J]
\end{aligned}$$

${}_GS^R$-model

$$\begin{aligned}
[\dot{p}_A^E] &= \kappa([\dot{p}_A] - [\dot{p}_S]); \quad [\dot{p}_C] = [E](\dot{v}/L - \dot{r}) - \kappa[\dot{p}_S] \\
\frac{d}{dt}[E] &= \kappa[\dot{p}_A] - [E]\dot{v}/L; \quad \dot{r} = \frac{[E]\dot{v}/L - \kappa[\dot{p}_S]}{[E_G] + [E]} \\
\dot{r}_B^{-1} &= \frac{3[E_G]}{\kappa[\dot{p}_M]} + \frac{3L_\infty}{\dot{v}} \quad \text{or} \quad \dot{r}_B^{-1} = \frac{3[E_G]}{[\dot{p}_M]} + \frac{3L_\infty}{\dot{v}} \\
L_\infty &= \frac{f\{\dot{p}_{Am}\}}{[\dot{p}_M]} \\
[\dot{p}_R] &= (1-\kappa)([\dot{p}_A] - [\dot{p}_S]) - [\dot{p}_J]
\end{aligned}$$

J-models

J-model

$$\begin{aligned}
[\dot{p}_A^E] &= [\dot{p}_A] - [\dot{p}_J]; \quad [\dot{p}_C] = [E](\dot{v}/L - \dot{r}) - [\dot{p}_J] \\
\frac{d}{dt}[E] &= [\dot{p}_A] - [E]\dot{v}/L; \quad \dot{r} = \frac{[E]\dot{v}/L - [\dot{p}_S] - [\dot{p}_J]}{[E_G]/\kappa + [E]} \\
\dot{r}_B^{-1} &= \frac{3L_\infty}{\dot{v}} + \frac{3[E_G]}{\kappa[\dot{p}_M]}\left(1 + \frac{\dot{k}_J E_H^p}{[\dot{p}_M]L_\infty^3}\right)^{-1} \quad \text{or} \quad \dot{r}_B^{-1} = \frac{3L_\infty}{\dot{v}} + \frac{3[E_G]}{[\dot{p}_M]}\left(1 + \frac{\dot{k}_J E_H^p}{[\dot{p}_M]L_\infty^3}\right)^{-1}
\end{aligned}$$

$$
\begin{aligned}
[\dot{p}_M] &= \frac{f\{\dot{p}_{Am}\}}{L_\infty} - \frac{\dot{k}_J E_H^p}{L_\infty^3} \\
[\dot{p}_R] &= (1-\kappa)([E](\dot{v}/L - \dot{r}) - [\dot{p}_J] - [\dot{p}_S])
\end{aligned}
$$

J_G-model

$$
\begin{aligned}
[\dot{p}_A^E] &= [\dot{p}_A] - [\dot{p}_J]; \quad [\dot{p}_C] = [E](\dot{v}/L - \dot{r}) - [\dot{p}_J] \\
\frac{d}{dt}[E] &= [\dot{p}_A] - [E]\dot{v}/L; \quad \dot{r} = \frac{[E]\dot{v}/L - [\dot{p}_S]/\kappa - [\dot{p}_J]}{[E_G]/\kappa + [E]} \\
\dot{r}_B^{-1} &= \frac{3L_\infty}{\dot{v}} + \frac{3[E_G]/[\dot{p}_M]}{1 + \frac{\kappa \dot{k}_J E_H^p}{[\dot{p}_M] L_\infty^3}} \quad \text{or} \quad \dot{r}_B^{-1} = \frac{3L_\infty}{\dot{v}} + \frac{3(1 - L_\infty/L_\kappa)[E_G]/[\dot{p}_M]}{1 + \left(1 - \frac{L_\infty}{L_\kappa}\right) \frac{\dot{k}_J E_H^p}{[\dot{p}_M] L_\infty^3}} \\
\frac{[\dot{p}_M]}{\kappa} &= \frac{f\{\dot{p}_{Am}\}}{L_\infty} + \frac{\dot{k}_J E_H^p}{L_\infty^3} \quad \text{or} \quad \frac{[\dot{p}_M]}{1 - L_\infty/L_\kappa} = \frac{f\{\dot{p}_{Am}\}}{L_\infty} + \frac{\dot{k}_J E_H^p}{L_\infty^3} \\
[\dot{p}_R] &= (1-\kappa)([E](\dot{v}/L - \dot{r}) - [\dot{p}_J])
\end{aligned}
$$

${}_GJ_{G0}$-model

$$
\begin{aligned}
[\dot{p}_A^E] &= \kappa([\dot{p}_A] - [\dot{p}_J]) - [\dot{p}_S]; \quad [\dot{p}_C] = [E](\dot{v}/L - \dot{r}) - \kappa[\dot{p}_J] - [\dot{p}_S] \\
\frac{d}{dt}[E] &= \kappa[\dot{p}_A] - [E]\dot{v}/L; \quad \dot{r} = \frac{[E]\dot{v}/L - [\dot{p}_S] - \kappa[\dot{p}_J]}{[E_G] + [E]} \\
\dot{r}_B^{-1} &= \frac{3L_\infty}{\dot{v}} + \frac{3}{\frac{[\dot{p}_M]}{[E_G]} + \frac{\kappa \dot{k}_J E_H^p}{[E_G] L_\infty^3}} \quad \text{or} \quad \dot{r}_B^{-1} = \frac{3L_\infty}{\dot{v}} + \frac{3(1 - L_\infty/L_\kappa)[E_G]/[\dot{p}_M]}{1 + \left(1 - \frac{L_\infty}{L_\kappa}\right) \frac{\dot{k}_J E_H^p}{[\dot{p}_M] L_\infty^3}} \\
\frac{[\dot{p}_M]}{\kappa} &= \frac{f\{\dot{p}_{Am}\}}{L_\infty} - \frac{\dot{k}_J E_H^p}{L_\infty^3} \quad \text{or} \quad \frac{[\dot{p}_M]}{1 - L_\infty/L_\kappa} = \frac{f\{\dot{p}_{Am}\}}{L_\infty} - \frac{\dot{k}_J E_H^p}{L_\infty^3} \\
[\dot{p}_R] &= (1-\kappa)([\dot{p}_A] - [\dot{p}_J])
\end{aligned}
$$

${}_GJ_{G1}$-model

$$
\begin{aligned}
[\dot{p}_A^E] &= \kappa([\dot{p}_A] - [\dot{p}_J]); \quad [\dot{p}_C] = [E](\dot{v}/L - \dot{r}) - \kappa[\dot{p}_J] \\
\frac{d}{dt}[E] &= \kappa[\dot{p}_A] - [E]\dot{v}/L; \quad \dot{r} = \frac{[E]\dot{v}/L - [\dot{p}_S] - \kappa[\dot{p}_J]}{[E_G] + [E]} \\
\dot{r}_B^{-1} &= \frac{3L_\infty}{\dot{v}} + \frac{3}{\frac{[\dot{p}_M]}{[E_G]} + \frac{\kappa \dot{k}_J E_H^p}{[E_G] L_\infty^3}} \quad \text{or} \quad \dot{r}_B^{-1} = \frac{3L_\infty}{\dot{v}} + \frac{3(1 - L_\infty/L_\kappa)[E_G]/[\dot{p}_M]}{1 + \left(1 - \frac{L_\infty}{L_\kappa}\right) \frac{\dot{k}_J E_H^p}{[\dot{p}_M] L_\infty^3}} \\
\frac{[\dot{p}_M]}{\kappa} &= \frac{f\{\dot{p}_{Am}\}}{L_\infty} - \frac{\dot{k}_J E_H^p}{L_\infty^3} \quad \text{or} \quad \frac{[\dot{p}_M]}{1 - L_\infty/L_\kappa} = \frac{f\{\dot{p}_{Am}\}}{L_\infty} - \frac{\dot{k}_J E_H^p}{L_\infty^3} \\
[\dot{p}_R] &= (1-\kappa)([\dot{p}_A] - [\dot{p}_J])
\end{aligned}
$$

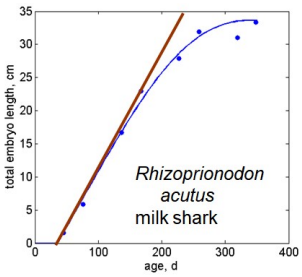

$\frac{d}{dt}L(0) = \frac{\dot{v}}{3}$

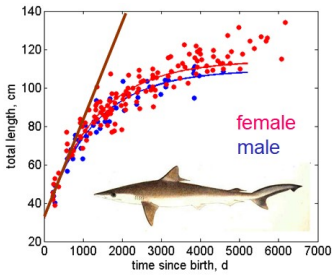

$\frac{d}{dt}L(a_b) = \frac{\dot{v}}{3}\frac{e-l_b}{e+g}$

Figure 11.5: Prenatal and postnatal growth of the milk shark *Rhizoprionodon acutus*. Length of both embryos and neonates initially grow linearly in time, but at different rates. Data from [1528].

${}_RJ_G$-model

$$
\begin{aligned}
[\dot{p}_A^E] &= (1-\kappa)([\dot{p}_A]-[\dot{p}_J]); \quad [\dot{p}_C] = [E](\dot{v}/L - \dot{r}) - (1-\kappa)[\dot{p}_J] \\
\frac{d}{dt}[E] &= (1-\kappa)[\dot{p}_A] - [E]\dot{v}/L; \quad \dot{r} = \frac{[\dot{p}_A] - [\dot{p}_S]/\kappa - [\dot{p}_J]}{[E_G]/\kappa} \\
\dot{r}_B^{-1} &= \frac{3[E_G]}{[\dot{p}_M] + \kappa \dot{k}_J E_H^p/L_\infty^3} \quad \text{or} \quad \dot{r}_B^{-1} = \frac{3[E_G]}{[\dot{p}_M]/(1-L_\infty/L_\kappa) + \dot{k}_J E_H^p/L_\infty^3} \\
\frac{[\dot{p}_M]}{\kappa} &= \frac{f\{\dot{p}_{Am}\}}{L_\infty} - \frac{\dot{k}_J E_H^p}{L_\infty^3} \quad \text{or} \quad \frac{[\dot{p}_M]}{1-L_\infty/L_\kappa} = \frac{f\{\dot{p}_{Am}\}}{L_\infty} - \frac{\dot{k}_J E_H^p}{L_\infty^3} \\
[\dot{p}_R] &= [E](\dot{v}/L - \dot{r}) - (1-\kappa)[\dot{p}_J]
\end{aligned}
$$

11.4 Variations on the standard DEB model

In our efforts to fit the standard DEB model to the species in the AmP collection, it became clear that we need some extensions, see the DEBtool manual. These extensions are minor and fit patterns that are evolutionarily consistent and order, rather than species, dependent.

Several variations on the standard (std) model have been proposed, for simplicity's sake. Kooijman [764], for instance, observed that if $\dot{k}_M = \dot{k}_J$, maturity density remains constant, implying that life history events (birth, puberty), still occur at fixed maturity thresholds, but now also at fixed values for structure. This reduction in number of state variables certainly simplifies the mathematics, but gave problems in particular applications. Another example is the DEBkiss model [660, 655], which is very close to the Kooijman-Metz model [794]. It is, in fact, another special case of the std model, with $\dot{v} \to \infty$. The odd implications for embryo development are fixed with a new embryo development module, which boils down to introducing a new state variable, yolk, which is mobilised such that the von Bertalanffy growth curve is back-extrapolated into the embryo stage, starting from structure zero, and yolk is zero at birth. In the std model length of the embryo and the neonate initially grows linearly as well, but at different rates (since growth depends on reserve density, which is infinitely large in the starting embryo, but not so in the neonate). See Fig. 11.5.

Although the motivation was to simplify the std model for routine applications in toxicity tests, it hardly does so in terms of number of state variable and parameters: yolk replaces reserve (so no less state variables), the yield of structure (i.e. biomass) on yolk replaces the yield of structure on reserve, the yield of yolk on food replaces the yield of reserve on food. The energy conductance is then the only parameter that is reduced, but at considerable loss of performance. If this really means a reduction in required number of parameters very much depends on the data that needs to be described. Males frequently differ for females, for instance, not only in ultimate size, but also in size at first maturity, in (von Bertalanffy) growth rate and in length-weight relationship. The standard DEB model can capture these differences, with a difference in max specific assimilation $\{\dot{p}_{Am}\}$ and maturity at puberty E_H^p only. Females of many rays and sharks are larger than males, meaning that they have a larger value for $\{\dot{p}_{Am}\}$, but with the same value for the energy conductance $\dot{v}$, female's reserve capacity $[E_m] = \{\dot{p}_{Am}\}/\dot{v}$ is larger, which contributes to weight. So females have a larger weight than males for the same length and they grow slower, since they have to build up this larger reserve. By a step-up of $\{\dot{p}_{Am}\}$, the female has automatically a smaller von Bertalanffy growth rate than the male in the std DEB model, but not in the DEBkiss model. The DEBkiss model can only capture the female-male couple with more parameters than the standard DEB model. Growth at different constant food levels shows a related problem. In the DEBkiss model growth (of biovolume) is given by $\frac{d}{dt}L^3 = \frac{\kappa f\{\dot{p}_{Am}\}L^2 - [\dot{p}_M]L^3}{[E_G]}$, which gives a von Bertalanffy growth rate of $\dot{r}_B = \dot{k}_M/3$ for $\dot{k}_M = [\dot{p}_M]/[E_G]$, while in the std model we have $\dot{r}_B = \frac{\dot{k}_M/3}{1+f/g}$ for energy investment ratio $g = \frac{[E_G]\dot{v}}{\kappa\{\dot{p}_{Am}\}}$. This is easy to check since $\dot{v} \to \infty$ means $g \to \infty$. So the von Bertalanffy growth rate $\dot{r}_B$ depends on food in the std model, but not so in the DEBkiss model. Ultimate length L_∞ depends on food in both models, implying that $\dot{r}_B$ does not depend on L_∞ in the DEBkiss model, but it does in the std model. Figure 2.3 of the comments confirms the latter for the waterflea, and Fig 2.4 for rat and mouse, while the AmP collection has many more convincing examples. The fundamental reason for this is easy to understand: reserve needs to build up during growth, this costs energy, which slows growth down since reserve per structure increases with the food level. It is as if food converts to less biomass at high food levels; a pattern that has been reported frequently in the literature (but frequently interpreted as a reduced digestion efficiency at high food levels). Adult humans can live happy with three meals per day, but babies want food more frequently. This naturally follows from std DEB model, since change in reserve density is linked to $\dot{v}/L$, but less so from the DEBkiss model.

The DEBkiss model has problems with the 6 compelling reasons for why reserve has been introduced, as listed in section 1.1.3 of [775]. As an implication, the DEBkiss model cannot handle the scatter in weights at certain length (at least for juveniles), which is widely used in ecology to quantify nutritional condition, and avoids the problem by not working with lengths. This cannot be avoided completely, however, since feeding depends on surface area, and maintenance on volume, while length is proportional to the ratio of the two for isomorphs. Moreover, the value for $\dot{v}$ can be estimated from data, even if it would be large and embryo data are omitted, but such very high values have not been found in the species in the AmP collection. Jager [655] inaccurately compares DEBkiss

with the std model in an appendix in a rather unfair way. The conclusion of Lika and Kooijman [859] was that the std model was the only model among the 21 topological alternatives with weak homeostasis that fitted a set of stylized facts; he left out these important restrictions and made a caricature of the arguments. The DEBkiss model is not a topological alternative (no reserve), nor does it sport weak homeostasis (for which you need more than one metabolic pool). Apart of the problem that the reproduction buffer is only present in adults, it hardly counts as a pool because those metabolites are already allocated to reproduction; the fact that it can be used otherwise under extreme starvation does not change its status. Due to its inherent pulsing nature, it certainly cannot be a second pool, next to structure, that follows weak homeostasis. The reproduction buffer is not indicated in the 21 diagrams of [859], because all models with an incrementally small allocation to reproduction in an incrementally small time period require a reproduction buffer and buffer handling rules, since eggs are not incrementally small. I wonder how the DEBkiss model would work out for species with foetal development, which don't need a reproduction buffer, since they can allocate incrementally small amounts directly to the foetus. The mapping by Jager to replace reserve by the reproduction buffer is incorrect, so is the mapping of the DEBkiss model to the ${}_R\kappa_G^{R0}$ model. Consistency with the empirical facts as listed by [859] was not the reason for introducing reserve, as stated by Jager, only to compare topological alternatives, which all have reserve (as well as a reproduction buffer that is not shown in the diagrams). Jager's argument that the parameters of the DEB model would be difficult to estimate from data is at odds with the demonstration that a bijection exists between (almost all) DEB parameters and a simple set of data [855], while the code for the mapping in both directions is offered in DEBtool. Moreover, the Add_my_Pet collection of thousands of animal species, where quite a few entries are really data-poor, demonstrates that the estimation of DEB parameter is hardly problem in practice. The DEBkiss model only applies to animals, according to Jager, not to other organisms, and has much less consistency with popular empirical models in the biological literature. Especially the inconsistency of the DEBkiss model with indirect calorimetry hurts: dissipating heat is a weighted sum of O_2-consumption and CO_2- and NH_3-production; the DEBkiss model can only accommodate 2 fluxes, not 3: this is at the root of metabolic theory. Users of the DEBkiss model should realize that several parameters look the same in notation, compared to the std model, but can have different values and the detailed interpretation is different. The specific somatic maintenance cost $[\dot{p}_M]$, for instance, relates in the DEBkiss model to all of the biomass, but in the std model to structure, which is only part of biomass. This different mapping affects other parameters as well, such as $\{\dot{p}_{Am}\}$, since the ratio with $[\dot{p}_M]$ controls ultimate size.

Sherborne et al [1294] proposed a decision tree for what model to use in what situation in ecotoxicity research, where the fist decision-question 'is reserve essential?' suggests that the answer depends on a technical detail that is only of interest for the specialist. A better rephrasing of this question would be 'is the step from results of a standarised toxicity test in the laboratory to field conditions (where food is varying) of importance to you?', or 'is the coherence of results of tests with animals and those with other organisms important for you?'. They incorrectly suggest that the std model requires more data than the DEBkiss model. These alternative decision-questions better illustrate that we are not talking about

a technical detail that one could avoid in a risk-assessment context. With a view on the data used in the AmP collection of 2650 animal species to estimate the parameters of the std model, I would not know any example where the DEBkiss model would need less data. So their suggestion that the std model needs more data is simply incorrect. The authors used parameter values from the collection in a DEBkiss model. This is misleading, as mentioned above. In the DEBkiss model the whole body needs somatic maintenance, for instance, in the std model only the structural part. This affects all other parameters. So user of the DEBkiss model should estimate DEBkiss parameters independently from data. Since large-bodied animals have relatively more reserve, the implication is that it will be much harder model to simulate ecosystems that have both small- and large-bodied species using the DEBkiss model, since the large-bodied species go extinct, even without the help of toxicants. Contrary to the DEBkiss model, the std model has a natural consistency with Kleibers law.

Martin, co-author of Sibly's model [1302], proposed a variation on the DEBkiss model specifically for fish, the DEBlipid model [914], to repair the problem that the DEBkiss model cannot handle changes in the composition of biomass (during the juvenile stage and across seasons). Apart that it inherits most problems of the DEBkiss model and ignores the embryo stage altogether, it introduces some new problems as well. Eggs cannot be synthesized from lipids, since initial egg mass needs to fuel embryo growth, while embryo structure has proteins. The DEBlipid model also deleted maturation and links stage transitions to size. In this way it cannot capture the supply-demand spectrum [855] (since the quantifier supply stress is proportional to maturity maintenance), that has strong empirical support in view of the segregation of large animal taxa along the supply-demand spectrum, and acceleration of maturation [1002] (where an decrease κ comes with an increase of respiration and maturation, leading to an earlier metamorphosis at a much smaller size), and the fact that size at puberty generally does depend on food level (smaller size at puberty at less food).

A weak aspect of the DEBlipid model is that it tries to capture season and size related changes in the chemical composition of salmon biomass, without having any information about food intake (or temperature), neither in quantity nor quality. Food intake in young salmon in rivers must be very different from that of large ones in the sea, with a transition from tiny, to small invertebrates, to a variety of fish species of increasing size (and swimming speed). Since the invertebrate-fish conversion efficiency is likely to be less efficient than the fish-fish conversion, later in life, an increase in reserve density during ontogeny is to be expected in a standard DEB context. Moreover, the increasing body size of fish prey partly relates to species of increasing maximum body size, which have larger reserve capacity, as expected by DEB theory and confirmed in the AmP collection. Reserve is likely to be richer in lipids in fish, compared to structure. Given a trajectory for temperature, I expect that it would be possible to reconstruct food intake from any lipid trajectory, like has been done for data on growth, reproduction and otolith size, see [775, Section 4.11]. The reason why DEB theory is chemically implicit is that taxa differ considerably in this respect. The 85000 species of molluscs, for instance, use carbohydrates rather than lipids as main energy storage. By working with fractional powers of energy, the DEBlipid model lost its connection with underlying physics.

11.4 DEB models have no alternatives

DEB theory aims to specify the metabolism of an individual thermodynamically in a changing environment, in terms of temperature and substrate availability, where metabolism includes feeding, digestion, growth, maintenance, development, respiration, excretion and, possibly, aging.

The theory as been set-up as a formal theory, where a set of consistent and coherent assumptions fully specify mathematical models. Many models for aspects of metabolism have been proposed, but the key issue revealed by DEB theory is that all have to be effective at the same time to specify the individual (thermo)dynamically. These processes do interact and have to be studied in coherence, while being consistent, realistic as well as general. This problem is much more complex, as illustrated in Section 11.1 of these comments, and restricts the possible class of models substantially.

Originally, in 1979, I intended to setup a DEB model based on a set of assumptions, as listed in [775, Table 2.4], and subsequently replace assumptions to arrive at a set of different models that can be compared for realism and other criteria. This is typically an effective way to gain insight. Despite considerable effort over the years, it turned out to be very hard to replace assumptions, however, which motivated research for the reasons. The standard DEB model can considered to be a canonical form among DEB models, and thought to be applicable to many animal species, which are metabolically simpler than other taxa due to the fact that they live of complex substrates, namely other organisms. Other DEB models are extensions of the standard one, including multiple reserves and structures, extra life stages, etc. The following 7-step reasoning leads to the conclusion that alternatives for the standard DEB model are impossible with a comparable level of complexity and consistency with a set of stylized facts, see Table 11.2 of the comments.

1. To specify the individual thermodynamically, we need mass balances for chemical elements. Since life exists in anaerobic environments [418], the use of dioxygen cannot be used as a quantifier for metabolic rate. Since some microbes absorb heat, rather then produce it [866], heat dissipation can also not be used as quantifier. The only quantifier that works is entropy dissipation [1343], but to access entropy of living biomass, we need an entropy balance, and, therefore, an energy balance. To create an energy balance, however, we need a mass balance, see [775, Section 4.8.1].

2. To create a mass balance, we need the strong homeostasis assumption: pools of metabolites that do not change in chemical composition. This excludes biochemical models that follow particular chemical compounds, because we need to follow all chemical compounds in an individual to create a mass balance, which is impossible. So the notion of pools of metabolites is unavoidable.

3. Given strong homeostasis, we need at least 2 pools. With a single pool, it will not be possible, for instance, to include (metabolic) memory, such as the nutritional status. [775, Section 1.1.3] gives additional arguments for why we minimally need 2 pools.

4. We need the weak homeostasis assumption, i.e. constant chemical composition of the whole body during growth in constant environments, to match stylized fact S2

in Table 11.2 and to access the chemical composition of the pools. If we cannot determine their chemical composition, we have a model that cannot be tested against reality on important traits, and we loose coherence with molecular biology.

5. Within the class of 2-pool models with weak homeostasis, the standard DEB model is the only one among the 21 topological alternatives that is consistent with a set of 8 stylized facts. See Section 11.4 of these comments and [859, 1343].

6. This still allows freedom in the relationship between food availability and ingestion rate. The Synthesizing Units, that DEB theory uses for specification [768], represent a very natural framework in the context of Markov processes, that can readily be extended to include behavioral modifications [536].

7. The final bit of freedom is how food intake relates to size. The DEB assumption that food intake is proportional to surface area has a nice link with underlying physics for transport, while the simplest, and parameter-free, way to relate surface area to volume results from the assumption of the standard DEB model that shape does not change during growth (isomorphy). This can readily be extended to include particular changes in shape during ontogeny, such as done to capture metabolic acceleration [778].

A remarkable observation in the context of lack of alternatives for the standard DEB model is that 26 popular empirical models for various aspects of metabolism turn out to be special cases of DEB models or very good numerical approximations, see [775, Table 11.1]. This suggests that the set of stylized facts constrain simple models more than is apparent on first sight, even without a formal context. Anyway, none of these modelers realized that they have been modeling different aspects of the same thing. It is, indeed, not self evident that the development of a bird egg [1146] has intimate relationships with the dynamics of (nutrient) cell quota of algae [358] and follow from the same set of assumptions.

Another remarkable observation is that the only way to access the entropy of living biomass, a notoriously difficult task indeed, is via the parameters of a DEB model. To get those parameters, we need to follow the individual throughout its life cycle and monitor what goes in and out. Gaps in knowledge of these dynamic budgets can partly be compensated with such (partial) knowledge of other species and/or estimate parameters in that context. DEB theory presently has quite a few handles for this, as demonstrated by the Add-my-Pet collection of over 2000 animal species.

It is possible, and frequently even necessary, as shown in many places [775], to extend the standard DEB model. Some details can be modified without much harm for the setup, such as the replacement of the assumption for maternal effect (i.e. the neonate has the reserve density of the mother at egg formation), but this costs at least an extra parameter and properties of such a model will be harder to analyze. Such minor modifications do not result in a really different model, in my opinion, but can be functional in particular cases.

What level of model complexity is actually required? The answer to this key question depends on the context of the research aims, so there is not a single answer. Simplicity is attractive for many reasons, but too much simplicity gives problems with reality. If

biodiversity cannot be accommodated, we also loose connection with the evolutionary context. Too much complexity, on the other hand, easily gives problems with practical applicability, since data will be lacking. [798] discusses the relationship between available data and parameters that can be estimated in the context of the standard DEB model, showing that the estimation of all primary parameters of the standard DEB model already frequently suffers from the problem of lack of data. While data completeness level 10 specifies the energy balance empirically, see [856], the mean completeness level in the AmP collection of 2026 animal species is only some 2.5, and the maximum one 6 at 2019/10/31. This motivated the development of context-based parameter estimation methods, while ideally all parameters should be determined accurately by data. This is presently way beyond scope. Much more complex models will have a strong tendency to be species-specific which hampers comparison with other species. They are also difficult to test and uncertainty about parameter values easily makes them useless.

In the document 'Basic methods for theoretical biology' and in [779], I warned for the 'Christmas tree syndrome': Just before Christmas, many people buy a Christmas tree for indoors; beautiful, but not beautiful enough. They start hanging balls, and other stuff, to enhance beauty, but if you continue too long with this, the Christmas tree will tumble over and you have nothing. The tree stands for the basic model structure, the balls for modules to include particular details. For me, the standard DEB model represents the tree without balls. My advice would be: don't forget to remove balls that are not needed (i.e. functional).

Bibliography

[1] K. Aagaard. Profundal chironimid populations during a fertilization experiment in Langvatn, Norway. *Holarct. Ecol.*, **5**:325–331, 1982.

[2] P. Abrams. Indirect interactions between species that share a predator: varieties of indirect effects. In W. C. Kerfoot and A. Sih, editors, *Predation; Direct and Indirect Impacts on Aquatic Communities*, pages 38–54. Univ. of New England Press, Hanover, 1987.

[3] R. A. Ackerman. Growth and gas exchange of embryonic sea turtles (*Chelonia*, *Caretta*). *Copeia*, **1981**:757–765, 1981.

[4] R. A. Ackerman. Oxygen consumption by sea turtle (*Chelonia*, *Caretta*) eggs during development. *Physiol. Zool.*, **54**:316–324, 1981.

[5] R. A. Ackerman, G. C. Whittow, C. V. Paganelli, and T. N. Pettit. Oxygen consumption, gas exchange, and growth of embryonic wedge-tailed shearwaters (*Puffinus pacificus chlororhynchus*). *Physiol. Zool.*, **53**:201–221, 1980.

[6] W. Agosta. *Bombardier Beetles and Fever Trees.* Addison Wesley, 1995.

[7] P. S. Agutter and J. A. Tuszynski. Analytic theories of allometric scaling. *J. Exp. Biol.*, **214**:1055–1062, 2011.

[8] V. Ahmadjian and S. Paracer. *Symbiosis; An Introduction to Biological Associations.* Univ. of New England Press, Hanover, 1986.

[9] D. L. Aksnes and J. K. Egge. A theoretical model for nutrient uptake in phytoplankton. *Mar. Ecol. Prog. Ser.*, **70**:65–72, 1991.

[10] A. H. Y. Al-Adhub and A. B. Bowers. Growth and breeding of *Dichelopandalus bonnieri* in Isle of Man Waters. *J. Mar. Biol. Assoc. U. K.*, **57**:229–238, 1977.

[11] M. Al-Habori. Macromolecular crowding and its role as intracellular signalling of cell volume regulation. *Int. J. Biochem. Cell Biol.*, **33**:844–864, 2001.

[12] A. W. H. Al-Hakim, M. I. A. Al-Mehdi, and A. H. J. Al-Salman. Determination of age, growth and sexual maturity of *Barbus grypus* in the Dukan reservoir of Iraq. *J. Fish Biol.*, **18**:299–308, 1981.

[13] O. Alda Alvarez, T. Jager, S. A. L. M. Kooijman, and J. E. Kammenga. Responses to stress of *Caenorhabditis elegans* populations with different reproductive strategies. *Func. Ecol.*, **19**:656–664, 2005.

[14] O. Alda Alvarez, T. Jager, E. Marco Redondo, and J. E. Kammenga. Assessing physiological modes of action of toxic stressors with the nematode *Acrobeloides nanus*. *Environ. Toxicol. Chem.*, **25**:3230–3237, 2006.

[15] M. Aleksiuk and I. M. Cowan. The winter metabolic depression in Arctic beavers (*Castor canadensis* Kuhl) with comparisons to California beavers. *Can. J. Zool.*, **47**:965–979, 1969.

[16] R. McN. Alexander. *Dynamics of Dinosaurs and Other Extinct Giants.* Columbia Univ, Press, New York, 1989.

[17] R. McN. Alexander. *Exploring Biomechanics; Animals in Motion.* Scientific American Library, New York, 1992.

[18] V. Y. Alexandrov. *Cells, Molecules and Temperature.* Springer-Verlag, Berlin, 1977.

[19] T. J. Algeo, S. E. Scheckler, and J. B. Maynard. Effects of the middle to late devonian spread of vascular land plants on weathering regimes, marine biotas, and global climate. In P. C. Gensel and D. Edwards, editors, *Plants Invade the Land; Evolutionary and Environmental Perspectives.* Columbio Univ. Press, New York, 2001.

[20] A. L. Alldredge. Abandoned larvacean houses. A unique food source in the pelagic environment. *Science*, **177**:885–887, 1972.

[21] A. L. Alldredge. Discarded appendicularian houses as sources of food, surface habitats and particulate organic matter in planktonic environments. *Limnol. Oceanogr.*, **21**:14–23, 1976.

[22] A. L. Alldredge. House morphology and mechanisms of feeding in *Oikopleuridae* (*Tunicata*, *Appendicularia*). *J. Zool. of Lond.*, **181**:175–188, 1977.

[23] F. Alonzo, P. Mayzaud, and S. Razouls. Egg production and energy storage in relation to feeding conditions in the subantarctic calanoid copepod *Drepanopus pectinatus*: an experimental study of reproductive strategy. *Mar. Ecol. Prog. Ser.*, **209**:231–242, 2001.

[24] J. P. Amend and E. L. Shock. Energetics of overall metabolic reactions of thermophilic and hyperthermophilic archaea and bacteria. *FEMS Microbiol. Rev.*, **25**:175–243, 2001.

[25] B. N. Ames, J. McCann, and E. Yamasaki. Methods for detecting carcinogens and mutagens with *Salmonella*/mammalian microsome mutagenicity test. *Mutat. Res.*, **31**:347–364, 1975.

[26] A. D. Anbar and A. H. Knoll. Proterozoic ocean chemistry and evolution: A bioinorganic bridge? *Science*, **1137**:1137–1142, 2002.

[27] J. S. Andersen, J. J. M. Bedaux, S. A. L. M. Kooijman, and H. Holst. The influence of design parameters on statistical inference in non-linear estimation; a simulation study based on survival data and hazard modelling. *J. Agric. Biol. Environ. Stat.*, **5**:323–341, 2000.

[28] R. A. Andersen. Biology and systematicss of heterokont and haptophyte algae. *Am. J. Bot.*, **91**:1508–1522, 2004.

[29] T. R. Andersen. *Pelagic Nutrient Cycles: Herbivores as Sources and Sinks.* Springer Verlag, Berlin, 1997.

[30] A. J. Anderson and E. A. Dawes. Occurrence, metabolism, metabolic control, and industrial uses of bacterial polyhydroxylkanoates. *Microbiol. Rev.*, **54**:450–472, 1990.

[31] S. G. E. Anderson, A. Zomorodipour, J. O. Andersson, T. Sicheritz-Pontén, U. C. M. Alsmark, R. M. Podowski, A. K. Näslund, A.-S. Eriksson, H. H. Winkler, and C. G. Kurland. The genome sequence of *Rickettsia prowazekii* and the origin of mitochondria. *Nature*, **396**:133–140, 1998.

[32] J. O. Andersson and A. J. Roger. A cyanobacterial gene in nonphotosynthetic protists; An early chloroplast acquisition in eukaryotes? *Curr. Biol.*, **12**:115–119, 2002.

[33] A. D. Ansell. Reproduction, growth and mortality of *Venus striatula* (Da Costa) in Kames Bay, Millport. *J. Mar. Biol. Assoc. U. K.*, **41**:191–215, 1961.

[34] M. E. F. Apol, R. S. Etienne, and H. Olff. Revisiting the evolutionary origin of allometric metabolic scaling in biology. *Funct. Ecol.*, **22**:1070–1080, 2008.

[35] T. M. Apostol. *Mathematical analysis.* Addison-Wesley Publishing co, Amsterdam, 1974.

[36] R. S. Appeldoorn. Variation in the growth rate of *Mya arenaria* and its relationship to the environment as analyzed through principal components analysis and the ω parameter of the von Bertalanffy equation. *J. Fish Biol.*, **81**:75–84, 1983.

[37] T. Appenzeller. Argentine dinos vie for heavyweight titles. *Science*, **266**:1085, 1994.

[38] A. Ar and H. Rahn. Interdependence of gas conductance, incubation length, and weight of the avian egg. In J. Piiper, editor, *Respiration Function in Birds.* Springer-Verlag, Berlin, 1978.

[39] K. Arbaĉiauskas and Z. Gasiūnaitė. Growth and fecundity of *Daphnia* after diapause and their impact on the development of a population. *Hydrobiologia*, **320**:209–222, 1996.

[40] R. Arking. *Biology of Aging.* Sinauer Assoc. Inc., Sunderland, Mass., 1998.

[41] E. A. Armstrong. *The Wren.* Collins, London, 1955.

[42] N. Armstrong, R. E. Chaplin, D. I. Chapman, and B. Smith. Observations on the reproduction of female wild and park Fallow deer (*Dama dama*) in southern England. *J. Zool. of Lond.*, **158**:27–37, 1969.

[43] D. K. Arrowsmith and C. M. Place. *An Introduction to Dynamical Systems.* Cambridge Univ. Press, 1990.

[44] D. K. Arrowsmith and C. M. Place. *Dynamical Systems. Differential Equations, Maps and Chaotic Behaviour.* Chapman & Hall, London, 1992.

[45] P. S. Ashton. Dipterocarp biology as a window to the understanding of tropical forest structure. *Ann Rev. Ecol. Syst.*, **19**:347–370, 1988.

[46] P. W. Atkins. *Physical Chemistry.* Oxford Univ. Press, 1989.

[47] P. W. Atkins. *Physical Chemistry.* Oxford Univ. Press, 1990.

[48] M. Atlas. The rate of oxygen consumption of frogs during embryonic development and growth. *Physiol. Zool.*, **11**:278–291, 1938.

[49] S. Augustine, B. Gagnaire, C. Adam, and S. A. L. M. Kooijman. Developmental energetics of zebrafish, Danio rerio. *Comp. Physiol. Biochem. A*, **159**:275–283, 2011.

[50] S. Augustine, K. Lika, and S. A. L. M. Kooijman. Altricial-precocial spectra in animal kingdom. *J. Sea Res*, **143**:27–34, 2019. .

[51] S. Augustine, K. Lika, and S. A. L. M. Kooijman. Why big-bodied animal species cannot evolve a waste-to-hurry strategy. *J. Sea Res.*, **143**:18–26, 2019. .

[52] S. Augustine, K. Lika, and S. A. L. M. Kooijman. The comparative energetics of the chondrichthyans reveals universal links between respiration, reproduction and life span. *J. Sea Res.*, **185**:1–20, 2022. .

[53] S. Augustine, M. K. Litvak, and S. A. L. M. Kooijman. Stochastic feeding in fish larvae and their metabolic handling of starvation. *J. Sea Res.*, **66**:411–418, 2011. .

[54] H. J. W. de Baar. Von Liebig's law of the minimum and plankton ecology. *Prog. Oceanogr.*, **33**:347–386, 1994.

[55] H. J. W. de Baar and P. W. Boyd. The role of iron in plankton ecology and carbon dioxide transfer of the global oceans. In R. B. Hanson, H. W. Ducklow, and J. G. Field, editors, *The Changing Ocean Carbon Cycle.*, pages 61–140. Cambridge Univ. Press, 2000.

[56] J. Baas, B. P. P. van Houte, C. A. M. van Gestel, and S. A. L. M. Kooijman. Modelling the effects of binary mixtures on survival in time. *Environ. Toxicol. Chem.*, **26**:1320–1327, 2007.

[57] J. Baas, T. Jager, and S. A. L. M. Kooijman. Estimation of no effect concentrations from exposure experiments when values scatter among individuals. *Ecotoxicol. Modell.*, **220**:411–418, 2009.

[58] J. Baas, T. Jager, and S. A. L. M. Kooijman. A model to analyze effects of complex mixtures on survival. *Ecotoxicol. Environ. Saf.*, **72**:669–676, 2009.

[59] J. Baas and S. A. L. M. Kooijman. Sensitivity of animals to chemical compounds links to metabolic rate. *Ecotoxicology*, **24**:657–663, 2015. .

[60] F. G. Bader. Analysis of double-substrate limited growth. *Biotechnol. Bioeng.*, **20**:183–202, 1978.

[61] T. Baekken. Growth patterns and food habits of *Baetis rhodani*, *Capnia pygmaea* and *Diura nanseni* in a west Norwegian river. *Holarct. Ecol.*, **4**:139–144, 1981.

[62] T. B. Bagenal. The growth rate of the hake, *Merluccius merluccius* (L.), in the Clyde and other Scottish sea areas. *J. Mar. Biol. Assoc. U. K.*, **33**:69–95, 1954.

[63] T. B. Bagenal. Notes on the biology of the schelly *Coregonus lavaretus* (L.) in Haweswater and Ullswater. *J. Fish Biol.*, **2**:137–154, 1970.

[64] J. E. Bailey and D. F. Ollis. *Biochemical Engineering Fundamentals.* McGraw-Hill, London, 1986.

[65] A.N. Baker, F.W.E. Rowe, and H.E.S. Clark. A new class of Echinodermata from New Zealand. *Nature*, **321**:862–864, 1986.

[66] B. Bakker. *Control and regulation of glycolysis in* Trypanosoma brucei. PhD thesis, Vrije Univ., 1998.

[67] R. Bakker. *The Dinosaur Heresies.* Longman, London, 1986.

[68] R. T. Bakker. Anatomical and ecological evidence of endothermy in dinosaurs. *Nature*, **238**:81–85, 1972.

[69] S. L. Baldauf, D. Bhattachary, J. Cockrill, P. Hugenholtz, and A. G. B. Pawlowski, J. ans Simpson. The tree of life. In J. Cracraft and M. J. Donoghue, editors, *Assembling the Tree of Life*, pages 43–75. Oxford Univ. Press, 2004.

[70] J. H. van Balen. A comparative study of the breeding ecology of the great tit *Parus major* in different habitats. *Ardea*, **61**:1–93, 1973.

[71] I. R. Ball and T. B. Reynoldson. *British planarians.*, volume 19 of *Synopses of the British Fauna.* Cambridge University Press, 1981.

[72] P. Ball. *A Biography of Water.* Weidenfeld & Nicolson, London, 1999.

[73] S. G. Ball and G. Peltier. The shaping and use of metabolic pathways in algae; Green factories. *Biochemical Journal Classic Papers*, **31**(3):20–23, 2009.

[74] H. Baltscheffsky. Energy conversion leading to the origin and early evolution of life: did inorganic pyrophosphate precede adenosine triphosphate? In H. Baltscheffsky, editor, *Origin and Evolution of Biological Energy Conversion.*, pages 1–9. VCH Publishers, Cambridge, 1996.

[75] M. Baltscheffsky, A. Schultz, and H. Baltscheffsky. H^+-PPases: a tightly membrane-bound family. *FEBS Letters*, **457**:527–533, 1999.

[76] C. A. M. Baltus. De effekten van voedselregime en lood op de eerste reproduktie van *Daphnia magna.* Technical report, Dienst DBW/RIZA, 1990.

[77] J. R. Banavar, M. E. Moses, J. H. Brown, J. Damuth, A. Rinaldo, R. M. Sibly, and A. Maritan. A general basis for quarter-power scaling in animals. *Proc. Natl. Acad. Sci. U. S. A.*, **107**:15816–15820, 2010.

[78] A. Bandyopadhyay, J. Stöckel, H. Min, L. A. Sherman, and H. B. Pakrasi. High rates of photobiological h_2 production by a cyanobacterium under aerobic conditions. *Nat. Comm.*, **1**(139):139, 2010. doi:10.1038/ncomms1139.

[79] M. C. Barber, L. A. Suárez, and R. R. Lassiter. Modeling bioconcentration of nonpolar organic pollutants by fish. *Environ. Toxicol. Chem.*, **7**:545–558, 1988.

[80] J. Barcroft, R. H. E. Elliott, L. B. Flexner, F. G. Hall, W. Herkel, E. F. McCarthy, T. McClurkin, and M. Talaat. Conditions of foetal respiration in the goat. *J. Physiol. (Lond.)*, **83**:192–214, 1935.

[81] D. R. Barneche, D. . Robertson, C. R. White, and D. J. Marshall. Fish reproductive-energy output increases disproportionately with body size. *Science*, **360**:642–645, 2018.

[82] C. Barreto, R. M. Albrecht, D. E. Bjorling, J. R. Horner, and N. J. Wilsman. Evidence of the growth plate and the growth of long bones in juvenile dinosaurs. *Science*, **262**:2020–2023, 1993.

[83] F. G. Barth. *Insects and Flowers.* Princeton Univ. Press, Princeton, 1991.

[84] G. A. Bartholomew and D. L. Goldstein. The energetics of development in a very large altricial bird, the brown pelican. In R. S. Seymour, editor, *Respiration and Metabolism of Embryonic Vertebrates*, pages 347–357. Dr. W. Junk Publishers, Dordrecht, 1984.

[85] I. V. Basawa and B. L. S. P. Rao. *Statistical Inference for Stochastic Processes.* Academic Press, London, 1980.

[86] G. C. Bateman and R. P. Balda. Growth, development, and food habits of young Pinon jays. *Auk*, **90**:39–61, 1973.

[87] J. F. Battey. Carbon metabolism in zooxanthellae-coelenterate symbioses. In W. Reisser, editor, *Algae and Symbioses*, pages 153–187. Biopress, Bristol, 1992.

[88] E. H. Battley. Calculation of entropy change accompanying growth of *Escherichia coli* K-12 on succinic acid. *Biotechnol. Bioeng.*, **41**:422–428, 1993.

[89] B. Baule. Zu Mitscherlichs Gesetz der physiologischen Beziehungen. *Landw. Jahrb.*, **51**:363–385, 1917.

[90] J. L. Baxter. A study of the yellowtail *Seriola dorsalis* (Gill). *Fish. Bull. (Dublin)*, **110**:1–96, 1960.

[91] B. L. Bayne, A. J. S. Hawkins, and E. Navarro. Feeding and digestion by the mussel *Mytilus edulis* L. (*Bivalvia*, *Mollusca*) in mixtures of silt and algal cells at low concentrations. *J. Exp. Mar. Biol. Ecol.*, **111**:1–22, 1987.

[92] B. L. Bayne, A. J. S. Hawkins, E. Navarro, and I. P. Iglesias. Effects of seston concentration on feeding, digestion and growth in the mussel *Mytilus edulis*. *Mar. Ecol. Prog. Ser.*, **55**:47–54, 1989.

[93] B. L. Bayne and R. C. Newell. Physiological energetics of marine molluscs. In A. S. M. Saleuddin and K. M. Wilbur, editors, *Physiology*, volume 4 of *The Mollusca*, chapter 1. Academic Press, London, 1983.

[94] M. J. Bazin and P. T. Saunders. Determination of critical variables in a microbial predator-prey system by catastrophe theory. *Nature*, **275**:52–54, 1978.

[95] T. D. Beacham and C. B. Murray. emperature, egg size, and development of embryos and alevins of 5 species of pacific salmon - a comparative-analysis. *Transactions of the American Fisheries Society*, **119**:927–945, 1990.

[96] R. C. Beason and E. C. Franks. Development of young horned larks. *Auk*, **90**:359–363, 1983.

[97] S. D. Beck and R. K. Bharadwaj. Reversed development and cellular aging in an insect. *Science*, **178**:1210–1211, 1972.

[98] J. R. Beddington. Mutual interference between parasites or predators and its effect on searching efficiency. *J. Anim. Ecol.*, **44**:331–340, 1975.

[99] W. N. Beer and J. J. Anderson. Modelling the growth of salmonid embryos. *J. theor. Biol.*, **189**:297–306, 1997.

[100] D. Beerling. *The Emerald Planet.* Oxford Univ. Press, 2007.

[101] D. J. Bell. *Mathematics of Linear and Nonlinear Systems.* Clarendon Press, Oxford, 1990.

[102] G. I. Bell and E. C. Anderson. Cell growth and division. *Biophys. J.*, **7**:329–351, 1967.

[103] P. J. L. Bell. Viral eukaryogenesis: was the ancestor of the nucleus a complex DNA virus? *J. Mol. Evol.*, **53**:251–256, 2001.

[104] P. J. L. Bell. Sex and the eukaryotic cell clycle is consistent with a viral ancestry for the eukaryotic nucleus. *J. theor. Biol.*, **243**:54–63, 2006.

[105] J. J. Beltrán, W. T. Butts, T. A. Olson, and M. Koger. Growth patterns of two lines of angus cattle selected using predicted growth parameters. *J Anim. Sci.*, **70**:734–741, 1992.

[106] S. Bengtson. *Early Life on Earth.* Columbia Univ. Press, New York, 1994.

[107] D. B. Bennett. Growth of the edible crab (*Cancer pagurus* L.) off south-west England. *J. Mar. Biol. Assoc. U. K.*, **54**:803–823, 1974.

[108] A. A. Benson and R. F. Lee. The role of wax in oceanic food chains. *Sci. Am.*, **3**:77–86, 1975.

[109] T. G. Benton, S. J. Plaistow, A. P. Beckerman, C. T. Lapsley, and S. Littlejohns. Changes in maternal investment in eggs can affect population dynamics. *Proc. R. Soc. Lond. Biol. Sci.*, **272**:1351–1356, 2005.

[110] J. Bereiter-Hahn. Behaviour of mitochondria in the living cell. *Int. Rev. Cytol.*, **122**:1–63, 1990.

[111] T. G. O. Berg and B. Ljunggren. The rate of growth of a single yeast cell. *Biotechnol. Bioeng.*, **24**:2739–2741, 1982.

[112] C. Bergmann. Über die Verhältnisse der Wärmeökonomie der Tiere zu ihrer Grösse. *Goett. Stud.*, **1**:595–708, 1847.

[113] H. Bergmann and H. Helb. *Stimmen der Vögel Europas.* BLV Verlagsgesellschaft, München, 1982.

[114] H. H. Bergmann, S. Klaus, F. Muller, and J. Wiesner. *Das Haselhuhn.* A. Ziemsen-Verlag, Wittenberg Lutherstadt, 1978.

[115] A. Bernard, C. Lécuyer, P. Vincent, R. Amiot, N. Bardet, E. Buffetaut, G. Cuny, F. Fourel, F. Martineau, J.-M. Mazin, and A. Prieur. Regulation of body temperature by some mesozoic marine reptiles. *Science*, **328**:1379–1382, 2010.

[116] C. Bernard, A. G. B. Simpson, and D. J. Patterson. Some free-living flagellates (Protista) from anoxic habitatats. *Ophelia*, **52**:113–142, 2000.

[117] J. Bernardo. Determinants of maturation in animals. *Trends Ecol. Evol.*, **8**:166–173, 1993.

[118] E. K. Berner and R. A. Berner. *Global Environment; Water, Air, and Geochemical Cycles.* Prentice-Hall, Englewood Cliffs, 1996.

[119] R. A. Berner. Atmospheric oxygen, tectonics and life. In S. H. Schneider and P. J. Boston, editors, *Scientists on Gaia.*, pages 161–173. MIT Press, Cambridge, Mass., 1991.

[120] D. R. Berry, editor. *Physiology of Industrial Fungi.* Blackwell Sci. Publ., Oxford, 1988.

[121] H. H. Berry. Hand-rearing lesser flamingos. In J. Kear and N. Duplaix-Hall, editors, *Flamingos.* T. & A. D. Poyser, Berkhamsted, 1975.

[122] L. von Bertalanffy. A quantitative theory of organic growth. *Hum. Biol.*, **10**:181–213, 1938.

[123] L. von Bertalanffy. Quantitative laws in metabolism and growth. *Q. Rev. Biol.*, **32**:217–231, 1957.

[124] L. von Bertalanffy. *General Systems Theory.* George Braziller, New York, 1968.

[125] L. von Bertalanffy. Basic concepts in quantitative biology of metabolism. *Helgol. Wiss. Meeresunters.*, **9**:5–34, 1969.

[126] J. Berthelin. Microbial weathering. In W. E. Krumbein, editor, *Microbial Geochemistry.*, pages 233–262. Blackwell Sci. Publ., Oxford, 1983.

[127] P. Berthold. Über den Einfluss der Nestlingsnahrung auf die Jugendentwickling, insbesondere auf das Flugelwachstum, bei der Mönchsgrasmücke (*Sylvia atricapilla*). *Vogelwarte*, **28**:257–263, 1976.

[128] D. F. Bertram and R. R. Strathmann. Effects of maternal and larval nutrition on growth and form of planktotrophic larvae. *Ecology*, **79**:315–327, 1998.

[129] J. Best. The influence on intracellular enzymatic properties for kinetics data obtained from living cells. *J. Cell. Comp. Physiol.*, **46**:1–27, 1955.

[130] J. J. Beun. *PHB metabolism and N-removal in sequencing batch granular sludge reactors.* PhD thesis, Univ. of Delft, 2001.

[131] R. J. H. Beverton and S. J. Holt. On the dynamics of exploited fish populations. *Fish. Invest. Ser. I*, **2**, 1957.

[132] R. J. Beyers. The metabolism of twelve aquatic laboratory microecosystems. *Ecol. Monogr.*, **33**:281–306, 1963.

[133] J. Bigay, P. Guonon, S. Robineau, and B. Antonny. Lipid packing sensed by arfgap1 couples copi coat disassembly to membrane bilayer curvature. *Nature*, **426**:563–566, 2003.

[134] R. Bijlsma. *De Boomvalk.* Kosmos, Amsterdam, 1980.

[135] R. J. Bijlsma. *Modelling whole-plant metabolism of carbon and nitrogen: a basis for comparative plant ecology and morphology.* PhD thesis, Vrije Univ., Amsterdam, 1999.

[136] T. Birkhead. *Great Auk Islands; a Field Biologist in the Arctic.* T. & A. D. Poyser, London, 1993.

[137] C. W. Birky. The inheritance of genes in mitochondria and chloroplasts: laws, mechanisms, and models. *Ann. Rev. Gen.*, **35**:125–148, 2001.

[138] E. C. Birney and D. D. Baird. Why do some mammals polyovulate to produce a litter of two? *Am. Nat.*, **126**:136–140, 1985.

[139] C. J. Bjerrum and D. E. Canfield. Ocean productivity before about 1.9 gyr ago limited by phosphorus adsorption onto iron oxides. *Nature*, **417**:159–162, 2002.

[140] D. G. Blackburn. Convergent evolution of viviparity, matrotrophy and specializations for fetal nutrition in reptiles and other vertebrates. *Am. Zool.*, **32**:313–321, 1992.

[141] F. F. Blackman. Optima and limiting factors. *Ann. Bot.*, **19**:281–295, 1905.

[142] W. U. Blanckenhorn and A. Heyland. The quantitative genetics of two life history trade-offs in the yellow dung fly in abundant and limited food environments. *Evol. Ecol.*, **18**:385–402, 2004.

[143] W. Bland and D. Rolls. *Weathering; an Introduction to the Scientific Principles.* Arnold, London, 1998.

[144] R. E. Blankenship and H. Hartman. Origin and early evolution of photosynthesis. *Photosynth. Res.*, **33**:91–111, 1992.

[145] R. E. Blankenship and H. Hartman. The origin and evolution of oxygenic photosynthesis. *Trends Biochem. Sci.*, **23**:94–97, 1998.

[146] J. H. S. Blaxter and J. R. Hunter. The biology of the clupoid fishes. In J. H. S. Balxter, F. S. Russell, and M. Yonge, editors, *Advances in Marine Biology*, volume 20, pages 1–223. Academic Press, London, 1982.

[147] K. Blaxter. *Energy Metabolism in Animals and Man.* Cambridge Univ. Press, 1989.

[148] C. I. Bliss. The method of probits. *Science*, **79**:38–39, 1934.

[149] J. Blondel and J. Aronson. *Biology and Wildlife of the Mediterranean Region.* Oxford University Press, Oxford, 1999.

[150] H. Blumel. *Die Rohrammer.* A. Ziemsen-Verlag, Wittenberg Lutherstadt, 1982.

[151] M. P. Boer. *The dynamics of tri-trophic food chains.* PhD thesis, Vrije Univ., Amsterdam, 2000.

[152] M. P. Boer, B. W. Kooi, and S. A. L. M. Kooijman. Food chain dynamics in the chemostat. *Math. Biosci.*, **150**:43–62, 1998.

[153] M. P. Boer, B. W. Kooi, and S. A. L. M. Kooijman. Homoclinic and heteroclinic orbits in a tri-trophic food chain. *J. Math. Biol.*, **39**:19–38, 1999.

[154] M. P. Boer, B. W. Kooi, and S. A. L. M. Kooijman. Multiple attractors and boundary crises in a tri-trophic food chain. *Math. Biosci.*, **169**:109–128, 2001.

[155] M. D. Boersma. Offspring size and parental fitness in *Daphnia magna*. *Evol. Ecol.*, **11**:439–450, 1997.

[156] P. D. Boersma, N. T. Wheelwright, M. K. Nerini, and E.S. Wheelwright. The breeding biology of the fork-tailed storm-petrel (*Oceanodroma furcata*). *Auk*, **97**:268–282, 1980.

[157] C. L. Boggs and C. L. Ross. The effect of adult food limitation on life-history traits in *Speyeria mormonia* (Lepidoptera, Nymphalidae). *Ecology*, **74**:433–441, 1993.

[158] S. Bohlken and J. Joosse. The effect of photoperiod on female reproductive activity and growth of the fresh water pulmonate snail *Lymnaea stagnalis* kept under laboratory conditions. *Int. J. Invertebr. Reprod.*, **4**:213–222, 1982.

[159] C. Bohr and K. A. Hasselbalch. Über die Kohlensäureproduction des Hühnerembryos. *Skand. Arch. Physiol.*, **10**:149–173, 1900.

[160] R. Bommarco. Stage sensitivity to food limitation far a generalist arthropod predator, *Pterostichus cupreus* (Coleoptera: Carabidae). *Environ. Entomol.*, **27**:863–869, 1998.

[161] J. T. Bonner. *Size and Cycle: an Essay on the Structure of Biology.* Princeton Univ. Press, 1965.

[162] T. A. Bookhout. Prenatal development of snowshoe hares. *J. Wildl. Manage.*, **28**:338–345, 1964.

[163] W. Booth and G.W. Schuett. Molecular genetic evidence for alternative reproductive strategies in North American pitvipers (Serpentes: Viperidae): long-term sperm storage and facultative parthenogenesis. *Biol. J. Linn. Soc.*, **104**:934–942, 2011.

[164] T. Borchardt. Influence of food quantity on the kinetics of cadmium uptake and loss via food and seawater in *Mytilus edulis*. *Mar. Biol.*, **76**:67–76, 1983.

[165] T. Borchardt. Relationships between carbon and cadmium uptake in *Mytilus edulis*. *Mar. Biol.*, **85**:233–244, 1985.

[166] F. van den Bosch. *The velocity of spatial population expansion.* PhD thesis, Univ. of Leiden, 1990.

[167] F. van den Bosch, J. A. J. Metz, and O. Diekmann. The velocity of spatial population expansion. *J. Math. Biol.*, **28**:529–565, 1990.

[168] Y. Bourles, M. Alunno-Bruscia, S. Pouvreau, G. Tollu, D. Leguay, C. Arnaud, P. Goulletquer, and S. A. L. M. Kooijman. Modelling growth and reproduction of the pacific oyster *Crassostrea gigas*: application of the oyster-DEB model in a coastal pond. *J. Sea Res.*, **62**:62–71, 2009.

[169] A. B. Bowers. Breeding and growth of whiting (*Gadus merlangus* L.) in Isle of Man waters. *J. Mar. Biol. Assoc. U. K.*, **33**:97–122, 1954.

[170] A. J. Boyce, M. L. Coleman, and M. J. Russell. Formation of fossil hydrothermal chimneys and mounds from Silvermines, Ireland. *Nature*, **306**:545–550, 1983.

[171] C. R. Boyden. Trace element content and body size in molluscs. *Nature*, **251**:311–314, 1974.

[172] D. F. Bradford and R. S. Seymour. Influence of water potential on growth and survival of the embryo, and gas conductance of the egg, in a terrestrial breeding frog, *Pseudophryne bibroni*. *Physiological Zoology*, **61**:470–474., 1988.

[173] A. E. Brafield and M. J. Llewellyn. *Animal Energetics.* Blackie, Glasgow, 1982.

[174] B. W. Brandt. *Realistic characterizations of biodegradation.* PhD thesis, Vrije Univ., Amsterdam, 2002.

[175] B. W. Brandt, F. D. L. Kelpin, I. M. M. van Leeuwen, and S. A. L. M. Kooijman. Modelling microbial adaptation to changing availability of substrates. *Water Res.*, **38**:1003–1013, 2004.

[176] B. W. Brandt and S. A. L. M. Kooijman. Two parameters account for the flocculated growth of microbes in biodegradation assays. *Biotechnol. Bioeng.*, **70**:677–684, 2000.

[177] B. W. Brandt, I. M. M. van Leeuwen, and S. A. L. M. Kooijman. A general model for multiple substrate biodegradation. Application to co-metabolism of non structurally analogous compounds. *Water Res.*, **37**:4843–4854, 2003.

[178] A. M. Branta. Studies on the physiology, genetics and evolution of some *Cladocera*. Technical report, Carnegie Institute, Washington, 1939.

[179] G. B. Brasseur, J. J. Orlando, and G. S. Tyndall. *Atmospheric Chemistry and Global Change.* Oxford Univ. Press, 1999.

[180] D. Brawand, W. Wahli, and H. Kaessmann. Loss of egg yolk genes in mammals and the origin of lactation and placentation. *PLoS Biol.*, **6**:0507–0517, 2008.

[181] P. R. Bregazzi and C. R. Kennedy. The biology of pike, *Esox lucius* L., in southern eutrophic lake. *J. Fish Biol.*, **17**:91–112, 1980.

[182] W. W. Brehm. Breeding the green-billed toucan at the Walsrode Bird park. *Int. Zoo Yearb.*, **9**:134–135, 1969.

[183] H. Bremer and P. P. Dennis. Modulation of chemical composition and other parameters of the cell by growth rate. In F. C. Neidhardt, editor, Escherichia coli *and* Salmonella typhimurium, pages 1527–1542. Am. Soc. Microbiol., Washington, 1987.

[184] H. Brendelberger and W. Geller. Variability of filter structures in eight *Daphnia* species: mesh sizes and filtering areas. *J. Plankton Res.*, **7**:473–486, 1985.

[185] J. R. Brett. The relation of size to rate of oxygen consumption and sustained swimming speed of sockeye salmon (*Oncorhynchus nerka*). *J. Fish. Res. Board Can.*, **22**:1491–1497, 1965.

[186] T. Brey, C. Müller-Wiegmann, Z. M. C. Zittier, and W. Hagen. Body composition in aquatic organisms - a global data bank of relationships between mass, elemental composition and energy content. *J. Sea Res.*, **64**:334–340, 2010.

[187] F. H. van den Brink. *Zoogdierengids*. Elsevier, Amsterdam, 1955.

[188] I. L. Brisbin Jr and L. J. Tally. Age-specific changes in the major body components and caloric value of growing Japanese quail. *Auk*, **90**:624–635, 1973.

[189] C Brochier-Armanet, S. Gribaldo, and P Forterre. A DNA topoisomerase ib in Thaumarchaeota testifies for the presence of this enzyme in the last common ancestor of Archaea and Eucarya. *Biol. Direct*, **3**:54, 2008.

[190] J. J. Brocks, G. A. Logan, R. Buick, and R. E. Summons. Archean molecular fossils and the early rise of eukaryotes. *Science*, **285**:1033–1036, 1999.

[191] J. M. Brockway, J.D. McDonald, and J. D. Pullar. The energy cost of reprodction in sheep. *J. Physiol.*, **167**:318–327, 1963.

[192] S. Brody. *Bioenergetics and Growth.* Rheinhold, New York, 1945.

[193] S. Broekhuizen. *Hazen in Nederland.* PhD thesis, Landbouw Hogeschool, Wageningen, 1982.

[194] L. T. Brooke, D. J. Call, and L. T. Brooke. *Acute Toxicities of Organic Chemicals to Fathead Minnow (*Pimephlus promelas*)*, volume IV of *Center for Lake Superior Environmental Studies*. Univ. of Wisconsin USA, 1988.

[195] L. T. Brooke, D. J. Call, and L. T. Brooke. *Acute Toxicities of Organic Chemicals to Fathead Minnow (*Pimephlus promelas*)*, volume V of *Center for Lake Superior Environmental Studies*. Univ. of Wisconsin USA, 1990.

[196] L. T. Brooke, D. L. Geiger, D. J. Call, and C. E. Northcott. *Acute Toxicities of Organic Chemicals to Fathead Minnow (*Pimephlus promelas*)*, volume I of *Center for Lake Superior Environmental Studies*. Univ. of Wisconsin USA, 1984.

[197] L. T. Brooke, S. H. Poirrier, and D. J. Call. *Acute Toxicities of Organic Chemicals to Fathead Minnow (*Pimephlus promelas*)*, volume III of *Center for Lake Superior Environmental Studies*. Univ. of Wisconsin USA, 1986.

[198] M. Brooke. *The Manx Shearwater*. T. & A. D. Poyser, London, 1990.

[199] J. L. Brooks and S. I. Dodson. Predation, body size, and composition of plankton. *Science*, **150**:28–35, 1965.

[200] S. P. J. Brooks, A. de Zwaan, G. van den Thillart, O. Cattani, and Corti. Differential survival of *Venus gallina* and *Scapharca inaequivalvis* during anoxic stress: covalent modification of phosphofructokinase and glycogen phosphorylase during anoxia. *J. Comp. Physiol.*, **161**:207–212, 1991.

[201] D. J. Brousseau. Analysis of growth rate in *Mya arenaria* using the von Bertalanffy equation. *Mar. Biol.*, **51**:221–227, 1979.

[202] E. Brouwer. On simple formulae for calculating the heat expenditure and the quantities of carbohydrate and fat metabolized in ruminants from data on gaseous exchange and urine N. In *1st Symp. on Energy Metabolism*, pages 182–194. European association for animal production, Rome, 1958.

[203] R. Brouwer and C. T. de Wit. A simulation model of plant grwoth with special attention to root growth and its consequences. In W. J. Whittington, editor, *Root Growth*, pages 224–279. Butterworth, London, 1969.

[204] L. W. Browder, C. A. Erickson, and Jeffery W. R. *Developmental Biology*. Saunders College Publishing, Philadelphia, 1991.

[205] G. H. Brown and J. J. Wolken. *Liquid Crystals and Biological Structures.* Academic Press, New York, 1979.

[206] J. H. Brown, J. F. Gillooly, A. P. Allen, V. M. Savage, and G. B. West. Toward a metabolic theory of ecology. *Ecology*, **85**:1771–1789, 2004.

[207] M. E. Brown. Experimental studies on growth. In M. E. Brown, editor, *The Physiology of Fishes*, volume 1, page 361. Academic Press, San Diego, 1957.

[208] W. Y. Brown. Growth and fledging age of sooty tern chicks. *Auk*, **93**:179–183, 1976.

[209] W. A. Bruggeman, L. B. J. M. Martron, D. Kooiman, and O. Hutzinger. Accumulation and elimination kinetics of di-, tri-and tetra chlorobiphenyls by goldfish after dietary and aqueous exposure. *Chemosphere*, **10**:811–832, 1981.

[210] L. W. Bruinzeel and T. Piersma. Cost reduction in the cold: heat generated by terrestrial locomotion partly substitutes for thermoregulation costs in knot *Calidris canutus*. *Ibis*, **140**:323–328, 1998.

[211] B. Bruun. *Gids voor de Vogels van Europa.* Elsevier, Amsterdam, 1970.

[212] C. Bryant. *Metazoan Life without Oxygen.* Chapman & Hall, London, 1991.

[213] M. M. Bryden. Growth of the south elephant seal *Mirounga leonina* (Linn.). *Growth*, **33**:69–82, 1969.

[214] T. L. Bucher. Parrot eggs, embryos, and nestlings: patterns and energetics of growth and development. *Physiol. Zool.*, **56**:465–483, 1983.

[215] L. J. Buckley. RNA-DNA ratio: an index of larval fish growth in the sea. *Mar. Biol.*, **80**:291–298, 1984.

[216] J. J. Bull. Sex determination mechanisms: an evolutionary perspective. In S. C. Stearns, editor, *The Evolution of Sex and Its Consequences*, pages 93–114. Birkhäuser, Basel, 1987.

[217] P. C. Bull and A. H. Whitaker. The amphibians, reptiles, birds and mammals. In G. Kuschel, editor, *Biogeography and Ecology in New Zealand*, pages 231–276. W. Junk b.v., Den Haag, 1975.

[218] B. A. Bulthuis. *Stoichiometry of growth and product-formation by* Bacillus licheniformis. PhD thesis, Vrije Univ., Amsterdam, 1990.

[219] S. Bunney. Some dinosaurs liked it cold. *New Sci.*, (8 April):27, 1989.

[220] C. W. Burns. The relationship between body size of filterfeeding cladocera and the maximum size of particles ingested. *Limnol. Oceanogr.*, **13**:675–678, 1968.

[221] S. S. Butcher, R. J. Charlson, G. H. Orians, and G. V. Wlofe. *Global Biochemical Cycles.* Academic Press, London, 1992.

[222] D. K. Button. Biochemical basis for whole-cell uptake kinetics: specific affinity, oligotrophic capacity, and the meaning of Michaelis constant. *Appl. Environ. Microbiol.*, **57**:2033–2038, 1991.

[223] M. Byrne. Viviparity and intragonadal cannibalism in the diminutive asterinid sea stars *Patiriella vivipara* and *P. parvivipara*. *Mar. Biol.*, **125**:551–567, 1996.

[224] P. L. Cadwallader and A. K. Eden. Food and growth of hatchery-produced chinook-salmon, *Oncorhynchus tschawytscha* (Walbaum), in landlocked lake Purrumbete, Victoria, Australia. *J. Fish Biol.*, **18**:321–330, 1981.

[225] A. G. Cairns-Smith, A. J. Hall, and M. J. Russell. Mineral theories of the origin of life and an iron sulphide example. *Origins Life Evol. Biosphere*, **22**:161–180, 1992.

[226] W. A. Calder III. The kiwi and egg design: evolution as a package deal. *Bioscience*, **29**:461–467, 1979.

[227] W. A. Calder III. *Size, Function and Life History.* Harvard Univ. Press, 1984.

[228] P. Calow and C. R. Townsend. Resource utilization in growth. In C. R. Townsend and P. Calow, editors, *Physiological Ecology*, pages 220–244. Blackwell Sci. Publ., 1981.

[229] N. Cameron. *The Measurement of Human Growth.* Croom Helm, London, 1984.

[230] R. N. Campbell. The growth of brown trout, *Salmo trutta* L. in northern Scottish lochs with special reference to the improvement of fisheries. *J. Fish Biol.*, **3**:1–28, 1971.

[231] D. E. Canfield, K. S. Habicht, and B. Thamdrup. The archean sulfur cycle and the early histroy of atmospheric oxygen. *Science*, **288**:658–661, 2000.

[232] H. Canter-Lund and J. W. G. Lund. *Freshwater Algae; Their Microscopic World Explored.* Biopress Ltd, Bristol, 1995.

[233] J. F. M. F. Cardoso. *Growth and reproduction in bivalves.* PhD thesis, Groningen Univ., 2007.

[234] J. F. M. F. Cardoso, H. W. van der Veer, and S. A. L. M. Kooijman. Body size scaling relationships in bivalves: a comparison of field data with predictions by dynamic energy budgets (DEB theory). *J. Sea Res.*, **56**:125–139, 2006.

[235] T. J. Case. Speculations on the growth rate and reproduction of some dinosaurs. *Paleobiol.*, **4**:320–328, 1978.

[236] M. Cashel and K. E. Rudd. The stringent response. In F. C. Neidhardt, editor, Escherichia coli *and* Salmonella typhimurium, volume 2, pages 1410–1438. Am. Soc. Microbiol., 1987.

[237] T. Cavalier-Smith. The origin of cells, a symbiosis between genes, catalysts and membranes. *Cold Spring Harbor Symp. on Quant. Biol.*, **52**:805–824, 1987.

[238] T. Cavalier-Smith. A revised six-kingdom system of life. *Biol. Rev.*, **73**:203–266, 1998.

[239] T. Cavalier-Smith. Membrane heredity and early chloroplast evolution. *Trends Plant Sci.*, **5**:174–182, 2000.

[240] T. A. Cavalier-Smith. Chloroplast evolution: Secondary symbiogenesis and multiple losses. *Curr. Biol.*, **12**:R62–R64, 2002.

[241] T. A. Cavalier-Smith. The phagotrophic origin of eukaryotes and phylogenetic classification of protozoa. *Int. J. Syst. Evol. Microbiol.*, **52**:297–354, 2002.

[242] L. Cazzador. Analysis of oscillations in yeast continuous cultures by a new simplified model. *Bull. Math. Biol.*, **53**:685–700, 1991.

[243] F. Chai, S. T. Lindley, J. R. Toggweiler, and R. R. Barber. Testing the importance of iron and grazing in the maintenance of the hogh nitrate condition in the equatorial pacific ocean: a physical-biological model study. In *The Changing Ocean Carbon Cycle.*, pages 155–186. Cambridge Univ. Press, 2000.

[244] G. Chapelle and L. Peck. Polar gigantism dictated by oxygen availability. *Nature*, **399**:114–115, 1999.

[245] D. J. Chapman and J. W. Schopf. Biological and chemical effects of the development of an aerobic environment. In J. W. Schopf, editor, *Earth's Earliest Biosphere: Its Origin and Evolution*, pages 302–320. Princeton, New York, 1983.

[246] S. Charlat and H. Mercot. *Wolbachia*, mitochondria and sterility. *Trends Ecol. Evol.*, **16**:431–432, 2001.

[247] R.J. Charlson. The vanishing climatic role of dimethyl sulfide. In G. M. Woodwell and F. T. Mackenzie, editors, *Biotic Feedbacks in the Global Climatic System.*, pages 251–277. Oxford Univ. Press, 1995.

[248] E. L. Charnov and D. Berrigan. Dimensionless numbers and the assembly rules for life histories. *Phil. Trans. R. Soc. Lond. B Biol. Sci.*, **332**:41–48, 1991.

[249] F. F. Chehab, K. Mounzih, R. Lu, and M. E. Lim. Early onset of reproductive function in normal female mice treated with leptin. *Science*, **275**:88–90, 1997.

[250] J. Chela-Flores. First step in eukaryogenesis: Physical phenomena in the origin and evolution of chromosome structure. *Origins Life Evol. Biosphere*, **28**:215–225, 1998.

[251] C. M. Chester. The effect of adult nutrition on the reproduction and development of the estuarine nudibranch, *Tenellia adspersa* (nordmann, 1845). *J. Exp. Mar. Biol. Ecol.*, **198**:113–130, 1996.

[252] S. G. Cheung and S. Lam. Effect of food availability on egg production and packaging in the intertidal scavenging gastropod *Nassarius festivus*. *Mar. Biol.*, **135**:281–287, 1999.

[253] L. Chistoserdova, C. Jenkins, M. G. Kalyuzhnaya, C. J. Marx, A. Lapidus, J. A. Vorholt, J. T. Stanley, and M. E. Lidstrom. The enigmatic Planctomycetes may hold a key to the origins of metanogenesis and methylotrophy. *Mol. Biol. Evol.*, **21**:1234–1241, 2004.

[254] D. Chivian, E. L. Brodie, et al. Environmental genomics reveals a single-species ecosystem deep within earth. *Science*, **322**:275–278, 2008.

[255] K. Christoffersen and A. Jespersen. Gut evacuation rates and ingestion rates of *Eudiaptomus graciloides* measured by means of gut fluorescence method. *J. Plankton Res.*, **8**:973–983, 1986.

[256] D. Claessen, A. M. de Roos, and L. Persson. Dwarfs and giants: cannibalism and competition in size-structured populations. *Am. Nat.*, **155**:219–237, 2008.

[257] B. M. Clark, N. F. Mangelson, L. L. St. Clair, L. B. Rees, G. S. Bench, and J. R. Southon. Measurement of age and growth rate in the crustose saxicolous lichen *Caloplaca trachyphylla* using ^{14}C accelerator mass spectrometry. *The Lichenologist*, **32**:399–403, 2000.

[258] T. D. Clark and A. P. Farrell. Effects of body mass on physiological and anatomical parameters of mature salmon: evidence against a universal heart rate scaling exponent. *J. Exp. Biol.*, **214**:887–893, 2011.

[259] A. Clarke. Temperature and embryonic development in polar marine invertebrates. *Int. J. Invertebr. Reprod.*, **5**:71–82, 1982.

[260] A. Clarke. *Principles of thermal ecology; Temperature, energy and life.* Oxford Univ. Press, Oxford, 2017.

[261] D. H. Clayton and J. Moore. *Host-parasite Evolution; General Principles & Avian Models.* Oxford Univ. Press, 1997.

[262] G. A. Clayton, C. Nixey, and G. Monaghan. Meat yield in turkeys. *Br. Poult. Sci.*, **19**:755–763, 1978.

[263] J. H. L. Cloethe. Prenatal growth in the merino sheep. *Onderstepoort J. Vet. Sci. Anim. Ind.*, **13**:417–558, 1939.

[264] H. M. Cochemé and M. P. Murphy. Mitochondria as a source of ROS. *Biochemical Journal Classic Papers*, **31**(3):28–31, 2009.

[265] J. F. Collins and M. H. Richmond. Rate of growth of *Bacillus cereus* between divisions. *J. Gen. Microbiol.*, **28**:15–33, 1962.

[266] R. Coma, M. Ribes, J.-M. Gili, and M. Zabala. Seasonality in coastal benthic ecosystems. *TREE*, **15**:448–453, 2000.

[267] A. Comfort. *The Biology of Senescence.* Churchill Livingstone, Edinburgh, 1979.

[268] A. Comfort. Effect of delayed and resumed growth on the longevity of a fish (*Lebistes reticulatus* Peters) in captivity. *Gerontologia (Basel)*, **8**:150–155, 1983.

[269] J. D. Congdon, D. W. Tinkle, and P. C. Rosen. Egg components and utilization during development in aquatic turtles. *Copeia*, **1983**:264–268, 1983.

[270] D. W. Connell and D. W. Hawker. Use of polynomial expressions to describe the bioconcentration of hydrophobic chemicals by fish. *Ecotoxicol. Environ. Saf.*, **16**:242–257, 1988.

[271] R. J. Conover. Transformation of organic matter. In O. Kinne, editor, *Marine Ecology.* J. Wiley, Chichester, 1978.

[272] G. D. Constanz. Growth of nestling rufous hummingbirds. *Auk*, **97**:622–624, 1980.

[273] C. L. Cooney, D. I. C. Wang, and R. I. Mateles. Measurement of heat evolution and correlation with oxygen consumption during microbial growth. *Biotechnol. Bioeng.*, **11**:269–281, 1968.

[274] S. Cooper. The constrained hoop: an explanation of the overschoot in cell length during a shift-up of *Escherichia coli*. *J. Bacteriol.*, **171**:5239–5243, 1989.

[275] A. Coors, M. Hammers-Wirtz, and H. T. Ratte. Adaptation to environmental stress in *Daphnia magna* simultaneously exposed to a xenobiotic. *Chemosphere*, **56**:395–404, 2004.

[276] P. S. Corbet. Stadia and growth ratios of odonata: a review. *International Journal of Odonatology*, **5**:45–73, 2002.

[277] J. D. Coronios. Development of behaviour in fetal cat. *Genet. Psychol. Monogr.*, **14**:283–330, 1933.

[278] R. R. Coutts and I. W. Rowlands. The reproductive cycle of the Skomer vole (*Clethrionomys glareolus skomerensis*). *J. Zool. of Lond.*, **158**:1–25, 1969.

[279] D. R. Cox. *Renewal Theory.* Methuen, London, 1962.

[280] D. R. Cox and D. Oakes. *Analysis of survival data.* Chapman & Hall, London, 1984.

[281] R. C. Crabtree and F. A. Bazzaz. Seedling response of four birch species to simulated nitrogen deposition - ammonium versus nitrate. *Ecol. Appl.*, **3**:315–321, 1993.

[282] D. Cragg-Hine and J. W. Jones. The growth of dace *Leuciscus leuciscus* (L.), roach *Rutilus rutilus* (L.) and chub *Sqalius cephalus* (L.) in Willow Brook, Northhamptonshire. *J. Fish Biol.*, **1**:59–82, 1969.

[283] J. F. Craig. A note on growth and mortality of trout, *Salmo trutta* L., in afferent streams of Windermere. *J. Fish Biol.*, **20**:423–429, 1982.

[284] G. Creutz. *Der Weiss-storch.* A. Ziemsen-Verlag, Wittenberg Lutherstadt, 1985.

[285] E. G. Crichton. Aspects of reproduction in the genus *Notomys* (*Muridae*). *Austral. J. Zool.*, **22**:439–447, 1974.

[286] R. E. Criss. *Principles of Stable Isotope Distribution.* Oxford Univ. Press, New York, 1999.

[287] N. Cronberg, R. Natcheva, and K. Hedlund. Microarthropods mediate sperm transfer in mosses. *Science*, **313**:1255, 2006.

[288] J. R. Cronmiller and C. F. Thompson. Experimental manipulation of brood size in red- winged blackbirds. *Auk*, **97**:559–565, 1980.

[289] C. J. Crossland and D. J. Barnes. The role of metabolic nitrogen in coral calcification. *Mar. Biol.*, pages 325–332, 1974.

[290] T. J. Crowley and G. R. North. *Paleoclimatology.* Oxford Univ. Press, 1991.

[291] H. Crum. *A Focus on Peatlands and Peat Mosses.* Univ. of Michican Press, Ann Abor, 1992.

[292] E. H. Curtis, J. J. Beauchamp, and B. G. Blaylock. Application of various mathematical models to data from the uptake of methyl mercury in bluegill sunfish (*Lepomis macrochirus*). *Ecol. Modell.*, **3**:273–284, 1977.

[293] J. M. Cushing. *An Introduction to Structured Population Dynamics.* SIAM, Philadelphia, 1998.

[294] J. Cuzin-Roudy and F. Buchholz. Ovarian development and spawning in relation the the moulting cycle in northern krill, (meganyctiphanes norvegica) (crustacea: Euphrasiacea), along a climatic gradient. *Mar. Biol*, **133**:267–281, 1999.

[295] H. Cyr and M. L. Pace. Allometric theory: extrapolations from individuals to communities. *Ecology*, **74**:1234–1245, 1993.

[296] J. B. Dacks and M. C. Field. Evolution of the eukaryotic mambrane-trafficking system: origin, tempo and mode. *J. Cell Sci.*, **120**:2977–2985, 2007.

[297] W. B. Dade, P. A. Jumars, and D. L. Penry. Supply-side optimization: maximizing absorptive rates. In R. N. Hughes, editor, *Behavioural Mechanisms of Food Selection*, volume 20, pages 531–555. Springer-Verlag, Berlin, 1990.

[298] M. J. Dagg. Complete carbon and nitrogen budgets for the carnivorous amphipod, *Calliopius laeviusculus* (Kroyer). *Int. Rev. Gesamten Hydrobiol.*, **61**:297–357, 1976.

[299] T. Dalsgaard, D. E. Canfield, J. Petersen, B. Thamdrup, and J. Acuna-Gonzalez. N-2 production by the anammox reaction in the anoxic water column of Golfo Dulce, Costa Rica. *Nature*, **422**:606–608, 2003.

[300] J. D. Damuth. Of size and abundance. *Nature*, **351**:268–269, 1991.

[301] J. D. Damuth. Taxon-free characterization of animal comminuties. In A. K. Behrensmeyer, J. D. Damuth, W. A. DiMichele, R. Potts, H.-D. Sues, and S. L. Wing, editors, *Terrestrial Ecosystems Through Time; Evolutionary Paleoecology of Terrestrial Plants and Animals.*, pages 183–203. Univ. of Chicago Press, 1992.

[302] N. Dan and S. E. R. Bailey. Growth, mortality, and feeding rates of the snail *Helix aspersa* at different population densities in the laboratory, and the depression of activity of helicid snails by other individuals, or their mucus. *J. Molluscan Stud.*, **48**:257–265, 1982.

[303] M. C. Dash and A. K. Hota. Density effects on the survival, growth rate, and metamorphosis of *Rana tigrina* tadpoles. *Ecology*, **61**:1025–1028, 1980.

[304] H. A. David and M. L. Moeschberger. *The Theory of Competing Risks.* C. Griffin & Co Ltd, 1978.

[305] P. J. Davoll and M. W. Silver. Marine snow aggregates: life history sequence and microbial community of abandoned larvacean houses from Monterey Bay, California. *Mar. Ecol. Prog. Ser.*, **33**:111–120, 1986.

[306] E. A. Dawes. The constrained hoop: an explanation of the overschoot in cell length during a shift-up of *Escherichia coli*. In T. R. Gray and J. R. Postgate, editors, *The Survival of Vegetative Microbes*, pages 19–53. Cambridge Univ. Press, 1976.

[307] W. R. Dawson. Evaporative losses of water by birds. *Biochem. Physiol.*, **71**:495–509, 1982.

[308] D. W. Deamer and R. M. Pashley. Amphiphilic components of the murchison carbonaceous chondrite; surface properties and membrane formation. *Orig. Life Evol. Biosphere*, **19**:21–38, 1989.

[309] J. Dean. *Lange's Handbook of Chemistry*. McGraw-Hill, 12^{th} Ed., New York, NY, 1979.

[310] D. L. DeAngelis, R. A. Goldstein, and R. V. O'Neill. A model for trophic interaction. *Ecology*, **56**:881–892, 1975.

[311] D. L. DeAngelis and L. J. Gross, editors. *Individual-Based Models and Approaches in Ecology*. Chapman & Hall, London, 1992.

[312] D. C. Deeming and M. W. J. Ferguson. Environmental regulation of sex determination in reptiles. *Phil. Trans. R. Soc. Lond. B Biol. Sci.*, **322**:19–39, 1988.

[313] D. C. Deeming and M. W. J. Ferguson. Effects of incubation temperature on growth and development of embryos of *Alligator mississippiensis*. *J. Comp. Physiol.*, **B159**:183–193, 1989.

[314] T. E. DeLaca, D. M. Karl, and J. H. Lipps. Direct use of dissolved organic carbon by agglutinated benthic foraminifera. *Nature*, **289**:287–289, 1981.

[315] T. H. DeLuca, O. Zackrisson, M.-C. Nilsson, and A. Sellstedt. Quantifying nitrogen-fixation in feather moss carpets of boreal forests. *Nature*, **429**:917–920, 2002.

[316] C. F. Delwiche. Tracing the thread of plastid diversity through the tapestry of life. *Am. Nat.*, **154**:S164–S177, 1999.

[317] C. F. Delwiche, R. A. Andersen, D. Bhattacharya, B. D. Mishler, and R. M. McCourt. Algal evolution and the early radiation of green plants. In J. Cracraft and M. J. Donoghue, editors, *Assembling the Tree of Life*, pages 121–167. Oxford Univ. Press, 2004.

[318] M. W. Demment and P. J. van Soest. A nutritional explanation for body size patterns of ruminant and non-ruminant herbivores. *Am. Nat.*, **125**:641–672, 1985.

[319] W. R. Demott. Feeding selectivities and relative ingestion rates of *Daphnia* and *Bosmina*. *Limnol. Oceanogr.*, **27**:518–527, 1982.

[320] C. Dennis. Close encounters of the jelly kind. *Nature*, **426**:12–14, 2003.

[321] V. E. Dent, M. J. Bazin, and P. T. Saunders. Behaviour of *Dictyostelium discoideum* amoebae and *Escherichia coli* grown together in chemostat culture. *Arch. Microbiol.*, **109**:187–194, 1976.

[322] E. Derelle, C. Ferraz, P. Lagoda, S. Eychenié, and others. DNA libraries for sequencing the genome of *Ostreococcus tauri* (*Chlorophyta, Prasinophyceae*): the smallest free-living eukaryotic cell. *J. Phycol.*, **38**:1150–1156, 2002.

[323] A. J. Desmond. *The Hot-Blooded Dinosaurs*. Futura Publications Ltd., London, 1975.

[324] R. L. Devaney. *An Introduction to Chaotic Dynamical Systems*. Addison-Wesley, Redwood City, CA, 1989.

[325] A. W. Diamond. The red-footed booby on Aldabra atoll, Indian Ocean. *Ardea*, **62**:196–218, 1974.

[326] J. M. Diamond and R. K. Buddington. Intestinal nutrient absorption in herbivores and carnivores. In P. Dejours, L. Bolis, C. R. Taylor, and E. R. Weibel, editors, *Comparative Physiology: Life in Water and on Land*. IX-Liviana Press, 1987.

[327] U. Dieckmann and R. Law. The mathematical theory of coevolution: a derivation from stochastic processes. *J. Math. Biol.*, **34**:579–612, 1996.

[328] O. Diekmann, H. J. A. M. Heijmans, and H. R. Thieme. On the stability of the cell size distribution. *J. Math. Biol.*, **19**:227–248, 1984.

[329] O. Diekmann, H. J. A. M. Heijmans, and H. R. Thieme. On the stability of the cell size distribution II: time periodic developmental rates. *Comp. & Math. with Appls.*, **12A**:491–512, 1985.

[330] O. Diekmann, H. A. Lauwerier, T. Aldenberg, and J. A. J. Metz. Growth, fission and the stable size distribution. *J. Math. Biol.*, **18**:135–148, 1983.

[331] C. Dijkstra. *Reproductive tactics in the kestrel* Falco tinnunculus*; a study in evolutionary biology*. PhD thesis, Univ. of Groningen, 1988.

[332] R. F. Dill, E. A. Shinn, A. T. Jones, K. Kelly, and R. P. Steinen. Giant subtidal stromatolites forming in normal salinity waters. *Nature*, **324**:55–58, 1986.

[333] J. G. Dillon and R. W. Castenholz. Scytonemin, a cyanobacterial sheath pigment, protects against uvc radiation: implications for early photosynthetic life. *J. Phycol.*, **35**:673–681, 1999.

[334] F. A. Dipper, C. R. Bridges, and A. Menz. Age, growth and feeding in the ballan wrasse *Labrus bergylta* Ascanius 1767. *J. Fish Biol.*, **11**:105–120, 1977.

[335] G. C. Dismukes, V. V. Klimov, S. V. Baranov, Dasguptam J. Kozlov, Yu. N., and A. Tyryshkin. The origin of atmospheric oxygen on earth: the innovation of oxygenic photosynthesis. *Proc. Natl. Acad. Sci. U. S. A.*, **98**:2170–2175, 2001.

[336] H. Dittberner and W. Dittberner. *Die Schafstelze.* A. Ziemsen-Verlag, Wittenberg Lutherstadt, 1984.

[337] P. S. Dixon. *Biology of the Rhodophyta.* Oliver & Boyd, Edinburgh, 1973.

[338] R. Docampo, W. de Souza, K. Miranda, P. Rohloff, and S. N. J. Moreno. Acidocalcisomes: conserved from bacteria to man. *Nature Rev. Microbiol.*, **3**:251–261, 2005.

[339] M. Doebeli. A model for the evolutionary dynamics of cross-feeding polymorphisms in microorganisms. *Pop. Ecol.*, **44**:59–70, 2002.

[340] E. J. Doedel, A. R. Champneys, T. F. Fairgrieve, Y. A. Kuznetsov, B. Sandstede, and X. Wang. Auto 97: Continuation and bifurcation software for ordinary differential equations. Technical report, Concordia Univ., Montreal, Canada, 1997.

[341] C. D. von Dohlen, S. Kohler, S. T. Alsop, and W. R. McManus. Mealybug β-proteobacterial endosymbionts contain γ-proteobacterial symbionts. *Nature*, **412**:433–436, 2001.

[342] D. Dolmen. Growth and size of *Triturus vulgaris* and *T. cristatus* (*Amphibia*) in different parts of Norway. *Holarct. Ecol.*, **6**:356–371, 1983.

[343] S. L. Domotor and C. F. D'Elia. Nutrient uptake kinetics and growth of zooxanthellae. *Mar. Biol.*, **80**:93–101, 1984.

[344] W. D. Donachie. Relationship between cell size and time of initiation of DNA replication. *Nature*, **219**:1077–1079, 1968.

[345] W. D. Donachie, K. G. Begg, and M. Vicente. Cell length, cell growth and cell division. *Nature*, **264**:328–333, 1976.

[346] W. F. Doolittle. Phylogenetic classification and the universal tree. *Science*, **284**:2124–2128, 1999.

[347] Q. Dortch. The interaction between ammonium and nitrate uptake in phytoplankton. *Mar. Ecol. Prog. Ser.*, **61**:183–201, 1990.

[348] P. G. Doucet and N. M. van Straalen. Analysis of hunger from feeding rate observations. *Anim. Behav.*, **28**:913–921, 1980.

[349] A. Douglas, P. J. McAuley, and P. S. Davies. Algal symbiosis in cnidaria. *J. Zool. of Lond.*, **231**:175–178, 1993.

[350] A. E. Douglas. *Symbiotic Interactions.* Oxford Univ. Press, 1994.

[351] S. E. Douglas. Plastid evolution: origin, diversity, trends. *Curr. Top. Gen. Dev.*, **8**:655–661, 1998.

[352] C. L. van Dover. *The Ecology of Deep-Sea Hydrothermal Vents.* Princeton Univ. Press, Princeton, 2000.

[353] W. L. Downing and J. A. Downing. Molluscan shell growth and loss. *Nature*, **362**:506, 1993.

[354] R. L. Draper. The prenatal growth of the guinea-pig. *Anat. Rec.*, **18**:369–392, 1920.

[355] P. G. Drazin. *Nonlinear Systems.* Cambridge Univ. Press, 1992.

[356] R. H. Drent. Functional aspects of incubation in the herring gull. *Behaviour, Suppl.*, **17**:1–132, 1970.

[357] M. R. Droop. Vitamin B_{12} and marine ecology. IV. the kinetics of uptake, growth and inhibition in *Monochrysis lutheri*. *J. Mar. Biol. Assoc. U. K.*, **48**:689–733, 1968.

[358] M. R. Droop. Some thoughts on nutrient limitation in algae. *J. Phycol.*, **9**:264–272, 1973.

[359] M. R. Droop. The nutrient status of algal cells in continuous culture. *J. Mar. Biol. Assoc. U. K.*, **54**:825–855, 1974.

[360] M. R. Droop. 25 years of algal growth kinetics. *Bot. Mar.*, **26**:99–112, 1983.

[361] G. L. Dryden. Growth and development of *Suncus murinus* in captivity on Guam. *J. Mammal.*, **49**:51–62, 1968.

[362] W. G. Du. Phenotypic plasticity in reproductive traits induced by food availability in a lacertid lizard, *Takydromus septentrionalis*. *Oikos*, **112**:363–369, 2006.

[363] N. Dubilier, C. Mulders, et al. Endosymbiotic sulphate-reducing and sulphide-oxidizing bacteria in an oligochaete worm. *Nature*, **411**:298–302, 2001.

[364] W. E. Duellman. Reproductive strategies of frogs. *Sci. Am.*, **7**:58–65, 1992.

[365] W. E. Duellman and L. Trueb. *Biology of Amphibians.* McGraw-Hill, 1986.

[366] G. C. A. Duineveld and M. I. Jenness. Difference in growth rates of the sea urchin *Echiocardium cordatum* as estimated by the parameter ω of the von Bertalanffy equation to skeletal rings. *Mar. Ecol.*, **19**:65–72, 1984.

[367] E. H. Dunn. Growth, body components and energy content of nestling double-crested cormorants. *Condor*, **77**:431–438, 1975.

[368] C. de Duve. *A Guided Tour of the Living Cell.* Scientific American Library, New York, 1984.

[369] M. Dworkin. *Developmental Biology of the Bacteria.* Benjamin-Cummings, Menlo Park, 1985.

[370] E. M. Dzialowski and P. R. Sotherland. Maternal effects of egg size on emu *Dromaius novaehollandiae* egg composition and hatchling phenotype. *J. Exp. Biol.*, **207**:597–606, 2004.

[371] R. A. Eagle, T. Thomas T¨utken, T. S. Martin, A. K. Tripati, H. C. Fricke, M. Connely, R. L. Cifelli, and J. M. Eiler. Dinosaur body temperatures determined from isotopic (^{13}C-^{18}O) ordering in fossil biominerals. *Science*, **333**:443–445, 2011.

[372] O. N. Eaton. Weight and length measurements of fetuses of karakul sheep and of goats. *Growth*, **16**:175–187, 1952.

[373] Muller E.B. and Nisbet R. M. Survival and production in variable resource environments. *Bulletin of Mathematical Biology*, **62**:1163–1189, 2000.

[374] B. Ebenman and L. Persson. *Size-Structured Populations. Ecology and Evolution.* Springer-Verlag, Berlin, 1988.

[375] K. J. Eckelbarger, P. A. Linley, and J. P. Grassle. Role of ovarian follicle cells in vitellogenesis and oocyte resorption in *Capitella* sp. I (Polychaeta). *Mar. Biol.*, pages 133–144, 1984.

[376] R. Eckert, D. Randall, and G. Augustine. *Animal Physiology.* W. H. Freeman and Company, New York, 1988.

[377] L. Edelstein-Keshet. *Mathematical Models in Biology.* Random House, New York, 1988.

[378] P. J Edwards, F. Fleischer-Dogley, and C. N.. and Kaiser-Bunbury. The nutrient economy of lodoicea maldivica, a monodominant palm producing the world's largest seed. *New Phytologist*, page DOI: 10.1111/nph.13272, 2015.

[379] D. A. Egloff and D. S. Palmer. Size relations of the filtering area of two *Daphnia* species. *Limnol. Oceanogr.*, **16**:900–905, 1971.

[380] M. Eichinger. *Bacterial degradation of dissolved organic carbon in the water column: an experimental and modelling approach.* PhD thesis, Univ. de Mediterranee & Vrije Univ., Marseille & Amsterdam, 2008.

[381] S. Einum and I. A. Fleming. Maternal effects of egg size in brown trout (*Salmo trutta*): norms of reaction to environmental quality. *Proc. R. Soc. Lond. Biol. Sci.*, **266**:2095–2095, 1999.

[382] J. F. Eisenberg. *The Mammalian Radiations. An Analysis of Trends in Evolutions, Adaptation, and Behaviour.* Univ. of Chicago Press, 1981.

[383] R. C. Elandt-Johnson and N. L. Johnson. *Survival Models and Data Analysis.* J. Wiley, Chichester, 1980.

[384] C. M. Elkin and M. L. Reid. Low energy reserves and energy allocation decisions affect reproduction by mountain pine beetles, *Dendroctonus ponderosae*. *Funct. Ecol.*, **19**:102–109, 2005.

[385] R. H. E. Elliott, F. G. Hall, and A. St. G. Huggett. The blood volume and oxygen capacity of the foetal blood in the goat. *J. Physiol. (Lond.)*, **82**:160–171, 1934.

[386] G. W. Elmes, J. A. Thomas, and J. C. Wardlaw. Larvae of *Maculinea rebeli*, a large-blue butterfly, and their *Myrmica* host ants: wild adoption and hehaviour in ant-nests. *J. Zool. of Lond.*, **223**:447–460, 1991.

[387] T. M. Embley and R. P. Hirt. Early branching eukaryotes? *Curr. Opin. Gen. Dev.*, **8**:624–629, 1998.

[388] S. Emerson. The growth phase in *Neurospora* corresponding to the logarithmic phase in unicellular organisms. *J. Bacteriol.*, **60**:221–223, 1950.

[389] L. H. Emmons and F. Feer. *Neotropical Rainforest Mammals.* Univ. of Chicago Press, 1990.

[390] J. Emsley. Potent painkiller from poisonous frog. *New Sci.*, **30**(May):14, 1992.

[391] R. H. Emson and P. V. Mladenov. Studies of the fissiparous holothurian *Holothuria parvula* (Selenka) (Echinodermata: Holothuroidea). *J. Exp. Mar. Biol. Ecol.*, **111**:195–211, 1987.

[392] H. Engler. *Die Teichralle.* A. Ziemsen-Verlag, Wittenberg Lutherstadt, 1983.

[393] F. van den Ent, L. A. Amos, and J. Löwe. Prokaryotic origin of the actin cytoskeleton. *Nature*, **413**:39–44, 2001.

[394] G. M. Erickson, D. K. Zelenitsky, D. I. Kay, and M. A. Norel. Dinosaur incubation periods directly determined from growth-line counts in embryonic teeth show reptilian-grade development. *PNAS*, **114**:201613716, 01 2017.

[395] G. Ernsting and J. A. Isaaks. Accelerated ageing: a cost of reproduction in the carabid beetle *Notiophilus biguttatus* F. *Funct. Ecol.*, **5**:229–303, 1991.

[396] G. Ernsting and J. A. Isaaks. Effects of temperature and season on egg size, hatchling size and adult size in *Notiophilus biguttatus*. *Ecol. Entomol.*, **22**:32–40, 1997.

[397] A. A. Esener, J. A. Roels, and N. W. F. Kossen. Dependence of the elemental composition of *K. pneumoniae* on the steady-state specific growth rate. *Biotechnol. Bioeng.*, **24**:1445–1449, 1982.

[398] A. A. Esener, J. A. Roels, and N. W. F. Kossen. Theory and applications of unstructured growth models: kinetic and energetic aspects. *Biotechnol. Bioeng.*, **25**:2803–2841, 1983.

[399] K. F. Ettwig, M. K. Butler, D. Le Paslier, E. Pelletier, et al. Nitrite-driven anaerobic methane oxidation by oxygenic bacteria. *Nature*, **464**:543–548, 2010.

[400] E. Evers and S. A. L. M. Kooijman. Feeding and oxygen consumption in *Daphnia magna*: a study in energy budgets. *Neth. J. Zool.*, **39**:56–78, 1989.

[401] N. Fairall. Prenatal development of the impala *Aepyceros melampus*. *Koedoe*, **12**:97–103, 1969.

[402] N. Fairall. Production parameters of the impala, *Aepyceros melampus*. *S. Afr. J. Anim. Sci.*, **13**:176–179, 1983.

[403] D. J. Fairbairn. *Odd couples; extraordinary differences between the sexes in the Animal Kingdom*. Princeton University Press, 2013.

[404] U. Falkengren-Grerup and H. Lakkenborg-Kristensen. Importance of ammonium and nitrate to the performance of herb-layer species from deciduous forests in southern Sweden. *Environ. Exp. Bot.*, **34**:31–38, 1994.

[405] P. G. Falkowski and J. A. Raven. *Aquatic Photosynthesis*. Blackwell Science, Oxford, 1997.

[406] A Farjon. *A Natural History of Conifers*. Timber Press, Portland, 2008.

[407] J. O. Farlow. A consideration of the trophic dynamics of a late Cretaceous large-dinosaur community (Oldman Formation). *Ecology*, **57**:841–857, 1976.

[408] J. O. Farlow and M. K. Brett-Surman. *The Complete Dinosaur*. Indiana Univ. Press, 1997.

[409] G. D. Farquhar. Models describing the kinetics of ribulose riphosphate carboxylase-oxygenase. *Arch. Biochem. Biophys.*, **193**:456–468, 1979.

[410] G. D. Farquhar, S. von Caemmerer, and J. A. Berry. A biochemical model of photosynthetic CO_2 assimilation in leaves of C_3 species. *Planta*, **149**:78–90, 1980.

[411] H. S. Fawcett. The temperature relations of growth in certain parasitic fungi. *Univ. Calif. Berkeley Publ. Agr. Sci.*, **4**:183–232, 1921.

[412] M. A. Fedak and H. J. Seeherman. Reappraisal of energetics of locomotion shows identical cost in bipeds and quadrupeds including ostrich and horse. *Nature*, **282**:713–716, 1979.

[413] R. Fenaux. Rhythm of secretion of oikopleurid's houses. *Bull. Mar. Sci.*, **37**:498–503, 1985.

[414] R. Fenaux and G. Gorsky. Cycle vital et croissance de l'appendiculaire *Oikopleura longicauda*. *Annu. Inst. Oceanogr.*, **59**:107–116, 1983.

[415] T. Fenchel. Intrinsic rate of natural increase: the relationship with body size. *Oecologia (Berlin)*, **14**:317–326, 1974.

[416] T. Fenchel. Eukaryotic life: anaerobic physiology. In D. McL. Roberts, P. Sharp, G. Alderson, and M Collins, editors, *Evolution of Microbial Life*, pages 185–203. Cambridge Univ. Press, 1996.

[417] T. Fenchel. *Origin & Early Evolution of Life*. Oxford Univ. Press, 2002.

[418] T. Fenchel and B. L. Finlays. *Ecology and Evolution in Anoxic Worlds*. Oxford Univ. Press, 1995.

[419] M. W. J. Ferguson. Palatal shelf elevation in the Wistar rat fetus. *J. Anat.*, **125**:555–577, 1978.

[420] S. Fernandez-Baca, W. Hansel, and C. Novoa. Embryonic mortality in the alpaca. *Biol. Reprod.*, **3**:243–251, 1970.

[421] J. G. Ferry. *Methanogenesis. Ecology, Physiology, Biochemistry & Genetics*. Chapman & Hall, New York, 1993.

[422] L. Fieseler, M. horn, M. Wagner, and U. Hentschel. Discovery of the novel candidate phylum "*Poribacteria*" in marine sponges. *Appl. Environ. Microbiol.*, **70**:3724–3732, 2004.

[423] C. E. Finch. *Longevity, Senescence, and the Genome*. Univ. of Chicago Press, 1990.

[424] G. A. Fines, J. S. Ballantyne, and P. A. Wright. Active urea transport and an unusual basolateral membrane composition in the gills of a marine elasmobranch. *Am. J. Physiol.*, **280**:R16–R24, 2001.

[425] M. S. Finkler, J. B. van Orman, and P. R. Sotherland. Experimental manipulation of egg quality in chickens: influence of albumen and yolk on the size and body composition of near-term embryos in a precocial bird. *J. Comp. Physiol. B*, **168**:17–24, 1998.

[426] B. J. Finlay and T. Fenchel. An anaerobic ciliate as a natural chemostat for the growth of endosymbiotic methanogens. *Eur. J. Protistol.*, **28**:127–137, 1992.

[427] R. A. Fisher and L. H. C. Tippitt. Limiting forms of the frequency distribution of the largest or the smallest memeber of a sample. *Proc. Camb. Phil. Soc.*, **24**:180–190, 1928.

[428] V. Fitsch. *Laborversuche und Simulationen zur kausalen Analyse der Populationsdynamik von* Daphnia magna. PhD thesis, Rheinisch-Westfälischen Technischen Hochschule Aachen, 1990.

[429] L. B. Flexner and H. A. Pohl. The transfer of radioactive sodium across the placenta of the white rat. *J. Cell. Comp. Physiol.*, **18**:49–59, 1941.

[430] P. R. Flood. Architecture of, and water circulation and flow rate in, the house of the planktonic tunicate *Oikopleura labradoriensis*. *Mar. Biol.*, **111**:95–111, 1991.

[431] G. L. Flynn and S. H. Yalkowsky. Correlation and prediction of mass transport across membranes I: influence of alkyl chain length on flux-determining properties of barrier and diffusant. *J. Pharm. Sci.*, **61**:838–852, 1972.

[432] K. J. Flynn, M. J. R. Fasham, and C. R. Hipkin. Modelling the interactions between ammonium and nitrate in marine phytoplankton. *Phil. Trans. R. Soc. Lond. B Biol. Sci.*, **352**:1625–1645, 1997.

[433] H. von Foerster. Some remarks on changing populations. In F. Stohlman, editor, *The Kinetics of Cellular Proliferation*. Grune and Stratton, 1959.

[434] J. Forsberg and C. Wiklund. Protandry in the green-veined white butterfly, *Pieris napi* L. (*Lepidoptera*; *Pieridae*). *Funct. Ecol.*, **2**:81–88, 1988.

[435] P. Forterre. Genomics and the early cellular evolution. the origin of the DNA world. *C. R. Acad. Sci.*, **324**:1067–1076, 2001.

[436] P. Forterre. The origin of DNA genomes and DNA replication proteins. *Curr. Opin. Microbiol.*, **5**:525–532, 2002.

[437] P. Forterre. The origin of virusses and their possible roles in major evolutionary transitions. *Virus Res.*, **117**:5–16, 2006.

[438] P. Forterre, A. Bergerat, and P. Lopez-Garvia. The unique DNA topology and DNA topoisomerase of hyperthermophilic archaea. *FEMS Microbiol. Rev.*, **18**:237–248, 1996.

[439] P. Forterre and S. Gribaldo. Bacteria with a eukaryotic touch: A glimpse of ancient evolution? *Proc. Natl. Acad. Sci. U. S. A.*, **107**:12739–12740, 2010.

[440] B. L. Foster Smith. The effect of concentration of suspension and inert material on the assimilation of algae by three bivalves. *J. Mar. Biol. Assoc. U. K.*, **55**:411–418, 1975.

[441] B. L. Foster Smith. The effect of concentration of suspension on the filtration rates and pseudofaecal production for *Mytilus edulis* L., *Cerastoderma edule* L. and *Venerupsis pullastra* (Montagu). *J. Exp. Mar. Biol. Ecol.*, **17**:1–22, 1975.

[442] D. R. Franz. Population age structure, growth and longevity of the marine gastropod *Uropalpinx cinerea* Say. *Biol. Bull. (Woods Hole)*, **140**:63–72, 1971.

[443] J. C. Frauenthal. Analysis of age-structured models. In T. G. Hallam and S. A. Levin, editors, *Mathematical Ecology*, pages 117–147. Springer-Verlag, Berlin, 1986.

[444] J. J. R. Fraústo da Silva and R. J. P. Williams. *The Biological Chemistry of the Elements. The Inorganic Chemistry of Life.* Clarendon Press, Oxford, 1993.

[445] A. G. Fredrickson, R. D. Megee III, and H. M. Tsuchiy. Mathematical models for fermentation processes. *Adv. Appl. Microbiol.*, **13**:419–465, 1970.

[446] B. Friedich. Genetics of energy converting systems in aerobic chemolithotrophs. In H. G. Schlegel and E. Bowien, editors, *Autotrophic Bacteria*, pages 415–436. Springer-Verlag, 1989.

[447] R. E. Frisch and R. Revelle. Height and weight at menarche and a hypothesis of menarche. *Archives of Disease in Childhood*, **46**:695–702, 1971.

[448] M. Fritsch, O. R. P. Bininda-Emonds, and S. Richter. Unraveling the origin of cladocera by identifying heterochrony in the developmental sequences of branchiopoda. *Frontiers in Zoology*, **10**(35):1–19, 2013.

[449] E. Frommhold. *Die Kreuzotter.* A. Ziemsen-Verlag, Wittenberg Lutherstadt, 1969.

[450] B. W. Frost. Effects of size and concentration of food particles on the feeding behaviour of the marine copepod *Calanus pacificus*. *Limnol. Oceanogr.*, **17**:805–815, 1972.

[451] B. W. Frost and N. C. Franzen. Grazing and iron limitation in the control of phytoplankton stock and nutrient concentration: a chemostat analogue of the pacific equatorial upwelling zone. *Mar. Ecol. Prog. Ser.*, **83**:291–303, 1992.

[452] W. E. Frost and C. Kipling. The growth of charr, *Salvinus willughbii* Gunther, in Windermere. *J. Fish Biol.*, **16**:279–289, 1980.

[453] B. Fry. *Stable Isotope Ecology.* Springer, New York, 2006.

[454] F. E. J. Fry. The effect of environmental factors on the physiology of fish. In W. S. Hoar and D. J. Randall, editors, *Fish Physiology*, volume 6, pages 1–87. Academic Press, London, 1971.

[455] G. Fryer. Evolution and adaptive radiation in *Macrothricidae* (*Crustacea*: *Cladocera*): a study in comparative functional morphology and ecology. *Proc. R. Soc. Lond. Biol. Sci.*, **269**:142–385, 1974.

[456] J. A. Fuerst. Intracellular compartmentation in planctomycetes. *Annu. Rev. Microbiol.*, **59**:299–328, 2005.

[457] J. Fuhrman. Genome sequences from the sea. *Nature*, **424**:1001–1002, 2003.

[458] E. Fuller, editor. *Kiwis.* Swan-Hill Press, Shrewsbury, 1991.

[459] T. W. Fulton. *The Sovereignty of the Seas.* Edinburgh, 1911.

[460] S. Fuma, H. Takeda, K. Miyamoto, K. Yanagisawa, Y. Inoue, N. Sato, M. Hirano, and Z. Kawabata. Effects of γ-rays on the populations of the steady state ecological microcosm. *Int. J. Radiat. Biol.*, **74**:145–150, 1998.

[461] R. W. Furness. *The Skuas.* T. & A. D. Poyser, Calton, 1987.

[462] V. F. Gallucci and T. J. Quinn. Reparameterizing, fitting, and testing a simple growth model. *Trans. Am. Fish. Soc.*, **108**:14–25, 1979.

[463] V. F. Gallucci and T. J. Quinn. Reproductive investment of several rotifer species. *Hydrobiologia*, **255**:317–324, 1993.

[464] L. Garby and P. Larsen. *Bioenergetics; its Thermodynamic Foundations.* Cambridge Univ. Press, 1995.

[465] W. Garstang. *Larval Forms and other zoological verses.* Blackwell, Oxford, 1951. Reprint: University of Chicago Press 1985.

[466] A. J. Gaston. *The Ancient Murrelet.* T. & A. D. Poyser, London, 1992.

[467] R. E. Gatten, K. Miller, and R. J. Full. Energetics at rest and during locomotion. In M. E. Feder and W. W. Burggren, editors, *Environmental Physiology of the Amphibians*, chapter 12, pages 314–377. Univ. of Chicago Press, 1992.

[468] M. Gatto, C. Ricci, and M. Loga. Assessing the response of demographic parameters to density in a rotifer population. *Ecol. Modell.*, **62**:209–232, 1992.

[469] J. Gaullaume, S. Kaushik, P. Bergot, and R. Metailler. *Nutrition en alimentation des poissons et crustacés.* INRA-IFREMER, Paris, 1999.

[470] H. Gee. *Across the bridge; Understanding the origin of the vertebrates.* The University of Chicago Press, Chicago, 2018.

[471] D. L. Geiger, C. E. Northcott, D. J. Call, and L. T. Brooke. *Acute Toxicities of Organic Chemicals to Fathead Minnow (*Pimephalus promelas*)*, volume II of *Center for Lake Superior Environmental Studies.* Univ. of Wisconsin USA, 1985.

[472] D.L. Geiger, L. T. Brooke, and D. J. Call. *Acute Toxicities of Organic Chemicals to Fathead Minnow (*Pimephales promelas*)*, volume 2-5 of *Center for Lake Superior Environmental Studies.* Univ. of Wisconsin-Superior, USA, 1985-1990.

[473] F. Geiser. Metabolic rate and body temperature reduction during hibernation and daily torpor. *Annu. Rev. Physiol.*, **66**:239–274, 2004.

[474] V. Geist. Bergmann's rule is invalid. *Can. J. Zool.*, **65**:1035–1038, 1987.

[475] W. Geller. Die Nahrungsaufname von *Daphnia pulex* in Aghängigkeit von der Futterkonzentration, der Temperatur, der Köpergrösse und dem Hungerzustand der Tiere. *Arch. Hydrobiol./ Suppl.*, **48**:47–107, 1975.

[476] W. Geller and H. Müller. Seasonal variability in the relationship between body length and individual dry weight as related to food abundance and clutch size in two coexisting *Daphnia*. *J. Plankton Res.*, **7**:1–18, 1985.

[477] R. B. Gennis. *Biomembranes. Molecular Structure and Function.* Springer-Verlag, Berlin, 1989.

[478] M. Genoud. Energetic strategies of shrews: ecological constraints and evolutionary implications. *Mammal Rev.*, **4**:173–193, 1988.

[479] G. S. Gerhard, E. J. Kauffman, X. Wang, R. Stewart, J. L. Moore, C. J. Kasales, E. Demidenko, and K. C. Cheng. Life spans and senescent phenotypes in two strains of zebrafish (*Danio rerio*). *Experimental Gerontology*, **37**:1055–1068, 2002.

[480] S. A. H. Geritz, É. Kisdi, G. Meszéna, and J. A. J. Metz. Evolutionarily singular strategies and the adaptive growth and branching of the evolutionary tree. *Evol. Ecol.*, **12**:35–57, 1998.

[481] A. A. M. Gerritsen. *The influence of body size, life stage, and sex on the toxicity of alkylphenols to* Daphnia magna. PhD thesis, Univ. of Utrecht, 1997.

[482] R. D. Gettinger, G. L. Paukstis, and W. H. N. Gutzke. Influence of hydric environment on oxygen consumption by embryonic turtles *Chelydra serpentina* and *Trionyx spiniferus*. *Physiol. Zool.*, **57**:468–473, 1984.

[483] W. Gewalt. *Der Weisswal (*Delphinapterus leucas*).* A. Ziemsen-Verlag, Wittenberg Lutherstadt, 1976.

[484] A. G. Gibbs. Biochemistry at depth. In D. J. Randall and A. P. Farrell, editors, *Deep-Sea Fishes.*, chapter 6, pages 239–278. Academic Press, San Diego, 1997.

[485] R. N. Gibson. Observations on the biology of the giant goby *Gobius cobitis* Pallas. *J. Fish Biol.*, **2**:281–288, 1970.

[486] R. N. Gibson and I. A. Ezzi. The biology of a Scottish population of Fries' goby, *Lesueurigobius friesii*. *J. Fish Biol.*, **12**:371–389, 1978.

[487] R. N. Gibson and I. A. Ezzi. The biology of the scaldfish, *Arnoglossus laterna* (Walbaum) on the west coast of Scotland. *J. Fish Biol.*, **17**:565–575, 1980.

[488] R. N. Gibson and I. A. Ezzi. The biology of the Norway goby, *Pomatoschistus norvegicus* (Collett), on the west coast of Scotland. *J. Fish Biol.*, **19**:697–714, 1981.

[489] A. Gierer. *Hydra* as a model for the development of biological form. *Sci. Am.*, **12**:44–54, 1974.

[490] M. A. Gilbert. Growth rate, longevity and maximum size of *Macoma baltica* (L.). *Biol. Bull. (Woods Hole)*, **145**:119–126, 1973.

[491] U. Gille and F. V. Salomon. Heart and body growth in ducks. *Growth Dev. Aging*, **58**:75–81, 1994.

[492] Samuel Ginther, Hayley Cameron, Craig R. White, and Dustin J. Marshall. Metabolic loads and the costs of metazoan reproduction. *Science*, **384**:763–767, 2024.

[493] S. J. Giovannoni, H. J. Tripp, S. Givan, M. Podar, K. L. Vergin, D. Baptista, L. Bibbs, J. Eads, T. H. Richardson, M. S. Noordewier, M. Rappé, J. M. Short, J. C. Carrington, and E. J. Mathur. Genome streamlining in a cosmopolitan oceanic bacterium. *Science*, **309**:1242–1245, 2005.

[494] M. Di Giulio. The universal ancestor and the ancestor of bacteria were hyperthermophiles. *J. Mol. Evol.*, **57**:721–730, 2003.

[495] S. Glasstone, K. J. Laidler, and H. Eyring. *The Theory of Rate Processes.* McGraw-Hill, London, 1941.

[496] D. S. Glazier. Effects of Food, Genotype, and Maternal Size and Age on Offspring Investment in *Daphnia Magna*. *Ecology*, **73**:910–926, 1992.

[497] D. S. Glazier. Does body storage act as a food-availability cue for adaptive adjustment of egg size and number in *Daphnia magna*? *Freshw. Biol.*, **40**:87–92, 1998.

[498] Z. M. Gliwicz. Food thresholds and body size in cladocerans. *Nature*, **343**:638–640, 1990.

[499] Z. M. Gliwicz and C. Guisande. Family planning in *Daphnia*: resistance to starvation in offspring born to mothers grown at different food levels. *Oecologia (Berlin)*, **91**:463–467, 1992.

[500] F. A. P. C. Gobas and A. Opperhuizen. Bioconcentration of hydrophobic chemicals in fish: relationship with membrane permeation. *Environ. Toxicol. Chem.*, **5**:637–646, 1986.

[501] K. Godfrey. *Compartment Models and Their Application.* Academic Press, New York, 1983.

[502] L. Godfrey, M. Sutherland, D. Boy, and N. Gomberg. Scaling of limb joint surface areas in anthropoid primates and other mammals. *J. Zool. of Lond.*, **223**:603–625, 1991.

[503] J. C. Goldman. Conceptual role for microaggregates in pelagic waters. *Bull. Mar. Sci.*, **35**:462–476, 1984.

[504] J. C. Goldman and E. J. Cerpenter. A kinetic approach of temperature on algal growth. *Limnol. Oceanogr.*, **19**:756–766, 1974.

[505] C. R. Goldspink. A note on the growth-rate and year-class strength of bream, *Abramis brama* (L.), in three eutrophic lakes, England. *J. Fish Biol.*, **19**:665–673, 1981.

[506] B. Gompertz. On the nature of the function expressive of the law of mortality, and on a new method of determining the value of life contingencies. *Phil. Trans. R. Soc. Lond. B Biol. Sci.*, **27**:513–585, 1825.

[507] M. Gophen and W. Geller. Filter mesh size and food particle uptake by *Daphnia*. *Oecologia (Berlin)*, **64**:408–412, 1984.

[508] R. W. Gordon, R. J. Beyers, E. P. Odum, and R. G. Eagon. Studies of a simple laboratory microecosystem: bacterial activities in a heterotrophic succession. *Ecology*, **50**:86–100, 1969.

[509] S. J. Gould. *Ontogeny and Phylogeny.* Belknap Press, Cambridge, 1977.

[510] C. E. Goulden, L. L. Henry, and A. J. Tessier. Body size, energy reserves, and competitive ability in three species of cladocera. *Ecology*, **63**:1780–1789, 1982.

[511] C. E. Goulden and L. L. Hornig. Population oscillations and energy reserves in planktonic cladocera and their consequences to competition. *Proc. Natl. Acad. Sci. U. S. A.*, **77**:1716–1720, 1980.

[512] B. W. Grant and W. P. Porter. Modelling global macroclimatic constraints on ectotherm energy budgets. *Am. Zool.*, **32**:154–178, 1992.

[513] C. J. Grant and A. V. Spain. Reproduction, growth and size allometry of *Liza vaigiensis* (Quoy & Gaimard) (*Pisces*: *Mugilidae*) from North Queensland inshore waters. *Austral. J. Zool.*, **23**:475–485, 1975.

[514] C. J. Grant and A. V. Spain. Reproduction, growth and size allometry of *Valamugil seheli* (Forskal) (*Pisces*: *Mugilidae*) from North Queensland inshore waters. *Austral. J. Zool.*, **23**:463–474, 1975.

[515] P. J. Graumann. Cytoskeletal elements in bacteria. *Annu. Rev. Microbiol.*, **61**:589–618, 2007.

[516] J. Gray. The growth of fish I. The relationship between embryo and yolk in *Salmo fario*. *J. Exp. Biol.*, **4**:215–225, 1926.

[517] N. D. Gray and M. Head. Ecology of giant sulfur bacteria. In M. G. Gadd, T. Semple, and H. M. Lappin-Scott, editors, *Micro-organisms and earth systems*, Advances in geomocrobiology. Cambridge University Press, 2005.

[518] R. H. Green. *Birds.* The Fauna of Tasmania. Potoroo Publishing, Launceton, 1995.

[519] W. Greve. Ökologische Untersuchungen an *Pleurobrachia pileus* 1. Freilanduntersuchungen. *Helgol. Wiss. Meeresunters.*, **22**:303–325, 1971.

[520] W. Greve. Ökologische Untersuchungen an *Pleurobrachia pileus* 2. Laboratoriumuntersuchungen. *Helgol. Wiss. Meeresunters.*, **23**:141–164, 1972.

[521] K. Grice, C. Cao, G. D Love, M. E. Böttcher, R. J. Twitchett, E. Grosjean, R. E. Summons, S. C. Turgeon, W. Dunning, and Y. Jin. Photic zone euxinia during the permian-triassic superanoxic event. *Science*, **307**:706–709, 2005.

[522] P. Groeneveld. *Control of specific growth rate and physiology of the yeast* Kluyveromyces marxianus*; a biothermokinetic approach.* PhD thesis, Vrije Univ., Amsterdam, 1999.

[523] R. S. de Groot. Origin, status and ecology of the owls in Galapagos. *Ardea*, **71**:167–182, 1983.

[524] R. K. Grosberg. Life-history variation within a population of the colonial ascidian *Botryllus schlosseri*. I. The genetic and environmental control of seasonal variation. *Evolution*, **42**:900–920, 1988.

[525] J. Gruenberg. The endocytic pathway: a mosaic of domains. *Nature Rev.*, **2**:721–730, 2001.

[526] R. Grundel. Determinants of nestling feeding rates and parental investment in the mountain chickadee. *Condor*, **89**:319–328, 1987.

[527] J. Guckenheimer and P. Holmes. *Nonlinear Oscillations, Dynamical Systems, and Bifurcations of Vector Fields.*, volume 42 of *Applied Mathematical Sciences*. Springer-Verlag, Berlin, 1983.

[528] R. Guerrero. Predation as prerequisite to organelle origin: *Daptobacter* as example. In L. Margulis and R. Fester, editors, *Symbiosis as a Source of Evolutionary Innovation.*, chapter 8, pages 106–117. MIT Press, Cambridge, Mass., 1991.

[529] M. A. Guinee, A. Gardner, A. E. Howard, S. A. West, and T. J. Little. The causes and consequences of variation in offspring size: a case study using *Daphnia*. *J. Evol. Biol.*, **20**:577–587, 2007.

[530] C. Guisande and Z. M. Gliwicz. Egg size and clutch size in 2 *Daphnia* species grown at different food levels. *J. Plankton Res.*, **14**:997–1007, 1992.

[531] R. Günther. *Die Wasserfrösche Europas*. A. Ziemsen-Verlag, Wittenberg Lutherstadt, 1990.

[532] R. S. Gupta. What are archaebacteria: life's third domain or monoderm prokaryotes related to gram-positive bacteria? A new proposal for the classification of prokaryotic organisms. *Mol. Microbiol.*, **29**:695–707, 1998.

[533] W. S. C Gurney and R. M. Nisbet. *Ecological Dynamics*. Oxford Univ. Press, 1998.

[534] W.C. Gurney and R. M. Nisbet. Resource allocation, hyperphagia and compensatory growth. *Bull. Math. Biol.*, **66**:1731–1753, 2004.

[535] R. Haase. *Thermodynamics of Irreversible Processes*. Dover Publications, New York, 1990.

[536] P. Haccou and E. Meelis. *Statistical Analysis of Behavioural Data; An Approach Based on Time-Structured Models*. Oxford Univ. Press, 1992.

[537] U. Halbach. Einfluss der Temperatur auf die Populationsdynamik der planktischer Radertieres *Brachionus calyciflorus* Pallas. *Oecologia (Berlin)*, **4**:176–207, 1970.

[538] B. K. Hall and M. H. Wake. *The origin and evolution of larval forms*. Academic Press, San Diego, 1999.

[539] D. O. Hall and K. K. Rao. *Photosynthesis*. Cambridge Univ. Press, 1999.

[540] S. R. Hall, C. Becker, and C. E. Cáceres. Parasitic castration,: a perspective of a model of dynamic energy budgets. *Integrative and Comparative Biology*, **47**:295–309, 2007.

[541] S. J. Hallam, N. Putnam, C. M. Preston, J. C. Detter, D. Rokhsar, P. M. Richardson, and E. F. DeLong. Revers methanogenesis: Testing the hypothesis with environmentl genomics. *Science*, **305**:1457–1462, 2004.

[542] T. G. Hallam, R. R. Lassiter, and S. A. L. M. Kooijman. Effects of toxicants on aquatic populations. In S. A. Levin, T. G. Hallam, and L. F. Gross, editors, *Mathematical Ecology.*, pages 352–382. Springer, London, 1989.

[543] T. G. Hallam, R. R. Lassiter, J. Li, and W. McKinney. An approach for modelling populations with continuous structured models. In D. L. DeAngelis and L. J. Gross, editors, *Individual Based Approaches and Models in Ecology*, pages 312–337. Springer-Verlag, 1992.

[544] T. G. Hallam, R. R. Lassiter, J. Li, and L. A. Suarez. Modelling individuals employing an integrated energy response: application to *Daphnia*. *Ecology*, **71**:938–954, 1990.

[545] T. G. Hallam and J. L. de Luna. Effects of toxicants on population: a qualitative approach. III. Environmental and food chain pathways. *J. theor. Biol.*, **109**:411–429, 1984.

[546] B. Halliwell and J. M. C. Gutteridge. *Free Radicals in Biology and Medicine*. Oxford Univ. Press, 1999.

[547] P. Hallock. Algal symbiosis: a mathematical analysis. *Mar. Biol.*, **62**:249–255, 1981.

[548] P. P. F. Hanegraaf. *Mass and energy fluxes in microorganisms according to the Dynamic Energy Budget theory for filaments*. PhD thesis, Vrije Univ., Amsterdam, 1997.

[549] P. P. F. Hanegraaf, B. W. Kooi, and S. A. L. M. Kooijman. The role of intracellular components in food chain dynamics. *C. R. Acad. Sci.*, **323**:99–111, 2000.

[550] R. J. F. van Haren and S. A. L. M. Kooijman. Application of the dynamic energy budget model to *Mytilus edulis* (L). *Neth. J. Sea Res.*, **31**:119–133, 1993.

[551] D. Harman. Role of free radicals in mutation, cancer, aging and maintenance of life. *Radiat. Res.*, **16**:752–763, 1962.

[552] D. Harman. The aging process. *Proc. Natl. Acad. Sci. U. S. A.*, **78**:7124–7128, 1981.

[553] F. M. Harold. *The Vital Force. A Study of Bioenergetics*. Freeman, New York, 1986.

[554] J. L. Harper. *Population Biology of Plants*. Academic Press, London, 1977.

[555] M. P. Harris. The biology of an endangered species, the dark-rumped petrel (*Pterodroma phaeopygia*), in the Galapagos Islands. *Condor*, **72**:76–84, 1970.

[556] C. Harrison. *A Field Guide to the Nests, Eggs and Nestlings of European Birds*. Collins, London, 1975.

[557] R. Harrison and G. G. Lunt. *Biological Membranes. Their Structure and Function*. Blackie, Glasgow, 1980.

[558] M. W. Hart. What are the costs of small egg size for a marine invertebrate with feeding planktonic larvae? *Am. Nat.*, **146**:415–426, 1995.

[559] H. Hartman. Speculations on the origin and evolution of metabolism. *J. Mol. Evol.*, **4**:359–370, 1975.

[560] H. Hartman. Photosynthesis and the origin of life. *Orig. life evol. biosphere*, **28**:515–521, 1998.

[561] R. J. Harvey, A. G. Marr, and P. R. Painter. Kinetics of growth of individual cells of *Escherichia coli* and *Azotobacter agilis*. *J. Bacteriol.*, **93**:605–617, 1967.

[562] S. C. Harvey and E. Orbidans. All eggs are not equal: The maternal environment affects progeny reproduction and developmental fate in *Caenorhabditis elegans*. *PLoS One*, **6**:e25840, 2011.

[563] K. A. Hasselbalch. Über den respiratorischen Stoffechsel des Hühnerembryos. *Skand. Arch. Physiol.*, **10**:353–402, 1900.

[564] A. Hastings. What equilibrium behaviour of Lotka-Volterra models does not tell us about food webs. In G. A. Polis and K. O. Winemiller, editors, *Food Webs*, pages 211–217. Chapman & Hall, London, 1996.

[565] A. Hastings. *Population Biology; Concepts and Models*. Springer, New York, 1997.

[566] A. Hastings and T. Powell. Chaos in a three-species food chain. *Ecology*, **72**:896–903, 1991.

[567] Ian A. Hattona, Andy P. Dobson, David Storch, Eric D. Galbraith, and Michel Loreau. Linking scaling laws across eukaryotes. *PNAS*, page 10.1073/pnas.1900492116, 2019.

[568] F. Haverschmidt. Notes on the life history of *Amazilia fimbriata* in Surinam. *Wilson Bull.*, **61**:69–79, 1952.

[569] D. W. Hawker and D. W. Connell. Relationships between partition coefficient, uptake rate constant, clearance rate constant and time to equilibrium for bioaccumulation. *Chemosphere*, **14**:1205–1219, 1985.

[570] D. W. Hawker and D. W. Connell. Bioconcentration of lipophilic compounds by some aquatic organisms. *Ecotoxicol. Environ. Saf.*, **11**:184–197, 1986.

[571] A. J. S. Hawkins and B. L. Bayne. Seasonal variations in the balance between physiological mechanisms of feeding and digestion in *Mytilus edulis* (*Bivalvia*, *Mollusca*). *Mar. Biol.*, **82**:233–240, 1984.

[572] J. M. Hayes. Global methanotrophy at the archeon-proterozoic transition. In S. Bengtson, editor, *Early life on Earth.*, volume 84 of *Nobel Symp.*, pages 220–236. Columbia Univ. Press, New York, 1994.

[573] D. D. Heath, C. W. Fox, and J. W. Heath. Maternal effects on offspring size: Variation through early development of chinook salmon. *Evol.*, **53**:1605–1611, 1999.

[574] P. D. N. Hebert. The genetics of *Cladocera*. In W. C. Kerfoot, editor, *Evolution and Ecology of Zooplankton Communities*, pages 329–336. Univ. of New England Press, 1980.

[575] P. D. N. Hebert. Genotypic characteristic of cyclic parthenogens and their obligately asexual derivates. In S. C. Stearns, editor, *The Evolution of Sex and Its Consequences*, pages 175–195. Birkhäuser, Basel, 1987.

[576] H. Heesterbeek. R_0. PhD thesis, Univ. of Leiden, 1992.

[577] H. J. A. M. Heijmans. Holling's 'hungry mantid' model for the invertebrate functional response considered as a Markov process. Part III: Stable satiation distribution. *J. Math. Biol.*, **21**:115–1431, 1984.

[578] H. J. A. M. Heijmans. *Dynamics of structured populations*. PhD thesis, Univ. of Amsterdam, 1985.

[579] J. J. Heijnen. A new thermodynamically based correlation of chemotrophic biomass yields. *Antonie van Leeuwenhoek*, **60**:235–256, 1991.

[580] J. J. Heijnen and J. P. van Dijken. In search of a thermodynamic description of biomass yields for the chemotrophic growth of micro organisms. *Biotechnol. Bioeng.*, **39**:833–858, 1992.

[581] J. J. Heijnen and J. A. Roels. A macroscopic model describing yield and maintenance relationships in aerobic fermentation. *Biotechnol. Bioeng.*, **23**:739–761, 1981.

[582] F. Heincke. Bericht über die Untersuchungen der Biologischen Anstalt auf Helgoland zur Naturgeschichte der Nutzfische. *Die Beteiligung Deutschlands an der Internationalen Meeresforschung*, **4/5**:67–155, 1908.

[583] B. Heinrich. *The Hot-Blooded Insects; Strategies and Mechanisms of Thermoregulation*. Harvard Univ. Press, Cambridge, Mass., 1993.

[584] R. Heinrich and S. Schuster. *The Regulation of Cellular Systems*. Chapman & Hall, New York, 1996.

[585] J. M. Hellawell. Age determination and growth of the grayling *Thymallus thymallus* (L.) of the River Lugg, Herefordshire. *J. Fish Biol.*, **1**:373–382, 1969.

[586] M. A. Hemminga. *Regulation of glycogen metabolism in the freshwater snail* Lymnaea stagnalis. PhD thesis, Vrije Univ., Amsterdam, 1984.

[587] A. M. Hemmingsen. Energy metabolism as related to body size and respiratory surfaces, and its evolution. *Rep. Steno. Mem. Hosp. Nordisk Insulinlaboratorium*, **9**:1–110, 1969.

[588] M. Hendrata and B. Birnir. Dynamic-energy-budget-driven fruiting-body formation in myxobacteria. *Phys Rev E Stat Nonlin Soft Matter Phys.*, **81**:DOI:10.1103/PhysRevE.81.061902, 2010.

[589] A. J. Hendriks. Modelling non-equilibrium concentrations of microcontaminants in organisms: comparative kinetics as a function of species size and octanol-water partitioning. *Chemosphere*, **30**:265–292, 1995.

[590] R. W. Hendrix, M. C. Smith, R. N. Burns, M. E. Ford, and G. F. Hatfull. Evolutionary relationships among diverse bacteriophages: all the world's a phage. *Proc. Natl. Acad. Sci. U. S. A.*, **96**:2192–2197, 1999.

[591] V. Henri. Théorie générale de l'action de quelques diastases. *C. R. Acad. Sci.*, **135**:916–919, 1902.

[592] W. G. Heptner and A. A. Nasimowitsch. *Der Elch (*Alces alces*)*. A. Ziemsen-Verlag, Wittenberg Lutherstadt, 1974.

[593] S. L. Herendeen, R. A. VanBogelen, and F. C. Neidhardt. Levels of major proteins of *Escherichia coli* during growth at different temperatures. *J. Bacteriol.*, **138**:185, 1979.

[594] C. F. Herreid II and B. Kessel. Thermal conductance in birds and mammals. *Comp. Biochem. Physiol.*, **21**:405–414, 1967.

[595] H. C. Hess. The evolution of parental care in brooding spirorbid polychaetes: the effect of scaling constraints. *Am. Nat.*, **141**:577–596, 1993.

[596] D. J. S. Hetzel. The growth and carcass characteristics of crosses between alabio and tegal ducks and muscovy and pekin drakes. *Br. Poult. Sci.*, **24**:555–563, 1983.

[597] E. H. W. Heugens, T. Jager, R. Creyghton, M. H. S. Kraak, A. J. Hendriks, N. M. van Straalen, and W. Admiraal. Temperature dependent effects of cadmium on *Daphnia magna*: accumulation versus sensitivity. *Environ. Sci. Technol.*, **37**:2145–2151, 2003.

[598] H. R. Hewer and K. M. Backhouse. Embryology and foetal growth of the grey seal, *Halichoerus grypus*. *J. Zool. of Lond.*, **155**:507–533, 1968.

[599] C. J. Hewett. Growth and moulting in the common lobster (*Homarus vulgaris* Milne-Edwards). *J. Mar. Biol. Assoc. U. K.*, **54**:379–391, 1974.

[600] P. S. Hewlett and R. L. Plackett. *The Interpretation of Quantal Responses in Biology.* Edward Arnold, London, 1979.

[601] L. C. Hewson. Age, maturity, spawning and food of burbot, *Lota lota*, in Lake Winnipeg. *J. Fish. Res. Board Can.*, **12**:930–940, 1955.

[602] D. S. Hibbet. When good relationships go bad. *Nature*, **419**:345–346, 2002.

[603] R. W. Hickman. Allometry and growth of the green-lipped mussel *Perna canaliculus* in New Zealand. *Mar. Biol.*, **51**:311–327, 1979.

[604] R. Hile. Age and growth of the cisco *Leuchichthys artedi* (Le Sueur) in lake of the north-eastern High Land Eisconsian. *Bull. Bur. Fish., Wash.*, **48**:211–317, 1936.

[605] H. V. Hill. The possible effects of aggregation on the molecules of haemoglobin on its dissociation curves. *J. Physiol. (Lond.)*, **40**:IV–VII, 1910.

[606] R. Hill and C. P. Whittingham. *Photosynthesis.* Methuen, London, 1955.

[607] T. L. Hill. *An Introduction to Statistical Thermodynamics.* Dover Publications, New York, 1986.

[608] S. S. Hillman, M. S. Lea, and J. M. Duerr. Osmotic effects on mitochondria from two species of amphibian, *Bufo marinus* and *Rana catesbeiana*. *Physiogical Zoology*, **64**:1552–1560, 1991.

[609] S. S. Hillman, P. C. Withers, and R. C. Drewes. Correlation of ventricle mass and dehydration tolerance in amphibians. *Herpetologica*, **56**:413–420, 2000.

[610] M. W. Hirsch and S. Smale. *Differential Equations, Dynamical Systems, and Linear Algebra.* Academic Press, London, 1974.

[611] A. G. Hirst, D. S. Glazier, and D. Atkinson. Body shape shifting during growth permits tests that distinguish between competing geometric theories of metabolic scaling. *Ecol. Let.*, page DOI 10.1111/ele.12334, 2014.

[612] P. W. Hochachka. *Living without Oxygen.* Harvard Univ. Press, Cambridge, Mass., 1980.

[613] P. W. Hochachka and M. Guppy. *Metabolic arrest and the control of biological time.* Harvard Univ. Press, Cambridge, Mass., 1987.

[614] P. W. Hochachka and G. N. Somero. *Biochemical Adaptation.* Princeton Univ. Press, 1984.

[615] P. A. R. Hockey. Growth and energetics of the African black oystercatcher *Haematopus moquini*. *Ardea*, **72**:111–117, 1984.

[616] J. K. M. Hodasi. The effects of different light regimes on the behaviour biology of *Achatina (Achatina) achatina* (Linne). *J. Molluscan Stud.*, **48**:283–293, 1982.

[617] C. van den Hoek, D. G. Mann, and H. M. Jahn. *Algae; An Introduction to Phycology.* Cambridge Univ. Press, 1995.

[618] N. van der Hoeven. The population dynamics of daphnia at constant food supply: a review, re-evaluation and analysis of experimental series from the literature. *Neth. J. Zool.*, **39**:126–155, 1989.

[619] N. van der Hoeven, S. A. L. M. Kooijman, and W. K. de Raat. Salmonella test: relation between mutagenicity and number of revertant colonies. *Mutat. Res.*, **234**:289–302, 1990.

[620] M. Hoffman. Yeast biology enters a surprising new phase. *Science*, **255**:1510–1511, 1992.

[621] M. A. Hofman. Energy metabolism, brain size and longevity in mammals. *Q. Rev. Biol.*, **58**:495–512, 1983.

[622] M. J. Holden. The growth rates of *Raja brachyura*, *R. clavata* and *R. montaqui* as determined from tagging data. *J. Physiol. (Lond.)*, **34**:161–168, 1972.

[623] H. D. Holland. *Early Proterozoic Atmospheric Change. In: Bengtson, S. (ed.) Early Life on Earth.* Columbia Univ. Press, New York, 1994.

[624] C. S. Holling. Some characteristics of simple types of predation and parasitism. *Can. Entomol.*, **91**:385–398, 1959.

[625] B. Holmes. The perils of planting pesticides. *New Sci.*, **28**:34–37, 1993.

[626] A. B. Hope and N. A. Walker. *The Physiology of Giant Algal Cells.* Cambridge Univ. Press, 1975.

[627] N. J. Horan. *Biological Wastewater Treatment Systems.* J. Wiley, Chichester, 1990.

[628] H. J. Horstmann. Sauerstoffverbrauch und Trockengewicht der Embryonen von *Lymnaea stagnalis* L. *Z. Vgl. Physiol.*, **41**:390–404, 1958.

[629] R. A. Horton, M. Rowan, K. E. Webster, and R. H. Peters. Browsing and grazing by cladoceran filter feeders. *Can. J. Zool.*, **57**:206–212, 1979.

[630] C. Hou, W. Zuo, M. E. Moses, W. H. Woodruff, J. H. Brown, and G. W. West. Energy uptake and allocation during ontogeny. *Science*, **322**:736–739, 2008.

[631] M. A. Houck, J. A. Gauthier, and R. E. Strauss. Allometric scaling in the earliest fossil bird, *Archaeopteryx lithographica*. *Science*, **247**:195–198, 1990.

[632] S. E. L. Houde and M. R. Roman. Effects of food quality on the functional ingestion response of the copepod *Acartia tonsa*. *Mar. Ecol. Prog. Ser.*, **48**:69–77, 1987.

[633] J. Hovekamp. *On the growth of larval plaice in the North Sea.* PhD thesis, Univ. of Groningen, 1991.

[634] R. A. How. Reproduction, growth and survival of young in the mountain possum, *Trichosurus caninus* (*Marsupialia*). *Austral. J. Zool.*, **24**:189–199, 1976.

[635] H. Huber, M. J. Hohn, R. Rachel, T. Fuchs, V. C. Wimmer, and K. O. Stetter. A new phylum of Archaea represented by nanosized hyperthermophilic symbiont. *Nature*, **417**:63–67, 2002.

[636] M. F. Hubert, P. Laroque, J. P. Gillet, and K. P. Keenan. The effects of dieet, ad libitum feeding, and moderate and severe dietary restriction on body weight, survival, clinical pathology parameters, and cause of death in control sprague-dawley rats. *Toxicol. Sci.*, **58**:195–207, 2000.

[637] J. Hugenholtz and L. G. Ljungdahl. Metabolism and energy generation in homoacetogenic clostridia. *FEMS Microbiol. Rev.*, **87**:383–389, 1990.

[638] A. St. G. Huggett and W. F. Widdas. The relationship between mammalian foetal weight and conception age. *J. Physiol. (Lond.)*, **114**:306–317, 1951.

[639] R. E. Hungate. The rumen microbial ecosystem. *Annu. Rev. Ecol. Syst.*, **6**:39–66, 1975.

[640] P. C. Hunt and J. W. Jones. Trout in Llyn Alaw, Anglesey, North Wales II. Growth. *J. Fish Biol.*, **4**:409–424, 1972.

[641] R. von Hutterer. Beobachtungen zur Geburt und Jugendentwicklung der Zwergspitzmaus, *Sorex minutus* L. (*Soricidae- Insectivora*). *Z. Sauegetierkd.*, **41**:1–22, 1976.

[642] J. S. Huxley. *Problems of Relative Growth.* Methuen, London, 1932.

[643] Juan Diego Ibánez-Álamo, Enrique Rubio, and Juan José Soler. Evolution of nestling faeces removal in avian phylogeny. *Animal Behaviour*, **124**:1–5, 2017.

[644] H. L. Ibsen. Prenatal growth in guinea-pigs with special reference to environmental factors affecting weight at birth. *J. Exp. Zool.*, **51**:51–91, 1928.

[645] T. D. Iles and P. O. Johnson. The correlation table analysis of a sprat (*Clupea sprattus* L.) year-class to separate two groups differing in growth characteristics. *J. Cons. Int. Explor. Mer.*, **27**:287–303, 1962.

[646] H. Ineichen, U. Riesen-Willi, and J. Fisher. Experimental contributions to the ecology of *Chironomus* (*Diptera*) II. Influence of the photoperiod on the development of *Chironomus plumosus* in the 4th larval instar. *Oecologia (Berlin)*, **39**:161–183, 1979.

[647] L. Ingle, T. R. Wood, and A. M. Banta. A study of longevity, growth, reproduction and heart rate in *Daphnia longispina* as influenced by limitations in quantity of food. *J. Exp. Zool.*, **76**:325–352, 1937.

[648] J. L. Ingraham. Growth of psychrophillic bacteria. *J. Bacteriol.*, **76**:75–80, 1958.

[649] J. L. Ingraham. *March of the microbes; sighting the unseen.* Cambridge, Mass., London, 2010.

[650] Y. K. Ip, A. M. Loong, S. M. L. Lee, J. L. Y. Ong, W.P. Wong, and S. F. Chew. The chinese soft-shelled turtle, *Pelodiscus sinensis*, excretes urea mainly through the mouth instead of the kidney. *J. Exp. Biol.*, **215**:3723–3733, 2012.

[651] R. Ivell. The biology and ecology of a brackish lagoon bivalve, *Cerastoderma glaucum* Bruguiere, in Lago Lungo, Italy. *J. Molluscan Stud.*, **45**:364–382, 1979.

[652] E. A. Jackson. *Perspectives of Nonlinear Dynamics.*, volume I, II. Cambridge Univ. Press, 1991.

[653] J. A. Jacquez. *Compartment Analysis in Biology and Medicine.* Elsevier Publ. Co., Amsterdam, 1972.

[654] D. A. Jaffe. The nitrogen cycle. In S. S. Butcher, R. J. Charlson, G. H. Orians, and G. V. Wolfe, editors, *Global Biogeochemical Cycles.*, pages 263–284. Academic Press, London, 1992.

[655] T. Jager. *DEBkiss, a simple framework for animal energy budgets.* 2016.

[656] T. Jager, O. Alda Alvarez, J. E. Kammenga, and S. A. L. M. Kooijman. Modelling nematode life cycles using dynamic energy budgets. *Funct. Ecol.*, **19**:136–144, 2005.

[657] T. Jager, T. Crommentuijn, C. A. M. van Gestel, and S. A. L. M. Kooijman. Simultaneous modelling of multiple endpoints in life-cycle toxicity tests. *Environ. Sci. Technol.*, **38**:2894–2900, 2004.

[658] T. Jager, T. Crommentuijn, C. A. M. van Gestel, and S. A. L. M. Kooijman. Chronic exposure to chlorpyrifos reveals two modes of action in the springtail *Folsomia candida*. *Environ. Pollut.*, **145**:452–458, 2007.

[659] T. Jager and S. A. L. M. Kooijman. Modeling receptor kinetics in the analysis of survival data for organophosphorus pesticides. *Environ. Sci. Technol.*, **39**:8307–8314, 2005.

[660] T. Jager, B. T. Martin, and E. I. Zimmer. Debkiss or the quest for the simplest generic model of animal life history. *Journal of Theoretical Biology*, **328**:9–18, 2013. .

[661] M. R. James. Distribution, biomass and production of the freshwater mussel, *Hyridella menziesi* (Gray), in Lake Taupo, New Zealand. *Freshwater Biol.*, **15**:307–314, 1985.

[662] M. J. W. Jansen and J. A. J. Metz. How many victims will a pitfall make? *Acta Biotheor.*, **28**:98–122, 1979.

[663] G. Janssen. *On the genetical ecology of springtails.* PhD thesis, Vrije Univ.", address = "Amsterdam, 1985.

[664] D. Jardine and M. K. Litvak. Direct yolk sac volume manipulation of zebrafish embryos and the relationship between offspring size and yolk sac volume. *J. Fish Biol.*, **63**:388–397, 2003.

[665] X. Ji, W.-G. Du, and W.-Q. Xu. Experimental manipulation of eggs size and hatling size in the cobra, *Naja naja atra* (*Elapidae*). *Neth. J. Zool.*, **49**:167–175, 1999.

[666] F. M. Jiggins, J. K. Bentley, M. E. N. Majerus, and G. D. D. Hurst. How many species are infected with *Wolbachia*? cryptic sex ratio distorters revealed to be common by intensive sampling. *Proc. R. Soc. Lond. Biol. Sci.*, **268**:1123–1126, 2001.

[667] M. Jobling. Mathematical models of gastric emptying and the estimation of daily rates of food consumption for fish. *J. Fish Biol.*, **19**:245–257, 1981.

[668] A. W. B. Johnston, J. L. Firmin, and L. Rosen. On the analysis of symbiotic genes in *Rhizobium*. *Symp. Soc. Gen. Microbiol.*, **42**:439–455, 1988.

[669] A.S.A. Johnston, M.E. Hodson, P. Thorbek, T. Alvarez, and R.M.Sibly. An energy budget agent-based model of earthworm populations and its application to study the effects of pesticides. *Ecological Modelling*, **280**:5–17, 2014.

[670] A. Jones. Studies on egg development and larval rearing of turbot, *Scophthalmus maximus* L. and brill, *Scophthalmus rhombus* L., in the laboratory. *J. Mar. Biol. Assoc. U. K.*, **52**:965–986, 1972.

[671] G. P. Jones. Contribution to the biology of the red-banded perch, *Ellerkeldia huntii* (Hector), with a discussion on hermaphroditism. *J. Fish Biol.*, **17**:197–207, 1980.

[672] H. G. Jones. *Plant and Microclimate. A Quantitative Approach to Environmental Plant Physiology.* Cambridge Univ. Press, 1992.

[673] J. W. Jones and H. B. N. Hynes. The age and growth of *Gasterosteus aculeatus*, *Pygosteus pungitius* and *Spinachia vulgaris*, as shown by their otoliths. *J. Anim. Ecol.*, **19**:59–73, 1950.

[674] M. de Jong-Brink. Parasites make use of multiple strategies to change energy budgetting in their host. In H. J. Th. et al Goos, editor, *Perspective in Comparative Endocrinology: Unity and Diversity.* Monduzzi Editore, International Proceedings Division., 2001.

[675] E. N. G. Joosse and J. B. Buker. Uptake and excretion of lead by litter-dwelling Collembola. *Environ. Pollut.*, **18**:235–240, 1979.

[676] E. N. G. Joosse and E. Veltkamp. Some aspects of growth, moulting and reproduction in five species of surface dwelling Collembola. *Neth. J. Zool.*, **20**:315–328, 1970.

[677] B. B. Jørgensen and V. A. Gallardo. *Thioploca* spp.: filamentous sulfur bacteria with nitrate vacuoles. *FEMS Microbiol. Rev.*, **28**:301–313, 1999.

[678] D. M. Joubert. A study of pre-natal growth and development in the sheep. *J. Agric. Sci.*, **47**:382–428, 1956.

[679] J. Juget, V. Goubier, and D. Barthélémy. Intrisic and extrinsic variables controlling the productivity of asexual populations of *Nais spp*, (*Naididae*, *Oligochaeta*). *Hydrobiologia*, **180**:177–184, 1989.

[680] M. Jusup, T. Klanjscek, H. Matsuda, and S. A. L. M. Kooijman. A full lifecycle bioenergetic model for bluefin tuna. *Plos Biology*, **6**:e21903, 2011. .

[681] H. Kaiser. Populationsdynamik und Eigenschaften einzelner Individuen. *Verh. Ges. Ökol. Erlangen*, pages 25–38, 1974.

[682] H. Kaiser. The dynamics of populations as result of the properties of individual animals. *Fortschr. Zool.*, **25**:109–136, 1979.

[683] J. D. Kalbfleisch and R. L. Prentice. *The Statistical Analysis of Failure Time Data.* J. Wiley, Chichester, 1980.

[684] E. Kamler. Parent-egg-progeny relationships in teleost fishes: an energetics perspective. *Rev. Fish. Biol. Fish.*, **15**:399–421, 2005.

[685] O. Kandler. The early diversification of life and the origin of the three domains: a proposal. In J. Wiegel and M. W. W. Adams, editors, *Thermophiles: The keys to Molecular Evolution and the Origin of Life.*, pages 19–31. Taylor & Francis, Washington, 1998.

[686] G. Kapocsy. *Weissbart- und Weissflugelseeschwalbe.* A. Ziemsen-Verlag, Wittenberg Lutherstadt, 1979.

[687] S. J. Karakashian. Growth of *Paramecium bursaria* as influenced by the presence of algal symbionts. *Physiol. Zool.*, **36**:52–68, 1963.

[688] W. H. Karasov. Daily energy expenditure and the cost of activity in mammals. *Am. Zool.*, **32**:238–248, 1992.

[689] P. Karell, P. Kontiainen, H. Pieti¨ainen, H. Siitari, and J. E. Brommer. Maternal effects on offspring igs and egg size in relation to natural and experimentally improved food supply. *Funct. Ecol.*, **22**:682–690, 2008.

[690] I. Karl, M. W. Lorenz, and K. Fisher. Energetics of reproduction: consequences of divergent selection on egg size, food limitation, and female age for egg composition and reproductive effort in a butterfly. *Biol. J. Linnean Soc.*, **91**:403–418, 2007.

[691] K. B. Karsten, L. N. Andriamandimbiarisoa, S. F. Fox, and C. J. Raxworthy. A unique life history among tetrapods: an annual chameleon living mostly as an egg. *Proc. Natl. Acad. Sci. U. S. A.*, **105**:8980–8984, 2008.

[692] V. V. Kashkin. Heat exchange of bird eggs during incubation. *Biophysics*, **6**:57–63, 1961.

[693] J. F. Kasting. The rise of atmospheric oxygen. *Science*, **293**:920–925, 2001.

[694] M. Kates. The phytanyl ether-linked polar lipids and isopreniod neutral lipids of extremely halophilic bacteria. *Lipids*, **15**:301–342, 1979.

[695] L. A. Katz. The tangled web: gene genealogies and the origin of eukaryotes. *Am. Nat.*, **154**:S137–S145, 1999.

[696] L. Kaufman. Innere und Äussere Wachstumsfactoren. Untersuchungen an Hühnern und Tauben. *Wilhelm Roux' Arch. Entwicklungsmech. Org.*, **6**:395–431, 1930.

[697] N. Kautsky. Quantitative studies on gonad cycle, fecundity, reproductive output and recruitment in a baltic *Mytilus edulis* population. *Mar. Biol.*, **67**:143–160, 1982.

[698] Z. Kawabata, K. Matsui, K. Okazaki, M. Nasu, N. Nakano, and T. Sugai. Synthesis of a species-defined microcosm with protozoa. *J. Protozool. Res.*, **5**:23–26, 1995.

[699] C. Kayser and A. Heusner. Étude comparative du métabolisme énergétiques dans la série animale. *J. Physiol. (Paris)*, **56**:489–524, 1964.

[700] M. Kearney. Reproductive hyperallometry does not challenge mechanistic growth models. *Trends in Ecology and Evolution*, **34**:265–276, 2019.

[701] M. Kearney, M. K. Fujita, and J. Ridenour. Lost sex in the reptiles: constraints and correlations. In I. Schon, K. Martens, and P. van Dijk, editors, *Lost sex: the evolutionary biology of parthogenesis.*, pages 447–474. Sprinter Scientific, Dordrecht, Netherlands, 2009.

[702] A.D. Keefe, S.L. Miller, and G. Bada. Investigation of the prebiotic synthesis of amino acids and RNA bases from CO_2 using FeS/H_2S as a reducing agent. *Proc. Natl. Acad. Sci. U. S. A.*, **92**:11904–11906, 1995.

[703] P. J. Keeling. A kingdom's progress: Archaezoa and the origin of eukaryotes. *BioEssays*, **20**:87–95, 1998.

[704] B. D. Keller. Coexistence of sea urchins in seagrass meadows: an experimental analysis of competition and predation. *Ecology*, **64**:1581–1598, 1983.

[705] C. M. Kemper. Growth and development of the Australian musid *Pseudomys novaehollandiae*. *Austral. J. Zool.*, **24**:27–37, 1976.

[706] S. C. Kendeigh. Factors affecting the length of incubation. *Auk*, **57**:499–513, 1940.

[707] M. Kennedy and P. Fitzmaurice. Some aspects of the biology of gudgeon *Gobio gobio* (L.) in Irish waters. *J. Fish Biol.*, **4**:425–440, 1972.

[708] R. A. Kent and D. Currie. Predicting algal sensitivity to a pesticide stress. *Environ. Toxicol. Chem.*, **14**:983–991, 1995.

[709] K. Kersting and W. Holterman. The feeding behaviour of *Daphnia magna*, studied with the coulter counter. *Mitt. Int. Ver. Theor. Angew. Limnol.*, **18**:1434–1440, 1973.

[710] M. Kessel and Y. Cohen. Ultrastructure of square bateria from a brine pool in southern Sinai. *J. Bacteriol.*, **150**:851–860, 1982.

[711] A. Keve. *Der Eichelhaher.* A. Ziemsen-Verlag, Wittenberg Lutherstadt, 1985.

[712] A. I. Khibnik, Yu. A. Kuznetsov, V. V. Levitin, and E. V. Nikolaev. Continuation techniques and interactive software for bifurcation analysis of ODEs and iterated maps. *Physica D*, **62**:360–371, 1993.

[713] S. S. Killen, I. Costa, J. A. Brown, and A. K. Gamperl. Little left in the tank: metabolic scaling in marine teleosts and its implications for aerobic scope. *Proc. R. Soc. B.*, **203**:431–438, 2007.

[714] C. B. Kimmel, W. W. Ballard, S. R. Kimmel, B. Ullmann, and T. F. Schilling. Stages of embryonic development of the zebrafish. *Developmental Dynamics*, **203**:253–310, 1995.

[715] P. Kindlmann and A. F. G. Dixon. Developmental constraints in the evolution of reproductive strategies: telescoping of generations in parthenogenetic aphids. *Funct. Ecol.*, **3**:531–537, 1989.

[716] C. M. King. *The Natural History of Weasels and Stoats.* C. Helm, London, 1989.

[717] P. Kingston. Some observations on the effects of temperature and salinity upon the growth of *Cardium edule* and *Cardium glaucum* larvae in the laboratory. *J. Mar. Biol. Assoc. U. K.*, **54**:309–317, 1974.

[718] F. C. Kinsky. The yearly cycle of the northern blue penguin (*Eudyptula minor novaehollandiae*) in the Wellington Harbour area. *Rec. Dom. Mus. (Wellington)*, **3**:145–215, 1960.

[719] T. Kiørboe, F. Møhlenberg, and O. Nøhr. Effect of suspended bottom material on growth and energetics in *Mytilus edulis*. *Mar. Biol.*, **61**:283–288, 1981.

[720] K. L. Kirk. Egg size, offspring quality and food level in planktonic rotifers. *Freshw. Biol.*, **37**:515–521, 1997.

[721] M. Kirkpatrick, editor. *The Evolution of Haploid-Diploid life cycles.*, volume 25 of *Lectures on Mathematics in the Life Sciences*. Am. Math. Soc., Providence, Rhode Island, 1993.

[722] M. Kirkpatrick and R. Lande. The evolution of maternal characters. *Evolution*, **43**:485–503, 1989.

[723] M. Klaassen, G. Slagsvold, and C. Beek. Metabolic rate and thermostability in relation to availability of yolk in hatchlings of black-legged kittiwake and domestic chicken. *Auk*, **104**:787–789, 1987.

[724] A. Klebanoff and A. Hastings. Chaos in a three-species food chain. *J. Math. Biol.*, **32**:427–451, 1994.

[725] M. Kleiber. Body size and metabolism. *Hilgardia*, **6**:315–353, 1932.

[726] O. T. Kleiven, P. Larsson, and A. Hobæk. Sexual reproduction in *Daphnia magna* requires three stimuli. *Oikos*, **64**:197–206, 1992.

[727] D. J. Klionsky. Regulated self-cannibalism. *Nature*, **431**:31–32, 2004.

[728] C. Klok and A. M. de Roos. Population level consequences of toxicological influences on individual growth and reproduction in *Lumbricus rubellus* (Lumbricidae, Oligochaeta). *Ecotoxicol. Environ. Saf.*, **33**:118–127, 1996.

[729] H. N. Kluyver. Food consumption in relation to habitat in breeding chickadees. *Auk*, **78**:532–550, 1961.

[730] A. H. Knoll. *Life on a Young Planet; the First Three Billion Years of Evolution on Earth.* Princeton Univ. Press, Princeton, 2003.

[731] A. L. Koch. Overall controls on the biosynthesis of ribosomes in growing bacteria. *J. theor. Biol.*, **28**:203–231, 1970.

[732] A. L. Koch. The macroeconomics of bacterial growth. In M. Fletcher and G. D. Floodgate, editors, *Bacteria in Their Natural Environment*, volume 16 of *Special publication of the Society for General Microbiology*, pages 1–42. Academic Press, 1985.

[733] A. L. Koch. The variability and individuality of the bacterium. In F. C. Neidhardt, editor, Escherichia coli *and* Salmonella typhimurium. *Cellular and Molecular Biology*, pages 1606–1614. Am. Soc. Microbiol., Washington, 1987.

[734] A. L. Koch. Diffusion. the crucial process in many aspects of the biology of bacteria. *Adv. Microb. Ecol.*, **11**:37–70, 1990.

[735] A. L. Koch. Quantitative aspects of cellular turnover. *Antonie van Leeuwenhoek*, **60**:175–191, 1991.

[736] A. L. Koch. Biomass growth rate during the prokaryote cell cycle. *Crit. Rev. Microbiol.*, **19**:17–42, 1993.

[737] A. L. Koch and M. Schaechter. A model for the statistics of the division process. *J. Gen. Microbiol.*, **29**:435–454, 1962.

[738] Y. Koga, T. Kyuragi, M. Nishhihara, and N. Sone. Did archaeal and bacterial cells arise independently from noncellular precursors? A hypothesis stating that the advent of membrane phospholipids with enantiomeric glycerophosphate backbones caused the separation of the two lines of decent. *J. Mol. Evol.*, **46**:54–63, 1998.

[739] A. C. Kohler. Variations in the growth of Atlantic cod (*Gadus morhua* L.). *J. Fish. Res. Board Can.*, **21**:57–100, 1964.

[740] T. Kolokotrones, V. Savage, E. J. Deeds, and W. Fontana. Curvature in metabolic scaling. *Nature*, **464**:753–756, 2010.

[741] M. Konarzewski. A model of growth in altricial birds based on changes in water content of the tissues. *Ornis Scand.*, **19**:290–296, 1988.

[742] A. S. Kondrashov. Evolutionary genetics of life cycles. *Annu. Rev. Ecol. Syst.*, **28**:391–435, 1997.

[743] W. H. Könemann. *Quantitative structure-activity relationships for kinetics and toxicity of aquatic pollutants and their mixtures in fish.* PhD thesis, Utrecht Univ., the Netherlands, 1980.

[744] W. H. Könemann. Quantitative structure-activity relationships in fish toxicity studies. 1. Relationship for 50 industrial pollutants. *Toxicology*, **19**:209–221, 1981.

[745] B. W. Kooi. Numerical bifurcation analysis of ecosystems in a spatially homogeneous environment. *Acta Biotheor.*, **51**:189–222, 2003.

[746] B. W. Kooi and M. P. Boer. Bifurcations in ecosystem models and their biological interpretation. *Appl. Anal.*, **77**:29–59, 2001.

[747] B. W. Kooi and M. P. Boer. Chaotic behaviour of a predator-prey system. *Dyn. Cont. Discr. Impul. Syst., Ser. B: Appl. Algor.*, **10**:259–272, 2003.

[748] B. W. Kooi, M. P. Boer, and S. A. L. M. Kooijman. Mass balance equation versus logistic equation in food chains. *J. Biol. Syst.*, **5**:77–85, 1997.

[749] B. W. Kooi, M. P. Boer, and S. A. L. M. Kooijman. Consequences of population models on the dynamics of food chains. *Math. Biosci.*, **153**:99–124, 1998.

[750] B. W. Kooi, M. P. Boer, and S. A. L. M. Kooijman. On the use of the logistic equation in food chains. *Bull. Math. Biol.*, **60**:231–246, 1998.

[751] B. W. Kooi, M. P. Boer, and S. A. L. M. Kooijman. Resistance of a food chain to invasion by a top predator. *Math. Biosci.*, **157**:217–236, 1999.

[752] B. W. Kooi and P. P. F. Hanegraaf. Bi-trophic food chain dynamics with multiple component populations. *Bull. Math. Biol.*, **63**:271–299, 2001.

[753] B. W. Kooi and F. D. L. Kelpin. Structured population dynamics: a modeling perspective. *Comm. Theor. Biol.*, **8**:125–168, 2003.

[754] B. W. Kooi and S. A. L. M. Kooijman. Invading species can stabilize simple trophic systems. *Ecol. Modell.*, **133**:57–72, 2000.

[755] B. W. Kooi, L. D. J. Kuijper, M. P. Boer, and S. A. L. M. Kooijman. Numerical bifurcation analysis of a tri-trophic food web with omnivory. *Math. Biosci.*, **177**:201–228, 2002.

[756] B. W. Kooi, L. D. J. Kuijper, and S. A. L. M. Kooijman. Consequences of symbiosis for food web dynamics. *J. Math. Biol.*, **3**:227–271, 2004.

[757] B. W. Kooi and T. A. Troost. Advantages of storage in a fluctuating environment. *Theor. Pop. Biol.*, **70**:527–541, 2006.

[758] S. A. L. M. Kooijman. Statistical aspects of the determination of mortality rates in bioassays. *Water Res.*, **17**:749–759, 1983.

[759] S. A. L. M. Kooijman. Toxicity at population level. In J. Cairns, editor, *Multispecies Toxicity Testing.*, pages 143–164. Pergamon Press, New York, 1985.

[760] S. A. L. M. Kooijman. Energy budgets can explain body size relations. *J. Theor. Biol.*, **121**:269–282, 1986. .

[761] S. A. L. M. Kooijman. Population dynamics on the basis of budgets. In J. A. J. Metz and O. Diekmann, editors, *The Dynamics of Physiologically Structured Populations.*, pages 266–297. Springer-Verlag, Berlin, 1986.

[762] S. A. L. M. Kooijman. What the hen can tell about her egg: egg development on the basis of budgets. *J. Math. Biol.*, **23**:163–185, 1986.

[763] S. A. L. M. Kooijman. The von Bertalanffy growth rate as a function of physiological parameters; a comparative analysis. In T. G. Hallam, L. J. Gross, and S. A. Levin, editors, *Mathematical Ecology.*, pages 3–45. World Scientific Press, Singapore, 1988.

[764] S. A. L. M. Kooijman. *Dynamic Energy Budgets in Biological Systems. Theory and Applications in Ecotoxicology.* Cambridge Univ. Press, 1993.

[765] S. A. L. M. Kooijman. Effects of temperature on birds. In E. J. M. Hagemeijer and T. J. Verstrael, editors, *Bird Numbers 1992. Distribution, monitoring and ecological aspects.*, pages 285–290. Statistics Netherlands, Voorburg/Heerlen, 1994.

[766] S. A. L. M. Kooijman. The stoichiometry of animal energetics. *J. theor. Biol.*, **177**:139–149, 1995.

[767] S. A. L. M. Kooijman. An alternative for NOEC exists, but the standard model has to be replaced first. *Oikos*, **75**:310–316, 1996.

[768] S. A. L. M. Kooijman. The synthesizing unit as model for the stoichiometric fusion and branching of metabolic fluxes. *Biophyscal Chemistry*, **73**:179–188, 1998.

[769] S. A. L. M. Kooijman. *Dynamic Energy and Mass Budgets in Biological Systems.* Cambridge Univ. Press, 2000.

[770] S. A. L. M. Kooijman. Quantitative aspects of metabolic organization; a discussion of concepts. *Phil. Trans. R. Soc. Lond. B Biol. Sci.*, **356**:331–349, 2001.

[771] S. A. L. M. Kooijman. On the coevolution of life and its environment. In J. Miller, P. J. Boston, S. H. Schneider, and E. Crist, editors, *Scientists Debate Gaia: The Next Century.*, pages 343–351. MIT Press, Cambridge, Mass., 2004.

[772] S. A. L. M. Kooijman. Pseudo-faeces production in bivalves. *J. Sea Res.*, **56**:103–106, 2006.

[773] S. A. L. M. Kooijman. Social interactions can affect feeding behaviour of fish in tanks. *J. Sea Res.*, **62**:175–178, 2009.

[774] S. A. L. M. Kooijman. What the egg can tell about its hen: embryo development on the basis of dynamic energy budgets. *J. Math. Biol.*, **58**:377–394, 2009.

[775] S. A. L. M. Kooijman. *Dynamic Energy Budget theory for metabolic organisation.* Cambridge University Press, 2010.

[776] S. A. L. M. Kooijman. Erratum to: Yolky eggs prepare for metabolic acceleration. *J. Math. Biol.*, **67**:1019–1021, 2013. .

[777] S. A. L. M. Kooijman. Waste to hurry: Dynamic energy budgets explain the need of wasting to fully exploit blooming resources. *Oikos*, **122**:348–357, 2013. .

[778] S. A. L. M. Kooijman. Metabolic acceleration in animal ontogeny: an evolutionary perspective. *J. Sea Res.*, **94**:128–137, 2014. .

[779] S. A. L. M. Kooijman. Models in stress research. *Ecological Complexity*, **34**:161–177, 2018. .

[780] S. A. L. M. Kooijman, T. R. Andersen, and B. W. Kooi. Dynamic energy budget representations of stoichiometric constraints to population models. *Ecology*, **85**:1230–1243, 2004.

[781] S. A. L. M. Kooijman, P. Auger, J. C. Poggiale, and B. W. Kooi. Quantitative steps in symbiogenesis and the evolution of homeostasis. *Biol. Rev.*, **78**:435–463, 2003.

[782] S. A. L. M. Kooijman, J. Baas, D. Bontje, M. Broerse, C. A. M. van Gestel, and T. Jager. Ecotoxicological applications of Dynamic Energy Budget theory. In J. Devillers, editor, *Ecotoxicology Modeling*, pages 237–259. Springer, 2009.

[783] S. A. L. M. Kooijman, J. Baas, D. Bontje, M. Broerse, T. Jager, C. van Gestel, and B. van Hattum. Scaling relationships based on partition coefficients and body sizes have similarities and interactions. *SAR and QSAR in Environ. Res.*, **18**:315–330, 2007.

[784] S. A. L. M. Kooijman and J. J. M. Bedaux. *The Analysis of Aquatic Toxicity Data.* Vrije Univ. Press, Amsterdam, 1996.

[785] S. A. L. M. Kooijman and J. J. M. Bedaux. Analysis of toxicity tests on *Daphnia* survival and reproduction. *Water Res.*, **30**:1711–1723, 1996.

[786] S. A. L. M. Kooijman and J. J. M. Bedaux. Dynamic effects of compounds on animal energetics and their population consequences. In J. E. Kammenga and R. Laskowski, editors, *Demography in Ecotoxicology.*, pages 27–41. J. Wiley, 2000.

[787] S. A. L. M. Kooijman, H. A. Dijkstra, and B. W. Kooi. Light-induced mass turnover in a mono-species community of mixotrophs. *J. theor. Biol.*, **214**:233–254, 2002.

[788] S. A. L. M. Kooijman, J. Grasman, and B. W. Kooi. A new class of non-linear stochastic population models with mass conservation. *Math. Biosci.*, **210**:378–394, 2007.

[789] S. A. L. M. Kooijman and R. J. F. van Haren. Animal energy budgets affect the kinetics of xenobiotics. *Chemosphere*, **21**:681–693, 1990.

[790] S. A. L. M. Kooijman and R. Hengeveld. The symbiontic nature of metabolic evolution. In T. A. C. Reydon and L. Hemerik, editors, *Current Themes in Theoretical Biology: A Dutch perspective.*, pages 159–202. Springer, Dordrecht, 2005.

[791] S. A. L. M. Kooijman, N. van der Hoeven, and D. C. van der Werf. Population consequences of a physiological model for individuals. *Funct. Ecol.*, **3**:325–336, 1989.

[792] S. A. L. M. Kooijman and K. Lika. Resource allocation to reproduction in animals. *Biol. Rev.*, **89**:849–859, 2014. .

[793] S. A. L. M. Kooijman, K. Lika, N. Marn, S. Augustine, and B. W. Kooi. The energetic basis of population growth in animal kingdom. *Ecol. Mod.*, **428**:109055, 2020. .

[794] S. A. L. M. Kooijman and J. A. J. Metz. On the dynamics of chemically stressed populations; the deduction of population consequences from effects on individuals. *Ecotox. Environ. Saf.*, **8**:254–274, 1984. .

[795] S. A. L. M. Kooijman and R. M. Nisbet. How light and nutrients affect life in a closed bottle. In S. E. Jørgensen, editor, *Thermodynamics and Ecological Modelling.*, pages 19–60. CRC Publ., Boca Raton, FL, USA, 2000.

[796] S. A. L. M. Kooijman, L. Pecquerie, S. Augustine, and M. Jusup. Scenarios for acceleration in fish development and the role of metamorphosis. *J. Sea Res.*, **66**:419–423, 2011. .

[797] S. A. L. M. Kooijman and L. A. Segel. How growth affects the fate of cellular substrates. *Bull. Math. Biol.*, **67**:57–77, 2005.

[798] S. A. L. M. Kooijman, T. Sousa, L. Pecquerie, J. van der Meer, and T. Jager. From food-dependent statistics to metabolic parameters, a practical guide to the use of dynamic energy budget theory. *Biol. Rev.*, **83**:533–552, 2008.

[799] S. A. L. M. Kooijman and T. A. Troost. Quantitative steps in the evolution of metabolic organisation as specified by the dynamic energy budget theory. *Biol. Rev.*, **82**:1–30, 2007.

[800] E. V. Koonin, K. S. Makarova, and L. Aravind. Horizontal gene transfer in prokaryotes: Quantification and classification. *Annu. Rev. Microbiol.*, **55**:709–742, 2001.

[801] L. J. H. Koppes, C. L. Woldringh, and N. Nanninga. Size variations and correlation of different cell cycle events in slow-growing *Escherichia coli*. *J. Bacteriol.*, **134**:423–433, 1978.

[802] A. Kowald and T. B. L. Kirkwood. Towards a network theory of ageing: a model combining the free radical theory and the protein error theory. *J. theor. Biol.*, **168**:75–94, 1994.

[803] A. Kowald and T. B. L. Kirkwood. A network theory of ageing: the interactions of defective mitochondria, aberrant proteins, free radicals and scavengers in the ageing process. *Mutat. Res.*, **316**:209–235, 1996.

[804] K. B. Krauskopf and D. K. Bird. *Introduction to Geochemistry.* McGraw-Hill, New York, 1995.

[805] J.-U. Kreft, G. Booth, and W. T. Wimpenny. BacSim, a simulator for individual-based modelling of bacterial colony growth. *Microbiology*, **144**:3275–3287, 1998.

[806] F. Kreit and W. Z. Black. *Basic Heat Transfer.* Harper & Row, 1980.

[807] H. J. Kreuzer. *Nonequilibrium Thermodynamics and its Statistical Foundations.* Clarendon Press, Oxford, 1981.

[808] A. Krogh. *The respiratory exchange of animals and man.* Longmans, Green and Co., London, 1916.

[809] H. J. Kronzucker, M. Y. Siddiqi, and A. D. M. Glass. Conifer root discrimination against soil nitrate and the ecology of forest succession. *Nature*, **385**:59–61, 1997.

[810] W. E. Krumbein and D. Werner. The microbial silica cycle. In W. E. Krumbein, editor, *Microbial Geochemistry.*, pages 125–157. Blackwell Scientific Publ., Oxford, 1983.

[811] M. Kshatriya and R. W. Blake. Theoretical model of migration energetics in the blue whale, *Balaenoptera musculus*. *J. theor. Biol.*, **133**:479–498, 1988.

[812] H. E. Kubitschek. Cell growth and abrupt doubling of membrane proteins in *Escherichia coli* during the division cycle. *J. Gen. Microbiol.*, **136**:599–606, 1990.

[813] S. W. Kuffler, J. G. Nicholls, and A. R. Martin. *From Neuron to Brain.* Sinauer, Sunderland, Mass., 1984.

[814] L. D. J. Kuijper. *The role of trophic flows in food web dynamics.* PhD thesis, Vrije Univ., Amsterdam, 2004.

[815] L. D. J. Kuijper, T. R. Anderson, and S. A. L. M. Kooijman. C and N gross efficiencies of copepod egg production studies using a dynamic energy budget model. *J. Plankton Res.*, **26**:1–15, 2003.

[816] L. D. J. Kuijper, B. W. Kooi, C. Zonneveld, and S. A. L. M. Kooijman. Omnivory and food web dynamics. *Ecol. Modell.*, **163**:19–32, 2003.

[817] Yu. A. Kuznetsov. *Elements of Applied Bifurcation Theory.*, volume 112 of *Applied Mathematical Sciences.* Springer-Verlag, Berlin, 1995.

[818] Yu. A. Kuznetsov and S. Rinaldi. Remarks on food chain dynamics. *Math. Biosci.*, **134**:1–33, 1996.

[819] Herrera M. L. G, N. Ramirez P., and L. Miron M. Ammonia excretion increased and urea excretion decreased in urine of a new world nectarivorous bat with decreased nitrogen intake. *Physiological and Biochemical Zoology*, **79**(4):801–809, 2006.

[820] D. Lack. *Ecological Adaptations for Breeding in Birds.* Methuen, London, 1968.

[821] A. K. Laird. Dynamics of tumor growth. *Br. J. Cancer*, **18**:490–502, 1964.

[822] J. A. Lake. Evidence for an early prokaryotic endosymbiosis. *Nature*, **460**:967–971, 2009.

[823] H. Lambers, F. S. Chapin III, and T. L. Pons. *Plant Physiological Ecology.* Springer-Verlag, New York, 1998.

[824] N. Lane. *Oxygen, the Molecule that Made the World.* Oxford Univ. Press, 2002.

[825] A. R. G. Lang and J. E. Begg. Movements of *Helianthus annuus* leaves and heads. *J. Appl. Ecol.*, **16**:299–306, 1979.

[826] E. Lanting. *Madagascar: A World Out of Time.* Aperture, New York, 1990.

[827] D. A. Lashof. Gaia on the brink: biogeochemical feedback processes in global warming. In S. H. Schneider and P. J. Boston, editors, *Scientists on Gaia.*, pages 393–404. MIT Press, Cambridge, Mass., 1991.

[828] R. R. Lassiter and T. G. Hallam. Survival of the fattest: a theory for assessing acute effects of hydrophobic, reversibly acting chemicals on populations. *Ecology*, **109**:411–429, 1988.

[829] D. M. Lavigne, W. Barchard, S. Innes, and N. A. Oritsland. *Pinniped Bioenergetics.*, volume IV of *FAO Fisheries Series No 5.* FAO, Rome, 1981.

[830] C. Lawrence, J. P. Ebersole, and R. V. Kesseli. Rapid growth and out-crossing promote female development in zebrafish (*Danio rerio*). *Environmental Biology of Fishes*, **81**:239–246, 2008.

[831] R. M. Laws. The elephant seal (*Mirounga leonina* Linn) I. Growth and age. *RIDS Sci. Rep.*, **8**:1–37, 1953.

[832] R. M. Laws. Age criteria for the African elephant, *Loxodonta a. africana* E. *Afr. Wildl.*, **4**:1–37, 1966.

[833] B. S. C Leadbeater. The 'droop equation'-michael droop and the legacy of the 'cell-quota' model of phytoplankton growth. *Protist*, **157**:345–358, 2006.

[834] M. LeCroy and C. T. Collins. Growth and survival of roseate and common tern chicks. *Auk*, **89**:595–611, 1972.

[835] J. J. Lee, G. F. Leedale, and P. Bradbury. *An Illustrated Guide to the Protozoa.* Society of Protozoologists, Lawrence, Kansas, 2000.

[836] I. M. M. van Leeuwen. *Mathematical models in cancer risk assessment.* PhD thesis, Vrije Univ., Amsterdam, 2003.

[837] I. M. M. van Leeuwen, F. D. L. Kelpin, and S. A. L. M. Kooijman. A mathematical model that accounts for the effects of caloric restriction on body weight and longevity. *Biogerontology*, **3**:373–381, 2002.

[838] I. M. M. van Leeuwen, C. Zonneveld, and S. A. L. M. Kooijman. The embedded tumor: host physiology is important for the interpretation of tumor growth. *Br. J. Cancer*, **89**:2254–2263, 2003.

[839] A. L. Lehninger. *Bioenergetics.* Benjamin/Cummings Publ. Co., Mnlo Park, Calif., 1973.

[840] R. A. Leigh and D. Sanders. *The Plant Vacuole.* Academic Press, San Diego, 1997.

[841] W. A. Lell. The relation of the volume of the amniotic fluid to the weight of the fetus at different stages of pregnancy in the rabbit. *Anat. Rec.*, **51**:119–123, 1931.

[842] V. Lemesle and L. Mailleret. Mechanistic investigation of the algae growth "Droop" model. *Acta Biotheor.*, **56**:87–102, 2008.

[843] B. J. Lempke. *De Nederlandse trekvlinders.* W.J. Thieme, Zutphen, 1972. Lepidoptera migration.

[844] J. W. Lengeler, G. Drews, and H. G. Schlegel, editors. *Biology of the Prokaryotes.* Thieme, Stuttgart, 1999.

[845] R. Leudeking and E. L. Piret. A kinetic study of the lactic acid fermentation. *J. Biochem. Microbiol. Technol. Eng.*, **1**:393, 1959.

[846] B. Levine and D. J. Klionsky. Development by self-digestion: Molecular mechanisms and biological functions of autophagy. *Devel. Cell*, **6**:463–477, 2004.

[847] G. Levy. Demonstration of michaelis-menten kinetics in man. *J. Pharm. Sci.*, **54**:496, 1965.

[848] G. Levy, A.W. Vogel, and L.P. Amsel. Capacity-limited salicylurate formation during prolonged administration of aspirin to healthy human subjects. *J. Pharm. Sci.*, **58**:503–504, 1969.

[849] S. M. Libes. *An Introduction to Marine Biogeochemistry.* J. Wiley, New York, 1992.

[850] J. von Liebig. *Chemistry in its Application to Agriculture and Physiology.* Taylor & Walton, London, 1840.

[851] N. Lifson and R. McClintock. Theory of use of the turnover rates of body water for measuring energy and material balance. *J. theor. Biol.*, **12**:46–74, 1966.

[852] J. D. Ligon. Still more responses of the poor-will to low temperatures. *Condor*, **72**:496–498, 1970.

[853] K. Lika, S. Augustine, and S. A. L. M. Kooijman. Body size as emergent property of metabolism. *J. Sea Res.*, **143**:8–17, 2019. .

[854] K. Lika, S. Augustine, and S. A. L. M. Kooijman. The use of augmented loss functions for estimating dynamic energy budget parameters. *Ecol. Mod.*, **428**:109110, 2020. .

[855] K. Lika, S. Augustine, L. Pecquerie, and S. A. L. M. Kooijman. The bijection from data to parameter space with the standard deb model quantifies the supply-demand spectrum. *J. Theor. Biol.*, **354**:35–47, 2014. .

[856] K. Lika, M. R. Kearney, V. Freitas, H. W. van der Veer, J. van der Meer, J. W. M. Wijsman, L. Pecquerie, and S. A. L. M. Kooijman. The 'covariation method' for estimating the parameters of the standard Dynamic Energy Budget model I: philosophy and approach. *J. Sea Res.*, **66**:270–277, 2011. .

[857] K. Lika, M. R. Kearney, and S. A. L. M. Kooijman. The 'covariation method' for estimating the parameters of the standard Dynamic Energy Budget model II: properties and preliminary patterns. *J. Sea Res.*, **66**:278–288, 2011. .

[858] K. Lika and S. A. L. M. Kooijman. Life history implications of allocation to growth versus reproduction in dynamic energy budgets. *Bull. Math. Biol.*, **65**:809–834, 2003.

[859] K. Lika and S. A. L. M. Kooijman. The comparative topology of energy allocation in budget models. *J. Sea Res.*, **66**:381–391, 2011. .

[860] K. Lika and R. M. Nisbet. A dynamic energy budget model based on partitioning of net production. *J. Math. Biol.*, **41**:361–386, 2000.

[861] K. Lika and N. Papandroulakis. Modeling feeding processes: a test of a new model for sea bream (*Sparus aurata*) larvae. *Can. J. Fish. Aquat. Sci.*, **99**:1–11, 2004.

[862] P. A. Lindahl and B. Chang. The evolution of acetyl-CoA synthase. *Orig. Life Evol. Biosphere*, **31**:403–434, 2001.

[863] M. R. Lindsay, R. J. Webb, M. Strouss, M. S. M. Jetten, M. K. Butler, R. J. Forde, and J. A. Fuerst. Cell compartmentalisation in planctomycetes: novel types of structural organisation for the bacterial cell. *Arch. Microbiol.*, **175**:413–429, 2001.

[864] G. N. Ling. *In Search of the Physical Basis of Life.* Plenum Press, New York, 1984.

[865] C. Little. *The colonisation of land; Origins and adaptations of terrestrial animals.* Cambridge University Press, Cambridge, 1983.

[866] J.-S. Liu, I. W. Marison, and U. von Stockar. Microbial growth by a net heat up-take: A calorimetric and thermodynamic study on acetotrophic methanogenesis by *Methanosarcina barkeri*. *Biotechnol. Bioeng.*, **75**:170–180, 2001.

[867] L. G. Ljungdahl. The acetyl-CoA pathway and the chemiosmotic generation of ATP during acetogenesis. In H. L. Drake, editor, *Acetogenesis.*, pages 63–87. Chapman & Hall, New York, 1994.

[868] C. Lockyer. Growth and energy budgets of large baleen whales from the southern hemisphere. In *Mammals in the Seas*, volume III of *FAO Fisheries series No 5*. FAO, Rome, 1981.

[869] H. Lodish, A. Berk, S. L. Zipursky, P. Matsudaira, D. Baltimore, and J. Darnell. *Molecular Cell Biology.* W. H. Freeman & Co, New York, 2000.

[870] B. E. Logan and J. R. Hunt. Bioflocculation as a microbial response to substrate limitations. *Biotechnol. Bioeng.*, **31**:91–101, 1988.

[871] B. E. Logan and D. L. Kirchman. Uptake of dissolved organics by marine bacteria as a function of fluid motion. *Mar. Biol.*, **111**:175–181, 1991.

[872] H. Lohrl. *Die Tannemeise.* A. Ziemsen-Verlag, Wittenberg Lutherstadt, 1977.

[873] J. Loman. Microevolution and maternal effects on tadpole *Rana temporaria* growth and development rate. *J. Zool. of Lond.*, **257**:93–99, 2002.

[874] A. Łomnicki. *Population Ecology of Individuals.* Princeton Univ. Press, 1988.

[875] J. A. Long, K. Trinajstic, G. C. Young, and T. Senden. Live birth in the Devonian period. *Nature*, **453**:650–651, 2008.

[876] T. G. A. Lonhiennea, E. Sagulenko, R. I. Webb, K.-C. Lee, J. Franke, D. P. Devos, A. Nouwens, B. J. Carroll, and J. A. Fuerst. Endocytosis-like protein uptake in the bacterium *Gemmata obscuriglobus*. *Proc. Natl. Acad. Sci. U. S. A.*, **107**:12883–12888, 2010.

[877] A. Lorena, G. Marques, S. A. L. M. Kooijman, and T. Sousa. Stylized facts in microalgal growth - interpretation in a DEB context. *Phil. Trans. R. Soc. B*, **365**:3509–3521, 2010.

[878] E. N. Lorenz. Deterministic non-periodic flow. *J. Atmospher. Sci.*, **20**:130–141, 1963.

[879] B. G. Loughton and S. S. Tobe. Blood volume in the African migratory locust. *Can. J. Zool.*, **47**:1333–1336, 1969.

[880] J.-C. Lousse and J. Donnez. Laparoscopic observation of spontaneus human ovulation. *Fertility and Sterility*, **90**:833–834, 2008.

[881] G. Louw. *Physiological Animal Ecology.* Longman, London, 1993.

[882] B. Lovegrove. *The Living Deserts of Southern Africa.* Fernwood Press, Vlaeberg, 1993.

[883] B. G. Lovegrove and C. Wissel. Sociality in molerats: Metabolic scaling and the role of risk sensitivity. *Oecologia (Berlin)*, **74**:600–606, 1988.

[884] Y. Loya and L. Fishelson. Ecology of fish breeding in brackish water ponds near the Dead Sea (Israel). *J. Fish Biol.*, **1**:261–278, 1969.

[885] A. G. Lyne. Observations on the breeding and growth of the marsupial *Pelametes nasuta* geoffroy, with notes on other bandicoots. *Austral. J. Zool.*, **12**:322–339, 1964.

[886] J. W. MacArthur and W. H. T. Baillie. Metabolic activity and duration of life. I. Influence of temperature on longevity in *Daphnia magna*. *J. Exp. Zool.*, **53**:221–242, 1929.

[887] R. H. MacArthur and E. O. Wilson. *The Theory of Island Biogeography.* Princeton Univ. Press, 1967.

[888] B. A. MacDonald and R. J. Thompson. Influence of temperature and food availability on ecological energetics of the giant scallop *Placopecten magellanicus* I. Growth rates of shell and somatic tissue. *Mar. Ecol. Prog. Ser.*, **25**:279–294, 1985.

[889] D. MacDonald. *European mammals; Evolution and behaviour.* HarperCollins, London, 1995.

[890] E. C. MacDowell, E. Allen, and C. G. Macdowell. The prenatal growth of the mouse. *J. Gen. Physiol.*, **11**:57–70, 1927.

[891] D. MacKay. Correlation of bioconcentration factors. *Environ. Sci. Technol.*, **16**:274–278, 1982.

[892] D. MacKay and S. Paterson. Calculating fugacity. *Environ. Sci. Technol.*, **15**:1006–1014, 1981.

[893] D. Mackay, W. Y. Shiu, and K. C. Ma. *Illustrated Handbook of Physical-Chemical Properties and Environmental Fate for Organic Chemicals.* Lewis publishers, Inc., Michigan, USA, 1992.

[894] R. S. MacKay and C. Tresser. Some flesh on the skeleton: the bifurcations of bimodal maps. *Physica D*, **27**:412–422, 1987.

[895] M. T. Madigan, J. M. Martinko, and J. Parker. *Brock Biology of Microorganisms.* Prentice-Hall, Englewood Cliffs, 2000.

[896] T. H. Mague, E. Friberg, D. J. Hughes, and I. Morris. Extracellular release of carbon by marine phytoplankton; a physiological approach. *Limnol. Oceanogr.*, **25**:262–279, 1980.

[897] R. A. Mah, D. M. Ward, L. Baresi, and T. L. Glass. Biogenesis of methane. *Annu. Rev. Microbiol.*, **31**:309–341, 1977.

[898] S. P. Mahoney and W. Threlfall. Notes on the eggs, embryos and chick growth of the common guillemots *Uria aalge* in Newfoundland. *Ibis*, **123**:211–218, 1981.

[899] U.-G. Maier, S. E. Douglas, and T. Cavalier-Smith. The nucleomorph genomes of cryptophytes and chlorarachniophytes. *Protist*, **151**:103–109, 2000.

[900] R. M. Malina. Secular trends in growth, maturation and physical performance: A review. *Anthropological Review*, **67**:3–31, 2004.

[901] S. E. Manahan. *Environmental Chemistry.* Lewis Publishers, 1994.

[902] K. H. Mann and J. R. N. Lazier. *Dynamics of Marine Ecosystems.* Blackwell Science, Oxford, 1996.

[903] R. H. K. Mann. The growth and reproductive stategy of the gudgeon, *Gobio gobio* (L.), in two hard-water rivers in southern England. *J. Fish Biol.*, **17**:163–176, 1980.

[904] S. C. Manolis, G. J. W. Webb, and K. E. Dempsey. Crocodile egg chemistry. In G. J. W. Webb, S. C. Manolis, and P. J. Whitehead, editors, *Wildlife Management: Crocodiles and Alligators*, pages 445–472. Beatty, Sydney, 1987.

[905] D. A. Manuwal. The natural history of Cassin's auklet (*Ptychoramphus aleuticus*). *Condor*, **76**:421–431, 1974.

[906] L. Margulis. *Origins of Eukaryotic Cells.* Freeman, San Fransico, 1970.

[907] L. Margulis. *Symbiosis in Cell Evolution.* Freeman, New York, 1993.

[908] L. Margulis and R. Fester, editors. *Symbiosis as a Source of Evolutionary Innovation.* MIT Press, Cambridge, Mass., 1991.

[909] D. M. Maron and B. N. Ames. Revised methods for the *Salmonella* mutagenicity test. *Mutat. Res.*, **113**:173–215, 1983.

[910] G. M. Marques, S. Augustine, K. Lika, L. Pecquerie, T. Domingos, and S. A. L. M. Kooijman. The amp project: Comparing species on the basis of dynamic energy budget parameters. *PLOS Computational Biology*, **14(5)**:e1006100, 2018. .

[911] G. M. Marques, K. Lika, S. Augustine, L. Pecquerie, and S. A. L. M. Kooijman. Fitting multiple models to multiple data sets. *J. Sea Res.*, **143**:48–56, 2019. .

[912] A. G. Marr, E. H. Nilson, and D. J. Clark. The maintenance requirement of *Escherichia coli*. *Annu. N. Y. Acad. Sci.*, **102**:536–548, 1963.

[913] A. G. Marr, P. R. Painter, and E. H. Nilson. Growth and division of individual bacteria. *Symp. Soc. Gen. Microbiol.*, **19**:237–261, 1969.

[914] B. T. Martin, R. Heintz, E. M. Danner, and R. M. Nisbet. Integrating lipid storage into general representations of fish energetics. *Journal of Animal Ecology*, 2017.

[915] M. M. Martin. *Invertebrate-Microbial Interactions: Ingested Fungal Enzymes in Arthropod Biology.* Explorations in Chemical Ecology. Comstock, Ithaca, 1987.

[916] W. Martin and M. Muller. The hydrogen hypothesis for the first eukaryote. *Nature*, **392**:37–41, 1998.

[917] W. Martin, C. Rotte, M. Hoffmeister, U. Theissen, g. Gelius-Dietrich, A. Ahr, and K. Henze. Early cell evolution, eukaryotes, anoxia, sulfide, oxygen, fungi first (?), and a thee of genomes revisited. *Life*, **55**:193–204, 2003.

[918] W. Martin, T. Rujan, E. Richly, A. Hansen, Cornelsen, S., T. Lins, D. Leister, B. Stoebe, M. Hasegawa, and D. Penny. Evolutionary analysis of arabidopsis, cyanobacterial, and chloroplast genomes reveals plastid phylogeny and thousands of cyanobacterial genes in the nucleus. *Proc. Natl. Acad. Sci. U. S. A.*, **99**:12246–12251, 2002.

[919] W. Martin and M. Russel. On the origin of cells: a hypothesis for the evolutionary transitions from abiotic geochemistry to chemoautotrophic prokaryotes and from prokaryotes to nucleated cell. *Phil. Trans. R. Soc. Lond. B Biol. Sci.*, **358**:59–85, 2003.

[920] W. Martin and C. Schnarrenberger. The evolution of the calvin cycle from prokaryotic to eukaryotic chromosomes: a case study of functional redundancy in ancient pathways through endosymbiosis. *Curr. Genet.*, **32**:1–18, 1997.

[921] W. Martin, B. Stoebe, V. Goremykin, S. Hansmann, M. Hasegawa, and K. V. Kowallik. Gene transfer to the nucleus and the evolution of chloroplasts. *Nature*, **393**:162–165, 1998.

[922] M. Q. Martindale. The ontogeny and maintenance of adult symmetry properties in the ctenophore *Mnemiopsis mccradyi*. *Devel. Biol*, **118**:556–576, 1986.

[923] D. Masman. *The annual cycle of the kestrel* Falco tinnunculus*; a study in behavioural energetics.* PhD thesis, Univ. of Groningen, 1986.

[924] N. Matscheko, S. Lundstedt, L. Svensson, M. Harju, and M. Tysklind. Accumulation and elimination of 16 polycyclic aromatic compounds in the earthworm (*Eisenia fetida*). *Environ. Toxicol. Chem.*, **21**:1724–1729, 2002.

[925] G. L. C. Matthaei. On the effect of temperature on carbon-dioxide assimilation. *Phil. Trans. R. Soc. Lond. B Biol. Sci.*, **197**:47–105, 1905.

[926] A. G. Matthysse, K. Deschet, M. Williams, M. Marry, A. R. White, and W. C. Smith. A functional cellulose synthase from ascidian epidermis. *Proc. Natl. Acad. Sci. U. S. A.*, **101**:986–991, 2004.

[927] J. Mauchline and L. R. Fisher. *The Biology of Euphausids.*, volume 7 of *Advances in Marine Biology*. Academic Press, 1969.

[928] J. E. Maunder and W. Threlfall. The breeding biology of the black-legged kittiwake in Newfoundland. *Auk*, **89**:789–816, 1972.

[929] R. M. May. *Stability and Complexity in Model Ecosystems*. Princeton Univ. Press, 1973.

[930] R. M. May. Simple mathematical models with very complicated dynamics. *Nature*, **261**:459, 1976.

[931] J. Maynard Smith, N. H. Smith, M. O'Rourke, and B. G. Spratt. How clonal are bacteria? *Proc. Natl. Acad. Sci. U. S. A.*, **90**:4384–4388, 1993.

[932] W. V. Mayneord. On a law of growth of Jensen's rat sarcoma. *Am. J. Cancer*, **16**:841–846, 1932.

[933] G. M. Maynes. Growth of the Parma wallaby, *Macropus parma* Waterhouse. *Austral. J. Zool.*, **24**:217–236, 1976.

[934] K. McCann and P. Yodzis. Nonlinear dynamics and population disappearances. *Am. Nat.*, **144**:873–879, 1994.

[935] K. McCann and P. Yodzis. Bifurcation structure of a tree-species food chain model. *Theor. Pop. Biol.*, **48**:93–125, 1995.

[936] E. McCauley, W. W. Murdoch, and R. M. Nisbet. Growth, reproduction, and mortality of *Daphnia pulex* Leydig: life at low food. *Funct. Ecol.*, **4**:505–514, 1990.

[937] M. D. McCue. Starvation physiology: Reviewing the different strategies animals use to survive a common challenge. *Comp. Biochem. Physiol. A*, **156**:1–18, 2010.

[938] P. McCullagh and J. A. Nelder. *Generalized Linear Models.* Monographs on Statistics and Applied Probability. Chapman & Hall, London, 1983.

[939] E. H. McEwan. Growth and development of the barren-ground caribou II. Postnatal growth rates. *Can. J. Zool.*, **46**:1023–1029, 1968.

[940] G. I. McFadden. Primary and secondary endosymbiosis and the origin of plastids. *J. Phycol.*, **37**:951–959, 2001.

[941] M. D. McGurk. Effects of delayed feeding and temperature on the age of irreversible starvation and on the rates of growth and mortality of pacific herring larvae. *Mar. Biol.*, **84**:13–26, 1984.

[942] G. S. McIntyre and R. H. Gooding. Egg size, contents, and quality: maternal-age and-size effects on house fly eggs. *Can. J. Zool.*, **78**:1544–1551, 2000.

[943] D. McKee and D. Ebert. The interactive effects of temperature, food level and maternal phenotype on offspring size in *Daphnia magna*. *Oecologia*, **107**:189–196, 1996.

[944] J. J. McMahon and W. C. Summers. Temperature effects on the developmental rate of squid (*Loligo pealei*) embryos. *Biol. Bull.*, **121**:561–567, 1971.

[945] J. W. McMahon. Some physical factors influencing the feeding behavior of *Daphnia magna* Straus. *Can. J. Zool.*, **43**:603–611, 1965.

[946] T. A. McMahon. Size and shape in biology. *Science*, **179**:1201–1204, 1973.

[947] T. A. McMahon and J. T. Bonner. *On Size and Life*. Freeman, New York, 1983.

[948] B. K. McNab. On the ecological significance of Bergmann's rule. *Ecology*, **52**:845–854, 1971.

[949] B. K. McNab. Energy expenditure: a short history. In T. E. Tomasi and T. H. Horton, editors, *Mammalian Energetics*, pages 1–15. Comstock Publ. Assoc., Ithaca, 1992.

[950] D.A. McQuarrie. Stochastic approach to chemical kinetics. *J. Appl. Prob.*, **4**:413–478, 1967.

[951] L. D. Mech, M. E. M. E. Nelson, and R. E. McRoberts. Effects of maternal and grandmaternal nutrition on deer mass and vulnerability to wolf predation. *J. Mammol.*, **72**:146–151, 1991.

[952] J. van der Meer. Metabolic theories in biology. *Trends Ecol. Evol.*, **21**:136–140, 2006.

[953] J. van der Meer. Metabolic theories in ecology: the dynamic energy budget (deb) theory and the metabolic theory of ecology (mte). In B. Fath, editor, *Encyclopedia of Ecology*. Elsevier, 2018.

[954] E. M. Meijer, H. W. van Verseveld, E. G. van der Beek, and A. H. Stouthamer. Energy conservation during aerobic growth in *Paracoccus denitrificans*. *Arch. Microbiol.*, **112**:25–34, 1977.

[955] T. H. M. Meijer. *Reproductive decisions in the kestrel* Falco tinnunculus*; a study in physiological ecology.* PhD thesis, Univ. of Groningen, 1988.

[956] T. H. M. Meijer, S. Daan, and M. Hall. Family planning in the kestrel (*Falco tinnuculus*): the proximate control of covariation of laying data and clutch size. *Behaviour*, **114**:117–136, 1990.

[957] E. Meléndez-Hevia. The game of the pentose phosphate cycle: a mathematical approach to study the optimization in design of metabolic pathways during evolution. *Biomed. Biochem. Acta*, **49**:903–916, 1990.

[958] E. Meléndez-Hevia and A. Isidoro. The game of the pentose phosphate cycle. *J. theor. Biol.*, **117**:251–263, 1985.

[959] W. de Melo and S. J. van Strien. *One-Dimensional Dynamics.* Springer-Verlag, Berlin, 1993.

[960] M. L. Mendelsohn. Cell proliferation and tumor growth. In L. F. Lamerton and R. J. M. Fry, editors, *Cell Proliferation*, pages 190–210. Blackwell, Oxford, 1963.

[961] J. A. J. Metz and F. H. D. van Batenburg. Holling's 'hungry mantid' model for the invertebrate functional response considered as a Markov process. I: The full model and some of its limits. *J. Math. Biol.*, **22**:209–238, 1985.

[962] J. A. J. Metz and F.H. D. van Batenburg. Holling's 'hungry mantid' model for the invertebrate functional response considered as a Markov process. II: Negligible handling time. *J. Math. Biol.*, **22**:239–257, 1985.

[963] J. A. J. Metz and O. Diekmann. *The Dynamics of Physiologically Structured Populations.*, volume 68 of *Lecture Notes in Biomathematics.* Springer-Verlag, Berlin, 1986.

[964] J. A. J. Metz and O. Diekmann. Exact finite dimensional representations of models for physiologically structured populations. I: The abstract foundations of linear chain trickery. In J. A. Goldstein, F. Kappel, and W. Schappacher, editors, *Differential Equations with Applications in Biology, Physics, and Engineering*, pages 269–289. Marcel Dekker, New York, 1991.

[965] J. A. J. Metz, S. A. H. Geritz, G. Meszéna, F. J. A. Jacobs, and J. S. van Heerwaarden. Adaptive dynamics, a geometrical study of the consequences of nearly faithful reproduction. In S. J. van Strien and S. M. Verduyn Lunel, editors, *Stochastic and Spatial Structures of Dynamical systems*, pages 183–231. North-Holland, Amsterdam, 1996.

[966] D. E. Metzler. *Biochemistry; the Chemical Reactions of Living Cells.* Academic Press, New York, 1977.

[967] E. A. Meuleman. Host-parasite interrelations between the freshwater pulmonate *Biomphalaria pfeifferi* and the trematode *Schistosoma mansoni. Neth. J. Zool.*, **22**:355–427, 1972.

[968] H. Meyer and L. Ahlswede. Über das intrauterine Wachstum und die Körperzusammensetzung von Fohlen sowie den Nährstoffbedarf tragender Stuten. *Übersicht. Tierernähr.*, **4**:263–292, 1976.

[969] D. G. Meyers. Egg development of a chydorid cladoceran, *Chydorus sphaericus*, exposed to constant and alternating temperatures: significance to secondary productivity in fresh water. *Ecology*, **61**:309–320, 1984.

[970] L. Michaelis and M. L. Menten. Die Kinetik der Invertwirkung. *Biochem. Z.*, **49**:333–369, 1913.

[971] W. Michaelis, R. Seifert, K. Nauhaus, and others. Microbial reefs in the black sea fuelled by anaerobic oxidation of methane. *Science*, **297**:1013–836, 2002.

[972] R. Mikelsaar. A view of early cellular evolution. *J. Mol. Evol.*, **25**:168–183, 1987.

[973] H. Mikkola. *Der Bartkauz.* A. Ziemsen-Verlag, Wittenberg Lutherstadt, 1981.

[974] T. T. Milby and E. W. Henderson. The comparative growth rates of turkeys, ducks, geese and pheasants. *Poult. Sci.*, **16**:155–165, 1937.

[975] S. Milius. Sea slug steals genes for greens, makes chlorophyll like a plant. *ScienceNews*, **117**:10, 2010.

[976] J. S. Millar. Post partum reproductive characteristics of eutherian mammals. *Evolution*, **35**:1149–1163, 1981.

[977] A. R. Millard. The body temperature of *Tyrannosaurus rex. Science*, **267**:1666–1667, 1995.

[978] P. J. Miller. Age, growth, and reproduction of the rock goby, *Gobius paganellus* L., in the Isle of Man. *J. Mar. Biol. Assoc. U. K.*, **41**:737–769, 1961.

[979] P. Milton. Biology of littoral blenniid fishes on the coast of south-west England. *J. Mar. Biol. Assoc. U. K.*, **63**:223–237, 1983.

[980] A. Mira. Why is meiosis arrested? *J. theor. Biol.*, **194**:275–287, 1998.

[981] J. K. Misra and R. W. Lichtwardt. *Illustrated Genera of Trichomycetes; Fungal Symbionts of Insects and Other Arthropods.* Science Publishers, Enfield, NH, USA, 2000.

[982] N. J. Mitchell. Low tolerance of embryonic desiccation in the terrestrial nesting frog *Bryobatrachus nimbus* (anura: Myobatrachinae). *Copeia*, **2**:364–373, 2002.

[983] J. M. Mitchison. The growth of single cells III: *Streptococcus faecalis. Exp. Cell Res.*, **22**:208–225, 1961.

[984] G. G. Mittelbach. Predation and resource patitioning in two sunfishes (*Centrarchidae*). *Ecology*, **65**:499–513, 1984.

[985] L. F. Møller, J. M. Canon, and P. Tiselius. Bioenergetics and growth in the ctenophore *Pleurobrachia pileus. Hydrobiologia*, **645**:167–178, 2010.

[986] J. Monod. *Recherches sur la Croissance des Cultures Bactériennes.* Hermann, Paris, 2nd edition, 1942.

[987] R. Montani. Warm-blooded 'seadragons'? *Science*, **328**:1361–1362, 2010.

[988] J. L. Monteith and M. H. Unsworth. *Principles of Environmental Physics.* E. Arnold, London, 1990.

[989] K. L. Montheith, L. E. Schmitz, J. A. Jenks, J. A. Delger, and R. T. Bowyer. Growth of male white-tailed deer: consequences of maternal effects. *Journal of Mammalogy*, **90**:651–660, 2009.

[990] M. Montserrat, C. Bas, S. Magelhães, M. W. Sabelis, A. de Roos, and S. Janssen. Predators induce egg retention in prey. *Oecologia*, **150**:699–705, 2007.

[991] D. Moore. *Fungal Morphogenesis.* Cambridge Univ. Press, 1998.

[992] D. Moran and R. M. G. Wells. Ontogenetic scaling of fish metabolism in the mouse-to-elephant mass magnitude range. *Comp.Biochem. Physiol. A*, **148**:611–620, 2007.

[993] N. Moran and P. Baumann. Phylogenetics of cytoplasmically inherited microorganisms of arthropods. *Trends Ecol. Evol.*, **9**:15–20, 1994.

[994] F. M. M. Morel. Kinetics of nutrient uptake and growth in phytoplankton. *J. Phycol.*, **23**:137–150, 1987.

[995] S. Moreno, P. Nurse, and P. Russell. Regulation of mitosis by cyclic accumulation of $p80^{cdc25}$ mitotic inducer in fission yeast. *Nature*, **344**:549–552, 1990.

[996] Y. Moret, P. Juchault, and T. Rigaud. *Wolbachia* endosymbiont responsible for cytoplasmic incompatibility in a terrestrial crustacean: effects in natural and foreign hosts. *Heredity*, **86**:325–332, 2001.

[997] S. A. Morley, R. S. Batty, A. J. Geffen, and P. Tytler. Egg size manipulation: a technique for investigating maternal effects on the hatching characteristics of herring. *J. Fish Biol.*, **55 (suppl. A)**:233–238, 1999.

[998] H. J. Morowitz, J. D. Kosttelrik, J. Yang, and G. D. Cody. The origin of intermediary metabolism. *Proc. Natl. Acad. Sci. U. S. A.*, **97**:7704–7708, 2000.

[999] J. A. Morrison, C. E. Trainer, and P. L. Wright. Breeding season in elk as determined from known-age embryos. *J. Wildl. Manage.*, **23**:27–34, 1959.

[1000] G. J. Morton, D. E. Cummings, D. G. Baskin, G. S. Barsh, and M. W. Schwartz. Central nervous system control of food intake and body weight. *Nature*, **443**:289–294, 2006.

[1001] J. Moya-Laraño. Senescence and food limitation in a slowly ageing spider. *Funct. Ecol.*, **16**:734–741, 2002.

[1002] C. Mueller, A. Augustine, S. A. L. M. Kooijman, M. R. Kearney, and R. Seymour. The trade-off between maturation and growth during accelerated development in frogs. *Comp. Physiol. Biochem. A*, **163**:103–110, 2012. .

[1003] B. S. Muir. Comparison of growth rates for native and hatchery-stocked populations of *Esox masquinongy* in Nogies Creek, Ontario. *J. Fish. Res. Board Can.*, **17**:919–927, 1960.

[1004] Y. Mukohata, editor. *New Era of Bioenergetics.* Academic Press, London, 1991.

[1005] M. M. Mulder. *Energetic aspects of bacterial growth: a mosaic non-equilibrium thermodynamic approach.* PhD thesis, Amsterdam Univ., 1988.

[1006] E. B. Muller. *Bacterial energetics in aerobic wastewater treatment.* PhD thesis, Vrije Univ., 1994.

[1007] E. B. Muller, R. M. Nisbet, S. A. L. M. Kooijman, J. J. Elser, and E. McCauley. Stoichiometric food quality and herbivore dynamics. *Ecol. Lett.*, **4**:519–529, 2001.

[1008] M. T. Murphy. Ecological aspects of the reproductive biology of eastern kingbirds: geographic comparisons. *Ecology*, **64**:914–928, 1983.

[1009] A. W. Murray and M. W. Kirschner. What controls the cell cycle? *Sci. Am.*, **3**:34–41, 1991.

[1010] L. Muscatine and H. M. Lenhoff. Symbiosis of hydra and algae. II. Effects of limited food and starvation on growth of symbiotic and aposymbiotic hydra. *Biol. Bull. (Woods Hole)*, **129**:316–328, 1965.

[1011] L. Muscatine, L. R. McCloskey, and R. E. Marian. Estimating the daily contribution of carbon from zooxanthellae to coral animal respiration. *Limnol. Oceanogr.*, **26**:601–611, 1981.

[1012] L. Muscatine and V. Weis. Productivity of zooxanthellae and biogeochemical cycles. In P. G. Falkowski and A. D. Woodhed, editors, *Primary Productivity and Biochemical Cycles in the Sea*, pages 257–271. Plenum Press, New York, 1992.

[1013] S. Nagasawa. Parasitism and diseases in chaetognats. In Q. Bone, H. Kapp, and A. C. Pierrot-Bults, editors, *The Biology of Chaetognats.* Oxford Univ. Press, 1991.

[1014] S. Nagasawa and T. Nemoto. Presence of bacteria in guts of marine crustaceans on their fecal pellets. *J. Plankton Res.*, **8**:505–517, 1988.

[1015] R. G. Nager, P. Monaghan, and D. C. Houston. Within-clutch trade-offs between the number and quality of eggs: experimental manipulations in gulls. *Ecology*, **81**:1339–1350, 2000.

[1016] R. G. Nager, P. Monaghan, D. C. Houston, K. E. Arnold, J. D. Blount, and N. Berboven. Maternal effects through the avian egg. *Acta Zoologica Sinica*, **52 (suppl)**:658–661, 2006.

[1017] H. Nakajima and Z. Kawabata. Sensitivity analysis in microbial cummunities. In Colwell *et al.* editor, *Microbial Diversity in Time and Space*, pages 85–91. Plenum Press, New York, 1996.

[1018] A. Narang, A. Konopka, and D. Ramkrishna. New patterns of mixed substrate growth in batch cultures of *Escherichia coli* K12. *Biotechnol. Bioeng.*, **55**:747–757, 1997.

[1019] R. D. M. Nash. The biology of Fries' goby, *Lesueurigobius friesii* (Malm) in the Firth of Clyde, Scotland, and a comparison with other stocks. *J. Fish Biol.*, **21**:69–85, 1982.

[1020] Richard D. M. Nash, Antonio H. Valencia, and Audrey J. Geffen. The origin of Fulton's condition factor - setting the record straight. *Fisheries*, **31(5)**:236–238, 2006.

[1021] S. Nee, A. F. Read, J. D. Greenwood, and P. H. Harvey. The relationship between abundance and body size in British birds. *Nature*, **351**:312–313, 1991.

[1022] F. C. Neidhardt, J. L. Ingraham, and M. Schaechter. *Physiology of the Bacterial Cell: a Molecular Approach.* Sinauer, Sunderland, MA, 1990.

[1023] J. A. Nelder. The fitting of a generalization of the logistic curve. *Biometrics*, **17**:89–110, 1961.

[1024] B. Nelissen, Y. van der Peer, A. Wilmotte, and R. de Wachter. An early origin of plastids within the cyanobacterial divergence is suggested by evolutionary trees based on complete 16S rRNA sequneces. *Mol. Biol. Evol.*, **12**:1166–1173, 1995.

[1025] B. Nelson. *The Gannet.* T. & A. D. Poyser, Berkhamsted, 1978.

[1026] E. Nestaas and D. I. C. Wang. Computer control of the penicillum fermentation using the filtration probe in conjunction with a structured model. *Biotechnol. Bioeng.*, **25**:781–796, 1983.

[1027] M. C. Newman and D. K. Doubet. Size dependence of mercury (II) accumulation in the mosquitofish *Gambusia affinis* (Baird and Girard). *Arch. Environ. Contam. Toxicol.*, **18**:819–825, 1989.

[1028] M. C. Newman and S. V. Mitz. Size dependence of zinc elimination and uptake from water by mosquitofish *Gambusia affinis* (baird and girard). *Aquat. Toxicol.*, **12**:17–32, 1988.

[1029] I. Newton. *The Migration Ecology of Birds.* Elsevier, Amsterdam, 2008.

[1030] M. M. Nice. Development of behavior in precocial birds. *Trans. Linn. Soc. (NY)*, **13**:211pp, 1962.

[1031] D. G. Nicholls. *Bioenergetics. An Introduction to the Chemiosmotic Theory.* Academic Press, New York, 1982.

[1032] A. J. Niimi and B. G. Oliver. Distribution of polychlorinated biphenyl congeners and other hydrocarbons in whole fish and muscle among Ontario salmonids. *Environ. Sci. Technol.*, **23**:83–88, 1989.

[1033] K. J. Niklas. *Plant Allometry; The Scaling of Form and Process.* Chicago Univ. Press, Chicago, 1994.

[1034] M. M. Ninness, E. D. Stevens, and P. A. Wright. Removal of the chorion before hatching results in increased movement and accelerated growth in rainbow trout (oncorhynchus mykiss) embryos. *Journal of Experimental Biology*, **209**:1874–1882, 2006.

[1035] B. Nisbet. *Nutrition and Feeding Strategies in Protozoa.* Croom Helm, London, 1984.

[1036] E. G. Nisbet and C. M. R. Fowler. Archaean metabolic evolution of microbial mate. *Proc. R. Soc. Lond. Biol. Sci.*, **266**:2375–2382, 1999.

[1037] R. M. Nisbet, A. Cunningham, and W. S. C. Gurney. Endogenous metabolism and the stability of microbial prey-predator systems. *Biotechnol. Bioeng.*, **25**:301–306, 1983.

[1038] R. M. Nisbet and W. S. C. Gurney. Model of material cycling in a closed ecosystem. *Nature*, **264**:633–634, 1976.

[1039] R. M. Nisbet, A. H. Ross, and A. J. Brooks. Empirically-based dynamic energy budget models: theory and application to ecotoxicology. *Nonlinear World*, **3**:85–106, 1996.

[1040] P. S. Nobel. *Physicochemical and Environmental Plant Physiology.* Academic Press, San Diego, 1999.

[1041] D. R. Nobles and R. M. Brown. The pivotal role of cyanobacteria in the evolution of cellulose synthase and cellulose synthase-like proteins. *Cellulose*, **11**:437–448, 2004.

[1042] V. Norris and D. J. Raine. A fission-fusion origin for life. *Orig. Life Evol. Biosphere*, **29**:523–537, 1998.

[1043] T. H. Y. Nose and Y. Hiyama. Age determination and growth of yellowfin tuna, *Thunnus albacares* Bonnaterre by vertebrae. *Bull. Jpn. Soc. Sci. Fish.*, **31**:414–422, 1965.

[1044] W. J. O'Brian. The dynamics of nutrient limitation of phytoplankron algae: a model reconsidered. *Ecology*, **55**:135–141, 1974.

[1045] N. Okamoto and I. Inouye. A secondary symbiosis in progress? *Science*, **310**:287, 2005.

[1046] A. Okubo. *Diffusion and Ecological Problems: Mathematical Models.* Springer-Verlag, Berlin, 1980.

[1047] B. G. Oliver and A. J. Niimi. Trophodynamic analysis of polychlorinated biphenyl congeners and other chlorinated hydrocarbons in Lake Ontario ecosystem. *Environ. Sci. Technol.*, **22**:388–397, 1988.

[1048] G. J. Olsen and C. R. Woese. Lessons from an archaeal genome: what are we learning from *Methanococcus jannaschii*? *Trends Genet.*, **12**:377–379, 1996.

[1049] A. W. Omta. *Eddies and algal stoichiometry: Physical and biological influences on the organic carbon pump.* PhD thesis, Vrije Univ., 2009.

[1050] A. W. Omta, J. Bruggeman, S. A. L. M. Kooijman, and H. A. Dijkstra. The biological carbon pump revisited: feedback mechanisms between climate and the redfield ratio. *Geophys. Res. Lett.*, **33**:L14613, 2006.

[1051] R. V. O'Neill, D. L. DeAngelis, J. J. Pastor, B. J. Jackson, and W. M. Post. Multiple nutrient limitations in ecological models. *Ecol. Modell.*, **46**:147–163, 1989.

[1052] A. Opperhuizen. *Bioconcentration in fish and other distribution processes of hydrophobic chemicals in aquatic environments.* PhD thesis, Univ. of Amsterdam, 1986.

[1053] F. I. Opute. Lipid and fatty-acid composition of diatoms. *J. Exp. Bot.*, **25**:823–835., 1974.

[1054] L. E. Orgel. Self-organizing biochemical cycles. *Proc. Natl. Acad. Sci. U. S. A.*, **97**:12503–12507, 2000.

[1055] R. Österberg. On the prebiotic role of iron and sulfur. *Orig. Life Evol. Biosphere*, **27**:481–484, 1997.

[1056] K. W. Osteryoung and J. Nunnari. The division of endosymbiotic organelles. *Science*, **302**:1698–1704, 2003.

[1057] A. Y. Ota and M. R. Landry. Nucleic acids as growth rate indicators for early developmental stages of *Calanus pacificus* Brodsky. *J. Exp. Mar. Biol. Ecol.*, **80**:147–160, 1984.

[1058] S. Otte, J. G. Kuenen, L. P. Nielsen, H. W. Pearl, J. Zopfi, H. N. Schulz, A. Teska, B. Strotmann, V. A. Gallardo, and B. B. Jørgenssen. Nitrogen, carbon, and sulfur metabolism in natural *Tioploca* samples. *Appl. Environ. Microbiol.*, **65**:3148–3157, 1999.

[1059] G. C. Packard. Water relations of Chelonian eggs and embryos: Is wetter better? *Amer. Zool.*, **39**:289–303, 1999.

[1060] M. J. Packard, G. C. Packard, and W. H. N. Gutzke. Calcium metabolism in embryos of the oviparous snake *Coluber constrictor*. *J. Exp. Biol.*, **110**:99–112, 1984.

[1061] M. J. Packard, G. C. Packard, J. D. Miller, M. E. Jones, and W. H. N. Gutzke. Calcium mobilization, water balance, and growth in embryos of the agamid lizard *Amphibolurus barbatus*. *J. Exp. Zool.*, **235**:349–357, 1985.

[1062] M. J. Packard, T. M. Short, G. C. Packard, and T. A. Gorell. Sources of calcium for embryonic development in eggs of the snapping turtle *Chelydra serpentina*. *J. Exp. Zool.*, **230**:81–87, 1984.

[1063] R. T. Paine. Growth and size distribution of the brachiopod *Terebratalia transversa* Sowerby. *Pac. Sci.*, **23**:337–343, 1969.

[1064] P. R. Painter and A. G. Marr. Mathematics of microbial populations. *Annu. Rev. Microbiol.*, **22**:519–548, 1968.

[1065] J. E. Paloheimo, S. J. Crabtree, and W. D. Taylor. Growth model for *Daphnia*. *Can. J. Fish. Aquat. Sci.*, **39**:598–606, 1982.

[1066] D. Pantaloni, C. Le Clainche, and M.-F. Carlier. Mechanism of actin-based motility. *Science*, **292**:1502–1506, 2001.

[1067] S. Papa and V. P. Skulacheve. Reactive oxygen species, mitochondria, apoptosis and aging. *Mol. Cell Biochem.*, **174**:305–319, 1997.

[1068] D. Papineau, J. J. Walker, S. J. Moizsis, and N. R. Pace. Composition and structure of microbial communities from stromatolites of Hamelin Pool in Shark Bay, Wesern Australia. *Appl. Environ. Microbiol.*, **71**:4822–4832, 2005.

[1069] D. M. Parichy, M. R. Elizondo, M. G. Mills, T. N. Gordon, and R. E. Engeszer. Normal table of postembryonic zebrafish development: staging by externally visible anatomy of the living fish. *Developmental Dynamics*, **238**:2975–3015, 2009.

[1070] J. R. Parks. *A Theory of Feeding and Growth of Animals.* Springer-Verlag, Berlin, 1982.

[1071] M. Parniske and J. A. Downie. Lock, keys and symbioses. *Nature*, **425**:569–570, 2003.

[1072] G. D. Parry. The influence of the cost of growth on ectotherm metabolism. *J. theor. Biol.*, **101**:453–477, 1983.

[1073] S. J. Parulekar, G. B. Semones, M. J. Rolf, J. C. Lievense, and H. C. Lim. Induction and elimination of oscillations in continuous cultures of *Saccharomyces cerevisiae*. *Biotechnol. Bioeng.*, **28**:700–710, 1986.

[1074] D. J. Patterson. The diversity of eukaryotes. *Am. Nat.*, **154**:S96–S124, 1999.

[1075] M. R. Patterson. A chemical engineering view of cnidarian symbioses. *Am. Zool.*, **32**:566–582, 1992.

[1076] D. Pauly and P. Martosubroto. The population dynamics of *Nemipterus marginatus* (Cuvier & Val.) off Western Kalimantan, South China Sea. *J. Fish Biol.*, **17**:263–273, 1980.

[1077] P. R. Payne and E. F. Wheeler. Growth of the foetus. *Nature*, **215**:849–850, 1967.

[1078] R. Pearl. The growth of populations. *Q. Rev. Biol.*, **2**:532–548, 1927.

[1079] L. Pecquerie. *Bioenergetic modelling of the growth, development and reproduction of a small pelagic fish: the Bay of Biscay anchovy.* PhD thesis, Agrocampus Rennes & Vrije Univ., Amsterdam, 2008.

[1080] L. Pecquerie, P. Petitgas, and S. A. L. M. Kooijman. Modelling fish growth and reproduction in the context of the Dynamic Energy Budget theory to predict environmental impact on anchovy spawning duration. *J. Sea Res.*, **62**:93–105, 2009.

[1081] T. J. Pedley. *Scale Effects in Animal Locomotion.* Academic Press, London, 1977.

[1082] E. Pennisi. Plant wannabes. *Science*, **313**:1229, 2006.

[1083] D. L. Penry and P. A. Jumars. Chemical reactor analysis and optimal digestion. *Bioscience*, **36**:310–315, 1986.

[1084] D. L. Penry and P. A. Jumars. Modeling animal guts as chemical reactors. *Am. Nat.*, **129**:69–96, 1987.

[1085] B. Peretz and L. Adkins. An index of age when birthdate is unknown in *Aplysia californica*: shell size and growth in long-term maricultured animals. *Biol. Bull. (Woods Hole)*, **162**:333–344, 1982.

[1086] L. Persson, D. Claessen, A. M. de Roos, P. Byström, S. Sjöberggren, R. Svanbäck, E. Wahlström, and E. Westman. Cannibalism in a size-structured population: energy extraction and control. *Ecological monographs*, **74**:135–157, 2004.

[1087] A. R. R. Péry, J. J. M. Bedaux, C. Zonneveld, and S. A. L. M. Kooijman. Analysis of bioassays with time-varying concentrations. *Water Res.*, **35**:3825–3832, 2001.

[1088] A. R. R. Péry, P. Flammarion, B. Vollat, J. J. M. Bedaux, S. A. L. M. Kooijman, and J. Garric. Using a biology-based model (DEBtox) to analyse bioassays in ecotoxicology: Opportunities and recommendations. *Environ. Toxicol. Chem.*, **21**:459–465, 2002.

[1089] R. H. Peters. *The Ecological Implications of Body Size.* Cambridge Univ. Press, 1983.

[1090] T. N. Pettit, G. S. Grant, G. C. Whittow, H. Rahn, and C. V. Paganelli. Respiratory gas exchange and growth of white tern embryos. *Condor*, **83**:355–361, 1981.

[1091] T. N. Pettit, G. S. Grant, G. C. Whittow, H. Rahn, and C. V. Paganelli. Embryonic oxygen consumption and growth of laysan and black-footed albatross. *Am. J. Physiol.*, **242**:121–128, 1982.

[1092] T. N. Pettit and G. C. Whittow. Embryonic respiration and growth in two species of noddy terns. *Physiol. Zool.*, **56**:455–464, 1983.

[1093] T. N. Pettit, G. C. Whittow, and G. S. Grant. Caloric content and energetic budget of tropical seabird eggs. In G. C. Whittow and H. Rahn, editors, *Seabird Energetics*, pages 113–138. Plenum Press, New York, 1984.

[1094] H. G. Petzold. *Die Anakondas.* A. Ziemsen-Verlag, Wittenberg Lutherstadt, 1984.

[1095] C. Pfeffer, S. Larsen, J. Song, M. Dong, F. Besenbacher, R. L. Meyer, K. U. Kjeldsen, L. Schreiber, Y. A. Gorby, M. Y. El-Naggar, K. M. Leung, A. Schramm, N. Risgaard-Petersen, and L. Peter Nielsen. Filamentous bacteria transport electrons over centimetre distances. *Nature*, page doi:10.1038/nature11586, 2012.

[1096] J. Phillipson. Bioenergetic options and phylogeny. In C. R. Townsend and P. Calow, editors, *Physiological Ecology.* Blackwell Sci. Publ., Oxford, 1981.

[1097] E. R. Pianka. On r and K selection. *Am. Nat.*, **104**:592–597, 1970.

[1098] E. R. Pianka. *Evolutionary Ecology.* Harper & Row, London, 1978.

[1099] E. R. Pianka. *Ecology and Natural History of Desert Lizards; Analyses of the Ecological Niche of Community Structure.* Princeton Univ. Press, 1986.

[1100] T. Piersma. Estimating energy reserves of great crested grebes *Podiceps cristatus* on the basis of body dimensions. *Ardea*, **72**:119–126, 1984.

[1101] T. Piersma, N. Cadée, and S. Daan. Seasonality in basal metabolic rate and thermal conductance in a long-distance migrant shorebird, the knot (*Calidris canutus*). *J. Comp. Physiol. B*, **165**:37–45, 1995.

[1102] T. Piersma and R. I. G. Morrison. Energy expenditure and water turnover of incubating ruddy turnstones: high costs under high arctic climatic conditions. *Auk*, **111**:366–376, 1994.

[1103] B. K. Pierson, H. K. Mitchell, and A. L. Ruff-Roberts. *Chloroflexus aurantiacus* and ultraviolet radiation: implications for Archean shallow-water stromatolites. *Orig. Life Evol. Biosphere*, **23**:243–260, 1993.

[1104] J. Pilarska. Eco-physiological studies on *Brachionus rubens* Ehrbg (*Rotatoria*) I. Food selectivity and feeding rate. *Pol. Arch. Hydrobiol.*, **24**:319–328, 1977.

[1105] E. M. del Pino. Marsupial frogs. *Sci. Am.*, **5**:76–84, 1989.

[1106] S. Piraino, F. Boero, B. Aeschbach, and V. Schmid. Reversing the life cycle: Medusae transforming into polyps and cell transdifferentiation in *Turritopsis nutricula* (cnidaria, hydrozoa). *Biological Bulletin*, **190**:302–312, 1996.

[1107] S. J. Pirt. The maintenance energy of bacteria in growing cultures. *Proc. R. Soc. Lond. Biol. Sci.*, **163**:224–231, 1965.

[1108] S. J. Pirt. *Principles of Microbe and Cell Cultivation.* Blackwell Sci. Publ., Oxford, 1975.

[1109] S. J. Pirt and D. S. Callow. Studies of the growth of *Penicillium chrysogenum* in continuous flow culture with reference to penicillin production. *J. Appl. Bacteriol.*, **23**:87–98, 1960.

[1110] P. Planquette, P. Keith, and P.-Y. le Bail. *Atlas des poissons d'eau douce de Guyane. Tome 1. Collection Patrimoines Naturels 22.* Publications scientifiques du Muséum national d'Histoire naturelle., Paris, 1996. 429p.

[1111] G. Pohle and M. Telford. Post-larval growth of *Dissodactylus primitivus* Bouvier, 1917 (*Brachyura*: *Pinnotheridae*) under laboratory conditions. *Biol. Bull. (Woods Hole)*, **163**:211–224, 1982.

[1112] J. S. Poindexter. Oligotrophy: fast and famine existence. *Adv. Microb. Ecol.*, **5**:63–89, 1981.

[1113] A. Polle. Mehler reaction: Friend or foe in photosynthesis? *Bot. Acta*, **109**:84–89, 1996.

[1114] D. E. Pomeroy. Some aspects of the ecology of the land snail, *Helicella virgata*, in South Australia. *Austral. J. Zool.*, **17**:495–514, 1969.

[1115] R. W. Pomeroy. Infertility and neonatal mortality in the sow. III: Neonatal mortality and foetal development. *J. Agric. Sci.*, **54**:31–56, 1960.

[1116] W. E. Poole. Breeding biology and current status of the grey kangaroo, *Macropus fuliginosus fuliginosus*, of Kangaroo Island, South Australia. *Austral. J. Zool.*, **24**:169–187, 1976.

[1117] H. Poorbagher, M. D. Lamare, M. F. Barker, and W. Rayment. Relative importance of parental diet versus larval nutrition on development and phenotypic plasticity of *Pseudechinus huttoni* larvae (Echinodermata: Echinoidea). *Mar. Biol. Res.*, **6**:302–314, 2010.

[1118] D. Poppe and B. Vos. *De Buizerd.* Kosmos, Amsterdam, 1982.

[1119] R. Porley and N. Hodgetts. *Mosses and Liverworts.* Collins, London, 2005.

[1120] K. G. Porter, J. Gerritsen, and J. D. Orcutt. The effect of food concentration on swimming patterns, feeding behavior, ingestion, assimilation and respiration by *Daphnia*. *Limnol. Oceanogr.*, **27**:935–949, 1982.

[1121] K. G. Porter, M. L. Pace, and J. F. Battey. Ciliate protozoans as links in freshwater planktonic food chains. *Nature*, **277**:563–564, 1979.

[1122] R. K. Porter and M. D. Brand. Body mass dependence of H^+ leak in mitochondria and its relevance to metabolic rate. *Nature*, **362**:628–630, 1993.

[1123] J. R. Post and J. A. Lee. Metabolic ontogeny of teleost fishes. *Can. J. Fish. Aquat. Sci.*, **53**:910–923, 1996.

[1124] L. Posthuma, R. F. Hogervorst, E. N. G. Joosse, and N. M. van Straalen. Genetic variation and covariation for characteristics associated with cadmium tolerance in natural populations of the springtail *Orchesella cincta* (L.). *Evolution*, **47**:619–631, 1993.

[1125] L. Posthuma, R. F. Hogervorst, and N. M. van Straalen. Adaptation to soil pollution by cadmium excretion in natural populations of *Orchesella cincta*(L.) (*Collembola*). *Arch. Environ. Contam. Toxicol.*, **22**:146–156, 1992.

[1126] E. Postma, W. A. Scheffers, and J. P. van Dijken. Kinetics of growth and glucose transport in glucose-limited chemostat cultures of *Saccharomyces cerevisiae* cbs 8086. *Yeast*, **5**:159–165, 1989.

[1127] E. Postma, C. Verduyn, W. A. Scheffers, and J. P. van Dijken. Enzyme analysis of the crabtree effect in glucose-limited chemostat cultures of *Saccharomyces cerevisiae*. *Appl. Environ. Microbiol.*, **55**:468–477, 1989.

[1128] S. Pouvreau, Y. Bourles, S. Lefebvre, A. Gangnery, and M. Alunno-Bruscia. Application of a dynamic energy budget model to the pacific oyster *Crassostrea gigas*, reared under various environmental conditions. *J. Sea Res.*, **56**:156–167, 2006.

[1129] D. M. Prescott. Relations between cell growth and cell division. In D. Rudnick, editor, *Rythmic and Synthetic Processes in Growth*, pages 59–74. Princeton Univ. Press, 1957.

[1130] G. D. Prestwich. The chemical defences of termites. *Sci. Am.*, **249**:68–75, 1983.

[1131] C. A. Price, J. F. Gillooly, A. P. Allen, J. S. Weitz, and K. J. Niklas. The metabolic theory of ecology: prospects and challenges for plant biology. *New Phytologist*, **188**:696–710, 2010.

[1132] H. H. Prince, P. B. Siegel, and G. W. Cornwell. Embryonic growth of mallard and pekin ducks. *Growth*, **32**:225–233, 1968.

[1133] R. Prinzinger, V. Dietz, and B. Nagel. Respiratory quatient and embryological development of metabolic heat production in the rhea (*Rhea americana*). *J. therm. Biol.*, **22**:223–226, 1997.

[1134] W. G. Pritchard. Scaling in the animal kingdom. *Bull. Math. Biol.*, **55**:111–129, 1993.

[1135] M. Proctor and P. Yeo. *The Pollination of Flowers.* Collins, London, 1973.

[1136] D. R. Prothero and W. A. Berggren, editors. *Eocene-Oligocene Climatic and Biotic Evolution.* Princeton Univ. Press, 1992.

[1137] L. Psihoyos. *Hunting Dinosaurs.* Random House, New York, 1994.

[1138] D. M. Purdy and H. H. Hillemann. Prenatal growth in the golden hamster (*Cricetus auratus*). *Anat. Rec.*, **106**:591–597, 1950.

[1139] A. Pütter. Studien über physiologische Ähnlichkeit. VI Wachstumsähnlichkeiten. *Arch. Gesamte Physiol. Mench. Tiere*, **180**:298–340, 1920.

[1140] H. Qian and D. A. Beard. Metabolic futile cycles and their functions: a systems analysis of energy and control. *Syst. Biol. (Stevenage)*, **153**:192–200, 2006.

[1141] P. A. Racey and S. M. Swift. Variations in gestation length in a colony of pipistrelle bats (*Pipistrellus pipistrellus*) from year to year. *J. Reprod. Fertil.*, **61**:123–129, 1981.

[1142] R. Radder and R. Shine. Thermally induced torpor in fullterm lizard embryos synchronizes hatching with ambient conditions. *Biol. Lett.*, **22**:415–416, 2006.

[1143] E. C. Raff, E. M. Popodi, B. J. Sly, F. R. Turner, J. T. Villinski, and R. A. Raff. A novel ontogenetic pathway in hybrid embryos between species with different modes of development. *Development*, **126**:1937–1945, 1999.

[1144] R. A. Raff, B. A. Parr, A. L. Parks, and G. A. Wray. Heterochrony and other mechanisms of radical evolutionary change in early development. In M. H. Nitecki, editor, *Evolutionary innovations.*, pages 71–98. Univ. of Chicago Press, Chicago, 1990.

[1145] U. Rahm. *Die Afrikanische Wurzelratte.* A. Ziemsen-Verlag, Wittenberg Lutherstadt, 1980.

[1146] H. Rahn and A. Ar. The avian egg: incubation time and water loss. *Condor*, **76**:147–152, 1974.

[1147] H. Rahn, A. Ar, and C. V. Paganelli. How bird eggs breathe. *Sci. Am.*, **2**:38–47, 1979.

[1148] H. Rahn and C. V. Paganelli. Gas fluxes in avian eggs: Driving forces and the pathway for exchange. *Comp. Biochem. Physiol.*, **95A**:1–15, 1990.

[1149] H. Rahn, C. V. Paganelli, and A. Ar. Relation of avian egg weight to body weight. *Auk*, **92**:750–765, 1975.

[1150] A. N. Rai, E. Soderback, and B. Bergman. Cyanobacterium-plant symbioses. *New Phytologist*, **147**:449–481, 2000.

[1151] K. Raman. *Transport Phenomena in Plants.* Narosa Publ. House, London, 1997.

[1152] J. E. Randall, G. R. Allen, and R. C. Steen. *Fishes of the Great Barrier Reef and Coral Sea.* Univ. of Hawai Press, Honolulu, 1990.

[1153] M. S. Rappé, S. A. Connon, K. L. Vergin, and S. J. Giovannoni. Cultivation of the ubiquitous SAR11 marine bacterioplankton clade. *Nature*, **438**:630–633, 2002.

[1154] B. Rasmussen, I. R. Fletcher, J. J. Brocks, and M. R. Kilburn. Reassessing the first appreearance of eukaryotes and cyanobacteria. *Nature*, **455**:1101–1104, 2008.

[1155] C. Ratledge. Biotechnology as applied to the oils and fats industry. *Fette Seifen Anstrichm.*, **86**:379–389, 1984.

[1156] D. M. Raup. Geometric analysis of shell coiling: General problems. *J. Paleontol.*, **40**:1178–1190, 1966.

[1157] D. M. Raup. Geometric analysis of shell coiling: Coiling in ammonoids. *J. Paleontol.*, **41**:43–65, 1967.

[1158] J. A. Raven. *Energetics and Transport in Aquatic Plants.*, volume 4 of *MBL Lectures in Biology.* Alan R. Liss, Inc., New York, 1984.

[1159] J. A. Raven. The vacuole: a cost-benefit analysis. In R. A. Leigh and D. Sanders, editors, *The Plant Vacuole.*, pages 59–86. Academic Press, San Diego, 1997.

[1160] J. A. Raven and C. Brownlee. Understanding membrane function. *J. Phycol.*, **37**:960–967, 2001.

[1161] J. A. Raven and D. Edwards. Roots: evolutionary origins and biogeochemical significance. *J. Exp. Bot.*, **52**:381–401, 2001.

[1162] J. A. Raven and Z. H. Yin. The past, present and future of nitrogenous compounds in the atmosphere, and their interactions with plants. *New Phytol.*, **139**:205–219, 1998.

[1163] S. Raviv, S. Parnes, and A. Sagi. Coordination of reproduction and molt in decapods. In E. Mente, editor, *Reproductive Biology of Crustaceans*, chapter 9, pages 365–390. Science Publishers, Enfield, NH, 2008.

[1164] P. J. Reay. Some aspects of the biology of the sandeel, *Ammodytes tobianus* L., in Langstone Harbour, Hampshire. *J. Mar. Biol. Assoc. U. K.*, **53**:325–346, 1973.

[1165] C. Reder. Metabolic control theory: a structural approach. *J. theor. Biol.*, **135**:175–201, 1988.

[1166] A. C. Redfield. The biological control of chemical factors in the environment. *Am. Sci.*, **46**:205–221, 1958.

[1167] M. R. Reeve. The biology of *Chaetognatha* I. Quantitative aspects of growth and egg production in *Sagitta hispida.* In J. H. Steele, editor, *Marine Food Chains.* Univ. of California Press, Berkeley, 1970.

[1168] M. R. Reeve and L. D. Baker. Production of two planktonic carnivores (Chaetognath and Ctenophore) in south Florida inshore waters. *Fish. Bull. (Dublin)*, **73**:238–248, 1975.

[1169] M. J. Reiss. *The Allometry of Growth and Reproduction.* Cambridge Univ. Press, 1989.

[1170] W. Reisser. *Algae and Symbioses.* Biopress Ltd, Bristol, 1992.

[1171] W. Reisser, R. Meier, and B. Kurmeier. The regulation of the endosymbiotic algal population size in ciliate-algae associations. An ecological model. In H. E. A. Schenk and W. Schwemmler, editors, *Endocytobiology*, volume 2, pages 533–543. W. de Gruyter, Berlin, 1983.

[1172] R. F. Rekker. The hydrophobic fragmental constant: a means of characterizing membrane systems. In W. Th. Nauta and R. F. Rekker, editors, *Pharmacochemistry Library*, pages 00–00. Elsevier, Amsterdam, 1977.

[1173] H. Remmert. *Artic Animal Ecology.* Springer-Verlag, Berlin, 1980.

[1174] D. Reznick, H. Callahan, and R. Llauredo. Maternal effects on offspring quality in poeciliid fishes. *Am. Zool.*, **36**:147–156, 1996.

[1175] D. N. Reznick, M. Mateos, and M. S. Springer. Independent origins and rapid evolution of the placenta in the fish genus *Poeciliopsis.* *Science*, **298**:1018–1020, 2002.

[1176] A. Ricciardi and E. Bourget. Weight-to-weight conversion factors for marine benthic macroinvertebrates. *Mar. Ecol. Prog. Ser.*, **163**:245–251, 1998.

[1177] F. J. Richards. A flexible growth function for empirical use. *J. Exp. Bot.*, **10**:290–300, 1959.

[1178] S. W. Richards, D. Merriman, and L. H. Calhoun. Studies on the marine resources of southern New England. IX. The biology of the little skate, *Raja erinacea* Mitchill. *Bull. Bingham Oceanogr. Collect. Yale Univ.*, **18**:5–67, 1963.

[1179] D. Richardson. *The Vanishing Lichens: Their History, Biology and Importance.* David and Charles, Newton Abbot, 1975.

[1180] M. L. Richardson and S. Gangolli. *The Dictionary of Substances and Their Effects.* Roy. Soc. Chem., Cambridge, 1995.

[1181] S. Richman. The transformation of energy by *Daphnia pulex*. *Ecol. Monogr.*, **28**:273–291, 1958.

[1182] D. Rickard, I.B. Butler, and A. Olroyd. A novel iron sulphide switch and its implications for earth and planetary science. *Earth Planet. Sci. Lett.*, **189**:85–91, 2001.

[1183] R. E. Ricklefs. Patterns of growth in birds. *Ibis*, **110**:419–451, 1968.

[1184] R. E. Ricklefs. Patterns of growth in birds III. Growth and development of the cactus wren. *Condor*, **77**:34–45, 1975.

[1185] R. E. Ricklefs. Composition of eggs of several bird species. *The Auk*, **94**:350–356, 1977.

[1186] R. E. Ricklefs. Adaptation, constraint, and compromise in avian postnatal development. *Biol. Rev.*, **54**:269–290, 1979.

[1187] R. E. Ricklefs, M. Konarzewski, and S. Daan. The relationship between basal metabolic rate and daily energy expenditure in birds and mammals. *Am. Nat.*, **147**:1047–1071, 1996.

[1188] R. E. Ricklefs and A. Scheuerlein. Biological implications of the Weibull and Gompertz models of aging. *J. Gerontology*, **57A**:B69–B76, 2002.

[1189] R. E. Ricklefs and T. Webb. Water content, thermoregulation, and the growth rate of skeletal muscles in the European starling. *Auk*, **102**:369–377, 1985.

[1190] R. E. Ricklefs, S. White, and J. Cullen. Postnatal development of Leach's storm-petrel. *Auk*, **97**:768–781, 1980.

[1191] U. Riebesell, D. A. Wolf-Gladrow, and V. Smetacek. Carbon dioxide limitation of marine phytoplankton growth rates. *Nature*, **361**:249–251, 1993.

[1192] F. H. Rigler. Zooplankton. In W. T. Edmondson, editor, *A Manual on Methods for the Assessment of Secondary Productivity in Fresh Waters*, number 17 in IBP handbook, pages 228–255. Bartholomew Press, Dorking, 1971.

[1193] H. U. Riisgård, E. Bjornestad, and F. Møhlenberg. Accumulation of cadmium in the mussel *Mytilus edulis*: kinetics and importance of uptake via food and sea water. *Mar. Biol.*, **96**:349–353, 1987.

[1194] H. U. Riisgård and F. Møhlenberg. An improved automatic recording apparatus for determining the filtration rate of *Mytilus edulis* as a function of size and algal concentration. *Mar. Biol.*, **66**:259–265, 1979.

[1195] H. U. Riisgård and A. Randløv. Energy budgets, growth and filtration rates in *Mytilus edulis* at different algal concentrations. *Mar. Biol.*, **61**:227–234, 1981.

[1196] M. A. Riley and J. E. Wertz. Bacteriochins: Evolution, ecology and application. *Annu. Rev. Microbiol.*, **56**:117–137, 2002.

[1197] N. Risgaard-Petersen, A. M. Langezaal, S. Ingvardsen, M. C. Schmid, M. S. M. Jetten, H. J. M. op den Camp, J. W. M. Derksen, E. Piña Ochoa, S. P. Eriksson, L. P. Nielsen, N. P. Revsbech, T. Cedhagen, and G. J. van der Zwaan. Evidence for complete denitrification in a benthic foraminifer. *Nature*, **443**:93–96, 2006.

[1198] M. Rizzotti. *Early Evolution.* Birkh´auser, Basel, 2000.

[1199] C. T. Robbins and A. N. Moen. Uterine composition and growth in pregnant white-tailed deer. *J. Wildl. Manage.*, **39**:684–691, 1975.

[1200] D. V. Roberts. *Enzyme Kinetics.* Cambridge Univ. Press, 1977.

[1201] J. R. Robertson and G. W. Salt. Responses in growth, mortality, and reproduction to variable food levels by the rotifer *Asplanchna girodi*. *Ecology*, **62**:1585–1596, 1981.

[1202] P. G. Rodhouse, C. M. Roden, G. M. Burnell, M. P. Hensey, T. McMahon, B. Ottway, and T. H. Ryan. Food resource, gametogenesis and growth of *Mytilus edulis* on the shore and in suspended culture: Killary Harbour, Ireland. *Mar. Biol.*, **64**:513–529, 1984.

[1203] N. Rodriguez-Ezpeleta, H. Brinkmann, S. C. Burey, B. Roure, G. Burger, W. Loffelhardt, H. J. Bohnert, H. Philippe, and B. F. Lang. Monophyly of primary photosynthetic eukaryotes: green plants, red algae, and glaucophytes. *Curr. Biol.*, **15**:1325–1330, 2005.

[1204] J. A. Roels. *Energetics and Kinetics in Biotechnology.* Elsevier, Amsterdam, 1983.

[1205] D. A. Roff. A motion for the retirement of the von Bertalanffy function. *Can. J. Fish. Aquat. Sci.*, **37**:127–129, 1980.

[1206] D. A. Roff. *The Evolution of Life Histories.* Chapman & Hall, New York, 1992.

[1207] A. J. Roger. Reconstructing early events in eukaryotic evolution. *Am. Nat.*, **154**:S146–S163, 1999.

[1208] K. Rohde. *Ecology of Marine Parasites.* CAB International, Wallingford, 1993.

[1209] A. h. Romano and T. Conway. Evolution of carbohydrate metabolic pathways. *Res. Microbiol.*, **147**:448–455, 1996.

[1210] A. L. Romanov. *The Avian Embryo.* MacMillan, New York, 1960.

[1211] C. Romijn and W. Lokhorst. Foetal respiration in the hen. *Physiol. Zool.*, **2**:187–197, 1951.

[1212] A. de Roos. Numerical methods for structured population models: the escalator boxcar train. *Num. Meth. Part. Diff. Eq.*, **4**:173–195, 1988.

[1213] A. M. de Roos. Escalator boxcar train package. http://staff.science.uva.nl/~aroos/Ebt.htm, 2007.

[1214] M. R. Rose. Laboratory evolution of postponed senescence in *Drosophila melanogaster*. *Evolution*, **38**:1004–1010, 1984.

[1215] R. W.. Rose. Embryonic growth rates of marsupials with a note on monotremes. *J. Zool., Lond.*, **218**:11–16, 1989.

[1216] J. L. Roseberry and W. D. Klimstra. Annual weight cycles in male and female bobwhite quail. *Auk*, **88**:116–123, 1971.

[1217] M. L. Rosenzweig. Paradox of enrichment: destabilization of exploitation ecosystems in ecological time. *Science*, **171**:385–387, 1971.

[1218] A. H. Ross and R. M. Nisbet. Dynamic models of growth and reproduction of the mussel *Mytilus edulis* L. *Funct. Ecol.*, **4**:777–787, 1990.

[1219] M. C. Rossiter. Environmentally-based maternal effects: a hidden force in insect population dynamics? *Oecologia*, **87**:288–294, 1991.

[1220] M. C. Rossiter. Maternal effects generate variation in life history: consequences of egg weight plasticity in the gypsy moth. *Funct. Ecol.*, **5**:386–393, 1991.

[1221] M. E. Rothenberg and Y.-N. Jan. The hyppo hypothesis. *Nature*, **425**:469–470, 2003.

[1222] G. W. Rouse, K. Worsaae, S. B. Johnson, W. J. Jones, and R. C. Vrijenhoek. Acquisition of dwarf male 'harems' by recently settles females of *Osedax roseus* n. sp. (siboglinidae; annelida). *Biol. Bull.*, **214**:67–82, 2008.

[1223] J. A. Ruben, W. J. Hillenius, N. R. Geist, A. Leitch, T. D. Jones, P. J. Currie, J. R. Horner, and G. Espe III. The metabolic status of some late cretaceous dinosaurs. *Science*, **273**:1204–2023, 1996.

[1224] M. Rubner. Über den Einfluss der Körpergrösse auf Stoff- und Kraftwechsel. *Z. Biol.*, **19**:535–562, 1883.

[1225] W. Rudolph. *Die Hausenten.* A. Ziemsen-Verlag, Wittenberg Lutherstadt, 1978.

[1226] M. J. S. Rudwick. The growth and form of brachiopod shells. *Geol. Mag.*, **96**:1–24, 1959.

[1227] M. J. S. Rudwick. Some analytic methods in the study of ontogeny in fossils with accretionary skeletons. *Paleont. Soc., Mem.*, **2**:35–59, 1968.

[1228] D. Ruelle. *Elements of Differentiable Dynamics and Bifurcation Theory.* Academic Press, San Diego, 1989.

[1229] P. C. de Ruiter and G. Ernsting. Effects of ration on energy allocation in a carabid beetle. *Funct. Ecol.*, **1**:109–116, 1987.

[1230] J. B. Russel and G. M. Cook. Energetics of bacterial growth: Balance of anabolic and catabolic reactions. *Microbiol. Rev.*, **59**:48–62, 1995.

[1231] R. W. Russel and F. A. P. C. Gobas. Calibration of the freshwater mussel *Elliptio complanata*, for quantitative monitoring of hexachlorobenzene and octachlorostyrene in aquatic systems. *Bull. Environ. Contam. Toxicol.*, **43**:576–582, 1989.

[1232] M. J. Russell and A. J. Hall. The emergence of life from iron monosulphide bubbles ar a submarine hydrothermal redox and pH front. *J. Geol. Soc. Lond.*, **154**:377–402, 1997.

[1233] M. J. Russell and A. J. Hall. From geochemistry to biochemistry: chemiosmotic coupling and transition element clusters in the onset of life and photosynthesis. *Geochem. News*, **133**(October):6–12, 2002.

[1234] M. J. Russell, Daniel R. M., A. J. Hall, and J. A. Sherringham. A hydrothermally precipitated catalytic iron sulfide membrane as a first step toward life. *J. Mol. Evol.*, **39**:231–243, 1994.

[1235] R. L. Rusting. Why do we age? *Sci. Am.*, **12**:86–95, 1992.

[1236] M. Rutgers. *Control and thermodynamics of microbial growth.* PhD thesis, Univ. of Amsterdam, 1990.

[1237] M. Rutgers, M. J. Teixeira de Mattos, P. W. Postma, and K. van Dam. Establishment of the steady state in glucose-limited chemostat cultures of *Kleibsiella pneumoniae*. *J. Gen. Microbiol.*, **133**:445–453, 1987.

[1238] A. J. Rutter and F. H. Whitehead. *The Water Relations of Plants.* Blackwell, London, 1963.

[1239] I. Ružić. Two-compartment model of radionuclide accumulation into marine organisms. I. Accumulation from a medium of constant activity. *Mar. Biol.*, **15**:105–112, 1972.

[1240] F. Ryan. *Darwin's Blind Spot.* Texere, New York, 2003.

[1241] T. L. Saaty. *Elements of Queueing Theory with Applications.* Dover Publications, New York, 1961.

[1242] S. I. Sandler and H. Orbey. On the thermodynamics of microbial growth processes. *Biotechnol. Bioeng.*, **38**:697–718, 1991.

[1243] R. Santarella-Mellwig, J. Franke, A. Jaedicke, M. Gorjanacz, Bauer U., Budd A., I. W. Mattaj, and D. P. Devos. The compartmentalized bacteria of the planctomycetes- verrucomicrobia-chlamydiae superphylum have membrane coat-like proteins. *Plos Biol.*, **8**(1000281):e1000281, 2010.

[1244] S. Saraiva, J. van der Meer, S. A. L. M. Kooijman, and Sousa T. Modelling feeding processes in bivalves; a mechanistic approach. *Ecol. Modelling*, **222**:514–523, 2011.

[1245] J. R. Sargent. Marine wax esters. *Sci. Prog.*, **65**:437–458, 1978.

[1246] Sarrus and Rameaux. Mémoire adressé à l'Académie Royale. *Bull. Acad. R. Med.*, **3**:1094–1100, 1839.

[1247] M.R. Sartori, E.W. Taylor, and A.S. Abe. Nitrogen excretion during embryonic development of the green iguana, iguana iguana (reptilia; squamata). *Comparative Biochemistry and Physiology, Part A*, **163**:210–214, 2012.

[1248] J. Sarvala. Effect of temperature on the duration of egg, nauplius and copepodite development of some freshwater benthic copepoda. *Freshwater Biol.*, **9**:515–534, 1979.

[1249] G. W. Saunders and M. H. Hommersand. Assessing red algal supraordinal diversity and taxonomy in the context of contemporary systematic data. *Am. J. Bot.*, **91**:1494–1507, 2004.

[1250] P. T. Saunders. *An Introduction to Catastrophe Theory.* Cambridge Univ. Press, 1980.

[1251] J. Schalk. *A study of the metabolic pathway of anaerobic ammonium oxidation.* PhD thesis, Univ. of Delft, 2000.

[1252] H. Schatzmann. *Anaerobes Wachstum von* Saccharomyces cervisiae*: Regulatorische Aspekte des glycolytischen und respirativen Stoffwechsels.* Diss. eth 5504, ETH, Zürich, 1975.

[1253] H. G. Schegel. *Algemeine Mikrobiologie.* Thieme, 1981.

[1254] H. Scheufler and A. Stiefel. *Der Kampflaufer.* A. Ziemsen-Verlag, Wittenberg Lutherstadt, 1985.

[1255] D. E. Schindel. Unoccupied morphospace and the coiled geometry of gastropods: Architectural constraint or geometric covariance? In R. M. Ross and W. D. Allmon, editors, *Causes of Evolution. A Paleontological Perspective.* The Univ. of Chicago Press, 1990.

[1256] D. W. Schindler. Feeding, assimilation and respiration rates of *Daphnia magna* under various environmental conditions and their relation to production estimates. *J. Anim. Ecol.*, **37**:369–385, 1968.

[1257] B. Schink, editor. *Advances in Microbial ecology*, volume 16. Kluwer Academic, New York, 2000.

[1258] I. I. Schmalhausen and E. Syngajewskaja. Studien über Wachstum und Differenzierung. I. Die individuelle Wachtumskurve von *Paramaecium caudatum. Roux's Arch. Dev. Biol.*, **105**:711–717, 1925.

[1259] U. Schmidt. *Vampirfledermäuse.* A. Ziemsen-Verlag, Wittenberg, 1978.

[1260] K. Schmidt-Nielsen. *Scaling: Why is Animal Size so Important?* Cambridge Univ. Press, 1984.

[1261] R. Schneider. Polychlorinated biphenyls (PCBs) in cod tissues from the Western Baltic: significance of equilibrium partitioning and lipid composition in the bioaccumulation of lipophilic pollutants in gill-breathing animals. *Meeresforschung*, **29**:69–79, 1982.

[1262] S. A. Schoenberg, A. E. Maccubbin, and R. E. Hodson. Cellulose digestion by freshwater microcrustacea. *Limnol. Oceanogr.*, **29**:1132–1136, 1984.

[1263] P. F. Scholander. Evolution of climatic adaptation in homeotherms. *Evolution*, **9**:15–26, 1955.

[1264] M. Schonfeld. *Der Fitislaubsanger.* A. Ziemsen-Verlag, Wittenberg Lutherstadt, 1982.

[1265] P. Schönheit and T. Schafer. Metabolism of hyperthermophiles. *World J. Microbiol. Biotechnol.*, **11**:26–57, 1995.

[1266] S. Schonn. *Der Sperlingskauz.* A. Ziemsen-Verlag, Wittenberg Lutherstadt, 1980.

[1267] R. M. Schoolfield, P. J. H. Sharpe, and C. E. Magnuson. Non-linear regression of biological temperature-dependent rate models based on absolute reaction-rate theory. *J. theor. Biol.*, **88**:719–731, 1981.

[1268] M. A. A. Schoonen, Y. Xu, and J. Bebie. Energetics and kinetics of the prebiotic synthesis of simple organic and amino acids with the FeS-H_2S/FeS_2 redox couple as a reductant. *Orig. Life Evol. Biosphere*, **29**:5–32, 1999.

[1269] L. M. Schoonhoven, T. Jermy, and J. J. A. van Loon. *Insect-Plant Biology; From Physiology to Ecology.* Chapman & Hall, London, 1998.

[1270] H. N. Schulz, T. Brinkhoff, T. G. Ferdelman, M. Hernández Marineé, A. Teske, and B. B. Jørgensen. Dense populations of a giant sulfur bacterium in Namibian shelf sediments. *Science*, **284**:493–495, 1999.

[1271] H. N. Schulz and B. B. Jørgensen. Big bacteria. *Annu. Rev. Microbiol.*, **55**:105–137, 2001.

[1272] K. L. Schulze and R. S. Lipe. Relationship between substrate concentration, growth rate, and respiration rate of *Escherichia coli* in continuous culture. *Arch. Mikrobiol.*, **48**:1–20, 1964.

[1273] A. Schüssler. Molecular phylogeny, taxonomy, and evolution of *Geosiphon pyriformis* and arbuscular mycorrhizal fungi. *Plant and Soil*, **244**:75–83, 2002.

[1274] K. Schütz, S. Kerje, Ö. Carlborg, L. Jacobsson, L. Andersson, and P. Jensen. QTL Analysis of a Red Junglefowl × White Leghorn intercross reveals trade-off in resource allocation between behavior and production traits. *Behav. Genet.*, **32**:423–433, 2002.

[1275] V. Schwartz. *Vergleichende Entwicklungsgeschichte der Tiere.* G. Thieme Verlag, Stuttgart, 1973.

[1276] R. P. Schwarzenbach, P. M. Gschwend, and D. M. Imboden. *Enviromental Organic Chemistry.* J. Wiley, New York, 1993.

[1277] D. E. Scott and M. R. Fore. The effect of food limitation on lipid levels, growth, and reproduction in the marbled salamander, *Ambystoma opacum. Herpetologica*, **51**:462–471, 1995.

[1278] W. A. Searcy. Optimum body sizes at different ambient temperatures: an energetics explanation of Bergmann's rule. *J. theor. Biol.*, **83**:579–593, 1980.

[1279] P. Sébert. Pressure effects on shallow-water fishes. In D. J. Randall and A. P. Farrell, editors, *Deep-Sea Fishes.*, chapter 7, pages 279–324. Academic Press, San Diego, 1997.

[1280] L. A. Segel. *Modeling Dynamic Phenomena in Molecular and Cellular Biology.* Cambridge Univ. Press, 1984.

[1281] L. A. Segel. *Biological Kinetics.*, volume 12 of *Cambridge Studies in Mathematical Biology.* Cambridge Univ. Press, 1991.

[1282] L. A. Segel. Diffuse feedback from a diffuse informational network. In L. A. Segel and I. Cohen, editors, *Design Principles for the Immune System and Other Distributed Autonomous Systems*, pages 203–226. Oxford Univ. Press, 2001.

[1283] D. Segré, D. Ben-Eli, D. W. Deamer, and D. Lancet. The lipid world. *Orig. Life Evol. Biosphere*, **31**:119–145, 2001.

[1284] M. Selig, K. B. Xavier, H. Santos, and P. Schönheit. Comparative analysis of Embden-Meyerhof and Entner-Doudoroff glycolytic pathways in hyperthermophilic archaea and the bacterium *Thermotoga. Arch. Microbiol.*, **167**:217–232, 1997.

[1285] M.-A. Selosse and F. Le Tacon. The land flora: a phototroph-fungus partnership? *Trends Ecol. Evol.*, **13**:15–20, 1998.

[1286] H. P. Senn. *Kinetik und Regulation des Zuckerabbaus von* Escherichia coli *ML 30 bei tiefen Zucker Konzentrationen.* PhD thesis, Techn. Hochschule Zurich, 1989.

[1287] R. V. Sequeira. *Nutritional and physiological ecology of insect host - parasitoid interactions: the pea aphid - Aphidius ervi system.* PhD thesis, Simon Fraser University, 1991.

[1288] M. Shafi and P. S. Maitland. The age and growth of perch (*Perca fluviatilis* L.) in two Scottish lochs. *J. Fish Biol.*, **3**:39–57, 1971.

[1289] M. Shafiei, A. P. Moczek, and H. F. Nijhout. Food availability controls the onset of metamorphosis in the dung beetle *Onthophagus taurus (Coleoptera: Scarabaeidae). Physiol. Entomol.*, **26**:173–180, 2001.

[1290] J. A. Shapiro. Bacteria as multicellular organisms. *Sci. Am.*, **6**:62–69, 1988.

[1291] P. J. H. Sharpe and D. W. DeMichele. Reaction kinetics of poikilotherm development. *J. theor. Biol.*, **64**:649–670, 1977.

[1292] J. E. Shelbourne. A predator-prey relationship for plaice larvae feeding on *Oikopleura. J. Mar. Biol. Assoc. U. K.*, **42**:243–252, 1962.

[1293] Y. Shen and R. Buick. The antiquity of microbial sulfate reduction. *Earth Sci. Rev.*, **64**:243–272, 2004.

[1294] N. Sherborne, N. Galic, and R. Ashauer. Sublethal effect modelling for environmental risk assessment of chemicals: Problem definition, model variants, application and challenges. *Sci. Tot. Environ.*, **745**:141027, 2020.

[1295] J. M. Shick. *A Functional Biology of Sea Anemones.* Chapman & Hall, London, 1991.

[1296] R. Shine. Why is sex determined by nest temperature in many reptiles? *Trends Ecol. Evol.*, **14**:186–189, 1999.

[1297] R. Shine and E. L. Charnov. Patterns of survival, growth, and maturation in snakes and lizards. *Am. Nat.*, **139**:1257–1269, 1992.

[1298] Y. Shlesinger and Y. Loya. Coral community reproductive pattern: Red Sea versus the Great Barrier Reef. *Science*, **228**:1333–1335, 1985.

[1299] R. V. Short. Species differences in reproductive mechanisms. In C. R. Austin and R. V. Short, editors, *Reproductive Fitness*, volume 4 of *Reproduction in mammals.*, pages 24–61. Cambridge Univ. Press, 1984.

[1300] R. M. Sibly, J. Baker, S. M. Grady, J. M. andLuna, A. Kodric-Brown, C. Venditti, and J. H. Brown. Fundamental insights into ontogenetic growth from theory and fish. *PNAS*, **112**:13934–13939, 2015.

[1301] R. M. Sibly and J. H. Brown. Toward a physiological explanation of juvenile growth curves. *J. Zool.*, **xx**:xx–xx, 2020.

[1302] R. M. Sibly, V. Grimm, B. Martin, A. S. A. Johnston, K. Kulakowska, C. J. Topping, P. Calow, J. Nabe-Nielsen, P. Thorbek, and D. L. DeAngelis. Representing the acquisition and use of energy by individuals in agent-based models of animal populations. *Methods in Ecology and Evolution*, **4**:151–161, 2013.

[1303] J. M. Siegel. The REM sleep-memory consilidation hypothesis. *Science*, **294**:1058–1063, 2001.

[1304] J. M. Siegel. Why we sleep. *Sci. Am.*, **289**(5):72–77, 2003.

[1305] L. Sigmund. Die postembryonale Entwicklung der Wasserralle. *Sylvia*, **15**:85–118, 1958.

[1306] A. Sih. Predators and prey lifestyles: an evolutionary and ecological overview. In W. C. Kerfoot and A. Sih, editors, *Predation; Direct and Indirect Impacts on Aquatic Communities*, pages 203–224. Univ. of New England Press, Hanover, 1987.

[1307] D. T. H. M. Sijm, K. W. Broersen, D. F. de Roode, and P. Mayer. Bioconcentration kinetics of hydrophobic chemicals in different densities of *Chlorella pyrenoidosa*. *Environ. Toxicol. Chem.*, **17**:1695–1704, 1998.

[1308] D. T. H. M. Sijm and A. van der Linde. Size-dependent bioconcentration kinetics of hydrophobic organic chemicals in fish based on diffusive mass transfer and allometric relationships. *Environ. Sci. Technol.*, **29**:2769–2777, 1995.

[1309] D. T. H. M. Sijm, G. Schüürmann, P. J. Vries, and A. Opperhuizen. Aqueous solubility, octanol solubility, and octanol/water partition coefficient of nine hydrophobic dyes. *Environ. Toxicol. Chem.*, **18**:1109–1117, 1999.

[1310] D. T. H. M. Sijm, W. Seinen, and A. Opperhuizen. Life-cycle biomagnification study in fish. *Environ. Sci. Technol.*, **26**:2162–2174, 1992.

[1311] D. T. H. M. Sijm, M. E. Verberne, W. J. de Jonge, P. Pärt, and A. Opperhuizen. Allometry in the uptake of hydrophobic chemicals determined *in vivo* and in isolated perfused gills. *Toxicol. Appl. Pharmacol.*, **131**:130–135, 1995.

[1312] A. G. Simpson and A. J. Roger. Eukaryotic evolution: getting to the root of the problem. *Curr. Biol.*, **12**:R691–R693, 2002.

[1313] A. G. B. Simpson, J. van den Hoff, C. Bernard, H. R. Burton, and D. J. Patterson. The ultrastructure and systematic position of the euglenozoon *Postgaardi mariagerensis*, Fenchel et al. *Arch. Protistenkd.*, **147**:213–225, 1996.

[1314] G. G. Simpson. *Penguins. Past and Present, Here and There.* Yale Univ. Press, New Haven, 1976.

[1315] M. R. Simpson and S. Boutin. Muskrat life history: a comparison of a northern and southern population. *Ecography*, **16**:5–10, 1993.

[1316] P. G. Simpson and W. B. Whitman. Anabolic pathways in methanogens. In J. G. Ferry, editor, *Methanogenesis.*, pages 445–472. Chapman & Hall, New York, 1993.

[1317] B. Sinervo. The evolution of maternal investment in lizard. An experimental and comparative analysis of egg size and its effect on offspring performance. *Evolution*, **44**:279–294, 1990.

[1318] D. Singer. Stable orbits and bifurcation of maps of the interval. *SIAM J. Appl. Math.*, **35**:260–267, 1978.

[1319] J. W. Sinko and W. Streifer. A model for populations reproducing by fission. *Ecology*, **52**:330–335, 1967.

[1320] P. Sitte, S. Eschbach, and M. Maerz. The role of symbiosis in algal evolution. In W. Reisser, editor, *Algae and Symbioses*, pages 711–733. Biopress, Bristol, 1992.

[1321] S. Sjöberg. Zooplankton feeding and queueing theory. *Ecol. Modell.*, **10**:215–225, 1980.

[1322] J. G. Skellam. The formulation and interpretation of mathematical models of diffusionary processes in population biology. In M. S. Bartlett and R. W. Hiorns, editors, *The Mathematical Theory of the Dynamics of Biological Populations*, pages 63–85. Academic Press, San Diego, 1973.

[1323] R. O. Slatyer. *Plant-Water Relationships.* Academic Press, London, 1967.

[1324] W. Slob and C. Janse. A quantitative method to evaluate the quality of interrupted animal cultures in aging studies. *Mech. Ageing Dev.*, **42**:275–290, 1988.

[1325] L. B. Slobodkin. Population dynamics in *Daphnia obtusa* Kurz. *Ecol. Monogr.*, **24**:69–88, 1954.

[1326] J. F. Sluiters. *Parasite-host relationship of the avian schistosome* Trichobilharzia ocellata *and the hermaphrodite gastropod* Lymnea stagnalis. PhD thesis, Vrije Univ.", address = "Amsterdam, 1983.

[1327] G. L. Small. *The Blue Whale.* Columbia Univ. Press, 1971.

[1328] D. C. Smith and A. E. Douglas. *The Biology of Symbiosis.* Arnold, London, 1987.

[1329] D. J. Smith and G. J. C. Underwood. The production of extracellular carbohydrates by estuarine benthic diatoms: the effects of growth phase and light and dark treatment. *J. Phycol.*, **36**:321–333, 2000.

[1330] F. A. Smith and N. A. Walker. Photosynthesis by aquatic plants: effects of unstirred layers in relation to assimilation of CO_2 and HCO_3^- and to carbon isotopic discrimination. *New Phytol.*, **86**:245–259, 1980.

[1331] H. L. Smith and P. Waltman. *The Theory of the Chemostat.* Cambridge Univ. Press, 1994.

[1332] M. L. Smith, J. N. Bruhn, and J. B. Anderson. The fungus *Armillaria bulbosa* is among the largest and oldest living organsism. *Nature*, **356**:428–431, 1992.

[1333] S. Smith. Early development and hatching. In M. E. Brown, editor, *The Physiology of Fishes*, volume 1, pages 323–359. Academic Press, San Diego, 1957.

[1334] S. M. Smith. *The Black-Capped Chickadee. Behavioral Ecology and Natural History.* Comstock Publishing Associates, Ithaca, 1991.

[1335] S. V. Smith. The Houtman Abrolhos Islands: Carbon metabolism of coral reefs at high latitude. *Limnol. Oceanogr.*, **26**:612–621, 1981.

[1336] S. V. Smith and D. W. Kinsey. Calcium carbonate production, coral reef growth, and sea level change. *Science*, **194**:937–939, 1976.

[1337] O. Snell. Die Abhängigkeit des Hirngewichtes von dem Körpergewicht und den geistigen Fähigkeiten. *Arch. Psychiatr. Nervenkr.*, **23**:436–446, 1891.

[1338] B. Snow and D. Snow. *Birds and Berries.* Poyser, Calton, 1988.

[1339] D. W. Snow. The natural history of the oilbird, *Steatornis caripensis* in Trinidad, W.I. part 1. General behaviour and breeding habits. *Zoologica (New York)*, **46**:27–48, 1961.

[1340] T. Sousa, T. Domingos, and S. A. L. M. Kooijman. From empirical patterns to theory: A formal metabolic theory of life. *Phil. Trans. R. Soc. Lond. B Biol. Sci.*, **363**:2453–2464, 2008.

[1341] T. Sousa, T. Domingos, J.-C. Poggiale, and S. A. L. M. Kooijman. Formalised DEB theory restores coherence in core biology. *Phil. Trans. R. Soc. Lond. B Biol. Sci.*, **365**:?, 2010.

[1342] T. Sousa, G. M. Marques, and T. Domingos. Comment on 'energy uptake and allocation during ontogeny'. *Science*, **325**:1206–b, 2009.

[1343] T. Sousa, R. Mota, T. Domingos, and S. A. L. M. Kooijman. The thermodynamics of organisms in the context of DEB theory. *Physi. Rev. E*, **74**:1–15, 2006.

[1344] G. M. Southward. A method of calculating body lengths from otolith measurements for pacific halibut and its application to Portlock-Albatross Grounds data between 1935 and 1957. *J. Fish. Res. Board Can.*, **19**:339–362, 1962.

[1345] G. R. Southworth, J. J. Beauchamp, and P. K. Schmieder. Bioaccumulation potential and acute toxicity of synthetic fuel effluents in freshwater biota: Azaarenes. *Environ. Sci. Technol.*, **12**:1062–1066, 1978.

[1346] A. L. Spaans. On the feeding ecology of the herring gull *Larus argentatus* Pont. in the northern part of the Netherlands. *Ardea*, **59**:75–188, 1971.

[1347] G. Spitzer. Jahreszeitliche Aspekte der Biologie der Bartmeise (*Panurus biarmicus*). *J. Ornithol.*, **11**:241–275, 1972.

[1348] J. R. Spotila and E. A. Standora. Energy budgets of ectothermic vertebrates. *Am. Zool.*, **25**:973–986, 1985.

[1349] J. B. Sprague. Measurement of pollutant toxicity to fish i. bioassay methods for acute toxicity. *Water Res.*, **3**:793–821, 1969.

[1350] J. I. Sprent. *The Ecology of the Nitrogen Cycle.* Cambridge Univ. Press, 1987.

[1351] M. Sprung. Physiological energetics of mussel larvae (*Mytilus edulis*) I. Shell growth and biomass. *Mar. Ecol. Prog. Ser.*, **17**:283–293, 1984.

[1352] J. T. Staley, M. P. Bryant, N. Pfennig, and J. G. Holt. *Bergeys Manual of Systematic Bacteriology.* Williams & Wilkins, Baltimore, 1989.

[1353] M. W. Stanier, L. E. Mount, and J. Bligh. *Energy Balance and Temperature Regulation.* Cambridge Univ. Press, 1984.

[1354] R. Y. Stanier, E. A. Adelberg, and J. L. Ingraham. *General Microbiology.* MacMillan, London, 1976.

[1355] R. Y. Stanier, J. L. Ingraham, M. L. Wheelis, and P. R. Painter. *The Microbial World.* Prentice-Hall, Englewood Cliffs, 1986.

[1356] J. M. Starck. Evolution of avian ontogenies. *Curr. Orn.*, **10**:275–366, 1993.

[1357] J. M. Starck and R. E. Ricklefs. Patterns of development: The altricial-precocial spectrum. In J. M. Starck and R. E. Ricklefs, editors, *Avian Growth and Development. Evolution within the altricial precocial spectrum*, chapter 1, pages 1–30. Oxford University Press, New York, 1998.

[1358] P. Starke-Reed. Oxygen radicals and aging. In C. E. Thomas and B. Kalyanaman, editors, *Oxygen Radicals and the Disease Process.* Hardwood, Amsterdam, 1997.

[1359] S. C. Stearns. *The Evolution of Life Histories.* Oxford Univ. Press, 1992.

[1360] A. Stechmann and T. Cavalier-Smith. Rooting the eukaryote tree by using a derived gene fusion. *Science*, **297**:89–91, 2002.

[1361] G. G. Steel. *Growth Kinetics of Tumors.* Clarendon Press, Oxford, 1977.

[1362] J. H. Steele. *The Structure of Marine Ecosystems.* Oxford Univ. Press, 1993.

[1363] P. Steemans and C. H. Wellman. Miospores and the emergence of land plants. In B. Webby, F. Paris, M. L. Droser, and I. C. Percival, editors, *The Great Ordovician Biodiversification Event.*, pages 361–366. Columbia Univ. Press, New York, 2004.

[1364] R. G. Steen. The bioenergetics of symbiotic sea anemones (*Anthozoa: Actinaria*). *Symbiosis*, **5**:103–142, 1988.

[1365] E. T. Steenkamp, J. Wright, and S. L. Baldauf. The protistan origins of animals and fungi. *Mol. Biol. Evol.*, **23**:93–106, 2006.

[1366] R. Stein and J. J. Blum. On the analysis of futile cycles in metabolism. *J. theor. Biol.*, **72**:487–522, 1978.

[1367] D. Steinberg. Fatty acid metabolization - mechanisms of regulation and metabolic consequences. In J. K. Grant and G. Popják, editors, *The control of lipid metabolism*, pages 111–144. Acad. Press, London and New york, 1963.

[1368] C. P. Stelzer. Resource limitation and reproductive effort in a planktonic rotifer. *Ecology*, **82**:2521–2533, 2001.

[1369] R. S. Stemberger and J. J. Gilbert. Body size, food concentration, and population growth in planktonic rotifers. *Ecology*, **66**:1151–1159, 1985.

[1370] M. N. Stephens. The otter report. Universal Federation of Animal Welfare, Hertfordshire, 1957.

[1371] R. W. Sterner and J. J. Elser. *Ecological Stoichiometry.* Princeton Univ. Press, 2002.

[1372] J. D. Stevens. Vertebral rings as a means of age determination in the blue shark (*Prionace glauca* L.). *J. Mar. Biol. Assoc. U. K.*, **55**:657–665, 1975.

[1373] J. R. Steward and M. B. Thompson. Evolution of placentation amoung squamate reptiles: recent research and future directions. *Comp. Biochem. Physiol.*, **127**:411–431, 2000.

[1374] J. W. Stiller, D. C. Reel, and J. C. Johnson. A single origin of plastids revisited: convergent evolution in organellar genome content. *J. Phycol.*, **39**:95–105, 2003.

[1375] D. K. Stoecker and M. W. Silver. Replacement and aging of chloroplasts in *Strombidium capitatum* (*Ciliophora: Oligaotrichida*). *Mar. Biol.*, **107**:491–502, 1990.

[1376] M. D. Stokes. Larval locomotion of the lancelet *Branchiostoma floridae*. *J. Exp. Biol.*, **200**:1661–1680, 1997.

[1377] B. Stonehouse. The emperor penguin. I: Breeding behaviour and development. F.I.D.S. Scientific Reports 6, 1953.

[1378] B. Stonehouse. The brown skua of south georgia. F.I.D.S. Scientific Reports 14, 1956.

[1379] B. Stonehouse. The king penguin of south georgia I. breeding behaviour and development. F.I.D.S. Scientific Reports 23, 1960.

[1380] A. H. Stouthamer. Metabolic pathways in *Paracoccus denitrificans* and closely related bacteria in relation to the phylogeny of prokaryotes. *Antonie van Leeuwenhoek*, **61**:1–33, 1992.

[1381] A. H. Stouthamer, B. A. Bulthuis, and H. W. van Verseveld. Energetics of growth at low growth rates and its relevance for the maintenance concept. In R. K. Poole, M. J. Bazin, and C. W. Keevil, editors, *Microbial Growth Dynamics*, pages 85–102. IRL Press, Oxford, 1990.

[1382] A. H. Stouthamer and S. A. L. M. Kooijman. Why it pays for bacteria to delete disused DNA and to maintain megaplasmids. *Antonie van Leeuwenhoek*, **63**:39–43, 1993.

[1383] N. M. van Straalen, T. B. A. Burghouts, M. J. Doornhof, G. M. Groot, M. P. M. Janssen, E. N. G. Joosse, J. H. van Meerendonk, J. P. J. J. Theeuwen, H. A. Verhoef, and H. R. Zoomer. Efficiency of lead and cadmium excretion in populations of *Orchesalla cincta* (*Collembola*) from various contaminated forest soils. *J. Appl. Ecol.*, **24**:953–968, 1987.

[1384] S. Stracke, C. Kistner, S. Yoshida, et al. A plant receptor-like kinase required bor both bacterial and fungal symbiosis. *Nature*, **417**:959–962, 2002.

[1385] R. Strahan, editor. *The Complete Book of Australian Mammals.* Angus & Robertson, London, 1983.

[1386] R. R. Strathmann and M. F. Strathmann. The relationship between adult size and brooding in marine invertebrates. *Am. Nat.*, **119**:91–1011, 1982.

[1387] J. R. Strickler. Calanoid copepods, feeding currents and the role of gravity. *Science*, **218**:158–160, 1982.

[1388] S. J. van Strien. *Structures in dynamics*, chapter Interval Dynamics, pages 111–160. Elsevier, Amstrdam, 1991.

[1389] T. Strömgren and C. Cary. Growth in length of *Mytilus edulis* L. fed on differentalgal diets. *J. Mar. Biol. Assoc. U. K.*, **76**:23–34, 1984.

[1390] P. K. Strother, L. Battison, M. D. Brasier, and C. H. Wellman. Earth's earliest non-marine eukaryotes. *Nature*, 2011. doi:10.1038/nature09943.

[1391] M. Strous. *Microbiology of anaerobic ammonium oxidation.* PhD thesis, Univ. of Delft, 2000.

[1392] M. Strous and M. S. M. Jetten. Anaerobic oxidation of mathane and ammonium. *Annu. Rev. Microbiol.*, **58**:99–117, 2004.

[1393] L. Stryer. *Biochemistry.* W. H. Freeman and Comp., New York, 1988.

[1394] M. R. Sullivan, J. B. Waterbury, and S. W. Chisholm. Cyanophages infecting the oceanic cyanobacterium *Prochlorococcus*. *Nature*, **424**:1047–1050, 2003.

[1395] W. C. Summers. Age and growth of *Loligo pealei*, a population study of the common Atlantic coast squid. *Biol. Bull. (Woods Hole)*, **141**:189–201, 1971.

[1396] D. W. Sutcliffe, T. R. Carrick, and L.G. Willoughby. Effects of diet, body size, age and temperature on growth rates in the amphipod *Gammarus pulex*. *Freshwater Biol.*, **11**:183–214, 1981.

[1397] A. Suwanto and S. Kaplan. Physical and genetic mapping of the *Rhodobacter sphaeroides* 2.4.1. genome: presence of two unique circular chromosomes. *J. Bacteriol.*, **171**:5850–5859, 1989.

[1398] C. Swennen, M. F. Leopold, and M. Stock. Notes on growth and behaviour of the American razor clam *Ensis directus* in the Wadden Sea and the predation on it by birds. *Helgol. Wiss. Meeresunters.*, **39**:255–261, 1985.

[1399] E. Syngajewskaja. The individual growth of protozoa: *Blepharisma lateritia* and *Actinophrys sp. Trav. Inst. Zool. Biol. Acad. Sci. Ukr.*, **8**:151–157, 1935.

[1400] B. Taborsky. Mothers determine offspringsize in response to own juvenile growth conditions. *Biol. Lett.*, **2**:225–228, 2006.

[1401] H. Tappan. Possible eucaryotic algae (*Bangiophycidae*) among early Proterozoic microfossils. *Geol. Soc. Am. Bull.*, **87**:633–639, 1976.

[1402] W. M. Tattersall and E. M. Sheppard. Observations on the asteriod genus *Luidia*. In *James Johnstone Memorial Volume*, pages 35–61. Liverpool Univ. Press, 1934.

[1403] C. R. Taylor, K. Schmidt-Nielsen, and J. L. Raab. Scaling of energetic costs of running to body size in mammals. *Am. J. Physiol.*, **219**:1104–1107, 1970.

[1404] D. L. Taylor. Symbiotic marine algae: taxonomy and biological fitness. In W. B. Vernberg, editor, *Symbiosis in the Sea*, pages 245–262. Univ. of South Carolina Press, Columbia, 1974.

[1405] F. J. R. Taylor. Implications and extensions of the serial endosymbiosis theory of the origin of eukaryotes. *Taxon*, **23**:229–258, 1974.

[1406] I. R. Taylor. Oxygen consumption of individual pupae during metamorphosis,. *J. Morphol. Physiol.*, **44**:313–339, 1927.

[1407] J. M. Taylor and B. E. Horner. Sexual maturation in the Australian rodent *Rattus fuscipes assimilis*. *Austral. J. Zool.*, **19**:1–17, 1971.

[1408] J. W. Taylor, J. Spatafora, K. O'Donnell, F. Lutzoni, T. James, D. S. Hibbert, D. Geiser, T. D. Bruns, and M. Blackwell. The fungi. In J. Cracraft and M. J. Donoghue, editors, *Assembling the Tree of Life*, pages 171–194. Oxford Univ. Press, 2004.

[1409] P. Taylor, T. E. Rummery, and D. G. Owen. Reactions of iron monosulfide solids with aqueous hydrogen sulfide up to 160°c. *J. Inorgani. Nucl. Chem.*, **41**:1683–1687, 1979.

[1410] R. H. Taylor. Growth of adelie penguin (*Pygoscelis adeliae* Hombron and Jacquinot) chicks. *N. Z. J. Sci.*, **5**:191–197, 1962.

[1411] W. D. Taylor. Growth responses of ciliate protozoa to the abundance of their bacterial prey. *Microb. Ecol.*, **4**:207–214, 1978.

[1412] H. Tennekes. *De Wetten van de Vliegkunst; Over Stijgen, Dalen, Vliegen en Zweven.* Aramith Uitgevers, Bloemendaal, 1992.

[1413] A. J. Tessier and C. E. Goulden. Cladoceran juvenile growth. *Limnol. Oceanogr.*, **32**:680–685, 1987.

[1414] T. F. Thingstad, H. Havskum, K. Garde, and B. Riemann. On the strategy of "eating your competitor": a mathematical analysis of algal mixotrophy. *Ecology*, **77**:2108–2118, 1996.

[1415] R. V. Thomann. Bioaccumulation model of organic chemical distribution in aquatic food chains. *Environ. Sci. Technol.*, **23**:699–707, 1989.

[1416] T. W. Thomann and J. A. Mueller. *Principles of Surface Water Quality Modeling and Control.* Harper & Row, New York, 1987.

[1417] P. G. Thomas and T. Ikeda. Sexual regression, shrinkage, re-maturation and growth of spent female *Euphausia superba* in the laboratory. *Mar. Biol.*, **95**:357–363, 1987.

[1418] D'Archy W. Thompson. *Growth and Form.*, volume I & II. Cambridge Univ. Press, 1917.

[1419] J. M. T. Thompson and H. B. Stewart. *Nonlinear Dynamics and Chaos.* J. Wiley, Chichester, 1986.

[1420] K. S. Thompson. *Living Fossil: The Story of the Coelacanth.* Hutchinson Radius, London, 1991.

[1421] M. B. Thompson. Patterns of metabolism in embryonic reptiles. *Respir. Physiol.*, **76**:243–256, 1989.

[1422] W. M. Thornton. The relation of oxygen to the heat of combustion of organic compounds. *Phil. Mag.*, **33**(Ser 6):196–203, 1917.

[1423] S. T. Threlkeld. Starvation and the size structure of zooplankton communities. *Freshwater Biol.*, **6**:489–496, 1976.

[1424] E. V. Thuesen. The tetrodotoxin venom of chaetognaths. In Q. Bone, H. Kapp, and A. C. Pierrot-Bults, editors, *The Biology of Chaetognaths.* Oxford Univ. Press, 1991.

[1425] R. R. Tice and R. B. Setlow. DNA repair and replication in aging organisms and cells. In C. E. Finch and E. L. Schneider, editors, *Handbook of the Biology of Aging*, pages 173–224. Van Nostrand, New York, 1985.

[1426] W. L. N. Tickell. *The Biology of the Great Albatrosses,* Diomedea exulans *and* Diomedea epomophora, pages 1–55. American Geophysical Union, Washington, DC, 1968.

[1427] A. G. M. Tielens. Energy generation in parasitic helminths. *Parasitol. Today*, **10**:346–352, 1994.

[1428] A. G. M. Tielens and J. J. van Hellemond. Differences in energy metabolism between *Trypanosomatidae. Parasitol. Today*, **14**:265–271, 1998.

[1429] A. G. M. Tielens and J. J. van Hellemond. The electron transport chain in anaerobically functioning eukaryotes. *Biochim. Biophys. Acta*, **1365**:71–78, 1998.

[1430] A. G. M. Tielens, C. Rotte, J. J. van Hellemond, and W. Martin. Mitochondria as we don't know them. *Trends Biochem. Sci.*, **27**:564–572, 2002.

[1431] K. Tiews. Biologische Untersuchungen am Roten Thun (*Thunnus thynnus* [Linnaeus]) in der Nordsee. *Ber. Dtsch. Wiss. Komm. Meeresforsch.*, **14**:192–220, 1957.

[1432] C. Tolla. *Bacterial populations dynamics modelling: applied to the study of bioturbation effects on the nitrogen cycle in marine sediments.* PhD thesis, Univ. of Marseille & Vrije Univ., Amsterdam, 2006.

[1433] C. Tolla, S. A. L. M. Kooijman, and J. C. Poggiale. A kinetic inhibition mechanism for the maintenance process. *J. theor. Biol.*, **244**:576–587, 2007.

[1434] H. Topiwala and C. G. Sinclair. Temperature relationship in continuous culture. *Biotechnol. Bioeng.*, **13**:795–813, 1971.

[1435] N. R. Towers, J. K. Raison, G. M. Kellerman, and A. W. Linnane. Effects of temperature-induced phase changes in membranes on protein synthesis by bound ribosomes. *Biochim. Biophys. Acta*, **287**:301–311, 1972.

[1436] A. P. J. Trinci. A kinetic study of the growth of *Aspergillus nidulans* and other fungi. *J. Gen. Microbiol.*, **57**:11–24, 1969.

[1437] A. P. J. Trinci, G. D. Robson, M. G. Wiebe, B. Cunliffe, and T. W. Naylor. Growth and morphology of *Fusarium graminearum* and other fungi in batch and continuous culture. In R. K. Poole, M. J. Bazin, and C. W. Keevil, editors, *Microbial Growth Dynamics*, pages 17–38. IRL Press, Oxford, 1990.

[1438] T. Troost. *Evolution of community metabolism.* PhD thesis, Vrije Univ., Amsterdam, 2006.

[1439] T. A. Troost, B. W. Kooi, and S. A. L. M. Kooijman. Ecological specialization of mixotrophic plankton in a mixed water column. *Am. Nat.*, **166**:E45–E61, 2005.

[1440] T. A. Troost, B. W. Kooi, and S. A. L. M. Kooijman. When do mixotrophs specialize? Adaptive dynamics theory applied to a dynamic energy budget model. *Math. Biosci.*, **193**:159–182, 2005.

[1441] I. Trubetskova and W. Lampert. Egg size and egg mass of *Daphnia magna* response to food availability. *Hydrobiol.*, **307**:139–145, 1995.

[1442] F. J. Trueba. *A morphometric analysis of* Escherichia coli *and other rod-shaped bacteria.* PhD thesis, Univ. of Amsterdam, 1981.

[1443] S. Tuljapurkar and H. Caswell. *Structured-Population Models in Marine, Terrestrial, and Freshwater Systems.* Chapman & Hall, New York, 1996.

[1444] A. W. H. Turnpenny, R. N. Bamber, and P.A. Henderson. Biology of the sand-smelt (*Atherina presbyter* Valenciennes) around Fawlay power station. *J. Fish Biol.*, **18**:417–427, 1981.

[1445] B. M. Tyler, S. Tripathy, et al. *Phytophthora* genome sequences uncover evolutionary origins and mechanisms of pathogenesis. *Science*, **313**:1261–1266, 2006.

[1446] H. Tyndale-Biscoe. *Life of Marsupials.* E. Arnold, London, 1973.

[1447] T. Tyrell. The relative influences of nitrogen and phosphorous on oceanic primary production. *Nature*, **400**:525–531, 1999.

[1448] A. Tzur, R. Kafri, V. S. LeBleu, G. Lahav, and M. W. Kirschner. Cell growth and size homeostasis in proliferating animal cells. *Science*, **325**:167–171, 2009.

[1449] D. E. Ullrey, J. I. Sprague, D. E. Becker, and E. R. Miller. Growth of the swine fetus. *J. Anim. Sci.*, **24**:711–717, 1965.

[1450] F. A. Urquhart. *The Monarch Butterfly: International Traveler.* Nelson Hall, Chicago, 1987.

[1451] E. Ursin. A mathematical model of some aspects of fish growth, respiration, and mortality. *J. Fish. Res. Board Can.*, **24**:2355–2453, 1967.

[1452] K. Uvnäs-Moberg. The gastrointestinal tract in growth and reproduction. *Sci. Am.*, **7**:60–65, 1989.

[1453] J. C. Valmalette, A. Dombrivsky, C. Mertz, and M. Capovilla. Light- induced electron transfer and atp synthesis in a carotene synthesizing insect. *SCIENTIFIC REPORTS*, **2**:579, 2012. DOI: 10.1038/srep00579.

[1454] H. A. Vanderploeg, G.-A. Paffenhöfer, and J. R. Liebig. Concentration-variable interactions between calanoid copepods and particles of different food quality: observations and hypothesis. In R. N. Hughes, editor, *Behavioural Mechanisms of Food Selection*, volume G 20, pages 595–613. Springer-Verlag, Berlin, 1990.

[1455] K. Vánky. *Illustrated Genera of Smut Fungi.*, volume 1 of *Cryptogamic Studies*. Gustav Fischer Verlag, Stuttgart, 1987.

[1456] H. van der Veer, J. F. M. F. Cardoso, M. A. Peck, and S. A. L. M. Kooijman. Physiological performance of plaice *Pleuronectes platessa* (L.): from Static to Dynamic Energy Budgets. *J. Sea Res.*, **62**:83–92, 2009.

[1457] H. W. van der Veer, S. A. L. M. Kooijman, W. C. Leggett, and J. van der Meer. Body size scaling relationships in flatfish as predicted by dynamic energy bugets (DEB theory): implications for recruitment. *J. Sea Res.*, **50**:255–270, 2003.

[1458] H. W. van der Veer, S. A. L. M. Kooijman, and J. van der Meer. Intra- and interspecific comparison of energy flow in north atlantic flatfish species by means of dynamic energy budgets. *J. Sea Res.*, **45**:303–320, 2001.

[1459] N. Verboven and T. Piersma. Is the evaporative water loss of knot *Calidris canutus* higher in tropical than in temperate climates? *Ibis*, **137**:308–316, 1995.

[1460] C Verduyn. *Energetic aspects of metabolic fluxes in yeasts.* PhD thesis, Technical Univ., Delft, 1992.

[1461] K. Vermeer. The importance of plankton to Cassin's auklets during breeding. *J. Plankton Res.*, **3**:315–329, 1981.

[1462] H. W. van Verseveld, M. Braster, F. C. Boogerd, B. Chance, and A. H. Stouthamer. Energetic aspects of growth of *Paracoccus denitrificans*: oxygen-limitation and shift from anaerobic nitrate-limitation to aerobic succinate-limitation. *Arch. Microbiol.*, **135**:229–236, 1983.

[1463] H. W. van Verseveld and A. H. Stouthamer. Oxidative phosphorylation in *Micrococcus denitrificans*; calculation of the P/O ration in growing cells. *Arch. Microbiol.*, **107**:241–247, 1976.

[1464] H. W. van Verseveld and A. H. Stouthamer. Growth yields and the efficiency of oxydative phosphorylation during autotrophic growth of *Paracoccus denitrificans* on methanol and formate. *Arch. Microbiol.*, **118**:21–26, 1978.

[1465] H. W. van Verseveld and A. H. Stouthamer. Two-(carbon) substrate-limited growth of *Paracoccus denitrificans* on mannitol and formate. *FEMS Microbiol. Lett.*, **7**:207–211, 1980.

[1466] J. Vidal and T. E. Whitledge. Rates of metabolism of planktonic crustaceans as related to body weight and temperature of habitat. *J. Plankton Res.*, **4**:77–84, 1982.

[1467] R. K. Vijendravarma, S. Narasimha, and T. J. Kawecki. Effects of parental larval diet on egg size and offspring in *Drosophila*. *Biol. Lett.*, **6**:238–241, 2010.

[1468] J. Vijverberg. Effect of temperature in laboratory studies on development and growth of *Cladocera* and *Copepoda* from Tjeukemeer, The Netherlands. *Freshwater Biol.*, **10**:317–340, 1980.

[1469] T. A. Villareal. Evaluation of nitrogen fixation in the diatom genus *Rhizosolenia* Ehr. in the absence of its cyanobacterial symbiont *Richelia intracellularis* Schmidt. *J. Plankton Res.*, **9**:965–971, 1987.

[1470] T. A. Villareal. Nitrogen fixation of the cyanobacterial symbiont of the diatom genus *Hemiaulus*. *Mar. Ecol. Prog. Ser.*, **76**:201–204, 1991.

[1471] C. M. Vleck, D. F. Hoyt, and D. Vleck. Metabolism of embryonic embryos: patterns in altricial and precocial birds. *Physiol. Zool.*, **52**:363–377, 1979.

[1472] C. M. Vleck, D. Vleck, and D. F. Hoyt. Patterns of metabolism and growth in avian embryos. *Am. Zool.*, **20**:405–416, 1980.

[1473] D. Vleck, C. M. Vleck, and R. S. Seymour. Energetics of embryonic development in the megapode birds, mallee fowl *Leipoa ocellata* and brush turkey *Alectura lathami*. *Physiol. Zool.*, **57**:444–456, 1984.

[1474] N. J. Volkman and W. Trivelpiece. Growth in pygoscelid penguin chicks. *J. Zool. of Lond.*, **191**:521–530, 1980.

[1475] P. de Voogt, B. van Hattum, P. Leonards, J.C. Klamer, and H. Govers. Bioconcentration of polycyclic hydrocarbons in the guppy (*Poecilia reticulata*). *Aquat. Toxicol.*, **20**:169–194, 1991.

[1476] W. J. Voorn and A. L. Koch. Characterization of the stable size distribution of cultured cells by moments. In J. A. J. Metz and O. Diekmann, editors, *The Dynamics of Physiologically Structured Populations*, volume 68 of *Springer Lecture Notes in Biomathematics.*, pages 430–440. Springer-Verlag, Berlin, 1986.

[1477] G. Wächtershäuser. Before enzymes and templates: Theory of surface metabolism. *Microbiol. Rev.*, **52**:452–484, 1988.

[1478] G Wächtershäuser. Pyrite formation, the first energy source for life. a hypothesis. *System. Appl. Microbiol.*, **10**:207–210, 1988.

[1479] G Wächtershäuser. Evolution of the 1st metabolic cycles. *Proc. Natl. Acad. Sci. U. S. A.*, **87**:200–204, 1990.

[1480] T. G. Waddell, P. Repovic, E. Meléndez-Hevia, R. Heinrich, and F. Montero. Optimization of glycolysis: A new look at the efficiency of energy coupling. *Biochemical Education*, **25**:204–205, 1997.

[1481] J. G. Wagner. The kinetics of alcohol elimination in man. *Acta Pharmacol. Toxicol.*, **14**:265–289, 1958.

[1482] J. G. Wagner. A modern view in pharmacokinetics. *J. Pharmacokinet. Biopharm.*, **1**:363–401, 1973.

[1483] J. G. Wagner. Do you need a pharmacokinetic model, and, if so, which one? *J. Pharmacokinet. Biopharm.*, **3**:457–478, 1975.

[1484] J. G. Wagner. Time to reach steady state and prediction of steady-state concentrations for drugs obeying Michaelis-Menten elimination kinetics. *J. Pharmacokinet. Biopharm.*, **6**:209–225, 1978.

[1485] C. H. Walker. Kinetic model to predict bioaccumulation of pollutant. *Funct. Ecol.*, **4**:295–301, 1990.

[1486] E. P. Walker. *Mammals of the World.* Johns Hopkins Univ. Press, Baltimore, 1975.

[1487] G. M. Walker. *Yeast; Physiology and Biotechnology.* J. Wiley, Chichester, 1998.

[1488] M. R. Walker. Stromatolites: The main geological source of information on the evolution of the early benthos. In S. Bengtson, editor, *Early Life on Earth.*, volume 84 of *Nobel Symp.*, pages 270–286. Columbria Univ. Press, New York, 1994.

[1489] M. Walls, H. Caswell, and M. Ketola. Demographic costs of Chaoborus-induced defences in *Daphnia pulex*. *Oecologia*, **87**:43–50, 1991.

[1490] G. E. Walsberg and T. C. M. Hoffman. Using direct calorimetry to test the accuracy of indirect calorimetry in an ectotherm. *Physiological and Biochemical Zoology*, **79(4)**:830–835, 2006.

[1491] G. E. Walsberg and Ty. C. M. Hoffman. Direct calorimetry reveals large errors in respirometric estimates of energy expenditure. *J. Exp. Biol*, **208**:1035–1043, 2005.

[1492] A. E. Walsby. A square bacterium. *Nature*, **283**:69–73, 1980.

[1493] P. Ward. Precambrian strikes back. *New Sci.*, **February 9**(9 Feb):40–43, 2008.

[1494] S. Ward and J. S. Carrel. Fertilization and sperm competition in the nematode *Caenorhabditis elegans*. *Develop. Biol.*, **73**:304–321, 1979.

[1495] J. Warham. The crested penguins. In B. Stonehouse, editor, *The Biology of Penguins*, pages 189–269. MacMillan, London, 1975.

[1496] B. L. Warwick. Prenatal growth of swine. *J. Morphol.*, **46**:59–84, 1928.

[1497] I. Watanabe and S. Okada. Effects of temperature on growth rate of cultured mammalian cells (l5178y). *J. Cell Biol.*, **32**:309–323, 1967.

[1498] L. Watson. *Whales of the World.* Hutchinson, London, 1981.

[1499] E. Watts and S. Young. Components of *Daphnia* feeding behaviour. *J. Plankton Res.*, **2**:203–212, 1980.

[1500] J. van Waversveld, A. D. F. Addink, and G. van den Thillart. The anaerobic energy metabolism of goldfish determined by simultaneous direct and indirect calorimetry during anoxia and hypoxia. *J. Comp. Physiol.*, **159**:263–268, 1989.

[1501] J. van Waversveld, A. D. F. Addink, G. van den Thillart, and H. Smit. Heat production of fish: a literature review. *Comp. Biochem. Physiol.*, **92A**:159–162, 1989.

[1502] H. Wawrzyniak and G. Sohns. *Die Bartmeise.*, volume 553. A. Ziemsen-Verlag, Wittenberg Lutherstadt, 1986.

[1503] G. J. W. Webb, D. Choqeunot, and P. J. Whitehead. Nests, eggs, and embryonic development of *Carettochelys insculpta* (*Chelonia*: *Carettochelidae*) from Northern Australia. *J. Zool. of Lond.*, **B1**:521–550, 1986.

[1504] G. J. W. Webb, S. C. Manolis, K. E. Dempsey, and P. J. Whitehead. Crocodilian eggs: a functional overview. In G. J. W. Webb, S. C. Manolis, and P. J. Whitehead, editors, *Wildlife Management: Crocodiles and Alligators*, pages 417–422. Beatty, Sydney, 1987.

[1505] T. P. Weber and T. Piersma. Basal metabolic rate and the mass of tissues differing in metabolic scope: migration-related covariation between individual knots *Calidris canutus*. *J. Avian Biol.*, **27**:215–224, 1996.

[1506] W. Weibull. A statistical distribution of wide applicability. *J. Appl. Mech.*, **18**:293–297, 1951.

[1507] A. P. Weinbach. The human growth curve. I: Prenatal. *Growth*, **5**:217–233, 1941.

[1508] R. Weindruch, R. L. Walford, S. Fligiel, and D. Guthrie. The retardation of aging in mice by dietary restriction: Longevity, cancer, immunity and lifetime energy intake. *J. Nutr.*, **116**:641–654, 1986.

[1509] J. Weiner. Physiological limits to sustainable energy budgets in birds and mammals: ecological implications. *Trends Ecol. Evol.*, **7**:384–388, 1992.

[1510] T. F. Weis. *Cellular Biophysics.*, volume I Transport. MIT Press, Cambridge, Mass., 1996.

[1511] E. Weitnauer-Rudin. Mein vogel. aus dem leben der mauerseglers *Apus apus*. Basellandschaftlicher Natur- und Vogelschutzverband, Liestal., 1983.

[1512] M. J. Wells. Cephalopods do it differently. *New Sci.*, **3**:333–337, 1983.

[1513] J. van Wensum. *Isopods and pollutants in decomposing leaf litter.* PhD thesis, Vrije Univ., Amsterdam, 1992.

[1514] J. H. Werren. Evolution and consequences of *Wolbachia* symbioses in invertebrates. *Am. Zool.*, **40**:1255–1255, 2000.

[1515] D. F. Werschkul. Nestling mortality and the adaptive significance of early locomotion in the little blue heron. *Auk*, **96**:116–130, 1979.

[1516] G. B. West, J. H. Brown, and B. J. Enquist. A general model for the origin of allometric scaling laws in biology. *Science*, **276**:122–126, 1997.

[1517] G. B. West, J. H. Brown, and B. J. Enquist. A general model for the structure and allometry of vascular systems. *Nature*, **400**:664–668, 1999.

[1518] G. B. West, J. H. Brown, and B. J. Enquist. A general model for ontogenetic growth. *Nature*, **413**:628–631, 2001.

[1519] I. C. West. *The Biochemistry of Membrane Transport.* Chapman & Hall, London, 1983.

[1520] M. J. West-Eberhard. *Developmental plasticity and evolution.* Oxford University Press, Oxford, 2003.

[1521] P. Westbroek. *Life as a Geological Force; Dynamics of the Earth.* W. W. Norton, New York, 1991.

[1522] H. V. Westerhoff and K. van Dam. *Thermodynamics and Control of Biological Free Energy Transduction.* Elsevier, Amsterdam, 1987.

[1523] K. Westerterp. The energy budget of the nestling starling *Sturnus vulgaris*, a field study. *Ardea*, **61**:137–158, 1973.

[1524] D. F. Westlake. Some effects of low-velocity currents on the metabolism of aquatic macrophytes. *J. Exp. Bot.*, **18**:187–205, 1967.

[1525] R. Wette, I. N. Katz, and E. Y. Rodin. Stochastic processes for solid tumor kinetics: surface-regulated growth. *Math. Biosci.*, **19**:231–225, 1974.

[1526] C. R. White, M. R. Kearney, P. G. D. Matthews, S. A. L. M. Kooijman, and D. J. Marshall. A manipulative test of competing theories for metabolic scaling in animals. *Am. Nat.*, **178**:746–754, 2011. .

[1527] T. C. R. White. *The Inadequate Environment; Nitrogen and the Abundance of Animals.* Springer-Verlag, Berlin, 1993.

[1528] W. T. White. *Aspects of the biology of elasmobranchs in a subtropical embayment in Western Australia and of chondichthyan fisheries in Indonesia.* PhD thesis, Murdoch Univ, Western Australia, 2003.

[1529] P. J. Whitehead. Respiration of *Crocodylus johnstoni* embryos. In G. J. W. Webb, S. C. Manolis, and P. J. Whitehead, editors, *Wildlife Management: Crocodiles and Alligators*, pages 473–497. Beatty, Sydney, 1987.

[1530] P. J. Whitehead, G. J. W. Webb, and R. S. Seymour. Effect of incubation temperature on development of *Crocodylus johnstoni* embryos. *Physiol. Zool.*, **63**:949–964, 1990.

[1531] P. J. Whitfield. *The Biology of Parasitism: An Introduction to the Study of Associating Organisms.* E. Arnold, London, 1979.

[1532] J. N. C. Whyte, J. R. Englar, and B. L. Carswell. Biochemical-composition and energy reserves in *Crassostrea-gigas* exposed to different levels of nutrition. *Aquaculture*, **90**:157–172, 1990.

[1533] A. P. Wickens. *The Causes of Aging.* Harwood, Amsterdam, 1998.

[1534] J. Widdows, P. Fieth, and C. M. Worral. Relationship between seston, available food and feeding activity in the common mussel *Mytilus edulis*. *Mar. Biol.*, **50**:195–207, 1979.

[1535] E. Widmark and J. Tandberg. Über die bedingungen für die Akkumulation indifferenter narkoliken theoretische Bereckerunger. *Biochem. Z.*, **147**:358–369, 1924.

[1536] P. Wiersma and T. Piersma. Effects of microhabitat, flocking, climate and migratory goal on energy expenditure in the annual cycle of red knots. *Condor*, **96**:257–279, 1994.

[1537] H. Wijnandts. Ecological energetics of the long-eared owl (*Asio otus*). *Ardea*, **72**:1–92, 1984.

[1538] M. Wilbrink, M. Treskes, T. A. de Vlieger, and N.P.E. Vermeulen. Comparative toxicokinetics of 2,2'- and 4,4'-dichlorobiphenyls in the pond snail *Lymnaea stagnalis* (L.). *Arch. Environ. Contam. Toxicol.*, **19**:69–79, 1989.

[1539] H. M. Wilbur. Interactions of food level and population density in *Rana sylvatica*. *Ecology*, **58**:206–209, 1977.

[1540] L. W. Wilcox and G. J. Wedemayer. Dinoflagellate with blue-green chloroplasts derived from an ensosymbiotic eukaryote. *Science*, **227**:192–194, 1985.

[1541] M. Wilkelski and C. Thom. Marine iguanas shrink to survive el niño. *Nature*, **403**:37, 2000.

[1542] D. I. Williamson. *Larvae and Evolution.* Chapman & Hall, London, 1992.

[1543] P. Williamson and M. A. Kendall. Population age structure and growth of the trochid *Monodonta lineata* determined from shell rings. *J. Mar. Biol. Assoc. U. K.*, **61**:1011–1026, 1981.

[1544] D. B. Wingate. First successful hand-rearing of an abondoned Bermuda petrel chick. *Ibis*, **114**:97–101, 1972.

[1545] J. E. Winter. The filtration rate of *Mytilus edulis* and its dependence on algal concentrations, measured by a continuous automatic recording apparatus. *Mar. Biol.*, **22**:317–328, 1973.

[1546] L. M. Winters, W. W. Green, and R. E. Comstock. Prenatal development of the bovine. *Techn. Bull. Minn. Agric. Exp. Station*, **151**:1–50, 1942.

[1547] P. C. Withers. *Comparative Animal Physiology.* Saunders College Publishing, Fort Worth, 1992.

[1548] P. C. Withers and J. U. M. Jarvis. The effect of huddling on thermoregulation and oxygen consumption for the naked mole-rat. *Comp. Biochem. Physiol.*, **66**:215–219, 1980.

[1549] M. Witten. A return to time, cells, systems, and aging III: Gompertzian models of biological aging and some possible roles for critical elements. *Mech. Ageing Dev.*, **32**:141–177, 1985.

[1550] C. R. Woese. A proposal concerning the origin of life on the planet earth. *J. Mol. Evol.*, **12**:95–100, 1979.

[1551] C. R. Woese. Archaebacteria. *Sci. Am.*, **6**:98–122, 1981.

[1552] C. R. Woese. On the evolution of cells. *Proc. Natl. Acad. Sci. U. S. A.*, **99**:8742–8747, 2002.

[1553] W. de Wolf, J. H. Canton, J. W. Deneer, R. C. C. Wegman, and J. L. M. Hermens. Quantitative structure-activity relationships and mixture-toxicity studies of alcohols and chlorohydrocarbons: reproducibility of effects on growth and reproduction of *Daphnia magna*. *Aquat. Toxicol.*, **12**:39–49, 1988.

[1554] D. Wolf-Gladrow and U. Riebesell. Diffusion and reactions in the vicinity of plankton: a refined model for inorganic carbon transport. *Mar. Chem.*, **59**:17–34, 1997.

[1555] D. A. Wolf-Gladrow, J. Bijma, and R. E. Zeebe. Model simulation of the carbonate chemistry in the micro-environment of symbiont bearing foraminifera. *Mar. Chem.*, **94**:181–198, 1999.

[1556] R. Wood. *Reef evolution.* Oxford Univ. Press, 1999.

[1557] F. I. Woodward. *Climate and Plant Distribution.* Cambridge Univ. Press, 1987.

[1558] R. J. Wootton. *Ecology of Teleost Fishes.* Chapman & Hall, London, 1990.

[1559] T. R. Worsley, R. D. Nance, and J. B. Moody. Tectonics, carbon, life, and climate for the last three billion years: A unified system? In S. H. Schneider and P. J. Boston, editors, *Scientists on Gaia.*, pages 200–210. MIT Press, Cambridge, Mass., 1991.

[1560] J. P. Wourms. Viviparity: the maternal-fetal relationship in fishes. *Am. Zool.*, **21**:473–515, 1981.

[1561] J. P. Wourms and J. Lombardi. Reflections on the evolution of piscine viviparity. *Am. Zool.*, **32**:276–293, 1992.

[1562] G. A. Wray. Punctuated evolution of embryos. *Science*, **267**:1115–1116, 1995.

[1563] G. A. Wray and A. E. Bely. The evolution of echinoderm development is driven by several distinct factors. *Development*, **suppl.**:97–106, 1994.

[1564] G. A. Wray and R. A. Raff. The evolution of developmental strategy in marine invertebrates. *Trends Ecol. Evol.*, **6**:45–50, 1991.

[1565] J. R. Wright and R. G. Hartnoll. An energy budget for a population of the limpet *Patella vulgata*. *J. Mar. Biol. Assoc. U. K.*, **61**:627–646, 1981.

[1566] I. Wyllie. *The Cuckoo.* Batsford, London, 1981.

[1567] J. Xiong, W. M. Fisher, K. Inoue, et al. Molecular evidence for the early evolution of photosynthesis. *Science*, **289**:1724–1730, 2000.

[1568] A. Ykema. *Lipid production in the oleaginous yeast* Apiotrichum curvantum. PhD thesis, Vrije Univ., Amsterdam, 1989.

[1569] P. Yodzis. *Introduction to Theoretical Ecology.* Harper, New York, 1989.

[1570] S. H. Yoon, J. D. Hacket, C. Ciniglia, G. Pinto, and D. Bhattacharya. The single, ancient origin of chromist plastids. *Proc. Natl. Acad. Sci. U. S. A.*, **99**:15507–15512, 2002.

[1571] S. H. Yoon, J. D. Hacket, C. Ciniglia, G. Pinto, and D. Bhattacharya. A molecular timeline for the origin of photosynthetic eukaryotes. *Mol. Biol. Evol.*, **21**:809–818, 2004.

[1572] S. H. Yoon, A. Reyes-Prieton, M. Melkonian, and D. Bhattacharya. Minimal plastid genome evolution in the *Paulinella* endosymbiont. *Current Biology*, **14**:213–218, 2001.

[1573] T. Yoshinaga, A. Hagiwara, and K. Tsukamoto. Effect of periodical starvation on the survival of offspring in the rotifer *Brachionus plicatilis*. *Fish. Sci.*, **67**:373–374, 2001.

[1574] J. C. Zachos, M. W. Wara, S. Bohaty, M. L. Delaney, et al. A transient rise in tropical sea surface temperature during the Paeocene-Eocene thermal maximum. *Science*, **302**:1551–1554, 2003.

[1575] E. Zeuthen. *Body Size and Metabolic Rate in the Animal Kingdom.* H. Hagerup, Copenhagen, 1947.

[1576] C. Zhang and A. M. Cuervo. Restoration of chaperone-mediated autophagy in aging liver improves cellular maintenance and hepatic function. *Nature Med.*, **14**:959–965, 2008.

[1577] Y.J. Zhao, H. Y. Wu, H. L. Guo, M. Xu, K. Cheng, and H. Y. Zhu. Vacuolation induced by unfavorable pH in cyanobacteria. *Progr. Nat. Sci.*, **11**:931–936, 2001.

[1578] S. H. Zinder. Physiological ecology of methanogens. In J.G. Ferry, editor, *Methanogenesis; Ecology, Physiology, Biochemistry and Genetics*, pages 128–206. Chapman & Hall, London, 1993.

[1579] C. Zonneveld. A cell-based model for the chlorophyll 'a' to carbon ratio in phytoplankton. *Ecol. Modell.*, **113**:55–70, 1998.

[1580] C. Zonneveld. Photoinhibition as affected by photoacclimation in phytoplankton: a model approach. *J. theor. Biol.*, **193**:115–123, 1998.

[1581] C. Zonneveld and S. A. L. M. Kooijman. Application of a general energy budget model to *Lymnaea stagnalis*. *Funct. Ecol.*, **3**:269–278, 1989.

[1582] C. Zonneveld and S. A. L. M. Kooijman. Body temperature affects the shape of avian growth curves. *J. Biol. Syst.*, **1**:363–374, 1993.

[1583] C. Zonneveld and S. A. L. M. Kooijman. Comparative kinetics of embryo development. *Bull. Math. Biol.*, **3**:609–635, 1993.

[1584] G. Zubay. *Origins of life on earth and in the cosmos*. Academic Press, San Diego, 2000.

[1585] W. Zuo, M. E. Moses, C. Hou, W. H. Woodruff, G. B. West, and J. H. Brown. Response to comments on 'energy uptake and allocation during ontogeny'. *Science*, **325**:1206–c, 2009.

Notation and symbols

See the notation document.

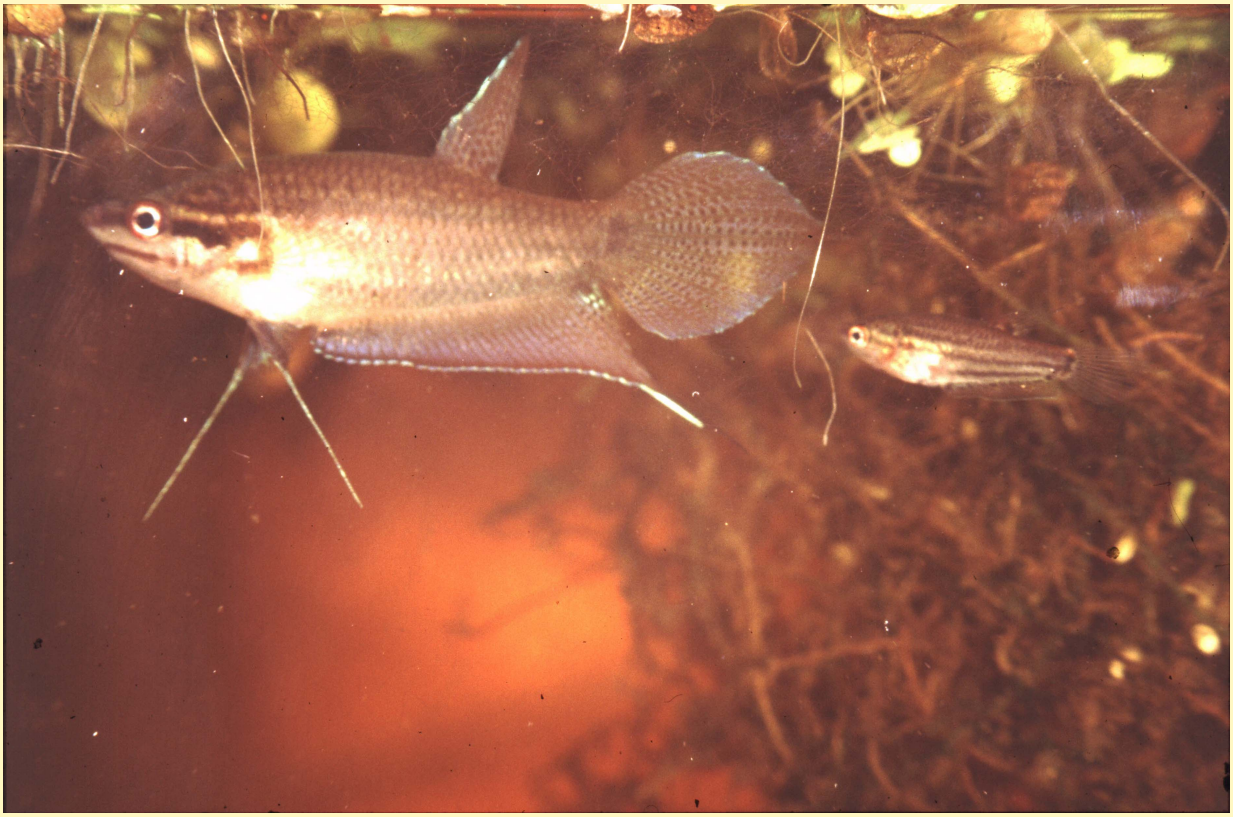

These talking gouramis, *Trichopsis vittatus*, come from the same brood and therefore are the same age. They also grew up in the same aquarium. The size difference resulted from competition for a limited amount of food chunks, which amplified tiny initial size differences. This illustrates that age cannot serve as a satisfactory basis for the description of growth and food intake should be included explicitly.

Dynamic Energy Budget (DEB) theory is a formal theory for the uptake and use of substrates (food, nutrients, light) by organisms and their use for maintenance, growth, maturation and propagation; it applies to all organisms (microorganisms, animals, plants). The document gives background, explanation and extension for the third edition of the DEB book.